Forecasting Resilience Loss for Flexible Pavement under the Impact of Temperature due to Climate Change

التنبؤ بمعدل فقدان الصلابة للطرق الأسفلتية تحت تأثيرالحراره بسب التغير المناخي

by

MOHAMMED MUFTAH ALARYANI

A thesis submitted in fulfilment

of the requirements for the degree of

DOCTOR OF PHILOSOPHY IN PROJECT MANAGEMENT

at

The British University in Dubai

June 2019

Forecasting Resilience Loss for Flexible Pavement under the Impact of Temperature due to Climate Change

التنبؤ بمعدل فقدان الصلابة للطرق الاسفلتية تحت تأثيرالحراره بسب التغير المناخي

by

MOHAMMED MUFTAH ALARYANIA

thesis submitted in fulfilment of the requirements for the degree of

DOCTOR OF PHILOSOPHY (PhD) in PROJECT MANAGEMENT

at

The British University in Dubai

June 2019

Thesis Supervisor

Professor Halim Boussabaine

Approved for award:

______________________________ ______________________________

Name Name

Designation Designation

______________________________ ______________________________

Name Name

Designation Designation

Date: _____________

DECLARATION

I warrant that the content of this research is the direct result of my own work and that any use made in it of published or unpublished copyright material falls within the limits permitted by international copyright conventions.

I understand that a copy of my research will be deposited in the University Library for permanent retention.

I hereby agree that the material mentioned above for which I am author and copyright holder may be copied and distributed by The British University in Dubai for the purposes of research, private study or education and that The British University in Dubai may recover from purchasers the costs incurred in such copying and distribution, where appropriate.

I understand that The British University in Dubai may make a digital copy available in the institutional repository.

I understand that I may apply to the University to retain the right to withhold or to restrict access to my thesis for a period which shall not normally exceed four calendar years from the congregation at which the degree is conferred, the length of the period to be specified in the application, together with the precise reasons for making that application.

____

Signature of the student

COPYRIGHT AND INFORMATION TO USERS

ABSTRACT

Projects and programmes for maintenance and rehabilitation works are crucial for pavement assets in order to achieve the required levels of safety and operability. It is well documented in the literature that pavement network infrastructures age with time, are underfunded and, more importantly, are designed based on historical conditions. The HDM-4 model, which is extensively used in pavement management systems, does not utilise future climate predictions. Climate change is likely to threaten pavement infrastructures' resilience through extreme weather events and chronically through gradual degradation. The objectives of the study were fivefold: firstly, to develop a modified HDM-4 model using pavement performance indicators (International Roughness Index and Pavement Condition Index) that assess the impacts of future climate change; secondly, to develop a Markov chain model for projection of pavement deterioration rate under different climate scenarios based on a modified HDM-4 model; thirdly, to establish the generic risk of pavement failure under the impact of climate change and quantify the risk interrelationships based on the received questionnaires using a deterministic risk analysis method; fourthly, to develop a system dynamics model for the projection of pavement deterioration rate for different risk scenarios; and, finally, to measure pavement resilience loss for the pavement network. The models were developed using data provided by the roads department in the Ministry of Public Works of the United Arab Emirates, Al Ain City Municipality, National Centre of Meteorology and Seismology, and questionnaires. A number of different methodologies were used such as linear and non-linear regression, simulation of system dynamics and probabilistic approach using a Markov chain. Both Markov chain and system dynamics models indicated that climate change impact can accelerate the rate of degradation for infrastructure assets. Moreover, the Markov chain model indicated resilience loss for the pavement network in the range of 27.86% to 32.4% for different climate change scenarios (2013, 2020, 2040 and 2060) over a period of 20 years' prediction. In addition, for the ultimate worse scenario, the resilience loss score was 73.57%. This record showed a value close to the range of resilience loss generated from the system dynamics model (range between 75.67% and 81.0% resilience loss). This research provides an increased understanding of modelling and managing uncertainty in pavement deterioration with respect to climate change impacts. Developing different tools such as a pavement condition index model, modified HDM-4, and probabilistic and system dynamics model will help the road and highway agency in the UAE to efficiently monitor the road pavement assets and establish the necessary maintenance plan for future years, and captures a real system which assists the policy decision makers in their pavement intervention programme.

تعد مشروعات وبرامج أعمال الصيانة وإعادة التأهيل ضرورية لأصول البنية التحتيه متمثله في أعمال الطرق من أجل تحقيق المستويات المطلوبة من السلامة المروريه ضمان التنقل المرن. تفيد الدراسات و الابحاث السابقه بأن البنية التحتية لشبكة الطرق تتهالك مع مرور الوقت ، وهي أيضا تعاني من نقص في التمويل ، والأهم من ذلك أنها مصممة حسب ظروف و معطيات مختلفه عن الوضع الحالي. على سبيل المثال ، نموذج (هج دي ام فور)، والذي يستخدم على نطاق واسع في أنظمة إدارة الطرق غير مصمم للتعاطي مع التغيرات المناخية المستقبلية. أن من المحتمل أن يهدد التغير المناخي مرونة و متانة البنية التحتية للطرق من خلال العواصف و الكوارث والطبيعيه أو من خلال التغير التدريجي في معدلات الظروف الجويه. تهدف هذه الدراسة إلى تحقيق خمسة أهداف: أولاً ، تطوير نموذج (هج دي ام فور) محدث باستخدام مؤشرات أداء الطرق (مؤشر خشونة الطرق ومؤشر حالة الرصف) حيث ستساهم هذه المؤشرات في تقيم الضرر المتوقع من ظاهرة التغير المناخ ؛ ثانياً ، تطوير نموذج سلسلة ماركوف للتنبؤ بمعدل تهالك الطرق في ظل سيناريوهات مناخية مختلفة بناءً على نموذج (هج دي ام فور) المعدل ؛ ثالثًا ، تحديد المخاطر المسببه لفشل الطرق تحت تأثير تغير المناخ وتحديد العلاقات المتبادلة للمخاطر استنادًا إلى الاستبيانات المستلمة باستخدام طريقة تحليل المخاطر الحتمية ؛ رابعا : تطوير نموذج لنظام ديناميكي قادر على التنبؤ بمعدل تهالك الطلرق لعدة سيناريوهات تحمل درجات مخاطر مختلفة ؛ وأخيراً قياس الفاقد من صلابة و مرونة شبكة الطرق. تم تطوير النماذج باستخدام البيانات التي قدمتها إدارة الطرق في كل من وزارة الأشغال العامة في دولة الإمارات العربية المتحدة وبلدية مدينة العين و أيضا المركز الوطني للأرصاد الجوية والزلازل والاستبيانات المجمعة. تم استخدام عدد من المنهجيات المختلفة في تحليل البيانات مثل الانحدار الخطي وغير الخطي ، محاكاة ديناميات النظام والنهج الاحتمالي. تثبت النتائج التي تم تحليلها باستخدام نماذج ماركوف وديناميكية النظام إلى أن ظاهر التغير المناخي يمكنها ان تزيد وتيرة معدلات تهالك أصول البنية التحتية. على سبيل المثال ، أشار نموذج سلسلة ماركوف إلى أن معدل فقدان المرونة و الصلابه لشبكة الطرق يتراوح ما بين 27.86 ٪ إلى 32.4 ٪ لمختلف سيناريوهات التغير المناخ للسنوات (2013 و 2020 و 2040 و 2060) على مدى فترة 20 عاما من التنبؤ. أما بخصوص السيناريو الأسوأ ، فان درجة فقدان المرونة و الصلابة لشبكة الطرق قد تصل الى 73.57٪. اما بخصوص تحليل النتائج عن طرق نظام نموذج ديناميات النظام فان معدل فقدان المرونة و الصلابة لشبكة الطرق يتراوح بين 75.67٪ و 81.0٪. تطوير ادوات مختلفه مثل نموذج (هج دي ام فور) المعدل ونموذج الاحتمالات وديناميكيات النظام سيساعد المؤسسات و الهيئات العامله في دولة الامارات لمراقبة أصول الطرق و البنية التحتيه بكفاءة ووضع خطة الصيانة اللازمة للسنوات المقبله.

Dedicated to

My Parents and My Family

ACKNOWLEDGEMENTS

I wish to express my sincere and deep appreciation to my mother, who made me believe that dreams are achievable. I wish to express my love and respect to my wife for her continuous patience, support and sacrifices during this journey. I am also very grateful for my daughters and sons, for their smiles that boost me day after day with energy and encourage me to confront challenges. Finally, I wish to express my sincere appreciation and thanks to my supervisor, Professor Halim Boussabaine.

Table of contents

LIST OF TABLES

LIST OF FIGURES

LIST OF ABBREVIATIONS

AADT	Average Annual Daily Traffic
ABS	Agent-based Simulation
ATC	Automatic Temporary Counts
CLD	Causal Loop Diagram
DES	Discrete-Event Simulation
EAD	Environment Agency – Abu Dhabi
ESAL	Equivalent Standard Axle Load
FWD	Falling Weight Deflectometer
HDM-4	Highway Development and Management Model
HDM-III	Highway Design and Maintenance Standards
HMA	Hot Mix Asphalt
HRA	Hot Rolled Asphalt
IPCC	the Intergovernmental Panel on Climate Change
IRI	the International Roughness Index
ITAE	Integral of the Time Absolute Error
M-E	Mechanistic-Empirical
NDT	Non-Destructive Testing
PCI	Pavement Condition Index
PMS	Project Management System
PSI	Present Serviceability Index
ROM	Regional Ocean Model
SD	System Dynamics
SN	Structural Number
TPM	Transition Probability Matrix
TPmax	Maximum Pavement Temperature
UNEP	United Nations Environment Programme
VIM	Voids in Mix
VOC	Vehicle Operating Costs
WRF	Weather Research and Forecasting model

VIM Voids in Mix

VOC Vehicle Operating Costs

WRF	Weather Research and Forecasting model
Tair	Maximum air temperature, ºC
P	Annual precipitation
PET	Adjusted potential evapotranspiration
TMI	Thornthwaite Moisture Index
RIa	Initial roughness of pavement at start of analysis year
ΔRI	Incremental change in roughness
RI	Total change in roughness
ΔRIs	Incremental change in roughness due to structural deterioration during analysis year, in m/km IRI
ΔRIc	Incremental change in roughness due to cracking during analysis year, in m/km IR
ΔRIr	Incremental change in roughness due to rutting during analysis year, in m/km IRI
ΔRIe	Incremental change in roughness due to the environment during analysis year, in m/km IRI
SNc	Modified structural number for the pavement at start of analysis year
AGE3	Age since last overlay or reconstruction, in years
YE4	Annual number of equivalent standard axles, in millions/lane
m	Environmental coefficient
ΔRDS	Incremental change in of rut depth during analysis year, in mm
VIM	Voids in mix for road asphalt material type m on road section i during year t
SP	Softening point of binder for road section i with material type m during year t
sh	Average speed of heavy vehicles on section i, in km/h during year t
PTmax	Maximum asphalt pavement temperature at 20mm below the surface in oC. TPmax is determined from mean daily maximum temperature during summer months
ΔACRA	Incremental change in area of total cracking during analysis year, in per cent
$\mathbf{F_{ikt}}$	The average annual daily traffic (AADT) of commercial vehicles class k in one direction on road section i during year t
W_k	The structural wear factor of commercial vehicle class k
GF	Traffic growth factor for adjusting existing traffic flow data to the desired year t
Pi	The proportion of commercial vehicles on the heavily loaded lane of road section i

LIST OF EQUATIONS

1. Chapter 1 Introduction

1.1. Introduction

This chapter describes the context and the background information of the research; it also explains the motivation for the study and identifies the research problem, aim and objectives, and research significance. The final section of this chapter provides an overview of the thesis structure.

1.2. Research Context and Background Information

Infrastructure is a crucial component for sustainable societies and healthy economies at the worldwide level. The Economic and Social Affairs Department at the United Nations (2014) has projected a world population of 9.7 billion by the middle of the 21st century. It is also expected that 66% of the world's inhabitants will be living in urban areas. Such increases in both urbanisation and population growth draw a completely new set of expectations for infrastructure worldwide (PWC 2014). Infrastructure is categorised into two areas. Economic infrastructure comprises utilities, energy, transport and telecommunication services. Social infrastructure consists of hospitals, schools and prisons (Panayiotou 2017).

Societies have a growing dependence on transportation infrastructure for their everyday activities, and the capability and ability of the transport system to continuously function to the levels of acceptable service is essential to people’s wellbeing. As individuals, companies, economies and societies evolve, reliable and resilient infrastructures are needed. For example, the national economy depends on transportation networks to support goods and mobility for people. The transportation infrastructure could be roads, bridges or airports. In the United States itself, such infrastructures represent more than 19,000 airports, 600,000 bridges and 4 million miles of roads (USDOT 2016). However, transportation infrastructures are not immune from deterioration.

Transportation infrastructure is expected to face a series of challenges over the coming decades. Markolf et al. (2019) mentioned that current transportation infrastructure receives insufficient and unstable funding, and is not well designed to cope with changes in external conditions or different utilisation. For instance, among transportation networks in the US, it is estimated that 65% of major roads are evaluated as being below good condition (The White House 2014). Climate change, also known as phenomena that cause destabilising changes in Earth systems, can exacerbate the challenges in current transport infrastructure. Climate change is not a short-term effect; it is a long-term phenomenon with a lot of uncertainty (Bhamidipati 2015), and little research has been conducted on how vulnerable transport infrastructure will be to climate change (Jaroszweski 2010).

Road pavement assets deteriorate over time. Such deterioration is a result of many factors such as asset ageing, traffic loading, environmental effects, construction deficiency and design inadequacy. Roads are usually constructed to have a design life of 20 to 40 years. Pavement scientists and practitioners have focused a great deal of attention on the use of a prediction deterioration model that can be applied to forecast how the future pavement is going to deteriorate. Kobayashi, Do and Han (2010) stated that keeping critical assets functional from an engineering perspective is very challenging. The deterioration rate is considered to be low at the beginning but with time this rate increases, dramatically increasing maintenance costs. Such deterioration occurs due to many factors such as asset ageing, traffic loading, environmental effects, construction deficiency, design inadequacy, etc. Pavement condition surveys of distress are periodically conducted to quantify pavement surface condition at a specific time. Highway agencies need to establish an efficient tool that correctly monitors the pavement performance (Thom 2014). However, funding limitations trigger the need to seek more cost-effective methods of pavement maintenance optimisation (Lamptey, Labi and Sinha 2004). If road assets managers and engineers had prior knowledge of the likely consequences of future climate change, this could help to ensure that maintenance strategies and activities are conducted at the right time with the right cost. Such an approach could lead to robust roads and highways. Anyala (2011) stated that achieving proper maintenance strategies tools that take into consideration key factors such as climate and traffic is possible and such tools will help in understanding the performance of our roads.

The impacts of climate change shorten such design lives. Mallick et al. (2014) stated that limited research has been conducted in the past to study the impact of climate change on pavement performance. Cechet (2005) stated that, the more knowledge road planners, designers and asset managers have of the expected impacts of future climate change, the better they can plan for such impacts, thus reducing future costs. Climate change impacts contribute to the degradation of infrastructure assets (Meyera and Weigel 2011). Climate change – both extreme and chronically gradual changes in weather events – is likely to threaten transportation infrastructures. Extreme weather events would cause substantial physical damage to the transportation infrastructure, which can lead to significant economic losses. For example, in New York City itself, $7.5 billion of damage to the transportation system occurred as a result of Hurricane Sandy, according to the United States Department of Commerce (USDOC 2013).

Climate change impacts are unavoidable events and there is a need for resilient transport networks that are able to withstand, mitigate and recover from the consequence of such adverse events. Such events have adversely affected the efficiency of transport systems over recent years (Rashidy 2014). Such catastrophic events trigger the need to enhance the performance of the transportation infrastructure. For example, some efforts to support the resilience of transportation systems to face the impact of climate change and other threats have started by incorporating robustness factors in such systems (Markolf et al. 2019). A focus on performance analyses with regard to resilience is also essential.

Resilience is not a new topic. In 1973, the first introduction of the resilience concept was made by Holling (1973), who defined resilience in ecological systems as a "*measure of perseverance of systems and their capability to absorb changes and disturbances, and still sustain the same relationships between populations or state variables*". It has also been widely used in multiple engineering fields (Bruneau et al. 2003; Cimellaro, Reinhorn and Bruneau 2009). Generally, resilience is the maximum degree of threat mitigation to respond to, minimise or remove long-term impacts to property and humans from hazards and the consequences of such risks (Godschalk 2003). Levina and Tirpak (2006) introduced two main elements of resilience. The first element is to observe a disruptive action without change to the original state of the system. The second element is the system recovering from the potential impact.

Maguire and Cartwright (2008) categorised resilience into three terminologies: stability, recovery and transformation. Godschalk (2003) emphasised the importance of measuring resilience to test the ability of the critical infrastructure to withstand and accommodate any change without catastrophic failure.

Freckleton et al. (2012) defined resilience in transportation systems as "*The ability for a transportation network to absorb disruptive events gracefully and return itself to a level of service equal to or greater than the pre-disruption level of service within a reasonable time frame*". Resilience analyses can lead to many benefits for the transportation infrastructure, for instance, improving safety relating to mobility and physical operability (Sun, Bocchini and Davison 2018). Moreover, interpretation of the exact characteristics of resilience allows transportation infrastructure managers to effectively draw the hazard line and quantitatively assess potential impacts of investment and policies (Cao 2015).

Disruptions to transportation infrastructures (or networks) trigger the vulnerability of the system, leading to delaying or stopping the movement of people and goods (Bagloee et al. 2017). The consequence of such disruption has become an area of rising concern to governmental institutions, and has led to the need to study the methods that achieve better understanding of these disruptions in order to make the systems more robust, and enable them to recover from disturbance events.

In terms of a safety system, resilience is a crucial indicator which can picture system-resilience measurements and define the roadmap for improving the system at the emergency level, planning level and response level (Zhao, Liu and Zhuo 2017). Rochas, Kuznecova and Romagnoli (2014) highlighted the main challenges in developing comprehensive resilience measurements, which have different natural inputs and outputs. Such problems include lack of information regarding historical events, different dynamics disruption scenarios, time-varying, interdependent system performance indicators and unknown system consequences.

Although many academics and researchers have conducted many kinds of studies on measuring resilience, a quantitative resilience metric with system performance scenarios still remains unsolved (Zhao, Liu and Zhuo 2017). Additionally, the current practice for measuring resilience quantitatively or qualitatively exhibits little standardisation and provides unclear guidance to asset managers (Francis and Bekera 2014). Bagloee et al. (2017) also added that, in the past, simple heuristic procedures were used to measure resilience for the entire road network. In order to make the measure of the resilience system more transparent and quantifiable, a comprehensive study should be conducted to allow application across a variety of scales (Hughes and Healy 2014).

Thus, the primary challenge is to measure the resilience of pavement infrastructure quantitatively through the concept of pavement performance with consideration of all the risk factors concerning climate change impacts and the consequences of such risk.

1.3. Research Problem

The lack of agreement on resilience measures has been the trigger for this research. There is no standard to guide engineers and managers on how resilience can be assessed (Murray-Tuite and Tech 2006; Cimellaro, Reinhorn and Bruneau 2010). Therefore, the main problem for this research originates from the gap in the literature on how to measure the resilience loss under climate change scenarios. There is a lack of integrated models for quantifying resilience analyses of pavement transport infrastructure using analytical methods and simulations. This problem can be classified into the following sub-problems:

1.3.1. Climate Change Impact

Climate change is having an increasing impact around the globe, either intensity wise, frequency wise or both (IPCC 2013). The World Bank (2013) classified infrastructure as the most critical sector of climate change adaptation due to its susceptibility to physical damage. Collins (2011) highlighted the importance of having a safe infrastructure due to its close association with the socioeconomic activities of a region; any failure of such assets will not be limited to structural failure losses and will also affect public security and safety. Protecting infrastructure systems such as roads, airports, dams and drainage systems is crucial. According to Ha et al. (2017), most infrastructure systems are built with a design life of over 50 years. Nevertheless, climate change is expected to continue in the future, leading to shortening the predicted life of these assets (Gledhill and Low 2010). Ha et al. (2017)

stated that enhancing the resilience of existing infrastructure is one of the adaptation options in the infrastructure sector. Moreover, new infrastructure can be designed to prevent and reduce the risk of climate change impacts.

1.3.2. Pavement Failure Risk

Insufficient pavement maintenance and rehabilitation programmes due to a limited budget leads to deterioration in pavement structure. The failure of a pavement can be seen in corrugation and waves on the pavement surface, rutting and shoving, unlevelled surface or a combination of several factors (Sorum, Guite and Martina 2014). Asset managers need to handle the complex risk factors related to pavement failure (pavement deterioration) in conjunction with the probability of occurrence of multiple failure modes, which they need to understand in detail (Al-Arkawazi 2017). Failure to identify the primary cause of pavement risk will lead to incorrect maintenance decisions (ill-chosen and ill-timed), which will poorly reflect on maintenance programmes and budget allocation. However, achieving accurate identification and precise assessment of the causes of pavement failure will support asset managers in making solid decisions on maintenance activities.

1.3.3. Current Deterioration Prediction Models

Until recently, there have been no reliable performance prediction models used by road authorities for defining the required annual budgets for maintenance and rehabilitation works (Mahmood 2015). Moreover, Anyala (2011) noted that the HDM-4 model, which is used as a decision support tool for road pavement deterioration models, is formulated on the base of a static climate assumption using past observations. However, a major problem with the results from such models is that they do not take into consideration pavement deterioration under future climate change scenarios.

1.3.4. Shortcomings of Deterministic Modelling

In deterministic modelling, the values of random variables such as the traffic and environmental impacts do not vary with time. Hong and Wang (2003) commented that this assumption might not be sufficient because, in practice, the traffic and the environmental actions do vary randomly with time. Therefore, they concluded that the deterioration in pavement performance could not be projected exactly because geometric variables, traffic loading, environmental impacts and the material properties are uncertain and therefore a deterministic approach cannot be reliable and predicted. For this reason, the authors also emphasised the importance of using a probabilistic framework to build such a model. Enright and Frangopol (2011) added that uncertainties are a big part of prediction deterioration due to complications related to isolating the individual random variable. Use of the Markov chain is suggested, which is a sophisticated technique to be applied in asset management systems for different types of assets such as roads, bridges and service utilities.

Moreover, the literature is sparse on the question of how to capture a real system of pavement deterioration under the impact of climate change by using system dynamics models. Building a casual loop diagram and simulating various stock and flow diagrams for a pavement deteriorating model as well as capturing the expected risk of pavement failure under climate change will expand our understanding of the impact of climate change on the performance of pavement deterioration.

1.4. Motivations for the Research

This study is academically and practically motivated. Academically, it measures resilience loss using a quantitative approach, defines pavement failure under the risk associated with climate change impact, establishes a pavement performance indicators model in terms of the International Roughness Index (IRI) and Pavement Condition Index (PCI), defines the relationship between these indicators, and, finally introduces a new pavement deterioration model using a Markov chain and system dynamics approach. Such an approach will create new knowledge and become an attractive field of research. On the other hand, recent study in the field of resilience has captured a great deal of attention. Thus, practically, highway agencies and organisations will be selective in the process of understanding how their pavement assets will deteriorate with respect to the impact of climate change, as they should have the required knowledge on assets' life shortening, and this phenomenon will trigger the need for maintenance interventions. Moreover, using the International Roughness Index (IRI) to investigate the pavement condition is an effective approach for deriving information to support decision-making.

Thus, this research is set to predict the rate of deterioration for pavement assets that belong to different highway agencies in the UAE (Al Ain City Municipality and the Ministry of Public Works) and the infrastructure resilience loss. Therefore, the knowledge gap in delivering successful, reliable deterioration models can be addressed through rigorous analysis of both collected pavement condition data and knowledge of expert judgement. The Highway Development and Management software (HDM-4), which is an accepted international tool for improving road investment appraisal techniques, provides a basis in this research. The main function of the HDM-4 is to optimise pavement performance wok. Moreover, the HDM-4 has the capability to handle other elements.

The HMD-4 model is used in this research to determine pavement performance variables such as roughness, rutting and cracking. Moreover, the HDM-4 depends on the application of the Thornthwaite Moisture Index (TMI) as the primary climatic factor embodied in the model. The research is keen to develop a new Thornthwaite Moisture Index (TMI) that matches UAE weather conditions and which will supply pavement engineers with a detailed plan for pavement performance predictions over time. It also gives a forecast on changes in the pavement condition in terms of roughness, structural cracking and rutting. The findings of the current study will provide decision makers with alternative ways of examination that will help in developing a further understanding about measures of infrastructure resilience to asset managers and engineer. Additionally, the study findings may aid highway agencies in gaining a clearer picture of the areas in which they may need to develop a pavement deterioration prediction model.

1.5. Research Significance and Knowledge Expansion

The growing number of climate change extremes globally, and specifically in the UAE, has drawn attention to the impact of such events on transport infrastructure networks (specifically, flexible pavement structure). The influence of such implications depends on the ability of infrastructure assets to mitigate, respond and recover. Recently, this approach has been introduced as the concept of resilience. Today there is no method, guidance or standard on how to measure the resilience of transport infrastructure. An assessment of the resilience of a pavement infrastructure may help asset managers and engineers to resolve several issues related to the performance of a pavement infrastructure and maintenance strategy with respect to climate change impact, deterioration rate, configuration and available capacity of such assets. Measuring resilience could increase awareness and guide transport authorities and agencies in formulating management policies. This approach will enhance the transport infrastructure performance under disruptive events as well as improving the daily operation of the network.

The study offers some important insights into the climate change risks that influence pavement deterioration. Furthermore, the study expands our understanding of the interaction between different constructs that influence pavement service life. Achieving accurate identification and precise assessment of the causes of pavement failure will support asset managers in establishing solid decisions on maintenance activities. The investigation will also provide an opportunity to advance our knowledge of three different areas:

Operational level:

- This project provides a substantial opportunity to advance the understanding of quantifying resilience analyses of transport infrastructure.

- Applying an analytical approach and simulations in order to deliver more comprehensive information about vulnerable components under the impact of climate change.

- Evaluating the requirements for achieving better road pavement maintenance strategies and policies that cope with the uncertainties of future climate change.

- Providing estimates for rate of deterioration of pavement condition for next 30 years using stochastic tools.

Strategic level:

- New decision support tools for the Ministry of Public Works in the UAE and Al Ain City Municipality.

Academic level:

- Build up a new environmental factor that incorporates the impact of climate change, which integrates with the pavement deterioration model based on UAE weather conditions.
- A new modified HDM-4 model to measure the rate of deterioration for the International Roughness Index (IRI) with respect to different climate change scenarios in the UAE.
- A new modified model that defines the relationship between International Roughness Index (IRI) and Pavement Condition Index (PCI) in the UAE.
- A new approach to build a Transition Probability Matrix using survey data of pavement conditions for different climate change scenarios (2013, 2020, 2040, 2060).
- Introduce a new Markov chain model for projection of pavement deterioration rate for different pavement performance indicators such as the Pavement Condition Index (PCI) and International Roughness Index (IRI) concerning impacts of future climate with different scenarios.
- A new holistic approach to define and assess the pavement risk under climate change impacts.
- Introduce a new system dynamics model (Casual Loop Diagram and Stock and Flow) that measures pavement deterioration rate for different pavement performance indicators such as Pavement Condition Index (PCI) and International Roughness Index (IRI) with respect to impacts of future climate change with and without pavement failure risk.

1.6. Aim, Objectives and Research Questions

1.6.1. Research Aim

The research is aimed at expanding the existing literature by integrating several methods for modelling pavement resilience using system dynamics and Markov chain (probabilistic) approach as well as evaluating the risk of climate change impact on road pavement performance.

Furthermore, this research proposes models (system dynamics and Markov chain) for use in assessing the climate change on road pavement performance. This model can be used by road engineers, project managers and highway engineering practitioners and provides sufficient tools for road maintenance management decisions in the light of uncertainties that exist in respect of future climate change.

1.6.2. Research Objectives

To achieve the research aim, the following objectives have been developed:

1. To accomplish a comprehensive literature review on climate change, modelling of pavement deterioration, Markov chain method, system dynamics method, pavement resilience, climate change and risk associated with pavement failure due to climate change.
2. To examine the relationship between pavement performance indicators (International Roughness Index and Pavement Condition Index). Moreover, to develop a modified HDM-4 model using these parameters to assess the impacts of future climate conditions in order to shape better strategies for adapting to unavoidable climate change and build a pavement deterioration model. A new, improved HDM-4 model will be produced with the development of new coefficients and equations.
3. To propose a Markov chain model for projection of pavement deterioration rate for different pavement performance indicators such as Pavement Condition Index (PCI) and International Roughness Index (IRI) concerning impacts of future climate change. A transition probability matrix is generated based on the results generated from step 2.
4. To propose a system dynamics model for projection of pavement deterioration rate for different pavement performance indicators such as Pavement Condition

Index (PCI) and International Roughness Index (IRI) with respect to impacts of future climate change. Model inputs are generated based on the results generated from step 2.

5. To establish generic risk events inherent in the pavement failure and incorporate all the risk interdependencies and interactions in the pavement deterioration model (SD). To quantify the risk interrelationships using the estimation of probability distribution generated from the questionnaire survey.
6. To propose a system dynamics model with pavement risk failure for projection of pavement deterioration rate for different pavement performance indicators such as Pavement Condition Index (PCI) and International Roughness Index (IRI) with respect to impacts of future climate change. Various risk factor scenarios will be introduced. Model inputs are generated based on the results produced from steps 2 and 5.
7. To determine a theoretical approach that can measure pavement resilience loss. Such a method is specific to a pavement deterioration models generated from both system dynamics and Markov chain.

1.6.3. Research Questions

(1) How to build a pavement deterioration prediction model using system dynamics and Markov chain under UAE climate change impact scenarios?

(2) What are the generic risk events inherent in the pavement failure and how to quantify the risk interrelationships and incorporate the risk interdependencies and interactions in a system dynamics model?

(3) How to measure pavement resilience quantitatively with respect to climate change in the UAE using system dynamics and Markov chain methods?

1.7. Thesis Structure

This thesis has 11 chapters plus references and appendices. The structure is as follows:

Chapter 1: **Introduction**. This chapter has introduced the need for a thorough understanding of the background information of the research. It also explains the motivation for the study and identifies the research problem, aim, objectives and research significance. The final section of this chapter provides an overview of the structure of this thesis.

Chapter 2: **Impact of Climate Change on Pavement Resilience** (Literature Review-Part 1). This chapter provides a review of the literature relevant to pavement infrastructure. It starts with a thorough examination of pavement performance that covers types of pavement performance indicators and pavement deterioration modelling theory relevant to this research, and the association between climate change and pavement failure. It also describes the existing literature about the Markov chain and system dynamics. Infrastructure resilience and measuring infrastructure resilience are also covered.

Chapter 3: **Theoretical Method for Modelling Pavement Deterioration** (Literature Review-Part 2). This chapter focuses on the climate change model, its impacts on road pavement structure and the measurement of impacts associated with future climate prediction. The chapter is also targeted at identifying the existing state of knowledge concerning pavement temperature, and the Thornthwaite Moisture Index in the United Arab Emirates (UAE). Defining pavement deterministic and probabilistic modelling with respect to the Pavement Condition Index (PCI) and the total change in roughness is also studied in more detail. Chapter 4 is a platform for building a theoretical background for the modelling of a pavement deterioration model. Total change in roughness is built from different elements: rutting component, cracking component and environmental component. The HDM-4 model is used to build new determination modelling with respect to the impact of climate change. Other models such as Markov chain model, pavement temperature and Thornthwaite Moisture Index are also determined. Measuring resilience is also studied.

Chapter 4: **Methodology**. The methodology of this research is focused on presenting a roadmap for the study. A detailed framework including all tasks is described, including the development of data sets, developing a deterministic model for pavement deterioration, determining the deterioration mode using the Markov chain method, determining the deterioration mode using the system dynamics method and the concept of measuring the pavement resilience and investigation of climate change.

Chapter 5: **Data Collection and Analysis**. This chapter explains the research data collection and analysis approach used to conduct the study. it examines the types of data and sources including International Roughness Index (IRI), asphalt surfacing rutting and cracking, traffic data, heavy vehicle speed (sh), asphalt surfacing thickness (Hs), asphaltic ageing and UAE weather data. This chapter represents a description of how the development of research model inputs is designed, such as development of predicted maximum air temperature (Tmax) in the UAE and pavement temperature (TPmax), predicted Thornthwaite Moisture Index (TMI) in the UAE, binder softening point (SP) and voids in mix (VIM). Information on questionnaires is also addressed. This chapter concludes with a description of the statistical methods that are used in the analysis, confidentiality issues and compliance with ethics. A summary of the variable inputs is finally drawn.

Chapter 6: **Developing Pavement Deterioration Indicators**. The methodology selected to develop the model was described in Chapter 2 and data collection and analysis was discussed in Chapter 5. This chapter’s goal is to estimate the pavement deterioration indicators that later will be used as parameters and inputs that shape the models in chapters 7, 8 and 9. Such indexes are built through the deterministic model concerning different climate change scenarios. The chapter explains the process used in the development of the model inputs using obtained analysed data discussed in Chapter 5. The chapter also provides details on the computation of the change in total roughness based on default HDM-4 equations. Developing new equations and coefficients is also investigated. Testing and comparison of the results are presented. Finally, the relationship between International Roughness Index and Pavement Condition Index is also investigated.

Chapter 7: **Forecasting Pavement Deterioration using a Markov Chain Method**. This chapter’s goal is to build the pavement deterioration model using a Markov chain with parameters developed in chapters 5 and 6. The model in this chapter is formed from two main elements, transition probability matrix and pavement condition rating. There are different methods for developing a transition probability matrix, as was highlighted in Chapter 4. The chapter explains the process of developing model inputs using computed analysed data which was discussed in Chapter 6 with different climate change scenarios for years 2013, 2020, 2040 and 2060. Finally, the chapter introduces pavement deterioration curves based on PCI and IRI with different climate change scenarios.

Chapter 8: **Causal Loop Diagrams for the Pavement Deterioration Model**. The purpose of this chapter is to forecast the pavement deterioration using system dynamics based on the established parameters from Chapter 6. The chapter investigates the impact of the pavement deterioration model with respect to generic risks that were developed in Chapter 3.The interdependencies between pavement failure risks due to climate change and pavement deterioration constructs were established by causal loop diagrams. These causal loop diagrams were used in the SD models as discussed in Chapter 9.

Chapter 9: **Modelling Pavement Deterioration Using System Dynamics**. Developing an understanding of risks associated with road pavement failure (pavement deterioration) was achieved and the risks were used as inputs into the system dynamics models as discussed in Chapter 8. This chapter explains the methodology adopted in the use of Stock and Flow modelling in system dynamics. Deterministic risk analysis is explained in this chapter. Vensim software was used to run the proposed model. Then, knowledge obtained on the risks related to pavement failure (pavement deterioration) will improve the success of the computational model through defining all the elements that could contribute to the change in IRI value and subsequently to PCI. Such an approach was developed from the stock and flow diagram to enrich the system in order to establish the dynamic behaviour for the selected variables. The pavement deterioration curve was introduced regarding pavement performance indicators PCI and IR with different risk scenarios. The chapter finally presents and discusses the results from the different modelling exercises.

Chapter 10: **Measuring Resilience Loss**. This chapter’s goal is to measure resilience loss for pavement networks. The pavement deterioration model using Markov chain and system dynamics with parameters developed in chapters 5 and 6 is used to determine the resilience loss. The model in this chapter is formed from two main elements, measuring the main performance by integrating the area under the survival curves and measuring resilience performance with respect to 100% perforce functionality of the pavement network. The chapter explains the process of development of resilience loss using a Markov chain model with different climate change scenarios for years 2013, 2020, 2040 and 2060. Also, a system dynamics model with different risks associated with climate change is developed. Comparison of the results between the two models is finally reported.

Chapter 11: **Discussion and Conclusion**. This chapter represents a comprehensive discussion of the findings and provides a clear picture about the relationships among the study variables, the degree to which the obtained results agree with or differ from the past empirical outcomes, and theoretical arguments. This chapter also presents a discussion of the key research objectives and themes analysed throughout this thesis. The first section presents a discussion on the findings of the eight objectives. This is followed by a discussion on the strengths of the research methodology and validation and implication. The last section presents the conclusion of the thesis covering the limitations of the research, summary of contributions, and future research and recommendations. This is achieved through discussing the main concepts of the research including the concepts of measuring pavement resilience and developing a pavement deterioration model using system dynamics and Markov chain.

2. Chapter 2 Impact of Climate Change on Pavement Resilience

2.1. Introduction

This chapter begins by setting out the theoretical dimensions of the research and focuses on how the impact of climate change affects pavement resilience. Knowledge on climate change from a scientific perspective in terms of its concept, causes, scenarios and importance is highlighted. Moreover, this chapter provides a review of the literature relevant to pavement infrastructure. It includes pavement performance that covers types of pavement performance indicators and pavement deterioration modelling theory relevant to this research, and the association between climate change and pavement failure. It also describes the existing literature about Markov chain and system dynamics. Infrastructure resilience and measuring infrastructure resilience are also covered.

2.2. Climate Change

This section first gives a brief overview of the recent history of climate change. Climate change or global warming within our environment is one of the factors that may affect our daily lives and the future in both positive or negative ways (Alzahrani 2015). The following sections define the theory of climate change.

2.2.1. Theory on Climate Change

Vast efforts have been made by paleoclimatologists to investigate past climates. It is believed that studying the history will answer how the Earth performed under conditions that are different to those nowadays. Many different palaeoarchives are applied to investigate the past, such as ice in different layers of an ancient glacier comprises trapped air bubbles and water over an extended period. Palaeoclimatologists believe that lake sediments, marine sediments and ice cores are the only palaeoclimate records which can be used extensively, especially around Antarctica. However, the history of ocean conditions is still unknown (Petit et al. 1999; Wolff 2005; Qiao 2015).

On the other hand, paleoclimatologists have concluded, after examining the isotopes of gases (oxygen or hydrogen), that the past climate change is shaped in the form of a linear relation between the isotopic composition and temperature (Petit et al. 1999). Moreover, tree rings can also be used to assess past climate condition (Petit et al. 1999). By studying climate variation such as precipitation and sunlight, paleoclimatologists can define accurate dating for tree growth. Moreover, ice ages, which resulted in extreme cold periods on the planet, are pure evidence of the natural variations in the climate. This has been seen through glaciers that covered large areas of the Earth. Today, the ice age has ended and glaciers have melted and retreated (Petit et al. 1999; Wolff 2005; Qiao 2015).

Scientists have developed a historical climate reading based on the ice core record to understand the Earth (Figure 2-1). They have defined four primary cycles that hit the Earth during ice ages over the past 400,000 years. Figure 2-1 shows the association between atmospheric carbon dioxide concentration and the estimated historical temperature. Nowadays we are in an increasing mode (too high temperature peaks) of heat, but it is assumed that the temperature will drop again after a certain period of time, based on temperature patterns that occurred during the past four primary ice ages. However, such a phenomenon is based on long-term trends, and temperature variations could happen in the short term (Petit et al. 1999, Qiao 2015).

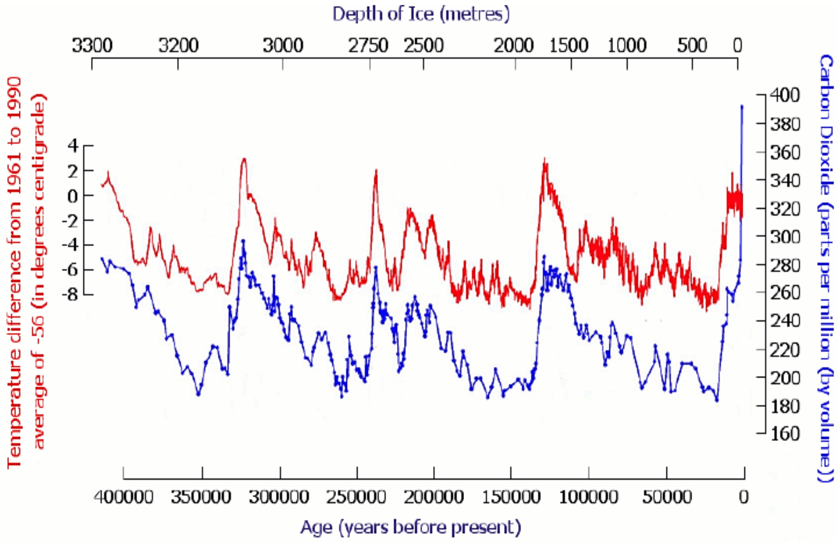

Figure 2-1: Atmospheric carbon dioxide concentration and estimated historical temperature (Petit et al. 1999)

Paleoclimatologists have not been able to define the reason behind the variations in the climate. However, they have established a better understanding of some significant factors such as the impact of the orbit of the Earth on climate change (Paillard 2001). This theory was first introduced by James Croll in the 1860s. In 1980, Imbire established a model to define the climate reaction to the orbital parameter of the Earth based on James Croll's theory. He used other influential factors such as changes in atmospheric compositions, variations in the solar output and change in the ocean current (Qiao 2015). As a system, the climate is on the equilibrium between heat reaching the Earth from the sun and the radiation of heat from the Earth into space. This balance is disturbed by the emission into the atmosphere of a number of gases (greenhouse gases), which will eventually lead to global climate change (Qiao, 2015). The occurrence of global climate change will impact the built infrastructure.

However, Alzahrani (2015) indicated that there are different views on climate change and the events that cause it. For example, one group of scientists and climate researchers believe that climate change stems from natural factors, whilst another group assumes that climate change was initiated before human existence by natural elements but has increased as a result of human activity. Moreover, there is another group of scientists who question the presence of climate change, stating that there are no changes in the climate and no need to invest significant funds into carrying out studies of it. Burnett (2001) also stated that it is difficult to define the size and degree of climate change, its direction and future predictions in terms of global temperature. While a variety of theories about the term climate change have been suggested, this research will use the theory first suggested by James Croll in the 1860s.

Qiao et al. (2015) also stated that the phenomenon of climate change is certain.Various signs in the natural forces point to the fact that the Earth has always had a changing climate (Chapman 2007), even though human activity has also contributed to this since the industrial revolution (Karl and Trenberth 2003). It is believed that human influences exaggerate climate change through inducing changes in atmospheric composition through the emission of greenhouse gases (NRC 2008). The trend of global climate change can be seen in the form of temperature increases as a result of warmer winters, drier summers and rising sea levels, together with unusual weather patterns and a higher number of floods (IPCC 2007). The phenomena of extreme weather events and associated natural hazards can also be generated as a result of climate change (Stewart and Deng 2015). The NRC (2008) has defined climate change as "*a statistically significant variation in either the mean state of the climate or its variability over an extended period, typically decades or longer, that can be attributed to either natural causes or human activity weather refers to the familiar hour-by-hour, day-by-day changes in temperature, cloudiness, precipitation, and other atmospheric phenomena*". Also, the term '*global warming'* is defined in terms of the increase in global average temperature resulting in the accumulation of greenhouse gases in the atmosphere (Wuebbles and Jain 2001).

In 1988, the Intergovernmental Panel on Climate Change (IPCC) was founded to study the problems associated with climate change and its impacts. The primary objective of the IPCC is to investigate the potential effects of climate change and advise the world community of the consequences of such phenomena. This action is conducted through continual monitoring and assessment in order to report the policy frameworks needed to address the climate change using a technical, scientific and socio-economic approach (IPCC 2013).

2.2.2. Climate Change Projection

Greenhouse gases such as methane, carbon dioxide and nitrous oxide have acted as a preventative layer to stop part of radiated heat escaping into space. Such gases will increase the Earth's temperature (Pavlopoulos 2010). The thickness of the preventative layer in the atmosphere has become very dense due to the concentration of carbon dioxide (CO_2). An IPCC (2007) report showed that the level of CO_2 had increased dramatically in last 50 years. Such phenomena have started to draw more attention as the temperature reading has shown a continuous increase since the previous 100 years, especially since 1970. It has been recorded that the average global temperature has increased by 0.74 degrees C (Pavlopoulos 2010).

Moreover, Nakicenovic and Swart (2000) summarised that the CO_2 levels based on IPCC data are forecasted to increase over the next century to a level between 540 and 970 parts per million. Eventually, this will be reflected in the average global temperatures. Watson (2001) mentioned that such increases in temperature could be between 1.4 and 5.8 C, resulting from extreme weather events such as rising sea levels (either by glacial melting or thermal expansion of the oceans). On the other hand, Chapman (2007) stated that there is vast uncertainty in making predictions of climate change based on emission scenarios. Nevertheless, the fact is that the concentration of CO_2 emissions has reached 400–450 parts per million, which is considered as an unbalanced scenario, and it will soon exceed the level required for equilibrium (Bristow et al. 2004).

2.2.3. Observations on Climate Change

Climate change can be seen in the form of changes in the temperature, precipitation and sea level, as discussed below.

2.2.3.1. Temperature

Based on the data from the IPCC, average global temperatures have increased by 0.74°C during the past 100 years (Qiao 2015). Results revealed that the increase in temperature over the most recent 50 years is almost double that of the past 100 years (Qiao 2015).

Estimation of temperature change by climate models shows a warmer forecast for the future. For example, based on the IPCC report, it is forecasted that average global warming will increase in the range from 1.1°C to 6.4°C by the end of the 21st century (see Figure 2-2). This phenomenon has recently been seen in the decline of the occurrence of cold days and nights and also the increase of hot days and hot nights. Moreover, heat waves have become more regular occurrences (IPCC 2007; Pavlopoulos 2010).

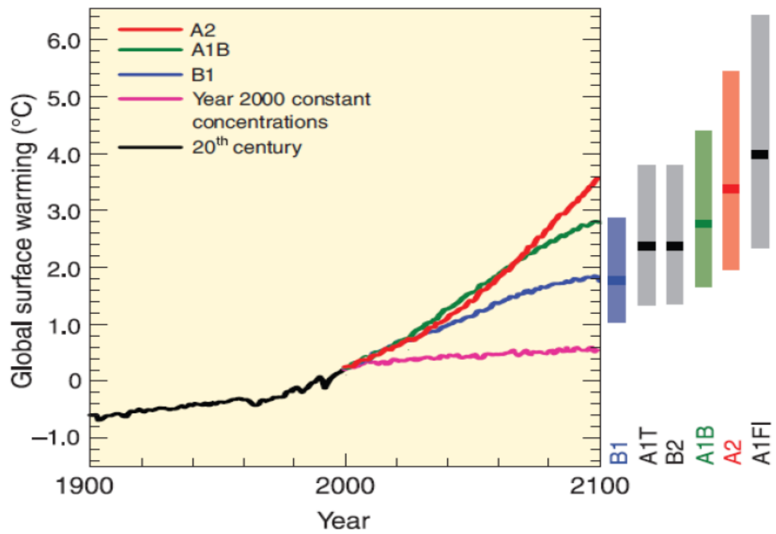

Figure 2-2: Global surface temperature change (IPCC 2007)

2.2.3.2. Precipitation

The International Panel on Climate Change (IPCC) report stated that precipitation across the world is varied. It has defined some areas, such as North and South America, northern Europe, and northern and central Asia that recorded a dramatic increase in precipitation between 1900 and 2005, whilst other places in the world such as the Mediterranean, southern Africa and parts of South Asia recorded less rainfall for the same period (IPCC 2007). An example of high precipitation occurred during a UK storm on 28 June 2012, which resulted in extensive disruption to the whole country, for instance, severing the main rail links between England and Scotland, causing delays of 10,000 minutes to services across the nation (Jaroszweski et al. 2015). It was also recorded that, within a period of five minutes, there were over 1000 lightning strikes in the UK and a total of over 50,000 were recorded during the day (Jaroszweski et al. 2015).

2.2.3.3. Sea Level Rise

The IPCC report indicates that the yearly increase in global sea level between 1961 and 2003 was at a rate of 1.8 mm with a total rise of 1.7 m in the 20th century (Pavlopoulos 2010). By considering the future impact of climate change on the global sea level rise, Church et al. (2008) stated that more increases will occur and could reach as much as 0.97 m by 2100 due to both glacial melting and thermal expansion. Furthermore, Demirel, Kompil and Nemry (2015) stated that the degree to which the sea level rises is not constant across the globe. For example, an additional 15–20 cm could be added for the area of northern Europe. On the other hand, fluctuation in atmospheric pressure can also result in changes in the sea level, which may lead to catastrophic storms with strong onshore winds followed by very high coastal sea levels (storm surges) (Demirel, Kompil and Nemry 2015). Such an event was recorded on the United Kingdom’s North Sea coast, when a high tide level of more than 2 m occurred during the winter of 2013/2014. This storm resulted in severe damage in the east of England (Huntingford et al. 2014).

2.2.3.4. Snow and Ice

As was discussed earlier, the temperature has started to rise, and the consequences of this action will lead to snow and ice melting. Overall, the IPCC report defined that the annual average speed of ice retreat in the Arctic Ocean was found to be 2.7% per decade, which will eventually lead to increases in sea level (IPCC 2007; Qiao 2015).

2.2.3.5. Extreme Weather

Extreme weather consists of heat waves, heavy precipitation and extremely high sea levels (Pavlopoulos 2010). This phenomenon has become more frequent in the last 50 years. For example, cyclones (typhoons and hurricanes) could become more intense, with more significant peak wind speeds and heavier precipitation (IPCC 2007).

Based on the highlighted literature, part of the research is to examine the emerging role of temperature in the context of climate change impact. Therefore, the research only considers the element of increases in temperature. More details are explained in sections 3.2.1 and 5.11.2

2.2.4. Impact of Climate Change in the UAE

2.2.4.1. Background

The UAE lies in a hot and water-scarce (water deficit rises every day) arid region. The country's climate is classified by high temperature in summer, moderate winter, deficient rainfall, high evaporation rate and limited non-renewable groundwater (Chowdhury, Mohamed and Murad 2016). In the UAE, the months of summer are April to September. These months are extremely hot as temperatures reach 48˚C in coastal cities and 50°C in the southern desert area (AlRustamani 2014). Moreover, the humidity levels reach 90% in coastal cities and drop in the southern desert area. According to statistics, the average yearly rainfall can be 140-200 mm and sometimes reach 350 mm in the mountainous regions along the north-east coast (Chowdhury, Mohamed and Murad 2016). Most of this rainfall occurs between December and April (Chowdhury, Mohamed and Murad 2016). It has also been forecasted that the temperature in the UAE will rise by between 2.79 ^{o}C and 3.8 ^{o}C (AlRustamani 2014; Chowdhury, Mohamed and Murad 2016).

2.2.4.2. Climate Change Projection in the UAE

According to the IPCC (2013), global warming is virtually guaranteed. For instance, in 2016, the world experienced the hottest year ever (Venturini et al. 2017). The Environment Agency - Abu Dhabi (EAD) in conjunction with the United Nations

Environment Programme (UNEP) developed the Weather Research and Forecasting (WRF) model and Regional Ocean Model (ROM). The findings of the WRF model in conjunction with the IPCC for the UAE are summarised as shown in Table 2-1.

Table 2-1: UAE climate change model outcomes by Venturini et al. (2017)

Climate parameter	Expected change	Rate of change
Temperature	*Suggests a strong upward trend in average temperature in the UAE*	*Increase of between 2 and 3°C during the summer months by 2060-2079* *1°C by 2020 and between 1.5 and 2°C by the 2040s*
Humidity	*Suggests an increase in humidity*	*Suggests an increase in humidity of about 10% over the entire Arabian Gulf by 2060-2079*
Precipitation	*Suggests an increase in average annual precipitation. This trend is stronger during the usually drier summer months and is associated with a reduction in the number of 'wet days'*	*Possible increases of up to 200% in the annual maximum 1-day precipitation*
Marine and coastal	*Suggests that the Sea Surface Temperatures (SSTs) of the Arabian Gulf could be warmer*	*1°C to 2°C by the end of the century*
Sea level	*Sea level globally is likely to rise*	*Around 0.06 m by mid-century (1.5 mm per year over the next 40 years)*
Storms	*There is some evidence that the Arabian Gulf coast of the UAE could be exposed to tropical cyclones in the future*	*Tropical cyclones could be less frequent but more intense (2-11% increase) and produce substantially higher rainfall rates (10-15%)*

Finally, the UAE is not isolated from climate change impacts. The signs of variations in temperature, precipitation and sea level conditions can be observed as such impacts are already being felt by people living in the country. The main climate change risk facing the UAE can be seen as heat and water stress. The area is strongly prone to rising temperatures and lack of water. UAE climate change model outcomes highlighted by Venturini et al. (2017) are applied in this research. More details are provided in sections 3.2.1and 5.10 .

2.2.5. Climate Change Impact on Pavement Structure

Climate change is not a short-term effect; it is a long-term phenomenon with a lot of uncertainty (Bhamidipati 2015), which means that the more knowledge that road planners, designers and asset managers have on the expected impacts of future climate change, the more cost savings can be made in the long run (Cechet 2005). The main principle is to prepare the road infrastructure (existing) to better deal with climate change (Cechet 2005). Roads are constructed with a design life of 20 to 40 years (Mallick et al. 2015). However, limited research was conducted in the past to study the impact of climate change on pavement performance (Mallick et al. 2015). Theoretically, increasing disturbance in pavement structure will eventually accelerate the rate of deterioration, leading to shortening the life of the assets and triggering the need for maintenance. According to statistics, the US spends nearly $20 million on daily maintenance activities (Mallick et al. 2015). Witczak, Zapata and Houston (2006) stated that the performance of flexible pavements could be affected significantly by climate conditions. Enríquez-de-Salamanca (2017) added that variations in climate change might impact flexible pavements in a negative or positive fashion in terms of degradation (reduction or increase in degradation). Cechet (2005) also stated that climate change could affect road infrastructure by both direct and indirect impacts. An example presented by Enríquez-de-Salamanca (2017) for indirect impacts is related to traffic and noise. A direct influence can be seen on the poor condition of the pavement surface, leading to safety issues and increasing travelling times. Mallick et al. (2015) presented the effect of climate change on the pavement as shown in Table 2-2.

Table 2-2: Climate change impact on pavement by Mallick et al. (2015)

Phenomenon	Effect
Rise in air temperatures	*Decreasing modulus of asphaltic pavement*
Increase in average annual rainfall	*Affects duration for which the subgrade soil can be expected to be at or close to saturation, and hence affects the modulus of the subgrade soil*
Increase in sea water level	*Increases the number of inundation (flooding) occurrences, and hence causes a lowering of the modulus of asphaltic pavement and subgrade*

Change in temperature due to the impact of climate change is the central element in the proposed research. Increase in temperature can contribute significantly to the degradation of pavement structure . Cechet (2005) concluded that temperature plays a crucial role in the ageing of bitumen, leading to an increase in cracking, leading to the pavement surface losing its waterproof feature. This can be seen when water is freely penetrating the pavement structure, causing fatigue cracking (Cechet 2005).

Engineers and infrastructure managers should start to embrace the impact of climate change through mitigation (reduction of the causes) and adaptation (reduction of consequences) (Bhamidipati 2015). For the proposed research, the elements of temperature and Thornthwaite Moisture Index are selected. Further discussion is provided in sections 3.3.2 and 5.11.3.

2.3. Pavement Structure

Highway pavements are classified into two groups, flexible and rigid. A typical flexible pavement is widely used, and its structure comprises of the top layer of surface course (asphaltic) and underneath layers: base and sub-base courses (see Figure 3-2). A subgrade soil provides the pavement foundation (Nguyen and Mohajerani 2016). For this research, flexible pavement is selected as it is widely used in the UAE. In the long term, pavement performance decreases based on stress and strain state theory. In brief, the load pulse applies when a dynamic load (traffic wheel) moves on the pavement surface. Such pressure penetrates the multi-layer pavement system, including the subgrade level (Qiao et al. 2016). Finally, this will cause, over time, more deterioration to the pavement until structure failure occurs. This scenario can occur due to both the impact magnitudes and the number of repetitions of stresses and strains (Mamlouk 1997). The stress-strain response in the pavement can be obtained by the resilient modulus of each layer. The resilient modulus is a crucial element that is used in flexible pavement design. It is considered as an input to the multilayer elastic theory to evaluate the pavement development under traffic loading, which designers use to decide on the optimum thickness of both new pavement designs and pavement rehabilitation (Ji 2006). Shafabakhsh and Tanakizadeh (2015) defined many elements affecting the resilient modulus of asphalt such as temperature, duration of loading pulse, rest periods between the stress level and time of loading.

There are also many physical properties that affect the resilient modulus of materials. For example, in terms of granular materials, the shape of aggregates has a potential impact on the resilient modulus. Hence, the selection of the physical properties of every layer is crucial; the more strength a material's particles have, the higher the resilient modulus that can be achieved (Allen and Thompson 1974). There is an unambiguous relationship between physical properties and the deterioration rate of a pavement section. Such a component is tested as a risk factor and more details are discussed in the pavement failure risk section (2.4.1).

Regarding the environment, the temperature can also have a potential impact on the stiffness of asphalt concrete. For instance, high heat can make asphalt binder soften and lose stiffness (Buttlar, 1996). Moreover, Hu et al. (2009) commented that the impact of loading time on an asphalt layer is not a constant factor. These factors change based on vehicle speed, asphalt layer thickness, depth and the ratio of asphalt layer modulus to base layer modulus. More details on the failure of pavement due to climate change are discussed in section 2.4.1.4.

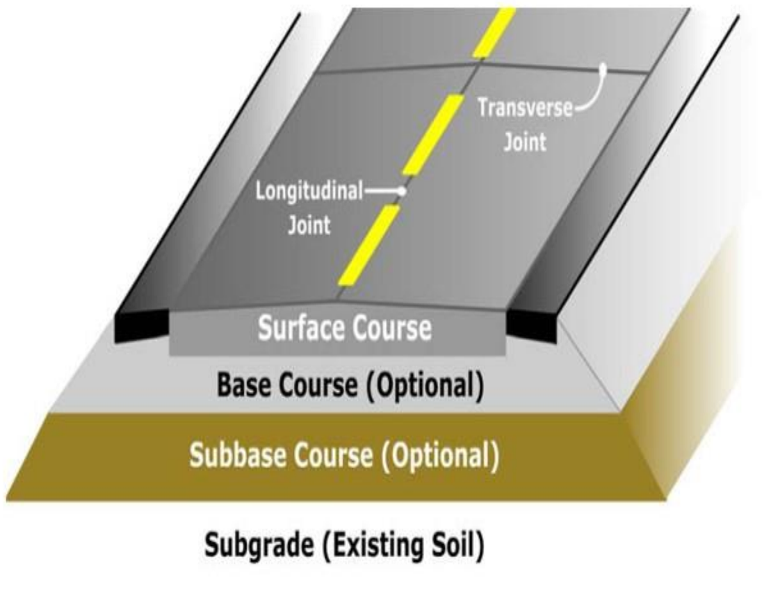

Figure 2-3:The typical section of flexible pavement stracture by Fwa (2006)

2.4. Pavement Deterioration

Haas, Hudson and Zaniewski (1994) concluded that pavements are arguably the most critical of all infrastructure assets, accounting for approximately 60% of the total infrastructure in the US. Park et al. (2008) added that the US federal government allocates approximately $60 billion a year for the transportation budget and the majority of the budget goes on road and highway repairs each year. Kobayashi, Do and Han (2010) stated that keeping critical assets functional from an engineering perspective is very challenging. Highway agencies need to establish an efficient tool that correctly monitors the performance of pavement (Thom 2014). However, funding limitations trigger the need to seek more cost-effective methods of pavement maintenance optimisation (Lamptey, Labi and Sinha 2004).

The deterioration of a pavement usually takes place once it is opened to traffic. The deterioration rate is considered to be low at the beginning but with time this rate increases, dramatically increasing maintenance costs. Mubaraki (2010) stated that within 20 years 60% of highway pavements (roads) achieve functional failure. On the other hand, according to Qiao et al. (2015), the phenomenon of climate change will impact flexible pavement by shortening the life span (typically 20–40 years). To this end, pavement scientists and practitioners have focused a great deal of attention on the use of prediction deterioration models that can be applied to forecast how the future pavement is going to deteriorate under the impact of climate change. The highway pavement assets decline over time. Such deterioration occurs due to many factors such as asset ageing, traffic loading, environmental effects, construction deficiency, design inadequacy, etc. Pavement condition surveys of distress are periodically conducted to quantify pavement surface condition at a specific time.

2.4.1. Pavement Failure

2.4.1.1. Review of Causes of Failure

Al-Arkawazi (2017) defined pavement failure (deterioration) as a phenomenon which appears immediately after opening the road (pavement) to traffic. Sorum, Guite and Martina (2014) highlighted that pavement failure comprises various pavement distresses such as potholes, ruts, crack settlement, localised depression. Kumar and Gupta (2010) considered pavement failure as decreases in the serviceability of the pavement. Al-Arkawazi (2017) also mentioned that pavement failure starts gradually, and may not be noticeable at the beginning; however, over time it accelerates dramatically.

Al-Arkawazi (2017) placed emphasis on monitoring the pavement assets during the whole life cycle (planning, designing, construction and maintenance) to minimise the impact of pavement failure risk. He also added that insufficient maintenance and programmes of evaluation of pavement failure under a limited budget leads to deterioration of the pavement structure. Pavement failure can be seen in corrugation and waves on the pavement surface, rutting and shoving, unlevelled surface or a combination of several factors (Sorum, Guite and Martina 2014). Reigle (2002) emphasised the difficulty to understand road pavement failure. He stated that such failure is a unique phenomenon which cannot be analysed using artificial repeat inputs in the computational models. Schlotjes (2013) added that understanding the risk of pavement failure (pavement deterioration) can be achieved by defining the mechanisms surrounding road pavement failure. He also expressed that, due to the variety of factors triggering the risk of pavement failure, pointing out the single main factor is very challenging. Asset managers need to handle the complex risk factors related to pavement failure (pavement deterioration) in conjunction with the probability of occurrence of multiple failure modes. The failure to identify the primary cause of such risk will lead to incorrect maintenance decisions (ill-chosen and ill-timed), which will poorly reflect on the maintenance programme and budget allocation. However, achieving accurate identification and precise assessment of the causes of pavement failure will support asset managers in establishing solid decisions on maintenance activities.

2.4.1.2. Risks Contributing to Pavement Deterioration

Alaswadko (2016) stated that the risk factors that impact the pavement assets can be classified into two different phases named initiation and progression phases. Hassan, McManus and Holden (2007) highlighted some of the risk factors that occur at the initiation phase such as construction quality, construction procedures, insufficient pavement design and pavement materials. The rate of pavement deterioration entirely depends on these risk factors. Roberts and Martin (1998) observed that these risks develop significantly once the rate of pavement degradation rises. Due to variations, interactions and consequences of risk factors generated at the initiation phase, the progression phase will develop different deterioration modes. These different deterioration modes affect driver safety and comfort, and are expressed in roughness, rutting and cracking, etc. Structural pavement failure usually occurs due to underestimated design load (bearing capacity) or traffic, and environmental load surpassing the original design loading calculated in the first place (Schlotjes 2013). Pavement failure can also be a single risk factor or multiple risk factors, for example, change in climate (rise in temperature) alone or combined failure of poorly designed pavement and climate change. Haas (2001) listed many risk factors that affect pavement deterioration, which are shown in Figure 2-4: traffic loading, climate, pavement composition, pavement strength, subgrade soil, maintenance, pavement age and drainage. Al-Arkawazi (2017) followed the factors put forward by Haas (2001) with slight changes. He introduced five elements, which are traffic volume and load, moisture or water, subgrade soil, construction quality and maintenance. Schlotjes (2013) classified the effects of pavement failure risk (pavement deterioration) into five main groups of factors, which are defined based on engineering knowledge. These factors are traffic loading, climate, pavement composition, pavement strength and subgrade soil, as is shown in Figure 2-5.

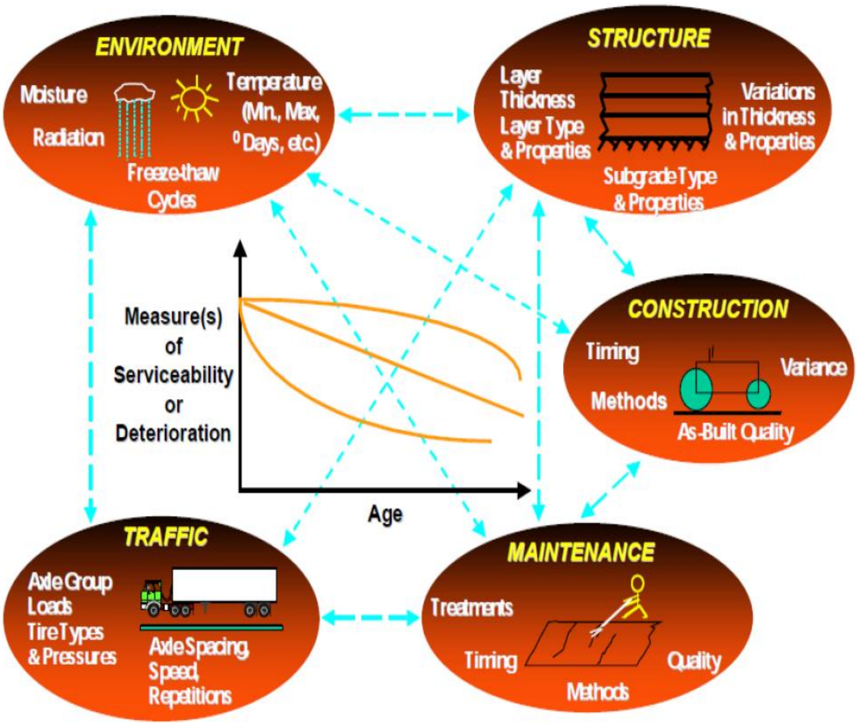

Figure 2-4: Factors influencing pavement performance by Haas (2001)

Schlotjes, Henning and Burrow (2011) stated that variability in traffic loading, environmental conditions, design and materials could lead to pavement failure happening earlier than planned in its intended design life. This phenomenon is considered to be complex and very challenging for asset managers. Schlotjes, Henning and Burrow (2011) have questioned studies that focused on a single risk when it comes to a pavement performance model. They also emphasised the importance of combining engineering knowledge with the cause of pavement failure risks in order to improve the modelling process and establish an accurate maintenance strategic plan. Such an approach is followed by the author to build a model based on engineering knowledge and pavement failure risk; more details are presented in Chapter 8 section 8.2.2 and Chapter 9 section 9.3.1.

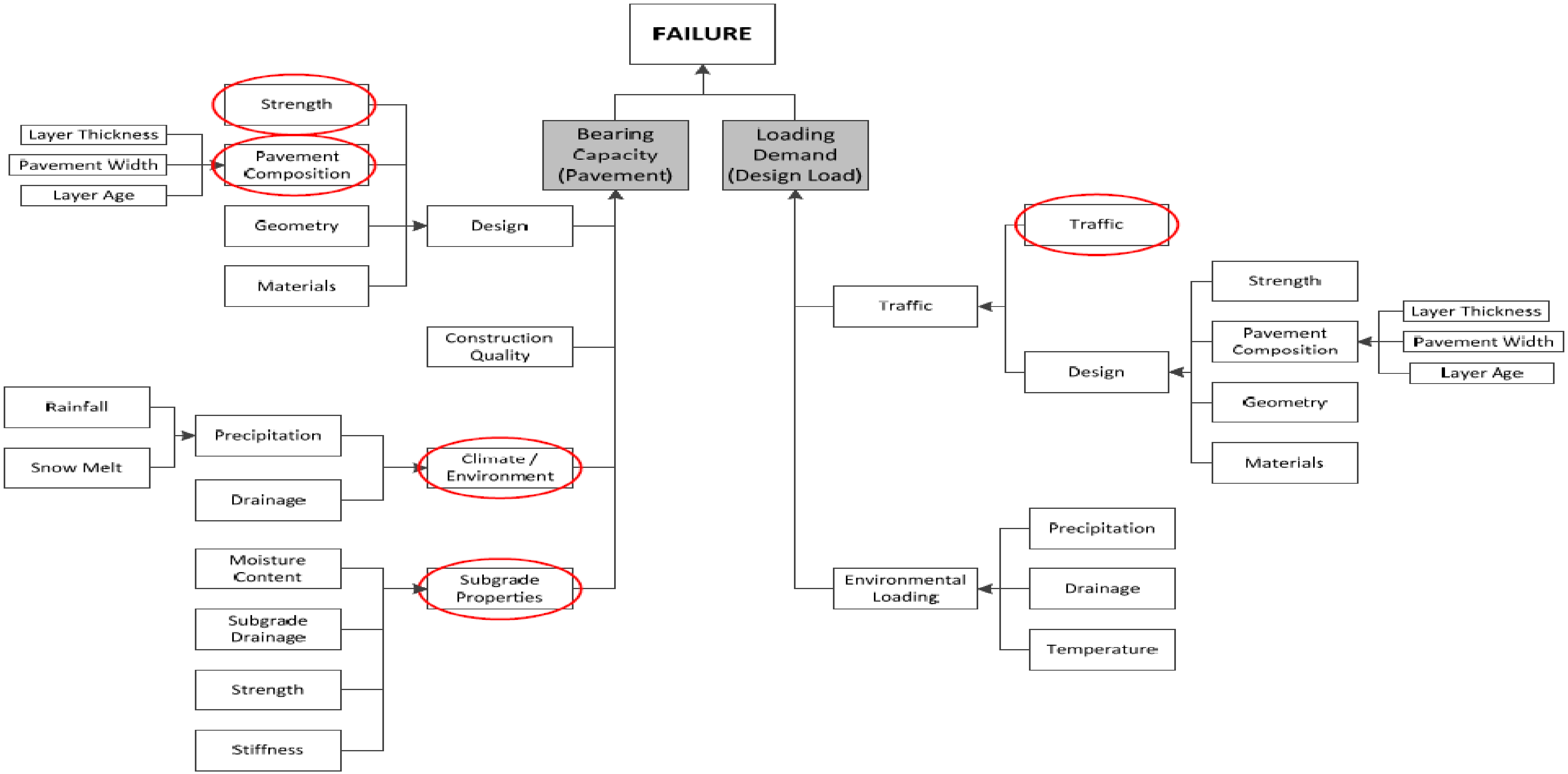

Figure 2-5: Generic failure paths for road pavements developed by Schlotjes (2013)

2.4.1.3. Risk due to Traffic Loading

In terms of pavement design, Schlotjes (2013) expressed that the primary function is to meet the expected traffic loadings during design life. However, any miscalculation on the principles will contribute to early failure of pavement assets. Martin (2011) raised a concern about the deterioration of pavements assets in Australia due to increasing axle loads. Lin et al. (2005) highlighted that the leading cause of the development of different deterioration modes such as roughness, rutting and cracking is the high volume of heavy trucks. Typically, due to both static and dynamic tyre load, a pavement structure is subjected to severe damage. Such loads are considered to be mainly received from the frequent passing of heavy vehicles. Cebon (1999) summarised the parameters that contribute to the traffic loading such as axle group type, tyre configuration, gross vehicle mass and dynamic wheel loading. A pavement structure is always designed to withstand the existing and future increase of applied traffic loading. However, under the phenomenon of unexpected repeated load, horizontal tensile strains and vertical compressive strains will be generated. Such horizontal strain leads to cracking inbound layers, and the vertical compressive stresses induce rutting (Sharp 2009; Alaswadko 2016).

Sen (2012) supported Martin's (2011) statement as he concluded that high traffic loading leads to high progression rates in rutting. Alaswadko (2016) also stated that traffic loading impact is a crucial primary factor in deterioration progression in all pavement types. The study introduced by Mun et al. (2012) showed that in pavements the remaining service life was reduced by as much as 26.5% upon receiving an 8% increase in traffic load. Moffatt (2013) added that the relationship between the rate of pavement deterioration and traffic loading is linear. Mclean and Ramsay (1996) had earlier reported that the dynamic component of truck axle loads increases with increasing road roughness.

Mikhail and Mamlouk (1998) reported that vehicle speed affects pavement performance. They stated that displacement generated from speed is around 10 times more at a speed of 20 km/hr in comparison with 130 km/hr. Loizos and Plati (2008) supported this theory. They concluded that vehicle characteristics and speed affect the riding quality as well as pavement roughness. Therefore, many studies have found that traffic load is a risk factor that plays a crucial rule in pavement performance. Traffic loading risk is discussed in Chapter 8 section 8.2.2 and Chapter 9 section 9.3.1.

2.4.1.4. Risk due to Environmental Loading

Climate conditions have a substantial impact on pavement performance. Accurate knowledge of climate is a crucial step in developing very reliable pavement performance models (Byrne and Aguiar 2010). Schlotjes (2013) stated that an unexpected climate (environmental loading) could damage a pavement significantly. Climate (environmental loading) can be seen in the form of precipitation, weathering and temperature (high or low temperature). Change in temperature impacts the pavement surface; for example, in the case of high temperature, some pavement surface may deform due to an expected loading generated from upper turning and braking stresses (Alaswadko 2016). Heat is the main risk factor for accelerating the rate of ageing/oxidation as well as the viscosity of asphaltic layers (Roberts and Martin 1998). For instance, low temperature results in stiff and brittle asphaltic layers, which consequently leads to fatigue cracking, whereas high temperatures increase the softness and viscoelasticity of the asphaltic layer, leading to permanent deformation (rutting) in the pavement structure (Harvey et al. 2004). In addition, Qi-sen, Yu-liang and Xue-lian (2009) reported that rutting is the main distress mode in asphaltic pavement layers, especially in higher summer temperatures.

Precipitation also has a substantial impact on pavement deterioration rate. Typically, the rate of the precipitation impact differs based on intensity and distribution, which subsequently affect the level of pavement moisture balance (Harvey et al. 2004). For example, in a wet climate, pavement strength is changed with the level of water content, especially with an insufficiently drained subgrade layer (Roberts and Martin 1998). Metehan and Murat (2016) concluded that increases in the amount of moisture content increase pavement deterioration. Moreover, Zuo, Drumm and Meier (2006) indicated that differences in subgrade water content in each season influence the remaining service life of a pavement structure. Pavement temperature risk and moisture risk are explained in Chapter 8 section 8.2.2 and Chapter 9 section 9.3.1.

2.4.1.5. Risk due to Pavement Composition

Pavement composition can be classified into two essential elements, which are material quality and pavement thickness. These two elements are important for achieving pavement performance (Harvey et al. 2004). The pavement structure is designed to withstand the effects of traffic loading and environment. Therefore, it is crucial to achieved sufficient pavement layer thickness and apply adequate material stiffness (Sharp 2009). In terms of pavement materials, typically, a pavement structure comprises different layers of different material properties. Material properties (physical and chemical properties) react differently under load (Paterson 1989). Each material layer has a stiffness value. For example, the asphalt layer stiffness is higher than that of the base and subgrade layers (Zuo, Drumm and Meier 2006).

On the other hand, pavement thickness depends on the available material. In practice, top layers always have less depth than the ones below. Most of the time, the thickness of the asphaltic layers is standard, while the thickness of the road base and sub-base depends on the traffic loading (Pearson 2011). The occurrence of rutting and/or cracking in a pavement can be controlled by achieving adequate pavement thickness with sufficient quality of pavement or surfacing materials (Harvey et al. 2004). To avoid rutting, the underneath layers such as the base and sub-base layers should be designed with adequate thickness that meets any traffic loading increases. Bae et al. (2008) emphasised the importance of achieving sufficient thickness. They concluded that longitudinal roughness deterioration could be minimised dramatically as the pavement thickness increased. Bitumen quality has been questioned over the last 30 years due to the reduction in crude oil quality and oil refining processes (White 2016). Changes in bitumen supply and quality contribute to many asphalt surface failures. For example, the bitumen quality affects pavements in terms of early life shearing, premature ageing and early life top-down cracking (White and Embleton 2015). Further discussion on the pavement composition risk is provided in Chapter 8 section 8.2.2 and Chapter 9 section 9.3.1.

2.4.1.6. Risk due to Pavement Strength

Generally, the pavement contains various layers of materials with different properties that react differently under load (Alaswadko 2016). In terms of pavement strength, Paterson (1989) stated that a pavement structure could withstand as much as nearly an eight times increase in equivalent standard axle load (ESAL) if the pavement structure receives 50% improvement and modification of its specification. However, insufficient pavement strength will lead to the development of rutting. Moreover, achieving pavement resilience modulus value of 20-35% less than that of its original design value will increase the probability of cracking and patching areas by more than 17% and the rate of rutting by more than 15 mm. Pavement strength is measured through the value of structural number (SN), which is considered a general parameter of the pavement layer strength (Paterson 1989). The bearing strength of the pavement is an essential metric of pavement performance (Schlotjes 2013). Further analysis of pavement strength risk is provided in Chapter 8 section 8.2.2 and Chapter 9 section 9.3.1.

2.4.1.7. Risk due to Subgrade Soil

Schlotjes (2013) and Sharp (2009) defined two primary functions of the subgrade layer. The first is to withstand the stresses generated on the layer due to various loads, whilst the second is to provide enough support to the upper layers of the pavement structure. The construction of roads and highways takes place on different soil types. Austroads (2018) emphasised the importance of subgrade selection as roads are designed to deteriorate over time; however, a suitable subgrade can delay the deterioration rate (Mann 2003). The main impact on the subgrade can be from water moisture content. For example, fluctuation in the level of water content can result in swelling or shrinkage of the subgrade layer, and eventually pavement settlement will occur (Jones and Jefferson 2012). Bae et al. (2008) also highlighted the risk associated with variation of water moisture content in the development of a faster rate of deterioration on pavement structure. For this research, subgrade soil risk is discussed in Chapter 8 section 8.2.2 and Chapter 9 section 9.3.1.

2.4.1.8. Risk due to Pavement Ageing

In pavement engineering, Martin and Choummanivong (2010) described pavement age as the date of original construction or last rehabilitation cycle. According to Harvey at el (2004), flexible pavement structure is designed to last 20-40 years, providing an adequate service that meets the comfort and safety of drivers. However, a consistently satisfactory service cannot be achieved during the whole period due to due to changes in traffic loading, climate, soil, etc. (Harvey et al. 2004). Therefore, a continuous maintenance cycle (preventive and corrective) should be applied during the service life cycle. Many investigations have highlighted the significance of the relationship between pavement deterioration and pavement age (Alaswadko 2016). For example, Shiyab, Al Fahim and Nikraz (2006) put forward the hypothesis that pavement age contributes to about 9% of the pavement performance model prediction. Mubaraki (2010) emphasised the importance of the pavement age factor in building a prediction model for pavement deterioration. In this research, pavement ageing risk is discussed in Chapter 8 section 8.2.2 and Chapter 9 section 9.3.1.

2.4.1.9. Risk due to Drainage

The impact of drainage risk can be observed in the level of water moisture content, which affects the subgrade layer and strength of pavement materials (Austroads 2018). Haas, Hudson and Zaniewski (1994) defined three main elements that measure the efficiency of pavement drainage: porosity, permeability and subjectivity. These measures are documented in terms of a poor, fair or good drainage system. An example of the pavement permeability index can be seen in the degradation of the bond between pavement layers or stripping of the binder from the aggregate. The distress of ravelling and delimitation of the pavement surface will occur. Therefore, pavement designers should always consider including a pavement drainage system to achieve equilibrium of moisture content for both asphaltic pavement layers and subgrade layers (Pearson 2011). Pearson (2011) also highlighted the impact of the existence of water on the pavement. Such an impact results in stripping the binder from the aggregate, lowering the asphalt homogeneity and damaging the bond between the several layers of the pavement. Due to the fluctuation of the natural water table in any ground resulting from the changing seasons, it is challenging to maintain equilibrium in the moisture content of the pavement foundation. According to statistics, the cost of drainage maintenance represents 7% of the whole cost of maintenance in the UK (Pearson 2011). Increase in the moisture content of base and sub-base layers leads to a loss in the bearing capacity and consequentially accelerates the rate of pavement deterioration and shortens the service life. Drainage risk is discussed in detail in Chapter 8 section 8.2.2 and Chapter 9 section 9.3.1.

2.4.1.10. Risk due to Excess Water

Christopher and McGuffey (1997) emphasised that excess water shortens pavement structure life by more than half. Raad, Minassian and Gartin (1992) stated that, in the US, the cost to preserve pavement assets could be significantly reduced if the water impact on the pavement response was well understood and taken into consideration during the design process. Christopher, Schwartz and Boudreau (2006) supported this statement, observing that poor drainage of the excess water increases the cost of initial construction by about 44% per lane-mile. Excess moisture content degrades the pavement's mechanical response (Roberson and Siekmeier 2002). Saad (2014) highlighted some of the studies on the influence of excess moisture content on the mechanical response of the pavement structure, as is shown Table 2-3.

Table 2-3: The impact of excess moisture content by Saad (2014)

Percentage of water content	Impact on resilient modulus/pavement structure/pavement service life	Study
Saturated only 10% of its life	*Stability factor only about 50% of its fully drained performance period*	Cedergren (1987)
5% increase in relative water content	*Leads to a 400% reduction in the pavement life*	Vuong et al. (1994)
Estimated 2% change in seasonal water content	*Decrease in the subgrade resilient modulus of 27%.*	Guan, Drumm and Jackson (1998)
Increase in moisture content	*Loss of stiffness of unbound aggregate base and sub-base and subgrade by 50% or more*	Christopher, Schwartz and Boudreau (2006)
Increase in moisture content	*Faster rutting occurrence in comparison with one with a low water table*	Korkiala-Tanttu and Dawson (2007)

2.4.1.11. Risk due to Maintenance

The primary goal of pavement maintenance and rehabilitation activities is to ensure the pavement condition is on the satisfactory level in terms of road safety, driver comfort and ride. Generally, the rate of pavement deterioration (roughness and rutting) is influenced by pavement maintenance and rehabilitation treatment plan. There are three types of maintenance strategies. These are routine maintenance (apply for minor defects), periodic maintenance (timely surface interventions to reduce future pavement deterioration) and rehabilitation activates (target roads which are significantly deteriorated), (Alaswadko 2016). Therefore, there is a need to ensure that maintenance activity is taking place at the right time with the right strategy. Adlinge and Gupta (2013) highlighted that, even if the pavement is well built, it will deteriorate over time. However, the main risk comes from delaying maintenance. Typically, postponing maintenance is due to budget limitation and constraints, which will lead to a significant financial impact within the pavement life cycle. Maintenance risk is discussed in detail in Chapter 8 section 8.2.2 and Chapter 9 section 9.3.1.

2.4.1.12. Risk due to Construction Quality

Adlinge and Gupta (2013) stated that risk in construction quality could be seen in inadequate moisture conditions during construction, improper quality of materials, inadequate compaction and incorrect layer thickness. Construction quality procedures should be used in the development of infrastructures (Abas et al. 2015). In the field of pavement construction, Deacon, Monismith and Harvey (2001) defined quality as a critical element in measuring how well a pavement sustains under various traffic loads and environmental impacts. The primary objective of the project owner in a highway construction project is to construct pavement assets that achieve good serviceability (Webb 1986). Pavement performance is affected by quality in construction pavement projects. Table 2-4 summarises the studies that identify the leading causes of the risk associated with construction quality.

Table 2-4: Some studies highlighting the main causes of the risk associated with construction quality

Main Factors	Sub-factors	Authors
Design and specification	*Pavement not designed to the regional conditions, consistency of specification interpretation of aggregate quality, amount of filler materials in the mixture, and availability of the specified material quality*	Al-Hassan (1993)
	Poor pavement design and asphalt quality and type used in the construction process	Abu El-Maaty, Akal and El-Hamrawy (2016)
	Specifications-related factors, namely structural design, aggregate quality, asphalt mix design, mix composition, and asphalt characteristics	Bubshait (2002)
Construction process	*Practice-related factors, namely aggregate characteristics, placement and compaction process, uniformity of materials, mixing operation control, and acceptable procedure*	Bubshait (2002)
Managerial Managerial	*The qualifications of the owner's inspection team and the contractor's personnel, the contractor's experience, the contractor's workforce and equipment capability, the contractor's qualifications, delay in progress payment, and amount of work subcontracted*	Bubshait (2002)
	(1) Availability of experienced staff of owner and contractor, (2) efficiency of the owner's inspection team, (3) clarity of responsibilities and roles for each owner, consultant and contractor	Abu El-Maaty, Akal and El-Hamrawy (2016)

Construction quality risk is discussed in detail in Chapter 8 section 8.2.2 and Chapter 9 section 9.3.1.

2.4.2. Pavement Deterioration Distress Risks

Overall, pavement distress is a sign that such assets are deteriorating. Such a sign could have resulted from many factors such as traffic loading, environment impact (temperature, moisture), ageing, construction practice, and deficiency of materials and maintenance practice as discussed in section 2.4.1. Pavement distress can be classified into the following areas: structural or functional. Cracking, rutting and roughness are the most common and very critical areas of distress (NRC 1993). In flexible pavement, distress surveys usually cover various deterioration data such as severity, location and distress types. Fwa (2006) classified distress into five groups, which are cracking, patching and potholes, surface deformation, surface defects and miscellaneous distresses as per Table 2-5.

Table 2-5: Flexible pavement distress types by Mahmood (2015)

Distress group	Distress type	Measure unit	Severity level
Cracking	*Alligator cracking*	*m2*	*Low, medium, high*
	Block cracking	*m2*	*Low, medium, high*
	Longitudinal and transverse	*m2*	*Low, medium, high*
	Edge cracking	*m2*	*Low, medium, high*
	Joint reflection cracking	*m2*	*Low, medium, high*
Patching and Potholes	*Patching*	*m2*	*Low, medium, high*
	Potholes	*Number*	*Low, medium, high*
Surface Deformation	*Rutting*	*m2*	*Low, medium, high*
	Shoving	*m2*	*Low, medium, high*
Surface Defects	*Bleeding*	*m2*	*Low, medium, high*
	Ravelling	*m2*	*Low, medium, high*
	Polished aggregate	*m2*	*N/A*
Miscellaneous distress	*Lane to shoulder drop off*	*m*	*Low, medium, high*
	Water bleeding and pumping	*m*	*N/A*

Factors found to be influencing pavement distress have been explored in section 2.4.1. Rutting and cracking of asphaltic pavements are the two most crucial elements of distress that present overall pavement condition. Rutting and cracking are fundamental modes of deterioration. In flexible road pavement design, the primary purpose of the design is to resist cracking (fatigue) of asphaltic layers and structural rutting of the subgrade (Yang et al. 2006). Rutting is also the most common distress within the asphalt layer of long-life pavements (Merrill, Van Dommelen and Gáspár 2006).

2.4.2.1. Cracking

One of the fundamental phenomena that occur on the surface of the flexible pavement, as a failure sign, is cracking. Moffatt and Hassan (2006) stated that cracking should be taken into consideration as a vital element regarding new pavement design thickness or rehabilitation activities, especially on overlaying an existing pavement. According to Alaswadko et al. (2016), cracking is a very active segment which gives a high weight when assessing pavement condition. Cracks are a sign of pavement defect. Qiao (2015) introduced cracking as a phenomenon that may appear either as small openings or partial fractures. Such cracking can be seen on pavement surfaces or bottoms of asphaltic layers. Fwa (2006) described cracks as "*fractures [that] exist on the pavement surface in various forms ranging from single cracks to interconnected patterns*". He also added that the main reasons for cracking are fatigue failure of the asphalt concrete, shrinkage, deformation, crack reflection from underlying pavement layers and poor construction joints of the asphalt concrete, and daily temperature cycling. AASHTO (1993) defines cracks as having a minimum length of 25 mm and a minimum width of 1 mm (NCHRP 2004). Cracks can result from traffic loading, environmental impact or both. Commonly, cracks spread on the pavement structure by two methods: top-down propagation and bottom-up propagation. In practice, if the cracks appear on the surface, the continuous load will make them wider, and with time this creates a path; thus, infiltration of water penetrates the pavement sub-layers and finally accelerates pavement deterioration to failure (Rohde 1995a; NCHRP 2004). There are several types of cracks (see figure 2-6). For example, the NCHRP (2004) defined fatigue cracking, longitudinal cracking, and transverse cracking and block cracking. Park et al. (2008) defined longitudinal cracking as it "*consists of cracks or breaks that run approximately parallel to the pavement centreline and is measured as the total length in linear feet per road segment*". Moreover, alligator cracking or fatigue can be classified as significant structural distress. Such cracks can be considered as a series of longitudinal and interconnected cracks caused by repeated traffic loading, leading to a severely damaged road (Huang 2004). This phenomenon occurs because of repeated bending stresses on the top layer. Consequently, over time, cracks occur at the bottom of the asphalt layer, leading to surface deficiency.

The traffic loading and environmental impact are the main factors for cracking (Moffatt and Hassan 2006). Cracking can be generated from traffic loads and overstressing from heavy vehicles (more details were provided earlier, in 2.4.1.3 Risk due to traffic loading). Moreover, the impact of environmental conditions leads to pavement structure moisture fluctuation as well as to the expansion of subgrade soils. Oxidation or chemical shrinkage is also a sign of environmental impact (see section 2.4.1.4 Risk due to environmental loading for more details).

On the other hand, the rate of pavement deterioration will increase dramatically in cases where widespread cracking occurs in pavement surface layers. The reason why pavement deterioration speeds up is because water is allowed to penetrate the pavement layers, which eventually will weaken both asphaltic subgrade layers (Paterson 1987). In other words, Paterson (1987) defied cracking in two stages. Stage one is the initiation stage. In this phase, the cracking starts to appear on the pavement surface after construction due to reasons discussed earlier. Then, the second stage, called the progression stage, begins. Cracking starts to develop gradually both vertically (widening) and horizontally (extending over the surface area). The climate change phenomenon worsens the rate of pavement deterioration in the form of cracking. More details of the impact of climate change on the pavement were discussed earlier in this chapter, in section 3.4.1.

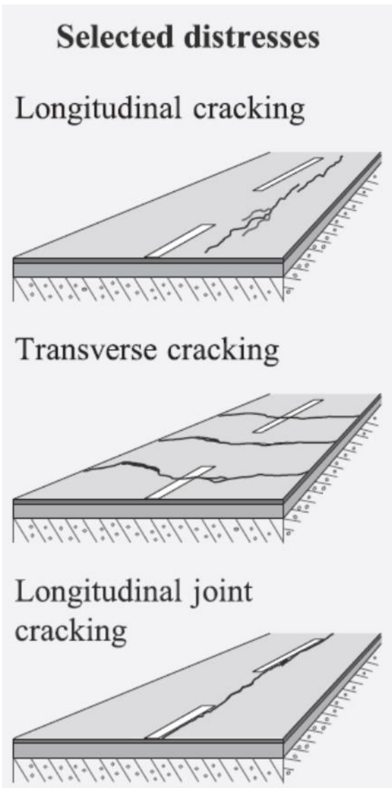

Figure 2-6: Example of cracking types by Fwa (2006)

2.4.2.2. Rutting

Papagiannakis and Masad (2012) described rutting as a phenomenon that appears in wheel paths of the pavement segment. It usually deforms as longitudinal depressions in the pavement. Such events result from structural failure of the sub-layers under wheel loadings. Paterson (1987) presented another description of surface rutting. He stated that rutting appears in the shape of plastic flow of the asphaltic material generated from stress. Fwa (2006) defined rutting as permanent deformation in the wheel path. Rutting can result for many reasons such as unstable hot mix asphalt (too much asphalt or too soft asphalt binder), densification of hot mix asphalt (poor compaction during construction) or deep settlement in the subgrade (drainage or weak subgrade). Technically, stress that occurs as a result of the traffic load that exceeds the shear strength of the asphaltic material is another reason for surface rutting. TRL (1993) stated that the increase in axle loads, channelised traffic, high maximum temperatures, and slowing and stopping of travelling vehicles could shape the rutting phenomenon. However, Morosiuk, Riley and Odoki (2004) argued that those factors are not the leading cause of rutting as these elements are always taken into consideration by pavement designers. Therefore, they suggested taking asphalt properties into account as a crucial element. Table 2-6 summarises the influence of asphalt material on rutting failure (Sousa, Craus and Carl 1991).

Table 2-6: Implication of material properties and other factors on rutting (Sousa, Craus and Carl 1991)

Material Properties/Factor	Change in Material Properties	Resistance of Asphalt Mixture to Rutting
Binder Stiffness	*increase*	*increase*
Air Void Contents	*increase*	*decrease*
Voids in Mineral Aggregate	*increase*	*decrease*
Temperature	*increase*	*decrease*
State of Stress/Strain	*increase in tyre pressure*	*decrease*
Load Repetition	*increase*	*decrease*

Rutting could occur at two levels, either on lower layers of the pavement or upper pavement layers. It is believed that, if the rutting is wide and evenly-shaped, then it can be classified as a failure in the pavement lower layers, whereas narrow and sharp ruts indicate pavement upper layer failure (CASRA 1992). Byrne and Aguiar (2010) stated that rutting can result from many factors such as climate change. For example, the consequences resulting from climate change impact can either reduce or magnify the cost of road construction and maintenance costs, depending on the location and area (Chinowsky, Price and Neumann 2013). Therefore, in this research, rutting and cracking distress are studied in conjunction with the change in roughness. More details are provided in Chapter 5 section 5.4 and Chapter 6 sections 6.2 and 6.3. More details on the impact of climate change on the pavement are also provided in Chapter 3 section 3.2. A considerable amount of literature on pavement failure has been discussed. A summary of the main and sub-risks is provided in Table 2-7. It is proposed to use this and the earlier tables in designing the questionnaire. More details are provided in Chapter 5.

Table 2-7: Generic pavement failure developed by the author

Code	Sub-Risk Factors	Main Risk Factor	Evidence
S.1	High volume of heavy trucks	R.1 Traffic Loading	Lin et al. (2005)
S.2	Axle group type	R.1 Traffic Loading	Cebon (1999)
S.3	Tyre configuration	R.1 Traffic Loading	Cebon (1999)
S.4	Gross vehicle mass	R.1 Traffic Loading	Cebon (1999)
S.5	Dynamic wheel loading	R.1 Traffic Loading	Cebon (1999)
S.6	High traffic loading (all vehicles type)	R.1 Traffic Loading	Sen (2012)
S.7	Vehicle speed	R.1 Traffic Loading	Mikhail and Mamlouk (1998)
S.8	Precipitation	R.2 Climate Change	Schlotjes (2013) and Alaswadko (2016)
S.9	Weathering	R.2 Climate Change	Schlotjes (2013) and Alaswadko (2016)
S.10	High temperature	R.2 Climate Change	Schlotjes (2013) and Alaswadko (2016)
S.11	Low temperature	R.2 Climate Change	Schlotjes (2013) and Alaswadko (2016)
S.12	Drainage	R.2 Climate Change	Schlotjes (2013) and Alaswadko (2016)
R.5	Pavement ageing	R.2 Climate Change	Roberts and Martin (1998)
S.14	Increased oxidation	R.2 Climate Change	Roberts and Martin (1998)
S.15	Increased viscosity and softness	R.2 Climate Change	Roberts and Martin (1998)
S.16	Increased brittle of asphaltic layer	R.2 Climate Change	Roberts and Martin (1998)
S.17	Increased moisture/excess water	R.2 Climate Change	Harvey et al. (2004)
S.18	Material quality and properties (Aggregate/soil)	R.3 Pavement Composition	Zuo, Drumm and Meier (2006)

S.19	Pavement thickness	R.3 Pavement Composition	Harvey et al. (2004)
S.20	Availability of material	R.3 Pavement Composition	Pearson (2011)
S.21	Bitumen supply and quality	R.3 Pavement Composition	White and Embleton (2015)
R.1	Traffic loading	R.4 Pavement Strength	Pearson (2011)
S.22	Insufficient value of structural number (SN)	R.4 Pavement Strength	Pearson (2011)
R.2	Climate change	R.5 Pavement Ageing	Harvey et al. (2004)
R.1	Traffic loading	R.5 Pavement Ageing	Harvey et al. (2004)
R.6	Subgrade soil	R.5 Pavement Ageing	Harvey et al. (2004)
R.8	Maintenance	R.5 Pavement Ageing	Harvey et al. (2004)
S.17	Increased moisture/excess water	R.6 Subgrade Soil	Jones and Jefferson (2012)
S.13	Selection of construction soil	R.6 Subgrade Soil	Austroadds (2018)
S.17	Increased moisture/excess water	R.7 Drainage	Haas, Hudson and Zaniewski (1994)
S.23	Insufficient drainage system	R.7 Drainage	Haas, Hudson and Zaniewski (1994)
S.24	Delay maintenance	R.8 Maintenance	Harvey et al. (2004)
S.25	Maintenance priorities/plan	R.8 Maintenance	Harvey et al. (2004)
S.26	Limited budget	R.8 Maintenance	Adlinge and Gupta (2013)
S.27	Design and specification	R.9 Construction Quality	Bubshait (2002) and Abu El-Maaty, Akal and El-Hamrawy (2016)
S.28	Construction process	R.9 Construction Quality	Bubshait (2002)
S.29	Construction management	R.9 Construction Quality	Abu El-Maaty, Akal and El-Hamrawy (2016)

2.5. Pavement Performance

Pavement performance is considered to be a crucial component in the design philosophy of pavement structures (Haas, Hudson and Zaniewski 1994; Huang 2004; Shahin 2005). Arimbi (2015) introduced pavement performance as a tool to measure the deformation of pavement condition and functionality. Abaza (2004) emphasised the importance of pavement performance in terms of pavement rehabilitation and management applications. Lytton (1987) concluded that pavement performance could only be monitored by determining the current condition of the pavement and then using the collected data to establish a management plan. Moreover, Amin (2015) stated that pavement management system optimisation for maintenance treatments is achieved through performance models. Furthermore, measuring the forecasted maintenance operations for pavement condition is one of the performance model outcomes. Arimbi

(2015) added that the state of a pavement would decline due to many factors such as asset ageing and accumulated axle loads. The primary objective is to capture the condition over time; thus, the deterioration rate can be measured. Therefore, many maintenance or rehabilitation alternatives can be introduced to upgrade the condition parameters. Abaza (2004) stated that the condition assessment of a pavement structure at a given period could be conducted using three important performance measurements. These are Pavement Condition Index (PCI) (presents the distresses on pavement sections), Present Serviceability Index (PSI) (presents the functional condition in terms of ride quality) and International Roughness Index (IRI) (measures the roughness along road profile) (Sayers 1995). Many scholars and engineers have agreed that cracking and excessive deformation of pavement sections, as well as disintegration of pavement material, result from repeated traffic loadings and environmental impacts, which lead to degradation of pavement performance (Haas, Hudson and Zaniewski 1994).

Data collection is a crucial element in assessing pavement performance. In practice, pavement condition data can be gathered using automated or manual methods. Every agency or municipality establishes their own approach for data collection methodologies, applied software programs and pavement management processes. Concerning data type, there are four general categories of pavement condition used in maintenance planning for pavements: Surface distress (Pavement Condition Index – PCI), Ride quality (International Roughness Index – IRI), Structural capacity (Falling Weight Deflectometer – FWD) and Friction (Skid resistance). More details are provided in Chapter 5 section 5.4.3.

2.5.1. Pavement Condition Index (PCI)

In the 1980s, the US Army Corps of Engineers introduced the Pavement Condition Index (PCI) rating system. Shiyab (2007) states that the PCI technique has been extensively implemented for airfield pavements, roads and parking lots by various highway authorities worldwide. The primary objective of the PCI is to give a good sign of structural integrity and operational condition of the pavement surface. Mahmood (2015) emphasised the importance of PCI application for highway agencies; he also stated that the PCI covers all types of distress such as cracking, rutting, shoving, etc. Moreover, the weights of both severity and quantity are expressed in PCI. Abaza (2004) concluded that the PCI techniques had been applied mainly in pavement management applications. Mahmood (2015) adopted the PCI in his research as it gives an excellent presentation of the pavement condition of a network regarding both functional and structural conditions. The PCI measure (or rating) is achieved by visual inspection of pavement distress. The rates of PCI for the surface condition of the pavement depend on the distresses monitored from the surface of the pavement. The primary objective of the data collection is to present the structural integrity and surface operational condition of the pavement section (ASTM 2011). The rating ranges from 0-100, where 100 is the best condition and 0 is the worst. Further analysis is provided in Chapter 5 section 5.4.3. Also, the PCI was used as a pavement indicator for the deterioration model. More information is presented in Chapter 6 section 6.5.

2.5.2. International Roughness Index

ASTM (2003) defined roughness as "*the deviation of a surface from a true planar surface with characteristic dimensions that affect vehicle dynamics and ride quality*". Sayers, Gillespie and Queiroz (1986) introduced another definition of roughness. They stated that it is "*variations in elevation of the surface that induce vibrations in traversing vehicles at a given point of time*". Fwa (2006) added another definition: "*the irregularities in the pavement profile which causes uncomfortable, unsafe, and economical riding*". Qiao (2015) presented roughness as the measurement of the longitudinal unevenness of the pavement. Overall, roughness is a crucial sign of vehicle operating costs and the safety, comfort and speed of travel. The rougher the pavement, the higher the in-road user's cost (Archondo-Callao and Faiz 1994). Basically, a higher roughness magnitude affects pavement serviceability and has more impact on vehicle operating costs (VOCs). Haas, Hudson and Zaniewski (1994) classified the rating of roughness based on vehicle speed, vehicle passengers' and driver's patience and attitude. On the other hand, Gillespie (1992) defined the main factors that cause roughness in a pavement such as environmental impact, traffic loads and defective material applied in the construction of the pavement. A newly constructed pavement segment is also considered to have some initial roughness. For such a section, the roughness value will start to increase with time due to pavement deterioration generated from both traffic loads and environmental impact. Therefore, missing of inadequate maintenance measures will lead to increase the severity and magnitude of distresses, which will eventually affect vehicle speed, and the safety and comfort of road users (Sayers, Gillespie and Queiroz 1986). The road roughness is not only a crucial element in achieving the pavement performance, it is also widely applied in forming the rehabilitation and maintenance priorities plan, especially with a limited budget (Shahin 2005). Therefore, many countries consider road roughness as a valuable tool for defining vehicle operating costs (VOCs).

To measure the roughness, in the 1970s the World Bank introduced a calibration standard that was first applied and tested in Brazil. Finally, a conceptual International Roughness Index (IRI) was developed to achieve an accepted scale that evaluated roughness using a fixed index. The International Roughness Index (IRI) model consists of a series of differential equations that link to the motions of a simulated quarter-car and the road profile. The International Roughness Index (IRI) is expressed in metres per km. Figure 2-7 shows IRI roughness with different scale.

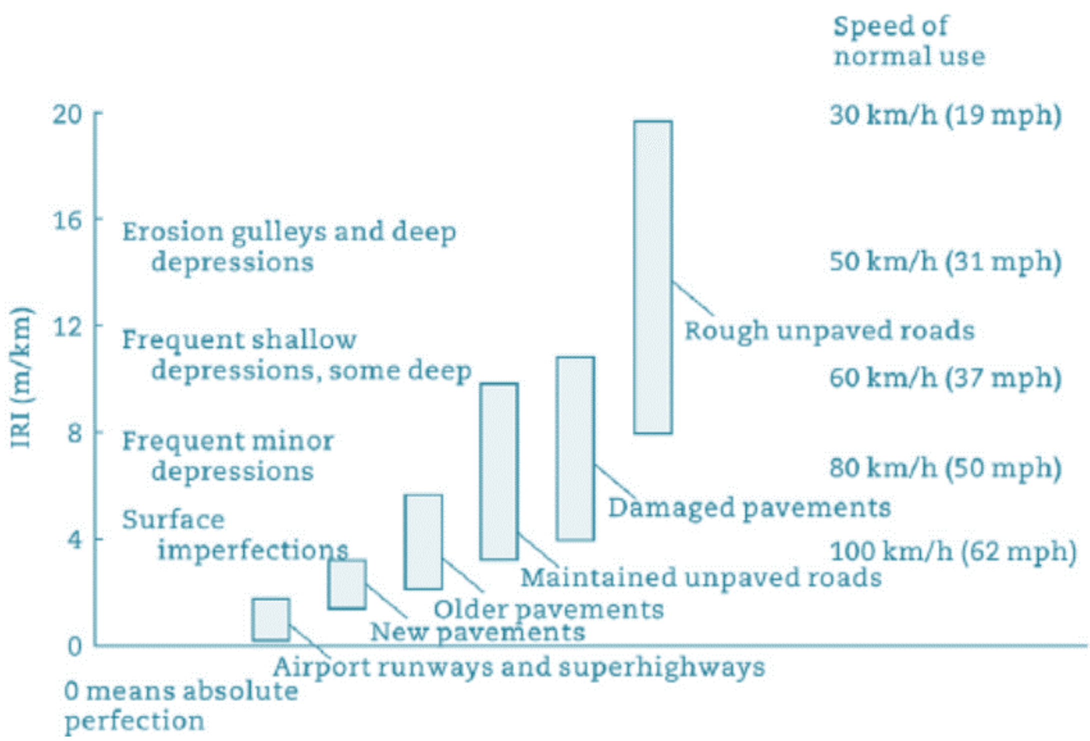

Figure 2-7: IRI roughness scale (Source: Sayers, Gillespie and Queiroz 1998)

Many different studies have been conducted on roughness to identify the progression trends and factors affecting roughness value (Kargah-Ostadi, Stoffels and Tabatabaee 2010). Many limitations were recorded in these studies such as complexity of the equations, a large number of variables applied, difficulties in collecting data relating to the variables (especially for the mechanistic-empirical models), and the limited and short period of prediction (Madanat, Nakat and Sathaye 2005). Therefore, it has been concluded that research is still required to discover a more efficient empirical model to be used at the network level. This is still an ongoing matter for pavement scientists and practitioners. In this study, it is proposed to establish a pavement performance indicators model in terms of International Roughness Index (IRI) and Pavement Condition Index (PCI) and then introduce a new pavement deterioration model using Markov chain and system dynamics. Chapter 6 section 6.5 introduces the proposal of an empirical model that concludes on how the International Roughness Index (IRI) can be measured with respect to different climate change impact scenarios.

2.5.3. Pavement Structural Condition

Rebecchi and Sharp (2009) discussed pavement structural condition through the pavement surface deflection under an applied load (traffic load). Alaswadko (2016) added that pavement strength is indicated by the Structural Number (SN). Paterson (1987) considered that Structural Number (SN) is widely used as a strength parameter in roughness progression models. Abd El-Raof et al. (2018) defined the structural number of existing pavement as "*a numerical value used as indicator of the pavement strength and its structural capacity at any age*". Moreover, recently, the pavement strength concept was developed to quantify the contribution of all pavement layers (pavement structures and subgrade) through an adjusted or modified structural number (SNP) (Rolt and Parkman, 2000). This new concept is incorporated in the HDM-4 model (Morosiuk, Riley and Odoki 2004). The primary goal of applying Non-Destructive Testing (NDT) is to quantify the pavement structural responses to heavy dynamic loads produced by heavy trucks. 'Falling Weight Deflectometer' is the most popular Deflection Measuring System for Non-Destructive Testing (NDT). The FWD is a device used to obtain the readings of stress/strain parameters of pavement structures including subgrades.

The strength data obtained from the Falling Weight Deflectometer (FWD) measure the surface deflection. The modified structural number (SNC) has been used to highlight the total strength of both the pavement and the subgrade. Such a combination can easily predict the performance of asphalt pavement structures at a network level (Watanatada et al., 1987). The variable of the SNC is the essential element in the equation of structural component of roughness based on default HDM-4 model. More details are presented in Chapter 6 sections 6.2.1 and 6.3.1.

2.6. Resilience Review

2.6.1. Resilience Background and Definitions

It is believed that, before studying the resilience of a local or global infrastructure, it is crucial to understand the definition of resilience in conjunction with the variety of disciplines of resilience itself. According to Gibbs (2009), the interpretation of the components of a system resilience needs more attention, and it is not straightforward; he concluded that the first move towards establishing what is called a 'system resilience' is through a better understanding of the definition itself. Furthermore, Bouch et al. (2012) suggested that the definition of resilience has a wider interpretation which slightly differs from discipline to discipline. The word resilience was initially extracted from the Latin "*resillo*", which means "*to jump back*" (Cimellaro, Reinhorn and Bruneau 2010), or "*resilience*", which means to "*bounce back*" (Hosseini, Barker and Ramirez-Marquez 2016). There are vast numbers of definitions for resilience depending on the context of the discipline in question, such as ecology, materials science, psychology, economics and engineering (Hosseini, Barker and Ramirez-Marquez 2016). According to Hosseini, Barker and Ramirez-Marquez (2016), the definition of resilience could be linked to some existing theories such as flexibility, robustness, survivability and agility.

Resilience is not a new topic. In 1973, Holling first introduced the resilience concept. During his research, he defined resilience in ecological systems as a "*measure of [the] perseverance of systems and their capability to absorb changes and disturbances, and still sustain the same relationships between populations or state variables*" (Holling 1973). Resilience can be considered as the maximum degree of threat mitigation to respond to, minimise or remove long-term impacts to property and humans from hazards and the consequences of such risks (Godschalk 2003a). The concept of resilience consists of various disciplines which shape the definition of resilient approaches. Levina and Tirpak (2006) introduced two main elements in resilience definitions. First, elements could undergo a disruptive action without change to the original state of the system. Second, features are the system's ability to recover from the potential impact. Maguire and Cartwright (2008) categorised resilience into three terminologies: stability, recovery and transformation. Hosseini, Barker and Ramirez-Marquez (2016) developed some resilience definitions that present different disciplines from a collection of previous studies. For example, Allenby and Fink (2005) introduced system resilience as the system having the ability to protect itself regarding functionality in case of both internal and external change.

Moreover, system resilience should be graceful enough to adopt such a change when degradation occurs. Pregenzer (2011) defined resilience as the "*measure of a system's ability to absorb continuous and unpredictable change and still maintain its vital functions*". Haimes (2009) explained resilience as a system which has both the ability and capacity to endure significant disruptive events causing accepted degradation parameters and to return to its original state within appropriate risks, time and costs.

Hollnagel and Woods (2006) have also questioned resilience concerning time recovery. They believe that the system should be measured against a timescale for recovery to define how effectively and quickly it can return to its original state after the occurrence of disruption.

Regarding transport networks, the DfT (2014) defined resilience as "*the ability of the transport network to withstand the impacts of extreme weather, to operate in the face of such weather and to recover promptly from its effects*". Murray-Tuite (2006) presented some essential elements in terms of the efficiency of the road transport network. Those elements depend on certain factors such as speed of recovery (time) and the magnitude of external support. These factors help the system to achieve refunctioning of its original performance.

2.6.2. Resilience Dimensions

Hosseini, Barker and Ramirez-Marquez (2016) summarised the approach suggested by Bruneau et al. (2003) for resilience classification. They proposed four resilience domains, namely social, engineering, economic and organisational. Such designations may differ based on the author's perspective. For example, Kahan, Allen and George (2009) divided resilience dimensions, which focus on organisations and infrastructure, into two fields: '*hard*' and '*soft*' resilience. Soft resilience focuses on human requirements, behaviours, relationships, psychology and endeavours. It is related to family, community and society. On the other hand, hard systems cover the area affecting the structural, mechanical and technical infrastructure.

Hughes and Healy (2014) concluded that the four domains (or dimensions) introduced by Bruneau et al. (2003) could not be assessed or evaluated as one component in terms of system performance. It is suggested that an individual study should be applied for each system. There is another classification, made by the US National Infrastructure Advisory Council (NIAC 2010), which establishes the categories of resilience system domains (or dimensions) into fields: practice and process. Practice focuses on people whereas process focuses on the structure of the infrastructure and asset. In their study, Hughes and Healy (2014) mentioned how important the four domains (organisational, engineering, economic and social) of system resilience are. Nevertheless, they concluded that focusing on the area of engineering and organisational system resilience is sufficient in terms of the transport system. The reason behind this approach where both social and economic domains are considered is implicit in the system (engineering and organisational). In this study, resilience is viewed in terms of the engineering dimension only. More details are provided in section 2.6.3.

2.6.3. Resilience in the Transport Context

The transportation system is an essential sector of any community. However, risks and uncertainty relating to all types of disruptions can affect transportation systems. For example, both natural disasters and human-made hazards can be the root cause for such disturbances. Natural disasters consist of earthquakes, hurricanes, floods, tsunamis, heavy snow, etc., whilst human-made hazards include terrorist attacks, group events, strikes and system breakdown. All these disturbances may lead to immense economic losses to society (Cao 2015). In terms of the transportation system, it has become increasingly important to integrate sustainability with resilience in management and development of local transport infrastructure (Bouch et al. 2012). To establish the long-term optimisation of engineered structures and efficient management systems, both managerial aspects and physical aspects should be equally taken into account. They are critical elements for a resilient transport infrastructure under different phenomena (Bouch et al. 2012). The more efficient organisational management there is, the more rapid the recovery in the transport system (DfT 2014). Cao (2015) concluded that the interpretation of the specific characteristics of resilience should allow transportation managers to draw the hazard line efficiently. Table 2-8 elaborates on the definition of resilience in terms of the transportation system developed by Cao (2015), who carried out research where he classified such interpretation based on the transportation area.

While a variety of definitions of the term transportation resilience have been suggested, this study will use the definition of Mansouri, Nilchiani and Mostashari (2010). The focus will be on the concept of the function of a system.

Table 2-8: Definition of resilience for different transport contexts, developed by Cao (2015)

Definition of Resilience	Source	Research Object
The ability of the system to absorb shock as well as to recover from a disruption so that it can return to its original service delivery level or close to it.	Mayada et al. (2012)	Maritime transportation system
A function of a system's vulnerability against potential disruption, and its adaptive capacity in recovering to an acceptable level of service within a reasonable time frame after being affected by disruption.	Mansouri, Nilchiani and Mostashari (2010)	Maritime infrastructure and transportation systems

Capability of a system to provide and maintain an acceptable level of service in the face of major changes or disruptions to the environment	Mansouri, Nilchiani and Mostashari (2010)	Port infrastructure systems
"The ability for the system to maintain its demonstrated level of service or to restore itself to that level of service in specified time frame."	Nayel et al. (2011)	Transportation network
"The ability for a transportation network to absorb disruptive events gracefully and return itself to a level of service equal to or greater than the pre-disruption level of service within a reasonable time frame..	Freckleton et al. (2012)	Transportation networks
"Both the network's inherent ability to cope with disruption via its topological and operational attributes and potential actions that can be taken in the immediate aftermath of a disruption or disaster event."	Miller-Hooks, Zhang and Faturechi (2012)	Freight transportation networks

2.6.4. The Relationship between the Climate Change Risk and Resilience

ISO (2018) defines risk as the: "*effect of uncertainty on objectives*". In terms of risk analysis, Khan and Haddara (2003) provide another definition: "*Risk analysis is a technique for identifying, characterising, quantifying, and evaluating the loss from an event"*. The primary objective of risk analysis concerns the efforts to answer the question of what makes system failure occur. Burnett (2013) highlighted the importance of identifying the critical assets. He also added that this approach will provide support in prioritising and planning a maintenance and rehabilitation plan. Risk consideration should be taken into account in all activities and procedures; thus, the risk can be well controlled. He also stated that there are various methods to measure risk. According to Park et al. (2013), risk analysis, under emergent disruptive events, should be studied with the conjunction of resilience analysis to achieve accepted protection of critical infrastructure systems like a transport network. Rashidy (2014) added that, in terms of resilience, identifying risk and consequences of such risk is a very challenging step in the risk analysis process. She also classified risk into two categories. One is risk in the context of climate change phenomena (natural impact) and consequent impacts, the other is human-made risk events (for example, terrorist attacks). For this research, the subject of human-made risk is excluded as the study is mainly focusing on the impact of climate change in terms of pavement infrastructure.

2.7. Review of Pavement Deterioration and Resilience Prediction Models

A prediction deterioration model is a mathematical approach that can be applied to forecast how the future pavement is going to deteriorate. The model depends on the existing pavement condition, deterioration factors and previous maintenance (OCED) 1987). Arimbi (2015) classified prediction deterioration into two categories in the deterministic model (prediction as an exact value based on mathematical functions from observed decay) and probabilistic models (prediction of the pavement condition as the probability of the occurrence of a range of possible outcomes) (Ortiz-García, Costello and Snaith 2006). In theory, probabilistic models are applied for pavement evaluation at the network level, where the deterministic model is the only appropriate tool for project-level performance. According to Osorio-Lird et al. (2018), the World Bank introduced many performance models under the umbrella of Highway Design and Maintenance Standards (HDM-III) and the Highway Development and Management Model (HDM-4). Odoki and Kerali (2006) stated that HDM-4 and HDM-3 have been applied mainly by many highway agencies across the world for more than 20 years.

2.7.1. Deterministic Model

In engineering practice, there is much to be explained about a mechanistic approach to pavement design. In simple engineering words, ‘mechanistic’ involves calculation of critical stress, strain or deflection in the pavement mathematically. ‘Empirical’ means to forecast the resulting damages caused by some empirical failure criteria (NCHRP 2004; Abo-Hashema 2009). According to George, Rajagopal and Lim (1989), the mode of determination comprises structural performance, functional performance, damage models and initial response. Anyala, Odoki and Baker (2014) defined deterministic models as they “*predict condition as precise values using mathematical functions*”. Determination of the pavement performance should be a function of a set of random variables that do not change over time. However, Hong and Wang (2003) indicated that environmental and traffic actions are random variables that vary with time. They encourage more stochastic processes. Amin (2015) also drew some limitations on using a deterministic model. One restriction is that the deterministic model fails to explain issues related to the randomness of traffic loads, environmental conditions and the non-linearity between the model elements. Moreover, there is poor evaluation of pavement distress as there is always room for bias. Therefore, for this research, the author has opted for the stochastic approach, which will be explained in Chapter 7. However, the deterministic approach is also used in chapters 5 and 6. Anyala, Odoki and Baker (2014) and Amin (2015) stated that there are different categories of deterministic models, such as mechanistic-empirical models, mechanistic models and regression or empirical models, which are discussed below.

2.7.1.1. Mechanistic Models

In terms of pavement responses, mechanistic models are mainly used to define the actual behaviour of the specimen with respect to stresses, strains and deflection. Such models have been questioned and are seen as being limited in application due to being data-intensive as well as the difficulty in measuring parameters in practice (Prozzi and Madanat 2003; Morosiuk, Riley and Odoki 2004). Moreover, Li, W-C and Haas (1996) concluded that mechanistic models shape the relationship between response parameters such as stress, strain and deflection.

2.7.1.2. Mechanistic-Empirical Models

Many transportation agencies have changed the flexible pavement design from the Empirical to Mechanistic-Empirical (M-E) procedure. Technically, the new approach has been introduced to overcome the limitations of the AASHTO (1993) design guide (NCHRP 2004). In comparison with a fixable pavement design, the main difference of the M-E pavement design procedure is that it applies a mechanistic calculation to forecast the induced pavement responses, which eventually interprets empirically in terms of pavement distress such as fatigue cracking and rutting (Schwartz and Carvalho 2007). Moreover, in order to apply a mechanistic-empirical design, advances in computational mechanics are needed. Such a system will solve complex calculations and finally the outcomes will be in the form of prediction of pavement response to both load and climate effects. According to the design guideline AASHTO

2002, the proposed Mechanistic-Empirical (M-E) Pavement Design takes into consideration a number of critical factors such as the expected future traffic, the structuring capacity of each pavement layer, and the variation of the pavement material properties due to seasonal environmental changes, especially the temperature and moisture. The primary objective is to calculate the required thickness (Bayomy and Abo-Hashema 2000 ; Abo-Hashema 2013). Anyala, Odoki and Baker (2014) stated that mechanistic-empirical models could be utilised at other locations if they have been appropriately calibrated. Unlike the mechanistic model, the mechanistic-empirical models are driven by regression models that shape the association between roughness, cracking and traffic loading, and other performance parameters such as PCI.

2.7.1.3. Empirical Models

Finally, empirical models are the most appropriate models in the pavement field. The dependent variable is associated with one or more explanatory variables (independent) such as pavement age, environmental loading and traffic loading. Jiménez and Mrawira (2012) stated that empirical modelling uses a regression technique to match observations of response to causal factors. Empirical models are being utilised through the statistical application. Nevertheless, they are only valid for a specific location and absolute time (Paterson 1987). Unlike mechanistic-empirical models, empirical models are sufficient to study the impact of climate change through the HDM-4 model. Further details are presented in Chapter 5 section 5.11 and Chapter 6 section 6.4.

2.7.1.4. Measuring Resilience Using a Deterministic Approach

To make the measurement of a resilient system more transparent and quantifiable, a comprehensive study should be conducted to allow application across a variety of scales (Hughes and Healy 2014). Moreover, defining the resilience evaluation process applied in practice is crucial. Hosseini, Barker and Ramirez-Marquez (2016) stated that the quantitative methods are always interested in engineering systems. An example of the application of the deterministic approach for measuring resilience was conducted by Bruneau et al. (2003) to identify four community resilience domains, which are organisational, technical, economic and social. They introduced resilience properties such as robustness, rapidity, resourcefulness and redundancy. The authors expressed four domains of resilience in the area of civil infrastructure: robustness, which presents the ability of the system; rapidity, which presents how fast the system can refunction after the disruptive event; resourcefulness, which is the ability to utilise resources such as materials; and redundancy, which means the extra capacity the system has to reduce the potential impact of the disruption. For example, as per Figure 2-8, a reading of 100% indicates no degradation in service where 0% means no service exists. In the case of an extreme natural event such as an earthquake, expectation of a drop in service will occur over a certain period; after that, restoration of the infrastructure will be achieved (indicated by the quality of 100%).

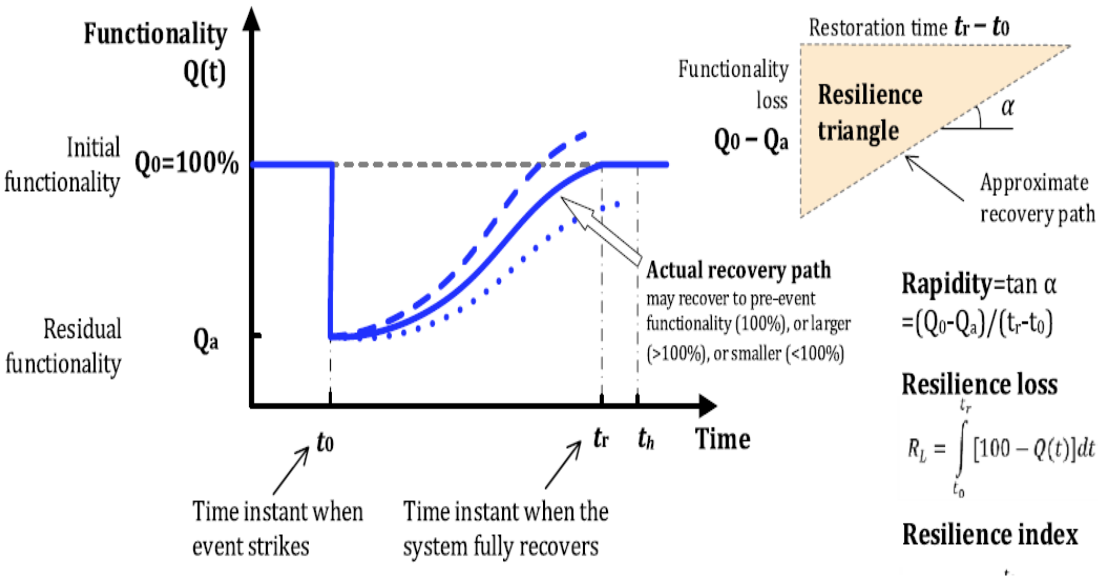

Figure 2-8: Resilience loss measurement from the resilience triangle (adapted from Bruneau et al. 2003)

In other words, resilience triangle-related measurements that were introduced by Bruneau et al. (2003) defined the theory based on the functionality recovery curve. The basic principle of the resilience triangle was a sudden and significant drop of functionality due to an extreme event at a specific period, then gradually functionality recovered, until the system reached its full functionality. Sun, Bocchini and Davison (2018) stated that measuring resilience using the resilience triangle approach may extensively represent the functionality loss. The methodological approach taken in this study is a quantitative methodology based on Bruneau et al.'s (2003) theory in order to measure pavement resilience loss. Bruneau et al. (2003) introduced an equation to measure the resilience loss which indicates that the larger values of resilience loss mean less resilient systems.

$$RL = \int_{t_0}^{t_1} [100 - Q(t)]dt$$

Equation 2-1: Bruneau et al. (2003)

- t0: The time at which the disruption occurs
- t1: The time at which the community returns to its normal pre-disruption state
- Q(t): The quality of the community infrastructure at time t

As a general concept, this method could be widely applied to infrastructure (system) performance. However, Hosseini, Barker and Ramirez-Marquez (2016) defined some limitations to Bruneau et al.'s (2003) approach. For example, it was assumed that the quality of the infrastructure (system) is 100% before the disruptive event (earthquake), which is not a usual scenario. Zobel (2011) stated that Bruneau et al.'s (2003) resilience measure might have various rates within each of the four domains previously explained, depending on the type and magnitude of a disruptive event. Zobel (2011) also depended on the four domains introduced by Bruneau et al. (2003) to develop his theory regarding measuring resilience. He focused on metrics to calculate the percentage of all the possible losses during the particular time interval.

2.7.2. Probabilistic Deterioration

Pavement scientists and practitioners have paid a great deal of attention to the use of stochastic models. Theoretically, pavement performance is considered to be a function of a set of random variables. In deterministic modelling, the values of random variables such as the traffic actions and environmental conditions do not vary with time. Hong and Wang (2003) commented that this assumption might not be sufficient because, in practice, the traffic and the environmental actions do vary randomly with time. Therefore, they concluded that deterioration of pavement performance could not be projected exactly because geometric variables, environmental impacts, traffic loading and the material properties are uncertain, and therefore the deterministic approach is not reliable or predictable. For this reason, Hong and Wang (2003) also emphasised the importance of using a probabilistic framework to build such a model.

Enright and Frangopol (2011) added that uncertainties are a big part of prediction deterioration due to complications related to isolating the individual random variable.

Haas (2001) stated that Markov chains are the most accurate techniques for prediction models since the future state of the model element is estimated solely for the current state of the component. The first Markov chain model was in American standards through the application called PONTIS. Moreover, it is common practice in the implementation of bridge management systems (FHWA 1993). Arimbi (2015) stated that Markov chains had been used extensively to build pavement performance through indication of the probable 'before' and 'after' condition of the pavement. Nevertheless, Madanat, Mishalani and Ibrahim (2002) stated that current approaches used to predict these transition probabilities from survey data (asset condition) are mostly ad hoc processes. On the other hand, NAMS (2009) added that the Markov chain is a sophisticated technique to be applied in asset management systems for different types of assets such as roads, bridges and service utilities.

Many studies such as Micevski, Kuczera and Coombes (2002) have stated that using a Markov chain performance model is crucial for generating sufficient and reliable performance models that can predict future conditions in a probabilistic shape. One example of applying the Markov chain was presented by Hassan, Lin and Thananjeyan (2017). They proposed forecasting the surface inspection rating for a specific road section based on five distresses. This study has also opted to use the Markov method. The process is explained in Chapter 7 section 7.3.

2.7.2.1. Markov Chain Process

The main application of the Markov chain is to predict the next condition state, taking into consideration that the current state or condition is known. Markov chain is a good example for such a model which is widely used in forecasting deterioration condition in many infrastructure assets such as pavements, bridges and buried infrastructure (Butt et al. 1994; Abaza, Ashur and Al-Khatib 2004; Park 2004). The Markov method requires transition probability matrices (TPMs) to express the transition from one pavement condition state to another. For the case of pavements, Lytton (1987) defined transition probability matrices (TPMs) as a collection of pavements of similar age or traffic level that shift from one state of distress to another within an identified period. To conduct the Markov chain, it is crucial to estimate the probability of shift from one condition state to another, which is usually done by expert judgement or based on the analysis of available previous information and data. The fundamental rule in Markov chains is that the probability of shifting from one state to another is independent of an item's earlier condition history (Black, Brint and Brailsford 2005; Austroads 2012). Amin (2015) stated that developing the transition probability matric (TPM) is the most challenging segment in building a stochastic model.

Parzen (1987) expressed a discrete-time Markov technique. In such a method the future process only depends on the present and not on the past. In discrete-time Markovian-based models, there are several versions of the model for pavement performance. Abaza (2016) stated that the most popular model could be built based on either homogeneous or heterogeneous type. For a homogeneous approach, the Markov chain is developed based on the assumption that steady transition probabilities occur over time, taking into consideration no change in traffic loading and progressive weakening of the pavement structure. On the other hand, the heterogeneous Markov chain can incorporate a different set of transition probabilities for each transition (i.e. time interval) within an analysis period comprised of transitions. Cheetham et al. (2007) commented on the Markov chain's limitation that such a process requires an enormous number of roughly consistent families related to pavement characteristics. In this study, a similar limitation occurred in developing a Markov chain model. More details are provided in Chapter 7 section 7.2. For this research, the selection of an homogeneous approach for Markov chain analysis is presented in Chapter 7 section 7.2.2

2.7.2.2. Markov Chain States

In a Markov chain model, defining the model condition states is crucial. Bryant (2014) stated that model states for any asset are typically assigned in separate numbers which are related to a particular condition. The model state is normally defined corresponding to these highlighted conditions of rating systems such as good, fail, poor, etc. An example of previous studies that determined different conditions was provided by Bryant (2014), as per Table 2-9.

Table 2-9: Previous studies that determined different conditions, introduced by Bryant (2014)

Number of states	Rating system	State description	References
10	*0,1,…,8,9*	*Failed, imminent failure… very good, excellent condition.*	*Madanat, Mishalani and Ibrahim (2002)*
7	*3,4,…,8,9*	*Poor, marginal… good, new*	*Scherer and Glagola (1994)*
6	*1,2,…,5,6*	*Critical, urgent… good, very good*	*Morcous (2006)*
4	*6,7,8,9*	*Satisfactory, good, very good, excellent condition*	*SOBANJO (2011)*
5	*1,2,3,4,5*	*Do nothing, preventative, corrective maintenance, minor, major rehabilitation*	*SOBANJO (2011)*

2.7.2.3. Transition Probability Matrix Using Data

There are two procedures frequently used to create the transition probability matrix from the pavement condition rating data. The first method is a regression-based optimisation (expected value), which requires only one set of data. Such a method estimates the transition probability matrix by solving the non-linear optimisation problem that minimises the sum of absolute differences between the regression curve that best fits the condition data and the conditions predicted using the Markov chain model. The second method is percentage prediction (frequency), which is a quite commonly used method. It involves at least two groups of inspection data without any maintenance and rehabilitation interventions.

Arce and Zhang (2019) defined two types of transition probability matrix which are generally used to model infrastructure deterioration. The defined transition probability matrix is either a progressive TPM or a sequential TPM. Both types receive no maintenance or rehabilitation treatment. In both procedures, the condition changes from a higher condition state to a lower condition state. For progressive TPMs, the condition of all transitions is restrained. In sequential TPMs, the control section of the model is changed by no more than one state in each cycle. Thus, the condition of the infrastructure assets is forced to transit through all the states before reaching the worse state. Such a transition is defined to move from one state to another only for a specific period (Arce and Zhang 2019). The sequential TPM is applied in this research. More details are provided in Chapter 7.

$$p = \begin{bmatrix} p_{11} & p_{12} & p_{13} & p_{14} \\ 0 & p_{22} & p_{23} & p_{24} \\ 0 & 0 & p_{33} & p_{34} \\ 0 & 0 & 0 & 1 \end{bmatrix}$$

Equation 2-2: Progressive TPM

$$p = \begin{bmatrix} p_{11} & 1 - p_{11} & 0 & 0 \\ 0 & p_{22} & 1 - p_{22} & 0 \\ 0 & 0 & p_{33} & 1 - p_{33} \\ 0 & 0 & 0 & 1 \end{bmatrix}$$

Equation 2-3: Sequential TPM

2.7.2.4. Measuring Resilience Using Probabilistic Approaches

Chang and Shinozuka (2004) provided an example of measuring resilience using a probabilistic approach. They used this technique for assessing resilience associated with an earthquake. Originally, their studies were based on Bruneau et al. (2003). They defined resilience associated with various infrastructure systems under seismic stress such as an earthquake. They also developed a notion of integrating all dimensions of community resilience using probabilistic frameworks. Two variable factors were applied in measuring the resilience: loss of performance and length of recovery (Hosseini, Barker and Ramirez-Marquez 2016; Tamvakis and Xenidis 2013). Hosseini, Barker and Ramirez-Marquez (2016) stated that Chang and Shinozuka's (2004) approach could be applied not only to quantify infrastructure resilience and communities' resilience following an earthquake but also to any other systems and disruptions. However, they highlighted some limitations when the two variables (loss of performance and recovery length) surpass their maximum satisfactory values.

Hosseini, Barker and Ramirez-Marquez (2016) also summarised a few examples where quantification of resilience was carried out based on probabilistic approaches. For instance, Franchin and Cavalieri (2015) tested the system resilience under the event of an earthquake, and their philosophy was based on the efficiency and accuracy of defining the position of an infrastructure network. Hosseini, Barker and Ramirez-Marquez (2016) concluded that their method could also be applicable for other infrastructures such as power plants and potable water networks. Mubaraki (2010) summarised the deterministic and probabilistic models, as detailed in Table 2-10. Moreover Summary of different pavement deterioration models are shown in Table 2-11.

Table 2-10: Models' comparison proposed by Mubaraki (2010)

Model	Advantage	Disadvantage
Regression	*1. Microcomputer software packages are now widely available for analysis which makes modelling easy and less time consuming. 2. These models can be easily installed in a PMS. 3. Models take less time and storage to run.*	*1. Needs large database for a better model. 2. Works only within the range of input data. 3. Faulty data sometimes get mixed up and induce poor prediction. 4. Needs data censorship. 5. Selection of proper form is difficult and time consuming.*
Mechanistic	*Prediction is based on cause-and effect relationship, hence gives the best result.*	*1. Needs maximum computer power, storage and time. 2. Uses large number of variables (e.g. material properties, environment conditions, geometric elements, loading characteristics, etc.). 3. Predicts only basic material responses.*
Mechanistic-empirical	*1. Primarily based on cause-and-effect relationship, hence its prediction is better. 2. Easy to work with the final empirical model. 3. Needs less computer power and time.*	*1. Depends on field data for the development of empirical model. 2. Does not lend itself to subjective inputs. 3. Works within a fixed domain of independent variable. 4. Generally works with large number of input variables (material properties, environment conditions, geometric elements, etc.) which are often not available in a PMS.*
Markov	*1. Provides a convenient way to incorporate data feedback. 2. Reflects performance trends regardless of non-linear trends.*	*1. No ready-made software is available. 2. Past performance has no influence 3. It does not provide guidance on physical factors which contribute to change. 4. Needs large computer storage and time.*

Table 2-11: Summary of different pavement deterioration models by the author

Author(s)	Model Name	Model Type	Independent Variables	Output (Dependent)
Kargah-Ostadi, Stoffels and Tabatabaee (2010)	Artificial Neural Networks (ANNs) for Roughness	Artificial Intelligence	Initial roughness, pavement age, traffic, climatic conditions, pavement structural properties, subgrade properties, drainage type and conditions, and maintenance and rehabilitation treatments	Predicted future roughness trends
Lorino et al. (2012)	Non-linear mixed-effects modelling	Deterministic	Ageing	Progression in cracking
Lethanh and (Adey 2013)	Exponential hidden Markov	Probabilistic	Ageing	Deterioration of road sections
Park et al. (2008)	Bayesian distress prediction utilising Markov chain Monte Carlo (MCMC) methods	Probabilistic	Ageing	Longitudinal cracking
Obaidat and Al- kheder (2006)	Multiple regression	Deterministic	ADT(traffic), distance from maintenance unit (R), section area and pavement age	Distresses quantities
Abaza (2016)	discrete-time Markov model	Probabilistic	Distress (cracking and deformation)	Predicting future pavement condition (deterioration rate)
Anyala, Odoki and Baker (2014)	Bayesian regression	Probabilistic	Climate, traffic, properties of materials and the design of pavements	Predict rutting in asphalt surfacing
Mubaraki (2016)	Linear regression	Deterministic	Three distresses (cracking, rutting, and ravelling)	International Roughness Index (IRI)
Bianchini and Bandini (2010)	Neuro-fuzzy	Artificial Intelligence	Indicators of the structural and functional serviceability of the pavement structure. For example, pavement conditions, traffic increment, and change in pavement serviceability	Performance of flexible (SPI, IRI) pavements

Amador-Jiménez and Mrawira (2012)	Rut depth progression model/Bayesian regression	Probabilistic	Traffic loading and pavement deflection under a moving standard dual wheel (single axle) for which pavement layer thickness and material properties were given	Rut depth
Amador-Jiménez and Mrawira (2009)	Markov chain deterioration	Probabilistic	Ageing	PCI
Abaza (2004)	Unique performance curve	Deterministic	Aging, traffic and potential pavement design	Present Serviceability Index (PSI)
Hong and Wang (2003)	Non-homogeneous Markov chain	Probabilistic	Ageing	Pavement performance degradation
Mandiartha et al. (2017)	Markov chain/The network-level effectiveness model	Probabilistic	International Roughness Index (IRI)	Predicted IRI

In terms of the deterministic approach, a strategy similar to that of Mubaraki (2016) was applied in this research to measure the pavement resilience. Mubaraki (2016) investigated the relationship between independent variables of three distresses (cracking, rutting and ravelling) and the dependent variable of the International Roughness Index (IRI) using linear regression. The proposed research is carried out to define the relationship between the independent variable of the International Roughness Index (IRI) and the dependent variable of the Pavement Condition Index (PCI). More details are shown in Chapter 6 section 6.5 and Chapter 10 section 10.2.

In terms of the stochastic approach, the discrete-time Markov model proposed by Abaza (2016) was applied with different proposed outcomes (International Roughness Index, IRI) to measure pavement resilience. The transitions probability matrix was determined from an empirical approach. More details are provided in Chapter 7 section 7.3 and Chapter 10 section 10.3

2.7.3. Simulation Models

The structural-based model is a mathematical approach to examine the impact of resilience. The simulation approach is a widely used method. Rashedi (2016) defined simulation as a useful tool that examines the action of real systems as well as the consequences of such action. Various techniques exist to simulate and model the behaviour of an actual system, such as system dynamics (SD), discrete-event simulation (DES) and agent-based simulation (ABS). Rashedi (2016) stated that the choice of one of these models relies on different justifications, for example, problem characteristics, decision-making level related to the model, either strategic or tactical, type and accuracy of information, phenomenon period (i.e., discrete or continuous) and the kind of system elements that need to be studied. Table 2-12 presents a general comparison of the different simulation methods.

Table 2-12: A general comparison of the different simulation methods by Rashedi (2016)

	System Dynamics (SD)	Discreet Event Simulation (DES)	Agent-Based Simulation (ABS)
Level of Detail	*Low*	*Medium/High*	*High*
Decision-Making	*Strategic*	*Tactical/Operational*	*Mostly Operational*
Main Components	*Stock variables, flows, feedback loops*	*Servers, Consumers, Inter-arrival Times*	*Individual agents, drivers, interactions*
Time Dependency	*Continuous*	*Discrete*	*Continuous*
Applications	*Policy Investigation, Strategy Evaluation, etc.*	*Production Analysis, Manufacturing Systems, etc.*	*Consumer Behaviour, Network Effects, etc.*
Analysis Point of View	*Policy Maker*	*Operator*	*User*
Example (Amusement Park)	*Strategies of number of rides, discounts, pricing and future improvements, etc.*	*Analysis of ride time, waiting time, service time, average number of users in queue, etc.*	*Analysis of user (agent) satisfaction, pattern of selection (rides, food), etc.*
Sample Software	*Vensim, Stella*	*Simul8, Arena*	*AnyLogic*

Banks et al. (2004) highlighted that the system dynamics model requires many fewer details in comparison with Discrete Event Simulation (DES) and Agent-Based Simulation (ABS). Therefore, the system dynamics model is sufficient for strategic modelling. Sterman (2000) emphasised the importance of system dynamics as the most reliable simulation technique in the field of policy optimisation. He also described the system as "*a method to enhance learning in complex systems. Just as an airline uses flight simulators to help pilots learn, system dynamics is, partly, a method for* *developing management flight simulators, often computer simulation models, to help us learn about dynamic complexity, understand the sources of policy resistance, and design more effective policies*". Shepherd (2014) described system dynamics as a very sophisticated tool distilled from system theory, information science, organisational theory, control theory, tactical decision-making, cybernetics and military games. Mallick et al. (2015) defined system dynamics as an "*approach that helps develop a strategic view of a 'system', which could be an industry, society or a nation, by modelling the different parts and simulating the dynamics of interaction among the different parts*". They also emphasised that system dynamics determines the changes over time. Finally, Sterman (2000) observed that system dynamics helps to change the policy and social aspects in a very efficient way. On the other hand, Sterman (2000) supported the application of system dynamics in the real world in a very holistic feedback view to avoid any problem or resistance that may be generated by other parties seeking to restore the upset balance.

2.7.3.1. Development of Simulation Models Using System Dynamics

Mallick et al. (2015) described the historical development of system dynamics. They stated that Forrester was the first to introduce system dynamics in the 1950–1960s. In 1971, he developed a sustainability model of world dynamics. Recently, Sterman (2011) provided a significant improvement to the system dynamics model (Rashedi 2016). The application of system dynamics was seen through modelling and simulation of an extensive variety of problems such as population growth and natural resources, social, industrial, business and sustainability (Shepherd 2014).

Rashedi (2016) stated that the application of system dynamics could be seen in many fields such as business and engineering (construction, projects and policies). The business management field was the first to practise system dynamics; however, over the past few decades, system dynamics has become a favourite tool in other areas such as healthcare, the automobile industry and urban studies (Sterman 2000). For example, Homer et al. (1993) introduced system dynamics in the field of engineering as he handled operations for huge and complex construction projects in great detail. Lee et al. (2006) applied system dynamics to establish a model for managing construction work through improving productivity. Alvanchi, Lee and AbouRizk (2011) built a model from system dynamics and discrete event simulation (DES) for the conceptual phase milestone.

Xu and Coors (2012) introduced a model in developing a residential urban plan by utilising system dynamics for GIS and 3D visualisation in sustainability assessment. In modelling, the principle of system dynamics is establishing connections between qualitative and quantitative models. Mallick et al. (2015) concluded that the primary objective of system dynamics is to achieve the ability to connect parameters and model the interdependencies of the various disciplines through loops with respect to the time. System dynamics consists of elements that shape and investigate a feedback model of strategic systems. To develop system dynamics into a sufficient model, it is crucial to introduce a stock and flow model with respect to the causal loop diagram (CLD). According to Rashedi (2016), the model consists of four primary elements named stocks (denote key system variables), flow variables that produce quantities gathered into inflows or out of outflows (the stocks), valves (flow generators) and clouds (entry or exit boundary points in the model. In practice, there are various types of computer software packages that can be applied for system dynamics modelling, Table 2-13 summarised some these model such as Vensim, Analogic, iThink and Stella.

Table 2-13: SD useful background information about software packages (Azar 2012)

Package	Information
Dynamo	"*It is the first SD simulation language originally developed by Jack Pugh at MIT; the language was made commercially available from Pugh-Roberts in the early 1960s. DYNAMO is originally designed for batch processing on mainframe computers. It was made available on minicomputers in the late 1970s and became available as 'micro-dynamo' on personal computers in the early 1980s. DYNAMO today runs on PC compatibles under Dos/Windows*."
iThink/STELLA	"*Originally developed in by isee systems (http://www.iseesystems.com) in 1985 by Barry Richmond. IThink and Stella software provided a graphically oriented front end for the development of SD models. They offer a practical way to dynamically visualise and communicate how complex systems and ideas work. Diagrams, charts and animation help visual learners discover relationships*
PowerSim-Studio	"*In the mid-1980s, the Norwegian government-sponsored research aimed at improving the quality of high school education using SD models. Powersim was later developed as a Windows-based environment for the development of SD models that also facilitates packaging as interactive games or learning*

Vensim	*"Originally developed in the mid-1980s for use in consulting projects. Ven- sim was made commercially available in 1992 by Ventana Systems, Inc. (Harvard, Massachusetts) (http://www.vensim.com). It is an integrated environment for the development and analysis of SD models. Vensim runs on Windows and Macintosh computers to simulate the dynamic behaviour of systems that are impossible to analyse without appropriate simulation software, because they are unpredictable due to many influences, feedback, etc. It helps with causality loops identification and finding leverage points. "*

The author has considered only Vensim as the software package to build the SD models. Vensim is a software package which is extensively applied to build and run system dynamics models (Khan, Luo and Ahmad 2009; Rashedi and Hegazy 2015). Wang and Yuan (2016) defined four categories of variables that prevail in Vensim software, which are followed by the author. These four categories are defined in the Table 2-14.

Table 2-14: The four categories of variables that prevail in Vensim software, by Wang and Yuan (2016)

Level variable	Presents the current state or condition of the system
Rate variable	Describes dynamic changes in the system over a definite time
Auxiliary variable	Is generated from other variables at a given period
Constant	Whose value does not change over time. In the software, the link between the types of variables is usually presented through arrows which indicate the relationship between variables in the form of information.

Causal loop diagrams (CLDs) are a crucial component in the system dynamics skeleton. According to Rashedi (2016), CLDs are responsible for defining theory and interactions among various variables as well as representing the cause-effect that makes variables dynamic. CLDs shape the critical feedbacks in strategic systems. A causal loop diagram is comprised of different elements or variables that are attached by links presenting the causal effects among them. Rashedi (2016) described that such links impact the relationship between variables by link polarities. CLDs present feedback loops which are either positive (self-reinforcing) or negative (self-correcting or balancing). In practice, if the element in the system which links to other components receives an effect of expansion or increase, it will proportionally lead to an increase in another, which will eventually lead to what is called exponential growth – this phenomenon is called reinforcing loops. With balancing loops, the relationships will be the reverse. It is opposing change, thus an increase in one entity is reflected in a decrease in another. A system can reach dynamic equilibrium when balancing and reinforcing loops occur (Sterman 2000; Shepherd 2014). In the simplified case of determining the impact of pavement condition over time using system dynamics, an assumption was made to define all pavement condition effects that are linked to dynamic time-dependent processes such as asset deterioration, maintenance and rehabilitation plan, rideability and driver safety. Rashedi and Hegazy (2015) emphasised the importance of system dynamics to establish a holistic view for strategic decision-making regarding pavement infrastructure rehabilitation through simulating the important dynamics among rehabilitation actions, cost accumulation and asset deterioration. Such an approach will give a better decision in the budgeting and planning process.

2.7.3.2. Using Simulation Models for Measuring Resilience

Albores and Shaw (2008) gave an example of simulation models used in quantifying system resilience. They introduced a discrete event simulation modelling to analyse the preparedness based on how a firefighting and rescue service reacts in case of an accident. Moreover, they determined different variables such as the scenario of multiple separate incidents occurring at various locations. The study mainly focused on the hazards that result from a terrorist attack. The authors presented two simulation models, one to deal with mass decontamination of a population focusing on resources such as vehicles, equipment and workforce, whilst the second deals with the allocation of resources focusing on level and response times.

In the context of the supply chain, Carvalho et al. (2012) introduced a study of simulation for a real case related to automotives in Portugal. Their simulation is to quantify the resilience of the supply chain. They mainly focused on improving supply chain resilience by devolving mitigation strategies. For the simulation model, two approaches (flexibility and redundancy) were applied and six scenarios were also designed to achieve system resilience. Redundancy was simulated by providing additional inventory (buffer stock) to successfully bear disruption if it occurs, while flexibility was simulated by limiting the extent of disruption to the transportation network.

Carvalho et al. (2012) also studied resilience for the supply chain. They concluded that the use of Integral Time Absolute Error (ITAE), which is mainly used in control engineering, is the most reliable technique for measuring resilience, especially on inventory levels and shipment rates. They used the application of a dynamic simulation supply chain resilience by taking into consideration three key resilience elements: readiness (preparedness), responsiveness and recovery. The simulation model mainly focused on achieving the minimum value of ITAE, which indicates the most appropriate response and recovery (Carvalho et al. 2012).

In conclusion, Bruneau et al.'s (2003) theory that established a relationship between resilience loss and the recovery time of the system was selected in this research to measure pavement resilience loss using a system dynamics method. More details are provided in Chapter 3 section 3.7 and Chapter 10 section 10.4.

2.8. Measuring Resilience through Pavement Performance

How to measure resilience is a challenging question (Schoon 2005). Previous sections (2.7.1.4, 2.7.2.2 and 2.7.3.2.) highlighted different approaches on how to quantitatively assess potential impacts on the infrastructure system. A resilient transportation infrastructure system indicates that such a system allows for a slight probability of failure, less recovery time, and limited impact propagations and redundant connectivity (Sun, Bocchini and Davison 2018). Transportation infrastructure resilience should also be evaluated in both socioeconomic and functional aspects. In this research, the focus is on the foundation of functionality measure. A resilience triangle-related measurement was introduced by Bruneau et al. (2003). Their theory is based on the functionality recovery curve. Sun, Bocchini and Davison (2018) stated that measuring resilience using the resilience triangle approach may extensively represent the functionality loss. More details were discussed in section 2.7.1.4. The resilience triangle theory is applied in this research to study the measured pavement infrastructure resilience loss through the concept of pavement performance.

The specific measures of resilience loss have been developed through the application of a pavement performance prediction model (Markov and system dynamics; more details are provided in chapters 7, 8 and 9). In theory, there are three essential types of pavement prediction models: deterministic, probabilistic and simulation (see sections 2.7.1 and 2.7.2). The three methods of deterministic, probabilistic and simulation approach have been selected in this research through the application of both Markov chain and system dynamics technique. The primary objective is to define the future prediction of pavement performance using Markov chain and system dynamics for different types of pavement assets. Then, the deterioration curve will be obtained for each type of pavement asset. From the obtained deterioration curves, resilience loss will be measured, as shown in Figures 2-9 and 2-10. The area under the curve presents the performance. A high value (area under the curve) indicates that the asset has a high resilience value and a lower value will present low resilience (classified as less than desirable or poor performance). In other words, achieving less resilience loss will indicate that the performance quality of specific assets will function sufficiently depending on their age and received maintenance activities (type, frequency, etc.). However, more resilience loss can occur due to fast deterioration in pavement performance.

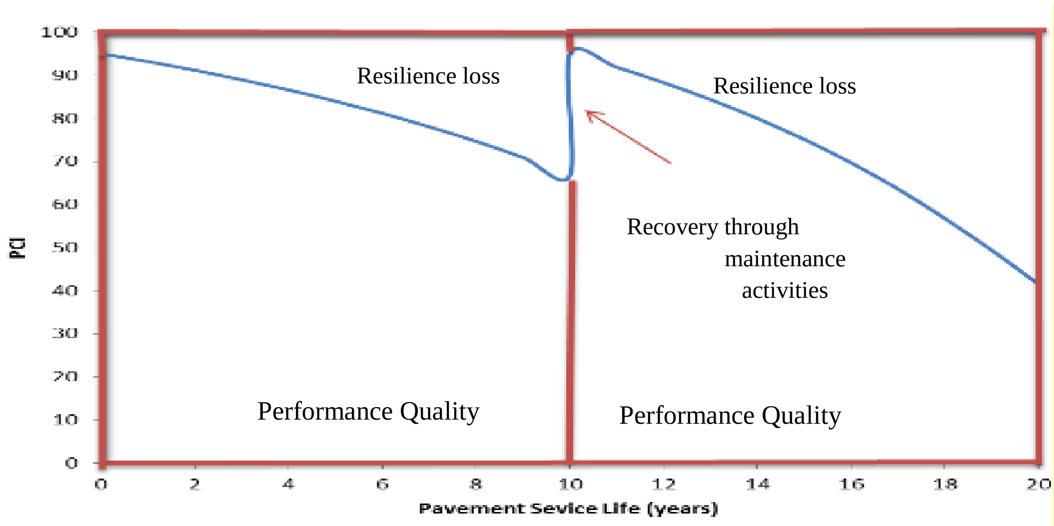

Figure 2-9: Performance with major maintenance and rehabilitation intervention (recovery)

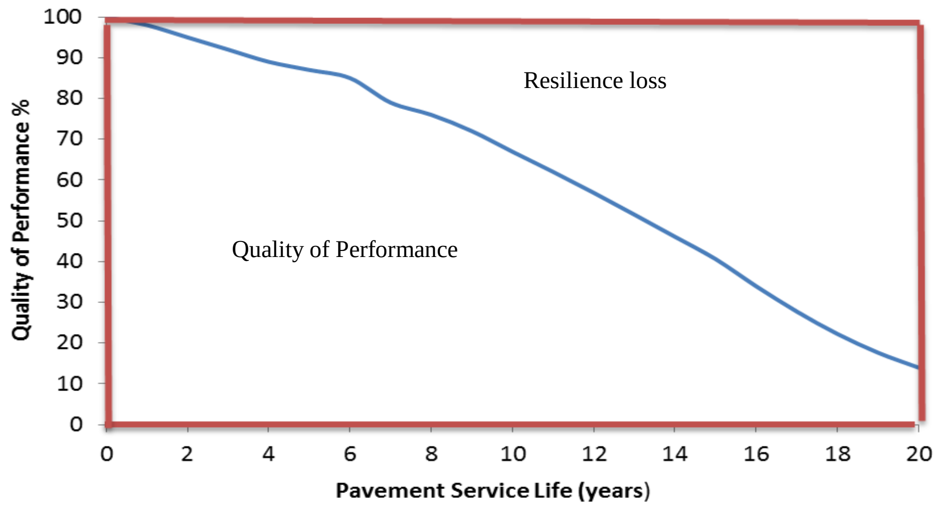

Figure 2-10: Performance without maintenance intervention (recovery)

2.9. Summary

In summary, this chapter has presented a thorough literature review about climate change, pavement performance, pavement structure and resilience. It has articulated how climate change impacts pavement structure. Projection of climate change for the UAE was addressed. Pavement failure risks were also reviewed and summarised. For the concept of resilience, definition, dimension and measurement were addressed. Finally, the measurement of resilience loss was highlighted.

3. Chapter 3 Theoretical Methods for Modelling Pavement Deterioration

3.1. Introduction

This chapter focuses on the climate change model, its impacts on road pavement structure and the measurement of impacts associated with future climate prediction. The chapter is also targeted at identifying the existing state of knowledge concerning pavement temperature and Thornthwaite Moisture Index in the United Arab Emirates (UAE). Defining pavement deterministic and probabilistic modelling with respect to Pavement Condition Index (PCI) and the total change in roughness is also studied in more detail. Figure 3-1 presents the roadmap for Chapter 3; it highlights the area of concern and how it is integrated with other chapters. Chapter 3 is a platform for building a theoretical background for the modelling of pavement deterioration models. Total change in roughness is built from different elements, which are rutting component, cracking component and environmental component. The HDM-4 model is used to build new determination modelling with respect to the impact of climate change. Other models such as Markov chain model, pavement temperature and Thornthwaite Moisture Index are also determined. Finally, risk analysis and measuring pavement resilience are addressed.

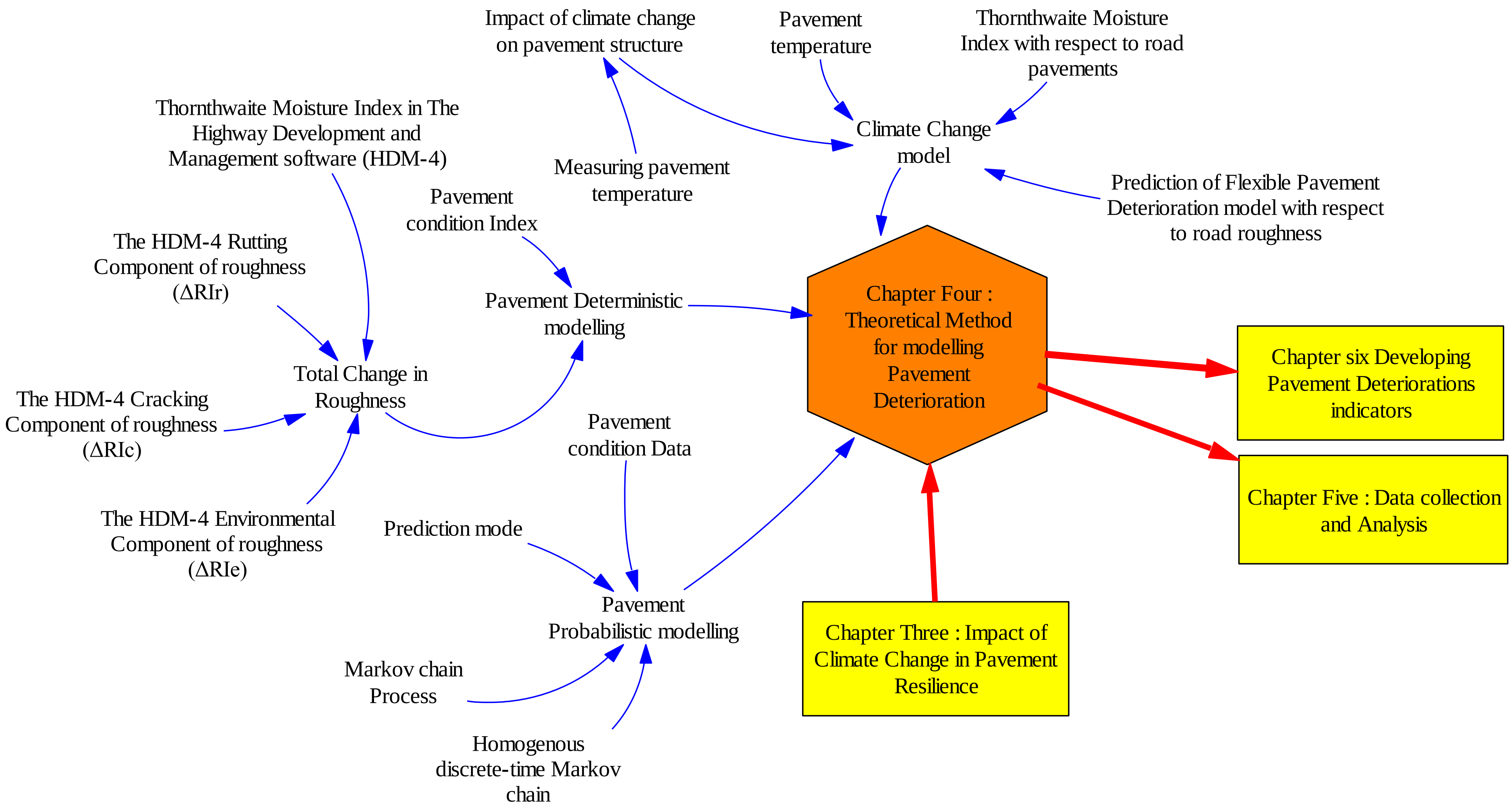

Figure 3-1: Chapter 3 roadmap

3.2. Climate Change Model

Climate change can be seen in the form of increasing temperatures, snow and ice, extreme weather, precipitation and sea levels. The selection of the change in temperature due to the impact of climate change is based on the author's interests, and other factors are not studied in the research. For the element of change in temperature, the following sections focus on the components used for determining the impact of the change in temperature with respect to pavement infrastructure.

3.2.1. Pavement Temperature Model

Temperature is a critical element in asphalt mixtures. It mainly affects the mechanical properties of asphalt mix materials. Temperature affects the strength or structural capacity of the asphaltic mix. Arangi and Jain (2015) emphasised the risk of heat. They stated that temperature could be a main cause of pavement distresses that lead to shortening the lifespan of a pavement. Matic et al. (2012) advised that pavement temperature be monitored accurately through the means of air temperatures, which will help the pavement engineer to calculate the resilient modulus and estimate pavement deflections.

Hot mix asphalt is classified as a viscoelastic material (viscous and elastic material), which means that pavement material will act as an elastic solid at low temperatures. Therefore, at low temperatures, permanent deformation is not likely to occur. However, at high temperatures, the pavement material will act as a viscous fluid. If the increase in temperature exceeds the design limit, strain will start to take place, leading to rutting (Asbahan and Vandenbossche 2011). Arangi and Jain (2015) also stated that, at a low temperature, the asphaltic mix could be hard, brittle and vulnerable, which eventually leads to cracking, and, at a high temperature, it becomes soft and susceptible to permanent deformation. Asbahan and Vandenbossche (2011) defined many factors that affect the temperature such as solar radiation, ambient temperature, wind speed and reflectance of the pavement.

Many scholars have broadly studied prediction of pavement temperature. Barber (1957) was the first scholar who investigated the changes in pavement temperature. Dempsey and Thompson (1970) introduced nomographs to measure the pavement temperature at both the surface and at a depth of 50 mm. Khraibani et al. (2010) developed a pavement temperature prediction model through computer simulation based on the theory of heat transfer. Arangi and Jain (2015) introduced a linear model for maximum pavement temperature which depended on asphalt binder type besides other factors. Al-Abdul Wahhab and Balghunaim (1994) conducted a study to quantify the pavement temperature in Saudi Arabia based on an annual measurement of pavement temperatures at various sections. Their findings showed that maximum pavement temperatures were recorded between 3°C and 72°C in an arid environment, while the temperature fluctuated between 4°C and 65°C in seaside zones. Moreover, Hassan et al. (2004) studied the pavement highest temperature at a depth of 20 mm below the ground surface for 445 days of collected data. The study took place in Oman, which is considered to have similar weather conditions to the UAE. Hassan et al. (2004) proposed a linear regression model by applying the highest air temperature as the independent variable and the highest 20 mm pavement temperature as a predictor, as per the equation 3-1 and Figure 3-2. (The equation achieved R^2 of 0.847.)

$$\boldsymbol{T_{20mm} = 3.160 + 1.139 \times T_{air}}$$

Equation 3-1: Pavement temperature model developed by Hassan et al. (2004)

- T20mm= Pavement temperature at 20 mm depth, ºC
- Tair = Maximum air temperature, ºC.

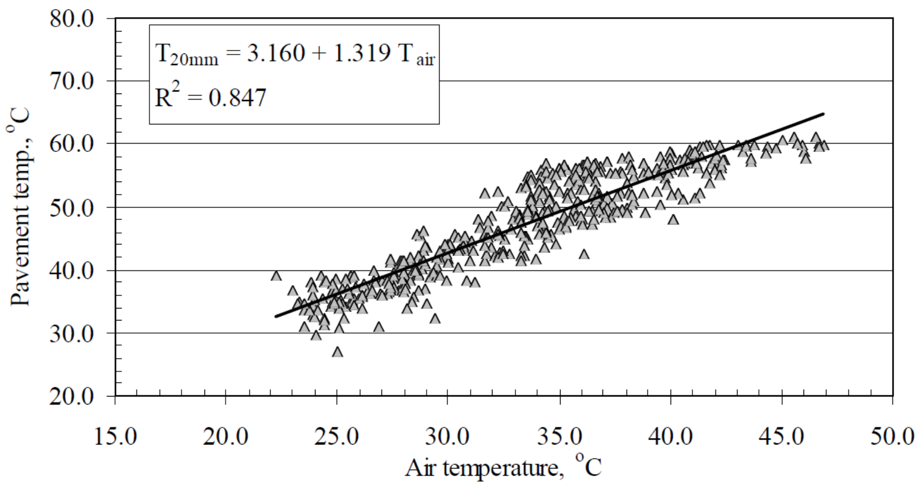

Figure 3-2: Pavement temperature measure developed by Hassan et al. (2004)

Hassan et al.'s (2004) experiment underwent similar weather conditions to UAE weather. Scoring a high value in the regression model provides more confidence in using such an equation. Hassan et al.'s (2004) model is used in this research to determine the maximum pavement temperature. Further explanation is provided in Chapter 5 section 5.11.

3.2.2. Thornthwaite Moisture Index model for pavements

Thornthwaite Moisture Index was first introduced in 1948 by C. W. Thornthwaite. The primary purpose of the system was to provide a new climate model for a specific community. Sun (2015) highlighted that the Thornthwaite Moisture Index (TMI) is widely applied to estimating the variation of climate. The climatic parameter (TMI) is a dimensionless parameter that represents a climate condition for a specific location generated from a function of evaporation and rainfall. The TMI is a yearly index and its value will differ based on various equations, methods and study periods. It presents many climate types. Martin and Choummanivong (2010) stated that TMI "*describes the aridity or humidity of the soil and climate of a region and is calculated from the collective effects of precipitation, evapotranspiration, soil water storage, moisture deficit, and runoff* ". Taylor and Philp (2016) emphasised the importance of using the TMI. They added that it is broadly used in the area of highway engineering such as pavement deterioration model and maintenance and rehabilitation planning climate indicator. Sun (2015) added that the positive index of the TMI indicates a humid climate with soil that has a high moisture conten while the negative index indicates an arid climate with less moisture in the soil. TMI application is widely accepted in the engineering field because it is a simple method and more practical than others. Thornthwaite introduced the TMI equation in 1948. Sun (2015) stated that this equation has been recognised and widely accepted by many scholars and practitioners over the past several decades. However, there are limitations as the equation needs to be computed yearly with water-balance analysis and such a procedure requires enormous information and data recording. Moreover, some of these data have to be estimated because they do not exist, while others are difficult to obtain (Sun 2015). The following two equations were introduced by Mather (1974) and Witczak, Zapata and Houston (2006) respectively to overcome the shortage in Thornthwaite's original equation in 1948:

$$TMI = 100\left(\frac{P}{PET} - 1\right)$$

Equation 3-2: Thornthwaite Moisture Index equation developed by Mather (1974)

Where,

- P = Annual precipitation,
- PET = Adjusted potential evapotranspiration

$$TMI = 75\left(\frac{P}{PET} - 1\right) + 10$$

Equation 3-3: Thornthwaite Moisture Index equation developed by Witczak et al. (2006)

Where,

- P = Annual precipitation,
- PET = Adjusted potential evapotranspiration

Equations 3-2 and 3-3 are default equations proposed by Mather (1974) and Witczak, Zapata and Houston (2006). To build a new TMI value that matches UAE conditions, an assessment of UAE weather data is needed. The highlighted equations (3-2 and 3-3) are used to define the most reliable model for TMI that matches UAE weather. Further explanation is provided in Chapter 5 section 5.11.3.

3.3. Highway Development and Management Model (HDM-4)

Various models are used for road maintenance optimisation. The highway development and management model (HDM-4) is one of the most accepted models across the world (Bannour et al. 2017). Morosiuk, Kerali and Greg (2000) stated that road investment appraisal techniques and maintenance optimisation have been continually updated for the last 30 years. The use of such a model has benefited many countries. For example, the HDM-4, which was published in 2000, has been used in 98 different countries for different projects (Morosiuk, Kerali and Greg 2000). HDM-4 is also an accepted universal tool for improving road investment appraisal techniques. Its primary function is to optimise pavement performance wok. Moreover, the HDM-4 can handle other elements. For example, the application of environmental impact in conjunction with greenhouse gas emissions can be investigated through HDM-4 (ISOHDM 2002). The HDM-4 performance prediction models are considered to be empirical regression models. In terms of road deterioration models, the HDM-4 can handle the complex interaction between the different variables such as the environment, vehicles and the pavement structure (Bannour et al. 2017). However, such a model must go through a configuration and calibration process before being applied to the level of a local context. The consequences of no calibration can be seen in the generation of significant deviations in the results that do not match the reality of the local context (Bannour et al. 2017). More details on how HDM-4 is related to the selected pavement distress (rutting and cracking) are presented later in this chapter (section 3.4.3) and in Chapter 6 section 6.2.

3.3.1. Calibration of Highway Development and Management Software (HDM-4)

It is crucial for local highway agencies using HDM-4 for the first time to calibrate and configure the model. For example, in terms of a pavement deterioration model, the calibration approach should facilitate more reliable and rational tools for the road assets network (Bannour et al. 2017). Bannour et al. (2017) stated that the consequences of using default equations in HDM-4 without configuration and calibration could generate inaccurate and inadequate pavement performance prediction. Therefore, calibration is essential to fine-tune the variable coefficients to forecast more acceptable outputs. According to Thube (2013), the calibration process involves introducing the adjustment factors, which are linear multipliers for modifying the predictions to meet the conditions of the selected area. Such factors work on achieving the best agreements between the field data and the model's prediction. In this study, the calibration factors for pavement deterioration models under the impact of climate change are determined with the conjunction of the default equation HDM-4 model for total change in roughness due to cracking and environment. Further explanation is provided in Chapter 5 section 5.11 and Chapter 6 section 6.2

3.3.2. Thornthwaite Moisture Index in the HDM-4 Model

Some of the default HDM-4 model sections depend on the application of TMI as the primary climatic factor embodied in the model. Taylor and Philp (2016) stated that the main function of the HDM-4 model is to supply pavement engineers with a detailed plan on pavement performance predictions over time. It also gives a forecast on changes in the pavement condition regarding roughness, structure, cracking and rutting. They also emphasised the importance of HDM-4 for estimating total life-cycle costs for roads (user and agency costs) as well as routine maintenance costs.

HDM-4 road deterioration models are widely utilised worldwide. Alaswadko (2016) stated that researchers in Australia and New Zealand have applied road deterioration modelling in conjunction with HDM-4 for different cases such as spray-sealed pavements. Australian and New Zealand researchers modified the deterioration model using local observational data. It has been documented that climate impact makes a significant contribution to the deterioration rate (Alaswadko 2016). In the HDM-4 model, the environmental component consists of five moisture classifications in terms of TMI, as per Table 3-1.

Table 3-1: Moisture classification developed by HDM-4 (Morosiuk, Riley and Odoki 2004)

Moisture Classification	Description	Thornthwaite Moisture Index	Annual Precipitation
Arid	Very low rainfall, high evaporation	-100 to –61	< 300
Semi-arid	Low rainfall	-60 to –21	300 to 800
Sub-humid	Moderate rainfall, or strongly seasonal rainfall	-20 to +19	800 to 1600
Humid	Moderate warm seasonal rainfall	+20 to +100	1500 to 3000
Per-humid	High rainfall, or very many wet-surface days	> 100	> 2400

Moreover, the TMI was also used as the climatic conditions parameter for the pavement deterioration model introduced by the Australian Road Research Board (ARRB) Group. For example, it was applied to investigate the cost associated with heavy vehicle road wear for various road types among other parameters such as road condition traffic, road type and road location (urban or rural) (National Transport Commission Australia 2011). Taylor and Philp (2016) stated that the TMI has been used in pavement maintenance and rehabilitation strategies. Alaswadko (2016) stated that environmental factors such as temperature and precipitation, humidity or moisture affect road roughness. In terms of the TMI, Martin and Choummanivong (2010) carried out a project to build a model to evaluate the strength of pavement or subgrade using a modified structural number (SNC). They concluded that there is a relationship between the strength of a pavement and its ageing, its design life and the TMI.

Moreover, Zareie, Amin and Amador-Jiménez (2016) studied the impact of the TMI on pavement structure using the International Roughness Index (IRI). In their research, they quantified the TMI value from 34 stations using different scenarios from 1961 through to 1990 (present scenario), 2011–2040 (future scenario), 2041–2070 (future scenario) and 2071–2100 (future scenario). They applied a downscaled average of monthly temperature and rainfall. The authors concluded that the IRI prediction of regional highways reported that the roughness progression would rise for higher TMI. Taylor and Philp (2015) examined the impact of climate change on the design of the asset in South Australia using the Austroads model (Byrne and Aguiar 2010). They predicted the value of IRI with different climate scenarios.

Moreover, the Austroads model can sufficiently calculate the roughness in terms of climate change. However, the model is limited to Australian networks, which are constructed to have a pavement section that consists of granular layers and is surfaced with sprayed (chip) seals (Byrne and Aguiar 2010; Oliver (1999). Generally, around 95% of Australia's rural arterial roads are sealed granular pavements (Oliver 1999), which is not the case for UAE roads, which are entirely built with a full asphaltic layer rather than a sprayed (chip) seals layer. In this research, pavement structure is considered to be full asphaltic. All the collected data for pavement thickness and layer types show that pavement cross sections are fully asphaltic (Valor 2013). Further explanation of pavement features in UAE is provided in Chapter 5. In this research, developing a Thornthwaite Moisture Index (TMI) adapted to UAE weather conditions is one of the primary objectives. More details are provided in Chapter 5 section 5.11.3. Moreover, comparisons between UAE TMI value and default TMI (as per the HDM-4 model) are also presented in Chapter 5 section 5.11.4. The TMI value is going to be used in the modified HDM-4 model; more details are provided in Chapter 6 section 6.4.

3.4. Modelling Pavement Indicators

3.4.1. Deriving the Relationship between PCI and IRI

The Pavement Condition Index (PCI) is organised to range from zero to 100, where 100 indicates that the pavement condition is excellent (new). Mubaraki (2016) stated that the PCI values are obtained based on many elements, which are the pavement distress type, severity of distress and assessment of collected distress through visual inspection. Mubaraki (2016) added that quantifying the procedure for the PCI, especially for pavement network level covering an area the size of a city, is tedious, inefficient, time-consuming and very expensive. Therefore, the pavement roughness measure can be used instead of the PCI measure. Pavement roughness is fundamentally linked to pavement serviceability, which quantifies physical features of pavement surface, and can be considered as a cheap solution for picturing the condition of pavement assets. Al-Suleiman and Shiyab (2003) stated that the

International Roughness Index (IRI) had gained increasing attention as an essential planning measure for pavement performance prediction in order to support maintenance and rehabilitation strategies. Dewan and Smith (2002) investigated the relationship of the pavement condition of asphalt pavement to its roughness. Their study measured the applicability of the IRI as a predictor variable of the PCI. Another model was introduced (Lin, Yau and Hsiao 2003) in San Francisco Bay, California, which confirmed the existence of strong relationships between both the variables (pavement distress and IRI) with adjusted R^2 of 0.52. Park, Thomas and Wayne (2007) investigated the relationship between the IRI and the PCI. They applied the power regression model formulated PCI in terms of IRI shown in Equation 3-4.

$$log\ PCI\ = 2 + \ K_2(log\frac{IRI}{0.727})$$

Equation 3-4: Developed by Park et al. (2007) for the relationship between the International Roughness Index (IRI) and the Pavement Condition Index (PCI)

The independent variable was International Roughness Index (IRI) and the dependent variable was Pavement Condition Index (PCI). The derived model was able to explained 59.0% of the variation in the existing data. The K coefficient, which is estimated to be -0.481

Park, Thomas and Wayne (2007) summarised the relationship between IRI and PCI as per Figure 3-3. In this research, investigation of the relationship between PCI on IRI is conducted based on their model. The process of data collection, derivation of equation and coefficients is discussed in Chapter 5

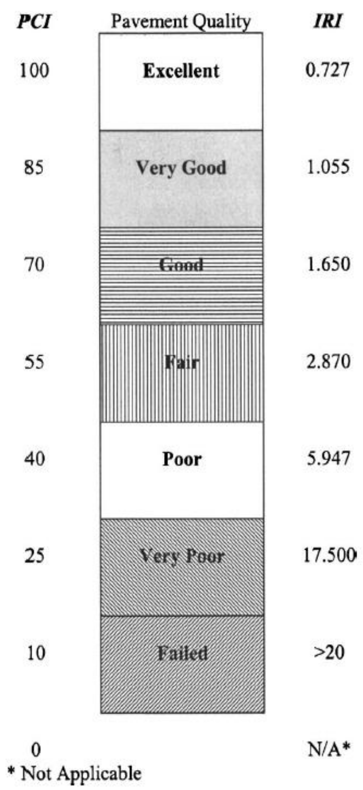

Figure 3-3: Park et al.'s (2007) summary of the relationship between IRI and PCI

3.4.2. Deriving the Relationship between Pavement Distress (Rutting and Cracking) and IRI

Some studies have stated that roughness can result from different individual pavement distresses such as potholes, cracking, patching, rutting and ravelling (Paterson 1987). However, not enough researchers have drawn conclusions about the development of models that define the roughness at a given point of time as a function of given distresses on the pavement. For example, the findings of Al-Omari and Darter's (1995) study on devolving rutting on the estimation of pavement roughness were not significant. Another research project was conducted by the NCHRP (2004) to develop a series of models that predict the pavement roughness from the distresses with respect to different parameters such as plasticity index of the subgrade material and annual precipitation. Another study was conducted by Karim and Lee (2001) to minimise the dependency on visual inspection for data collection. Their study investigated the relationship between pavement distress and IRI. Their findings showed that the use of IRI measurement helped to avoid the impact of poor and inconsistent results gathered by personal factors for pavement index value. They concluded that the correlation coefficient between the pavement distress and IRI was as high as 0.944.

Moreover, the application of various maintenance activities on pavement roughness was also studied by Hall, Correa and Simpson (2002). They examined the impact of using chip seal, slurry seal, overlays and crack seal, and suggested that only the overlay method has a significant effect on pavement roughness, whereas other maintenance activities were recorded as not significant. Li, Kazmierowski and Sharma (2001) examined the relationship between IRI, rutting and pavement cracking. The study covered more than 650 km of highway road. They proved statistically that there was a significant relationship between IRI and both cracking and rutting. Nevertheless, they concluded that such a relationship is not adequate to apply IRI as a surrogate measure for cracking and rutting. Moreover, Elghriany et al. (2016) found that a significant relationship exists between pavement roughness and traffic safety. They investigated the impact of IRI value on the rates of crashes. A recent study was conducted by Mubaraki (2016) who examined the relationship of IRI values to three types of distresses: rutting, ravelling and cracking. The results also matched Li, Kazmierowski and Sharma's (2001) findings. Mubaraki concluded that a significant relationship exists between IRI and the other three distresses. However, such a relationship is not strong enough for IRI to replace the measures of pavement condition (Mubaraki 2016).

One of the main objectives of this research is to investigate the relationship between pavement distress (rutting, cracking) and International Roughness Index (IRI). In conclusion, based on previous literature, the relationship between the multiple variables (rutting, cracking and IRI) needs to be studied with respect to climate change factor. Therefore, in this research, the climate factor component needs to be added into the model.

3.4.3. Total Change in Roughness Model

As was highlighted earlier, in Chapter 3, roughness has been defined as a distress measure present in components of deformation. Roughness is due to elements such as depth variation from rutting, surface defects from cracking, asphalt ageing and environmental impact, and traffic loading (Hunt and Bunker 2001). Thus, monitoring pavement roughness progression is crucial for ensuring that the road network is in a satisfactory condition (Alaswadko et al. 2017). To achieve a reliable model for pavement roughness, the empirical regression modelling technique is the most accepted method. It is considered to be a fairly simple method which can combine all the measurable variables of roughness prediction (Haas, Hudson and Zaniewski 1994; Mubaraki 2010). Toole (2009) highlighted various elements affecting pavement roughness and deterioration such as pavement ageing, traffic loading, environmental impact, type of subgrade soil, geometrical design of the road section, maintenance intervention programme, pavement type, and strength of asphaltic layer and subgrade soil. To develop models that assess the impact of climate change on road roughness, the HDM-4 model is used. Total Change in Roughness is a summation of the complete annual incremental change in roughness and initial roughness value as per the following equation, 3-5.

$$RI_{total} = RI_a + \Delta RI$$

Equation 3-5: Total roughness based on HDM-4

Where,

- RIa: Initial pavement roughness at start of analysis year
- ΔRI: Incremental change in roughness
- RI (total): Total Change in Roughness

Based on the HDM-4 model, the total annual incremental change in roughness is the sum of the various components, such as rutting, cracking, environmental and structural components. The total incremental change in roughness in HDM-4 is given by Equation 3-6 and defined in Table 3-2:

$$\Delta RI = \Delta RI_s + \Delta RI_c + \Delta RI_r + \Delta RI_e \ldots$$

Equation 3-6: The total incremental change in roughness in HDM-4 (Morosiuk, Riley and Odoki, 2004)

Table 3-2: The total annual incremental change based on HDM-4 by Morosiuk, Riley and Odoki (2004)

Main Equation	Variable	Description
The HDM-4 structural component of roughness	ΔRIs	• Incremental change in roughness due to structural deterioration during analysis year, in m/km IRI
The HDM-4 cracking component of roughness	ΔRIc	• Incremental change in roughness due to cracking during analysis year, in m/km IR
The HDM-4 rutting component of roughness	ΔRIr	• Incremental change in roughness due to rutting during analysis year, in m/km IRI
The HDM-4 environmental component of roughness	ΔRIe	• Incremental change in roughness due to the environment during analysis year, in m/km IRI

3.4.4. Modelling The HDM-4 Structural Component of Roughness (ΔRIs)

Structural deformation is the main phenomenon of pavement deterioration. Basically, structural deformation is the result of pavement materials receiving shear stresses by traffic loading. The impact of environmental factors is also a crucial element in structural deformation. Other features such as material strength are also considered. Both HDM-3 and HDM-4 considered the effect of the structural component of roughness as per the Table 3-3.

Table 3-3: Structural component of roughness (ΔRIs) based on HDM-4 by Morosiuk, Riley and Odoki (2004)

Main Equation 1	Variable	Description
$\mathbf{\Delta RIs = Kgs\ a0\ exp[Kgm\ (m)\ (AGE3)]\ (1 + SNc)^{-5} YE4)}$ The structural component of roughness in HDM-4 uses the adjusted structural number (SNP) as the pavement strength indicator, rather than the modified structural number (SNC) that was used in HDM-III. For this research, the selection of SNC = modified structural number for the pavement is made.		
The HDM-4 structural component of roughness	ΔRIs	Incremental change in roughness due to structural deterioration during analysis year, in m/km IRI
	SNc	Modified structural number for the pavement at start of analysis year

	AGE3	Age since last overlay or reconstruction, in years
	YE4	Annual number of equivalent standard axles, in millions/lane
	m	Environmental coefficient
	Kgm	Calibration factor for environmental coefficient =1
	Kgs	Calibration factor for the structural component of roughness=1
	a0	The coefficient values (a0 = 134)

3.4.5. Modelling The HDM-4 Rutting Component of Roughness

The incremental change in roughness due to rutting during analysis year is given by Equation 3-7.

$$\Delta RI_r = +Kg_r a_0 \, (\Delta RDS)$$

Equation 3-7: Incremental change in roughness due to rutting based on HDM-4

- ΔRIr = Incremental change in roughness due to rutting during analysis year, in m/km IRI
- ΔRDS = Incremental change in of rut depth during analysis year, in mm
- Kgr = Calibration factor for the rutting component of roughness

For this research, Equation 3-7 of the Highway Development and Management System (HDM-4) for change in rutting is adopted and tested, as discussed in Chapter 6.

3.4.6. Development Change in Rutting (ΔRDS) Model based on Climate Change

It is believed that the incremental change in rutting can be directly linked to many elements such as the impact of temperature on the pavement materials' properties. Anyala (2011) and MacDonald (2006) argued that the proposed equation (3-7), which was introduced by Morosiuk, Riley and Odoki (2004), does not fully cover the elements of asphalt material properties and pavement temperature. Morosiuk, Riley and Odoki (2004) justified the reason for not considering these elements as being due to difficulties in obtaining reliable values of pavement temperature and material properties. Anyala (2011) questioned the application of the Highway Development and Management System (HDM-4) for making decisions on road management policies. He claimed that the current prediction model for pavement deterioration in HDM-4 applied for rutting is limited to static climate (averages of past climate records). He emphasised the importance of establishing a new prediction model that is able to handle the prediction of impacts associated with future climate change. Therefore, the four essential elements in the HDM-4 rutting model named surface wear, structural deformation, initial densification and plastic deformation, which were introduced Morosiuk, Riley and Odoki (2004), are studied and investigated as per the following sections in order to establish a theoretical model which can be later investigated and tested. More details are provided in Chapter 6.

3.4.6.1. Initial Densification Factor

Adlinge and Gupta (2013) stated that risk on construction quality could be seen in achieving inadequate moisture conditions during construction, improper compaction, poor quality of materials and imprecise layer thickness. Quality should have existed in the development of infrastructures and measures concerning cost and time (Abas et al. 2015). In the field of pavement construction, Deacon, Monismith and Harvey (2001) defined quality as a critical element in measuring how well a pavement will perform under various traffic loads and environmental impacts. The important of construction quality was taken into account through the HDM-4 model. The component of initial densification is linked to the degree of compaction the pavement structure layers receive during the construction phase and traffic loading. The primary approach of the HDM-4 initial densification model is to ensure the elimination of the fast-initial increase in rutting once traffic is allowed onto newly constructed pavements. Martin (2011) stated that high traffic loading leads to high progression rates in rutting. For this research, an assumption was made that the roads should be designed and built according to standards and specifications with the accepted construction quality. Therefore, the parameter of quality of construction was not considered as a part of the rutting equations.

On the other hand, Mamlouk (1997) reported that vehicle speed affects pavement performance. He stated that displacement generated from speed is around 10 times greater with a speed of 20 km/hr in comparison with 130 km/hr. Loizos and Plati (2008) supported Mikhail and Mamlouk’s (1998) theory, as many studies have concluded that traffic load is a risk factor that plays a crucial role in pavement performance. Anyala (2011) considered initial densification component as an essential factor. He applied material properties such as Voids in Mix (VIM) and Softening Point (SP) of binder instead. In this study, the author agrees with Anyala's (2011) approach. The speed of heavy vehicles, VIM and SP of the binder are factors that are included in rutting equations. More details on the importance of VIM and SP of the binder are provided in sub-section 3.4.6.4: Plastic deformation factor.

3.4.6.2. Surface Wear Factor

Morosiuk, Riley and Odoki (2004) highlighted that the surface wear model was introduced for prediction rutting resulting from studded tyres wear. It predicts seasonal surface wear which occurs in areas where vehicles use snow chains. The UAE is located in a hot climate area; therefore, this factor is not considered in the proposed equation. Moreover, Anyala (2011) also did not consider such elements in his model. Therefore, for this research, the study focuses on the UAE, a country with hot climate conditions.

3.4.6.3. Structural Deformation Factor

Morosiuk, Riley and Odoki (2004) defined structural deformation based on the progression of rutting. It is believed that the rutting will progress linearly till cracking appears. Once cracking distress is taking place on the pavement surface, the rutting progression will increase faster. Anyala (2011) did not consider the cracking factor directly in the equation as he focused more on the main components that affect the strength and lead to cracking, such as pavement strength and traffic loading. The author of this research agrees with Anyala's (2011) approach and similar assumptions are included in the proposed model.

3.4.6.4. Plastic Deformation Factor

For the pavement structure, the surface deformation component is related to the asphalt surfacing layers while structural deformation impacts both the asphalt and foundation layers of the pavement. Morosiuk, Riley and Odoki (2004) highlighted the main component that affects rutting, which is plastic deformation. Generally, four elements present the conditions which lead to plastic deformation, which are summarised by TRL Road Note 31 (TRL 1993) as the following:

(1) High maximum temperature
(2) Stopping and slow-moving heavy traffic
(3) Channelised traffic
(4) Frequent heavy axle loads (heavy vehicles)

Nevertheless, Morosiuk, Riley and Odoki (2004) stated that the occurrence of any of the above does not result in plastic deformation if the asphaltic mix was designed to meet such impact. Anyala (2011) questioned the proposed model given by HDM-4 regarding surface deformation. He highlighted some limitations in the model such as the impacts of hot, dry summers are not considered. He also added other elements based on the TRL (1993) report, such as the gradient of the pavement section and properties of asphalt mix. In this research, the assumption was made that most of the roads in the UAE are flat; thus, the gradient element is not considered in the proposed equation of change in rutting. However, properties of asphalt mix such as asphalt binder viscosity are deemed important, and are discussed in detail in section 3.4.6.5.

3.4.6.5. Asphalt Material Properties

Morosiuk, Riley and Odoki (2004) stated that various elements affect the mixing properties of asphalt, which eventually affects the performance of asphaltic layers. NDLI (1995) highlighted the criteria used for evaluation of these elements, such as the ability to measure changes in performance, easily obtained without sophisticated tools or equipment, and availability in a typical application. The authors shed light on the most significant mix properties for the plastic deformation model, which are asphalt binder viscosity and voids in mix (VIM). Anyala (2011) agreed with their statement and applied such properties for an improved deterioration model. A similar approach is adopted in this research.

Asphalt Binder Viscosity

Basically, at high pavement temperatures, binder viscosity has a significant effect on the stability of an asphalt mix. For such cases, the application softening point (SP) is introduced to measure the viscosity. Morosiuk, Riley and Odoki (2004) defined the softening point (SP) as "*the temperature at which bitumen attains a certain level of consistency*". Mixing and placement, voids in mix and pavement temperature are the three main factors that increase the softening point. For example, Daines (1992) highlighted that a high asphalt mix with high voids content is most likely to have age hardening because the softening point is increased. Morosiuk, Riley and Odoki (2004) added that pavement temperature also affects the rate of age hardening. At high pavement temperatures, binder viscosity has a significant effect on the stability of an asphalt mix.

Prediction of Softening Point Value

Rohde (1995) investigated the relationship between pavement age and softening point. He highlighted that the prediction of softening point can be modelled as shown in Figure 3-4.

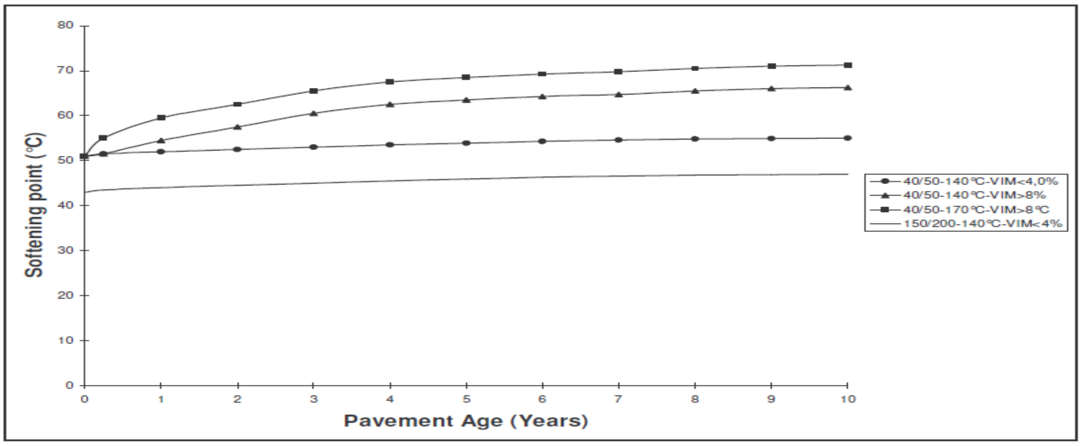

Figure 3-4: Expected increase in softening point over time by Rohde (1995)

According to Figure 4-4, the softening point rises at the start of the asphalt mix's life. Rohde (1995) stated that such an increase is due to the asphalt mix having high voids (VIM) content. However, as the pavement structure ages, then the voids in the mix (VIM) start to reduce. Mainly, such reduction is due to traffic load generated from heavy vehicles. Thus, the softening point will continue rising at a constant rate. Rohde (1995) named this phase the hardening stage as voids decrease in the asphalt mix. He concluded that voids designed in the mix range from 2.4% to 9%. Asphalt ageing is most likely to increase the softening point per year in the range from 0.1 °C to 2.9°C. And after 10 years it remains constant with no change. As per the conclusion delivered by Daines (1992), a high voids content is most likely to produce age hardening because the softening point is increased. Morosiuk, Riley and Odoki (2004) and Anyala (2011) agreed that pavement temperature affects the rate of age hardening. Anyala, Odoki and Baker (2014) considered softening point in their research model in conjunction with age (AGE) of the asphalt layer using the following equation, 3-8.

$$SP = a_0 \times \ln(AGE + 0.0001) + a_1$$

Equation 3-8:Softening point equation developed by Anyala, Odoki and Baker (2014)

The author follows their proposed equation. The reason behind this is that there are no recorded data that represent the softening point with respect to pavement age in either the Ministry of Public Works or Al Ain City Municipality (Valor 2013). Therefore, a similar coefficient will be used in this research, which is a0= 2.52 and a1= 70.5. In conclusion, softening point equation and coefficients used by Anyala, Odoki and Baker (2014) as per Equation 3-8 are adopted in this research to determine the change in rutting.

Voids in Mix (VIM)

There is no doubt that Percentage Voids in Mix (VIM) is crucial for asphalt mix property. VIM are related to the stability of the asphalt mix and contribute to the resistance to rutting. Generally, once a new road has been constructed, the level of VIM is considered to be in the high range while, with time, due to continuous traffic compaction, the level of VIM is known to be decreased (NDLI 1995; Nicholls et al. 2007). Rohde (1995) emphasised the importance of voids in the mix; their impact can be the reason for rutting occurrence, especially if they drop below 3%. Such a drop leads to unstable and plastic flow conditions. Axle loads and average speed of heavy vehicles are the leading causes for VIM drops. Basically, loads and duration of such loads will have an impact on the plastic deformation.

Rohde (1995) highlighted that the rate of decreasing the VIM variable for the first year is not the same for the rest of the mix's life. The reason for such behaviour occurs in the initial year when the mix receives loads from compaction effort applied during the construction period, then the VIM will receive much lower impact for the same conditions. Anyala, Odoki and Baker (2014) determined the VIM model in conjunction with age (AGE) of asphalt layer, as per Equation 4-9.

$$VIM = a_0 \times \ln(AGE + 0.0001) + a_1$$

Equation 3-9: VIM equation developed by Anyala, Odoki and Baker (2014)

The author follows this proposed equation. The reason behind this is that no recorded data represent the VIM concerning pavement age. Moreover, a similar coefficient will be used in this research, which is a0= -0.07 and a1= 1.39. In conclusion, the VIM equation and coefficients used by Anyala, Odoki and Baker (2014) as per Equation 3-9 are adopted in this research to determine the change in rutting.

3.4.6.6. Maximum Pavement Temperature

In the HDM-4 model, Harun and Morosiuk (1995) incorporated the element of pavement temperature, which indicates the pavement temperature (in °C) at a depth of 20 mm below the surface, during analysis year. Anyala, Odoki and Baker (2014) proposed a function of maximum pavement temperature (TPmax) in degrees Celsius (°C) at 20 mm (TPmax). Basically, Lavin (2003) stated that the surface pavement temperature is always higher than air temperature by an average of 7 degrees Celsius. For this research, the model developed by Hassan et al. (2004) is adopted. Such a model is discussed in section 3.2.1.Pavement temperature model. It was also decided to apply the maximum pavement temperature (TPmax) in degrees Celsius (°C) at 20 mm based on the highest air temperature that occurs in the UAE.

In conclusion, the development of change in rutting (ΔRDS) model based on climate change with respect to the previous literature, assumptions and discussion draws on the following equation (3-10) and details are highlighted in Table 3-4.

$$(\Delta RDS) = Krpd\ a0 \times YE4 \times (sh)^{a1} \times (HS)^{a2} \times \left(\frac{PTmax}{SP}\right)^{a3} \times (VIM)^{a4}$$

Equation 3-10: Development of change in rutting (ΔRDS) model

Table 3-4: Incremental change in rutting based on the HDM-4 model by Morosiuk, Riley and Odoki (2004)

Main Equation 4-10	Variable	Description
Incremental change in rut depth (ΔRDS) $(\Delta RDS) = Krpd\ a0 \times YE4 \times (sh)^{a1} \times (HS)^{a2} \times \left(\frac{PTmax}{SP}\right)^{a3} \times (VIM)^{a4}$		
The HDM-4 rutting component of roughness	**ΔRIr**	Incremental change in roughness due to rutting during analysis year, in m/km IRI
	Kgr	Calibration factor for the rutting component of roughness =1
	a0	the coefficient values = 0.088 for ΔRIr
	ΔRDS	Incremental change in standard deviation of rut depth during analysis year, in mm
	Krpd	Calibration factor for the change in rutting plastic deformation (ΔRDS) r =1
	YE4	Annual number of equivalent standard axles, in millions/lane
	HS	Thickness of asphalt layer on section i during year t, in mm
	PTmax	Maximum asphalt pavement temperature at 20mm below the surface in °C. TPmax is determined from mean daily maximum temperature during summer months
	SP	Softening point of binder for road section i with material type m during year t.
	VIM	Voids in Mix for road asphalt material type m on road section i during year t
	sh	Average speed of heavy vehicles on section i, in km/h during year t

For the change in rutting (ΔRDS) model, the coefficients are presented as per Table 3.5. The highlighted rutting coefficient for plastic deformation and the default HDM-4 rutting component of roughness (ΔRIr) are used to define the value of total change in roughness, as presented in Chapter 6 section 6.2.2. The comparison between default HDM-4 equations and new proposed modified HDM-4 equation is also discussed in Chapter 6 section 6.4.

Table 3-5: Rutting coefficient for plastic deformation based on HDM-4 model by Morosiuk, Riley and Odoki (2004)

a0	a1	a2	a3	a4
0.46	**-0.78**	**0.71**	**1.34**	**-1.26**

3.4.7. Modelling the HDM-4 Cracking Component of Roughness

The cracking component of roughness in HDM-4 is calculated based on the equation presented in Table 3-6.

Table 3-6: Cracking component of roughness (ΔRIc) based on the HDM-4 model by Morosiuk, Riley and Odoki (2004)

Main Equation 3	Variable	Description
ΔRIc = Kgr a0 ΔACRA .		
The HDM-4 Cracking component of roughness	ΔRIc	Incremental change in roughness due to cracking during analysis year, in m/km IRI
	Kgc	Calibration factor for the cracking component of roughness=1
	a0	The coefficient values =0.0066
	ΔACRA	Incremental change in area of total cracking during analysis year, in per cent

3.4.8. Modelling the HDM-4 Environmental Component of Roughness

The HDM-4 environmental component of roughness is calculated based on the following equation presented in Table 3-7.

Table 3-7: Environmental component of roughness (ΔRIe)

Main Equation 4	Variable	Description
ΔRIe = Kgm m RIa m = 0.197+ 0.000155 TMI		
ΔRIe	Incremental change in roughness due to the environment during analysis year, in m/km IRI	
Kgm	Calibration factor for the environmental component (default = 1.0)	
m	Environmental coefficient	
RIa	Roughness at the start of the analysis year, in m/km IRI	
TMI	Thornthwaite Moisture Index	

3.5. Pavement Deterioration Probabilistic Modelling

3.5.1. Modelling of Markov Chain

The prediction deterioration model is a mathematical approach that can be applied to forecast how the future pavement is going to deteriorate. A model entirely depends on the existing pavement condition, deterioration factors and previous maintenance (OCED1987). Arimbi (2015) classified the prediction deterioration model into two categories: the deterministic model (predicts as an exact value based on mathematical functions from observed deterioration) and probabilistic model (predicts the pavement condition as the probability of occurrence of a range of possible outcomes) (Ortiz-García, Costello and Snaith 2006). In theory, probabilistic models are applied for pavement evaluation at the network level, while the deterministic model is the only appropriate tool for project-level performance. Moreover, Haas, Hudson and Zaniewski (1994) stated that Markov chains are the most accurate techniques for prediction models since the future state of the model element is estimated solely for the current state of the component.

The Markov method requires transition probability matrices (TPMs) to express the transition from one pavement condition state to another. For the case of pavements, in order to conduct a Markov chain, it is crucial to estimate the probability of shifting from one condition state to another, which is usually done by expert judgement or based on the analysis of available previous information. The fundamental rule in Markov chains on the probability of shifting from one state to another is independent of an item’s prior condition history (Black, Brint and Brailsford 2005; Austroads 2012). Parzen (1987) expressed a discrete-time Markov technique that future process only depends on the present and not on the past.

Ha et al. (2017) stated that the Markov chain approach is a broadly accepted tool for deterioration modelling of infrastructure. Nevertheless, they added that such a tool has some limitations in the validity of its assumptions, according to Thomas and Sobanjo (2016). One of the critical limitations of the Markov chain approach depends on the probability of changing from one phase to another (independent of time). This theory is questionable because it indicates that changes in the future, such as environmental impact (weather condition), will not affect the transition probabilities (Lytton 1987).

3.5.1.1. Homogenous Discrete-time Markov Chain

State probabilities and state transition are the two major components in the discrete-time Markov model. State probabilities are estimated based on pavement condition states (e.g.: very good, good, poor… etc.) (Abaza 2016). The transition probability represents the probability of the pavement changing from one condition state to another during one specified period (Abaza 2016). The time interval is defined as a discrete period, which is in practice (for pavement assets) taken every one or two years, and each period represents one transition. In practice, quantifying state probabilities needs at least one cycle of pavement distress assessment, which is surveyed by the road and highway agencies. Typically, the pavement project is divided into small pavement sections to gather a better condition survey and reflect the certain present condition of the pavement. The numbers of pavement sections (Ni) assigned to various deployed condition states can then be used to estimate the state probabilities (Si), as defined in equations 3-11 and 3-12.

$$S_i = \frac{N_i}{N}$$

Equation 3-11: Equation for estimating the state probabilities by Abaza (2016)

$$N = \sum_{i=1}^{m} N_i$$

Equation 3-12: Equation for estimating total number of pavement sections used by Abaza (2016)

Where,

- S_i = is the ith state probability
- N_i = is the number of pavement sections assigned to the ith condition state
- N = is the total number of pavement sections used in the study (i.e. sample size)
- and m is the number of deployed pavement condition states.

In this research a homogenous Markov chain is adopted. It is assumed that the transition probabilities remain constant over time (steady-state condition). In order to forecast the state probabilities associated with the use of Equation 3-13, the model is built on the state and transition probabilities. Theoretically, the initial (i.e. present) state probabilities and transition probabilities are known. The initial state probabilities for new pavement can be assumed to take on the values of 1, 0, 0, . . . , 0.

$$
\begin{aligned}
&S^{(k)} = S^{(0)} P^{(k)} \\
&(k = 1,2,\ldots\ldots,n) \\
&S^{(k)} = (S_1^{(k)}, S_2^{(k)}, S_3^{(k)}, \ldots\ldots S_m^{(k)}), \\
&S^{(0)} = (S_1^{(0)}, S_2^{(0)}, S_3^{(0)}, \ldots\ldots S_m^{(0)}), \\
&\sum_{i=1}^{m} s_i^{(k)} = 1.0,
\end{aligned}
$$

Equation: 3-13: Equation for estimating state probabilities based on steady-state condition by Abaza (2016)

Where,

- $S^{(k)}$ = is the row vector representing state probabilities after k transitions
- $S^{(0)}$ = is the row vector representing initial state probabilities
- $P^{(k)}$ = is the transition matrix raised to the kth power
- m is the number of deployed pavement condition states
- n is the number of deployed discrete-time intervals (transitions)

The transition matrix is a square matrix (m × m) comprising all estimated transition probabilities. The matrix entries (Pi,i) represent the probability of pavements remaining in the same condition states after the elapse of one transition or the likelihood of the portion of the network in the state ‘i’ moving to state ‘j’ in one duty cycle. There are two scenarios for transitions. First is the deterioration transition probability (Pi,j; j > i), which indicates the probability that the pavement condition is transitioning to a worse condition state. This assumption is based on the fact that there is no maintenance and rehabilitation works. The other scenario is an improvement in the transition probabilities. The main diagonal ($P_{i,j}$; $j < i$) indicates the probability that the pavement condition is transitioning to a better condition state after one transition.

3.6. Risk Analysis for Pavement Failure

The part of the research related to pavement failure risk is planned and executed to accommodate a rich diversity of opinion for the impact of climate change on pavement structure. Such a view plans to be generated from specialists and related parties such as contractors, project owners, consultants and operators via a questionnaire. The primary objective of the questionnaire is to ascertain the risk associated with pavement failure due to the impact of climate change. The questionnaire is designed through a systematic process showing all the relevant risks that contribute to the failure of pavement as derived from the literature (see Chapter 2). The weights that the respondents give to the factors will be summarised in table form. There are different methods for risk analysis, deterministic (on numerical computations) and qualitative (based on the subjective system). For this research, the deterministic technique is adopted and discussed in the following section.

3.6.1. Deterministic Risk Analysis

The deterministic approach is the most relevant as it is embedded into the theme of risk management. The expected risk effect for pavement failure due to climate change is measured from a questionnaire survey which will be filled in by experts in the area of pavement engineering such as pavement material engineers, highway maintenance contractors, highway maintenance consultants, clients and asset managers. The results will be used to quantify the risk variables' relationship. Two methods can be used to define such relationships: multiple-regression analysis method (using three different scenarios named maximum risk factor, mean risk factor and minimum risk factor) and average probability method (using average results). Once the value of the expected risk effect for pavement failure due to climate change is determined using both methods, Equation 3-14 to 3-26 are used to achieve the final product value for the variable component with risk associated due to climate change.

3.6.1.1. Traffic Loading Modification to Risk

$$y_{R1.T} = Pv.F_T \times \prod_{i=1}^{i=n} R_{R.1T}$$

$$Pv.F_{R1.T} = y_{R1.T} + Pv.F_T$$

Equation 3-14: Equation for deterministic risk analysis for traffic loading

Where,

- $R_{R1.T}$ = Risk impact on a traffic loading
- $Pv.F_T$= Pavement failure due to traffic loading
- $Pv.F_{R1.T}$ =Pavement failure due to traffic loading and climate change impact risk

3.6.1.2. Environmental Loading Adjustment to Risk

$$y_{R2.CC} = Pv.F_{CC} \times \prod_{i=1}^{i=n} R_{R2.CC}$$

$$Pv.F_{R2.CC} = y_{R2.CC} + Pv.F_{CC}$$

Equation 3-15: Equation for deterministic risk analysis for environmental loading

Where,

- $R_{R2.CC}$ = Risk impact on an environmental loading
- $Pv.F_{CC}$= Pavement failure due to environmental loading
- $Pv.F_{R2.CC}$ =Pavement failure due to environmental loading and climate change impact risk

3.6.1.3. Pavement Composition Adjustment to Risk

$$y_{R3.PC} = Pv.F_{PC} \times \prod_{i=1}^{i=n} R_{R3.PC}$$

$$Pv.F_{R3.PC} = y_{R3.PC} + Pv.F_{PC}$$

Equation 3-16: Equation for deterministic risk analysis for pavement composition

Where,

- $R_{R3.PC}$ = Risk impact on pavement composition

- $Pv.F_{PC}$= Pavement failure due to pavement composition
- $Pv.F_{R3.PC}$ =Pavement failure due to pavement composition and climate change impact risk

3.6.1.4. Pavement Strength Adjustment to Risk

$$y_{R4.Ps} = Pv.F_{Ps} \times \prod_{i=1}^{i=n} R_{R4.Ps}$$

$$Pv.F_{R4.Ps} = y_{R4.Ps} + Pv.F_{Ps}$$

Equation 3-17: Equation for deterministic risk analysis for pavement strength

Where,

- $R_{R4.Ps}$ = Risk impact on pavement strength
- $Pv.F_{Ps}$= Pavement failure due to pavement strength
- $Pv.F_{R4.Ps}$ =Pavement failure due to pavement strength and climate change impact risk

3.6.1.5. Pavement Ageing Adjustment to Risk

$$y_{R5.PA} = Pv.F_{PA} \times \prod_{i=1}^{i=n} R_{R4.PA}$$

$$Pv.F_{R5.PA} = y_{R5.PA} + Pv.F_{PA}$$

Equation 3-18: Equation for deterministic risk analysis for pavement ageing

Where,

- $R_{R5.PA}$ = Risk impact on pavement ageing
- $Pv.F_{PA}$= Pavement failure due to pavement ageing
- $Pv.F_{R5.PA}$ =Pavement failure due to pavement ageing and climate change impact risk

3.6.1.6. Subgrade Soil Adjustment to Risk

$$y_{R6.ss} = Pv.F_{ss} \times \prod_{i=1}^{i=n} R_{R6.ss}$$

$$Pv.F_{R6.ss} = y_{R6.ss} + Pv.F_{ss}$$

Equation 3-19: Equation for deterministic risk analysis for subgrade soil

Where,

- $R_{R6.ss}$ = Risk impact on subgrade soil
- $Pv.F_{ss}$= Pavement failure due to subgrade soil
- $Pv.F_{R6.ss}$ =Pavement failure due to subgrade soil and climate change impact risk

3.6.1.7. Drainage Risk Adjustment to Risk

$$y_{R7.D} = Pv.F_D \times \prod_{i=1}^{i=n} R_{R7.D}$$

$$Pv.F_{R7.D} = y_{R7.D} + Pv.F_D$$

Equation 3-20: Equation for deterministic risk analysis for drainage

Where,

- $R_{R7.D}$ = Risk impact on drainage
- $Pv.F_D$= Pavement failure due to drainage
- $Pv.F_{R7.D}$ =Pavement failure due to drainage and climate change impact risk

3.6.1.8. Maintenance Adjustment to Risk

$$y_{R8.m} = Pv.F_m \times \prod_{i=1}^{i=n} R_{R8.m}$$

$$Pv.F_{R8.m} = y_{R8.m} + Pv.F_m$$

Equation 3-21: Equation for deterministic risk analysis for maintenance

Where,

- $R_{R8.m}$ = Risk impact on maintenance
- $Pv.F_m$= Pavement failure due to maintenance
- $Pv.F_{R8.m}$ =Pavement failure due to maintenance and climate change impact risk

3.6.1.9. Construction Quality Adjustment to Risk

$$y_{R9.cq} = Pv.F_{cq} \times \prod_{i=1}^{i=n} R_{R9.cq}$$

$$Pv.F_{R9.cq} = y_{R9.cq} + Pv.F_{cq}$$

Equation 3-22: Equation for deterministic risk analysis for construction quality

Where,

- $R_{R9.cq}$ = Risk impact on construction quality
- $Pv.F_{cq}$= Pavement failure due to construction quality
- $Pv.F_{R9.cq}$ =Pavement failure due to construction quality and climate change impact risk

3.6.1.10. Rutting Adjustment to Risk

$$y_{R.rut} = Pv.F_{rut} \times \prod_{i=1}^{i=n} R_{R.rut}$$

$$Pv.F_{R.rut} = y_{R.rut} + Pv.F_{rut}$$

Equation 3-23: Equation for deterministic risk analysis for rutting

Where,

- $R_{R.rut}$ = Risk impact on rutting
- $Pv.F_{rut}$= Pavement failure due to rutting
- $Pv.F_{R.rut}$ =Pavement failure due to rutting and climate change impact risk

3.6.1.11. Cracking Adjustment to Risk

$$y_{R.cra} = Pv.F_{cra} \times \prod_{i=1}^{i=n} R_{R.cra}$$

$$Pv.F_{R.cra} = y_{R.cra} + Pv.F_{cra}$$

Equation 3-24: Equation for deterministic risk analysis for cracking

Where,

- $R_{R.cra}$ = Risk impact on cracking
- $Pv.F_{cra}$= Pavement failure due to cracking
- $Pv.F_{R.cra}$ =Pavement failure due to cracking and climate change impact risk

3.6.1.12. Heavy Vehicle Speed Adjustment to Risk

$$y_{R.VS} = Pv.F_{VS} \times \prod_{i=1}^{i=n} R_{R.VS}$$

$$Pv.F_{R.VS} = y_{R.VS} + Pv.F_{VS}$$

Equation 3-25: Equation for deterministic risk analysis for heavy vehicle speed

Where,

- $R_{R.VS}$ = Risk impact on heavy vehicle speed
- $Pv.F_{VS}$= Pavement failure due to heavy vehicle speed
- $Pv.F_{R.VS}$ =Pavement failure due to heavy vehicle speed and climate change impact risk

3.6.1.13. Pavement Thickness Adjustment to Risk

$$y_{R.VT} = Pv.F_{VT} \times \prod_{i=1}^{i=n} R_{R.VT}$$

$$Pv.F_{R.VT} = y_{R.VT} + Pv.F_{VT}$$

Equation 3-26: Equation for deterministic risk analysis for pavement thickness risk category

Where,

- $R_{R.VT}$ = Risk impact on pavement thickness from the risk category
- $Pv.F_{VT}$= Pavement failure due to pavement thickness
- $Pv.F_{R.VT}$ =Pavement failure due to pavement thickness + the risk added due to climate change impact for the specific pavement thickness

3.6.2. Multiple-Regression Analysis

There is no doubt that the regression modelling technique is a very accepted method in the engineering discipline. The main principle of regression modelling is based on one variable, named the independent variable (x), to impose a change on another variable, named the dependent variable (y). Such a method is applied in this research to analyse the results generated from the survey questionnaires. The results shall be analysed using SPSS software by conducting an regression analysis

It was decided to follow a similar approach to that of Jang (2011) in this research to analyse the risk of climate change on the pavement failure. Therefore, a quadratic multiple regression models will be applied to quantify the risk and the functional relations for a dependent risk variable and its independent variables in pavement failure risk. The equation can be expressed as per 3-27:

$$\boldsymbol{Y}_{\mathbf{1}}=\boldsymbol{B_0}+\boldsymbol{B_1X_{i1}}+\boldsymbol{B_2X_{i2}}+\boldsymbol{B_3X_{i3}}+\boldsymbol{B_4X_{i4}}+\cdots+\boldsymbol{B_nX_{in}}+\in$$

Equation 3-27: Risk multiple-regression analysis equation

Where,

- $\boldsymbol{X_{i1} to X_{in}}$ = The value of the independent variable in risk category
- $\boldsymbol{B_0 to B_n}$ = Constant or regression coefficients

3.7. Measuring Resilience Loss for the Pavement Network

The resilience triangle theory is applied in this research to measure pavement infrastructure resilience loss through the concept of pavement performance (pavement network functionality). The specific measures of resilience loss will be achieved from the deterioration curve (survival curve). Such models are built using two different methods, which are Markov and system dynamics (more details are provided in Chapter 7 section 7.3 and Chapter 9 section 9.5) as per Equation 3-28. More details on resilience measurement are provided in Chapter 10 sections 10.3 and 10.4.

Equation 3-28: Measuring resilience loss based on different deterioration models

$$RL_{Markov.PCI} = Q(t)_{full} - \int_{t0}^{t1} Q(t)dt$$

$$RL_{SD.PCI} = Q(t)_{full} - \int_{t0}^{t1} Q(t)dt$$

Where,

- t0: The time at which the measuring of the performance of the pavement network starts
- t1: The time at which the measuring of the performance of the pavement network ends
- Q(t)full: System functionality, which is assumed to be 100% before the degradation in the system
- $RL_{SD.PCI}$: Resilience loss based on survival curve generated from system dynamics
- $RL_{Markov.PCI}$: Resilience loss based on survival curve generated from Markov chain
- $\int_{t0}^{t1} Q(t)dt$: Remaining pavement performance under the survival curve

3.8. Summary

In summary, this chapter has presented a theoretical method for different modelling pavement deterioration and climate change impacts.The HDM-4 model was used to build new deterioration modelling with respect to the impact of climate change. Other models such as Markov chain model, pavement temperature and Thornthwaite Moisture Index were also determined. Finally, risk analysis and measuring pavement resilience was highlighted

4. Chapter 4 Methodology

4.1. Introduction

This chapter is concerned with the methodology used for this study. The methodology of this research focused on presenting a roadmap for the study. The detailed framework including all tasks is described, including the development of data sets, developing a deterministic model for pavement deterioration, determining the deterioration model using the Markov chain method, determining the deterioration model using the system dynamics method, and the concept of measuring the pavement resilience and investigation of climate change.

4.2. Research Background

In the mid-1960s, the concept of a pavement management system was first introduced in order to systematise and manage all the pavement management activities for the purpose of achieving the best strategy for value for money (Karan, Haas and Walker 1981), especially with the increase in demand for highway rehabilitation and maintenance as well as the limitation of available resources and funds. Technically, there are three pavement condition indexes, which are commonly used for assessing the pavement condition. These are the Pavement Condition Index (PCI), which presents the distresses on pavement sections, the Present Serviceability Index (PSI), which presents the functional condition in terms of ride quality, and the International Roughness Index (IRI), which measures the roughness along the road profile (Sayers 1995; ASTM 2011). These performance indicators are essential for current maintenance optimisation that is built into the PMS. Arimbi (2015) stated that a shortage of data regarding the efficacy of maintenance treatments is one of the major problems in current maintenance optimisation modelling. Techniques to improve the capabilities of asset owners in optimally managing their investment decisions are of increasing interest to highway agencies (Weninger-Vycudil 2008). The Markov chain is an excellent example for such a model, which is widely used in forecasting deterioration in many infrastructure assets such as pavements, bridges and buried infrastructure (Butt et al. 1994; Abaza, Ashur and Al-Khatib 2004).

Future climate change and its impact on the road network performance is also another issue that is concerning road authorities. In many model forecasts, temperatures are likely to rise and fluctuation in precipitation intensity could occur. Such changes are expected to affect road performance negatively. To manage these changes, current pavement design practice as well as maintenance and rehabilitation plans may need to be amended to achieve better pavement performance and robust pavement resilience. There are vast numbers of resilience concepts in the context of different disciplines such as ecology, materials science, psychology, economics and engineering (Hosseini, Barker and Ramirez-Marquez 2016). According to Hosseini, Barker and Ramirez-Marquez (2016), resilience could be related to many concepts such as robustness, fault-tolerance, flexibility, survivability, and agility (Bruneau et al. 2003). The theory that establishes a relationship between resilience loss and the recovery time of the system was chosen in this research to define the pavement resilience loss. In this research, the application of system dynamics and Markov chain is selected to determine the pavement deterioration rate under climate change conditions with respect to different climate change scenarios. Shepherd (2014) described system dynamics as a very sophisticated tool distilled from system theory, information science, organisational theory, control theory, tactical decision-making, cybernetics and military games. Mallick et al. (2015) concluded that the primary objective of system dynamics is to achieve the ability to connect parameters and model the interdependencies of the various disciplines through loops with respect to the time. In terms of the stochastic approach, the discrete-time Markov model proposed by Abaza (2014) was applied with different proposed pavement indicators' outcomes (International Roughness Index (IRI)). A transitions probability matrix was also determined from the empirical approach. The methodological approach taken in this study is explained in the following sections.

4.3. Research Scope

This study aims to shine new light on these debates through an examination of the impact of climate change on pavement performance. Therefore, two methods are utilised in this research to determine the deterioration of pavement condition under climate change scenarios. System dynamics is the first methodological approach taken in this study. The primary objective of system dynamics (SD) is to study the dynamic interactions among the pavement performance indicators (Pavement Condition Index (PCI) and International Roughness Index (IRI)) concerning climate change to build a pavement deterioration prediction model. The second method uses the Markov chain to construct a probabilistic deterioration model using also pavement performance indicators (IRI and PCI), and more details are provided in chapters 6 to 9. Finally, measuring the pavement resilience is determined using both developed models (SD and Markov) (details are provided in Chapter 10). The proposed system dynamics model is also built to incorporate a risks network model of pavement failure under the impact of climate change. The estimated risk for interaction effects on pavement failure concerning climate change is achieved by conducting a survey questionnaire with experts. The research data in this thesis are drawn from three primary sources. Data are gathered from the roads department in the Ministry of Public Works of the United Arab Emirates, Al Ain City Municipality and the National Centre of Meteorology and Seismology. Historical data of both pavement distress (rutting, cracking, PCI, IRI) and weather data (air temperature, precipitation, etc.) are collected. These data are categorised, processed and analysed. Development of model coefficients, Transition Probability Matrix, Causal Loop Diagram (CLD), and Stock and Flow diagram is also carried out using several techniques. Finally, the SD model and the Markov model are used to model pavement deterioration under climate change scenarios. The results from these models are used to measure pavement resilience. The following conceptual framework in Figure 4-1 presents the thesis roadmaps.

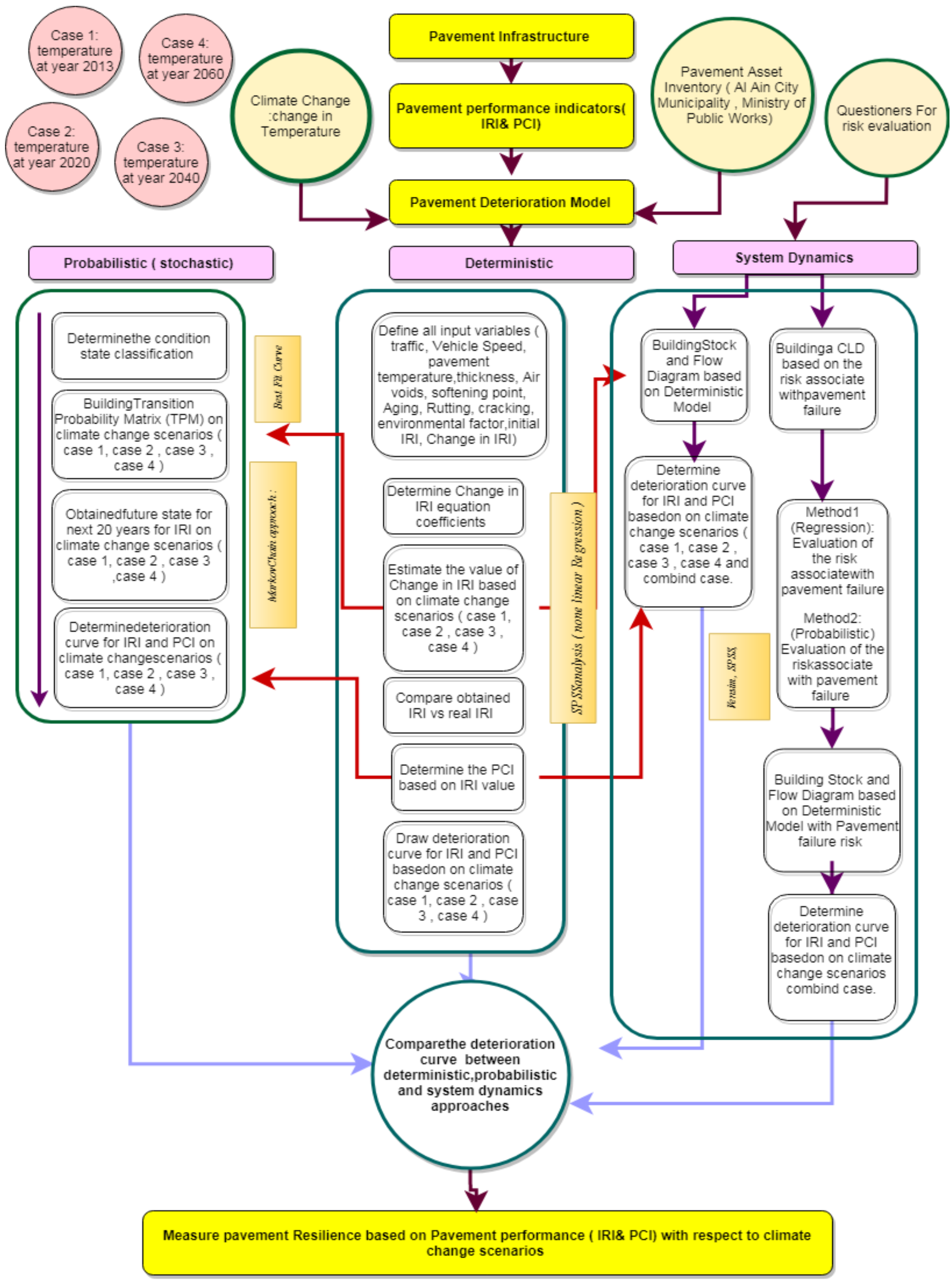

Figure 4-1: Conceptual framework presenting the thesis roadmaps

4.4. Delivery of Scope

In order to carry out the tasks highlighted in Figure 2-1, the following steps are followed:

- The study focuses on United Arab Emirates roads taking into consideration only federal roads and highways which are under the jurisdiction of the UAE Ministry of Public Works. Local authority roads are not included, except Al Ain City Municipality roads.
- The research investigates the main roads with a flexible pavement type. Other types such as composite or concrete are not part of the research scope.
- The assumption is made that, in general, there is one standard policy and specification for designing and constructing the roads and highways. And the built roads are delivered according to the UAE design standards.
- The assumption is made that maintenance activities are almost the same across all federal roads.
- The source of the pavement condition data (IRI, cracking, rutting), Annual Average Daily Traffic (AADT), pavement thickness, pavement age and heavy vehicle speed is the UAE Ministry of Public Works. Three sets of data for consecutive years are available. The data will be used to determine the modified HDM-4, Transition Probability Matrix and Pavement Condition Index. This process is similar to the studies conducted by Anyala (2011) and Abaza (2016).
- Weather data such as average, minimum and maximum mean monthly temperature and evaporation are collected from the National Centre of Meteorology and Seismology. This process is similar to the study conducted by Anyala (2011).
- Pavement Condition Index (PCI) data are collected from Al Ain City Municipality.

- The future rises in UAE temperature are estimated from the forecasting model developed by the Abu Dhabi environmental agency (Venturini et al. 2017), based on three different scenarios, 2020, 2040 and 2060.

- Maximum pavement temperature is developed based on three future climate change scenarios and calculated accordingly. This process is similar to the study conducted by Hassan et al. (2004).

- Determination of the change in roughness is structured based on the modified HDM-4 model. SPSS tools are applied to the model to define the relationship and variable coefficients between dependent and independent variables. A similar method was used by Mubaraki (2010) and Anyala (2011).

- The relationship between PCI and IRI is modelled using SPSS. A similar method was used by Park, Thomas and Lee (2007).

- The modified equations of change in roughness based on HDM-4 with new coefficients are applied to build a Transition Probability Matrix with different climate change scenarios (2013,2020, 2040 and 2060). The Transition Probability Matrix is delivered using @RISK software. The author modified the approach carried out by Abaza (2016).

- For building the Markov chain model, the pavement network in the UAE is assumed to be in excellent condition and classification of pavement condition is made according to IRI classification. A similar approach was defined by the UAE Ministry of Public Works. However, the author modified the classification of condition states based on the literature.

- Determination of Markovian deterioration curve based on IRI and PCI with different climate change scenarios (2013,2020, 2040 and 2060) is made. A similar method was used by Arimbi (2015).

- Building the system dynamics model through casual loop diagram and stock and flow using variables from the modified HDM-4 model (change in roughness). Modified equations and coefficients are applied to cement the relationship between dynamic variables in the Vensim software. This process is similar to the studies conducted by Mallick et al. (2015) and Rashedi (2016).

- Deterioration curve modelling is based on the proposed system dynamics model of PCI and IRI.
- Investigation of the risk associated with pavement failure under the impact of climate change is determined from the literature and examined by the survey. Results are analysed using regression method and probability method. This process is similar to the study conducted by Jang (2011).
- Risk is incorporated into the built system dynamics methods with different scenarios and the deterioration curve is modelled under different climate change scenarios. This process is similar to the study conducted by Jang (2011).
- Measuring resilience loss of the pavement network in the UAE under different climate change scenarios and different risks by using deterioration curves generated from both system dynamics model and Markov chain model. This process is similar to the studies conducted by Bruneau et al. (2003) and Sun, Bocchini and Davison (2018).

4.5. Dataset Development

The primary source of the data is the UAE Federal Road Network. Moreover, other road data relating to the research are gathered from Al Ain City Municipality. Concerning weather data, the National Centre of Meteorology and Seismology is the primary source for climate data. The data types are collected under the following groups: International Roughness Index, Pavement Condition Index, climate, traffic and asphalt material properties. The approaches used to obtain the data and their sample sizes are presented in Chapter 5 section 5.4 to 5.10.

Data are collected and organised by considering that all the roads have a starting point and a final point. Some roads are divided into three sub-roads based on direction. To achieve a better data analysis for the classification of roads, the author decided to split the roads into two groups for data collection: forward roads and backward roads. For this research, only data occurring in slow lanes (number 1 and number 2), which are the lanes with the excessive proportion of heavy goods vehicles, are considered as these sections are prone to fast deterioration activities. This is similar to the study conducted by Anyala (2011). In the current study, the author follows the approach of Anyala (2011) and Mubaraki (2010) to analyse the received data. For the maximum air temperature, this study follows the method proposed by the Environment Agency – Abu Dhabi (EAD). The findings of the model in conjunction with the IPCC for the UAE shape the future predictions of air temperature for the UAE based on three different scenarios (2020, 2040, 2060-2079). For pavement temperature, the author follows the model developed by Hassan et al. (2004). Moreover, the maximum air temperature recorded in Al Ain in June 2016 is used. Regarding the Thornthwaite Moisture Index, there are various methods to determine such value. For this research, the equations introduced by Mather (1974) are selected and tested. More details are presented in Chapter 5 section 5.11.

4.6. Questionnaire

A questionnaire is a set of questions used to obtain the specific information and data required for fulfilment of a study's research objective (Parasuraman et al. 1991). The survey comprises different phases such as designing the questionnaire, distributing it and, finally, collecting the completed survey forms for the desired research investigations. It is a fast process compared to other research methods. The researcher designed a questionnaire survey based on the probability rating, scaling the risk contribution from 0.1 to 0.72, and following Jang's (2011) approach (see Chapter 5 section 5.14). The questionnaire survey is proposed to be completed by experts in the area of pavement engineering such as pavement material engineers, highway maintenance contractors, highway maintenance consultants, clients and asset managers. The nominated experts are asked to fill in the questions in order to achieve a constant scale of magnitude to estimate the anticipated risk effect for each risk event.

A similar methodology is also used by Jang (2011). More details are presented in Chapter 5 section 5.14 and Chapter 9 section 9.4.

4.7. Deterministic Model Approach

George, Rajagopal and Lim (1989) defined the deterministic model as comprising structural performance, functional performance, damage models and initial response. Anyala, Odoki and Baker (2014) outlined deterministic models as "*predicting condition as precise values using mathematical functions*". Determining the pavement performance should be a function of a set of random variables that do not change over time. The deterministic approach is used in this research to model pavement performance indicators (IRI and PCI) under the HDM-4 model. The following tools are used to analyse the received data.

4.7.1. Numerical Analysis

To date various methods have been developed and introduced to model pavement performance indicators (IRI and PCI). The numerical analysis method is one of the more practical ways of examining a deterministic model. This approach has a number of attractive features such as descriptive statistics. Descriptive statistics are used to handle the process of data organising, summarising and presenting in order to achieve a very convenient and informative set of data (Keller 2009). In terms of data analysis, Mubaraki (2010) stated that estimating a parameter for the distribution, to characterise the spread or variability, is an essential task in exploratory data analysis. For example, the most accepted measure of the central tendency of data distribution is the mean. Other parameters use the median, which defines the midpoint of a distribution. Standard deviation is the best method to rate the variability of a distribution. Further characterisation of the data including skewness and kurtosis can also be introduced to define the lack of symmetry and whether the data are peaked or flat with respect to a normal distribution respectively. All these analyses and tests are used in this research. To ease the process of analysis, SPSS software is utilised.

4.7.2. Non-linear Regression Modelling

For a statistical model, three major elements structure the principle of modelling, and these are the response variable (y), the mathematical function (x) and random errors (e). Regression methods are a widely accepted method in modelling. Regression is very powerful in cases regarding the description of the association between a response variable and one or more explanatory variables. In this research, such analysis is used to define the relationship between different variables in the HDM-4 model. Also, the relationship between IRI and PCI is determined. Furthermore, a similar method is used to analyse the results generated from the survey questionnaire. The results can be reported based on statistically significant (p-values).

4.7.3. Estimating Total Change in Roughness in the Default HDM-4 Model

The determination of the roughness model structure based on default equation and coefficients for the default HDM-4 model is conducted. Collecting, sampling and analysing the data, which are presented in Chapter 5, are used in this model. Assumptions are made that all road sections are built according to the standard. The coefficients and equations of change in roughness based on structural, rutting, cracking and environmental components for HDM-4 are studied. Once the model is built based on the HDM-4 equation and variables, the inputs of different climate change scenarios are tested and the results for the years 2013 (current weather data), 2020, 2040 and 2060 (future climate change scenarios) are recorded.

4.7.4. Estimating Total Change in Roughness on the Modified HDM-4 Model

There are different methods to develop pavement performance models. One of the most accepted methods is 'Statistical Regression Analysis' (Amador-Jiménez and Mrawira 2012). To develop new model coefficients and equations, descriptive statistical analysis with the help of the SPSS software program is used. Data preparation and cleaning such as removing any invalid data or outliers is carried out to obtain the most solid sample. The descriptive statistical analysis in this section includes measurement aspects of non-linear and linear regression analysis. The primary objective is to investigate the most reliable coefficient based on the available data gathered from the Ministry of Public Works in the UAE. Goodness fit test (ANOVA test), correlations test and parameter estimates test for change in roughness based on structural, rutting, cracking and environmental components is conducted. Three different experiments are carried out to compare the original HDM-4 model, observed data and the modified HDM-4. Two deficiencies are reported, and improvement is applied accordingly. The calibration process involves introducing the adjustment factors, which are linear multipliers for adjusting the predictions to meet the conditions of the selected area and are adapted in this study by following Thube's (2013) approach. Once the model is built based on the new, modified HDM-4 (equations, coefficients and calibration), it will be tested with different inputs of climate change scenarios (pavement temperature). These scenarios are for the year 2013 (current weather data), 2020, 2040 and 2060 (projected weather data).

4.7.5. Pavement Condition Index (PCI) Model

The Pavement Condition Index (PCI) ranges from zero to 100, where 100 represents an excellent pavement condition. Mubaraki (2016) stated that the PCI values are obtained based on many elements, which are the pavement distress type, severity of distress and assessment of collected distress through visual inspection. To obtain PCI value, the International Roughness Index is used in many model forecasts. This study tests the relationship between the PCI and the IRI; the author follows Park, Thomas and Lee's (2007) approach using available data gathered from Al Ain City Municipality. The SPSS software program is utilised. The data preparation is carried out to clean the data and remove any invalid data or outliers. This descriptive statistical analysis includes two different measurement aspects: correlation and regression analysis. A correlation test is used to represent how and to what extent two variables are associated. Regression analysis is used to predict one variable from existing information on one or more variables and to find significant relationships (residual square), since linear and non-linear regressions are used to estimate the result of a dependent Pavement Condition Index. More details are presented in Chapter 6 section 6.5.

4.7.6. Model Checking and Validation

For model checking and validation, the application of an independent T-test is used. Generally, an independent T-test (‘analysis of variance’) is used to study the comparison of the means of different independent groups (either two or more) in order to find out statistically if they are significantly different or not. It is a parametric test. For the developing model, the analysis is carried out only on the backward direction roads data (see Chapter 5 section 5.2). Model checking and validation is conducted by testing the modified HDM-4 with the calibrated factor in the forward direction data instead of the backward direction. For example, the traffic loading data for a road in the forward direction differs from that for one in the backward direction. A test is conducted to verify the reliability of the model with different variable inputs. Therefore, a comparison between two means (2013 forward results and 2013 backward results) is conducted.

4.8. Markov Chain Process

To simulate the pavement deterioration process and evaluate variations, the Markov chain method is used. The Markov method requires transition probability matrices (TPMs) to express the transition from one pavement condition state to another. The relevant data sets are from a pavement network of multiple roads and highways under the management of the UAE Ministry of Public Works. The research methodology of the Markov chain consists of four parts. The first part is defining the number of condition states and categories. The second part presents the method to estimate the transition probability matrix in conjunction with the available data. The third part is to determine the current distribution of the pavement condition, and the final part is a simulation and an exploration of the long-run behaviour of the model.

4.8.1. Define Number of Condition States

Many researchers have stated that the most challenging aspect of using the Markov modelling method is the state size. This is because system states need to be comprehensively described. Moreover, simulation of a Markov chain model with numerous condition states shall lead to a very complex system which challenges the available computer resources. Therefore, it is crucial to introduce a sufficient number of states. As mentioned in Chapter 4, the ‘Condition Rating System’ is a technique of physical deterioration classification to assess the condition of pavement assets. Although condition states for the IRI defined by the UAE Ministry of Public Works are rated on a scale of four classifications, five condition states are applied in this research. More details are presented in Chapter 7 section 7.2.

4.8.2. Determine Pavement Deterioration Rate (Transition Probability Matrix)

A transition matrix estimates pavement deterioration rate, which is a change in the existing pavement condition state to the next poor condition state within a specific period, normally one year. The transition probability matrix can be derived from historical condition data. However, estimating transition probability from incomplete data is very difficult (Jin and Mukherjee 2014). Estimation of the transition probabilities can be achieved using two methods. The first method is based on data on pavement condition over several years. Once the available data are obtained, a way of estimating the corresponding deterioration rates can be quickly developed using any of the pavement performance indicators such as PCI or IRI. The second method is to use the subject matter of experts to estimate the transition probabilities. By reviewing the available data (see Chapter 5 section 5.4) from both Al Ain City Municipality and the Ministry of Public Works, it was found that the only data sets available were for three consecutive years (2013, 2014 and 2015). Both methods are tested in this research. More details are presented in Chapter 7 section 7.2.2.

4.8.3. Determine Current Pavement Condition

Distribution of actual pavement condition states for the entire pavement network gives the condition state vector. In this study, the assumption of the initial state vector is (1 0 0 0 0). The assumption is made that the pavement conditions of the study area are in excellent condition state. Once this initial condition state vector is determined, the transient probabilities for the pavement for every year can be calculated by multiplying this condition state vector with the deterioration matrix. More details are presented in Chapter 7 section 7.2.

4.8.4. Model Simulation

In exploring the behaviour of system prediction performance using the Markov chain, it is presumed that at time step zero all pavement conditions are new (excellent condition). Typically, four strategies are involved in this research. Hence, to explore the system's behaviour under different approaches, four strategies that are linked to different climate change scenarios are examined, as follows: Strategy 1, current weather condition (based on 2013 weather data). Strategy 2, all pavement sections are determined under 2020 predicted conditions. Strategy 3, all pavement sections are determined under 2040 predicted weather conditions. Strategy 4, all pavement sections are determined under 2060-2079 predicted weather conditions. For each case, the transition process is performed in Excel (Microsoft software) and outcomes will be plotted on different graphs (more details are provided in Chapter 7 section 7.3). The forecasted period is set for 30 cycles (usual pavement section design life). Each cycle presents a single year. The results of determining IRI for different climate scenarios are listed in Appendix 4.

4.8.5. Markov Model Assumptions

Lytton (1987) and Panthi (2009) described the assumption for the Markov model process which is also adopted by the author:

(1) The transition probabilities rely only on the present condition state.

(2) The probability of transition from one condition state to another is time independent. (The transition process is stationary.)

(3) Increase in condition rating due to maintenance intervention is not considered in this research as the pavement section is assumed to have deteriorated on its own. Also, condition ratings will be assumed to be constant or decrease with time.

(4) Deterioration process is occurring as a single state condition in one year. More than a single state is not allowed to deteriorate.

(5) Transition probability matrix is assumed to be homogenous, meaning that the transition probability for deterioration from one year to the next is always the same. Even though this assumption is generally not valid for pavement conditions, since changes can occur in the weather or the traffic load, the author decided to follow an homogenous Markov chain.

4.9. System Dynamics

One of the most reliable simulation methods used in the field of policy optimisation is system dynamics. Rashedi (2016) stated that the application of system dynamics could be seen in many areas such as business and engineering (construction, projects and policies). In the modelling process, the principle of system dynamics establishes connections between quantitative and qualitative models. A system dynamics model consists of elements that shape and investigate a feedback model of strategic systems. In general, Rashedi (2016) shed light on various essential features that are involved in applying system dynamics for strategic modelling. These elements are strategic variables, causal loop diagram, and stock and flow diagram, as shown in Figure 4-2 below.

Figure 4-2: System dynamics modelling procedure by Rashedi (2016)

A system dynamics model consists of elements that shape and investigate a feedback model of strategic systems. It is crucial to answer two questions in modelling system dynamics. The first question is how the quantities for the defined problem (variables) vary through time and the second question concerns defining the substantial feedback relationship between the variables. To answer these questions, a model which is a simplification of real-world phenomena is the best method to make the problem more understandable. Shire (2018) stated that system dynamics modellers are not following any guidelines, standards or specific modelling process. In this thesis, the SD modelling stages proposed by Sterman (2000) are followed, as shown in Figure 4-3.

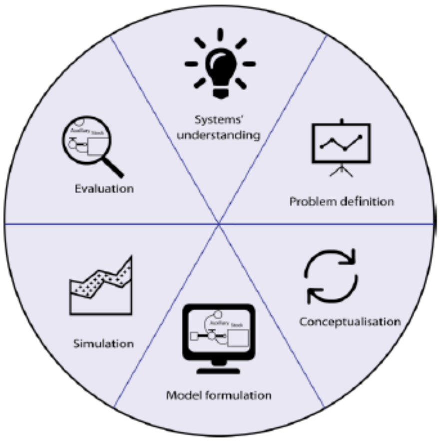

Figure 4-3: SD modelling process – adapted from Sterman (2000)

4.9.1. Stage 1 – Problem Definition

The first stage in the system dynamics model is to define the problem by focusing on drafting a research plan. The literature review presented in Chapter 2 section 2.7.3 is used to develop the system dynamics model in this research. The modified HDM-4 model, critical information from risks associated with climate change, and the factors related to pavement failures and deteriorations (see sections 2.4.1 and 8.2.2) are the main inputs for defining the system dynamics problem. The outcomes are a literature-based systems model that shapes key system concepts, variables and behaviour. Such variables contain quantities that vary over time.

4.9.2. Stage 2 – System Conceptualisation

This phase involves the system mapping process. Such a process presents important influences that interact within the proposed system. Shire (2018) added that group model-building, which defines how causal loop diagrams are prepared, is the primary function of the conceptual modelling stage. It also involves how the key variables are linked and how feedback structures are built. For this study, the conceptual model is derived from the modified HDM-4 model, which is discussed in Chapter 6. The proposed systems may be drafted on paper in several fashions to construct the causal loop diagram, then the models are represented in the form of computer code that can be fed into the proposed software package. The author has considered only Vensim as the software package to build the SD models.

4.9.3. Stage 3 – Data Collection

The data required is discussed in the section on data sets. For pavements, failure risks are recorded and measured based on each of the likelihood and impact ratings of each risk event as per the risk matrix. The questionnaire survey is completed by experts in the area of pavement engineering such as pavement material engineers, highway maintenance contractors, highway maintenance consultants, clients and asset managers. The final output is used as data sets for stage 4.

Probabilit	Threats				
0.9	0.05 ( )	0.09 ( )	0.18 ( )	0.36 ( )	0.72 ( )
0.7	0.04 ( )	0.07 ( )	0.14 ( )	0.28 ( )	0.56 ( )
0.5	0.03 ( )	0.05 ( )	0.1 ( )	0.2 ( )	0.4 ( )
0.3	0.02 ( )	0.03 ( )	0.06 ( )	0.12 ( )	0.24 ( )
0.1	0.01 ( )	0.01 ( )	0.02 ( )	0.04 ( )	0.08 ( )
	0.05/ very low	0.10/ low	0.2/low	0.04/High	0.80/Very High

Figure 4-4: Risk matrix with risk effect scale numbering developed by the author

The results will be used to quantify risk variable relationships. The SPSS software is applied to investigate the most reliable coefficient of variable risk based on the received questionnaire. In order to examine the model with different risk factors under the multiple-regression analysis method, it was decided to apply three separate experiments for the variable inputs, which are average scenario, minimum scenario and maximum scenario.

4.9.4. Stage 4 – Simulation Model Formulation

According to Shire (2018), the simulation model formulation stage is to integrate it with the conceptual models generated at stage 2. This stage is formalised with equations, initial conditions and rate of change. Basically, in this phase, simulation is conducted to determine how all the variables within the system behave over a period. In this study, variables are specified in Chapter 6 based on the modified HDM-4 model that presents a deterministic method for pavement deterioration with respect to climate change. Measuring the risks associated with climate change is also determined from the questionnaire. Risk magnitudes are measured using multiple-regression analysis and probability measures.

4.9.5. Stage 5 – Evaluation

Several analyses are carried out to validate the model which involve the determination of the pavement deterioration curve based on the change in IRI and PCI. Tests under extreme conditions are conducted. Comparison of the simulated behaviour of the model to the actual practice is presented (see Chapter 9 section 9.5). Finally, the model is used to test alternative policies, options and scenarios that might be implemented in the system under the proposed study.

4.10. Measuring Resilience through Pavement Performance

For this research, pavement performance is selected as a domain for measurement of pavement resilience. The specific measures of resilience are developed through the application of a pavement performance prediction model (SD and Markov). In theory, there are two essential types of pavement prediction models: deterministic and probabilistic. The selection of the probabilistic approach is used through the application of the Markov chain technique while the deterministic approach is applied through the application of system dynamics. In the end, the deterioration curve is obtained for different models.

A resilience triangle-related measurement introduced by Bruneau et al. (2003) is followed by the author. Their theory is based on the functionality recovery curve. Sun, Bocchini and Davison (2018) stated that measuring resilience using a resilience triangle approach may extensively represent the functionality loss. The resilience triangle theory is applied in this research to study the measured pavement infrastructure resilience loss through the concept of pavement performance. The area under the curve presents the performance. Software called CurveExpert Professional is applied to measure the area under the curve using the generated deterioration pavement curve from the Markova chain model and system dynamics.

4.11. Summary

This chapter has described the conceptual model development. It has clarified that this research proposes different methods and theories. The methodology comprises the three major components: deterministic, probabilistic and system dynamics. It has also provided thorough information about the study area, study data and study criteria for development of a pavement deterioration model and consequently the measurement of resilience loss. A number of analysis tools and software packages were also defined.

5. Chapter 5 Data Collection and Analysis

5.1. Introduction

This chapter explains the research data collection and analysis approach used to conduct the study. This study examines the types of data and source such as International Roughness Index (IRI), asphalt surfacing rutting and cracking, traffic data, heavy vehicle speed (sh), asphalt surfacing thickness (Hs), asphaltic ageing and UAE weather data. This chapter represents a description of how the research model inputs are designed such as development of predicted maximum air temperature (Tmax) in the UAE and maximum pavement temperature (TPmax), predicted Thornthwaite Moisture Index (TMI) in the UAE, binder softening point (SP) and voids in mix (VIM). This chapter concludes with a description of the statistical methods that are used in the analysis and the questionnaire results for pavement failure risks. Finally, a summary of the variables' inputs is provided.

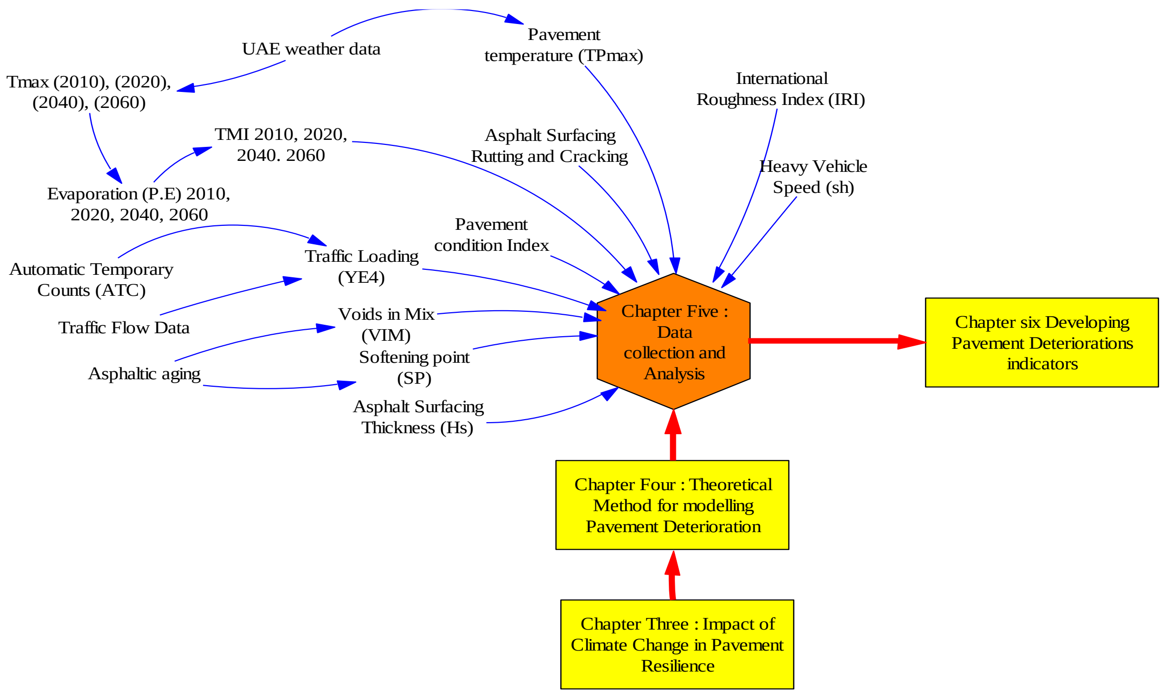

Figure 5-1: The chapter 5 roadmaps for outputs

5.2. The Study Area

The study was conducted in the United Arab Emirates. The primary source of the data is the federal road network in the UAE. The studied network contains the Northern Emirates roads under the control of the Ministry of Public Works. Moreover, other road data related to the research are gathered from Al Ain City Municipality. Concerning weather data, the National Centre of Meteorology and Seismology (NCMS) is the primary source for climate data in the UAE. NCMS can collect climatic data and assess different forms of climate data from many automatic stations across the UAE.

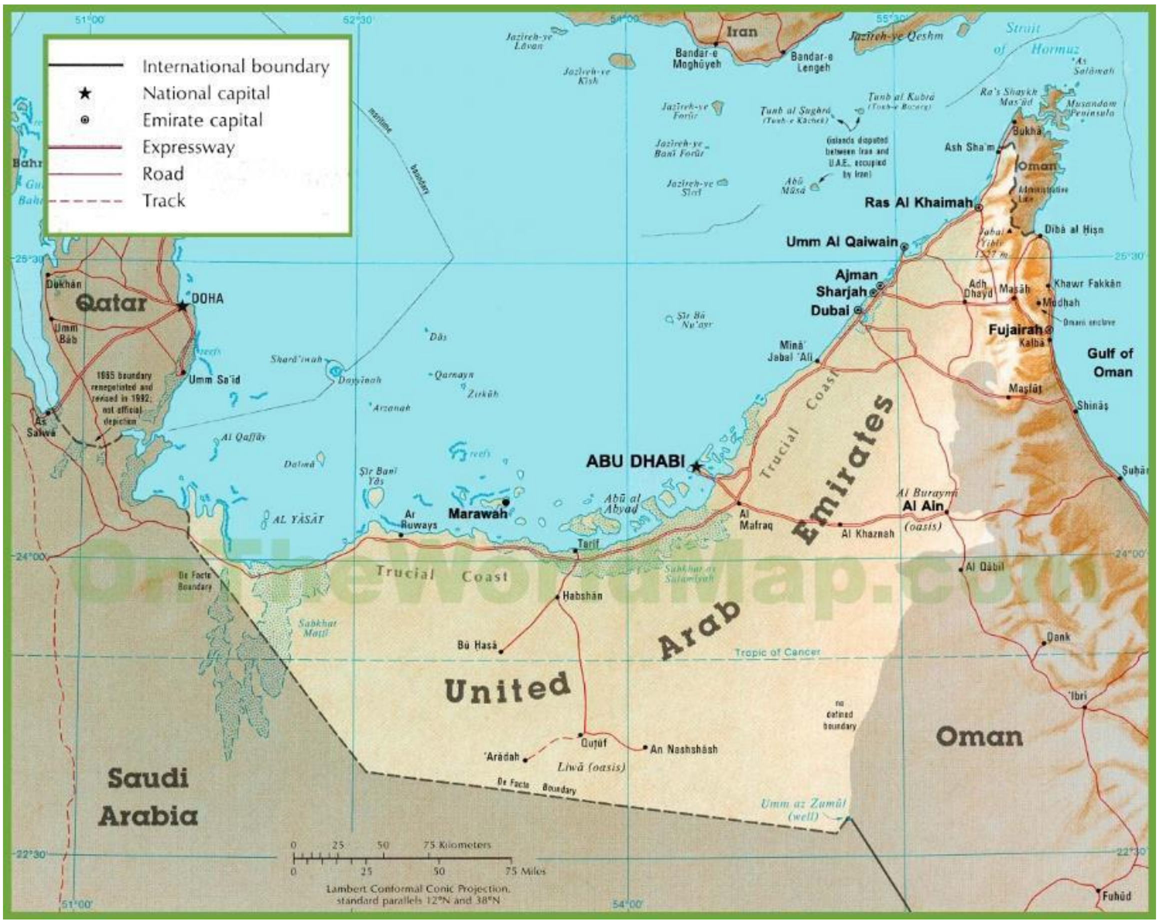

Figure 5-2: Study area map: UAE, from Valor (2013)

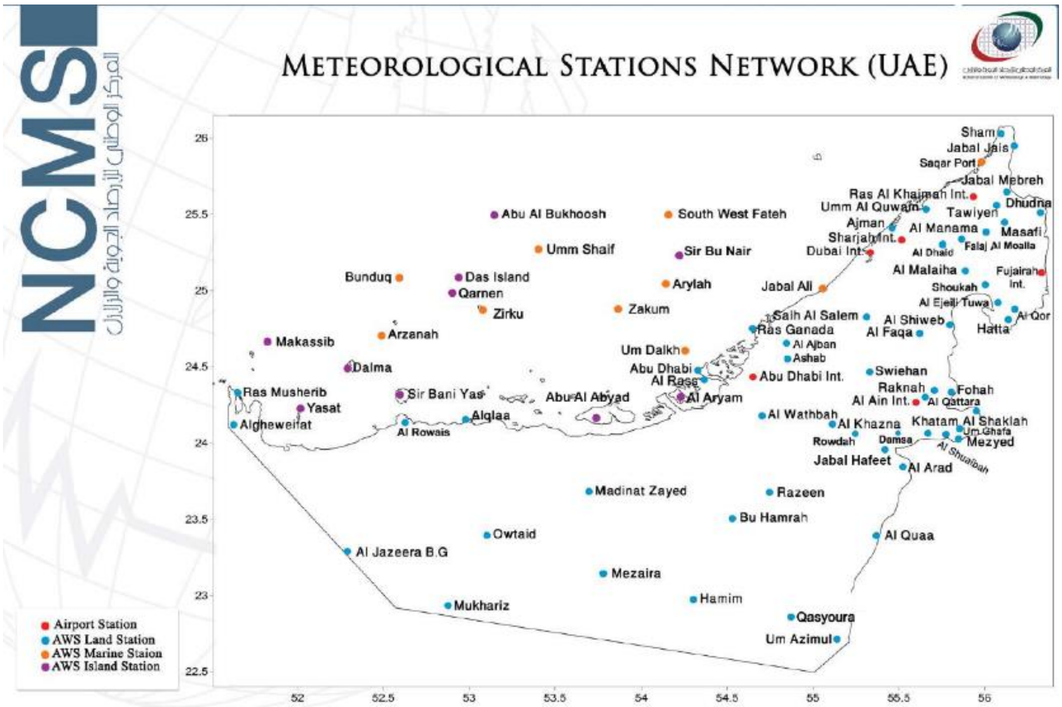

Figure 5-3: Meteorological Station Network UAE by NCMS (2018)

5.3. Study Background

A primary concern in this study is to achieve a reliable data set to develop reliable results. A summary of essential roads under the jurisdiction of the Ministry of Public Works in the UAE is highlighted in Appendix 1. An example is shown in the table below.

A summary of the length of roads used in the study is also given in Appendix 1. The roads to be investigated are selected based on the data availability. Table 5-1 shows an example list.

Table 5-1: Example of the roads selected based on the data availability by Valor (2013)

N	Code	Road	Direction	Length [m]
1	E.11	E-11. Ittihad road	RAK	47,560
2	E.11	E-11. Ittihad road	SHA	47,650
3	E18.1	E-18. Manama- RAK Airport	Rak Airport	41,640

4	E18.1	E-18. Manama- RAK Airport	Manama	41,550
5	E18.2	E-18. RAK Airport-Sha'am	Sha'am	53,360

According to the design manual followed by the UAE Ministry of Public Works, in terms of Data Assets Management, data are collected and organised by considering that all the nominated roads have a starting point and a final point. Some roads were divided into three sub-roads based on direction. For example, the E99 highway has been divided into three segments, E-99.1 (from Khor Fakkan to Dibba), E-99.2 (from Fujairah to Khor Fakkan) and E-99.3 (from Fujairah to Oman Border). To achieve a better data analysis for the road classification, it was decided to split the roads into two groups for data collection, named forward direction roads and backward direction roads, as per the tables in Appendix 1 (Valor 2013). An example is shown in Tables 5-2 and 5-3 for illustration purpose. Classification of the backward and forward roads follows the UAE Ministry of Public Works. Therefore, the two sets of data are organised accordingly.

Table 5-2: Example of roads classified as forward direction group based on Valor (2013)

N	Road Code	Road	Direction	Length [m]	Data Collection Approach
2	E.11	Ittihad road	SHA	47,650	Forward
4	E18.1	Manama- RAK Airport	Manama	41,550	Forward
6	E18.2	RAK Airport-Sha'am	Rak Airport	53,480	Forward

Table 5-3: Example of roads classified as backward direction group based on Valor (2013)

N	Road Code	Road	Direction	Length [m]	Data collection Approach
1	E.11	Ittihad road	RAK	47,560	Backward
3	E18.1	Manama- RAK Airport	Rak Airport	41,640	Backward
5	E18.2	RAK Airport-Sha'am	Sha'am	53,360	Backward
7	E311	Sheik Mohammed Bin Zayed	SHA	70,950	Backward

In order to build an effective and rigorous pavement deterioration model, there is a need for appropriate input data. Such data include information about inventory, for example, location and structural type of individual components. In general, Sun, Bocchini and Davison (2018) stated that data may be gathered from the field, or generated from simulations, experiments and expert surveys. However, having access to such data is difficult as some companies and highway agencies refuse to share their inventory data. Sun, Bocchini and Davison (2018) highlighted that national security and competitive advantage are the main reasons for not sharing these data. They also added that general scarcity of data leads to limited data validation and consequently difficulties in ensuring the accuracy of a deterioration model.

Every highway agency has a different approach to data collection and storing. According to the asset condition manual followed by the UAE Ministry of Public Works, in terms of Data Assets Management, the approach for data collection was based on lane numbering, as shown in Figure 5-4. The odd numbers were assigned to the lanes defined in the carriageway as moving from the starting point to the ending point of the road (forward direction), for example, the fast lane named as number 5 and the slow lane designated as number 1. On the other hand, the pair numbers were defined in the carriageway coming from the road ending point to the starting point (backward direction). The first fast lane was numbered 6, and the most right-sided lane (slow lane) was numbered 2 (Valor 2013). According to UAE traffic law, heavy vehicles are only allowed to travel in a slow lane. TRL Road Note 31 (TRL 1993) states that frequent heavy axle loads and slow-moving heavy traffic are the leading causes for road sections to undergo surface rutting. For this research, only data occurring in slow lanes (number 1 and number 2), which are the lanes with an excessive proportion of heavy goods vehicles, are considered in this research. These sections are prone to fast deterioration activities. Therefore, the model was built on the data generated from these slow lanes. Anyala (2011) also focused on the road used by heavy vehicles is his study. A similar approach is followed in this research.

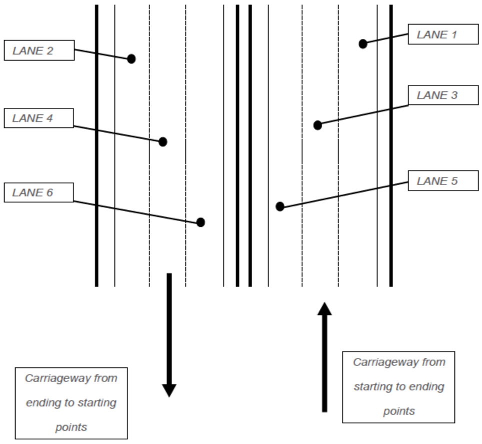

Figure 5-4: Data collection methodology for the selected roads (Valor 2013)

A complete inventory of all roads was obtained from the Ministry of Public Works and Al Ain City Municipality. In each section, data were collected for every 10 m for both directions with the focus on the two slow lanes. For instance, data for the forward direction included slow lane number 1 and the same approach was used for the backward direction with slow lane number 2.

In his study, Mubaraki (2010) used a sample unit of pavement distress such as cracking and rutting for the selected main roads of every 100-metre length. Anyala (2011) also applied the same as he used averaged rutting depth data over 100 m road sections on the road carriageway. It is worth pointing out that both studies used infrastructures that are very old. The infrastructure used in this study is still in very good condition. The author carried out a similar approach to analyse the received data. The average sample for the 100-metre section was taken into the analysis to define the sample value for International Roughness Index (IRI), cracking, rutting and Pavement Condition Index (PCI). The number of readings for each road was substantial. The total length of the network was 1,060,090 linear metres (1060 km) (see the Appendix 1 for road classification). Data analysis demonstrated that there is no variation in IRI, rutting and cracking at 100-metre interval sampling. This could be due to the fact that the network is new, as stated above. Several sampling experimental tests were conducted. The author was able to estimate the value of IRI, rutting and cracking based on average reading of 5000 metres (more details are provided in Chapter 6 section 6.3).

5.4. Data Types and Sources

The data needed for the development of pavement deterioration indicators in Chapter 6 are gathered under the following groups: International Roughness Index, Pavement Condition Index, climate, traffic and asphalt material properties. The approaches used to gather the data, and their sample sizes are presented in the following sections.

5.4.1. International Roughness Index (IRI)

The data for IRI are collected from the Federal Road Network in the UAE for three consecutive years (2013, 2014 and 2015) in order to determine the change in IRI. The Ministry of Public Works in the UAE used laser sensors and accelerometers that attached to survey vehicles in order to obtain the mean value of IRI. A complete table is presented in Appendix 1. The following table (5-4) gives an example of mean IRI value for backward direction roads.

Table 5-4: Example of IRI value for backward direction roads

Final distance	Initial distance	Road	Stretch	Stretch way	Lane	Right IRI	Left IRI	Average IRI
10	0	E84	Fujairah to Maliha	Backward	2	5.32	5.32	5.32
20	10	E84	Fujairah to Maliha	Backward	2	11.3	11.3	11.32
30	20	E84	Fujairah to Maliha	Backward	2	5.03	5.03	5.03

Concerning IRI data analysis, for example, road E84, there are three readings of IRI that were collected for every 10 metres. An average reading for every 5000 metres was taken instead of 10 metres for one reading, which is average IRI. A similar approach was conducted for the remaining roads, and the value reported. The final results are shown in Appendix 1. An example is presented below in Table 5-5.

Table 5-5: Example of mean IRI value for backward direction-based data collection

N	Road Code	Road	IRI
1	E.11	Ittihad road	1.16
3	E18.1	Manama- RAK Airport	0.98
5	E18.2	RAK Airport-Sha'am	1.73

Errors in IRI measurement due to circumstances related to the survey are likely to happen; however, with large sampling (taking one reading every 5000 readings) data accuracy and reliability can be achieved.

5.4.2. Asphalt Surfacing Rutting and Cracking

The data for rutting and cracking are collected from the Federal Road Network in the UAE for three consecutive years (2013, 2014 and 2015) in order to determine the change in rutting and cracking. Table 5-6 presents an example of cracking and rutting value for forward direction roads.

Table 5-6: Example of rutting value for forward direction roads

Road	Stretch	Stretch way	Campaign	Lane	Right ruts	Left ruts	Average ruts
E84	Maliha to Fujairah	Forward	2014	1	0.50	1.90	1.20
E84	Maliha to Fujairah	Forward	2014	5	1.00	0.00	0.50
E84	Maliha to Fujairah	Forward	2014	5	0.20	0.80	0.50

For cracking and rutting data, a similar approach to analysing IRI data was followed in order to obtain sufficient sample sizing. Also, average cracking and rutting for the slow lane (1 or 5) were selected.

Table 5-7: Example of cracking value for forward direction roads

Road	Stretch	Stretch way	Measurement date	Campaign	Lane	Total cracking
E84	Maliha to Fujairah	Forward	16/02/2015	2015	1	0.088
E84	Maliha to Fujairah	Forward	16/02/2015	2015	5	0.000
E84	Maliha to Fujairah	Forward	16/02/2015	2015	5	0.454

5.4.3. Pavement Condition Index

The PCI data are not available in the Ministry of Public Works assets inventory. A decision was made to compare the relationship between IRI and PCI based on the data available in a different transport agency. Al Ain City Municipality was selected as it uses PCI and IRI as primary indicators to evaluate pavement asset condition in the city. According to data collected from Al Ain City Municipality, for every single road, IRI value is recorded every 10 metres in the one road direction while PCI reading is recorded every 100 metres. For sampling size, an average PCI and IRI was prepared for every 1000 m for some of the main roads in Al Ain city, as is shown below in Table 5-8.

Table 5-8: Example of sampling of IRI and PCI from Al Ain City Municipality

sample	IRI	PCI
1	1.73	100.00
2	1.51	100.00
3	1.96	100.00
4	1.86	100.00
5	1.88	99.00
6	1.82	100.00
7	1.50	100.00
8	1.55	100.00
9	1.71	100.00
10	1.25	100.00

5.5. Reliability of Data from the Conditional Survey

The data used in this study are based on row data from the UAE Ministry of Public Works and AlAin City Municipality. The UAE highway agencies have restricted procedure for carrying out the pavement condition survey. All equipment used in the survey is calibrated and checked periodically. The data also are checked for consistency. The obtained data from the road conditional survey are summarised as follows:

Table 5-9: Data type and source

	Definition	Source of data
ΔRDS	Incremental change in standard deviation of rut depth during analysis year, in mm	Conditional survey done by Ministry of Public Works in the UAE
ΔACRA	Incremental change in area of total cracking during analysis year, in per cent	Conditional survey done by Ministry of Public Works in the UAE
ΔRI	Incremental change in roughness during analysis year, in m/km IRI	Conditional survey done by Ministry of Public Works in the UAE and from Al Ain City Municipality. (The set collected from Al Ain City Municipality is used for PCI model (same roads), the other set s used for IRI model.)
SNc	Modified Structural number	Data were not available in Ministry of Public Works in UAE. It was average data taken from another agency in the UAE (Al Ain City Municipality)
PCI	Pavement Condition Index	Al Ain City Municipality

5.6. Traffic Data

5.6.1. Automatic Temporary Counts (ATCs)

Traffic information is vital information to define the number and type of vehicles. Data related to the number of vehicles using the defined road and the types of vehicles that are classified as heavyweight vehicles were obtained by using a network of temporary and fixed counting stations. The Ministry of Public Works used automatic temporary counts (ATCs) as machine for collecting the traffic data.

5.6.2. Traffic Flow Data

The Average Annual Daily Traffic (AADT) of commercial vehicles (F) on roads in the research network was calculated from the Ministry of Public Works in the UAE. Traffic flow data are measured using the same vehicle detector equipment, which is the technology of compressed air to register the movement of all vehicles through two inflated tubes which send the information to a counting machine. Data related to the number of vehicles using the road and the types of vehicles that are classified as heavyweight were obtained. The data were recorded as shown in Appendix 1. An example is given in tables 5-10 and 5-11 below:

Table 5-10: Example of average daily traffic for backward data collection roads

Backward data collection roads					Average daily traffic		
N	**Road Code**	**Road**	**Direction**	**Length [m]**	**A.D.T**	**A.D.T Heavy**	**Heavy Vehicles %**
1	E.11	Ittihad road	RAK	47,560	18351	918	5
3	E18.1	Manama- RAK Airport	Rak Airport	41,640	4025	1146	28
5	E18.2	RAK Airport-Sha'am	Sha'am	53,360	4025	1006	25

Table 5-11: Average daily traffic for forward data collection roads

Forward data collection roads					average daily traffic		
N	**Road Code**	**Road**	**Direction**	**Length [m]**	**A.D.T**	**A.D.T Heavy**	**Heavy Vehicles%**
2	E.11	Ittihad road	SHA	47,650	18344	1101	6
4	E18.1	Manama- RAK Airport	Manama	41,550	4092	275	6
6	E18.2	RAK Airport-Sha'am	Rak Airport	53,480	4025	1146	28

5.6.3. Traffic Loading (YE4)

Pavement degradation is hugely impacted by traffic volume and vehicle types. Average Annual Daily Traffic (AADT) data were obtained for the selected main roads. As was explained earlier, the traffic loading is a contributing factor to both rutting and structural number which are represented in the proposed model structures given in Chapter 6. The model aimed to apply the annual number of equivalent standard axles (YE4) in millions per lane. YE4 on each road in the network area was obtained using the following equation (DMRB 2017):

$$YE4 = \sum_{K=1}^{K} \frac{365 \times F_{ikt} \times W_k \times GF_t \times P_i}{10^6}$$

Equation 5-1: Annual Daily Traffic (AADT) data (DMRB 2017)

Where,

- F_{ikt} = is the Average Annual Daily Traffic (AADT) of commercial vehicles class k in one direction on road section i during year t
- W_k= is the structural wear factor of commercial vehicle class k
- GF = is a traffic growth factor for adjusting existing traffic flow data to the desired year t
- Pi is the proportion of commercial vehicles on the heavily loaded lane of road section i

Wear factors are a measure of road pavement structural wear in the UAE. The wear factor applied in the UAE is 0.65 according to AASHTO 1993 (ESAL 2018). The annual number of equivalent standard axle loads (YE4) on each road (backward and forward direction) section was obtained using Equation 5-1 above. Average YE4 values were presented as per Table 5-12 and 5-13 below. No future growth was considered; it was assumed that future traffic will remain the same. Calculation of Annual Daily Traffic (AADT) is presented in Appendix 1. Table 5-12 below is an example.

Table 5-12: Annual daily traffic (AADT) data for forward data collection roads

Forward data collection roads			**Average Daily Traffic**		**EASL**					
N	**Road Code**	**Road**	**A.D.T**	**A.D.T Heavy**	**% Heavy Vehicles**	**LEF**	**DD**	**Growth factor**	**EASL**	**EASL m/lane**
2	E.11	Ittihad road	18344	1101	6	6.5	0.7	1	1827888	**1.83**
4	E18.1	Manama-RAK Airport	4092	275	6	6.5	0.7	1	407747	**0.41**
6	E18.2	RAK Airport-Sha'am	4025	1146	28	6.5	0.7	1	1871665	**1.87**

Table 5-13: Annual daily traffic (AADT) data for backward data collection roads

Backward data collection roads			**Average Daily Traffic**		**EASL**					
N	**Road Code**	**Road**	**A.D.T**	**A.D.T Heavy**	**% Heavy Vehicles**	**LEF**	**DD**	**Growth factor**	**EASL**	**EASL m/lane**
1	E.11	Ittihad road	18351	918	5	6.5	0.7	1	1523821	**1.52**

3	E18.1	Manama-RAK Airport	4025	1146	28	6.5	0.7	1	1871665	**1.87**
5	E18.2	RAK Airport-Sha'am	4025	1006	25	6.5	0.7	1	1671130	**1.67**

5.7. Heavy Vehicle Speed (sh)

Heavy vehicle speed (sh) is one of the explanatory variables that were also highlighted by HDM-4. Heavy vehicles range in type from two-axle to six-axle vehicles, as per the FHWA classification. For this research, the proposed variable of Heavy Vehicle Speed (sh) is considered in the model (see Chapter 3 section 3.4.6 and Chapter 6 section 6.2.2). Therefore, heavy vehicle speed data for each road are essential for assessing the model coefficients for the heavy vehicle speed variable. For data collection, vehicle speed data were obtained from the Ministry of Public Works. The data were collected using speed measuring equipment based on the machine of Vehicle Counting Cabinet and Weight in Motion. The machine records information about the vehicle axle number and vehicle weight using predefined vehicle lengths. Speed measurements were conducted for every hour for 24 hours and recorded in km per hour. An example of road data can be seen for Road E.88 Al David – Massif, as per Appendix 1.

Table 5-14: Example of speed measurements

E88 Al Dhaid - Masafi			
Date	**Time**	**Speed(km/h)**	**Axle**
7/8/2013	0:00:13	56	6
7/8/2013	0:00:24	65	6
7/8/2013	0:00:26	80	6
7/8/2013	0:00:42	87	6
7/8/2013	0:01:43	89	6

According to the statistics, the average speed for road E.88 Al Dhaid – Masafi is nearly 70km/hr. Such a reading occurs with the standard speed limit as it is uncommon to find a road in the UAE that allows heavy trucks to travel at more than 80 km/h. Therefore, it is proposed to apply a 70 km/has maximum vehicle speed. Nevertheless, vehicle speed depends on whether heavy vehicles are loaded with goods or not. As was discussed early, the heavier the vehicle, the slower the travelling speed, the more impact can be generated on the road. For this research, the worst case scenario is chosen, which is the minimum travelling speed (heavily loaded vehicles). More details are provided in Chapter 6 section 6.2.2.

5.8. Asphalt Surfacing Thickness (Hs)

One of the most critical variables is asphalt surfacing thickness. It reflects the strength of the pavement structure, which varies based on the material used and the size of each layer. The pavement designer applies the required thickness of the asphaltic layer based on many factors such as traffic type, traffic volume, etc. It was highlighted earlier that in Australia more than 90% of the asphaltic road is made with granular seal material in rural areas. In England, Anyala (2011) also considered the factor of asphalt surfacing thickness (HS) in his model for determining the change in rutting. It is crucial to obtain asphalt surface thickening data for each road, and the following table presents the essential information for the variables for determining the model predictor. These data are based on the original design thickness and an assumption was made that no maintenance and rehabilitation activities such as overlay works had been introduced. Thickness data are given in Appendix 1. Example of asphalt surfacing thickness (HS) for data collection forward and backward approach is presented in Tables 5-15 and 5-16.

Table 5-15: Example of asphalt surfacing thickness (HS) for data collection backward approach

N	Road Code	Road	Wearing course (mm)	Binder course (mm)	Base course (mm)	Wet mix macadam as base (mm)	road Base (mm)	granular sub-base (mm)	subgrade (mm)	total (mm)	asphaltic layer (mm)
1	E.11	Ittihad road	50	60	70	0	250	200	150	**780**	**180**
3	E18.1	Manama- RAK Airport	50	50	60	200	0	150	150	**660**	**160**
5	E18.2	RAK Airport-Sha'am	50	50	60	200	0	150	150	**660**	**160**

Table 5-16: Example of asphalt surfacing thickness (HS) for data collection forward approach

N	Road Code	Road	Wearing Course (mm)	Binder Course (mm)	Base course (mm)	Wet mix Macadam as Base (mm)	Road Base (mm)	Granular sub-base (mm)	subgrade (mm)	total (mm)	Asphaltic layer (mm)
2	E.11	Ittihad road	50	60	70	0	250	200	150	**780**	**180**
4	E18.1	Manama- RAK Airport	50	50	60	200	0	150	150	**660**	**160**
6	E18.2	RAK Airport-Sha'am	50	50	60	200	0	150	150	**660**	**160**

5.9. Asphaltic Ageing

Asphaltic age represents the date on which the pavement structure was constructed, or the last major maintenance and rehabilitation actives were made. For the defined roads, data of asphaltic age for each road section were collected. Mainly, the pavement age was directly taken in the model. Moreover, it was the source for determining both softening point and voids in the mix. According to the experts, the accuracy of pavement ageing is questionable as limited recording is available, especially regarding whether such assets have undergone maintenance activity. Data for pavement ageing are shown in Appendix 1. Example of asphaltic age for roads based on data collection forward and backward approach are presented in Tables 5-17 and 5-18.

Table 5-17: Example of asphaltic age for roads based on data collection (backward approach)

N	Road code	Road	Construction date	Major rehabilitation	Road age
1	E.11	Ittihad road	2006	no record	11
3	E18.1	Manama- RAK Airport	2006	no record	11

Table 5-18: Example of asphaltic age for roads based on data collection (forward approach)

N	Road code	Road	Construction date	Major rehabilitation	Road age
2	E.11	Ittihad road	2006	no record	11
4	E18.1	Manama- RAK Airport	2006	no record	11

5.10. UAE Weather Data

The National Centre of Meteorology and Seismology is the primary source for climate data in the UAE. NCMS can collect climatic data and assess different forms of climate data from many automatic stations across the UAE. There are 75 automatic stations for data collection. For this research, Al Ain Airport station was the selected station (Table 5-19).

Table 5-19: Al Ain Airport Meteorological station details

N°	Stations	Latitude	Longitude	Height (metres)	Period	Years
2	Al Ain Airport	24° 15 N	55° 37 E	264 m	1995-2016	22

The received data were from the years 2003 to 2016. In this research, the data of 2003 to 2016 from Al Ain Airport station were analysed and are presented as per the Figures (5-5), (5-6), (5-7), (5-8), (5-9) and (5-10).

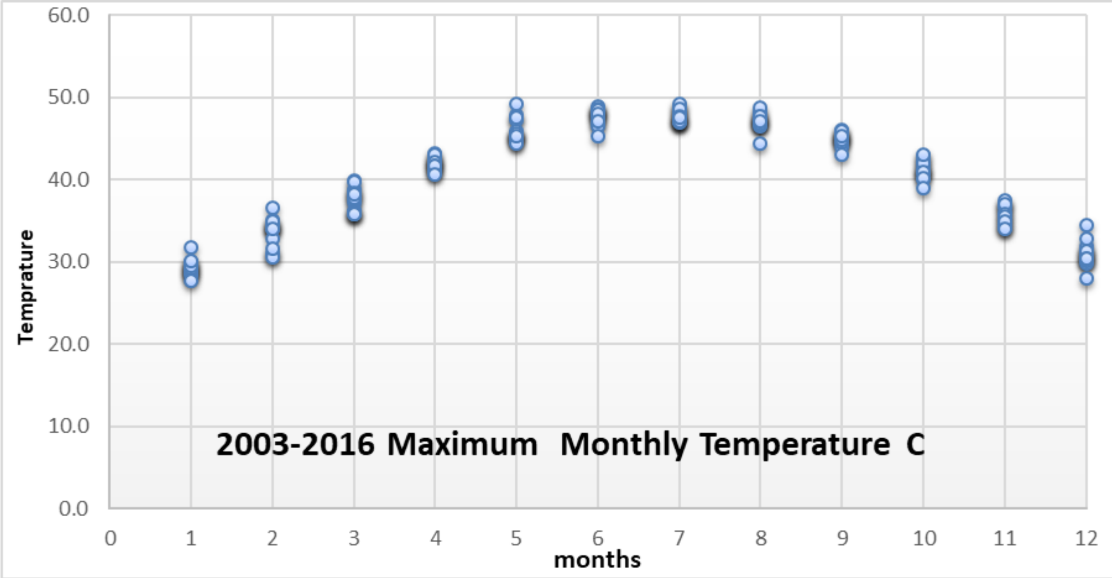

Figure 5-5: Maximum monthly temperature for the period 2003-2016 (Al Ain Airport station)

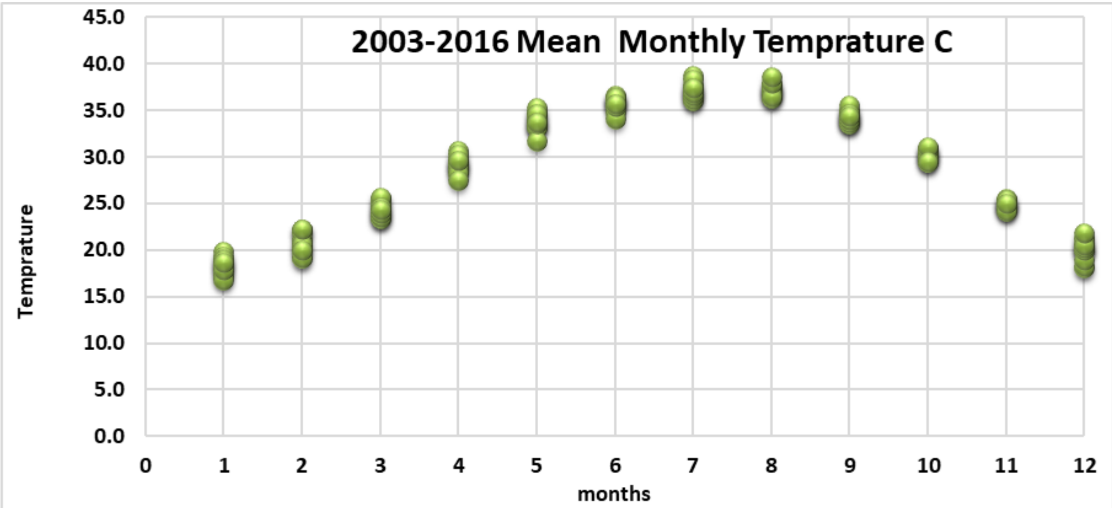

Figure 5-6: Mean monthly temperature for the period 2003-2016 (Al Ain Airport station)

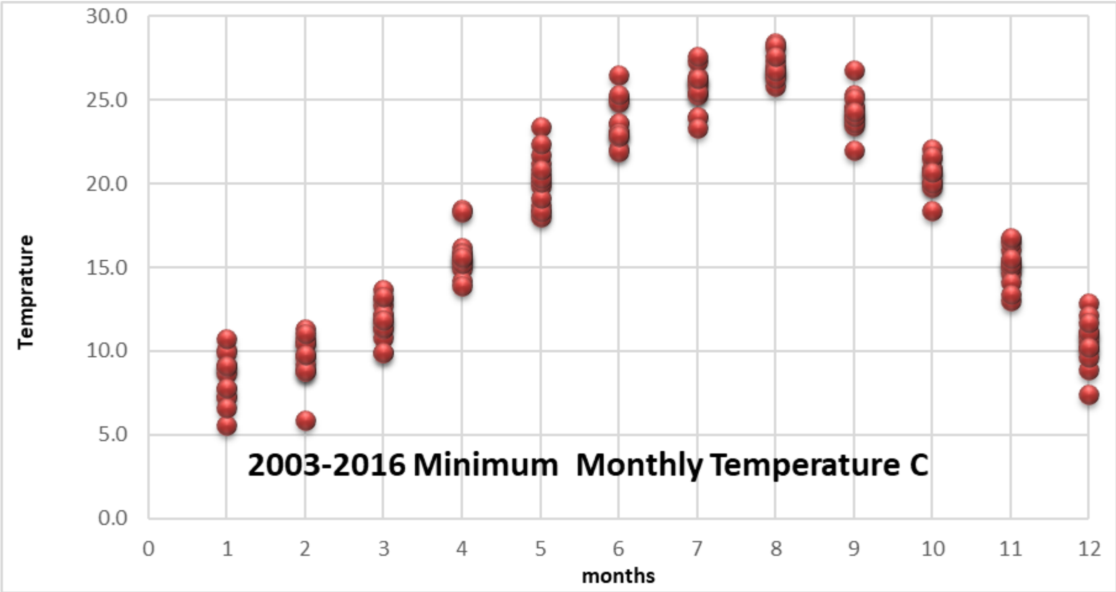

Figure 5-7: Minimum monthly temperature for the period 2003-2016 (Al Ain Airport station)

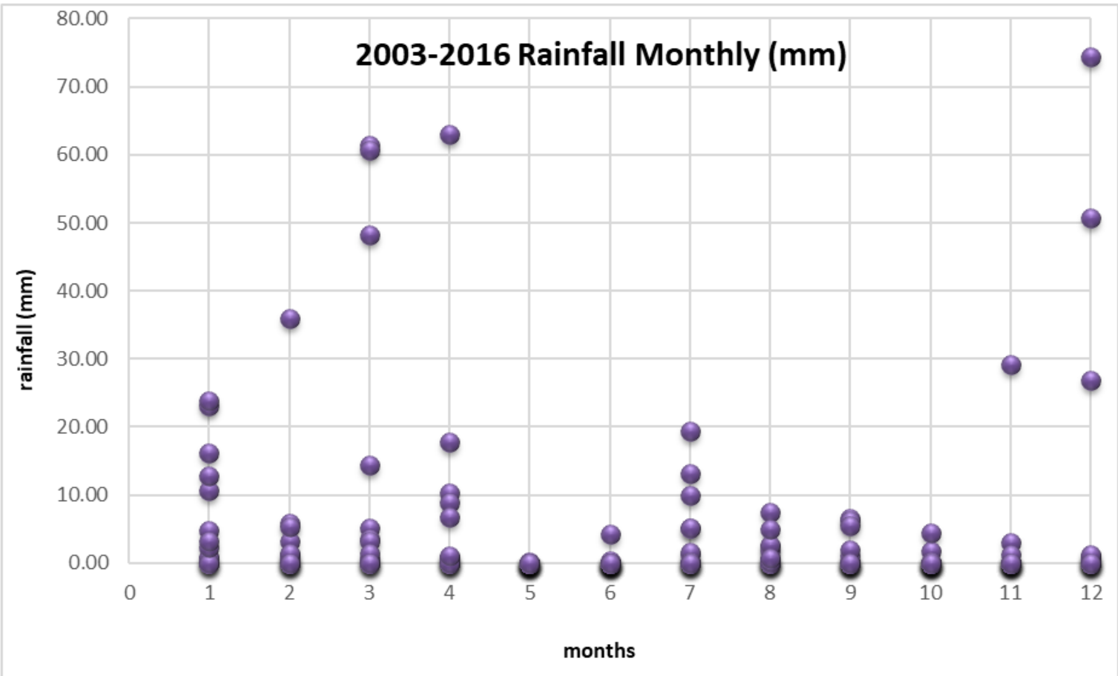

Figure 5-8: Monthly rainfall for the period 2003-2016 (Al Ain Airport station)

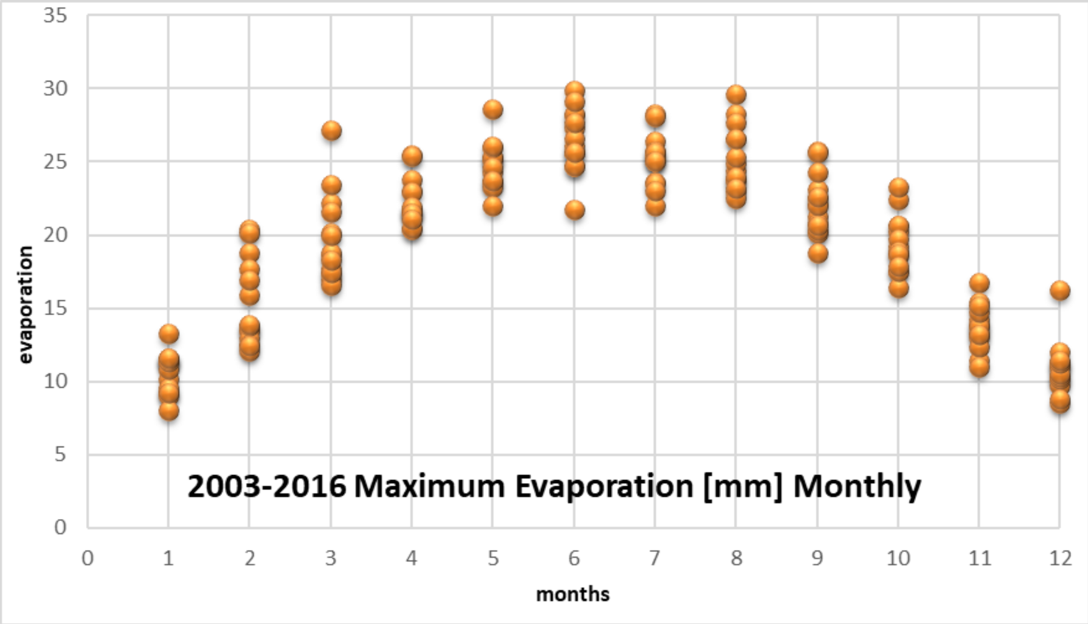

Figure 5-9: Maximum monthly evaporation for the period 2003-2016 (Al Ain Airport station)

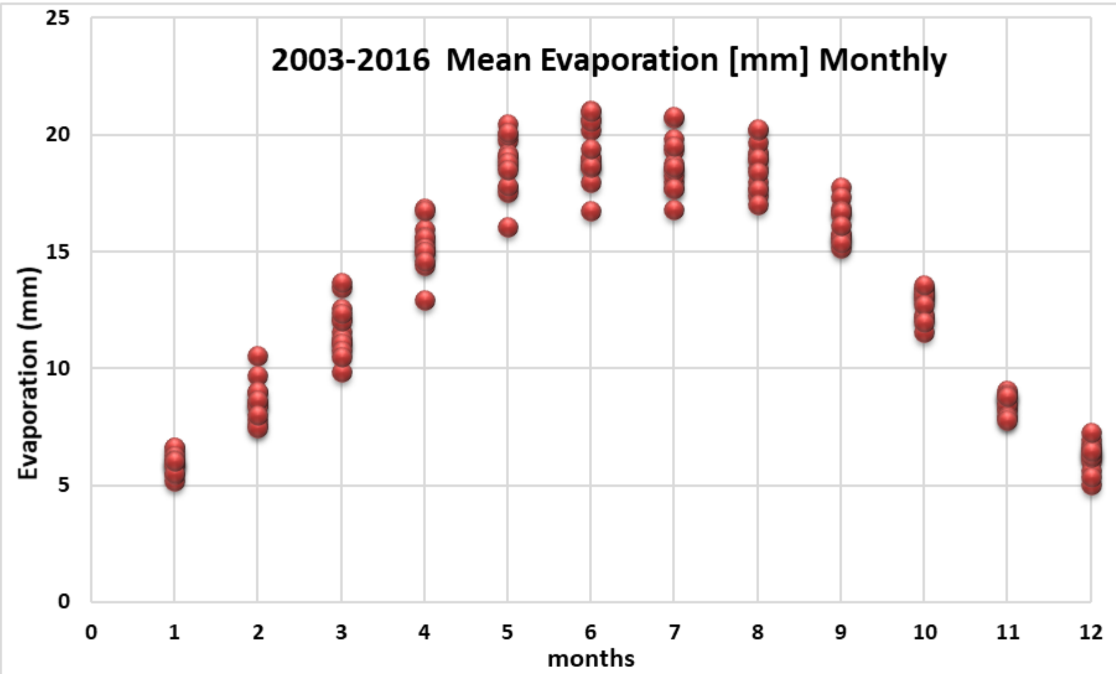

Figure 5-10: Mean monthly evaporation for the period 2003-2016 (Al Ain Airport station)

5.11. Developments of Model Inputs

5.11.1. Maximum Air temperature (Tmax) in the UAE

This study follows the method proposed by the Environment Agency - Abu Dhabi (EAD) in conjunction with the United Nations Environment Programme (UNEP) as they developed the Weather Research and Forecasting (WRF) model and Regional Ocean Model (ROM). The findings of the WRF model in conjunction with the IPCC for the UAE that shape the future predictions of air temperature for the UAE based on three different scenarios (2020, 2040, 2060-2079) for climate change are given in Appendix 1. Table 5-20 below presents the prediction for the air temperature based on the highest record.

Table 5-20: Predicted air temperature for the UAE based on three different scenarios (2020, 2040, 2060-2079)

Month	Max month Temp. Current (2010)	The highest reading ever in UAE	2020 TMax	2040 Tmax	2060-2079 Tamx
			Increase by 1°C	1.5 and 2°C	2 and 3°C
			Assume =1°C	Assume =2°C	Assume = 3°C
Month 6-2016		50.4	51.4	52.4	53.4

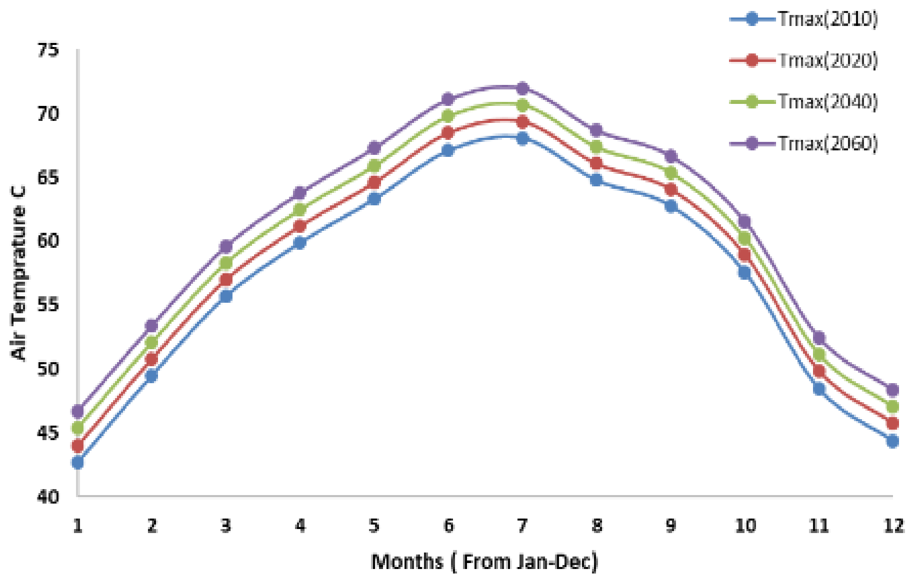

Figure 5-11: Predicted air temperature for the UAE based on three different scenarios (2020, 2040, 2060-2079)

Figure 5-11 presents the predicted air temperature for the UAE based on three different scenarios (2020, 2040, 2060-2079). The selection of the highest air temperature recorded in the UAE was made to develop the model based on the worst case scenarios. Therefore, a maximum air temperature of 50.4 recorded in Al Ain in June 2016 was applied for this research.

5.11.2. Pavement Temperature (TPmax)

The model developed by Hassan et al. (2004) which was earlier discussed in Chapter 3 section 3.2.1 was used to determine pavement temperature. Moreover, the maximum air temperature ever recorded was 50.4 in Al Ain in June 2016. Therefore, for this research, the weather data were taken based on Al Ain city.

$$T20mm = 3.160 + 1.319\ Tair$$

Equation 5-2: Hassan et al.'s (2004) model for measuring the pavement temperature

Where,

- T20mm= pavement temperature at 20 mm depth, °C and Tair = maximum air temperature, °C

Table 5-21: Predicted pavement temperature for the UAE based on three different scenarios (2020, 2040, 2060-2079)

Month	Max month Temp. Current (2010)	The highest reading ever in UAE	2020 TMax	2040 Tmax	2060-2079 Tamx	2013	2020	2040	2060-2079
			Increase by 1°C	1.5 and 2°C	2 and 3°C	TPmax	TPmax	TPmax	TPmax
			Assume =1°C	Assume =2°C	Assume = 3°C				
Month 6-2016		50.4	51.4	52.4	53.4	**69.6**	**71.0**	**72.3**	**73.6**

5.11.3. Thornthwaite Moisture Index (TMI) in UAE

As was explained earlier, in Chapter 2, there are various methods to determine the Thornthwaite Moisture Index value. For this research, the equations introduced by Mather (1974) and Witczak, Zapata and Houston (2006) are selected and tested based on the available data.

$$TMI = 100\left(\frac{P}{PET} - 1\right)\ method\ 1$$

Equation 5-3: Thornthwaite Moisture Index by Mather (1974)

$$TMI = 75\left(\frac{P}{PET} - 1\right) + 10\ \ method\ 2$$

Equation 5-4: Thornthwaite Moisture Index by Witczak, Zapata and Houston (2006)

Where,

- P = Annual precipitation
- PET = Adjusted potential evapotranspiration

Table 5-22: Thornthwaite Moisture Index (TMI) in the UAE based on two methods

Year	Evaporation [Cm] PE			Rainfall [Cm] P	TMI method 1 by Mather (1974)			TMI method 2 by Witczak et al. (2006)		
	Max	Mean	Min	Total	Max	Mean	Min	Max	Mean	Min
2003	25.38	16.70	8.97	7.99	-69	**-52**	-11	-41	**-29**	2
2004	24.14	16.72	10.87	3.31	-86	**-80**	-70	-55	**-50**	-42
2005	22.66	15.89	9.07	3.40	-85	**-79**	-63	-54	**-49**	-37
2006	24.21	16.45	10.10	9.53	-61	**-42**	-6	-35	**-22**	6
2007	23.65	16.33	10.20	6.85	-71	**-58**	-33	-43	**-34**	-15
2008	23.68	16.35	9.84	3.69	-84	**-77**	-63	-53	**-48**	-37
2009	23.93	15.99	9.23	11.51	-52	**-28**	25	-29	**-11**	29
2010	23.45	16.04	9.02	0.97	-96	**-94**	-89	-62	**-60**	-57
2011	22.20	15.43	10.05	2.47	-89	**-84**	-75	-57	**-53**	-47
2012	24.01	15.99	9.74	1.25	-95	**-92**	-87	-61	**-59**	-55
2013	22.18	14.79	8.98	8.13	-63	**-45**	-9	-38	**-24**	3
2014	22.53	15.34	9.06	6.49	-71	**-58**	-28	-43	**-33**	-11
2015	24.52	17.26	10.49	2.91	-88	**-83**	-72	-56	**-52**	-44
2016	23.41	15.91	9.52	7.51	-68	**-53**	-21	-41	**-30**	-6

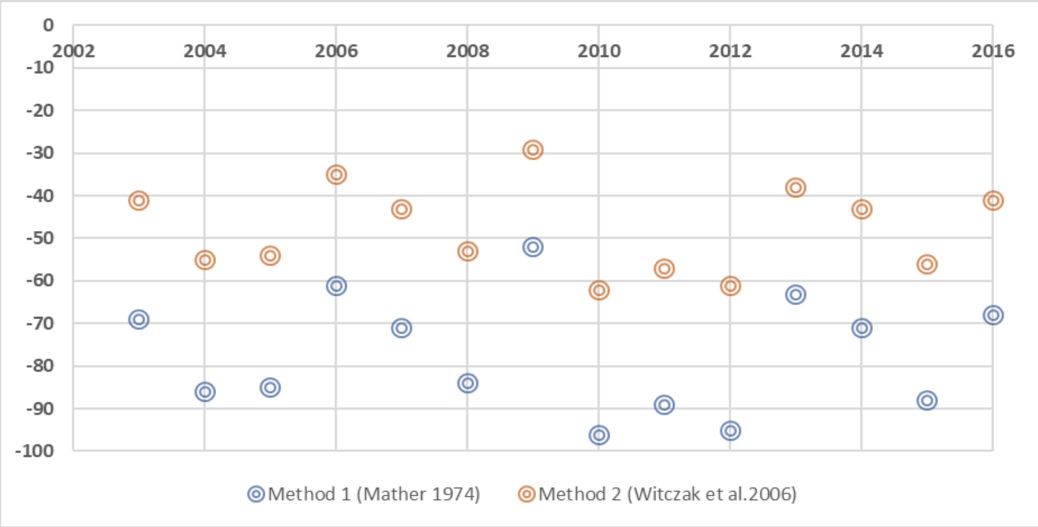

Figure 5-12: Comparison of the maximum TMI Method 1 and Method 2

Table 5-23: Comparison between predicted UAE TMI and HDM-4 TMI

Method	Moisture Classification	Annual Precipitation mm	TMI (Max)	TMI (Mean)	TMI (Min)	Final recommended Range
HDM-4	Arid	300<	-100 to –61	-100 to –61	-100 to –61	**Apply method 1 based on Maximum TMI <u>-96 to -52</u>**
TMI method 1 by Mather (1974)	Arid	12.5 to 110	-96 to -52	-92 to -42	-87 to -9	
Within the Range (HDM-4) Model	YES	YES	YES	NO	NO	
TMI method 2 by Witczak et al. (2006)	Arid	12.5 to 110	-62 to -29	-60 to -11	-57 to 2	
Within the Range (HDM-4) model	YES	YES	NO	NO	NO	

Based on tables 5-22 and 5-23, which present a comparison between two methods using Maximum, Mean and Minimum temperature and total precipitation for the period from 2003 to 2016 (Al Ain Airport stations), the HDM-4 value was used to set as a benchmark for the comparison. Therefore, two methods were tested to maximum temperature scenario to determine TMI value for Al Ain region. Method 1 was found to be in the most suitable range. Consequently, it was selected for this research.

5.11.4. TMI for Future Climate Change Scenario

As was early discussed, the Weather Research and Forecasting (WRF) model and Regional Ocean Model (ROM) introduced by the Environment Agency - Abu Dhabi (EAD) have forecasted the expected rise in temperature as follows:

Table 5-24: The expected rise in temperature based on Venturini et al. (2017)

2020	2040	2060-2079
Increase by 1°C	1.5 and 2°C	2 and 3°C
Assume =1°C	Assume =2°C	Assume = 3°C

Moreover, for the precipitation, there are possible increases of up to 200% in the maximum rain over one day (Venturini et al. 2017). For this research, it was decided to ignore the impact of extreme weather (thunderstorms) which is likely to occur as a result of climate change. Therefore, an assumption was made that the future precipitation shall remain consistent with the projection scenarios. On the other hand, for the future predicted model, the data for evaporation rate need to be predicted. Such a value is crucial for predicting the future TMI. Therefore, the predicted model for evaporation rate is developed using previously recorded data to define the relationship between air temperature and evaporation rate, and, based on the relationship, the new predicted evaporation data are determined.

5.11.4.1. Regression Model between Evaporation Rate and Air Temperature

The non-linear regression model was conducted to analyse the relation between evaporation (PE) rate and air temperature (T), where evaporation (PE) is the dependent variable (Y) and air temperature is independent variable (x), and b_0, b_1 are regression coefficients. This study follows the below equation to determine the relationship between maximum monthly temperature and evaporation (PE) rate $Y = b_0 + b_1X$.

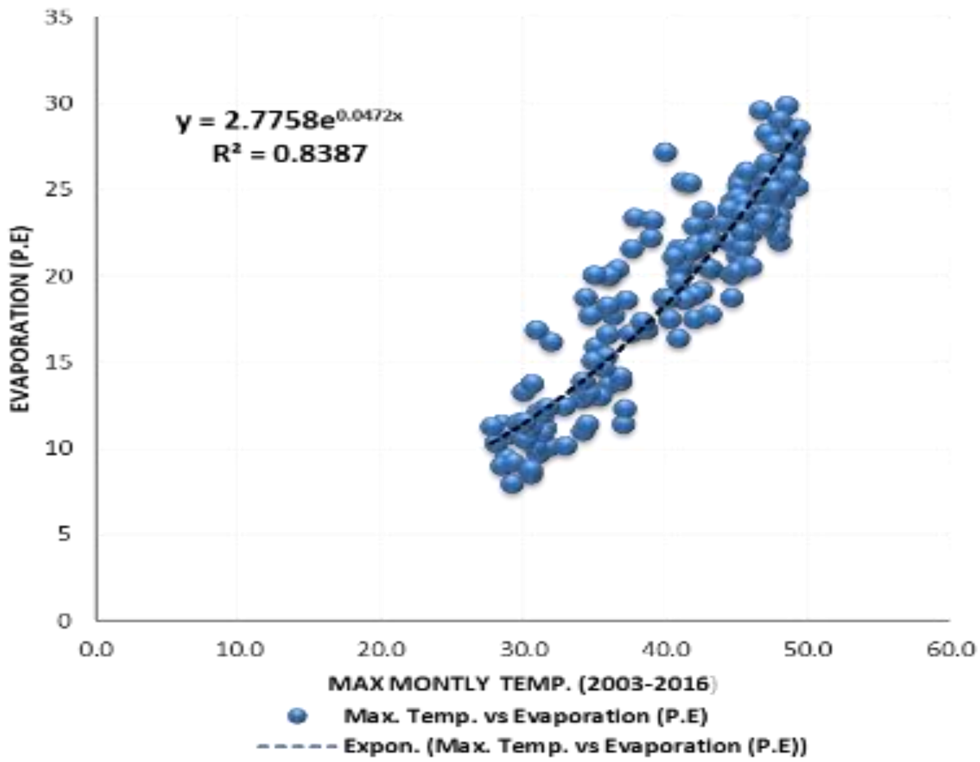

Figure 5-13: The relationship between maximum monthly temperature and evaporation (PE) 2003-2016

For the regression model, the results show a significant non-linear relationship between the evaporation (PE) and maximum temperature (Tmax) and the coefficient of multiple determinations (R^2) is 0.84, according to Figure 5-13. For average maximum months of air temperature based on the current records from 2003-2016, the following TMIs were obtained for the periods 2020, 2040, 2060-2079 using method 1.

$$TMI = 100\left(\frac{P}{PET} - 1\right) \qquad Eq(method\ 1)$$

Table 5-25: Obtained TMI for 2020 climate change scenario based on average maximum month temperature (2003-2016)

Month	Max month Temp. Current (2003-2016)	Max Month Temp. 2020	Predict of Evaporation based on 2020	Monthly Mean. Rainfall Current (2003-2016)	Monthly Mean. Rainfall Current (2020)	TMI (2020) The highest scenarios
Jan	31.8	32.8	13.1	7	7	**-79**
Feb	36.6	37.6	16.4	3.8	3.8	
March	39.9	40.9	19.1	14.2	14.2	
April	43.2	44.2	22.4	7.8	7.8	
May	49.3	50.3	29.8	0	0	
June	49	50	29.4	0	0	
July	49.2	50.2	29.7	3.9	3.9	
Aug	48.8	49.8	29.1	3.9	3.9	
Step	46.1	47.1	25.6	1.5	1.5	
Oct	43.1	44.1	22.3	0.5	0.5	
Nov	37.5	38.5	17.1	2.3	2.3	
Dec	34.5	35.5	14.8	11.1	11.1	
			268.7		**56**	

Table 5-26: Obtained TMI for 2040 climate change scenario based on average maximum month temperature (2003-2016)

Month	Max month Temp. Current (2003-2016)	Max Month Temp.2040	Predict of Evaporation based on 2040	monthly Mean. Rainfall Current (2003-2016)	monthly Mean. Rainfall Current (2040)	TMI (2040)
Jan	31.8	33.8	13.7	7	7	**-80**
Feb	36.6	38.6	17.2	3.8	3.8	
March	39.9	41.9	20.1	14.2	14.2	
April	43.2	45.2	23.4	7.8	7.8	
May	49.3	51.3	31.3	0	0	
June	49	51	30.8	0	0	
July	49.2	51.2	31.1	3.9	3.9	
Aug	48.8	50.8	30.5	3.9	3.9	
Step	46.1	48.1	26.9	1.5	1.5	
Oct	43.1	45.1	23.3	0.5	0.5	
Nov	37.5	39.5	17.9	2.3	2.3	
Dec	34.5	36.5	15.5	11.1	11.1	
			281.7		**56**	

Table 5-27: Obtained TMI for 2060-2079 climate change scenario based on average maximum month temperature (2003-2016)

Month	Max month Temp. Current (2003-2016)	Max Month Temp. 2060-2079	Predict of Evaporation based on 2060-2079	monthly Mean. Rainfall Current (2003-2016)	monthly Mean. Rainfall Current (2060-2079)	TMI (2060-2079)
Jan	31.8	34.8	14.3	7	7	**-81**
Feb	36.6	39.6	18.0	3.8	3.8	
March	39.9	42.9	21.0	14.2	14.2	
April	43.2	46.2	24.6	7.8	7.8	
May	49.3	52.3	32.8	0	0	
June	49	52	32.3	0	0	
July	49.2	52.2	32.6	3.9	3.9	
Aug	48.8	51.8	32.0	3.9	3.9	
Step	46.1	49.1	28.2	1.5	1.5	
Oct	43.1	46.1	24.5	0.5	0.5	
Nov	37.5	40.5	18.8	2.3	2.3	
Dec	34.5	37.5	16.3	11.1	11.1	
			295.3		**56**	

Among the weather data between the years 2003 and 2016, the year of 2010 scored the highest temperature. For this research, it was decided to select the worse record ever; thus, for maximum monthly temperature, 2010 was used. The obtained TMIs for the periods 2020, 2040, 2060-2079 are shown in the following Table 5-28:

Table 5-28: Obtained TMI for 2020 climate change scenario based on average maximum month temperature 2010

Month	Max month Temp. Current (2010)	Max Month Temp. 2020	Predict of Evaporation based on 2020	monthly Mean. Rainfall Current (2010)	monthly Mean. Rainfall Current (2020)	TMI (2020)
Jan	30	31	12.0	0.6	0.6	**-96.1**
Feb	35.1	36.1	15.3	3.1	3.1	
March	39.8	40.8	19.0	3.2	3.2	
April	43	44	22.1	0.02	0.02	
May	45.6	46.6	25.0	0.22	0.22	
June	48.5	49.5	28.7	0	0	
July	49.2	50.2	29.7	1.52	1.52	
Aug	46.7	47.7	26.4	0.04	0.04	
Step	45.2	46.2	24.6	0	0	
Oct	41.3	42.3	20.4	0	0	
Nov	34.4	35.4	14.8	0.02	0.02	
Dec	31.3	32.3	12.7	1	1	
			250.8		**9.72**	

Table 5-29: Obtained TMI for 2040 climate change scenario based on average maximum month temperature 2010

Month	Max month Temp. Current (2010)	Max Month Temp.2040	Predict of Evaporation based on 2040	monthly Mean. Rainfall Current (2010	monthly Mean. Rainfall Current (2040)	TMI (2040)
Jan	30	32	12.6	0.6	0.6	**-96.3**
Feb	35.1	37.1	16.0	3.1	3.1	
March	39.8	41.8	20.0	3.2	3.2	
April	43	45	23.2	0.02	0.02	
May	45.6	47.6	26.2	0.22	0.22	
June	48.5	50.5	30.1	0	0	
July	49.2	51.2	31.1	1.52	1.52	
Aug	46.7	48.7	27.6	0.04	0.04	
Step	45.2	47.2	25.8	0	0	
Oct	41.3	43.3	21.4	0	0	
Nov	34.4	36.4	15.5	0.02	0.02	
Dec	31.3	33.3	13.4	1	1	
			262.9		**9.72**	

Table 5-30: Obtained TMI for 2060-2079 climate change average maximum month temperature 2010

Month	Max month Temp. Current (2010)	Max Month Temp. 2060-2079	Predict of Evaporation based on 2060-2079	monthly Mean. Rainfall Current (2010)	monthly Mean. Rainfall Current (2060-2079)	TMI (2060-2079)
Jan	30	33	13.2	0.6	0.6	**-96.5**
Feb	35.1	38.1	16.8	3.1	3.1	
March	39.8	42.8	20.9	3.2	3.2	
April	43	46	24.3	0.02	0.02	
May	45.6	48.6	27.5	0.22	0.22	
June	48.5	51.5	31.6	0	0	
July	49.2	52.2	32.6	1.52	1.52	
Aug	46.7	49.7	29.0	0.04	0.04	
Step	45.2	48.2	27.0	0	0	
Oct	41.3	44.3	22.5	0	0	
Nov	34.4	37.4	16.2	0.02	0.02	
Dec	31.3	34.3	14.0	1	1	
			275.6		9.72	

Table 5-31: TMI range value for the three future scenarios

Year	Case 1	Case 2	Range	Propose TMI

2020	-79	-96.1	-79 to 96.1	-85
2040	-80	-96.3	-80 to 96.3	-90
2060-2079	-81	-96.6	-81 to 96.6	-96

The following results were selected as inputs of TMI value for the three future scenarios as minimum for 2020, average for 2040 and maximum for 2040-2079. More details are provided in Chapter 6 section 6.2.4 and 6.4.

Table 5-32: The inputs of TMI value for the three future scenarios

TMI (2020) Minimum scenario	TMI (2040) Average scenario	TMI (2040-2069) Maximum scenario
-85	**-90**	**-96**

5.12. Binder Softening Point (SP)

As was explained earlier, the author follows the proposed equation by Anyala (2011). The reason behind this is that there are no recorded data that represent the softening point concerning pavement age in either the Ministry of Public Works or Al Ain City Municipality. In practice, such data are not collected on a yearly basis. However, for research purposes, such data might be recorded. Anyala (2011) used previously received data to investigate the degradation of binder (hardening) which leads to an increase in softening point temperature. On the other side, coefficients introduced by Anyala, Odoki and Baker (2014) were used in this research, which were a1= 2.52 and a2= 70.5. The determination of softening point based on the pavement structure age in the UAE is shown in the table in Appendix 1; samples of the results are given in tables 5-33 and 5-34.

Table 5-33: Example of development of binder softening point (SP) for data collection backward approach

N	Road Code	Road	construction date	Major rehabilitation	road age	a1	a2	softening point
1	E.11	Ittihad road	2006	N/A	11	2.5	70.5	76.5
3	E18.1	Manama- RAK Airport	2006	N/A	11	2.5	70.5	76.5
5	E18.2	RAK Airport-Sha'am	2005	N/A	12	2.5	70.5	76.8

Table 5-34: Example of development of binder softening point (SP) for data collection forward approach

N	Road Code	Road	construction date	Major rehabilitation	road age	a1	a2	softening point
2	E.11	Ittihad road	2006	N/A	11	2.52	70.5	76.5
4	E18.1	Manama- RAK Airport	2006	N/A	11	2.52	70.5	76.5

5.13. Voids in Mix (VIM)

The author has also followed the equation proposed by Anyala (2011). The reason behind this is that there are no recorded data that represent the voids in mix (VIM) concerning pavement age. Moreover, a similar coefficient will be used in this research, which is B1= -0.07 and B2= 1.39. The determination of VIM is shown in the table in Appendix 1. Samples of the results are given in tables 5-35 and 5-36.

Table 5-35: Example of development of voids in mix (VIM) based on data collection backward

N	Road Code	Road	construction date	Major rehabilitation	road age	b1	b2	VIM%
1	E.11	Ittihad road	2006	no record	11	-0.07	1.39	1.22
3	E18.1	Manama- RAK Airport	2006	no record	11	-0.07	1.39	1.22

5	E18.2	RAK Airport-Sha'am	2005	no record	12	-0.07	1.39	1.22
7	E311	Sheik Mohammed Bin Zayed	2011	no record	6	-0.07	1.39	1.26

Table 5-36: Example of development of voids in mix (VIM) based on data collection forward

N	Road Code	Road	construction date	Major rehabilitation	road age	b1	b2	VIM
2	E.11	Ittihad road	2006	no record	11	-0.07	1.39	1.22
4	E18.1	Manama- RAK Airport	2006	no record	11	-0.07	1.39	1.22
6	E18.2	RAK Airport-Sha'am	2005	no record	12	-0.07	1.39	1.22

5.14. Pavement Failure Risk

5.14.1. Risk Rating Matrix

A risk matrix is applied to plot the pavement deterioration risk. The pavement risk factor was recorded and measured based on the likelihood and impact rating of each risk event. Mapping risks in a matrix for all the elements related to pavement failure (pavement deterioration) is discussed in Chapter 2. Generally, a questionnaire is a set of questions used to obtain the specific information and data required for fulfilment of a study's research objective (Parasuraman, Zeithaml and Berry 1991). The survey comprises different phases such as designing the questionnaire, distributing the design and, finally, collecting the completed survey forms for the desired research investigations. It is a fast process compared to other research methods. In this study, the researcher did introduce a probability rating as shown in Figure 5-14. The researcher designed a questionnaire survey based on the probability rating scaling the risk contribution from 0.1 to 0.72. It was proposed that the questionnaire survey would be completed by experts in the area of pavement engineering such as pavement material engineers, highway maintenance contractors, highway maintenance consultants, clients, asset managers, etc. The nominated experts were asked to complete the questions to achieve a constant scale of magnitude to rate and quantify the expected risk effect for each risk event.

Probabilit	Threats				
0.9	0.05 ( )	0.09 ( )	0.18 ( )	0.36 ( )	0.72 ( )
0.7	0.04 ( )	0.07 ( )	0.14 ( )	0.28 ( )	0.56 ( )
0.5	0.03 ( )	0.05 ( )	0.1 ( )	0.2 ( )	0.4 ( )
0.3	0.02 ( )	0.03 ( )	0.06 ( )	0.12 ( )	0.24 ( )
0.1	0.01 ( )	0.01 ( )	0.02 ( )	0.04 ( )	0.08 ( )
	0.05/ very low	0.10/ low	0.2/low	0.04/High	0.80/Very High

Figure 5-14: Risk matrix with risk effect scale numbering developed by the author

The primary objective of the questionnaire survey is to measure the expected risk effect of pavement failure due to climate change. The results quantify variable risk relationships. The plan for the questionnaire survey is provided in Appendix 2. Approximately 30 questionnaires were received from experts in the area of pavement engineering such as pavement material engineers, highway maintenance contractors, highway maintenance consultants, clients and asset managers. Such an approach is to reduce the potential bias arising from an individual judgement. The results of the questionnaires are shown in Appendix 2. The list of experts who participated in the survey is presented in Figure 5-15, while their years of experience are provided in Figure 5-16.

5.14.2. Respondents' General Information

Even though the target sample was 40 participants, requests to participate in the survey were made to 50 participants working in the asphalt field sector of the construction industry in the UAE. However, only 30 returned valid questionnaires with all sections fully responded to. Figures 5-15 and 5-16 summarise the participants' information.

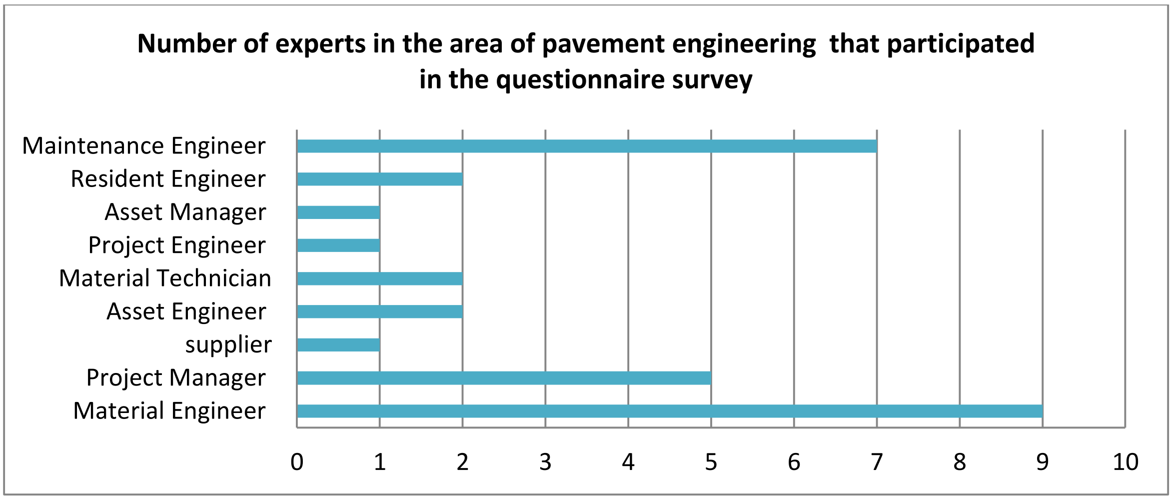

Figure 5-15 Number of experts in the area of pavement engineering that participated in the questionnaire survey

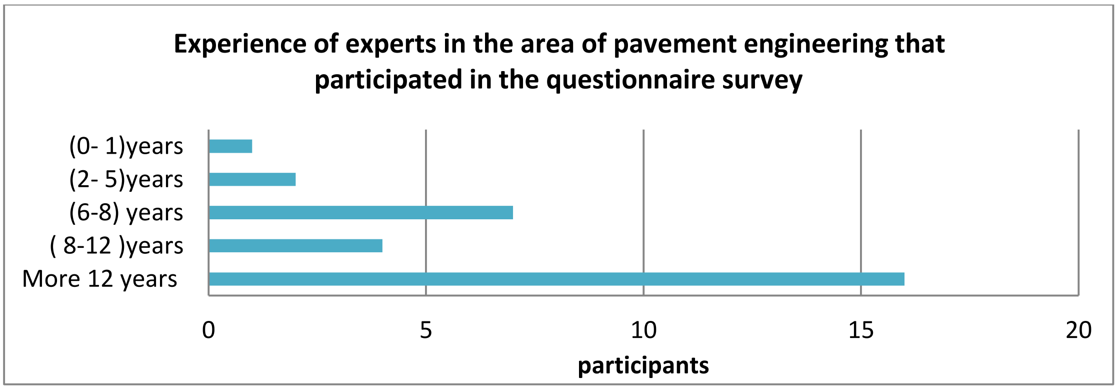

Figure 5-16: Experience of experts in the area of pavement engineering that participated in the questionnaire survey

5.14.3. Descriptive Statistics for Pavement Failure Risk

The primary objective of descriptive statistics is to handle the process of data organising, summarising and presenting to achieve a very convenient and informative set of data (Keller 2009). Descriptive statistics is the best technique to describe the key structures of a collection of data in quantitative terms. In terms of data analysis, Mubaraki (2010) stated that estimation of a parameter for the distribution, to characterise the spread or variability, is an essential task in exploratory data analysis. For example, the mean is the most accepted measure of the central tendency of a distribution of results. Other parameters use the median, which defines the midpoint of distribution, or standard deviation, which is also the most accepted measure of the variability of a distribution. Further characterisation of the data including skewness and kurtosis can also be introduced to define the lack of symmetry and whether the data are peaked or flat with respect to a normal distribution respectively.

The table (5-37) below explains the descriptive statistical analysis for significant risk associated with pavement failure. Such a study was carried out with the aid of the SPSS software program. Data preparation and cleaning such as removing any invalid data or outliers was carried out to obtain the most solid sample. The descriptive statistical analysis in this section includes measurement aspects of non-linear and linear regression analysis. The primary objective is to investigate the most reliable coefficient based on the available data gathered from the questionnaire on pavement failure risk. Further descriptive statistical analysis is presented to examine every single risk and related sub-risk. The Major risks associated with pavement failure due to climate change impacts are highlited in Table 5-38. More details are provided in Chapter 9 section 9.4.

Table 5-37: Descriptive statistics for major risk associated with pavement failure due to climate change impacts

	N	Minimum	Maximum	Sum	Mean	Std. Deviation	Variance	Skewness		Kurtosis	
Y1	30	0.01	0.36	4.86	0.162	0.09845	0.01	0.426	0.42	-0.734	0.833
Y2	30	0.02	0.72	8.35	0.278	0.2452	0.06	0.528	0.42	-1.158	0.833
Y4	30	0.03	0.56	3.97	0.132	0.11782	0.014	1.948	0.42	4.734	0.833
Y3	30	0.01	0.4	4.49	0.149	0.10074	0.01	1.07	0.42	0.597	0.833
Y5	30	0.02	0.56	5.09	0.169	0.12181	0.015	1.44	0.42	2.68	0.833
Y6	30	0.01	0.28	3.7	0.123	0.08759	0.008	0.44	0.42	-1.176	0.833
Y7	30	0	1	5	0.17	0.127	0.016	1.286	0.42	1.878	0.833
Y8	30	0.01	0.4	4.4	0.146	0.10104	0.01	0.661	0.42	-0.35	0.833
Y9	30	0.01	0.56	7.37	0.245	0.16021	0.026	0.068	0.42	-0.814	0.833
Y10	30	0.01	0.72	6.11	0.2037	0.19468	0.038	1.44	0.42	1.709	0.833
Y11	30	0.03	0.8	8.86	0.2953	0.25833	0.067	0.79	0.42	-0.994	0.833
Y12	30	0.01	0.4	2.32	0.0773	0.08741	0.008	2.274	0.42	6.089	0.833
Y13	30	0.01	0.72	7.21	0.2403	0.21386	0.046	0.969	0.42	-0.188	0.833

Table 5-38: Major risks associated with pavement failure due to climate change impacts

Y1	R1.Traffic
Y2	R2.Climate Change
Y3	R3.Pavement Composition
Y4	R4.Pavement Strength
Y5	R5.Pavement Ageing
Y6	R6.Subgrade Soil
Y7	R7.Drainage
Y8	R8.Maintenance
Y9	R9.Construction Quality
Y10	Rutting
Y11	Cracking
Y12	S7.Vehicle speed
Y13	S19.Pavement Thickness

5.15. Summary

This chapter has presented a comprehensive description of the data used in the study. Data suitable for use in the development of the proposed models in Chapter 6 are collected, analysed and summarised in this chapter. Such data are gathered from different transport and weather agencies. A summary of the data used in Chapter 6 for the determination of model coefficients is given in the Table 5-39 as it shown below:

Table 5-39: Model Inputs

Variables inputs	Data	Description
Tpmax(2013)	69.6	Maximum asphalt pavement temperature at 20 mm below the surface in °C. TPmax is determined from mean daily maximum temperature during summer months based on 2010 weather data and match 2013 scenario
Tpmax(2020)	71	Maximum asphalt pavement temperature at 20 mm below the surface in °C. TPmax is determined from mean daily maximum temperature during summer months based on 2010 weather data and match Prediction a pavement temperature based 2020 scenario
Tpmax(2040)	72.3	Maximum asphalt pavement temperature at 20 mm below the surface in °C. TPmax is determined from mean daily maximum temperature during summer months based on 2010 weather data and match Prediction a pavement temperature based 2040 scenario
Tpmax(2060)	73.6	Maximum asphalt pavement temperature at 20 mm below the surface in °C. TPmax is determined from mean daily maximum temperature during summer months based on 2010 weather data and match Prediction a pavement temperature based 2060 scenario
TMI(2013)	-80	Thornthwaite Moisture Index based on 2013 scenarios
TMI(2020)	-85	Thornthwaite Moisture Index based on 2020 scenarios

TMI(2040)	-90	Thornthwaite Moisture Index based on 2040 scenarios
TMI(2060)	-96	Thornthwaite Moisture Index based on 2060 scenarios
m	Data input	Environmental coefficient
AGE3	Data input	Age since last overlay or reconstruction, in years
YE4	Data input	Annual number of equivalent standard axles, in millions/lane
ΔRI	Data input	Incremental change in roughness in m/km IRI
YE4	Data input	Annual number of equivalent standard axles, in millions/lane
VIM%	Data input	Voids in Mix for road asphalt material type m on road section i during year t
SP	Data input	Softening point of binder for road section i with material type m during year t
HS	Data input	Thickness of asphalt layer on section i during year t, in mm
sh	Data input	Average speed of heavy vehicles on section i, in km/h during year t
TPmax	Data input	Maximum asphalt pavement temperature at 20 mm below the surface in ^{o}C
ΔRDS	Data input	Incremental change of rutting in mm
ΔACRA	Data input	Incremental change in area of total cracking during analysis year, in per cent
PCI	Output Results	Pavement Condition Index

6. Chapter 6 Developing Pavement Deteriorations Indicators

6.1. Introduction

The methodology selected to develop the model was described in Chapter 4 and data collection and analysis was discussed in Chapter 5. This chapter’s goal is to estimate the pavement deterioration indicators that later will be used as parameters and inputs that shape the models in Chapters 7, 8 and 9. Such indexes are built through the deterministic model concerning different climate change scenarios. The chapter explains the process used in the development of the model inputs using the obtained analysed data discussed in Chapter 5. The chapter also provides details on the computation of the change in total roughness based on default HDM-4 equations. Developing new equations and coefficients is also investigated, and the results and tested and compared. Finally, the relationship between the International Roughness Index and Pavement Condition Index is also examined. Figure 6-1 section 6.1.1 shows how this chapter is integrated with other chapters.

6.1.1. Chapter 6 Roadmap

Figure 6-2 illustrates the roadmap that structures the sections in this chapter. The main elements in the chapter are the generated data from Chapter 5 which include different climate change scenarios (2013, 2020, 2040, 2060), TMI value (for current year, 2020, 2040 and 2060) and maximum pavement temperature. Other important parameters such as traffic loading, heavy vehicle speed, pavement thickness and ageing were also used. Phase one was to build the model based the default equations and coefficients available in the HDM-4 model to generate the total roughness value. Phase two was to estimate new equations and coefficients based on the analysed data using SPSS. Phase three was to build a model based on the new obtained coefficient and equations in order to determine total change in roughness. Three different experiments were conducted to achieve better calibration of the model that matches reality. The final phase was to build the relationship between Pavement Condition Index (PCI) and Pavement Roughness Index (IRI).

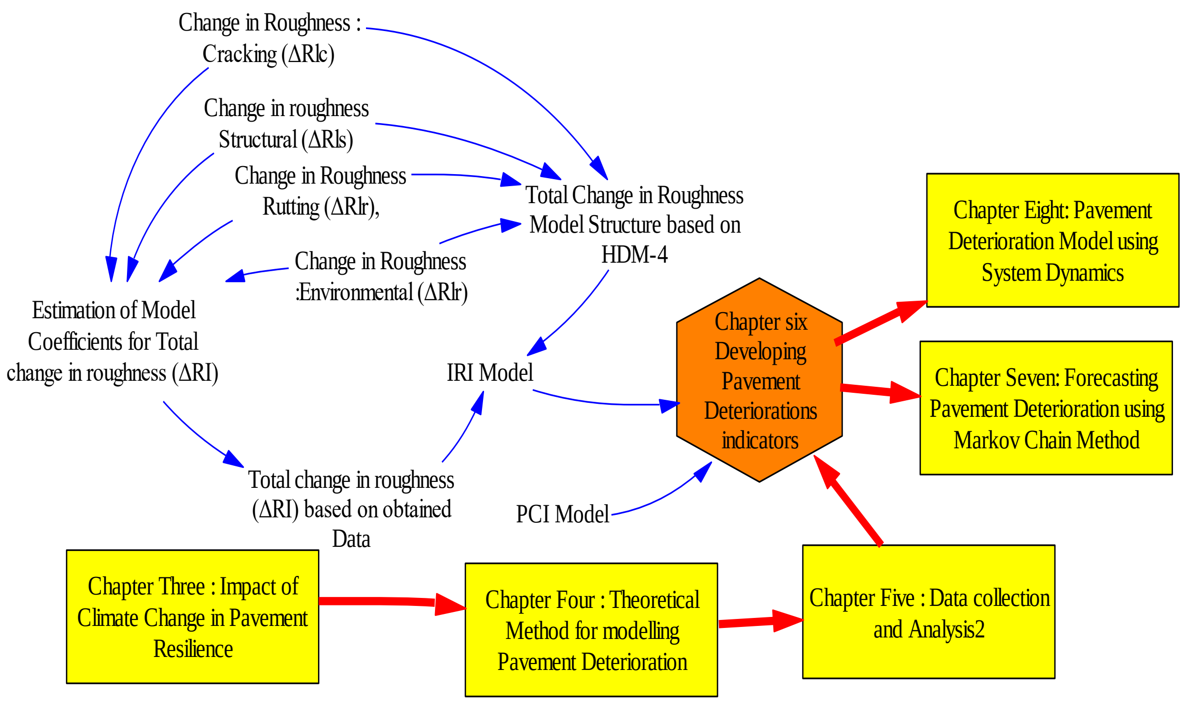

Figure 6-1: The integration of chapter six with other chapters

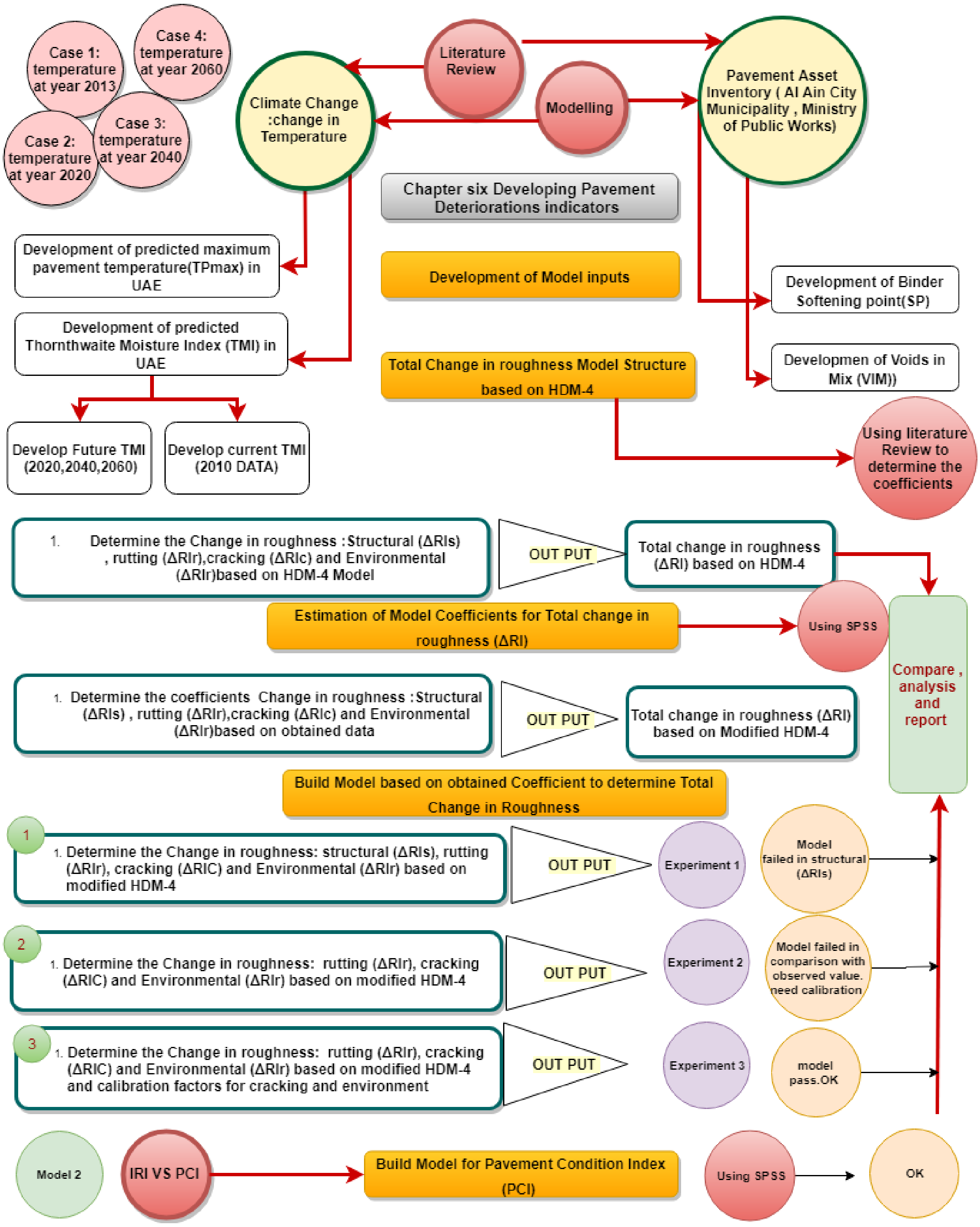

Figure 6-2: The structure of Chapter 6

6.2. Estimating Total Change in Roughness in the Default HDM-4 Model

As was discussed earlier, in chapters 2 and 3, there are different methods to develop pavement performance models. One of the most accepted methods is 'Statistical Regression Analysis' (Amador-Jiménez and Mrawira 2011). Regression models can be in the form of linear or non-linear relations. The statistical regression analysis method is an accepted tool which has been proved to be an effective method for data modelling and analysis (Dong, Huang and Richards 2014). However, this method generates a single value of the dependent variable and extrapolation beyond the limits of the experimental data is limited (Amador-Jiménez and Mrawira 2011). More details are provided in the following section, 6.2.1.

6.2.1. Structural Component of Roughness based on Default HDM-4 Model

Collecting, sampling and analysing the data were presented in Chapter 5. Collected data were grouped into the backward and forward directions. As discussed in Chapter 5, the data collection was carried out to cover the road sections in two directions (backward and forward); the elements of construction quality, the materials used and design criteria are neglected as it is assumed that all road sections were built according to the standard. For model development, the analysis was carried out only on the backward direction roads data. This study follows a similar process as advocated by the HDM-4 model which was discussed in chapters 2 and 3. For this research, in order to deliver the structural component of roughness based on default HDM-4 model, Table 6-1 highlighs the applied equation.

Table 6-1: Structural component of roughness (ΔRIs) based on HDM-4

Main Equation	Variable	Description
$\Delta RIs = Kgs\ a0\ \exp[Kgm\ (m)\ (AGE3)]\ (1 + SNc)^{-5} YE4$		
The structural component of roughness in HDM-4 uses the adjusted structural number (SNP) as the pavement strength indicator, rather than the modified structural number (SNC) that was used in HDM-III. For our case we shall apply SNC = modified structural number for the pavement		

The HDM-4 structural component of roughness	ΔRIs	Incremental change in roughness due to structural deterioration during analysis year, in m/km IRI
	SNc	Modified structural number for the pavement at start of analysis year
	AGE3	Age since last overlay or reconstruction, in years
	YE4	Annual number of equivalent standard axles, in millions/lane
	m	Environmental coefficient
	Kgm	Calibration factor for environmental coefficient =1
	Kgs	Calibration factor for the structural component of roughness=1
	a0	The coefficient values a0 = 134

The model variables input (data) for the structural component of roughness (ΔRIs) based on the highlighted equation is presented in Chapter 5, and the default coefficients are discussed in Chapter 3. The final results for the selected roads are shown in Appendix 3. A sample of the results is presented below in Table 6-2:

Table 6-2: Example of structural component of roughness (ΔRIs) based on HDM-4 model

N	Road	SNPKb	m	AGE	HS	Kgs	kgm	YE4	a0	ΔRls
1	Etihad road	3.5	0.008	11	180	1	1	1.52	134	0.121
3	Manama- RAK Airport	3.5	0.007	11	160	1	1	1.87	134	0.147
5	RAK Airport- Sha'am	3.5	0.013	12	160	1	1	1.67	134	0.141

6.2.2. Rutting Component of Roughness Based on Default HDM-4 Model

This study follows a similar process as advocated by the HDM-4 model which was discussed in chapters 2 and 3. Regarding data variables input and coefficient, the rutting component of roughness based on default HDM-4 model follows a similar approach as the change in roughness structure (ΔRls). The rutting component of roughness equation used is presented as following:

$$\Delta RIr = Kgr\ a0\ (\Delta RDS)$$

Equation 6-1: Rutting component of roughness (ΔRlr) equation based on HDM-4 model

- ΔRIr = Incremental change in roughness due to rutting during analysis year, in m/km IRI

- ΔRDS = Incremental change in of rutting during analysis year, in mm
- Kgr = Calibration factor for the rutting component of roughness

The incremental change in rutting can be directly linked to many elements such as the impact of temperature on the pavement materials' properties. Anyala (2011) questioned the application of the Highway Development and Management System (HDM-4) for shaping decisions on road management policies. He claimed that the current model used in HDM-4 to predict pavement deterioration is only limited to static climate (averages of past climate records). The author has selected Equation 6-1 to link it with the impact of climate change by establishing a new prediction model that is able to handle the prediction of impacts associated with future climate change. The model is based on the following equations and coefficients shown in Table 6-3 and 6-4:

Table 6-3: The HDM-4 rutting component of roughness (ΔRIr)

Main Equation 2	Variable	Description
Incremental change in rut depth due to Plastic deformation (ΔRDS) (ΔRDS) = Krpd a0 × YE4 × $(\boldsymbol{sh})^{a1} \times (\boldsymbol{HS})^{a2} \times (\frac{\boldsymbol{PTmax}}{\boldsymbol{SP}})^{a3} \times (\boldsymbol{VIM})^{a4}$		
The HDM-4 rutting component of roughness	ΔRIr	Incremental change in roughness due to rutting during analysis year, in m/km IRI
	Kgr	Calibration factor for the rutting component of roughness =1
	a0	The coefficient values = 0.088 for ΔRIr
	ΔRDS	Incremental change in standard deviation of rut depth during analysis year, in mm
	Krpd	Calibration factor for the change in rutting Plastic deformation (ΔRDS) r =1
	YE4	Annual number of equivalent standard axles, in millions/lane
	HS	Thickness of asphalt layer on section i during year t, in mm
	PTmax	Maximum asphalt pavement temperature at 20 mm below the surface in ^{o}C. TPmax is determined from mean daily maximum temperature during summer months
	SP	Softening point of binder for road section i with material type m during year t.
	VIM	Voids in Mix for road asphalt material type m on road section i during year t
	sh	Average speed of heavy vehicles on section i, in km/h during year t

Table 6-4: Rutting coefficient for plastic deformation based on default HDM-4 Model

a0	a1	a2	a3	a4
.46	-0.78	0.71	1.34	-1.26

The model variables input (data) for the rutting component of roughness (ΔRlr) is based on the above equation and is presented in Chapter 5, and the default coefficients are discussed in Chapter 3 and shown above in Table 6-4. The final results for the selected roads are shown in Appendix 3. A sample of the results is presented in Tables 6-5 and 6-6

Table 6-5: Example of change in rutting (ΔRDS) based on HDM-4

Road	YE4	VIM%	SP	HS	RIa	sh	TPmax	Krpd	ΔRDS
Ittihad road	1.52	1.222	76.54	180	1.160	48	69.64	1	4.99
Manama- RAK Airport	1.87	1.222	76.54	160	0.980	48	69.64	1	5.64
RAK Airport-Sha'am	1.67	1.216	76.76	160	1.730	50	69.64	1	4.89

Table 6-6: Example of rutting component of roughness (ΔRlr) based on HDM-4

Road	ΔRDS	ΔRIr	Kgr	c0
Ittihad road	4.99	0.44	1	0.088
Manama- RAK Airport	5.64	0.50	1	0.088
RAK Airport-Sha'am	4.80	0.43	1	0.088

6.2.3. Cracking Component of Roughness Based on Default HDM-4 Model

This study follows a similar process as advocated by the HDM-4 model which was discussed in chapters 2 and 3. Cracking component of roughness (ΔRIc) is based on HDM-4 coefficients, and the equations are presented below in Table 6-7:

Table 6-7: HDM-4 cracking component of roughness (ΔRIc)

Main Equation 3	Variable	Description

$\Delta RIc = Kgr\ a0\ \Delta ACRA$		
The HDM-4 cracking component of roughness	ΔRIc	Incremental change in roughness due to cracking during analysis year, in m/km IRI
	Kgc	Calibration factor for the cracking component of roughness=1
	a0	The coefficient values =0.0066
	$\Delta ACRA$	The incremental change in area of total cracking during analysis year, in per cent

The final results for the selected roads are shown in Appendix 3. A sample of the results is presented below in Table 6-8:

Table 6-8: Example of change in roughness due to cracking ΔRIc based on HDM-4

Road	ΔACRA	kgc	a0	ΔRIc
Ittihad road	3.6829	1	0.0066	0.024
Manama- RAK Airport	7.7311	1	0.0066	0.051
RAK Airport-Sha'am	4.4786	1	0.0066	0.030

6.2.4. Environmental Component of Roughness Based on Default HDM-4 Model

This study follows a similar process as advocated by the HDM-4 model which was discussed in chapters 2 and 3. Environmental component of roughness (ΔRIe) based on HDM-4 coefficients and equations is presented in Table 6-9.

Table 6-9: Environmental component of roughness (ΔRIe)

Main Equation 4	Variable	Description
$\Delta RIe = Kgm\ m\ Ria$ $m = 0.197 + 0.000155\ TMI$		
ΔRIe	Incremental change in roughness due to the environment during analysis year, in m/km IRI	
Kgm	Calibration factor for the environmental component (default = 1.0)	
m	Environmental coefficient	
RIa	Roughness at the start of the analysis year, in m/km IRI	
TMI	Thornthwaite Moisture Index	

The final results for the selected roads are shown in Appendix 3. A sample of the results is presented below in Table 6-10:

Table 6-10: Example of environmental component of roughness (ΔRIe) based on HDM-4

Road	ΔRIe	Kgm	m	RIa
Ittihad road	0.010	1	0.0085	1.160
Manama- RAK Airport	0.007	1	0.0072	0.980
RAK Airport-Sha'am	0.022	1	0.0126	1.730

6.2.5. Total Change in Roughness (ΔRI) Based on Default HDM-4

This study follows a similar process as advocated by the HDM-4 model which was discussed in chapters 2 and 3. Based on the HDM-4 model, the total annual incremental change in roughness is the sum of the various components, such as rutting, cracking, environmental and structural components (see Table 6-11). The total incremental change in roughness in HDM-4 is given by:

$$\Delta RI = \Delta RIs + \Delta RIc + \Delta RIr + \Delta RIe$$

Equation 6-2: The total incremental change in roughness in HDM-4

Table 6-11: The total annual incremental change

Main Equation	**Variable**	**Description**
The HDM-4 structural component of roughness	ΔRIs	Incremental change in roughness due to structural deterioration during analysis year, in m/km IRI
The HDM-4 Cracking component of roughness	ΔRIc	Incremental change in roughness due to cracking during analysis year, in m/km IRI
The HDM-4 rutting component of roughness	ΔRIr	Incremental change in roughness due to rutting during analysis year, in m/km IRI
The HDM-4 environmental component of roughness	ΔRIe	Incremental change in roughness due to the environment during analysis year, in m/km IRI

The final results for the selected roads are shown in Appendix 3. A sample of the results is presented below in Table 6-12:

Table 6-12: Example of total change in roughness (ΔRI) based on HDM-4

Road	**ΔRIs**	**ΔRIr**	**ΔRIc**	**ΔRIe**	**ΔRI**
Ittihad road	0.12	0.439	0.024	0.010	0.594
Manama- RAK Airport	0.15	0.497	0.051	0.007	0.702

RAK Airport-Sha'am	0.14	0.431	0.030	0.022	0.623

6.2.6. Results of Default HDM-4 Model

Once the model was built based on HDM-4 equation and variables, the inputs of different climate change scenarios (pavement temperature) were tested and the results for the year 2013 (current weather data), 2020 (projected weather data), 2040 (projected weather data) and 2060 (projected weather data) are recorded and shown in Appendix 3. Examples of all the different scenarios are explained below in tables 6-13, 6-14, 6-15 and 6-16.

Table 6-13: Example of results of HDM-4 model based on 2013 climate change scenario

N	Road Code	Road	Change in roughness structural (ΔRIs)	Change in roughness rutting ΔRIr	Change in roughness due to cracking ΔRIc	Environmental component of roughness (ΔRIe)	The total incremental change in roughness ΔRI
1	E.11	Ittihad road	0.121	0.438	0.024	0.214	0.798
1	E.11	Ittihad road	0.121	0.438	0.054	0.214	0.828
1	E.11	Ittihad road	0.121	0.438	0.079	0.214	0.853

Table 6-14: Example of results of HDM-4 model based on 2020 climate change scenario

N	Road Code	Road	Change in roughness structural (ΔRIs)	Change in roughness rutting ΔRIr	Change in roughness due to cracking ΔRIc	Environmental component of roughness (ΔRIe)	The total incremental change in roughness RI
1	E.11	Ittihad road	0.833	0.450	0.024	0.213	1.521
1	E.11	Ittihad road	0.833	0.450	0.054	0.213	1.551
1	E.11	Ittihad road	0.833	0.450	0.079	0.213	1.576

Table 6-15: Example of results of HDM-4 model based on 2040 climate change scenario

N	Road Code	Road	Change in roughness structura	Change in roughness rutting ΔRIr	Change in roughness due to cracking	Environmental component of roughness (ΔRIe)	The total incremental change in roughness ΔRI
1	E.11	Ittihad road	0.826	0.461	0.024	0.212	1.524

1	E.11	Ittihad road	0.826	0.461	0.054	0.212	1.555
1	E.11	Ittihad road	0.826	0.461	0.079	0.212	1.580

Table 6-16: Example of results of HDM-4 model based on 2060 climate change scenario

N	Road Code	Road	Change in roughness structural (ΔRIs)	Change in roughness rutting ΔRIr	Change in roughness due to cracking ΔRIc	Environmental component of roughness (ΔRIe)	The total incremental change in roughness ΔRI
1	E.11	Ittihad road	0.818	0.472	0.024	0.211	1.526
1	E.11	Ittihad road	0.818	0.472	0.054	0.211	1.556
1	E.11	Ittihad road	0.818	0.472	0.079	0.211	1.581

The default HDM-4 model was run based on the data highlighted in Chapter 5. Such data represented different road lengths with different variables input, such as speed of heavy vehicles, traffic load, pavement thickness, pavement ageing, softening point and VIM. It was tested with four different climate change scenarios; a combination of the results is shown in Figure 6-3. It can be seen that the sample roads showed a significant difference in total change in roughness with different climate change scenarios. The change in total roughness mainly depends on many variables that affect the deterioration of the road asphaltic pavement. The results prove that the rate of degradation of pavement assets is increasing with the increase in the pavement temperature (see the differences between 2013, 2020, 2040 and 2060). These phenomena reflect how the impact of climate change can be seen on pavement condition level. Other factors such as traffic load and composition also contribute significantly to the rate of deterioration.

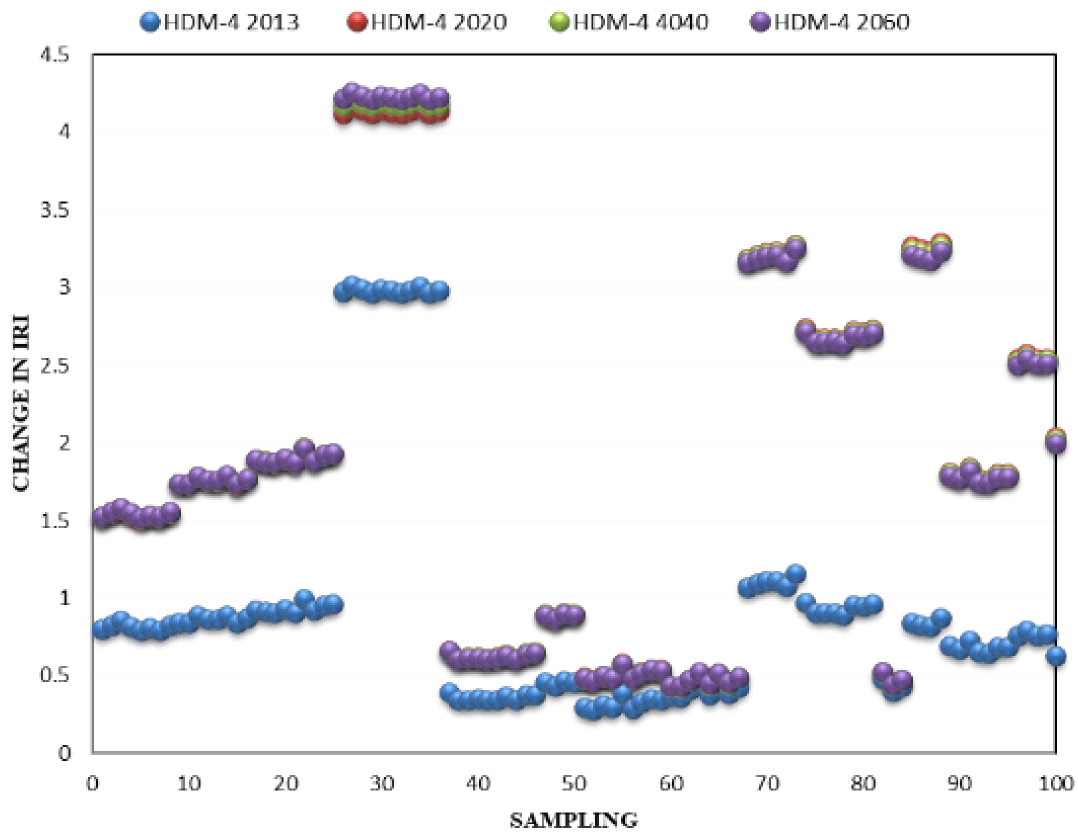

Figure 6-3: HDM-4 model change in IRI based on four different climate change scenarios

6.3. Estimation of the Model Coefficients and Equations for Total Change in Roughness (ΔRI)

A key objective of this section was to model coefficients and equations for the total change in roughness (ΔRI) which can be used for assessing the impact of future changes in climate on asphalt road networks in the UAE. To that end, model structures were developed and tested through three different experiments (1, 2 and 3). The results were compared with the previous default HDM-4 model which was discussed in section 6.2. The model was built using formulated data in Chapter 5 such as climate variable (TPmax), traffic load, heavy vehicle speed, asphaltic pavement thickness, softening point and voids in the mix. Also, cracking, rutting and roughness value for consecutive years as explained in Chapter 5 was applied. Therefore, a HDM-4 model was generated and its coefficients were estimated based on the obtained data. The goodness fit of the model was assessed using R^2 and p-values, as explained in the following sections.

6.3.1. Estimation of the Model Coefficients for Structural Component of Roughness

This sub-section explains the descriptive statistical analysis with the aid of the SPSS software program. Data preparation and cleaning such as removing any invalid data or outliers was carried out to obtain the most solid sample. This descriptive statistical analysis in this section includes measurement aspects of non-linear and linear regression analysis. The primary objective is to investigate the most reliable coefficient based on the available data gathered from the Ministry of Public Works in the UAE. The obtained results are presented below in Table 6-17, 6-18, 6-19 and 6-20.

Table 6-17: Descriptive analysis for data of structural component of roughness (ΔRls)

		YE4	SNPK	m	AGE	HS	ΔRls
N	Valid	89	89	89	89	89	89
	Missing	0	0	0	0	0	0
Mean		1.038	3.500	.009399	13.56	176.40	.219
Median		1.130	3.500	.008769	15.00	180.00	.205
Mode		.21	3.5	.0085	16	180	.027[a]
Std. Deviation		.685	.0000	.0020134	3.662	9.323	.118
Variance		.469	.000	.000	13.408	86.925	.014
Skewness		-.053		.167	-1.013	-.937	.364
Std. Error of		.255	.255	.255	.255	.255	.255
Kurtosis		-1.666		-.635	.269	-.317	-.598
Std. Error of Kurtosis		.506	.506	.506	.506	.506	.506
Range		1.84	.0	.0073	14	30	.484
Minimum		.14	3.5	.0059	5	160	.027
Maximum		1.98	3.5	.0132	19	190	.511
Sum		92.37	311.5	.8365	1207	15700	19.508

Table 6-18: Goodness fit of the structural component of roughness model (ΔRls)

ANOVA[a]			
Source	Sum of Squares	df	Mean Squares
Regression	50.888	7	7.270
Residual	5.574	82	.068
Uncorrected Total	56.462	89	
Corrected Total	7.629	88	
Dependent variable: log_RI[a]			
a. R squared = 1 - (Residual Sum of Squares) / (Corrected Sum of Squares) = .269.			

The goodness fit of the model is shown in Table 6-18. The independent variables were traffic (YE4), modified structural number (SNc), pavement thickness (HS), pavement age (AGE) and environmental factor (m) and the dependent variable was structural component of roughness (ΔRls). Several experiments were conducted to find the best fit model. Several transformations were considered including log, square roots, etc. The derived model was able to explain 26.9% of the variation in the existing data.

Table 6-19: Estimation coefficients for structural component of roughness (ΔRls)

Parameter Estimates				
Parameter	Estimate	Std. Error	95% Confidence Interval	
			Lower Bound	Upper Bound
a0	-1.039	.429	-1.891	-.186
a1	1.232	.245	.744	1.720
a2	-1.436	.963	-3.351	.479
a3	-1.824	.470	-2.759	-.888
a4	-2.832	1.550	-5.915	.252
a5	1.000	.000	1.000	1.000
a6	1.000	.000	1.000	1.000

Table 6-20: Correlations of parameter estimator structural component of roughness (ΔRls)

Correlations of Parameter Estimates							
	a0	a1	a2	a3	a4	a5	a6
a0	1.000	-.660	.345	.981	.344	.	.
a1	-.660	1.000	-.263	-.789	-.280	.	.
a2	.345	-.263	1.000	.306	.990	.	.
a3	.981	-.789	.306	1.000	.307	.	.
a4	.344	-.280	.990	.307	1.000	.	.
a5	.	.	.	.	.	.	.
a6	.	.	.	.	.	.	.

Structural component of roughness (ΔRls), parameter estimates column provides a gradient of the non-linear regression which is the regression coefficient **(a0= -1.039, a1=1.232 , a2-1.436, a3=-1.824 and a4=-2.832)**. Thus, the final equation for change in structural component of roughness (ΔRls) is derived as per equation 6-3 and Table 6-2.

$$\mathbf{LOG\ (\Delta RIs) = a0\times \log(m) + a1\times \log(AGE3) + a2 \times \log(YE4)^3 + a3 \times \log(HS) + (\log(SNc) \times \log(YE4)^2)\times a4}$$

Equation 6-3: New equation for structural component of roughness (ΔRls)

Table 6-21: The coefficient of structural component of roughness (ΔRIs) based on the obtained data (Improved HDM-4)

Main Equation	Variable	Description
LOG (ΔRIs) = a0× log(m) + a1× log (AGE3) + a2 × log (YE4)^3 + a3 × log (HS) + (log (SNc) × log (YE4)^2)× a4		
The obtained structural component of roughness (improved HDM-4)	ΔRIs	Incremental change in roughness due to structural deterioration during analysis year, in m/km IRI
	SNc	Modified structural number for the pavement at start of analysis year
	AGE3	Age since last overlay or reconstruction, in years
	YE4	Annual number of equivalent standard axles, in millions/lane
	m	Environmental coefficient
Coefficient	a0	-1.039
Coefficient	a1	1.232
Coefficient	a2	-1.436
Coefficient	a3	-1.824
Coefficient	a4	-2.832

6.3.2. Estimation of the Model Coefficients for Rutting Component of Roughness

6.3.2.1. Rutting (ΔRDS) based on Obtained Data

For analysing the change in rutting, a similar approach to structural component of roughness (ΔRIs) was conducted using descriptive statistical analysis with the aid of the SPSS software program. The obtained results are presented below in Table 6-22, 6-23, 6-24 and 6-25.

Table 6-22: Statistical descriptive analysis for change in rutting (ΔRDS) based on obtained data

Statistics									
		YE4	VIM%	SP	HS	sh	TPmax	Krpd	ΔRDS
N	Valid	116	116	116	116	116	116	116	116
Mean		2.086	1.219	76.612	175.86	44.88	69.637	1.00	1.1890
Median		1.520	1.216	76.7619	180.0	46.00	69.637	1.00	1.053
Mode		7.67	1.195	77.486	180	48	69.64	1	1.37
Std. Deviation		2.382	.028	1.088155	9.331	4.322	.00000	.000	.775
Variance		5.674	.001	1.184	87.07	18.68	.000	.000	.601
Skewness		1.629	.805	-.837	-.909	-.995			.843
Std. Error of Skewness		.225	.225	.225	.225	.225	.225	.225	.225
Kurtosis		1.284	-.677	-.580	-.524	.099			.259
Std. Error of Kurtosis		.446	.446	.446	.446	.446	.446	.446	.446
Range		7.53	.0897	3.956	30	15	.00	0	3.43
Minimum		.14	1.187	73.993	160	35	69.64	1	.17
Maximum		7.67	1.277	77.950	190	50	69.64	1	3.60

Table 6-23: Goodness fit of change in rutting (ΔRDS) based on obtained data

ANOVA[a]			
Source	Sum of Squares	df	Mean Squares
Regression	205.841	7	29.406
Residual	27.288	109	.250

Uncorrected Total	233.128	116
Corrected Total	69.132	115
Dependent variable: ΔRDS_M		
a. R squared = 1 - (Residual Sum of Squares) / (Corrected Sum of Squares) = **.605.**		

The goodness fit of the model is shown in Table 6-23. The independent variables were traffic (YE4), air voids (VIM%), pavement thickness (HS), softening point (SP), heavy vehicle speed (sh) and maximum pavement temperature (TPmax) and the dependent variable was change in rutting (ΔRDS). Several experiments were conducted to find the best fit model. Several transformations were considered including log, square roots, etc. The derived model was able to explain 60.5% of the variation in the existing data.

Table 6-24: Parameter estimates for change in rutting (ΔRDS) based on obtained data

Parameter Estimates				
Parameter	**Estimate**	**Std. Error**	**95% Confidence Interval**	
			Lower Bound	**Upper Bound**
a0	11.863	74194332.282	-147050742.643	147050766.369
a2	-7.234	1.792	-10.786	-3.682
a3	-3.131	4.362	-11.776	5.514
a1	-5.244	1.674	-8.562	-1.925
a4	15.729	1478900.941	-2931117.857	2931149.316
a5	.835	.260	.320	1.350
a6	.045	286189.793	-567218.819	567218.910

Table 6-25: Correlation of parameter estimates for change in rutting (ΔRDS) based on obtained data

Correlations of Parameter Estimates							
	a0	a2	a3	a1	a4	a5	a6
a0	1.000	.740	-.147	.647	-1.000	-.671	-1.000
a2	.740	1.000	.083	.762	-.740	-.644	-.740
a3	-.147	.083	1.000	.241	.147	.495	.147
a1	.647	.762	.241	1.000	-.647	-.647	-.647
a4	-1.000	-.740	.147	-.647	1.000	.671	1.000

a5	-.671	-.644	.495	-.647	.671	1.000	.671
a6	-1.000	-.740	.147	-.647	1.000	.671	1.000

For change in rutting (ΔRDS), the parameter estimates column provides a gradient of the non-linear regression which is the regression coefficients are **a0=11.863, a1= -5.244, a2= -7.234, a3=-3.131, a4= 15.729, a5= 0.835** and **a6=0.045**. Thus, the final equation for change in rutting (ΔRDS) is derived as per the equation 6-4 and Tables 6-26 and 6-27.

$$\Delta RDS = a0 \times (YE4)^{a5} \times (sh)^{a1} \times (HS)^{a2} \times (SP/VIM)^{a3}) \times TPmax \times a4 + a0 \times a6$$

Equation 6-4: New equation for change in rutting (ΔRDS)

Table 6-26: The coefficient of rutting component of roughness (ΔRIr) based on obtained equations

Main Equation 2	Variable	Description
Incremental change in rut depth due to plastic deformation (ΔRDS) $\Delta RDS = a0 \times (YE4)^{a5} \times (sh)^{a1} \times (HS)^{a2} \times (SP/VIM)^{a3}) \times TPmax \times a4 + a0 \times a6$		
The new rutting component (improved HDM-4) of roughness model with estimated coefficients	ΔRIr	Incremental change in roughness due to rutting during analysis year, in m/km IRI
	ΔRDS	Incremental change in standard deviation of rut depth during analysis year, in mm
	YE4	Annual number of equivalent standard axles, in millions/lane
	HS	Thickness of asphalt layer on section i during year t, in mm
	PTmax	Maximum asphalt pavement temperature at 20 mm below the surface in °C. TPmax is determined from mean daily maximum temperature during summer months
	SP	Softening point of binder for road section i with material type m during year t.
	VIM	Voids in Mix for road asphalt material type m on road section i during year t
	sh	Average speed of heavy vehicles on section i, in km/h during year t

Table 6-27: Rutting estimated coefficient new model develop by the author

a0	11.863
a2	-7.234
a3	-3.131
a1	-5.244
a4	15.729
a5	.835
a6	.045

6.3.2.2. Rutting Component of Roughness based on the Obtained Data

In terms of the default HDM-4, change in roughness – rutting (ΔRlr) equation used is presented as ΔRIr = Kgr a0 (ΔRDS). Based on the obtained data, the main objective is to determine the relationship between incremental change in rutting depth during analysis year, in mm (ΔRDS) and change in roughness due rutting component (ΔRlr) year, in m/km ΔRIr. The analysis was conducted using descriptive statistical analysis with the aid of the SPSS software program. The following graph (Figure 6-4) illustrates the relationship between incremental change in rutting depth during analysis year, in mm (ΔRDS) and rutting component of roughness (ΔRIr) year, in m/km ΔRIr ,which is a non-linear relationship. SPSS software was run to test the regression and correlation between the two independent and dependent variables. The obtained results are presented below in Table 6-28, 6-29 and 6-30.

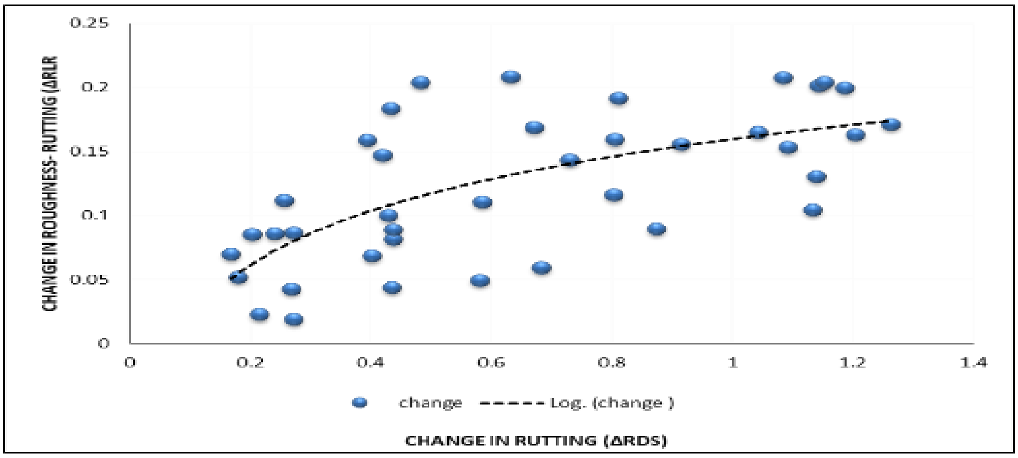

Figure 6-4: The relationship between change in rutting (ΔRDS) and rutting component of roughness (ΔRIr)

Table 6-28: Statistical descriptive analysis for rutting component of roughness (ΔRIr)

Statistics		ΔRDS	ΔRlr
N	Valid	39	39
	Missing	0	0
Mean		.653	.123
Median		.583	.116
Mode		.168[a]	.019[a]
Std. Deviation		.352	.057
Variance		.124	.003
Skewness		.301	-.085
Std. Error of Skewness		.378	.378
Kurtosis		-1.321	-1.195
Std. Error of Kurtosis		.741	.741
Range		1.095	.189
Minimum		.168	.019
Maximum		1.264	.209
Sum		25.468	4.813

Table 6-29: Goodness fit of rutting component of roughness (ΔRIr)

ANOVAa			
Source	Sum of Squares	df	Mean Squares
Regression	.648	3	.216
Residual	.071	36	.002
Uncorrected Total	.719	39	
Corrected Total	.125	38	
Dependent variable: ΔRls			
a. R squared = 1 - (Residual Sum of Squares) / (Corrected Sum of Squares) = .431.			

The goodness fit of the model is shown in Table 6-29. The independent variable was change in rutting (ΔRDS) and the dependent variable was rutting component of roughness (ΔRIr). Several experiments were conducted to find the best fit model. Several transformations were considered including log, square roots, etc. The derived model was able to explain 43.1% of the variation in the existing data.

Table 6-30: Parameter estimator for change in rutting (ΔRDS) based on obtained data

Parameter Estimates				
Parameter	Estimate	Std. Error	95% Confidence Interval	
			Lower Bound	Upper Bound
a 0	.061	.012	.037	.085
a 1	.160	.010	.140	.180

The rutting component of roughness (ΔRIr), parameter estimates column provides the gradient of the non-linear regression which is the regression coefficients are **a0=0.061 and a1= 0.160**.

$$\Delta RIr = a0 \times \ln(\Delta RDS) + a1$$

Equation 6-5: New equations for rutting component of roughness (ΔRIr)

6.3.3. Estimation of the Model Coefficients for Cracking Component of Roughness

For analysis of the cracking component of roughness (ΔRIc), a similar approach to that used for the structural component of roughness (ΔRls) was conducted using descriptive statistical analysis and non-linear regression with the aid of the SPSS software program. This study follows a similar process as suggested by the HDM-4 model. The obtained results are presented below in Table 6-31, 6-32, 6-33 and 6-25.

Table 6-31: Statistical descriptive analysis for cracking component of roughness (ΔRIc)

Statistics			
		ΔRIc	ΔACRA
N	Valid	73	73
	Missing	0	0
Mean		.254	4.020
Std. Error of Mean		.023	.535
Median		.202	2.861
Mode		.025[a]	.000
Std. Deviation		.196	4.573
Variance		.039	20.914
Skewness		1.353	1.824
Std. Error of Skewness		.281	.281

Kurtosis	1.296	3.737
Std. Error of Kurtosis	.555	.555
Range	.822	21.879
Minimum	.025	.000
Maximum	.847	21.879
Sum	18.602	293.527
a. Multiple modes exist. The smallest value is shown		

Table 6-32: Goodness fit cracking component of roughness (ΔRIc)

ANOVA[a]			
Source	Sum of Squares	df	Mean Squares
Regression	2.637	3	.879
Residual	.840	52	.016
Uncorrected Total	3.477	55	
Corrected Total	1.222	54	
Dependent variable: Change in roughness			
a. R squared = 1 - (Residual Sum of Squares)/(Corrected Sum of Squares) = .313			

The goodness fit of the model is shown in Table 6-32. The independent variable was change in cracking (ΔACRA) and the dependent variable was cracking component of roughness (ΔRIc). Several experiments were conducted to find the best fit model. Several transformations were considered including log, square roots, etc. The derived model was able to explained 31.3% of the variation in the existing data.

Table 6-33: Parameter estimator for cracking component of roughness (ΔRIc)

Parameter Estimates				
Parameter	Estimate	Std. Error	95% Confidence Interval	
			Lower Bound	Upper Bound
a0	-.003	.004	-.011	.005
a 1	.058	.024	.009	.107
a2	.104	.028	.047	.161

For change in cracking (ΔACRA), the parameter estimates column provides a gradient of the non-linear regression, which is the regression coefficients are **a0=-0.003, a1= 0.058 and a2= 0.104.**

$$\Delta RIc = a0\times (\Delta ACRA)^2 + a1\times \Delta ACRA + a2$$

Equation 6-6: New equations for cracking component of roughness (ΔRIc)

Table 6-34: Improved HDM-4 cracking component of roughness (ΔRIc)

Main Equation 3	Variable	Description
	$\Delta RIc = a0\times (\Delta ACRA)^2 + a1\times \Delta ACRA + a2$	
The improved HDM-4 cracking component of roughness	ΔRIc	Incremental change in roughness due to cracking during analysis year, in m/km IRI
	ΔACRA	Incremental change in area of total cracking during analysis year, in per cent

Table 6-35: Cracking component of roughness estimated coefficient new model develop by the author

Parameter	Estimate
a0	-0.003
a 1	0.058
a2	0.104

6.3.4. Estimation of the Model Coefficients for Environmental Component of Roughness

Environmental factor m was determined from TMI equation (m = 0.197+ 0.000155 TMI). For TMI value, the following results were selected as input TMI value for the three future scenarios as minimum for 2020, average for 2040 and maximum for 2040-2079 as per Table 6-36.

Table 6-36: The inputs of TMI value for the three future scenarios

TMI (2020) Minimum scenario	TMI (2040) Average scenario	TMI (2040-2069) Maximum scenario
-85	-90	96

There is no estimated coefficient for the environmental component (ΔRIe); therefore, a similar equation to the default HDM-4 was applied.

Default HDM-4 model and modified HDM-4 model in terms of the total incremental change in roughness are presented in Table 6-37 and Model inputs for both HDM-4 and proposed model inputs are shown in Table 6-38.

Table 6-37: Default HDM-4 model and modified HDM-4 model in terms of the total incremental change in roughness

Description	Author proposed Model	Default HDM-4
The total incremental change in roughness	**RI (total) = RIa + ΔRI**	**RI (total) = RIa + ΔRI**
The total incremental change in roughness	**ΔRI = ΔRIs + ΔRIc + ΔRIr + ΔRIe**	**ΔRI = ΔRIs + ΔRIc + ΔRIr + ΔRIe**
The HDM-4 structural component of roughness	**LOG (ΔRIs) = a0× log(m) + a1× log (AGE3) + a2 × log (YE4)^3 + a3 × log (HS) + (log (SNc) × log (YE4)^2)× a4**	**ΔRIs = Kgs a0 exp[Kgm (m) (AGE3)]** $(1 + SNc)^{-5}$**YE4**
The HDM-4 rutting component of roughness	**ΔRIr = a0× Ln (ΔRDS) + a1**	**ΔRIr = Kgr a0 (ΔRDS)**
Deformation for rutting ΔRDS	**(ΔRDS) = a0 ×** $(YE4)^{a5} \times (sh)^{a1} \times (HS)^{a2} \times (\frac{SP}{VIM})^{a3} \times$ **TPmax × a4 + a0 × a6**	**ΔRDS) = Krpd a0 × YE4 ×** $(sh)^{a1} \times (HS)^{a2} \times (\frac{PTmax}{SP})^{a3} \times (VIM)^{a4}$
Softening point	**SP = a0 × Ln(AGE + 0.0001) + a1**	**SP = a0 × Ln(AGE + 0.0001) +a1**
Voids in Air	**VIM = a0 × Ln(AGE + 0.0001) + a1**	**VIM = a0 × Ln(AGE + 0.0001) + a1**
The HDM-4 cracking component of roughness	**ΔRIc = a0× (ΔACRA)^2 + a1× ΔACRA + a2**	**ΔRIc = Kgr a0 ΔACRA**
The HDM-4 environmental component of roughness	**ΔRIe = Kgm m RIa**	**ΔRIe = Kgm m RIa**

Environmental coefficient	**m = 0.197+ 0.000155 TMI**	**m = 0.197+ 0.000155 TMI**

Table 6-38: Model inputs for both HDM-4 and proposed model

Case	Variables inputs	Author Model (Constant value, coefficients)	Default HDM-4 Model (Constant value, coefficients)	Description
Scenario 1	Tpmax(2013)	69.6	69.6	Maximum asphalt pavement temperature at 20 mm below the surface in °C. TPmax is determined from mean daily maximum temperature during summer months based on 2010 weather data and match 2013 scenario
Scenario 2	Tpmax(2020)	71	71	Maximum asphalt pavement temperature at 20 mm below the surface in °C. TPmax is determined from mean daily maximum temperature during summer months based on 2010 weather data and match Prediction of pavement temperature based 2020 scenario
Scenario 3	Tpmax(2040)	72.3	72.3	Maximum asphalt pavement temperature at 20 mm below the surface in °C. TPmax is determined from mean daily maximum temperature during summer months based on 2010 weather data and match Prediction of pavement temperature based 2040 scenario
Scenario 4	Tpmax(2060)	73.6	73.6	Maximum asphalt pavement temperature at 20 mm below the surface in °C. TPmax is determined from mean daily maximum temperature during summer months based on 2010 weather data and match Prediction of pavement temperature based 2060 scenario
Scenario 1	TMI (2013)	-80	-80	Thornthwaite Moisture Index based on 2013 scenarios
Scenario 2	TMI (2020)	-85	-85	Thornthwaite Moisture Index based on 2020 scenarios
Scenario 3	TMI (2040)	-90	-90	Thornthwaite Moisture Index based on 2040 scenarios
Scenario 4	TMI (2060)	-96	-96	Thornthwaite Moisture Index based on 2060 scenarios

The HDM-4 structural component of roughness	SNPKb	3.5	3.5	Modified structural number for the pavement at start of analysis year , Average value based on data from Alain city municipality is 3.5
	m	Data input	Data input	Environmental coefficient
	AGE3	Data input	Data input	Age since last overlay or reconstruction, in years
	Kgs	1	1	Calibration factor for environmental coefficient =1
	kgm	1	1	Calibration factor for the structural component of roughness=1
	YE4	Data input	Data input	Annual number of equivalent standard axles, in millions/lane
	a0	-1.039	a0=134	The coefficient values for change in roughness structural (ΔRls)
	a1	1.232		
	a2	-1.436		
	a3	-1.824		
	a4	-2.832		
	ΔRls	output Results	output Results	Incremental change in roughness due to structural deterioration during analysis year, in m/km IRI
Deformation for rutting ΔRDS	YE4	Data input	Data input	Annual number of equivalent standard axles, in millions/lane
	VIM%	Data input	Data input	Voids in Mix for road asphalt material type m on road section i during year t
	SP	Data input	Data input	Softening point of binder for road section i with material type m during year t.
	HS	Data input	Data input	Thickness of asphalt layer on section i during year t, in mm
	sh	Data input	Data input	Average speed of heavy vehicles on section i, in km/h during year t
	TPmax	based on year	based on year	Maximum asphalt pavement temperature at 20mm below the surface in oC
	Krpd	1	1	Calibration factor for the change in rutting Plastic deformation (ΔRDS) r =1
	b0	11.863	2.46	The coefficient values for deformation for rutting ΔRDS
	b1	-5.244	-0.78	
	b2	-7.234	0.71	
	b3	-3.131	1.34	
	b4	15.729	-1.26	
	b5	0.835	N/A	
	b6	0.045	N/A	
	ΔRDS	output Results	output Results	Incremental change in standard deviation of rut depth during analysis year, in mm

The HDM-4 rutting component of roughness	ΔRIr	output Results	output Results	Incremental change in roughness due to rutting during analysis year, in m/km IRI
	Kgr	1		Calibration factor for the rutting component of roughness =1
	c0	0.061	0.088	The coefficient values for ΔRIr
	c1	0.16	N/A	
The HDM-4 cracking component of roughness	$\Delta ACRA$	Data input	Data input	Incremental change in area of total cracking during analysis year, in per cent
	d0	-0.003	0.0066	The coefficient values for ΔRIc
	d1	0.058	N/A	
	d2	0.104	N/A	
	ΔRIc	output Results	output Results	Incremental change in roughness due to cracking during analysis year, in m/km IRI
	kgc	1	1	Calibration factor for the cracking component of roughness=1
The HDM-4 environmental component of roughness	ΔRIe	output Results	output Results	Incremental change in roughness due to the environment during analysis year, in m/km IRI
	Kgm	1	1	Calibration factor for the environmental component (default = 1.0)
	TMI	based on year	based on year	Thornthwaite Moisture Index
	m	Data input	Data input	Environmental coefficient
	RIa	Data input	Data input	Roughness at the start of the analysis year, in m/km IRI
The total incremental change in roughness	ΔRI	output Results	output Results	Total Change in Roughness

6.4. Modelling Total Change in Roughness

6.4.1. Experimental Model 1: Determine Total Change in Roughness

To develop a model that assesses the impact of climate change on road roughness, the HDM-4 model was improved with new equations, coefficients and variables. Based on the default HDM-4 model, the determination of the total annual incremental change in roughness can be achieved through the summation of the various components, such as rutting, cracking, environmental and structural elements ($\Delta RI = \Delta RIs + \Delta RIc + \Delta RIr + \Delta RIe$). The non-linear equation and coefficients for each component were determined as is discussed earlier, in sub-section 6.3. In such a model, the collected data (see Chapter 5 section 5.4) are applied to take into consideration one reading of various variables every 5000 m. Once the model was built based on the new modified HDM-4 equations and coefficients, it was tested with different inputs of climate change scenarios (pavement temperature). These scenarios were for the year 2013 (current weather data), 2020 (projected weather data), 2040 (projected weather data) and 2060 (projected weather data), and are recorded and shown in Appendix 3. Examples of all the different scenarios are provided in Tables 6-39, 6-40, 6-41and 6-42 below:

Table 6-39: Example of experiment model 1-total change in roughness 2013 scenario

N	Road Code	Road	Change in roughness structural (ΔRIs)	Change in roughness rutting ΔRIr	Change in roughness due to cracking ΔRIc	Environmental component of roughness (ΔRIe)	The total incremental change in roughness ΔRI
1	E.11	Ittihad road	0.0003	0.1478	0.276	0.214	0.64
1	E.11	Ittihad road	0.0003	0.1478	0.3783	0.214	0.74
1	E.11	Ittihad road	0.0003	0.1478	0.3679	0.214	0.73

Table 6-40: Example of experiment model 1-total change in roughness 2020 Scenario

N	Road Code	Road	Change in roughness structural (ΔRIs)	Change in roughness rutting ΔRIr	Change in roughness due to cracking ΔRIc	Environmental component of roughness (ΔRIe)	The total incremental change in roughness ΔRI
1	E.11	Ittihad road	0.0003	0.159	0.2769	0.183	0.6201
1	E.11	Ittihad road	0.0003	0.154	0.3783	0.2132	0.7469
1	E.11	Ittihad road	0.0003	0.154	0.3679	0.2132	0.7365

Table 6-41: Example of experiment model 1-total change in roughness 2040 Scenario

N	Road Code	Road	Change in roughness structural (ΔRIs)	Change in roughness rutting ΔRIr	Change in roughness due to cracking ΔRIc	Environmental component of roughness (ΔRIe)	The total incremental change in roughness ΔRI
1	E.11	Ittihad road	0.0003	0.1628	0.276	0.212	0.652
1	E.11	Ittihad road	0.0003	0.1628	0.378	0.212	0.754
1	E.11	Ittihad road	0.0003	0.1628	0.367	0.212	0.743

Table 6-42: Example of experiment model 1- total change in roughness 2060 Scenario

N	Road Code	Road	Change in roughness structural (ΔRIs)	Change in roughness rutting ΔRIr	Change in roughness due to cracking ΔRIc	Environmental component of roughness (ΔRIe)	The total incremental change in roughness ΔRI
1	E.11	Ittihad road	0.0003	0.171	0.276	0.211	0.660
1	E.11	Ittihad road	0.0003	0.171	0.378	0.211	0.761
1	E.11	Ittihad road	0.0003	0.171	0.367	0.211	0.751

6.4.1.1. Deficiency in Experiment Model 1

According to the default HDM-4 model, the determination of the total annual incremental change in roughness can be achieved through the summation of the various components. However, the results for some road sections with different traffic values achieved unexpected outcomes for the structural component of roughness (ΔRIs) (Table 6-42. It appears that the developed equation is very sensitive to the traffic loading.

$$LOG(\Delta RIs) = a0\times \log(m) + a1\times \log(AGE3) + a2 \times \log(YE4)^3 + a3 \times \log(HS) + (\log(SNc) \times \log(YE4)^2)\times a4$$

Moreover, accordingly, the goodness fit of the model is shown in Table 6-18. The independent variables were traffic (YE4), modified structural number (SNc), pavement thickness (HS), pavement age (AGE) and environmental factor (m), and the dependent variable was structural component of roughness (ΔRls). The derived model was able to explained 26.9% of the variation in the existing data. Such a value appears to be insignificant and contributes to the weakness of the results (see Table 6-43). Therefore, it is proposed to improve the equation by excluding the component of the change in roughness – structural (ΔRls). The final equation can be seen below:

$$\Delta RI = \Delta RIc + \Delta RIr + \Delta RIe$$

Equation 6-7: Modified total annual incremental change in roughness

The new modified total annual incremental change in roughness was tested through experiment 2.

Table 6-43: Example of deficiency in experiment model 1, 2013 climate change scenario

N	Road Code	Road	Change in roughness structural (ΔRls)	Change in roughness rutting ΔRIr	Change in roughness due to cracking ΔRIc	Environmental component of roughness (ΔRIe)	The total incremental change in roughness ΔRI
8	E55.1	Dhaid - Madam	**1382.844**	0.129	0.382	0.241	1383.599
8	E55.1	Dhaid - Madam	**1382.844**	0.129	0.236	0.241	1383.452
10	E55.2	Madam - Shiweb	**39.303**	0.131	0.367	0.278	40.081
10	E55.2	Madam - Shiweb	**39.303**	0.131	0.3728	0.278	40.086
12	E55.3	Umm Al Quwaim - Dhaid	**16618.800**	0.126	0.269	0.214	16619.469
12	E55.3	Umm Al Quwaim - Dhaid	**16618.850**	0.126	0.153	0.214	16619.351

6.4.2. Experiment 2: Determine Total Change in Roughness (Improving Equation)

Experiment 2 was based on testing the model with a new improved equation of total change in roughness ($\Delta RI = \Delta RIc + \Delta RIr + \Delta RIe$) using a similar approach as experiment 1 concerning coefficients and variables input; the model was conducted and it was also tested with different inputs of climate change scenarios (pavement temperature). The obtained results were recorded and are shown in Appendix 3. Examples of all the different scenarios are provided in Tables 6-44, 6-45, 6-46 and 6-47.

Table 6-44: Example of experiment model 2- total change in roughness 2013 climate change scenario

N	Road Code	Road	Change in roughness structural (ΔRIs)	Change in roughness rutting ΔRIr	Change in roughness due to cracking ΔRIc	Environmental component of roughness (ΔRIe)	The total incremental change in roughness RI
1	E.11	Ittihad road	0	0.147	0.276	0.214	0.638
3	E18.1	Manama- RAK Airport	0	0.177	0.249	0.180	0.607
5	E18.2	RAK Airport-Sha'am	0	0.166	0.2481	0.319	0.733

Table 6-45: Example of experiment model 2- total change in roughness 2020 climate change scenario

N	Road Code	Road	Change in roughness structural (ΔRIs)	Change in roughness rutting ΔRIr	Change in roughness due to cracking ΔRIc	Environmental component of roughness (ΔRIe)	The total incremental change in roughness ΔRI
1	E.11	Ittihad road	0	0.159	0.276	0.183	0.619
3	E18.1	Manama-RAK Airport	0	0.189	0.249	0.180	0.618
5	E18.2	RAK Airport-Sha'am	0	0.176	0.378	0.3180	0.872

Table 6-46: Example of experiment model 2- total change in roughness 2040 climate change scenario

N	Road Code	Road	Change in roughness structural (ΔRIs)	Change in roughness rutting ΔRIr	Change in roughness due to cracking ΔRIc	Environmental component of roughness (ΔRIe)	The total incremental change in roughness ΔRI
1	E.11	Ittihad road	0	0.162	0.276	0.212	0.652
3	E18.1	Manama- RAK Airport	0	0.201	0.373	0.179	0.753
5	E18.2	RAK Airport- Sha'am	0	0.187	0.303	0.316	0.807

Table 6-47: Example of experiment model 2- total change in roughness 2060 climate change scenario

N	Road Code	Road	Change in roughness structural (ΔRIs)	Change in roughness rutting ΔRIr	Change in roughness due to cracking ΔRIc	Environmental component of roughness (ΔRIe)	The total incremental change in roughness ΔRI
1	E.11	Ittihad road	0	0.171	0.276	0.211	0.660
3	E18.1	Manama- RAK Airport	0	0.214	0.249	0.178	0.642
5	E18.2	RAK Airport- Sha'am	0	0.198	0.303	0.315	0.817

The modified HDM-4 model (new equations and coefficients) tested data inputs including different roads with different variables such as speed of heavy vehicles, traffic load, pavement thickness, pavement ageing, softening point and VIM. The sampling test was made for every 5000 m of the road to represent the condition of the road segment based on the 2013 data scenario and with other forecasted scenarios of climate change (2020, 2040 and 2060). The combination of results is shown in Figure 6-5 below. It can be seen that the sample road sections showed a significant difference in change in roughness with different climate change impacts. The change in roughness mainly depends on many variables that affect the deterioration of the road asphaltic pavement. The results prove that the rate of degradation of pavement assets is increasing with the increase of the pavement temperature (see the differences between 2013, 2020, 2040 and 2060). These phenomena reflect how the impact of climate change can be seen on the pavement condition level. There is no doubt that other factors such as traffic load and composition contribute significantly to the rate of deterioration. Overall, the proposed model using the new improved equation of total change in roughness ($\Delta RI = \Delta RIc + \Delta RIr + \Delta RIe$) provides confidence in the outcome results; however, still there is a need to prove how accurate the model can be once compared with real data on roughness. Therefore, experiment 3 is conducted to test the reliability of the model, as discussed in the following section.

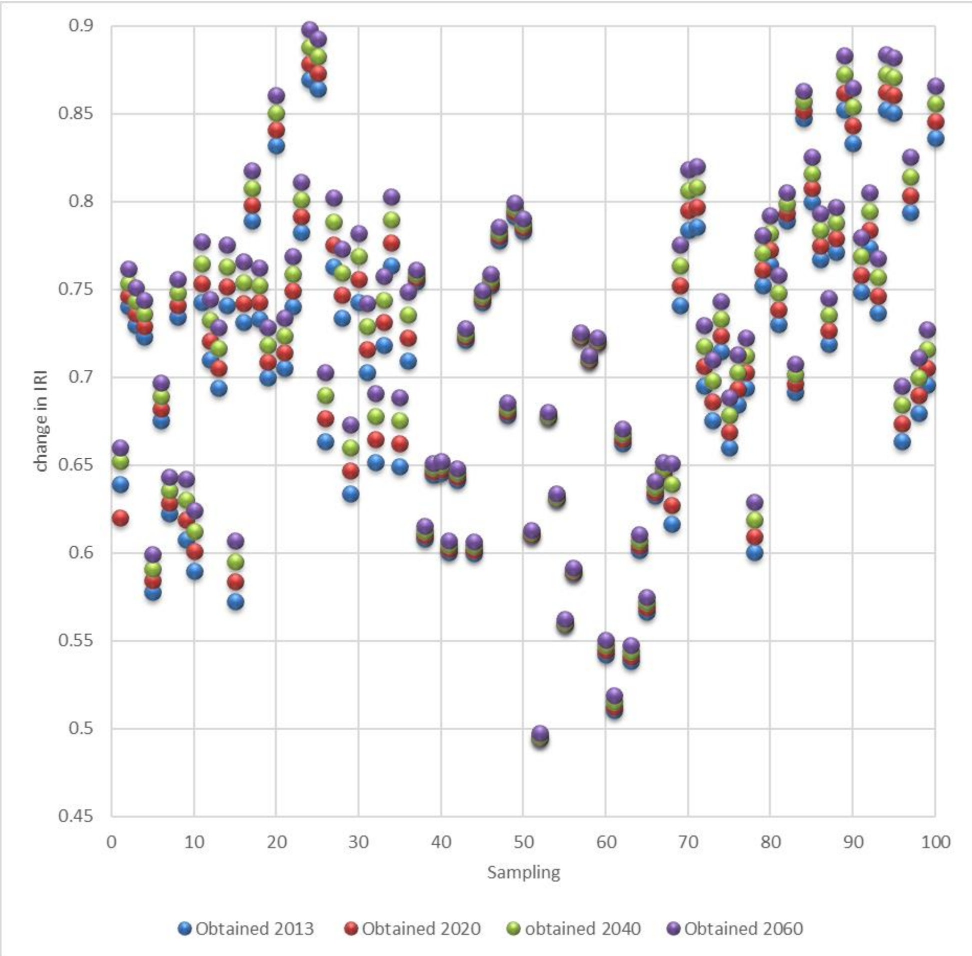

Figure 6-5: Experiment model 2- change in IRI for four different climate change scenarios

6.4.2.1. Deficiency in Experiment 2

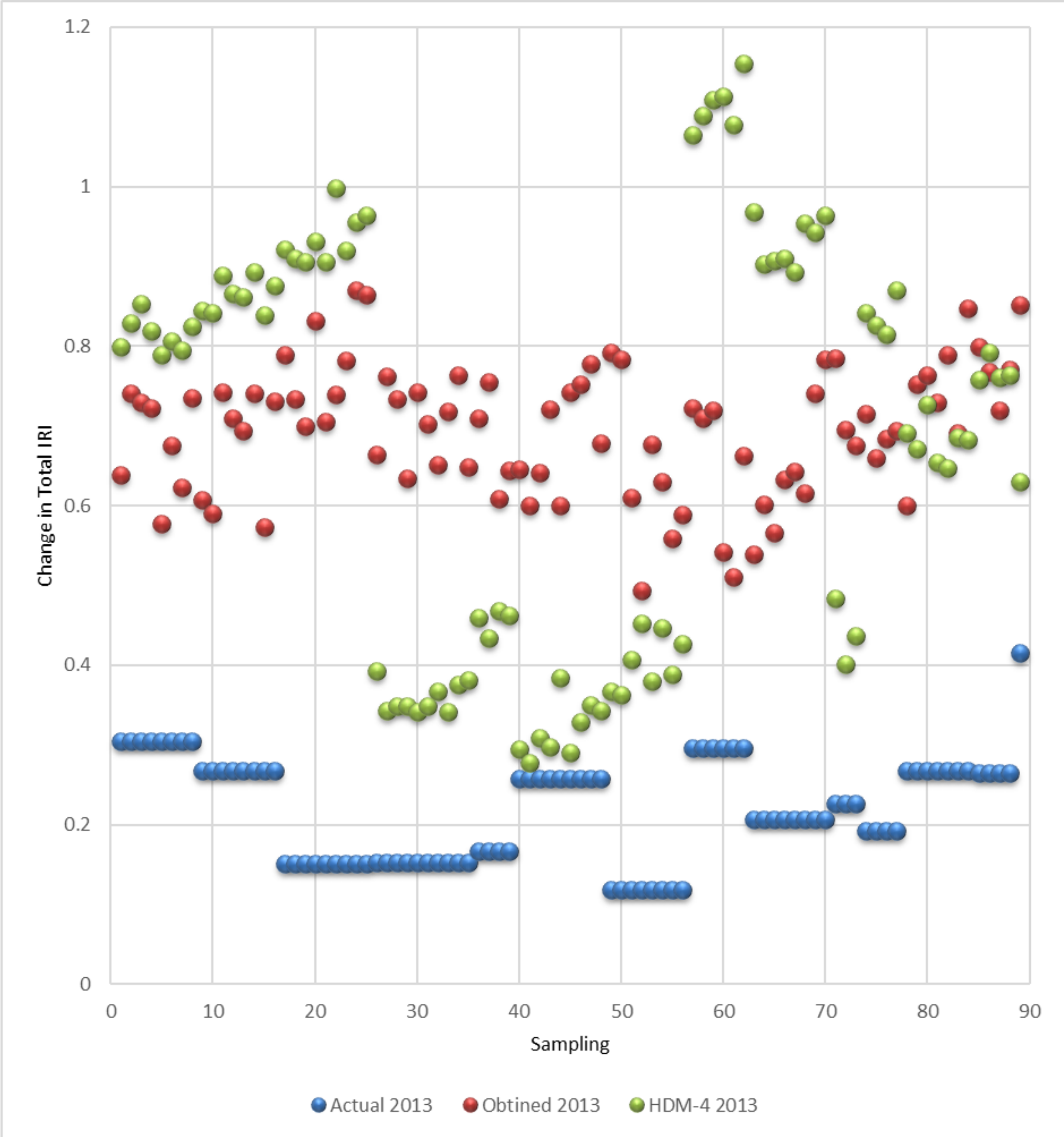

Figure 6-6: Comparing HDM-4 change in IRI with obtained model (2013) and actual Data

Figure 6-6 compares the two models' final results of the total change in IRI (modified and default HDM-4) with the real collected value from the selected roads (see Chapter 5 section 5.4). For modified and default HDM-4, the results are susceptible to variable inputs such as traffic loading, pavement maximum temperature, heavy vehicle speed and pavement thickness. It also shows inconsistency in comparison with other models. On the other hand, the improved HDM-4 based on new coefficients and equations is still scoring a higher value of total change in roughness in comparison with the real value. Such discrepancy could reach 50%. For example, the amount of change in roughness in Etihad road E.11 was recorded as 0.3 m/km when in the improved HDM-4 model it was 0.83 m/km. Bannour et al. (2017) stated that using default equations in HDM-4 without configuration and calibration could result in the generation of inaccurate and inadequate pavement performance prediction. Therefore, calibration is essential to modify the variable coefficients to forecast more accepted outputs. According to Thube (2013), the calibration process involves introducing the adjustment factors which are linear multipliers for adjusting the predictions in order to meet the conditions of the selected area. Such factors work on achieving the best agreements between the field data and model prediction. In this study, the calibration factors for pavement deterioration models under the impact of climate change were determined in conjunction with the default equation HDM-4 model for total change in roughness due to cracking and environment. Bannour et al. (2017) also stated that comparing the model outputs to the known data is a practical approach to assess the adequacy of the HDM-4 deterioration models. Therefore, in this study, Bannour et al. (2017) and Thube's (2013) approach was followed by the author to define calibration factors, which are linear multipliers for modifying the predictions to suit the modified HDM-4 model. Experiment 3 is conducted to introduce the calibration factor.

6.4.3. Experiment 3: Determine Total Change in Roughness (Calibration Factors)

The HDM-4 performance prediction models are empirical regression models. In terms of road deterioration models, the HDM-4 can handle the complex interaction between different variables such as the environment, vehicles and the pavement structure (Bannour et al. 2017). However, such a model must undergo a configuration and calibration process before being applied to the local context level. The consequences of no calibration can be seen in the generation of significant deviational results that do not match the reality the local context (Bannour et al. 2017). Bannour et al. (2017) added that the calibration is introduced by reducing the squares of the differences between computed and measured data. In this research, various trials for calibration factors have been attempted for road sections in the proposed model. Bannour et al. (2017) carried out a calibration process for HDM-4 by suggesting factors for predicting the deterioration model of roads in Morocco in terms of ravelling, structure, potholes, cracking, and their resultant roughness. The calibration approach was conducted on surface distress initiation factors. This process was based on determining the ratio between the observed values of the initiation of distress and the values obtained from uncalibrated performance models based on HDM-4. In this study, the principle for selecting the corresponding calibration factors was to minimise the value of change in roughness due to environmental component (ΔRIe) and cracking component (ΔRIc) in order to achieve an accepted total change in roughness value. Then, these models are compared with the HDM-4 model (having default calibration factors of 1.0). The suggested ratio between the observed values for environmental component of roughness (ΔRIe) and cracking component of roughness (ΔRIc) and the values predicted by the uncalibrated models generated from HDM-4 can be achieved. Several tests and experiments were carried out to find the most suitable calibrated value. It was found that calibration value of Kgm= 0.5 for the environmental (ΔRIe) equation (Table 6-48) and for the cracking component of roughness (ΔRIc) equation (Table 6-49) the calibration Kgc= 0.7 were appropriate for this study. This is based on the fact that the results from these calibration factors were very close to the real values of change in roughness.

Table 6-48: Environmental component of roughness (ΔRIe) with calibration Kgm= 0.5

Main Equation	Variable / Description
ΔRIe = Kgm m Ria m = 0.197+ 0.000155 TMI	
ΔRIe	Incremental change in roughness due to the environment during analysis year, in m/km IRI
Kgm	Calibration factor for the environmental component (default = 0.5)

Table 6-49: Improved HDM-4 cracking component of roughness (ΔRIc) with calibration Kgc= 0.7

Main Equation 3	Variable	Description
$\Delta RIc = (a0 \times (\Delta ACRA)^2 + a1 \times \Delta ACRA + a2) \times Kgc$.		
The improved HDM-4 Cracking	ΔRIc	Incremental change in roughness due to cracking during analysis year, in m/km IRI
	ΔACRA	Incremental change in area of total cracking during analysis year, in per cent

component of roughness	
Kgc	Calibration factor for the Cracking component (default = 0.7)

Experiment 3 was conducted by applying the new improved equation of total change in roughness (ΔRI = ΔRIc + ΔRIr + ΔRIe) with a calibration factor of Kgc =0.7 and Kge =0.5. The model was also tested with different inputs of climate change scenarios (pavement temperature). The obtained results were recorded and are shown in Appendix 6. Examples of all the different scenarios are shown below in Tables 6-49, 6-50, 6-51 and 6-52.

Table 6-50: Example of experiment 3 – total change in roughness 2013 climate Change Scenario

N	Road Code	Road	Change in roughness structural (ΔRIs)	Change in roughness rutting ΔRIr	Change in roughness due to cracking ΔRIc	Environmental component of roughness (ΔRIe)	The total incremental change in roughness ΔRI
1	E.11	Ittihad road	0	0.147	0.193	0.107	0.448
1	E.11	Ittihad road	0	0.147	0.264	0.107	0.519
1	E.11	Ittihad road	0	0.147	0.257	0.107	0.512

Table 6-51: Example of experiment 3 – total change in roughness 2020 climate change scenario

N	Road Code	Road	Change in roughness structural (ΔRIs)	Change in roughness rutting ΔRIr	Change in roughness due to cracking ΔRIc	Environmental component of roughness (ΔRIe)	The total incremental change in roughness ΔRI
1	E.11	Ittihad road	0	0.159	0.193	0.091	0.444
1	E.11	Ittihad road	0	0.154	0.264	0.106	0.526
1	E.11	Ittihad road	0	0.154	0.257	0.106	0.519

Table 6-52: Example of experiment 3 – total change in roughness 2040 climate change scenario

N	Road Code	Road	Change in roughness structural (ΔRIs)	Change in roughness rutting ΔRIr	Change in roughness due to cracking ΔRIc	Environmental component of roughness (ΔRIe)	The total incremental change in roughness ΔRI
1	E.11	Ittihad road	0	0.162	0.193	0.106	0.462
1	E.11	Ittihad road	0	0.162	0.264	0.106	0.533
1	E.11	Ittihad road	0	0.162	0.257	0.106	0.526

Table 6-53 Example of experiment 3 – total change in roughness 2060 climate change scenario

N	Road Code	Road	change in roughness structural (ΔRIs)	change in roughness rutting ΔRIr	change in roughness due to cracking ΔRIc	environmental component of roughness (ΔRIe)	The total incremental change in roughness ΔRI
1	E.11	Ittihad road	0	0.171	0.193	0.105	0.471
1	E.11	Ittihad road	0	0.171	0.264	0.105	0.542
	E.11	Ittihad road	0	0.171	0.257	0.105	0.535

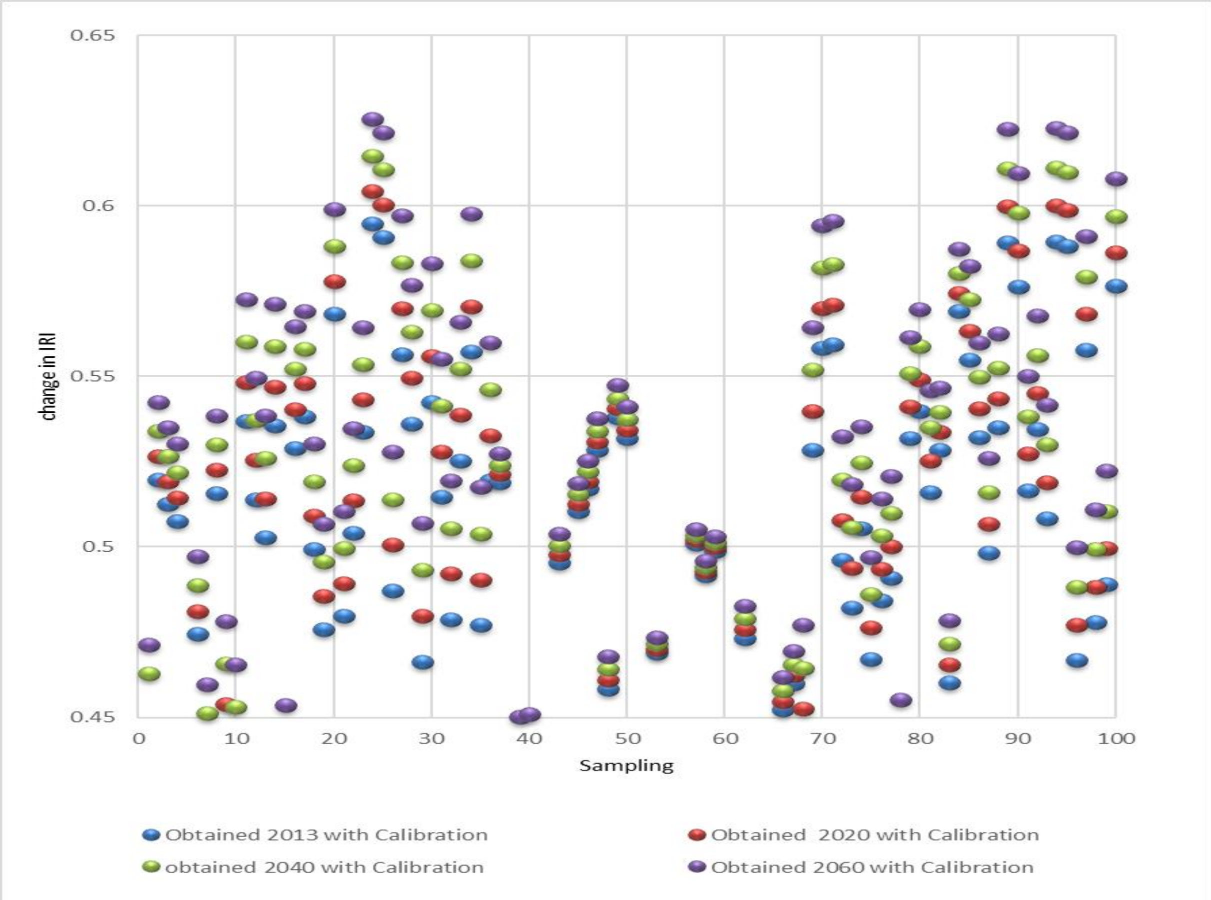

Figure 6-7: Experiment 3 – change in IRI for four different climate change scenarios

The new improved HDM-4 model (new equations and coefficients) with calibration factor for both change in roughness due to environmental component (ΔRIe) and cracking component (ΔRIc) was run for different roads with different variables input. The combination of results is shown in Figure 6-7. It can be seen that the sample roads showed a significant difference in total change in roughness with different climate change scenarios.

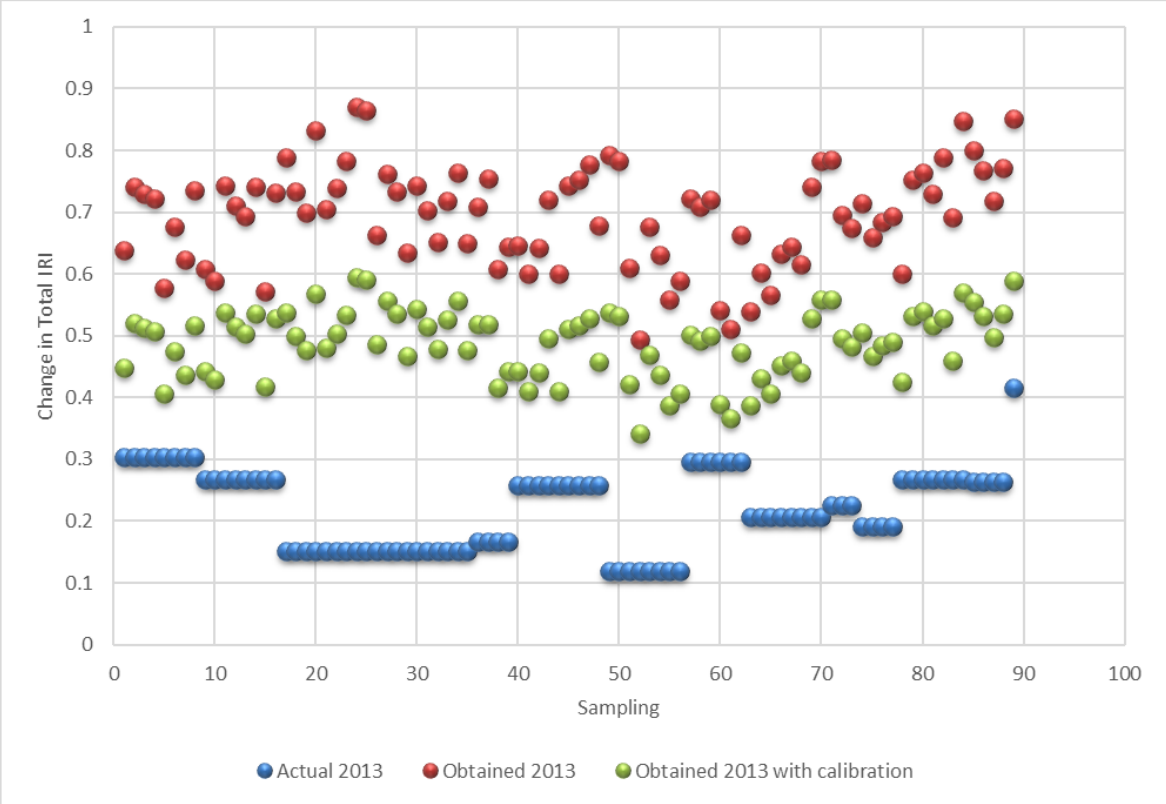

Figure 6-8: Comparing change in total roughness (improved HDM-4) with obtained data (2013), calibrated data and actual data

According to Figure 6-8, which compares the two improved HDM-4 models' (calibrated and non-calibrated) final results of the total change in IRI with the real collected value from the selected roads (see Chapter 5 section 5.4), the improved HDM-4 with calibrated factor showed an improvement. For example, the amount of change in roughness in Etihad road E.11 was recorded as 0.3 m/km (real value) when in the improved HDM-4 model without calibration it was 0.83 m/km, and, after calibration, the value dropped to 0.5 m/km. According to the results, there is correlation between observed values vs predicted values. Therefore, improved HDM-4 models with calibrated factors will be used later on in chapters 7, 8 and 9 to build the deterioration model.

6.5. Pavement Condition Index (PCI) Model

As was discussed earlier, in Chapter 4, the Pavement Condition Index (PCI) ranges from zero to 100, where 100 represents an excellent pavement condition. To test the relationship between PCI and International Roughness Index (IRI), the SPSS software program was applied. Data preparation was carried out to clean the data and remove any invalid data or outliers, as was discussed in Chapter 5 section 5.5. This descriptive statistical analysis includes two different measurement aspects, correlation and regression analysis, which are described in the next sub-sections. A correlation test is used to represent how and to what extent two variables are associated. Regression analysis is used to predict one variable from existing information of one or more variables and to find significant relationships (residual square), since linear and non-linear regressions are used to estimate the result of a dependent PCI. The obtained results are presented below in Table 6-54 and 6-55.

Table 6-54 : Statistical information of PCI and IRI

Statistics			
		IRI	**PCI**
N	Valid	275	275
	Missing	0	0
Mean		1.682	68.520
Std. Error of Mean		.033	1.163
Median		1.620	68.000
Mode		.95a	100.00
Std. Deviation		.55768	19.29291
Variance		.311	372.216
Skewness		.947	-.245
Std. Error of Skewness		.147	.147
Kurtosis		1.845	.485
Std. Error of Kurtosis		.293	.293
Minimum		.63	.0
Maximum		4.42	100.00
Sum		462.56	18843.01

Table 6-55: Correlation results between IRI and PCI

Correlations			
		IRI	**PCI**
IRI	Pearson Correlation	1	-.836**
	Sig. (2-tailed)		.000
	N	275	275

PCI	Pearson Correlation	-.836**	1
	Sig. (2-tailed)	.000	
	N	275	275
**. Correlation is significant at the 0.01 level (2-tailed).			

Table 6-54 indicates that International Roughness Index (IRI) as independent variable has a significant correlation with the dependent variable of Pavement Condition Index (PCI), and this correlations is negative. In summary, the highest correlations found for International Roughness Index (IRI) with the Pavement Condition Index (PCI) dependent variable were -0.836 at the p = 0.001 level.

6.5.1. Regression Analysis

Regression analysis uses knowledge of one or more variables to predict another variable and to look for significant relationships (Residual Square). Non-linear regression is applied to estimate the result of a dependent value of Pavement Condition Index (PCI). The model summary represents the R^2 values, which evaluate the goodness fit of the measured regression equations of every output model. These R^2 values represent the degree of data variation in the estimated equations. These parameters estimate the impact of the success in prediction of PCI. For the non-linear model the results are reported as shown below in Tables 6-56 and 6-57.

Table 6-56: Parameter estimates for the non-linear relationship of IRI And PCI

Parameter Estimates				
Parameter	Estimate	Std. Error	95% Confidence Interval	
			Lower Bound	Upper Bound
a1	144.932	4.353	136.362	153.502
a2	-.463	.020	-.502	-.425

Correlations of Parameter Estimates		
	a1	a2

a1	1.000	-0.955
a2	-0.955	1.000

Table 6-57: The goodness fit for IRI vs PCI

ANOVA[a]			
Source	Sum of Squares	df	Mean Squares
Regression	1363391.561	2	681695.781
Residual	29719.439	273	108.862
Uncorrected Total	1393111.000	275	
Corrected Total	101987.270	274	
Dependent variable: PCI[a]			
a. R squared = 1 - (Residual Sum of Squares) / (Corrected Sum of Squares) = .709.			

The goodness fit of the model is shown in Table 6-57. The independent variable was independent International Roughness Index (IRI) and the dependent variable was Pavement Condition Index (PCI). Several experiments were conducted to find the best fit model. Several transformations were considered including log, square roots, etc. The derived model was able to explained 70.9% of the variation in the existing data.

For Pavement Condition Index (PCI), the regression coefficients are **a1=144.932 and a2= -0.463**. Thus, the final equation for Pavement Condition Index (PCI) is derived as per equation 6-8 and Tables 6-58 and 6-59.

$$\mathbf{PCI = (a1\times e^{a2 \times IRI})}$$

Equation 6-8: New model for Pavement Condition Index (PCI)

Table 6-58: PCI model

Main Equation 3	Variable	Description
PCI = (a1× $e^{a2 \times IRI}$)		
PCI model	IRI	International Roughness Index, in m/km IRI
	PCI	Pavement Condition Index

Table 6-59: Estimated coefficient for PCI Model

Correlations of Parameter Estimates	
a1	144.932
a2	-0.463

6.6. Model Checking and Validation

In Chapter 5, it was suggested that the roads in the study area be divided into two groups for data collection, named forward roads and backward roads. For model development, the analysis was carried out only on data for roads in the backward direction. The reason behind the approach was because roads in the forward direction were in a similar condition to the backward direction roads. Example of roads classified as forward and backward group are shown in Tables 6-60 and 6-61.

Table 6-60: Example of roads classified as forward group

N	Road Code	Road	Direction	Length [m]	Data collection Approach
2	E.11	Ittihad road	SHA	47,650	Forward
4	E18.1	Manama- RAK Airport	Manama	41,550	Forward
6	E18.2	RAK Airport-Sha'am	Rak Airport	53,480	Forward

Table 6-61: Example of roads classified as backward group

N	Road Code	Road	Direction	Length [m]	Data collection Approach
1	E.11	Ittihad road	RAK	47,560	Backward
3	E18.1	Manama- RAK Airport	Rak Airport	41,640	Backward
5	E18.2	RAK Airport-Sha'am	Sha'am	53,360	Backward
7	E311	Sheik Mohammed Bin Zayed	SHA	70,950	Backward

Model checking and validation is conducted by testing the improved HDM-4 with the calibrated factor in the forward direction instead of in the backward direction. The forward and backward traffic loading is different. Hence using forward traffic loading to test models that were derived from backward traffic loading. Table 6-62 presents forward traffic loading data collection.

Table 6-62: Forward traffic loading data collection

N	Road Code	Road	EASL m/lane
2	E.11	Ittihad road	**1.52**
4	E18.1	Manama- RAK Airport	**1.87**
6	E18.2	RAK Airport-Sha'am	**1.67**
9	E55.1	Dhaid - Madam	**0.21**
11	E55.2	Madam - Shiweb	**0.34**
13	E55.3	Umm Al Quwaim - Dhaid	**0.15**
15	E611.1	Maliha Rd - Fallah Al Muala Rd	**4.94**
17	E611.2	Fallah Al Muala Rd - Shk Mohammed Bin Zayed Rd	**1.78**
19	E84	Sheikh Khalifa Rd	**0.55**
21	E88.1	Sharjah - Dhaid	**1.98**
23	E88.2	Dhaid - Masafi	**1.65**
25	E89.1	Masafi - Dibba (from Dibba to Ghona Bridge)	**0.14**
27	E89.3	Masafi - Fujairah	**1.27**

To validate the developed model using different data inputs, a test was conducted to verify the reliability of the model with different variable inputs. For example, the change in roughness based on rutting component for year 2013 was selected (using forward data as discussed in Chapter 5). Therefore, a comparison between two means (2013 forward results and 2013 backward results) is conducted using an independent T-test (analysis of variance), which is used to study the comparison of the means of different independent groups (either two or more) in order to find out statistically if there is a significant difference or not. It is a parametric test. The obtained results are presented below in Table 6-63 and 6-64.

Table 6-63: Independent t-test group statistics

Group Statistics					
	Direction	N	Mean	Std. Deviation	Std. Error Mean
ΔRIr	1	77	0.144	.0162	.0018
	2	77	0.149	.0194	.0022

Table 6-64: Independent samples test change in roughness rutting ΔRIr

Independent Samples Test										
		Levene's Test		t-test for Equality of Means						
		F	**Sig.**	**t**	**df**	**Sig. (2-tailed)**	**Mean Difference**	**Std. Error Difference**	**95% Confidence Interval of the Difference**	
									Lower	**Upper**
ΔRIr	Equal variances assumed	5.938	.016	-1.729	152	0.086	-0.0049	.00288	-.0106	.0007
	Equal variances not assumed			-1.729	147.263	0.086	-0.0049	.00288	-.01068	.0007

The t-test results for the prediction of pavement condition model (the forward direction) showed that the model (M = 0.145, SD = 0.0162) did not differ significantly in levels of change in roughness rutting ΔRIr than the backward direction (M = 0.150, SD = 0.0194), t(1) = -1.729, p > .05 (0.086).

6.7. Summary

In this study, historical data of pavement condition survey, traffic loading, pavement thickness, heavy vehicle speed, IRI and pavement ageing from both the Ministry of Public Works and Al Ain City Municipality have been employed in modelling the total change in roughness and PCI. The developed models could provide a reasonable prediction of pavement condition indicators with the adaptation of different scenarios of climate change impact. These models can be the basis for developing a Markov chain model (Chapter 7 section 7.3) and system dynamics model (Chapter 9 section 9.5).

7. Chapter 7 Forecasting Pavement Deterioration Using Markov Chain

7.1. Introduction

This chapter's goal is to build the pavement deterioration model using a Markov chain with parameters developed in chapters 5 and 6. The model in this chapter is formed from two main elements, transition probability matrix and pavement condition rating. There are different methods for developing a transition probability matrix, as was highlighted in Chapter 3. This chapter explains the process of developing the model inputs using computed analysed data which was discussed in Chapter 6 with different climate change scenarios for years 2013, 2020, 2040 and 2060. Finally, the chapter introduces pavement deterioration curves based on PCI and IRI with different climate change scenarios. Figure 7-1 shows how the chapter is integrated with other chapters.

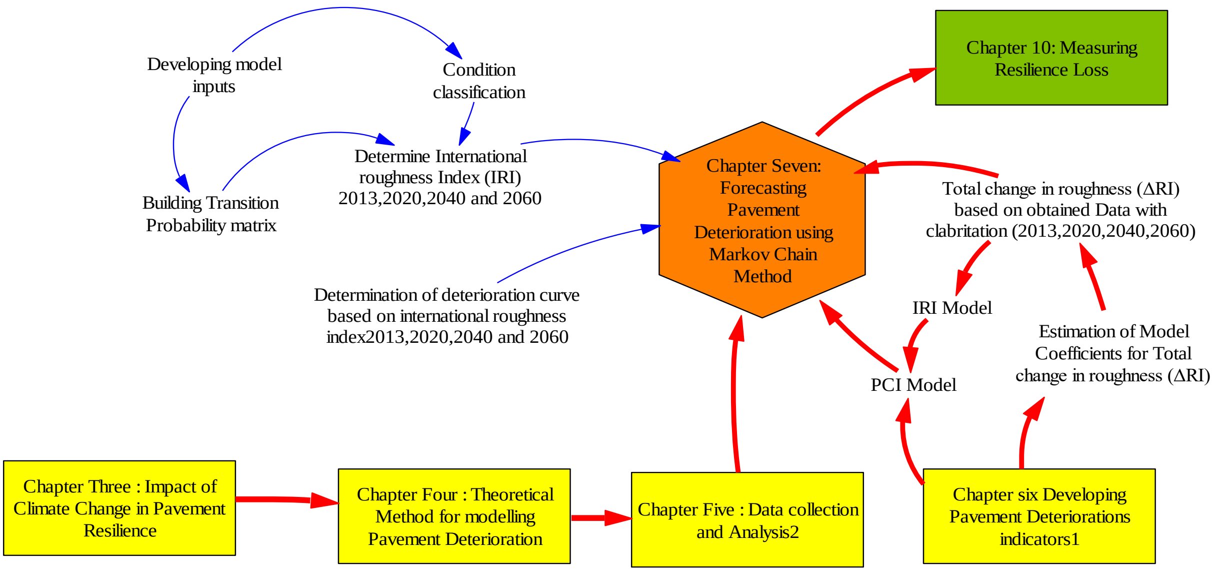

Figure 7-1: The integration of chapter 7 with other chapters

7.1.1. Chapter 7 Roadmap

Figure 7-2 illustrates the roadmap for this chapter starting from developing the model inputs and ending with deterioration curves. The central element in this chapter is building a Markov chain model that predicts the change in the assets' condition with respect to different climate change scenarios. First, the model was built from the parameters developed in Chapter 6. It included different climate change scenarios (2013, 2020, 2040 and 2060) and pavement deterioration indicators. The second step was to develop a pavement condition classification for IRI value and transition probability matrix. After that, the Markov chain model was built, and the results are presented in different deterioration scenarios: 2013, 2020, 2040 and 2060. For the Markov chain model, the deterioration curve showing the forecasted UAE pavement assets is drawn for the next 30 years under different climate change impact scenarios (2013, 2020, 2040 and 2060).

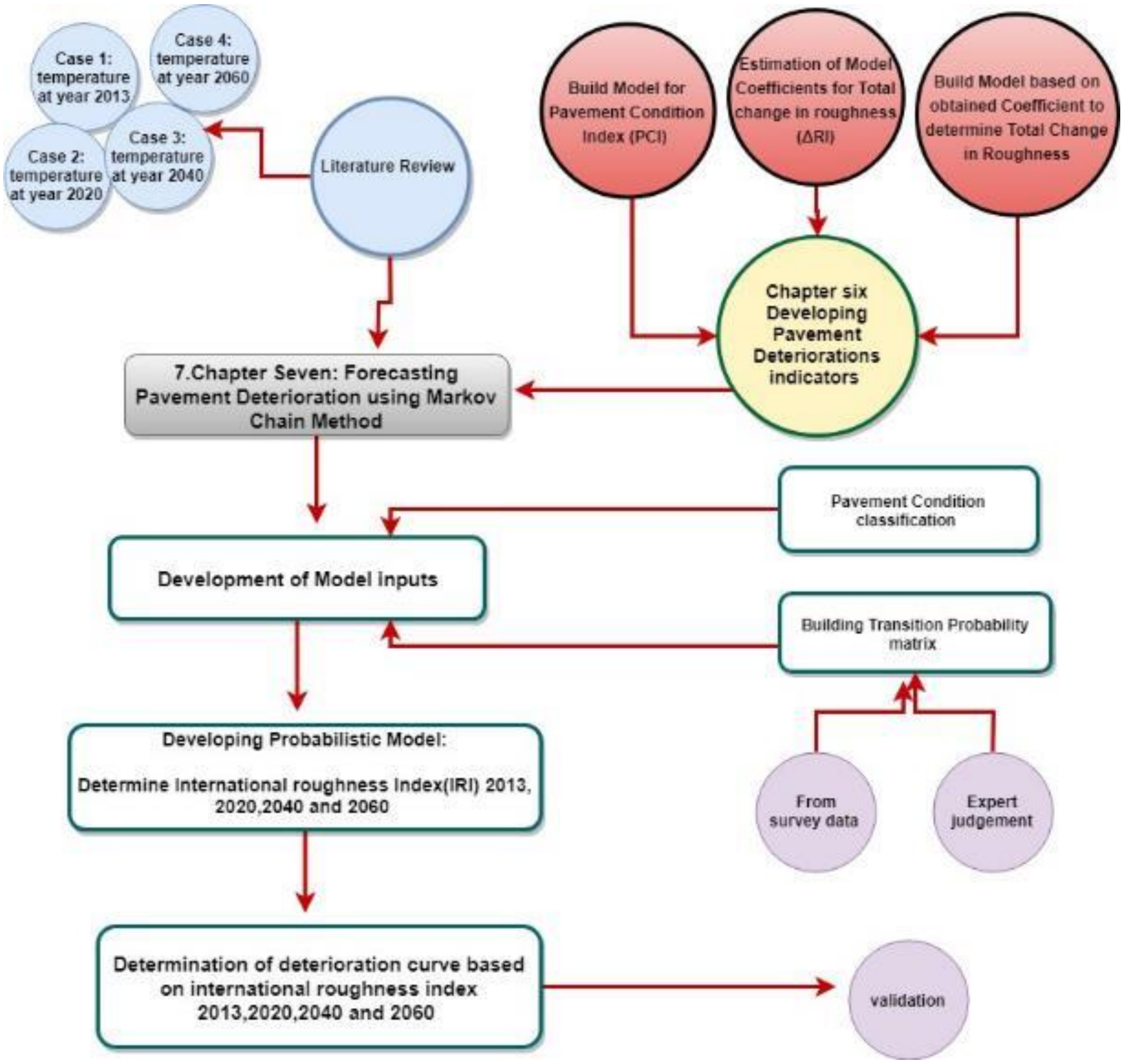

Figure 7-2: The structure of this chapter

7.2. Developing Model Inputs

As discussed in Chapter 3, the prediction deterioration model is a mathematical approach that can be applied to forecast how the future pavement is going to deteriorate. The model depends on the existing pavement condition, deterioration factors and previous maintenance (OCED) Organization for Economic Co-operation and Development 1987). In our case, probabilistic models (which predict the pavement condition as the probability of occurrence of a range of possible outcomes) are applied for using the Markov chain method, which are the most accurate techniques for prediction models. Building the transition probability matrix is a crucial element in developing the Markov chains model.

7.2.1. Condition Classification

As mentioned in the discussion in Chapter 3 section 3.5.1, the importance of collecting pavement condition data is to manage the assets. Such data practically impact the decision-making procedure of the asset management team as they are used to define at which stage the maintenance intervention occurs. However, these data should have a 'Condition Rating System', which is a technique of physical deterioration classification to assess the condition of pavement assets. For example, the most frequently accepted condition rating system across many highway agencies is a 1 to 5 rating, where state 5 is very poor assets and condition 1 is excellent or as new assets (NAMS 2009). Others use a scale ranging from 0-100, which is similar to the one used in the Pavement Condition Index by the US military. Example of Pavement Condition Index (PCI) classification is shown in Figure 7-3 and 7-4.

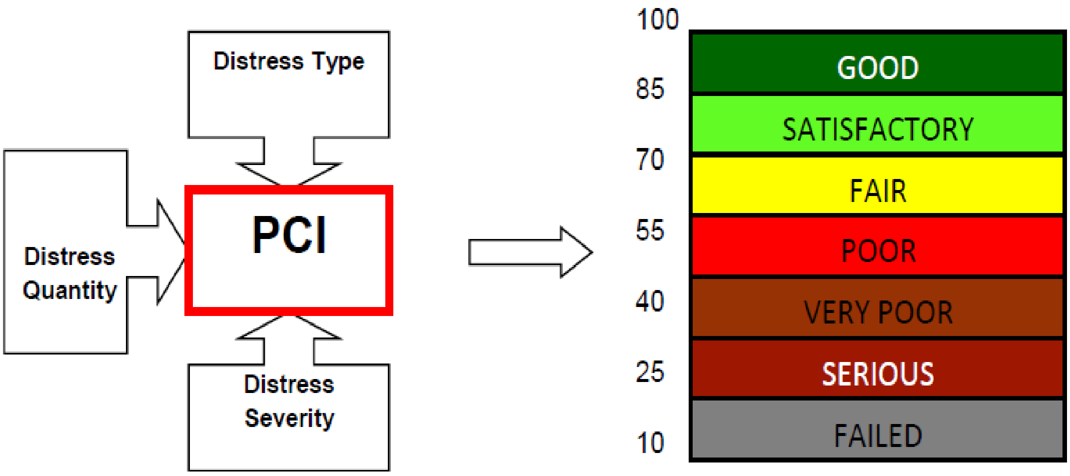

Figure 7-3: Pavement Condition Index (PCI) classification

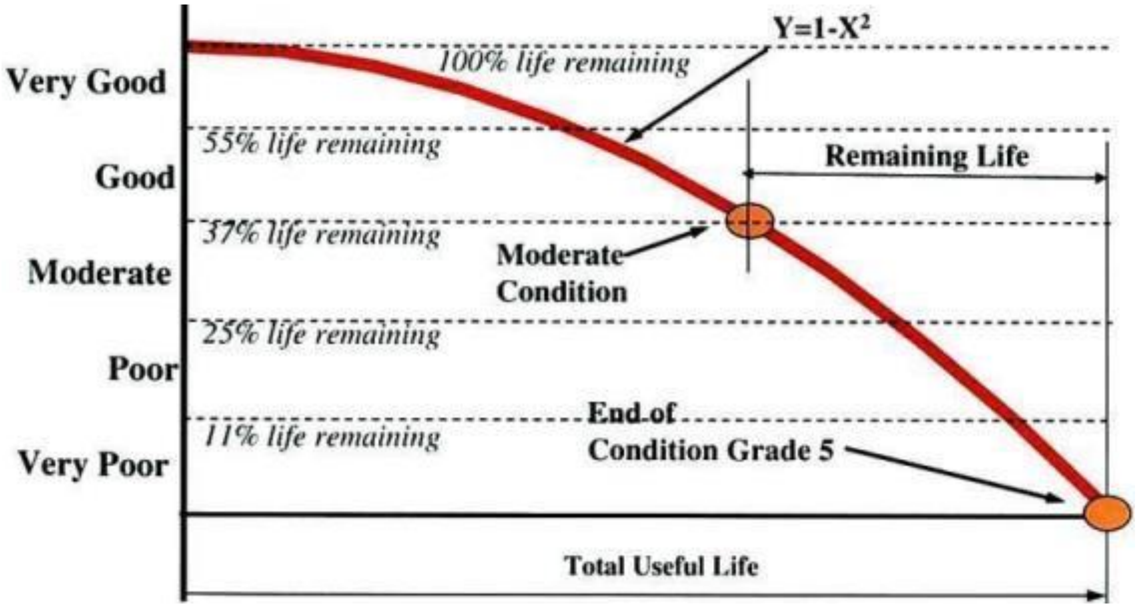

Figure 7-4: Example of an asset's condition over its life cycle

According to the Ministry of Public Works reports for asset management, which were discussed in Chapter 5, the International Roughness Index was used as the main parameter to reflect the condition of the road assets. This pavement indicator contains four classifications, as shown in Table 7-1. The IRI condition rating system was applied for the roads under the management of the UAE Ministry of Public Works.

Table 7-1: Condition rating system in the roads under the management of UAE Ministry of Public Works

State 1	State 2	State 3	State 4
<=1.5 m/km	<=2.0 m/km	<=2.5 m/km	>2.5 m/km

Overall, most of the roads in the UAE are in a good condition. As an example, based on the IRI, the road pavement condition of more than 75% of Etihad's roads is at state 1(Figure 7-5).

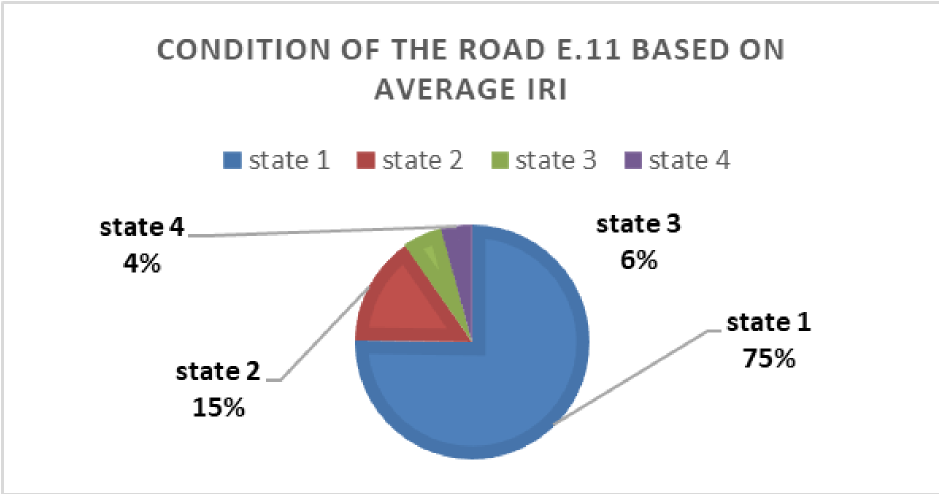

Figure 7-5: Example of Etihad road pavement condition based on IRI

The first step in Markov chain modelling is to evaluate the condition of the asset's elements (Sharabah, Setunge and Zeephongsekul 2006). In practice, pavement condition data can be gathered using automated or manual methods. Every agency or municipality establishes its own approach to data collection methodologies, applied software programs and pavement management processes. Moreira et al. (2016) stated that gathered parameters can be represented by their measured values in different units. Moreira et al. (2016) also highlighted that HDM-4 uses a global index such as Present Serviceability Rating. Other pavement indicators such as Pavement Condition Index (PCI) and International Roughness Index (IRI) can be used. Accuracy and availability of data on the condition of assets such as found in the PCI are critical elements in defining the current condition of the pavement network. Mandiartha et al. (2017) stated that distributing road conditions into different condition ratings has been proven to be a sufficient method to assist highway agencies in deciding a suitable choice of maintenance intervention. For example, Mandiartha et al. (2017) applied IRI value condition to build a Markov chain model that can assess the effectiveness of road network pavement maintenance. In this study, for the condition rating system, feedback on the subject matter from an expert was taken into consideration as he stated that UAE roads are considered to be new and most of the IRI value is 1.5 km/m and any value beyond 2.0 km/m is not accepted by the UAE highway agency's standards and regulations. He also stated that the level of acceptance of the rideability differs from one place to another and the UAE highway agency considers that any value beyond 2.0 km/m requires an immediate maintenance intervention depending on road type and location. According to NAMS (2009), the most accepted condition rating system among many infrastructure asset classes is the basic 1 to 5 rating, where class 5 is normally defined as very poor condition and class 1 is defined as very good condition. Nevertheless, there is no single classification for condition rating and it is practically accepted to use whichever scaling system works for a specific organisation (NAMS 2009). Sobanjo (2011) defined five condition states in his study for bridge evaluation. Therefore, after studying the data available, the 1 to 4 condition states introduced by the UAE Ministry of Public Works were expanded into the 1 to 5 condition states shown in Table 7-2.

Table 7-2: Condition rating system used in the research

Condition Rating System	Range
very good	0-1.25
Good	1.25-1.5
satisfaction	1.5-1.75
Fair	1.75-2.0
Poor	2.0 above

7.2.2. Building a Transition Probability Matrix

Arimbi (2015) stated that Markov chains have been used extensively to build pavement performance through indication of the probability ‘before’ and ‘after’ condition of the pavement. The Markov method requires transition probability matrices (TPMs) to express the transition from one pavement condition state to another. For the pavement case, in order to conduct a Markov chain, it is crucial to estimate the probability of shifting from one condition state to another, which is usually done by expert judgement or based on the analysis of available previous information (historical data). In this research, both methods were tested and are reported in the following sub-sections.

7.2.2.1. Building a Transition Probability Matrix from the Contribution of Expert Judgement

Mohseni (2012) stated that, in some industries where not enough data are available for building the transition probability matrix of the Markov chain for modelling deterioration prediction, the engineering judgement on the application of the Markov chain method would be the most appropriate solution for estimating the future condition of an element. The contribution of expert judgement in developing a transition probability matrix which presents the rate of deterioration of the road (flexible pavement) in the UAE can be achieved by using interviews or questionnaires. In the research, the rating matrix scale (example in Table 7-3) was used to evaluate the rate of degradation of UAE pavements. The results are attained from respondents working in different highway engineering industries (i.e. contractors, clients, consultants, suppliers, etc.) in the UAE (see Chapter 5 section 5.14. The actual survey is part of the completed risk measurement survey (see Chapter 9 section 9.3) and the results are shown in Appendix 4. For result collection, the researcher had to meet with experts and ask them to complete the questionnaire manually. Thirty experts completed the survey from the beginning of March 2018 to the end of April 2018. The results are presented (Table 7-4), and an average reading was taken to determine the rate of change for four different states using the PCI scale: very good state (100) to good state (80), good state (80) to satisfactory state (60), satisfactory state (60) to poor state (40) and, finally, poor state (40) to failure state (less than 40).

Table 7-3: Example of rating matrix scale that was used to evaluate the rate of degradation in UAE pavements

			Threats				
1. Pavement network classified in UAE into 4 condition states: how likely the risk of "Rate of pavement deterioration "**moved from Very good condition to good condition"** every year	probability	0.9	0.05 ( )	0.09 ( )	0.18 ( )	0.36 ( )	0.72 ( )
		0.7	0.04 ( )	0.07 ( )	0.14 ( )	0.28 ( )	0.56 ( )
		0.5	0.03 ( )	0.05 ( )	0.1 ( )	0.2 ( )	0.4 ( )
		0.3	0.02 ( )	0.03 ( )	0.06 ( )	0.12 ( )	0.24 ( )
		0.1	0.01 ( )	0.01 ( )	0.02 ( )	0.04 ( )	0.08 ( )
			0.05/Very Low	0.1/Low	0.2/Low	0.4/High	0.8/Very High

Table 7-4: The descriptive statistics of the questionnaire results based on 30 experts

Descriptive Statistics													
	N	Range	Minimum	Maximum	Sum	Mean		Std. Deviation	Variance	Skewness		Kurtosis	
State	Statistic	Statistic	Statistic	Statistic	Statistic	Statistic	Std. Error	Statistic	Statistic	Statistic	Std. Error	Statistic	Std. Error
Rate of deterioration in state 1	30	0.71	0.01	0.72	5.41	0.1803	0.03611	0.19779	0.039	1.637	0.427	2.173	0.833
Rate of deterioration in state 2	30	0.35	0.01	0.36	3.49	0.1163	0.0195	0.10679	0.011	0.846	0.427	-0.661	0.833
Rate of deterioration in state 3	30	0.35	0.01	0.36	3.85	0.1283	0.01888	0.10339	0.011	0.653	0.427	-0.812	0.833
Rate of deterioration in state 4	30	0.71	0.01	0.72	5	0.1667	0.0292	0.15994	0.026	1.592	0.427	3.549	0.833

For building the transition probability matrix, the average results for the contribution of expert judgement in determining the rate of change were applied. However, a restriction was added to the analysis of the results by allowing no more than one state deterioration in each cycle. Porras-Alvarado, Zhang and Salazar (2014) confirmed that such an approach is common practice in modelling pavement deterioration. The reason behind this is that pavement degradation occurs in a natural sequence which does not do more than one state at a time. The following TPM was developed based on the contribution of expert judgement and presented in Table 7-5.

Table 7-5: Transition probability matrix based on expert judgement

2013				
	State 1	**State 2**	**State 3**	**State 4**
Very good	0.820	0.180	0	0
Good	0	0.703	0.297	0
Satisfaction	0	0	0.575	0.4246
Poor	0	0	0	1

One of the primary objectives of the research is to develop a deterioration model under different climate change scenarios. However, the above transition probability matrix represents the rate of change only for the present climate. The impact of future predicted climate change scenarios cannot be incorporated into the model. Thus, TPM based on expert judgement cannot be valid for this case.

7.2.2.2. Building a Transition Probability Matrix from Survey Data

As was discussed in Chapter 4, two procedures are frequently used to create the transition probability matrix from the pavement condition rating data. The first method is a regression-based optimisation (expected value) which requires only one set of data. This method estimates the transition probability matrix by solving the non-linear optimisation problem that minimises the sum of absolute differences between the regression curve that best fits the condition data and the conditions predicted using the Markov chain model. The second method is percentage prediction (frequency), which is quite a commonly used method. It involves at least two groups of inspection data without any maintenance and rehabilitation interventions.

For frequency method, the estimation of the transition probabilities can be achieved in this research based on pavement condition data over a number of years. Once the available data are obtained, a way of estimating the corresponding deterioration rates can be quickly developed using any of the pavement performance indicators such as PCI or IRI. Abaza (2014) projected the transition probabilities using only two consecutive cycles of pavement distress assessment. However, the proposed transition probability matrix was estimated on the basis of a current climate assumption using past observations without considering the consequences of climate change impact, whereas one of the main goals of this research is to introduce a prediction model that can be used for measuring the impacts of future climate.

A regression-based approach (expected value) using modified HDM-4 was used to generate pavement performance (see example in Table 7-6) from Chapter 6. The output results of the regression model were fed into a software package named @RISK to determine the best fit of probability distribution that captures the pavement deterioration. Then, the survival probability curves of each pavement deterioration under each climate scenario were generated from the software. The survival probability curves were used to estimate the probability of each state in the transition matrix, as shown in Figure 7-6 and 7-7 . The collected results in Chapter 6 were used to define the probability distribution of deterioration for the occurrence of different future climate change impact scenarios, as per the example in Table 7-6. The analysis was carried out using analysis software named @RISK which can automatically empower the correct choice of distribution for a set of given data.

Table 7-6: Example of results from the deterministic model used to estimate the transition probability matrix

N	Road Code	Road	initial roughness RIa	ΔRIe 2013	IRI	ΔRIe 2020	IRI	ΔRIe 2040	IRI	ΔRIe 2060	IRI
1	E.11	Ittihad road	1.16	0.449	**1.609**	0.455	**1.615**	0.463	**1.623**	0.471	**1.631**
3	E18.1	Mnama-RAK Airport	0.98	0.442	**1.422**	0.454	**1.434**	0.466	**1.446**	0.478	**1.458**
5	E18.2	RAK Airport-Sha'am	1.73	0.538	**2.268**	0.548	**2.278**	0.558	**2.288**	0.569	**2.299**

Using such @RISK software takes into consideration that no more than one state deteriorates in each cycle. The probability distribution of the rate of degradation is generated and reported for pavement condition for change in IRI based on the four different climate change scenarios in Appendix 4. An example is shown below of the probability of pavement condition for change in IRI based on 2013 obtained results with calibration from Chapter 6 section 6.4.3.

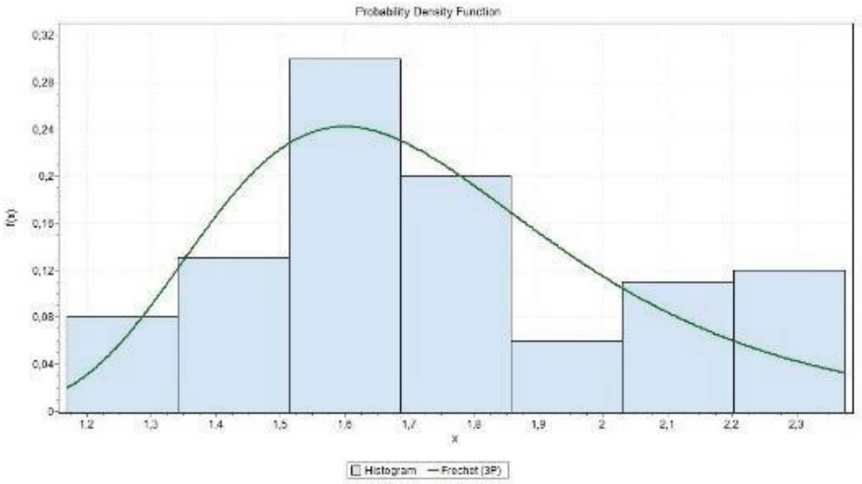

Figure 7-6: Probability of pavement condition for change in IRI based on 2013 obtained results from the modified HDM-4 model

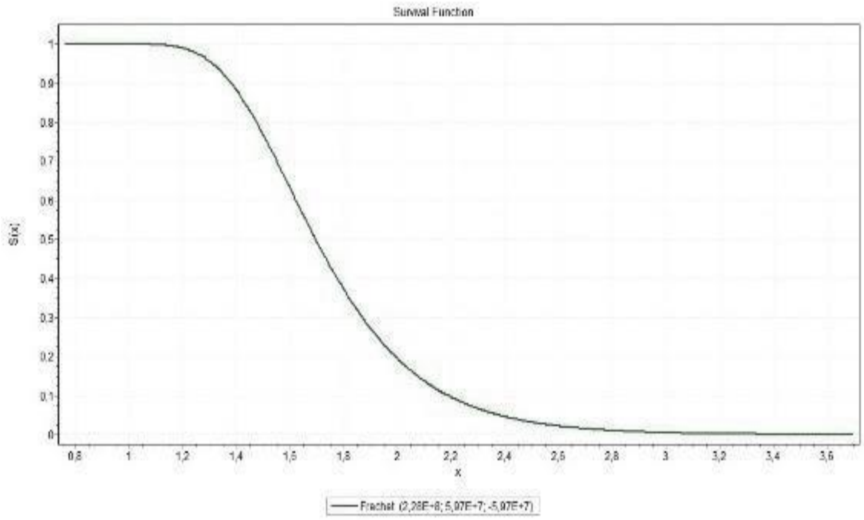

Figure 7-7: Survival curve for change in IRI based on 2013 obtained results from the modified HDM-4 model

Based on the probability of pavement condition and survival curve for the change in IRI, the determination of the transition probability matrix for four different climate change scenarios (2013, 2020, 2040 and 2060) is developed as shown in Tables 7-7, 7-8, 7-9, and 7-10.

Table 7-7: Transition probability matrix for 2013

2013					
	state 1	**state 2**	**state 3**	**state 4**	**state 5**
very good	0.87	0.13	0	0	0
Good	0	0.79	0.21	0	0
satisfaction	0	0	0.48	0.52	0
Fair	0	0	0	0.2	0.8
Poor	0	0	0	0	1

Table 7-8: Transition probability matrix for 2020

2020					
	state 1	**state 2**	**state 3**	**state 4**	**state 5**
very good	0.84	0.16	0	0	0
Good	0	0.76	0.24	0	0
satisfaction	0	0	0.45	0.55	0
Fair	0	0	0	0.2	0.8
Poor	0	0	0	0	1

Table 7-9: Transition Probability matrix for 2040

2040					
	state 1	**state 2**	**state 3**	**state 4**	**state 5**
very good	0.83	0.17	0	0	0
Good	0	0.75	0.25	0	0
satisfaction	0	0	0.44	0.56	0
Fair	0	0	0	0.19	0.81
Poor	0	0	0	0	1

Table 7-10: Transition probability matrix for 2060

2060					
	state 1	**state 2**	**state 3**	**state 4**	**state 5**
very good	0.82	0.18	0	0	0
Good	0	0.72	0.28	0	0
satisfaction	0	0	0.42	0.58	0
Fair	0	0	0	0.19	0.81
Poor	0	0	0	0	1

7.3. Developing the Probabilistic Model

As described in Chapter 3, the stochastic technique of the Markov chain using a discrete data set has been selected in the study to define the deterioration tendency of pavement assets with respect to different climate change scenarios.

7.3.1. Projection of Pavement Condition

The model can be run using either MATLAB or Excel Microsoft Office software. The forecasted period was set for 30 cycles. Each cycle represents a single year. The results of determination of IRI for different climate scenarios are listed in Appendix 4. An example of the results is shown below; consequently, the transient probabilities can be calculated, assuming that the initial state is 1 0 0 0 0. The assumption was made that the pavements of the study area are in the very good condition state. The results are shown in Appendix 4. Tables 7-11, 7-12, 7-13 and 7-14 below show examples of the International Roughness Index (IRI) values generated from the Markov chain model for a 30-year cycle based on the 2013 transition probability matrix.

Table 7-11: Example results of International Roughness Index (IRI) 2013 based on Markov chain model for a 30-year cycle

Years /cycle	state 1	state 2	state 3	state 4	state 5	IRI
0	1	0	0	0	0	0.9000
1	0.8700	0.1300	0.0000	0.0000	0.0000	0.9585
2	0.7569	0.2158	0.0273	0.0000	0.0000	1.0162
3	0.6585	0.2689	0.0584	0.0142	0.0000	1.0747
4	0.5729	0.2980	0.0845	0.0332	0.0114	1.1385

Table 7-12: Example results of International Roughness Index (IRI) 2020 based on Markov chain model for a 30-year cycle

Years/ cycle	state 1	state 2	state 3	state 4	state 5	IRI
0	1	0	0	0	0	0.9000
1	0.8400	0.1600	0.0000	0.0000	0.0000	0.9720
2	0.7056	0.2560	0.0384	0.0000	0.0000	1.0421
3	0.5927	0.3075	0.0787	0.0211	0.0000	1.1125
4	0.4979	0.3285	0.1092	0.0475	0.0169	1.1899

Table 7-13: Example results of International Roughness Index (IRI) 2040 based on Markov Chain Approach for 30-year cycle

Years /cycle	state 1	state 2	state 3	state 4	state 5	IRI
0	1	0	0	0	0	0.9000
1	0.8300	0.1700	0.00000	0.0000	0.0000	0.9765
2	0.6889	0.2686	0.0425	0.0000	0.0000	1.0506
3	0.5717	0.3185	0.0858	0.0238	0.0000	1.1248
4	0.4745	0.3361	0.1174	0.0526	0.01928	1.2068

Table 7-14: Example results of International Roughness Index (IRI) 2060 based on Markov Chain Approach for 30-year cycle

Years/ cycle	state 1	state 2	state 3	state 4	state 5	IRI
0	1	0	0	0	0	0.900
1	0.8200	0.1800	0.0000	0.0000	0.0000	0.9810
2	0.6724	0.2772	0.0504	0.0000	0.0000	1.0600
3	0.5513	0.3206	0.0987	0.0292	0.0000	1.1397

4	0.4521	0.3300	0.1312	0.0628	0.0236	1.2289

To observe the performance trend over the next 30 years for a pavement section, the results of the 2013, 2020, 2040 and 2040 scenarios were plotted into different graphs. Tables 7-11, 7-12, 7-13 and 7-14 show that the state condition probability of the pavement based on different scenarios (from 1 to 5) changes over the years. Figures 7-8, 7-9, 7-10 and 7-11 show the resulting graphs.

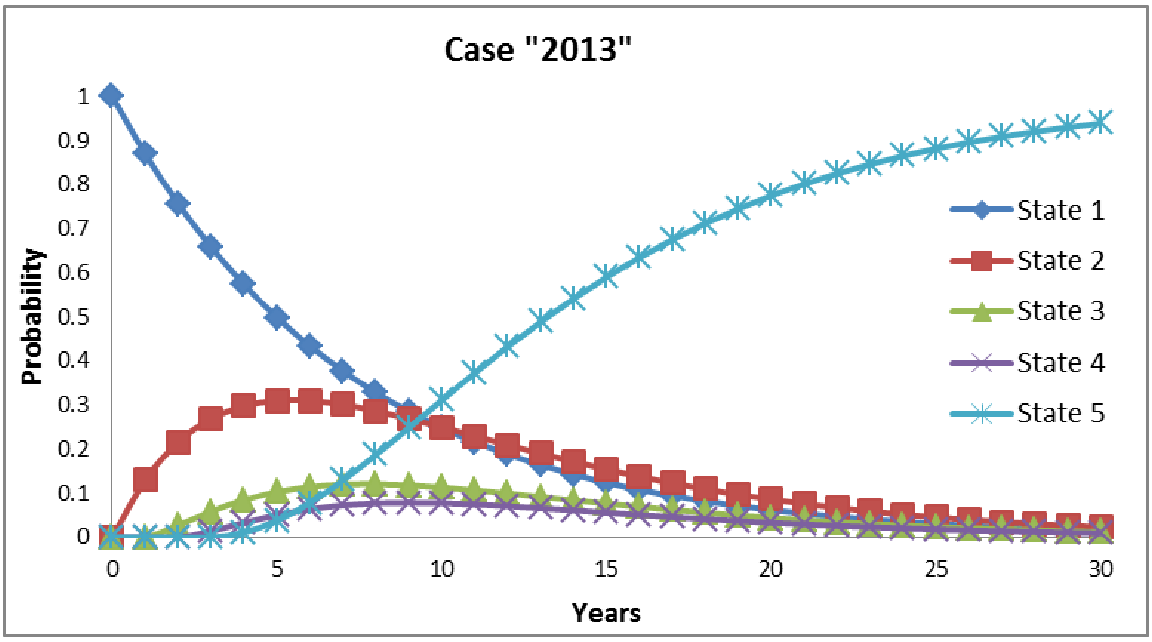

Figure 7-8: Probability graph for 2013 scenario

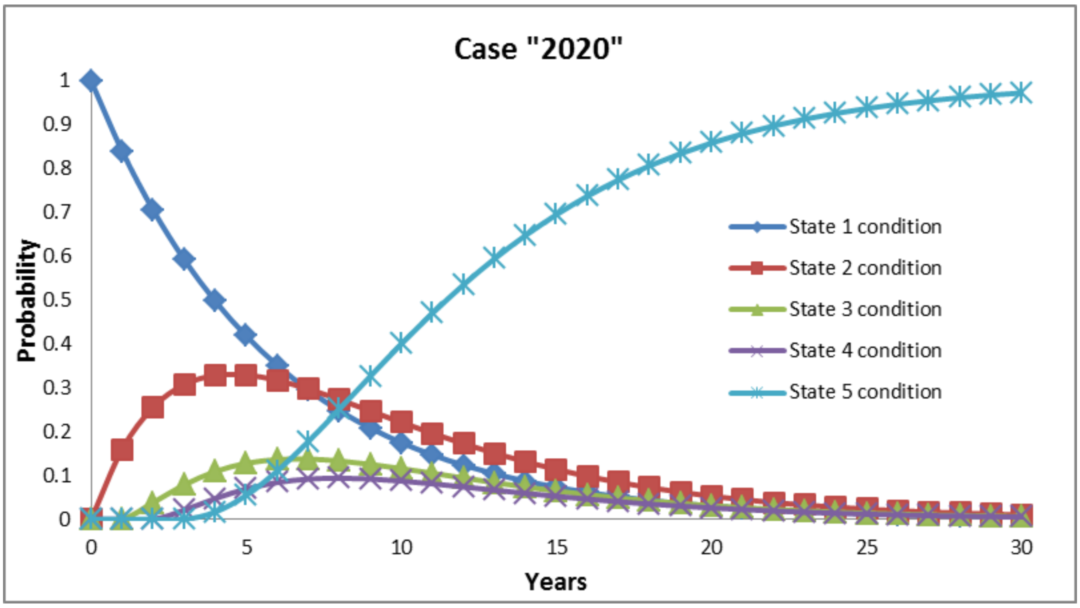

Figure 7-9: Probability graph for 2020 scenario

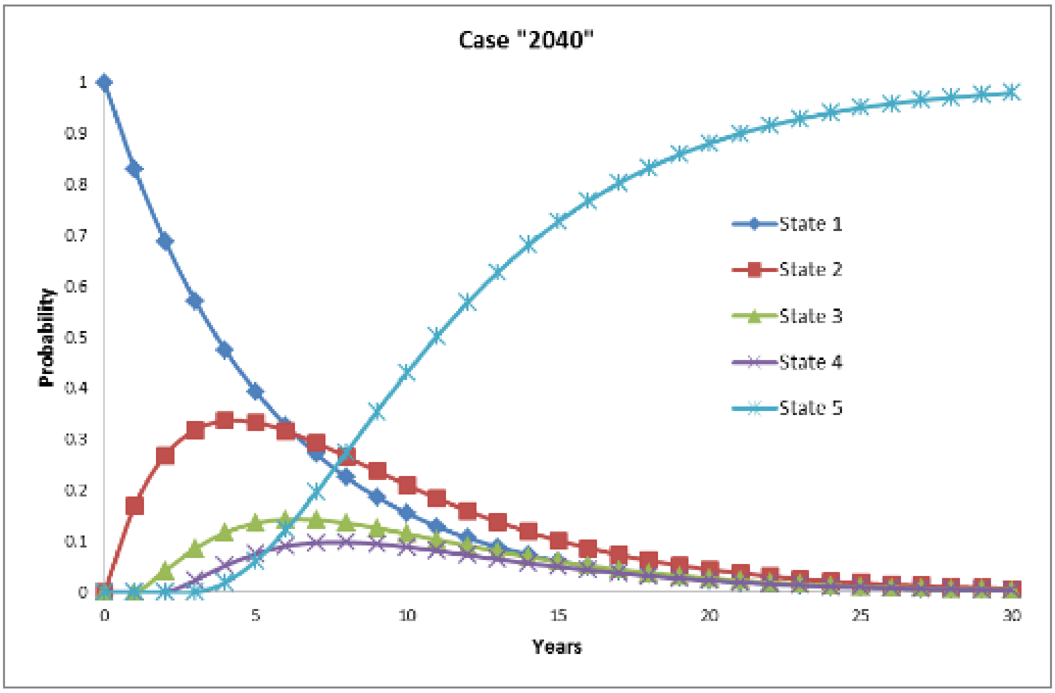

Figure 7-10: Probability graph for 2040 scenario

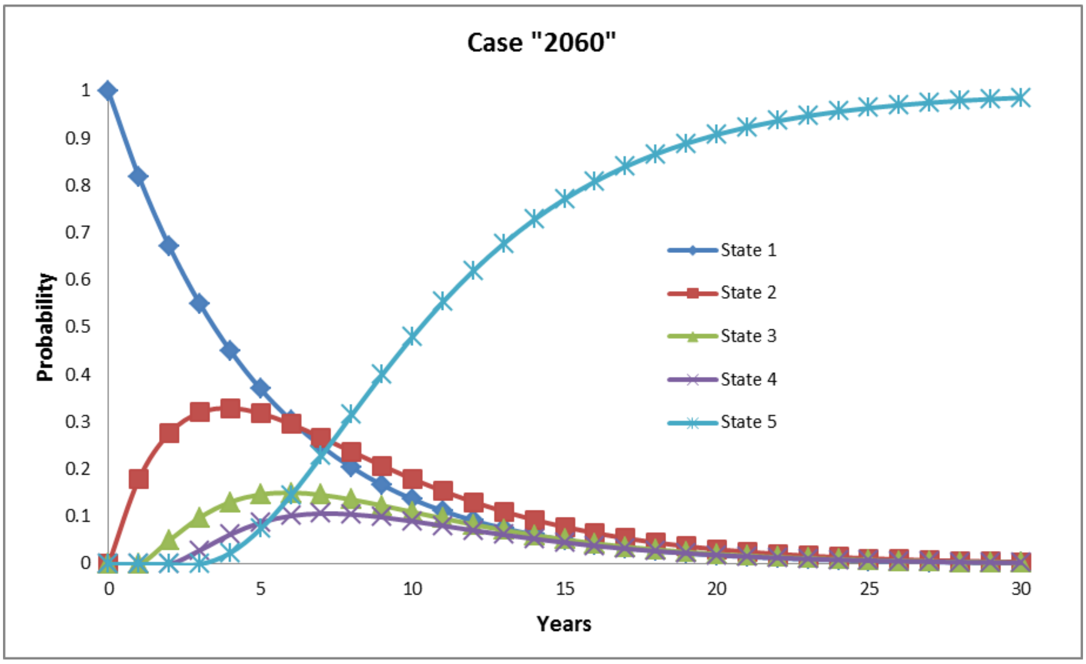

Figure 7-11: Probability graph for 2060 scenario

The simulation results are shown in the above figures, 7-8, 7-9, 7-10 and 7-11. The graphs express pavement deterioration based on IRI for different types of condition states. The initial start of condition S1, which represents the new pavement condition (good) with the actual probability of state value, is equal to 1. As explained earlier, the categories of state 1 represent the best condition whereas state 5 indicates the worst condition. According to the graph, the probability of the pavement being in a good condition (state 1) will deteriorate dramatically to achieve a probability below 5% for the next 30 years. Other conditions are behaving in the same manner. The change indicates the progressive deterioration that appears in the pavement condition at the network level. It can be seen that the probability of state 5 (the worst state) will keep rising over the years until it reaches the probability larger than state 1.

For example, Figure 7-8 illustrates the probabilistic deterioration curves for the flexible pavement component for the 2013 scenario. The probabilistic deterioration curve shows that there is a 25% chance that the component is still in condition 1 (very good) and performing to its optimal functionality after 10 years; on the other hand, the probabilistic deterioration curves show that this forecast (2013 scenario) has a high probability that the component will have deteriorated to condition 5 after 30 years, which is 93%. Table 7-15 presents the results for the probabilistic deterioration curves of tables 7-9 to 7-12 at different functional years (10 years, 20 years, 30 years).

Table 7-15: Results of pavement transition probability based on Markov model

condition state	**Year 10**				**Year 20**				**Year 30**			
scenarios	**2013**	**2020**	**2040**	**2060**	**2013**	**2020**	**2040**	**2060**	**2013**	**2020**	**2040**	**2060**
1	25.0%	17.5%	15.5%	14%	6.0%	3.1%	2.4%	1.9%	1.5%	0.5%	0.4%	0.3%
2	25.0%	22.1%	21.0%	18%	8.0%	5.3%	4.4%	3.1%	2.0%	1.0%	0.8%	0.5%
3	11.0%	11.6%	11.5%	11%	4.0%	3.1%	2.7%	2.1%	1.0%	0.6%	0.5%	0.3%
4	9.0%	8.7%	8.9%	9%	3.0%	2.6%	2.3%	1.9%	1.0%	0.5%	0.4%	0.3%
5	30.0%	40.1%	43.1%	48%	77.0%	85.9%	88.1%	90.9%	93.0%	97.3%	98.0%	98.7%

According to the obtained results from the Markov chain model for the four different climate change scenarios, the following figures (7-12, 7-13, 7-14 and 7-15) compare the results for every state concerning the climate case. It can be seen that the rate of deterioration for the 2060 example is the worst in all states (state 1, 2, 3, 4 and 5) over the projected period of 30 years, whereas 2013, which is the current scenario, has the lowest deterioration rate (states 1, 2, 3, 4 and 5). Such results conclude that climate change impact can accelerate the rate of degradation for infrastructure assets (pavement in the case study). And such degradation increases with increasing pavement temperature (assuming other variables are consistent).

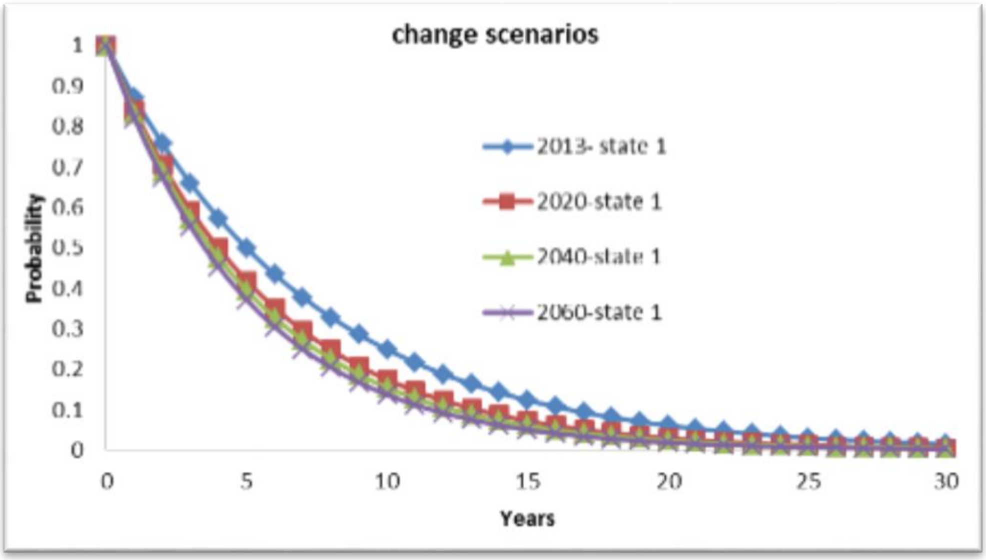

Figure 7-12: Change in state 1 condition based on different climate change scenarios

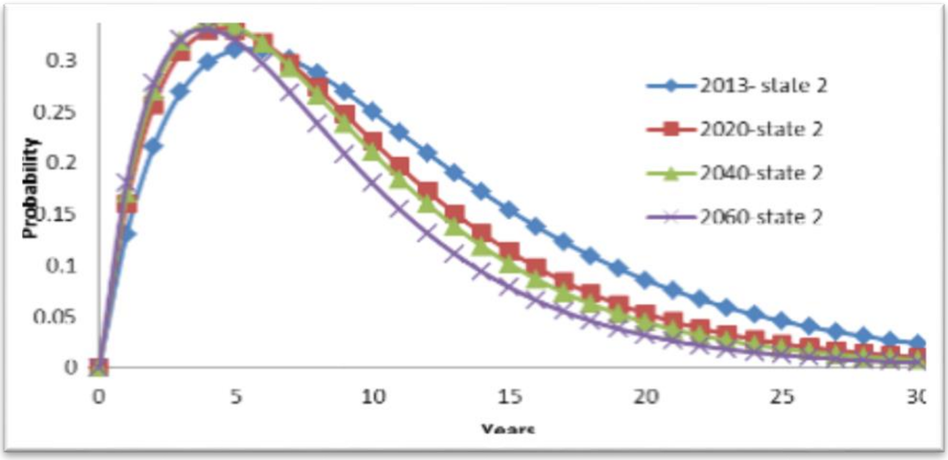

Figure 7-13: Change in state 2 condition based on different climate change scenarios

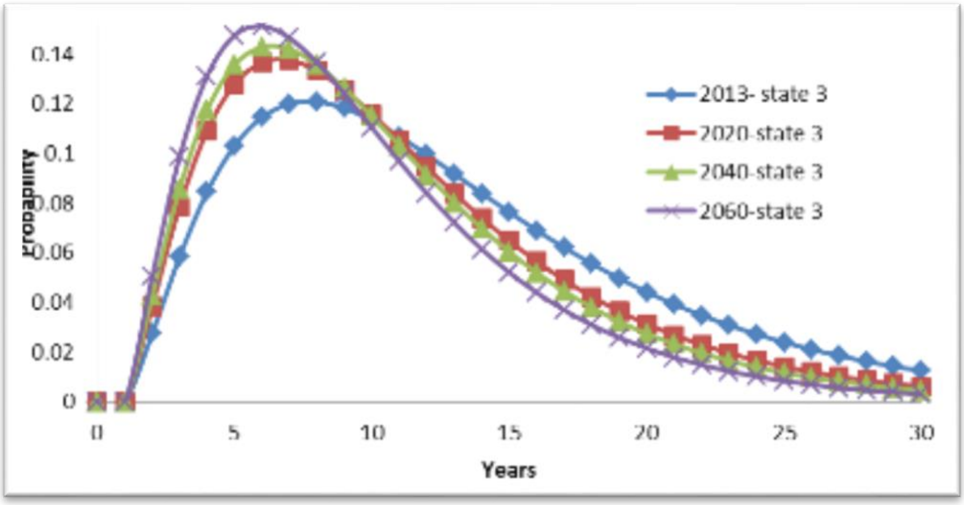

Figure 7-14: Change in state 3 condition based on different climate change scenarios

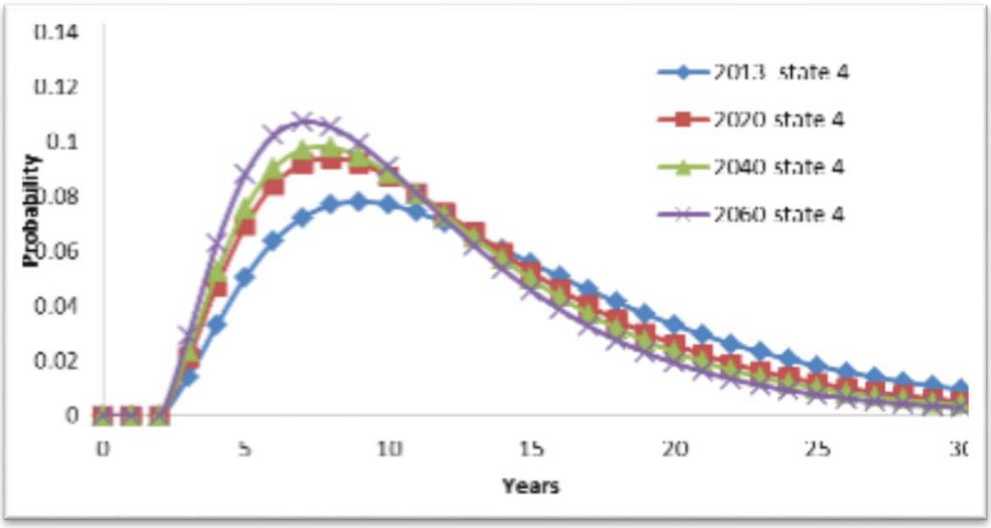

Figure 7-15: Change in state 4 condition based on different climate change scenarios

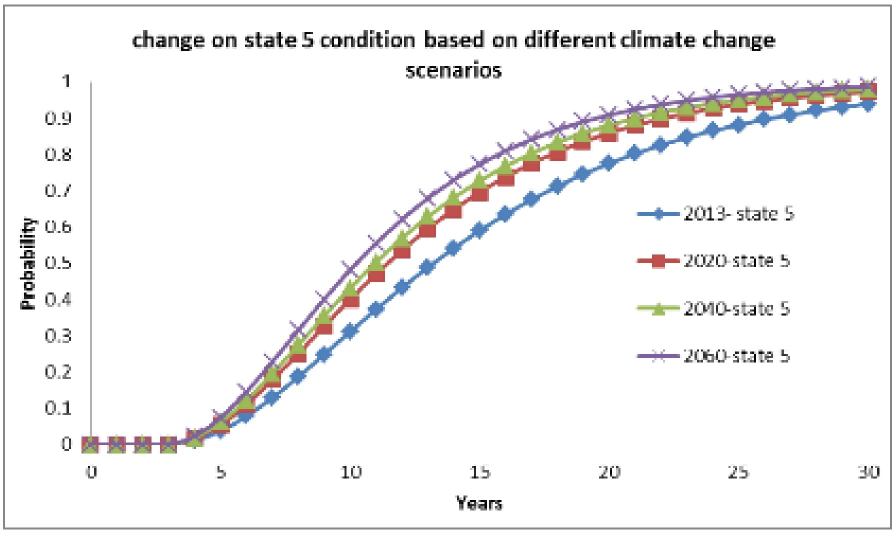

Figure 7-16: Change in state 5 condition based on different climate change scenarios

7.4. Determination of Deterioration Curve Based on International Roughness Index

There are different interpretations of the deterioration predictions function. Other researchers such as Mubaraki (2010) have found the traditional S-shaped or sigmoid function is the best presentation of the pavement deterioration predictions curve(Figure 7-17). Mohseni (2012) added that an S-shaped or sigmoid curve indicates that no deterioration occurs at the start of the asset's life. On the other hand, NAMS (2009) suggested taking an exponential approach to represent the deterioration curve.

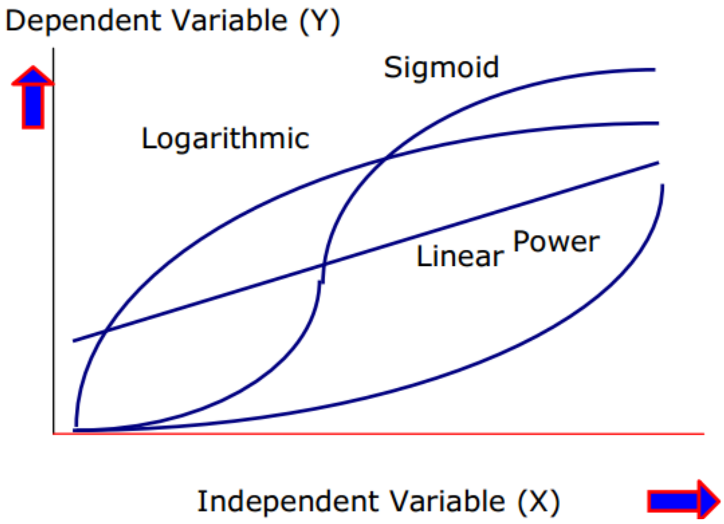

Figure 7-17: Types of pavement deterioration predictions curve by Mubaraki (2010)

According to Figure 7-18, the pavement deterioration curves based on the IRI value for different climate change impacts (2013, 2020, 2040 and 2060) obtained a logarithmic curve shape as a result of the Markov chain modelling.

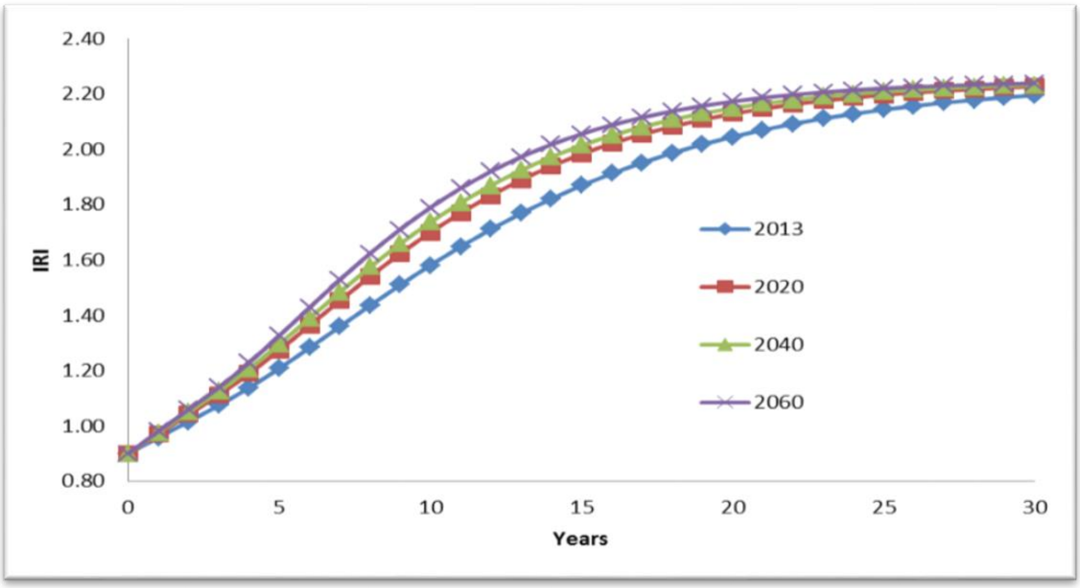

Figure 7-18: Pavement deterioration curves based on the IRI value for different climate change impacts (2013, 2020, 2040 and 2060)

The shape of the pavement deterioration curve does not match that of other researchers, who have found the sigmoid function is the best interpretation of curve deterioration (Mubaraki 2010). The logarithmic curve shape of the deterioration curve can be read as the pavement assets receive a sharp deterioration rate at the start, then a phase of smooth increase takes place till it reaches a consistent level. The occurrence of such a phenomenon could be a result of the interpretation of the condition survey data and how such data are being developed in the transition probability matrix. On the other hand, technically, some failure in the pavement can occur as soon as the pavement structure receives traffic loading. This could happen in cases of insufficient pavement strength or construction quality deficiency. Therefore, the rate of deterioration increases faster until consolidation has taken place.

On the other hand, the amount of IRI for the obtained results from the Markov chain model highlighted that the 2060 case contains a faster deterioration rate while the 2013 case has the lowest deterioration rate. These results show that climate change impact can accelerate the rate of degradation for infrastructure assets (pavement in the case study). And such degradation increases with increasing pavement temperature (assuming other variables are consistent).

7.5. Determining the Pavement Condition Index (PCI)

As was discussed early, the relationship of the pavement condition of asphalt pavement to its roughness was determined in Chapter 6 section 6.5. The model was introduced as per the equation in Table 7-16.

Table 7-16: PCI model

Main Equation 3	Variable	Description
PCI = (a1× $\boldsymbol{e}^{\boldsymbol{a2} \times \boldsymbol{IRI}}$)		
PCI model	IRI	International Roughness Index, in m/km IRI
	PCI	Pavement Condition Index

Using the obtained results from the Markov chain model for the four different climate change scenarios and the model highlighted in Chapter 6, the Pavement Condition Index was determined, and the results are reported in Appendix 4. The below table (7-17) provides an example of the results for the different climate change scenarios (2013, 2020, 2040 and 2060) for PCI value vs IRI.

Table 7-17: Example of PCI results obtained from IRI (Markov chain approach)

Years	2013		2020		2040		2060	
	IRI	PCI	IRI	PCI	IRI	PCI	IRI	PCI
0	0.90	95.54	0.90	95.54	0.90	95.54	0.90	95.54
1	0.96	92.99	0.97	92.41	0.98	92.22	0.98	92.03
2	1.02	90.54	1.04	89.46	1.05	89.11	1.06	88.72
3	1.07	88.12	1.11	86.59	1.12	86.09	1.14	85.50
4	1.14	85.55	1.19	83.54	1.21	82.89	1.23	82.04
5	1.21	82.83	1.27	80.33	1.30	79.52	1.33	78.41
6	1.28	80.03	1.36	77.09	1.39	76.14	1.43	74.81

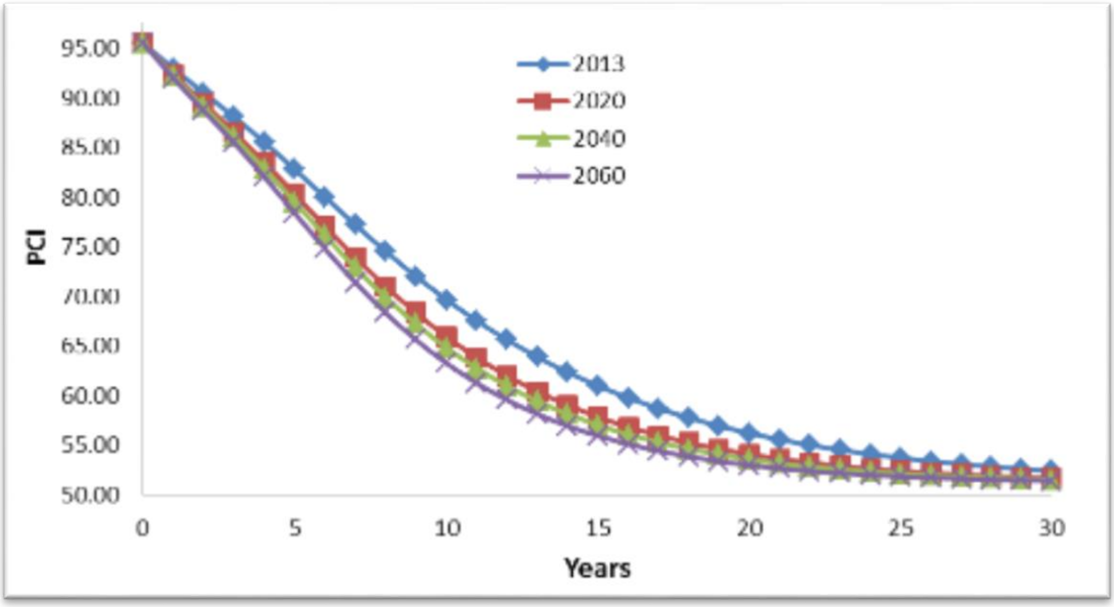

Figure 7-19: Deterioration curve for Pavement Condition Index for different climate change scenarios

Figure 7-19 represents the deterioration curves concerning the Pavement Condition index (PCI) for next predicted 30 years for the pavement network of the UAE Ministry of Public Works with different climate change scenarios. With a similar approach to the deterioration curve of IRI, the 2060 case received the worst deterioration scenario, whilst the 2013 case received the best one. Such results conclude that climate change impact can accelerate the rate of degradation for infrastructure assets (pavement in the case study). And such degradation increases with increasing pavement temperature (assuming other variables are consistent).

7.6. Summary

This chapter has presented a concept for generating a Markov chain model in order to determine deterioration prediction curves for the pavement network for the UAE Ministry of Public Works. Different climate change scenarios were modelled and tested. The challenges of deriving the transition probability matrix based on two methods were discussed. The proposed method was demonstrated using a sample set of condition data from Chapter 6 (modified HDM-4 model). The results showed that, for the deterioration curve of IRI, the 2060 case received the worse deterioration scenario while the 2013 case was the best one.

8. Chapter 8 Causal Loop Diagrams for the Pavement Deterioration Model

8.1. Introduction

The purpose of this chapter is to forecast the pavement deterioration using system dynamics based on the established parameters from Chapter 6. Moreover, the generic risks developed in Chapter 2 section 2.4.1 are studied in this chapter. The interdependencies between climate change risks and pavement deterioration model were constructed by causal loop diagrams. These causal loop diagrams shall be used in the SD models as discussed in Chapter 9 section 9.2.

8.2. Causal Loop Diagrams

As was discussed earlier, in Chapter 2, causal loop diagrams (CLDs) are a crucial component of the system dynamics skeleton. According to Rashedi (2016), CLDs are responsible for defining theory and interactions among various variables. He also stated that CLD links impact the relationship between variables by link polarities. CLDs present feedback loops which are either positive (self-reinforcing) or negative (self-correcting or balancing). In this chapter, the researcher explores the methodology based on the pavement deterioration model developed in Chapter 6 section 6.4. Using system dynamics will provide an understanding of how the pavement condition is changing over a period. To elaborate more, there is a need to investigate the proposed modified HDM-4 model developed in Chapter 6 by determining the CLDs based on the following principles and methods:

- In Chapter 3, the CLD variables were built to address the component interrelationships, which were based on the developed equations and coefficients for the improved HDM-4 model with calibration and taking into consideration the data described in Chapter 5 and current literature in Chapter 2.

- The causal loop diagrams for the proposed model were empirically confirmed by Chapter 6 model outputs which are used in this chapter to examine whether the CLDs could fit to be used in determining pavement condition.

- All of the model components such as change in roughness due to rutting, cracking and environmental component, including their direct variables and sub-variables, were encompassed in the causal loop.

- The modelling of the risk causal loop diagrams is considered through the investigation of the risk associated with pavement failure.

8.3. Casual Loop Diagram for Total Change in Roughness (ΔRI) and Pavement Condition Index (PCI)

As was discussed earlier, in Chapter 2, developing models that assess the impact of climate change on road roughness can be achieved using the HDM-4 model. Total change in roughness is a summation of the total annual incremental change in roughness and initial roughness. Based on HDM-4, the total annual incremental change in roughness is the sum of the various components such as rutting, cracking, environmental and structural components. The modified total change in roughness is used as per the following equation:

$$\Delta RI = \Delta RIc + \Delta RIr + \Delta RIe$$

Equation 8-1:Total change in roughness

Figure 8-1 presents the variables that represent the casual loop diagram for total roughness and PCI based on modified HDM-4.

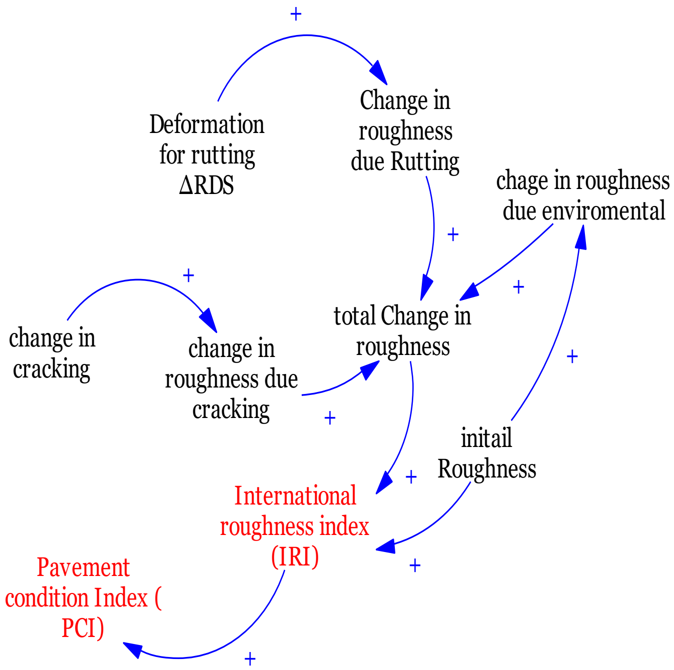

Figure 8-1: CLD for the total incremental change in roughness and PCI

8.3.1. Rutting Component of Roughness (ΔRlr)

The change in roughness – rutting (ΔRlr) based on improved HDM-4 with calibration factor was discussed in Chapter 6. Figure 8-2 presents the variables. Causal loop diagrams (CLDs) present feedback loops which are either positive (self-reinforcing) or negative (self-correcting or balancing). According to the CLD for rutting component of roughness (ΔRlr), most of the elements in the system such as traffic loading, pavement thickness, speed of heavy vehicles, maximum pavement temperature and rutting are linked to each other and receive an effect of expansion or increase based on equations 8-2 and 8-3. This approach, over time, will magnify the system, leading to what is called exponential growth.

$$\Delta\mathbf{RIr} = \mathbf{a0} \times \mathbf{Ln}\ (\Delta\mathbf{RDS}) + \mathbf{a1}$$

Equation 8-2: Rutting component of roughness (ΔRlr)

$$(\Delta\mathbf{RDS}) = \mathbf{a0} \times (\boldsymbol{YE4})^{\boldsymbol{a5}} \times (\boldsymbol{sh})^{\boldsymbol{a1}} \times (\boldsymbol{HS})^{\boldsymbol{a2}} \times \left(\frac{\boldsymbol{SP}}{\boldsymbol{VIM}}\right)^{\boldsymbol{a3}} \times \mathbf{TPmax} \times \mathbf{a4} + \mathbf{a0} \times \mathbf{a6}$$

Equation 8-3: Deformation for rutting ΔRDS

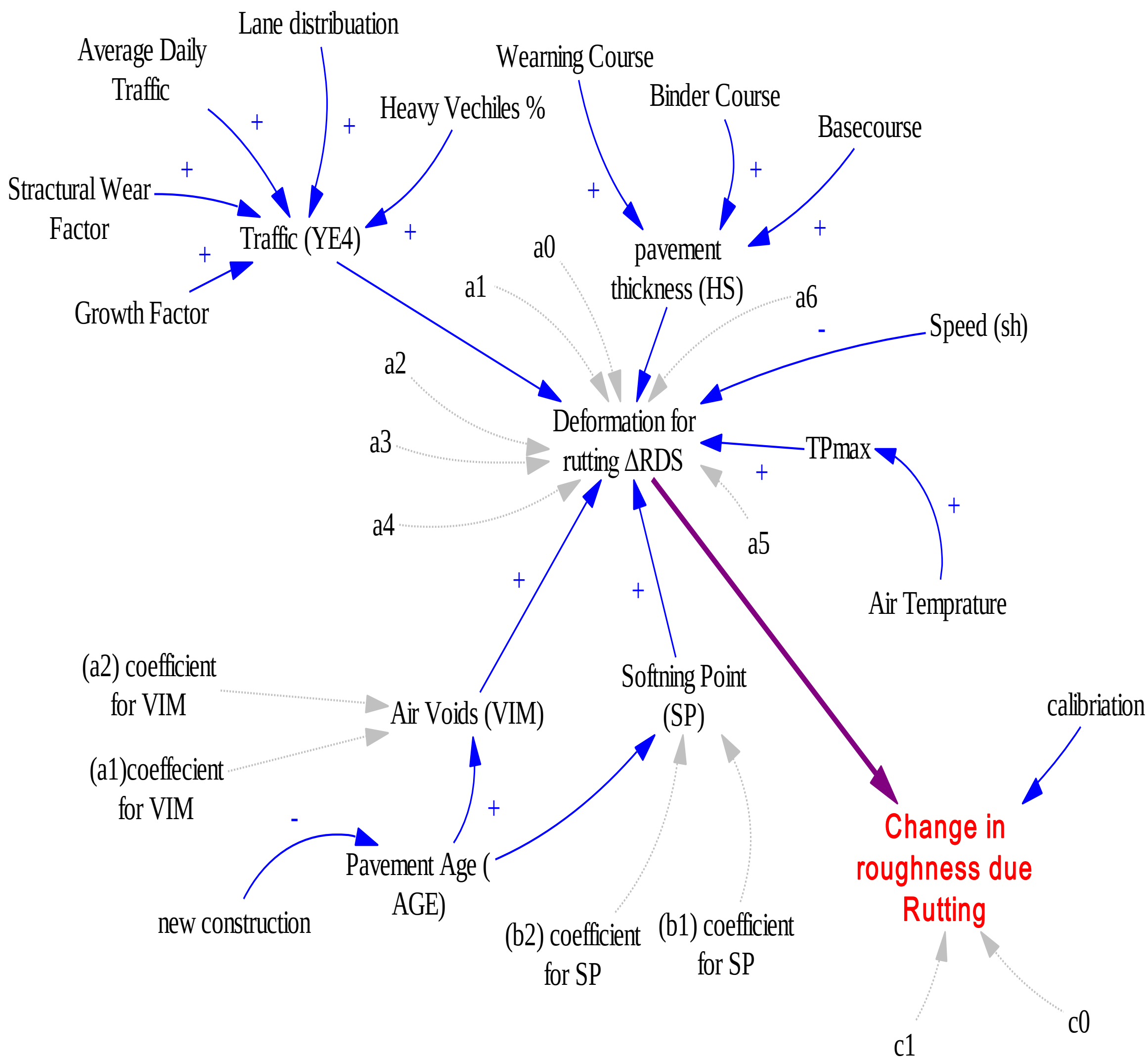

Figure 8-2: Casual loop diagram for rutting component of roughness (ΔRlr)

8.3.2. Cracking and Environmental Component of Roughness

Components for investigating the pavement deterioration model such as change in roughness due to cracking ΔRIc and environmental (ΔRIe) components were also discussed (see Chapter 6). The following variables are used to build the casual loop diagram. Change in roughness due to cracking component consists of incremental change in the area of total cracking during analysis year, in per cent, which is always a real input from the condition survey, unlike the change in rutting, which is determined from different variables. Moreover, the environmental component of roughness (ΔRIe) is also considered (see Figure 8-3 and Figure 8-4).

$$\mathbf{\Delta RIc = d0\times (\Delta ACRA)^2 + d1\times \Delta ACRA + d2}$$

Equation 8-4:Change in roughness due to cracking component

The coefficients are d0, d1, d2

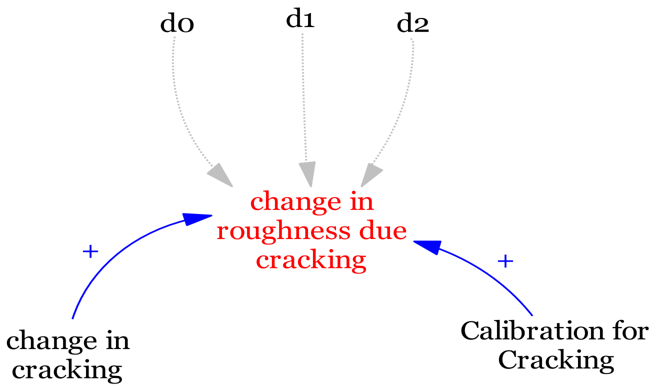

Figure 8-3: CLD change in roughness due to cracking component ΔRIc

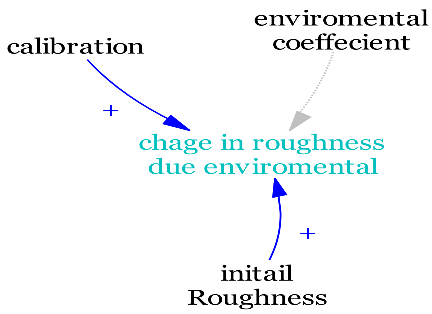

Figure 8-4: CLD Change in roughness due to environmental component (ΔRIe)

ΔRIe = Kgm m Ria

Equation 8-5: Environmental component of roughness (ΔRIe)

Both CLDs are positive (self-reinforcing) for change in roughness due to cracking ΔRIc and environmental (ΔRIe) components. The highlighted variables for the two components are in the expansion direction over time, which will be read as exponential growth. The use of calibration and coefficients remains constant. Finally, the combination of all sub-models to develop CLDs for the pavement deterioration model is illustrated in Figure 8-5 .

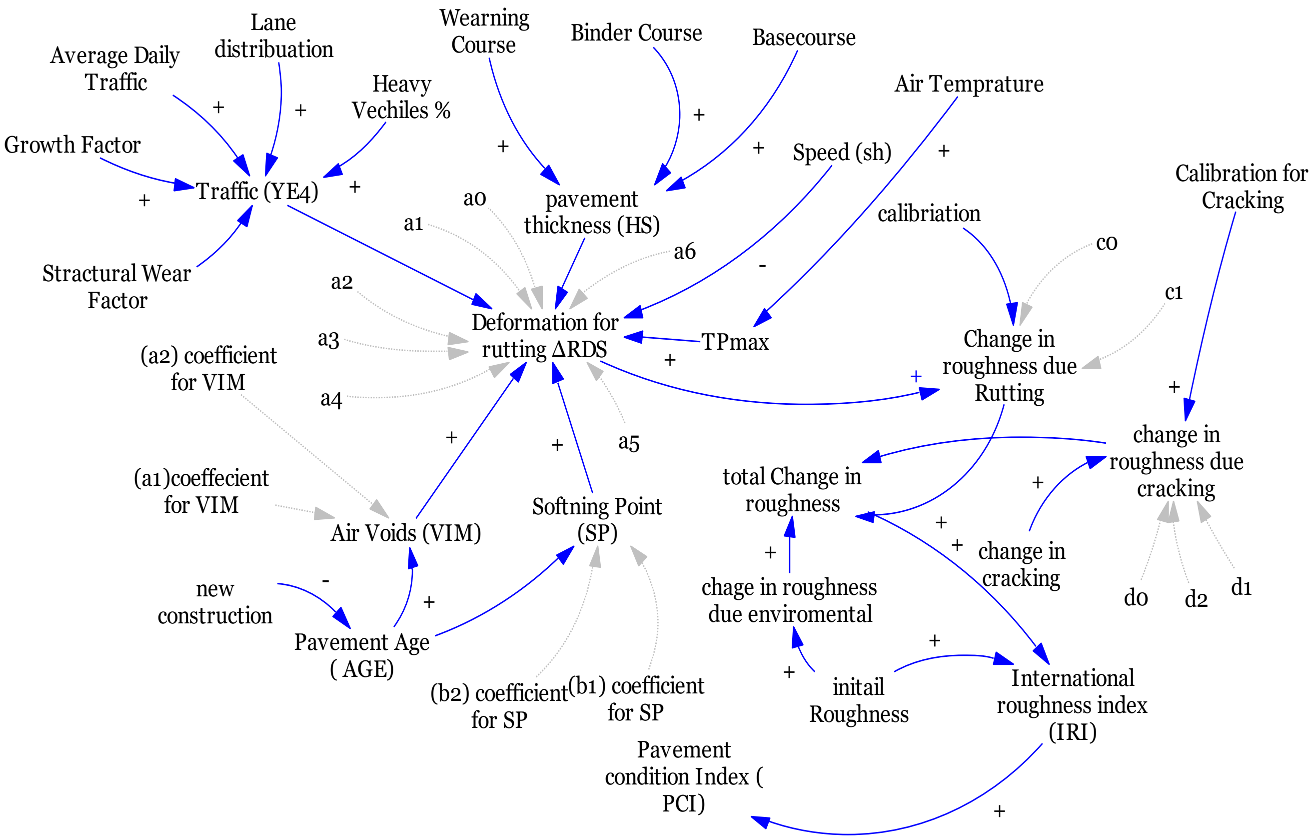

Figure 8-5: Casual loop diagram for pavement deterioration model based on modified HDM-4 without risk

8.4. Risk Causal Loop Diagrams for Pavement Deterioration Model under Climate Change Impact

8.4.1. Pavement Failure Risk

In Chapter 2, the definition of pavement failure was introduced. For example, Al-Arkawazi (2017) mentioned that pavement failure usually start gradually, and may not be noticeable at the beginning; however, over time it accelerates dramatically. The importance of understanding the risk associated with road pavement failure (pavement deterioration) was discussed in Chapter 2. Understanding the risk of road pavement failure is not straightforward (Reigle 2002). However, Schlotjes (2013) stated that understanding this risk can be achieved by defining the mechanisms surrounding road pavement failure. Based on Schlotjes' (2013) approach, the primary goal of this chapter is to describe the variety of factors that can trigger the risk of pavement failure using a system dynamics approach. The risk factors related to pavement failure (pavement deterioration) in conjunction with the probability of occurrence of multiple failure modes are complex; therefore, the researcher used different methods to analyse the complexity of pavement failure risk and how it can be integrated into the proposed model of pavement deterioration (this is discussed in detail later, in Chapter 9; see section 9.2). Identification and assessment of the causes of pavement failure will support highway agencies such as the Ministry of Public Works in the UAE in establishing a solid understanding of how such risk contributes to the rate of deterioration in pavement condition. Table 8-1 presents generic pavement failure developed by the author.

Table 8-1: Generic pavement failure developed by the author

Code	Sub-Risk Factors	Main Risk Factor	Evidence
S.1	High volume of heavy trucks	R.1 Traffic Loading	Graves et al. (2005)
S.2	Axle Group Type	R.1 Traffic Loading	Cebon (1999)
S.3	Tyre configuration	R.1 Traffic Loading	Cebon (1999)
S.4	Gross vehicle mass	R.1 Traffic Loading	Cebon (1999)
S.5	Dynamic Wheel Loading	R.1 Traffic Loading	Cebon (1999)
S.6	High traffic loading (all vehicles type)	R.1 Traffic Loading	Sen (2012)

S.7	Vehicle speed	R.1 Traffic Loading	Mikhail and Mamlouk (1997)
S.8	Precipitation	R.2 Climate Change	Schlotjes (2013) Alaswadko (2016)
S.9	Weathering	R.2 Climate Change	Schlotjes (2013),Alaswadko (2016)
S.10	High Temperature	R.2 Climate Change	Schlotjes (2013) Alaswadko (2016)
S.11	Low Temperature	R.2 Climate Change	Schlotjes (2013) Alaswadko (2016)
S.12	Drainage	R.2 Climate Change	Schlotjes (2013) Alaswadko (2016)
R.5	Pavement Ageing	R.2 Climate Change	Roberts and Martin (1998)
S.14	Increase oxidation	R.2 Climate Change	Roberts and Martin (1998)
S.15	Increase viscosity and softness	R.2 Climate Change	Roberts and Martin (1998)
S.16	Increase Brittle of asphaltic layer	R.2 Climate Change	Roberts and Martin (1998)
S.17	Increase Moisture/ Excess water	R.2 Climate Change	Harvey et al. (2004)
S.18	Material Quality and Properties (Aggregate/soil)	R.3 Pavement composition	Zuo et al. (2007) and Harvey et al. (2004)
S.19	Pavement Thickness	R.3 Pavement composition	Harvey et al. (2004)
S.20	Availability of Material	R.3 Pavement composition	Pearson (2012)
S.21	Bitumen Supply and Quality	R.3 Pavement composition	White (2016)
R.1	Traffic Loading	R.4 Pavement Strength	Pearson (2012)
S.22	Insufficient value of Structural Number (SN)	R.4 Pavement Strength	Pearson (2012)
R.2	Climate Change	R.5 Pavement Ageing	Harvey et al. (2004)
R.1	Traffic Loading	R.5 Pavement Ageing	Harvey et al. (2004)
R.6	Subgrade Soil	R.5 Pavement Ageing	Harvey et al. (2004)
R.8	Maintenance	R.5 Pavement Ageing	Harvey et al. (2004)
S.17	Increase Moisture/ Excess water	R.6 Subgrade Soil	Jones and Jefferson (2012)
S.13	Selection of construction soil	R.6 Subgrade Soil	Jameson (2008)
S.17	Increase Moisture/ Excess water	R.7 Drainage	Haas et al. (1994)
S.23	Insufficient drainage system	R.7 Drainage	Haas et al. (1994)
S.24	Delay maintenance	R.8 Maintenance	Martin (2004)
S.25	Maintenance priorities/plan	R.8 Maintenance	Martin (2004)
S.26	Limited Budget	R.8 Maintenance	Adlinge and Gupta (2013)
S.27	Design and Specification	R.9 Construction Quality	Bubshait (2001), Al-Hassan (1993) and Abu El-Maaty (2016)
S.28	Construction Process	R.9 Construction Quality	Bubshait (2001)

8.4.2. Pavement Failure Risk Causal Loop Diagrams

One of the core mechanisms of pavement failure is risk identification so that the asset managers and pavement designer work together efficiently and adequately in order to handle the risks for better performance of the pavement assets. The pavement failure risk presented in the literature review by various authors can be considered as incomplete and unrepresentative because the assessment conducted by previous studies only found single direct risks. A list of generic risk factors has been extracted from various literature and was discussed in Chapter 2. The researcher also explored the effects of pavement failure to define a clear picture to start risk allocation through a framework of risk causal loop diagrams (CLDs). Therefore, the risk causal loop diagrams were modelled based on the significant risk variables that can occur during the pavement life cycle, including all risks and their direct and intermediate variables.

8.4.2.1. Causal Loop Diagrams (CLDs) for Traffic Loading Risks

A traffic loading risk event would cause deterioration in the pavement. Factors such as increase in axle loads, high volume of heavy trucks and vehicle speed can cause the development of different deterioration modes such as roughness, rutting and cracking. CLDs present feedback loops which are either positive (self-reinforcing) or negative (self-correcting or balancing). According to the CLD for Traffic Loading (Figure 8-6), all of the elements in the system such as high volume of heavy trucks, axle group type, tyre configuration, gross vehicle mass, dynamic wheel loading, high traffic loading (all vehicles type) and vehicle speed which are linked to each other receive an effect of expansion or increase. Such an approach, over time, will magnify the system, leading to what is called exponential growth. The interrelationship between each element is discussed later, in Chapter 9 section 9.3.

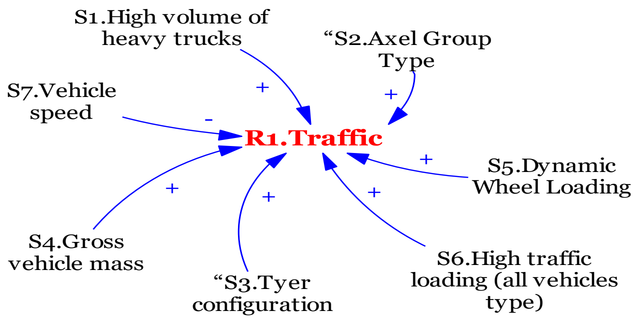

Figure 8-6: Causal loop diagram of traffic loading risk and sub-risks

8.4.2.2. Climate (Environmental Loading) Risks

Climate (environmental loading) is a crucial component for the pavement failure risk. As was mentioned in Chapter 2, climate risk (environmental loading) has a substantial impact on pavement performance. The CLDs are positive (self-reinforcing) for climate (environmental loading). The highlighted variables for the component (Figure 8-7), which are the precipitation, weathering, high temperature, drainage, pavement ageing, increased oxidation, increased viscosity and softness, increased brittleness of an asphaltic layer, increased moisture/excess water and low temperature, are in the expansion direction over time, which will be read as exponential growth, as discussed in Chapter 2 section 2.4.1 and Chapter 4 section 4.6.

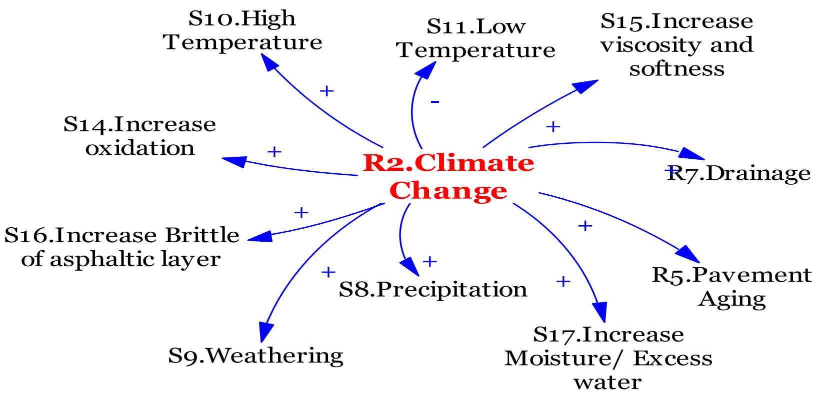

Figure 8-7: Causal loop diagrams of climate (environmental loading) risk and sub-risks

8.4.2.3. Pavement Composition Risks

Causal loop diagrams (CLDs) for pavement composition highlighted variables shaping the risk associated with it. There are four elements (Figure 8-8) , which are material quality and properties (aggregate/soil), pavement thickness, availability of material, and bitumen supply and quality. The material quality and pavement thickness are the two essential elements for achieving pavement performance, and any deficiency in these elements will lead to pavement failure risk. For example, to avoid rutting, the underneath layers such as the base and sub-base layers should be designed with an adequate thickness that meets any traffic loading increases. Another example is the change in bitumen supply and quality, which contributes to many asphalt surface failures. Therefore, the risk of achieving insufficient pavement composition is shown as in Chapter 2 section 2.4.1 and Chapter 3 section 3.6.

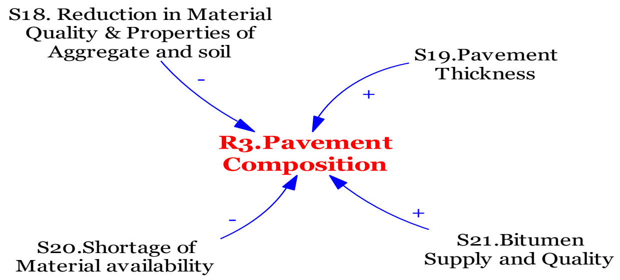

Figure 8-8: Causal loop diagrams of pavement composition risk and sub-risks

8.4.2.4. Pavement Strength Risks

Risk associated with pavement strength is impacted by the two elements: the insufficient value of Structural Number (SN) and traffic loading (see Figure 8-9). Traffic loading is a significant risk which is linked to many other features which are discussed in the previous sub-section. Concerning pavement strength, Paterson (1987) stated that pavement structure could withstand as much as nearly eight times an increased equivalent standard axle load (ESAL) if the pavement structure received 50% improvement and modification of pavement specification. However, insufficient pavement strength will lead to the development of rutting. Therefore, the risk of pavement strength is measured by the value of Structural Number (SN). The CLDs represent feedback loops that are both positive (self-reinforcing) for traffic loading and associated sub-elements and negative (self-correcting or balancing) for pavement strength associated with Traffic Loading and insufficient value of Structural Number (SN). The interrelationship between each element is discussed later in Chapter 9 section 9.3.

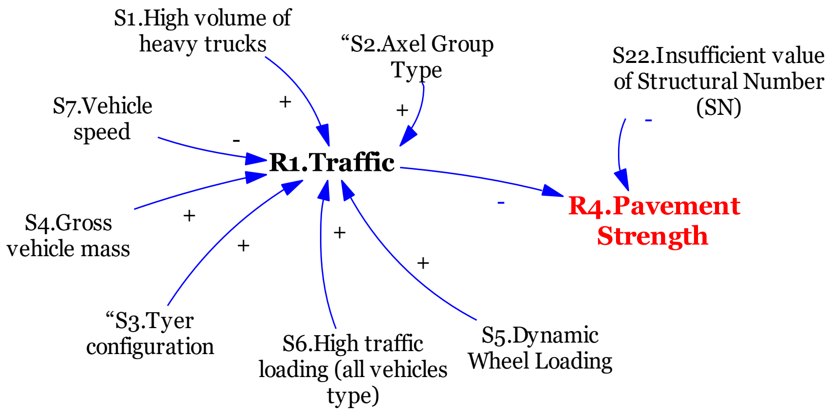

Figure 8-9: Causal loop diagrams of pavement strength risk and sub-risks

8.4.2.5. Subgrade Soil Risks

Selection of a suitable subgrade can delay the deterioration rate (Mann 2003) and the main impact on the subgrade can be received from water moisture content. Bae et al. (2008) also highlighted the risk associated with variation of water moisture content on developing a faster rate of deterioration in the pavement structure. According to the CLD for subgrade soil (Figure 8-10), all of the elements in the system such as the selection of construction soil and increased moisture/excess which are linked to each other have a balancing effect on each other. The interrelationship between each element is discussed later in the Chapter 9 section 9.3.

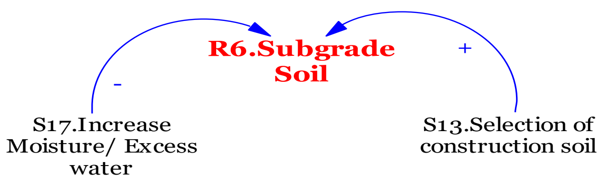

Figure 8-10: Causal loop diagrams of subgrade soil risk and sub-risks

8.4.2.6. Pavement Ageing Risks

Details of pavement ageing risk were highlighted in Chapter 2, section 2.4.1 In pavement engineering, Martin and Choummanivong (2010) described pavement age as the date of original construction or last rehabilitation cycle. According to Harvey et al. (2004), a flexible pavement structure is designed to last 20-40 years, providing an adequate service that meets the comfort and safety of drivers. The pavement ageing risk event is associated with four significant elements: traffic loading, climate, subgrade soil and continuous maintenance. Many investigations have presented how vital the relationship between pavement deterioration and pavement age is (Alaswadko 2016). For example, Shiyab, Al Fahim and Nikraz (2006) distilled the hypothesis that the pavement age contributed about 9% of the model's prediction of flexible pavement performance. Mubaraki (2010) emphasised the importance of the pavement age factor in building a predicting model for pavement deterioration. For the CLD for pavement ageing risk (Figure 8-11), all of the elements in the system such as traffic loading, climate, subgrade soil and continuous maintenance are linked to each other and receive a different effect.

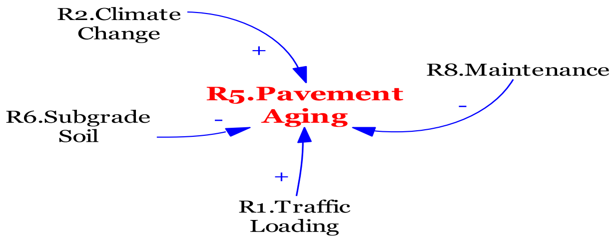

Figure 8-11: Causal loop diagram of pavement ageing risk and sub-risks

8.4.2.7. Drainage Risks

The impact of drainage risk can be observed in the level of water moisture content which affects the subgrade layer and strength of pavement materials (Austroads 2018). Increases in the moisture content of the base and sub-base layers lead to a loss in the bearing capacity, and consequential acceleration in the rate of pavement deterioration and shortening of service life. For the CLD of the drainage risk, two elements are linked (Figure 8-12). These are increased moisture/excess water and insufficient drainage system.

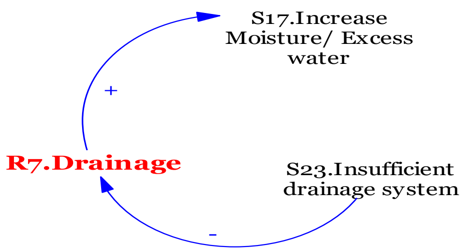

Figure 8-12: Causal loop diagrams of drainage risk and sub-risks

8.4.2.8. Maintenance Risks

The primary goal of pavement maintenance and rehabilitation activities is to ensure the pavement condition is at a satisfactory level in terms of road safety, driver comfort and ride. In general, the rate of pavement deterioration (roughness and rutting) is influenced by the pavement maintenance and rehabilitation treatment plan (Martin 2011). Adlinge and Gupta (2013) highlighted that, even if the pavement is well built, it will deteriorate over time. However, the main risk comes from delaying maintenance. Typically, postponing maintenance is due to budget limitations and constraints, which will lead to a significant financial impact on the pavement life cycle. In conclusion, limited budget, maintenance priorities/plan and delay in maintenance intervention are the elements that build the CLD for the maintenance risk as per Figure 8-13.

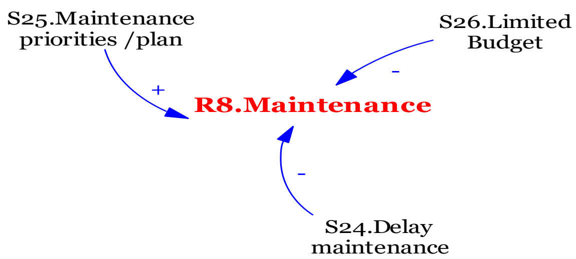

Figure 8-13: Causal loop diagrams of maintenance risk and sub-risks

8.4.2.9. Construction Quality Risks

Adlinge and Gupta (2013) stated that risk in construction quality could be seen in achieving inadequate compaction and inadequate moisture conditions during construction, poor quality of materials, and imprecise layer thickness. In the field of pavement construction, Deacon, Monismith and Harvey (2001) defined quality as a critical element of measuring performance. A pavement's performance is affected by the quality of construction . For the CLD of construction risk, three aspects in are linked. These are construction process, construction management, and design and specification.

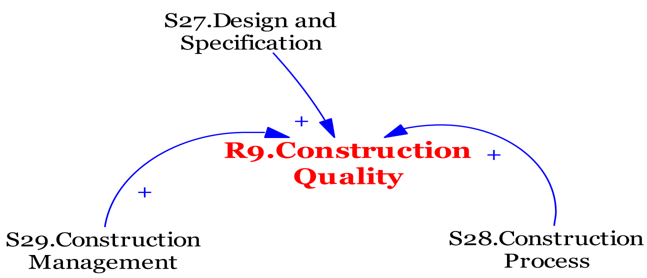

Figure 8-14: Causal loop diagrams of construction quality risk and sub-risks

8.4.2.10. Rutting Risks

Rutting risk can result for many reasons, such as unstable HMA (too much asphalt or too soft asphalt binder), densification of HMA (poor compaction during construction) and deep settlement in the subgrade (drainage or weak subgrade). Technically, the stresses that occur result from traffic load that exceeds the shared strength of the asphaltic material. Other reasons for surface rutting introduced by TRL (1993) are the increase in axle loads, channelised traffic, high maximum temperatures, and slowing and stopping travel vehicles. To summarise the risk associated with rutting, the following CLD is drawn as per Figure 8-15, showing that climate change, pavement strength, subgrade soil, pavement composition and construction quality are the risk elements.

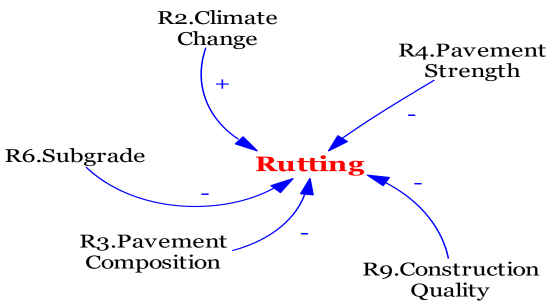

Figure 8-15: Causal loop diagrams of rutting risk and sub-risks

8.4.2.11. Cracking Risks

According to Alaswadko et al. (2016), cracking is a very active segment which gives a high weight in assessing pavement condition. The risk of crack is a sign of pavement defect. Fwa (2006) stated that the main reason for cracking risk is fatigue failure of the asphalt concrete, shrinkage, deformation, crack reflection from underlying pavement layers and poor construction joints of the asphalt concrete, and daily temperature cycling. Cracks can also result from traffic loading, the environmental impact or both. Paterson (1987) and Harvey et al. (2004) defined some of these causes such as pavement structure overloading, moisture movement and volume change, ingress of water into pavement layers, ageing, hardening of pavement surface (oxidation) and the impact of climate change (for example, heat and precipitation). To summarise the risk associated with cracking, the following CLD is drawn showing that climate change, pavement strength, subgrade soil, pavement composition and construction quality are the risk elements (Figure 8-16).

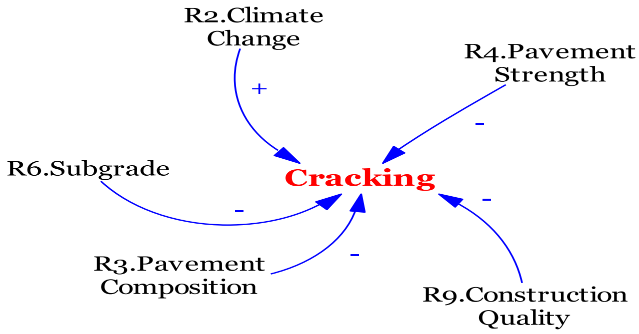

Figure 8-16: Causal loop diagrams of cracking risk and sub-risks

8.4.2.12. Heavy Vehicle Speed Risks

The primary goal of pavement maintenance and rehabilitation activities is to ensure the pavement's condition is satisfactory in terms of road safety, driver comfort and ride. The speed range is affected by the road condition, and if there was no maintenance then a slow speed for travelling vehicles would have to be introduced. This means that more impact could be generated if the vehicle slows down. On the other hand, it is not only maintenance that can affect the travelling speed: pavement ageing and the drainage system available on the road can also have an effect. The risk associated with heavy vehicle speed can be linked to three elements, pavement ageing, maintenance and drainage. The CLD in Figure (8-17) shows the shape of the risk.

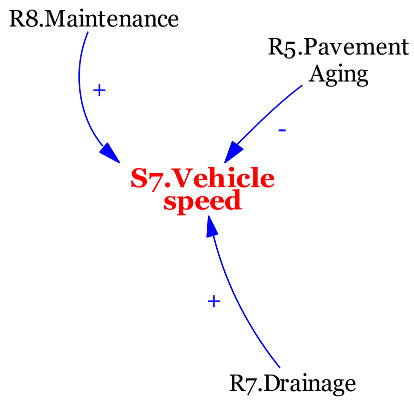

Figure 8-17: Causal loop diagrams of vehicle speed risk and sub-risks

8.4.2.13. Pavement Thickness Risks

Pavement thickness depends on the available material. The occurrence of rutting and cracking on a pavement can be controlled by achieving adequate pavement thickness with sufficient quality of pavement or surfacing materials (Harvey 2004). To avoid rutting, the underneath layers such as the base and sub-base layers should be designed with an adequate thickness that meets any traffic loading increases. Bae et al. (2008) emphasised the importance of achieving sufficient thickness. They concluded that longitudinal roughness deterioration could be minimised dramatically as the pavement thickness increased. Therefore, it is believed that construction quality is the major contributor to the risk of pavement thickness. The CLD that defines the relationship between construction quality risk and pavement thickness is shown in Figure (8-18).

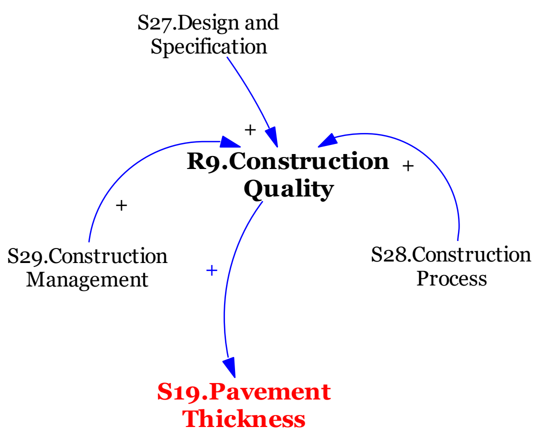

Figure 8-18: Causal loop diagrams of pavement thickness risk and sub-risks

8.5. Summary

This chapter has presented the development of causal loop diagrams for the modified HDM-4 model variables. Also, all the risk failures under the impact of climate change were captured using causal loop diagrams. Causal loop diagrams provided an understanding of how the pavement condition is changing over a period. The model is set up in order to include stock and flow models with different risk scenarios. CLD for all risk scenarios of the proposed pavement deterioration model is shown in Figure (8-19)

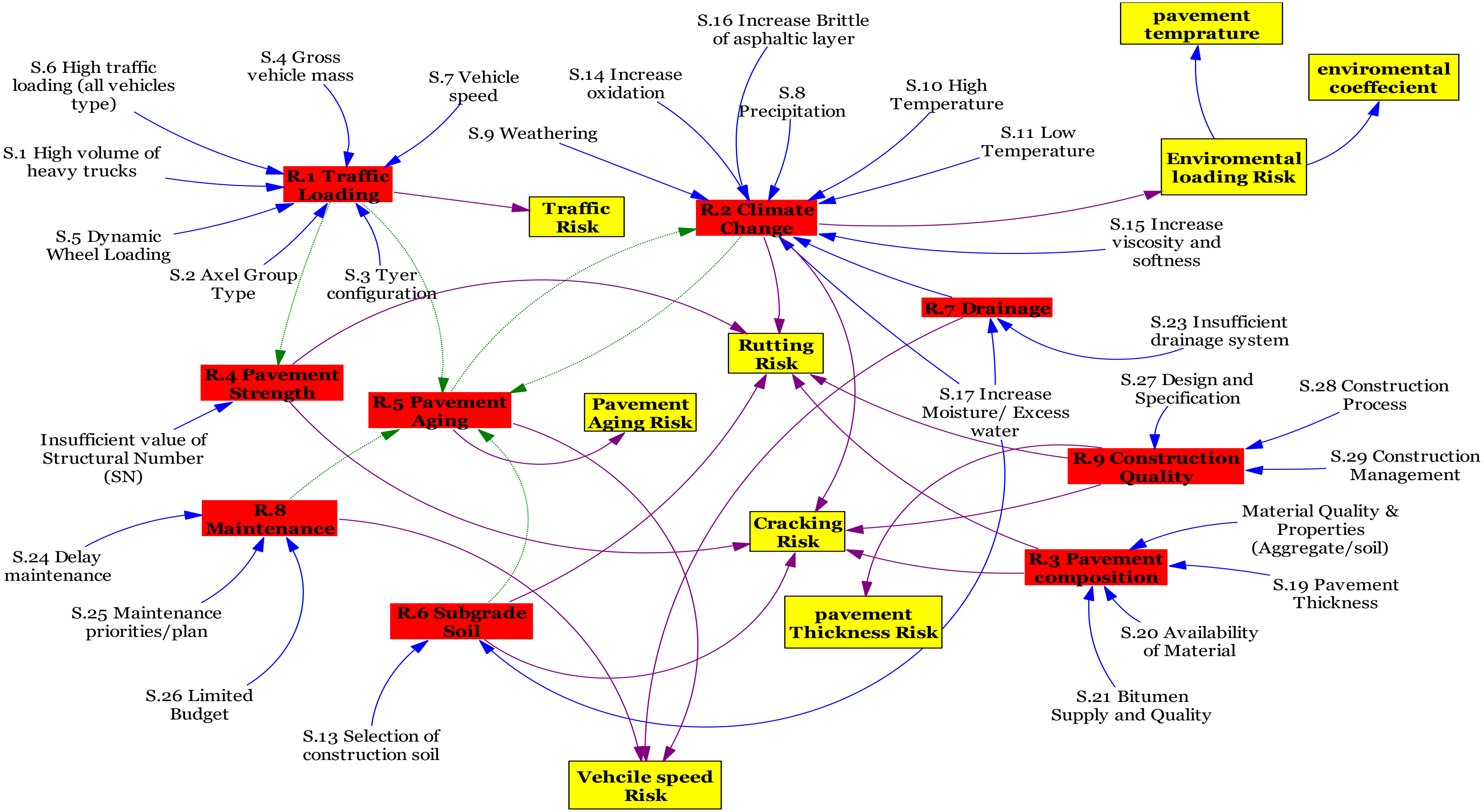

Figure 8-19: CLD for risk scenarios of the pavement deterioration model

9. Chapter 9 Modelling Pavement Deterioration Using System Dynamics

9.1. Introduction

Developing an understanding of risk associated with road pavement failure (pavement deterioration) under the impact of climate change was achieved and used as inputs into the system dynamics models, as discussed in Chapter 8. This chapter explains the methodology adopted in the use of stock and flow modelling in system dynamics. Vensim software was used to run the proposed model. Then, knowledge obtained on the risk related to pavement failure (pavement deterioration) was used to improve the success of the computational model through defining all the elements that could contribute to the change in IRI value and subsequently to PCI. Such an approach was developed from the stock and flow diagram to enrich the system in order to establish the dynamic behaviour for the selected variables. The pavement deterioration curve was obtained regarding pavement performance indicators PCI and IRI with different risk scenarios. The chapter finally presents and discusses the results from the different modelling exercises.

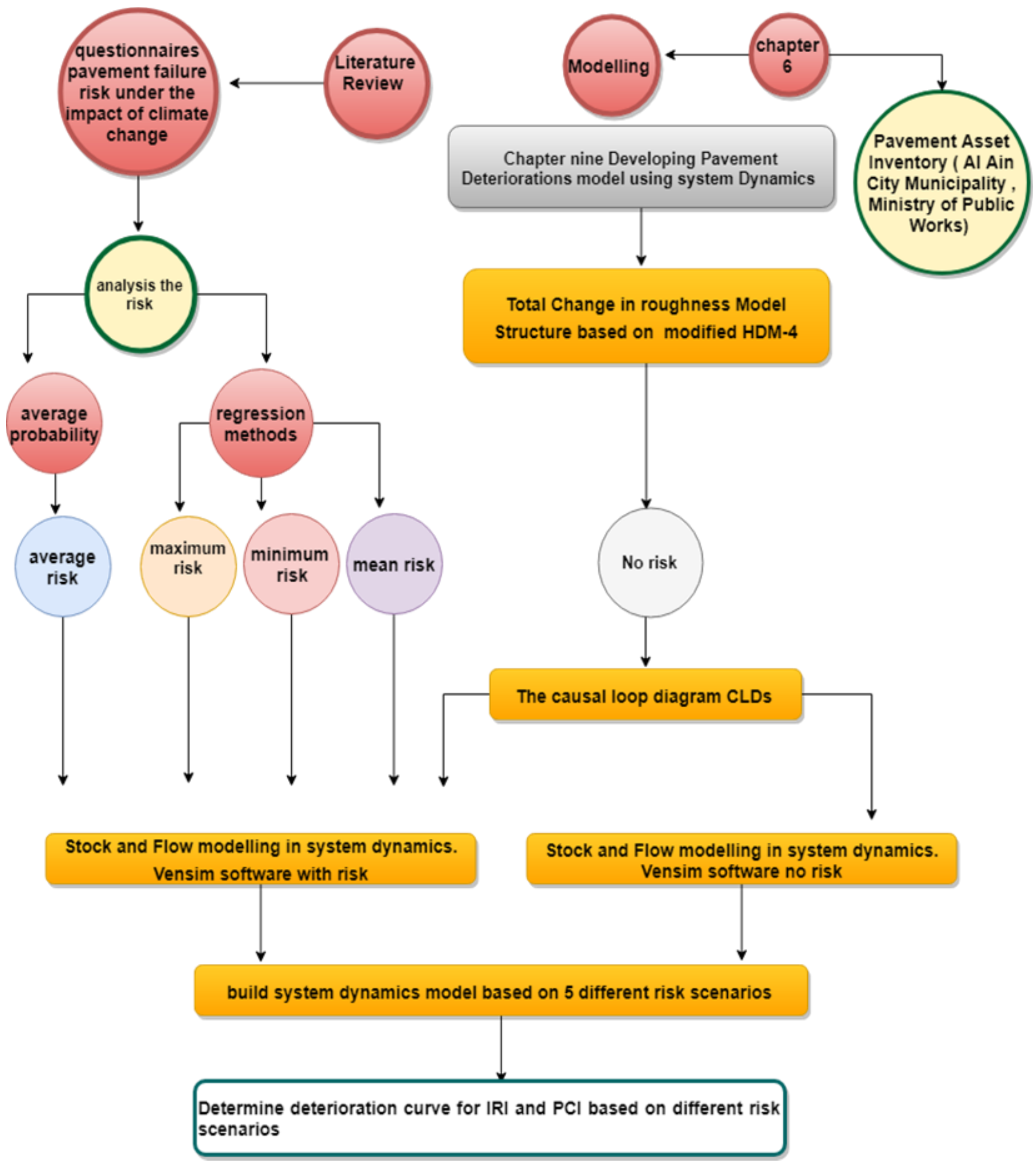

Figure 9-1: Roadmap of Chapter 9

9.2. Modelling and Simulation for Pavement Deterioration

The stock and flow model is a crucial element in SD models. According to Rashedi (2016), the model consists of four primary elements stocks (denote key system variables), flows (variables that produce quantities accumulated into inflows or out of outflows in the stocks), valves (flow generators) and clouds (entry or exit boundary points in the model). For this research, it is proposed to use Vensim as the software package for system dynamics modelling. Vensim software consists of various tools such as causal tracing analysis tools, variables diagram tree and SD models that quantify the Stock-Flow diagram (Rashedi 2016).

The proposed model was designed to receive the worst case scenarios at all levels. In practice, this could not always be the case; however, highway designers always compose a pavement structure design based on maximum historical or predicted data. In this study, a similar approach was carried out by introducing the ultimate values of the variable to seek the stage where the failure could occur under different climate scenarios and with different risk magnitudes.

9.2.1. Modelling of Total Change in Roughness and Pavement Condition Index

The tool of the HDM-4 model was applied to develop models that assess the impact of climate change on road roughness. Total change in roughness is a summation of the total annual incremental change in roughness and initial roughness value, as per Equation 9-1, and the total annual incremental change in roughness is the sum of the various components, such as rutting, cracking and environmental components, as per Equation 9-2. These equations were applied to define the relationship in the system dynamics modelling between the variables.

$$RI_{total} = RI_a + \Delta RI$$

Equation 9-1: Total roughness based on HDM-4

$$\boldsymbol{\Delta RI = \Delta RI_s + \Delta RI_c + \Delta RI_r + \Delta RI_e \ldots}$$

Equation 9-2: The total incremental change in roughness in HDM-4

9.2.1.1. Rutting Component of Roughness (ΔRIr) Sub-Model

The causal loop diagrams (CLDs) were developed and transformed into quantitative stock-flow diagrams to operationalise the model of pavement deterioration. One of the sub-models is the change in roughness due to rutting (ΔRIr). Rutting component of roughness (ΔRlr) is derived from the modified HDM-4 model, as discussed in Chapter 6 section 6.3.2 and as per equations 9-3 and 9-4, which define the relationship between the variables in the model.

$$\Delta RIr = a0 \times Ln(\Delta RDS) + a1$$

Equation 9-3: New equation for rutting component of roughness (ΔRlr) based on modified HDM-4

For change in rutting (ΔRDS), it is derived as per the following:

$$\Delta RDS = a0 \times (YE4)^{a5} \times (sh)^{a1} \times (HS)^{a2} \times (SP/VIM)^{a3}) \times TPmax \times a4 + a0 \times a6$$

Equation 9-4: New equation for change in rutting (ΔRDS) based on modified HDM-4

It was decided to investigate the range for every single variable in the proposed models. These variables are the pavement thickness, pavement temperature, pavement ageing, traffic loading and the speed of heavy vehicles, as per Equation 9-4. The following sections discuss the variables' model input range in more detail.

9.2.1.2. Pavement Thickness (HS)

Generally, the thickness of the pavement layer differs from one road to another due to many factors such as traffic loading, road type, availability of materials and pavement design life. According to the analysed data in Chapter 5, roads that belong to the UAE Ministry of Public Works consist of different pavement thickness sizes; an example is shown Table 9-1 below (more details were presented in Chapter 5 section 5.8). For this research, it was decided to run the entire model for 20 years, unlike the Markov chain model, which was 30 years (see Chapter 7 section 7.3).

Table 9-1: An example of asphalt surfacing thickness (HS) for data collection for the backward approach

N	Road Code	Road	Wearing Course (mm)	Binder Course (mm)	Base course (mm)	Wet mix Macadam as Base (mm)	Road Base (mm)	Granular sub-base (mm)	subgrade (mm)	total (mm)	Asphaltic layer (mm)
1	E.11	Ittihad road	50	60	70	0	250	200	150	780	180
3	E18.1	Manama- RAK Airport	50	50	60	200	0	150	150	660	160
5	E18.2	RAK Airport-Sha'am	50	50	60	200	0	150	150	660	160

To build the stock and flow diagram, it is necessary to compute the rate of change for pavement thickness in every interval year. Moreover, other information such as the initial value and simulation of the total period are needed. Thus, the model can match the real design thickness and achieve realistic results. For pavement thickness (HS), Pearson (2011) stated that each lower layer of a pavement is thicker than the one above it. The thickness of the surface and asphaltic layer is fairly standard, which depends on the traffic loading. For example, a study by Nunn et al. (1997) investigated the rates of asphalt rutting on more than 40 sites located on trunk roads in England with different pavement thicknesses ranging from 100 mm to 300 mm, as per the following Figure, 9-2.

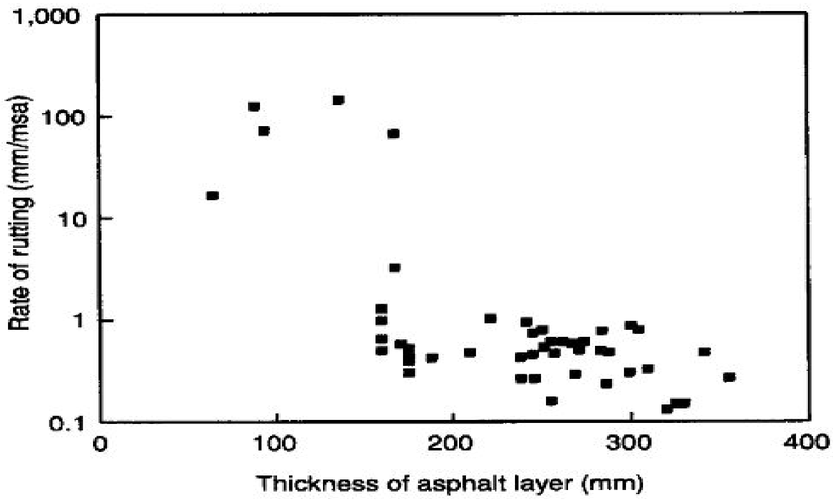

Figure 9-2: Rates of asphalt rutting with thickness on trunk roads in England (Nunn et al. 1997)

Anyala (2011) also investigated different thicknesses of asphalt layers of pavement based on trunk roads in England. The sample data collected for year 2003 that covered the Hot Rolled Asphalt (HRA) type of pavement thickness were in the approximate range 120 mm to 440 mm. After reviewing the UAE manuals for pavement design in conjunction with data collected from the Ministry of Public Works, it was decided to use the range between 120 mm and 220 mm of asphaltic thickness with consistent rate change (assumed linear relationship). The thickness stock and flow were tested, and the highlighted variable becomes a dynamic element, as per Figure 9-2. The rate of change for the pavement thickness was based on a linear approach (consistent rate of accumulation). It was also decided to build the stock and flow model to start with the lower scenario and move towards the most critical variable inputs. Figure 9-3 presents stock and flow for pavement thickness with proposed accepted range

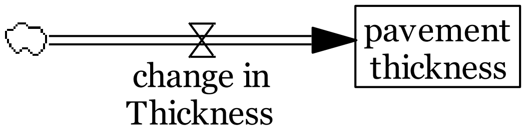

Figure 9-3: Stock and flow pavement thickness with proposed accepted range

9.2.1.3. Speed of Heavy Vehicles (sh)

In a similar approach to the pavement thickness factor, speed of heavy vehicles was determined to establish a stock and flow diagram. The analysis in Chapter 5 showed that the speed of heavy vehicles depends on whether the vehicle is loaded with goods or not. In Anyala's (2011) study, sampled heavy vehicle speed data included annual average speed values from 2001 to 2006 for speed measurement ranging from 15 km/h to 110 km/h. In the UAE, all heavy vehicles must travel at speeds no greater than the speed displayed on the relevant speed limit sign. Some signs have two speeds listed, one for light motor vehicles and one for heavy trucks. In most cases, 80 km/h is the maximum limit for heavy vehicles; however, the speed limit may not always be the safe speed for a heavy vehicle because of the vehicle's performance and weight of the loaded goods. Therefore, heavily loaded vehicles travel at slower speeds, which means they have more impact on pavement deterioration. To compute the speed of heavy vehicles variable into the system, it was decided to range the speed value from 80 km/h to 20 km /h (in descending order with a linear relationship), as per Figure 9-4. The stock and flow model for the variable was tested and run for a consecutive period of 20 years. The author also suggested that the stock and flow model should be built to start with the less impactful scenario and move towards the most critical variable inputs, and in this case, the heavy vehicle speed of 20 km/h is the most extreme input. Mikhail and Mamlouk (1998) reported that vehicle speed affects pavement performance as the displacement generated from speed is around 10 times more at a speed of 20 km/hr in comparison with 130 km/hr. Example of speed measurements is presented in Table 9-2.

Table 9-2: Example of speed measurements

E88 Al Dhaid - Masafi			
Date	**Time**	**Speed(km/h)**	**Axle**
7/8/2013	0:00:13	56	6
7/8/2013	0:00:24	65	6
7/8/2013	0:00:26	80	6
7/8/2013	0:00:42	87	6
7/8/2013	0:01:43	89	6

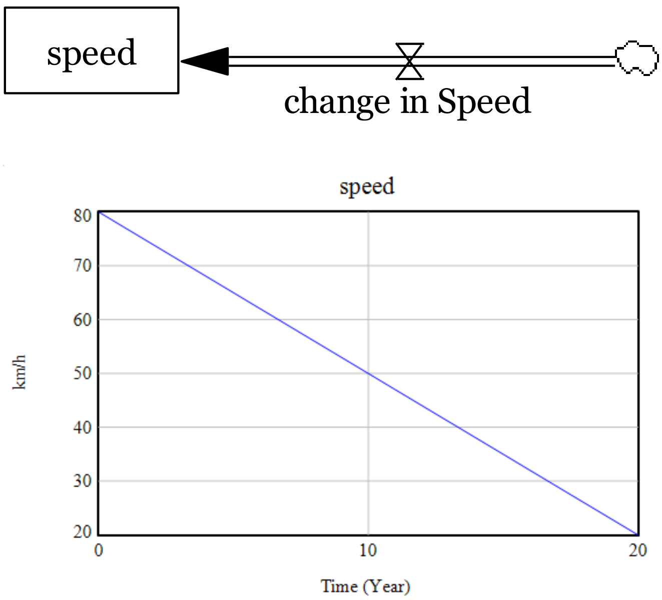

Figure 9-4: Stock and flow for speed of heavy vehicles with proposed accepted range

9.2.1.4. Pavement Temperature (TPmax)

As discussed in Chapter 5, for this research, Hassan et al.'s (2004) model was adopted (Table 9-3) and the following equation, which measures the pavement temperature, is used.

T20mm = 3.160 + 1.319 Tair

Equation 9-5: Hassan et al.'s (2004) model for measuring the pavement temperature

Table 9-3: Predicted pavement temperature for UAE based on three different scenarios (2020, 2040, 2060-2079)

Month	Max month Temp. Current (2010)	The highest reading ever in UAE	2020 TMax	2040Tmax	2060-2079 Tamx	2013	2020	2040	2060-2079
			Increase by 1°C	1.5 and 2°C	2 and 3°C	TPmax	TPmax	TPmax	TPmax
			Assume =1°C	Assume =2°C	Assume = 3°C				
Month 6-2016		50.4	51.4	52.4	53.4	**69.6**	**71.0**	**72.3**	**73.6**

For the current case (based on 2013 data), the pavement temperature is recorded at approximately 69 ºC, as per Table 9-3. Nevertheless, the model needs to cope with future climate change scenarios. Unlike the previous deterioration model using Markov chain (see Chapter 7 section 7.3), which was run for four separate different climate change scenarios (2013, 2020, 2040 and 2060), the structure of system dynamics for the pavement temperature model was developed as one dynamics variable that ranged from the 2013 current climate condition (best scenario to the future 2060 condition which is the most critical scenarios. Therefore, the stock and flow model for the pavement temperature was developed to have a range of inputs for 20 years from 69 ºC to 79 ºC with consistent rate change (assumed linear relationship), as is shown in figures 9-5 and 9-6 below:

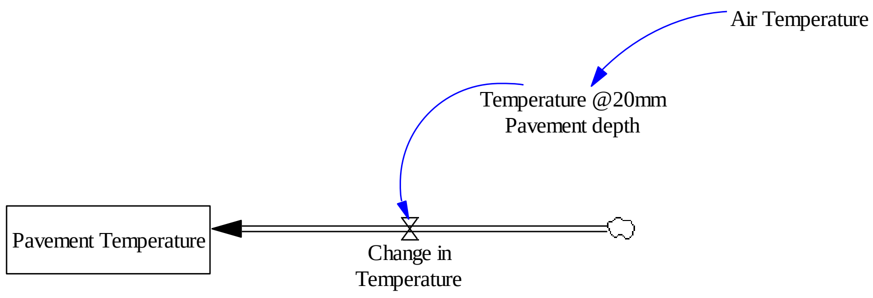

Figure 9-5: Stock and flow for pavement temperature

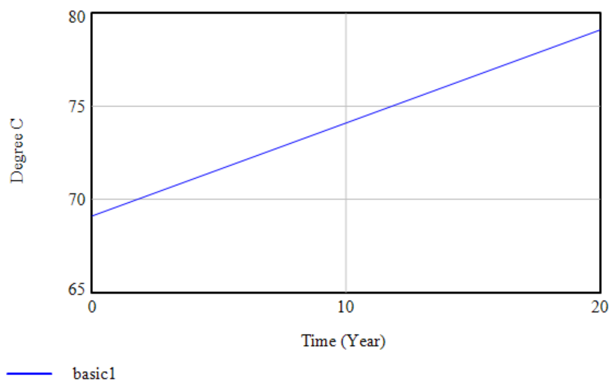

Figure 9-6: Pavement temperature with proposed accepted range for SD model

9.2.1.5. Pavement Ageing

Asphaltic age was discussed and analysed in Chapter 5 section 5.9. According to the collected data, the age of the pavement structure can be related to the date of construction or the date of the last major maintenance and rehabilitation activities. For example, if the date of construction was the year 2000, the age of the pavement structure is 13 years (assuming the data were collected in year 2013). Asphaltic age is the source for determining both softening point and voids in the mix. The pavement ageing used the following equations to shape the relationship between the variables (softening point and voids in air). An example of asphaltic age for roads based on data collection (backward approach) is shown in Table 9-4.

$$SP = a0 \times \mathrm{Ln}(AGE + 0.0001) + a1$$

Equation 9-6:Relationship between softening point and age

$$VIM = a0 \times Ln(AGE + 0.0001) + a1$$

Equation 9-7: Relationship between voids in air and age

Table 9-4: An example of asphaltic age for roads based on data collection (backward approach)

N	Road Code	Road	Construction date	Major rehabilitation	Road age
1	E.11	Ittihad road	2006	no record	11
3	E18.1	Manama- RAK Airport	2006	no record	11

The records showed that the pavement ageing value ranged from eight years to 18 years (see Chapter 5, section 5.9). Therefore, the stock and flow diagram for pavement ageing (Figure 9-7) was built to achieve dynamic variables ranging from eight years to 18 years (in ascending order) over a certain period of time (20 years). The simulation period for the model was selected to be year interval. The higher the value of the age, the higher the value of both softening point and air voids based on the relationship highlighted in equations 9-6 and 9-7. The final stocks and flows are presented in Figures 9-8, 9-9 and 9-10.

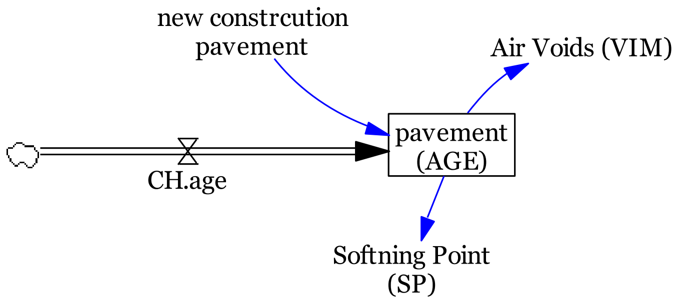

Figure 9-7: Stock and flow for pavement ageing

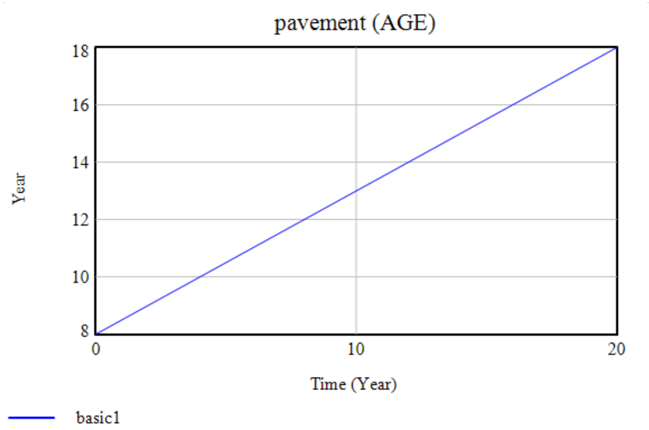

Figure 9-8: Pavement ageing and proposed accepted range for SD model

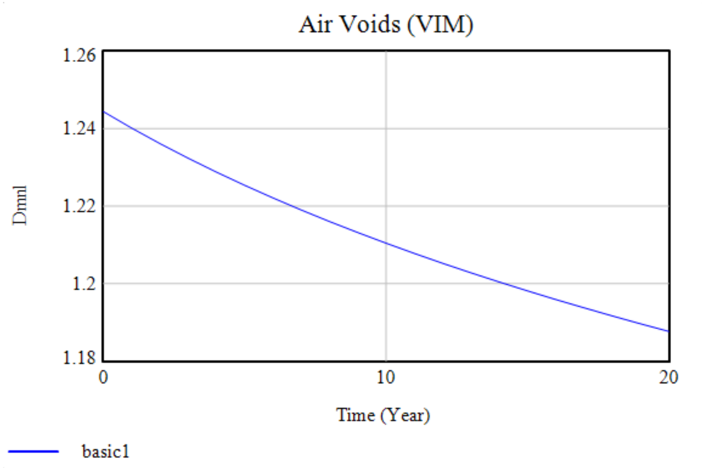

Figure 9-9: The range of air voids based on SD model based on Equation 9-7

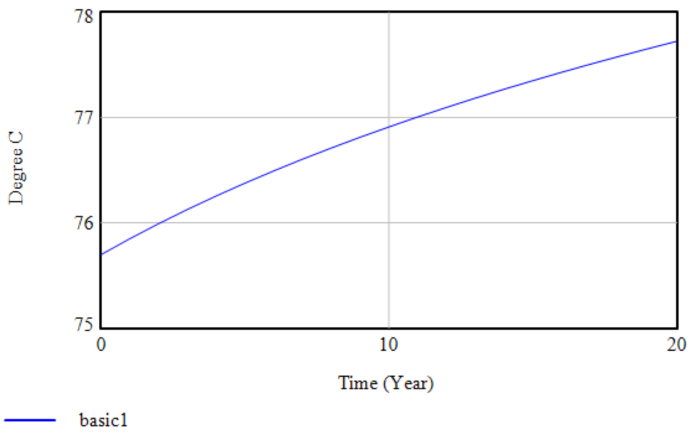

Figure 9-10: The range of softening point based on SD model based on Equation 9-6

9.2.1.6. Traffic Loading (YE4)

A similar approach to the previous sub-section was utilised to determine the stock and flow for traffic loading. The size of traffic moving on a particular road is not constant. Based on the data analysis in Chapter 5 section 5.6, the federal roads follow the UAE Ministry of Public Works' recorded different Average Annual Daily Traffic (AADT), as per Table 9-5.

Table 9-5: Example of the average Annual Daily Traffic (AADT)

Backward data collection roads			
N	**Road Code**	**Road**	**m EASL**
1	E.11	Ittihad road	**1.52**
7	E311	Sheik Mohammed Bin Zayed	**7.67**
8	E55.1	Dhaid - Madam	**0.21**
10	E55.2	Madam - Shiweb	**0.34**

12	E55.3	Umm Al Quwaim - Dhaid	**0.15**
14	E611.1	Maliha Rd - Fallah Al Muala Rd	**4.94**
16	E611.2	Fallah Al Muala Rd - Shk Mohammed Bin Zayed	**1.78**
18	E84	Sheikh Khalifa Rd	**0.55**
20	E88.1	Sharjah - Dhaid	**1.98**
22	E88.2	Dhaid - Masafi	**1.65**
30	E99.3	Fujairah - Oman	**0.61**
31	Siji link	Siji link	**0.97**

The higher the traffic loading, the worse the impacts that the pavement receives. Therefore, the stock and flow diagram was prepared to achieve dynamic variables. The traffic loading started from 0.1 m ESAL to 8 m EASL within 20 years (using a non-linear relationship), as per Figures 9-11 and 9-12.

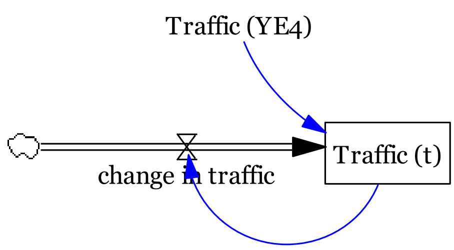

Figure 9-11: Stock and flow for traffic loading (YE4)

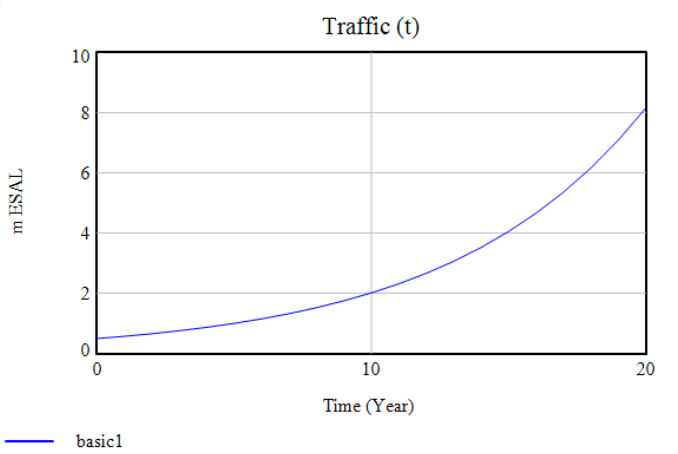

Figure 9-12: Traffic loading (YE4) proposed accepted range for SD model

To build the deformation for the rutting ΔRDS model, first, every single variable in the sub-models such as pavement thickness, pavement temperature, pavement ageing, traffic loading and the speed of heavy vehicles was developed as a stock and flow diagram and was simulated with different ranges. Running the simulation range for dynamic variables over the period of 20 years was also achieved. Therefore, the final step was to synchronise all the stocks and flows discussed earlier into one major sub-model which is deformation for rutting (ΔRDS) and subsequently change in roughness rutting (ΔRIr), as per Figure 9-13. Equation 9-4 was used to address the components' interrelationships, which were based on the developed equations and coefficients of the improved HDM-4 with calibration. Once the sub-model was organised and fully integrated, the running process started by accumulating the stock and flow for the defined variables in the sub-model, leading to the results that present the change in roughness rutting (ΔRIr).

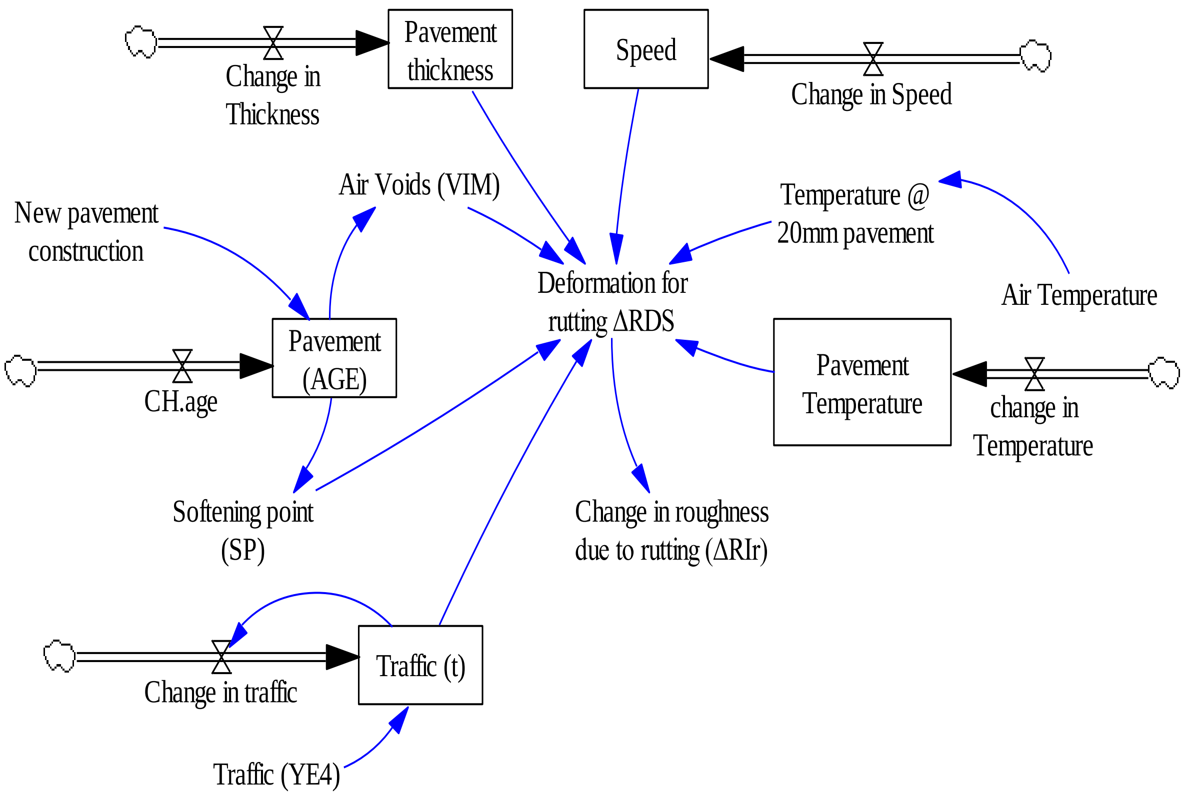

Figure 9-13: Stock and flow diagram for sub-model change in roughness due to rutting

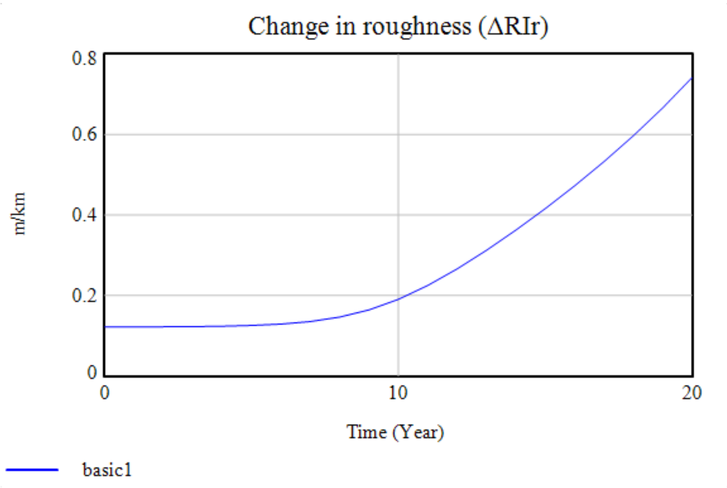

Figure 9-14: Rate of change for roughness rutting (ΔRIr)

Figure 9-14 presents the rate of change for roughness rutting (ΔRIr) over a period of 20 years' projections taking into consideration all the dynamic variables highlighted earlier.

9.2.1.7. Cracking (ΔRIc) and Environmental (ΔRIe) components of Roughness Sub-models

The following equations (9-8 and 9-9) which were developed in Chapter 6 are used to shape the stock and flow for the total change in roughness. It was assumed that no stock and flow shall be applied for the change in roughness due to cracking (ΔRIc) and environmental (ΔRIe) components as these components cannot be dynamic variables with constant value. Nevertheless, they were used to draw the final model of total change in roughness as per Figures 9-15 and 9-16.

$$\Delta RIc = a0 \times (\Delta ACRA)^2 + a1 \times \Delta ACRA + a2$$

Equation 9-8:Change in roughness due to cracking component (ΔRIc)

$$\Delta RIe = Kgm\ m\ Ria$$

$$m = 0.197 + 0.000155\ TMI$$

Equation 9-9:Environmental component of roughness (ΔRIe)

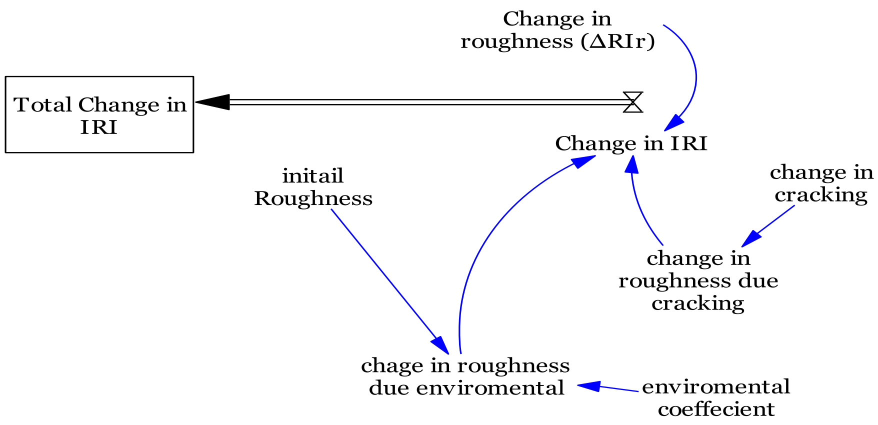

Figure 9-15: Stock and flow diagram for total change in roughness

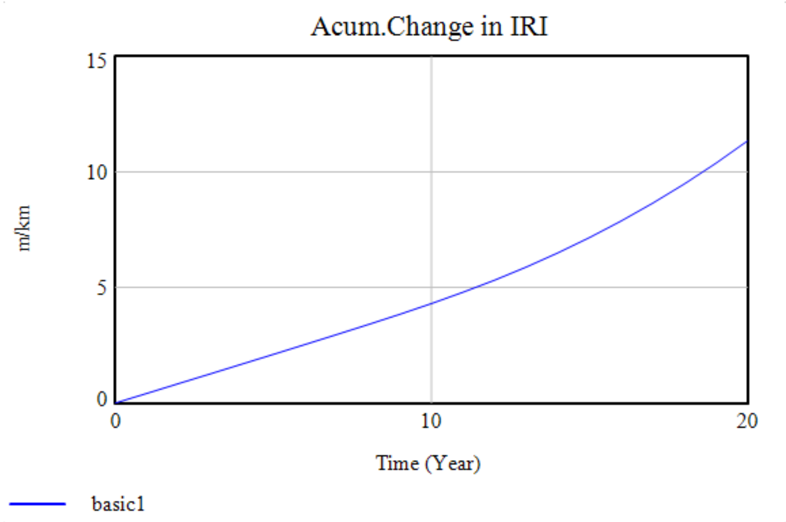

Figure 9-16: The results of total change in roughness using SD

The final equation for presenting the relationship between change in roughness (IRI) and Pavement Condition Index (PCI) is derived as per Equation 9-10 and the final stock and flow model was determined as per Figure 9-17.

$$\mathbf{PCI = (a1\times e^{a2\times IRI})}$$

Equation 9-10: The new model for Pavement Condition Index (PCI)

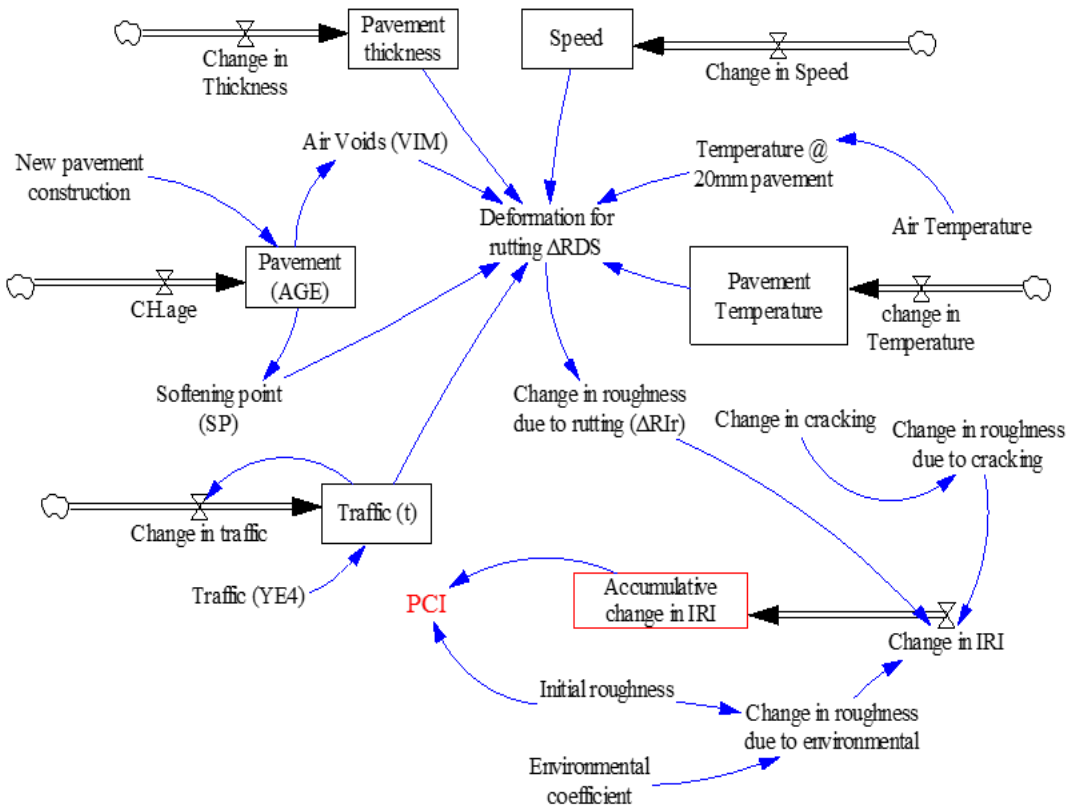

Figure 9-17: Stock and flow diagram pavement deterioration model

9.3. Modelling and Simulation for Pavement Failure

9.3.1. Pavement Failure Risk Analysis

9.3.1.1. Risk Analysis Using Average Probability Based on the Questionnaire

As discussed in Chapter 5 section 5.14, pavement risks were recorded and measured based on each of the likelihoods and impact ratings of each risk event. The questionnaire survey was completed by experts in the area of pavement engineering such as pavement material engineers, highway maintenance contractors, highway maintenance consultants, clients and asset managers. The results were used to quantify risk variable relationships as per the following:

9.3.1.2. Traffic Loading

The questionnaire was structured so that the risk of traffic loading was split into seven elements: S1. High Volume of Heavy Trucks, S2. Axle Group Type, S3.Tyre Configuration, S4. Gross Vehicle Mass, S5. Dynamic Wheel Loading, S6. High Traffic Loading (all vehicle type) and S7. Vehicle Speed. To analyse the results, Table 9-6 represents the rating for each element and Equation 9-11 was applied to define the value of pavement failure due to traffic loading including climate change impact risks.

$$y_{R1.T} = Pv.F_T \times \prod_{i=1}^{i=n} R_{R.1T}$$

$$Pv.F_{R1.T} = y_{R1.T} + Pv.F_T$$

Equation 9-11: Equation for deterministic risk analysis for traffic loading

Where,

- $R_{R1.T}$ = Risk impact on a traffic loading
- $Pv.F_T$= Pavement failure due to traffic loading
- $Pv.F_{R1.T}$ =Pavement failure due to traffic loading and climate change impact risks

The average probability for traffic loading risk was directly quoted from the questionnaire as per Table 9-6.

Table 9-6: Risk analysis for traffic loading using average probability

R1.	S1	S2	S3	S4	S5	S6	S7
Y1	X1.1	X1.2	X1.3	X1.4	X1.5	X1.6	X1.7
R1.Traffic	S1.High volume of heavy trucks	“S2.Axel Group Type	“S3.Tyer configuration	S4.Gross vehicle mass	S5.Dynamic Wheel Loading	S6.High traffic loading (all vehicles type)	S7.Vehicle speed
Average Rate	**0.339**	**0.221**	**0.087**	**0.186**	**0.141**	**0.189**	**0.072**
	Risk impact on an traffic loading from the risk Category						
$R_{R1.T}$	**0.176**						

9.3.1.3. Environmental Loading

The risk of environmental loading consisted of 10 sub-risks named S8. Precipitation, S9. Weathering, S10. High Temperature, S11. Low Temperature, R7. Drainage, R5. Pavement Ageing, S14. Increased Oxidation, S15. Increased Viscosity and Softness, S16. Increased Brittleness of Asphaltic Layer and, finally, S17. Increased Moisture/Excess Water. To measure the risk of such variables, Table 9-7 represents the rating for each element and Equation 9-12 was applied to define pavement failure due to environmental loading including climate change impact risk.

$$y_{R2.CC} = Pv.F_{CC} \times \prod_{i=1}^{i=n} R_{R2.CC}$$

$$Pv.F_{R2.CC} = y_{R2.CC} + Pv.F_{CC}$$

Equation: 9-12 Equation for deterministic risk analysis for environmental loading

Where,

- $R_{R2.CC}$ = Risk impact on an environmental loading
- $Pv.F_{CC}$= Pavement failure due to environmental loading
- $Pv.F_{R2.CC}$ =Pavement failure due to environmental loading and climate change impact risks

The average probability for environmental loading risk was directly quoted from the questionnaire as per Table 9-7.

Table 9-7: Risk analysis for climate change using probability method

R2.	S8	S9	S10	S11	R7	R5	S14	S15	S16	S17
Y2	X2.1	X2.2	X2.3	X2.4	X2.5	X2.6	X2.7	X2.8	X2.9	X2.10
R2.Climate Change	S8.Precipitation	S9.Weathering	S10.High Temperature	S11.Low Temperature	R7.Drainage	R5.Pavement Ageing	S14.Increase oxidation	S15.Increase viscosity and softness	S16.Increase Brittle of asphaltic layer	S17.Increase Moisture/ Excess water
Average Rate	0.169	0.146	0.310	0.098	0.189	0.172	0.191	0.121	0.198	0.126
	Probability risk analysis for environmental loading risk category									
$R_{R2.CC}$	**0.172**									

9.3.1.4. Pavement Composition

Unlike the risk of environmental loading, the risk of pavement composition is comprised of only four sub-risks, which are S18. Reduction in Material Quality and Properties of Aggregate and Soil, S19. Pavement Thickness, S20. Shortage of Material availability, and S21. Bitumen Supply and Quality. To measure the risk of these variables, Table 9-8 represents the rating for each element and Equation 9-13 was applied to define pavement failure due to pavement composition including climate change impact risk.

$$y_{R3.PC} = Pv.F_{PC} \times \prod_{i=1}^{i=n} R_{R3.PC}$$

$$Pv.F_{R3.PC} = y_{R3.PC} + Pv.F_{PC}$$

Equation 9-13: Equation for deterministic risk analysis for pavement composition

Where,

- $R_{R3.PC}$ = Risk impact on pavement composition
- $Pv.F_{PC}$= Pavement failure due to pavement composition
- $Pv.F_{R3.PC}$ =Pavement failure due to pavement composition and climate change impact risks

The average probability for pavement composition risk was directly quoted from the questionnaire as per Table 9-8.

Table 9-8: Risk analysis for pavement composition using probability method

R3.	**S18**	**S19**	**S20**	**S21**
Y3	X3.1	X3.2	X3.3	X3.4
R3.Pavement Composition	S18. Reduction in Material Quality and Properties of Aggregate and soil	S19.Pavement Thickness	S20.Shortage of Material availability	S21.Bitumen Supply and Quality
Average Rate	**0.240**	**0.213**	**0.132**	**0.212**
	Probability risk analysis for Pavement composition risk category			
$R_{R3.PC}$	**0.199**			

9.3.1.5. Pavement Strength

Two sub-risks form the main risk to pavement strength. These are R1. Traffic Loading and S22. Insufficient Value of Structural Number (SN). To measure the risk of these variables, Table 9-9 represents the rating for each element and Equation 9-14 was applied to define pavement failure due to pavement strength including climate change impact risk.

$$y_{R4.Ps} = Pv.F_{Ps} \times \prod_{i=1}^{i=n} R_{R4.Ps}$$

$$Pv.F_{R4.Ps} = y_{R4.Ps} + Pv.F_{Ps}$$

Equation 9-14 Equation for deterministic risk analysis for pavement strength

Where,

- $R_{R4.Ps}$ = Risk impact on pavement strength
- $Pv.F_{Ps}$= Pavement failure due to pavement strength
- $Pv.F_{R4.Ps}$ =Pavement failure due to pavement strength and climate change impact risks

The average probability for pavement strength risk was directly quoted from the questionnaire as per Table 9-9.

Table 9-9: Risk analysis for pavement strength using probability method

D		
R4	S1	S22
Y4	X4.1	X4.2
R4.Pavement Strength	R1.Traffic Loading	S22.Insufficient value of Structural Number (SN)
Average Rate	0.196	0.225
	probability risk analysis for Pavement strength risk category	
$\boldsymbol{R_{R4.Ps}}$	**0.211**	

9.3.1.6. Pavement Ageing

R2. Climate Change, R1. Traffic Loading and R6. Subgrade Soil are the sub-risks of the pavement ageing risk. Table 9-10 represents the rating for each element which was used to measure the risk. Also, Equation 9-15 was applied to define pavement failure due to pavement strength including climate change impact risk.

$$y_{R5.PA} = Pv.F_{PA} \times \prod_{i=1}^{i=n} R_{R5.PA}$$

$$Pv.F_{R5.PA} = y_{R5.PA} + Pv.F_{PA}$$

Equation 9-15: Equation for deterministic risk analysis for pavement ageing

Where,

- $R_{R5.PA}$ = Risk impact on pavement ageing
- $Pv.F_{PA}$= Pavement failure due to pavement ageing
- $Pv.F_{R5.PA}$ =Pavement failure due to pavement ageing and climate change impact risks

The average probability for pavement ageing risk was directly quoted from the questionnaire as per Table 9-10.

Table 9-10: Risk analysis for pavement strength using probability method

c				
R3.	R2	R1	R6	R8
Y5	X5.1	X5.2	X5.3	X5.4
R5.Pavement Ageing	R2.Climate Change	R1.Traffic Loading	R6.Subgrade Soil	R8.Maintenance
Average Rate	**0.182**	**0.214**	**0.168**	**0.139**
	probability risk analysis for Pavement Ageing risk category			
$R_{R5.PA}$	**0.176**			

9.3.1.7. Subgrade Soil

S17. Increased Moisture/Excess Water and S13. Selection of Construction Soil are the sub-risks of the subgrade soil risk. Table 9-11 represents the rating for each element used to measure the risk. Also, Equation 9-16 was applied to define pavement failure due to subgrade soil including climate change impact risks.

$$y_{R6.ss} = Pv.F_{ss} \times \prod_{i=1}^{i=n} R_{R6.ss}$$

$$Pv.F_{R6.ss} = y_{R6.ss} + Pv.F_{ss}$$

Equation 9-16: Equation for deterministic risk analysis for subgrade soil

Where,

- $R_{R6.ss}$ = Risk impact on subgrade soil
- $Pv.F_{ss}$= Pavement failure due to subgrade soil
- $Pv.F_{R6.ss}$ =Pavement failure due to subgrade soil and climate change impact risks

The average probability for the subgrade soil risk was directly quoted from the questionnaire as per Table 9-11.

Table 9-11: Risk analysis for subgrade soil using probability method

c		
R3.	S17	S13
Y6	X6.1	X6.2
R6.Subgrade Soil	S17.Increase Moisture/ Excess water	S13.Selection of construction soil
Average Rate	**0.137**	**0.213**
	probability risk analysis for Subgrade Soil risk category	
$\boldsymbol{R_{R6.ss}}$	**0.175**	

9.3.1.8. Drainage Risk

S17. Increased Moisture/Excess Water and S23. Insufficient Drainage System are the sub-risks of the drainage risk. Table 9-12 represents the rating for each element used to measure the risk. Also, Equation 9-17 was applied to define pavement failure due to drainage risk including climate change impact risks.

$$y_{R7.D} = Pv.F_D \times \prod_{i=1}^{i=n} R_{R7.D}$$

$$Pv.F_{R7.D} = y_{R7.D} + Pv.F_D$$

Equation 9-17: Equation for deterministic risk analysis for drainage

Where,

- $R_{R7.D}$ = Risk impact on drainage
- $Pv.F_D$= Pavement failure due to drainage
- $Pv.F_{R7.D}$ =Pavement failure due to drainage and climate change impact risks

The average probability for drainage risk was directly quoted from the questionnaire as per Table 9-12.

Table 9-12: Risk analysis for drainage using probability method

R3.	**S17**	**S23**
Y7	X7.1	X7.2
R7.Drainage	S17.Increase Moisture/ Excess water	S23.Insufficient drainage system
Average Rate	**0.163**	**0.294**
	Probability risk analysis for Drainage risk category	
$\boldsymbol{R_{R7.D}}$	**0.228**	

9.3.1.9. Maintenance

S24. Delay Maintenance, S.25. Maintenance Priorities/Plan and S26. Limited Budget are the sub-risks of the maintenance risk. Table 9-13 represents the rating for each element used to measure the risk. Also, Equation 9-18 was applied to define pavement failure due to maintenance risk including climate change impact risk.

$$y_{R8.m} = Pv.F_m \times \prod_{i=1}^{i=n} R_{R8.m}$$

$$Pv.F_{R8.m} = y_{R8.m} + Pv.F_m$$

Equation 9-18: Equation for deterministic risk analysis for maintenance

Where,

- $R_{R8.m}$ = Risk impact on maintenance
- $Pv.F_m$= Pavement failure due to maintenance
- $Pv.F_{R8.m}$ =Pavement failure due to maintenance and climate change impact risks

The average probability for maintenance risk was directly quoted from the questionnaire as per Table 9-13.

Table 9-13: Risk analysis for maintenance using probability method

	c		
R8	S24	S25	S26
Y8	X8.1	X8.2	X8.3
R8.Maintenance	S24.Delay maintenance	S25.Maintenance priorities /plan	S26.Limited Budget
Rate	**0.274**	**0.269**	**0.240**
	probability risk analysis for Maintenance risk category		
$\boldsymbol{R_{R8.m}}$	**0.261**		

9.3.1.10. Construction Quality

S27. Design and Specification, S28. Construction Process and S29. Construction Management are the sub-risks of the construction quality risk. Table 9-14 represents the rating for each element used to measure the risk. Also, Equation 9-19 was employed to adjust pavement failure due to construction quality risk including climate change impact risk.

$$y_{R9.cq} = Pv.F_{cq} \times \prod_{i=1}^{i=n} R_{R9.cq}$$

$$Pv.F_{R9.cq} = y_{R9.cq} + Pv.F_{cq}$$

Equation 9-19: Equation for deterministic risk analysis for construction quality risk

Where,

- $R_{R9.cq}$ = Risk impact on construction quality
- $Pv.F_{cq}$= Pavement failure due to construction quality
- $Pv.F_{R9.cq}$ =Pavement failure due to construction quality and climate change impact risks

The average probability for construction quality risk was directly quoted from the questionnaire as per Table 9-14.

Table 9-14: Risk analysis for construction using probability method

c			
R9	S27	S28	S29
Y9	X9.1	X9.2	X9.3
R9. Construction Quality	S27.Design and Specification	S28.Construction Process	S29.Construction Management
Rate	**0.230**	**0.165**	**0.216**
	Probability risk analysis for construction quality risk category		
$R_{R9.cq}$	**0.204**		

9.3.1.11. Rutting

R2. Climate Change, R3. Pavement Composition, R9. Construction Quality, R4. Pavement Strength and R6. Subgrade are the sub-risks of the rutting risk. Table 9-15 represents the rating for each element used to measure the risk. Also, Equation 9-20 was used to define pavement failure due to rutting risk including the risk due to climate change impact.

$$y_{R.rut} = Pv.F_{rut} \times \prod_{i=1}^{i=n} R_{R.rut}$$

$$Pv.F_{R.rut} = y_{R.rut} + Pv.F_{rut}$$

Equation 9-20: Equation for deterministic risk analysis for rutting

Where,

- $R_{R.rut}$ = Risk impact on rutting
- $Pv.F_{rut}$= Pavement failure due to rutting
- $Pv.F_{R.rut}$ =Pavement failure due to rutting and climate change impact risks

The average probability for rutting risk was directly quoted from the questionnaire as per Table 9-15.

Table 9-15: Risk analysis for rutting using probability method

c					
R10.	**R2**	**R3**	**R9**	**R4**	**R6**
Y10	X10.1	X10.2	X10.3	X10.4	X10.5
Rutting	R2.Climate Change	R3.Pavement Composition	R9.Construction Quality	R4.Pavement Strength	R6.Subgrade
Rate	**0.148**	**0.203**	**0.227**	**0.213**	**0.221**
	probability risk analysis for Rutting risk category				
$\boldsymbol{R_{R.rut}}$	**0.203**				

9.3.1.12. Cracking

X11.1 Climate Change, X11.2 Pavement Composition, X11.3 Construction Quality, X11.4 Pavement Strength and X11.5 Subgrade are the sub-risks of the cracking risk. Table 9-15 represents the rating for each element used to measure the risk. Also, Equation 9-21 was used to define pavement failure due to cracking risk including the risk due to climate change impact.

$$y_{R.cra} = Pv.F_{cra} \times \prod_{i=1}^{i=n} R_{R.cra}$$

$$Pv.F_{R.cra} = y_{R.cra} + Pv.F_{cra}$$

Equation 9-21: Equation for deterministic risk analysis for cracking

Where,

- $R_{R.cra}$ = Risk impact on cracking
- $Pv.F_{cra}$= Pavement failure due to cracking
- $Pv.F_{R.cra}$ =Pavement failure due to cracking and climate change impact risks

The average probability for cracking risk was directly quoted from the questionnaire as per Table 9-16.

Table 9-16: Risk analysis for cracking using probability method

R11.	R2	R3	R9	R4	R6
Y11	X11.1	X11.2	X11.3	X11.4	X11.5
Cracking	R2.Climate Change	R3.Pavement Composition	R9.Construction Quality	R4.Pavement Strength	R6.Subgrade
Rate	**0.243**	**0.145**	**0.182**	**0.162**	**0.111**
	probability risk analysis for Cracking risk category				
$R_{R.cra}$	**0.169**				

9.3.1.13. Heavy Vehicle Speed

X12.1 Pavement Ageing, X12.3 Drainage and X12.4 Maintenance are the sub-risks of the heavy vehicle speed risk. Table 9-17 represents the rating for each element used to measure the risk. Also, Equation 9-22 was applied to define pavement failure due to heavy vehicle speed risk including the risk due to climate change impact.

$$y_{R.VS} = Pv.F_{sh} \times \prod_{i=1}^{i=n} R_{R.sh}$$

$$Pv.F_{R.sh} = y_{R.sh} + Pv.F_{sh}$$

Equation: 9-22: Equation for deterministic risk analysis for heavy vehicle speed

Where,

- $R_{R.sh}$ = Risk impact on vehicle speed
- $Pv.F_{sh}$= Pavement failure due to vehicle speed
- $Pv.F_{R.sh}$ =Pavement failure due to vehicle speed and climate change impact risks

The average probability for vehicle speed risk was directly quoted from the questionnaire as per Table 9-17.

Table 9-17: Risk analysis for heavy vehicle speed using probability method

S7	R2	R1	R6
Y12	X12.1	X12.2	X12.3
S7.Vehicle speed	R5.Pavement Ageing	R7.Drainage	R8.Maintenance
Rate	**0.094**	**0.135**	**0.159**
	probability risk analysis for Heavy Vehicle speed risk category		
$R_{R.VS}$	**<u>0.129</u>**		

9.3.1.14. Pavement Thickness

X13.1 Construction Quality is the sub-risk of the pavement thickness risk. Table 9-18 represents the rating for pavement thickness which is used to measure the risk. Also, Equation 9-21 was applied to define pavement failure due to heavy vehicle speed risk including the risk due to climate change impact.

$$y_{R.VT} = Pv.F_{VT} \times \prod_{i=1}^{i=n} R_{R.VT}$$

$$Pv.F_{R.VT} = y_{R.VT} + Pv.F_{VT}$$

Equation 9-23 Equation for deterministic risk analysis for pavement thickness

Where,

- $R_{R.VT}$ = Risk impact on pavement thickness
- $Pv.F_{VT}$= Pavement failure due to pavement thickness
- $Pv.F_{R.VT}$ =Pavement failure due to pavement thickness and climate change impact risks

The average probability for pavement thickness risk was directly quoted from the questionnaire as per Table 9-18.

Table 9-18: Risk analysis for pavement thickness using probability method

S7	R2
Y13	X13.1
S19.Pavement Thickness	R9.Construction Quality
Rate	**0.237**

	Probability risk analysis for Pavement thickness risk category
$R_{R.VT}$	**0.237**

9.3.2. Risk Analysis Using Multiple-Regression Analysis

The main principle of regression modelling is based on one of the independent variables (x) that statistically impose a change on the dependent variable (y). Such a technique was applied in this research to analyse the results generated from the survey questionnaires. The results were analysed using SPSS software and by conducting a regression analysis.

1.1.1.1.1 Traffic Loading

To analyse the risk of climate change on the pavement failure due to traffic loading, a quadratic multiple regression model was used to quantify the risk and the associations between the dependent variable and the independent variables. The SPSS software was used to investigate the most reliable coefficient based on the received questionnaires. The obtained results are shown in Appendix 5 and were reported as follows:

Table 9-19: Statistical analysis results from SPSS for traffic loading risks

Model	R	R Square	Adjusted R Square	Std. Error of the Estimate
1	.657[a]	.431	.250	.08524

a. Predictors: (Constant), X1.7, X1.2, X1.3, X1.5, X1.1, X1.6, X1.4

ANOVA

Model		Sum of Squares	df	Mean Square	F	Sig.
1	Regression	.121	7	.017	2.384	.056[b]
	Residual	.160	22	.007		
	Total	.281	29			

a. Dependent Variable: Y1

a. Predictors: (Constant), X1.7, X1.2, X1.3, X1.5, X1.1, X1.6, X1.4 as it shown in Table 9-20

Coefficients[a]

Model		Unstandardised Coefficients B	Std. Error	Standardised Coefficients Beta	t	Sig.
1	(Constant)	.062	.038		1.604	.123
	X1.1	-.103	.113	-.189	-.913	.371
	X1.2	.225	.138	.337	1.627	.118
	X1.3	-.067	.198	-.066	-.341	.736
	X1.4	.036	.154	.059	.231	.819
	X1.5	.079	.134	.137	.591	.561
	X1.6	.247	.183	.315	1.346	.192
	X1.7	.378	.205	.345	1.843	.079

a. Dependent Variable: Y1: R1.Traffic loading

Table 9-20: Traffic loading risks and sub-risks

Y1	X1.1	X1.2	X1.3	X1.4	X1.5	X1.6	X1.7
R1.Traffic loading	S1.High volume of heavy trucks	“S2.Axel Group Type	“S3.Tyer configuration	S4.Gross vehicle mass	S5.Dynamic Wheel Loading	S6.High traffic loading (all vehicles type)	S7.Vehicle speed

A quadratic multiple regression was considered for estimating the regression coefficients

$$\boldsymbol{Y}_{\text{traffic}=B_0}+a_1X_{i1}+a_2X_{i2}+a_3X_{i3}+a_4X_{i4}+a_5X_{i5}+a_6X_{i6}+a_7X_{i7}$$

Equation 9-24: Risk factor coefficients analysis for traffic loading due to climate change impact

The results are shown in Table 19-9 to define the relationship between the independent variable sub-risks: high volume of heavy trucks, axle group type, tyre configuration, gross vehicle mass, dynamic wheel loading, high traffic loading (all vehicle type) and vehicle speed (traffic), and the dependent variable traffic loading. The quadratic multiple regression model explained 43.1% of the variance of the data set. The model was significant at 0.056. This is marginally above P<0.05. The regression coefficients are **a1= -0.103, a2=0.225, a3-0.067, a4=0.036, a5=0.079, a6=0.247 and a7= 0.378**.

$$Y_{\text{traffic}} = 0.062 - 0.103 \times X_{i1} + 0.225 \times X_{i2} - 0.067 \times X_{i3} + 0.036 X_{i4} + 0.079 X_{i5} + 0.247 X_{i6} + 0.379 X_{i7}$$

9.3.2.1. Environmental Loading Risk

To analyse the risk of climate change on the pavement failure due to environmental loading, a quadratic multiple regression model was used to quantify the risk and the associations between the dependent variable and the independent variables. The SPSS software was used to investigate the most reliable coefficient based on the received questionnaires. The obtained results are shown in Appendix 5 and were reported as follows:

Table 9-21: Statistical analysis results from SPSS for environmental loading risk

Model Summary

Model	R	R Square	Adjusted R Square	Std. Error of the Estimate
1	.820a	.673	.500	.17333

a. Predictors: (Constant), X2.10, X2.1, X2.6, X2.8, X2.4, X2.7, X2.5, X2.2, X2.3, X2.9

ANOVAa

Model		Sum of Squares	df	Mean Square	F	Sig.
1	Regression	1.173	10	.117	3.904	.005b
	Residual	.571	19	.030		
	Total	1.744	29			

a. Dependent Variable: Y2

b. Predictors: (Constant), X2.10, X2.1, X2.6, X2.8, X2.4, X2.7, X2.5, X2.2, X2.3, X2.9 as per Table 9-22

Coefficients[a]

Model		Unstandardised Coefficients		Standardised Coefficients	t	Sig.
		B	Std. Error	Beta		
1	(Constant)	-.053	.084		-.635	.533
	X2.1	-.988	.424	-.603	-2.330	.031
	X2.2	.193	.347	.110	.557	.584
	X2.3	.090	.272	.073	.332	.744

X2.4	.660	.304	.383	2.171	.043
X2.5	1.527	.313	.952	4.882	.000
X2.6	-.524	.482	-.237	-1.088	.290
X2.7	.203	.324	.122	.626	.538
X2.8	-.160	.342	-.075	-.468	.645
X2.9	.672	.461	.371	1.459	.161
X2.10	.216	.420	.089	.515	.613

a. Dependent Variable: Y2: Environmental loading

Table 9-22: Environmental loading risk and sub-risks

Y2	X2.1	X2.2	X2.3	X2.4	X2.5	X2.6	X2.7	X2.8	X2.9	X2.10
R2. Environmental loading	S8.Precipitation	S9.Weathering	S10.High Temperature	S11.Low Temperature	R7.Drainage	R5.Pavement Ageing	S14.Increase oxidation	S15.Increase viscosity and softness	S16.Increase Brittle of asphaltic layer	S17.Increase Moisture/ Excess water

A quadratic multiple regression was considered for estimating the regression coefficients

$$Y_{\text{climate}} = B_0 + a_1 X_{i1} + a_2 X_{i2} + a_3 X_{i3} + a_4 X_{i4} + a_5 X_{i5} + a_6 X_{i6} + a_7 X_{i7} + a_8 X_{i8} + a_9 X_{i9} + a_{10} X_{i10}$$

Equation 9-25: Risk factor coefficients analysis for environmental loading due to climate change impact

The results are shown in Table 9-21 to define the relationship between the independent variable sub-risks: precipitation, weathering, high temperature, low temperature, drainage, pavement ageing, increased oxidation, increased viscosity and softness, increased brittleness of asphaltic layer and increased moisture/excess water, and the dependent variable environmental loading. The quadratic multiple regression model explained 67.3% of the variance of the data set. The model was significant at .005 (P<0.05). The regression coefficients are **a1= -0.988, a2=0.193, a3=0.090, a4=0.660, a5=1.527, a6=-0.524 and a7= 0.203, a8= -0.160, a9=0.672 and 0.216**.

$$Y_{\text{climate}} = -0.053 - 0.988 \times X_{i1} + 0.193 \times X_{i2} + 0.090 \times X_{i3} + 0.660 \times X_{i4} + 1.527 \times X_{i5} - 0.524 \times X_{i6} + 0.203 \times X_{i7} - 0.160 \times X_{i8} + 0.672 \times X_{i9} + 0.216 \times X_{i10}$$

9.3.2.2. Pavement Composition

To analyse the risk of climate change on the pavement failure due to Pavement composition, a quadratic multiple regression model was used to quantify the risk and the associations between the dependent variable and the independent variables. The SPSS software was used to investigate the most reliable coefficient based on the received questionnaires. The obtained results are shown in Appendix 5 and were reported as follows:

Table 9-23: Statistical analysis results from SPSS for pavement composition risk

Model Summary

Model	R	R Square	Adjusted R Square	Std. Error of the Estimate
1	.536a	.287	.173	.09161

a. Predictors: (Constant), X3.4, X3.2, X3.3, X3.1

ANOVAa

Model		Sum of Squares	df	Mean Square	F	Sig.
1	Regression	.084	4	.021	2.517	.067b
	Residual	.210	25	.008		
	Total	.294	29			

a. Dependent Variable: Y3: R3.Pavement Composition

b. Predictors: (Constant), X3.4, X3.2, X3.3, X3.1as per Table 9-24

Coefficientsa

Model		Unstandardised Coefficients		Standardised Coefficients	t	Sig.
		B	Std. Error	Beta		
1	(Constant)	.052	.037		1.382	.179
	X3.1	0.273	.195	.369	1.397	.175
	X3.2	0.193	.113	.331	1.705	.101
	X3.3	-0.064	.173	-.077	-.371	.714
	X3.4	7.057E-05	.130	.000	.001	1.000

a. Dependent Variable: Y3: R3.Pavement Composition

Table 9-24: Pavement composition risks and sub-risks

Y3	X3.1	X3.2	X3.3	X3.4
R3.Pavement Composition	S18. Reduction in Material Quality and Properties of Aggregate and soil	S19.Pavement Thickness	S20.Shortage of Material availability	S21.Bitumen Supply and Quality

A quadratic multiple regression was considered for estimating the regression coefficients.

$$Y_{\text{comps}} = B_0 + a_1 X_{i1} + a_2 X_{i2} + a_3 X_{i3} + a_4 X_{i4}$$

Equation 9-26: Risk factor coefficients analysis for pavement composition due to climate change impact

The results are shown Table 9-23 to define the relationship between the independent variable sub-risks: reduction in material quality and properties of aggregate and soil pavement thickness, shortage of material availability, and bitumen supply and quality, and the dependent variable pavement composition. The quadratic multiple regression model explained 28.7% of the variance of the data set. The model was significant at .067. This is marginally above ($P<0.05$). The regression coefficient are **a1= 0.273, a2=0.193, a3=-0.064 and a4=7.057E-05**.

$$Y_{\text{comps}} = 0.052 + 0.273 \times X_{i1} + 0.193 \times X_{i2} - 0.064 \times X_{i3} + 7.057 \times 10^{-5} X_{i4}$$

9.3.2.3. Pavement Strength

To analyse the risk of climate change on the pavement failure due to pavement strength, a multiple regression model was used to quantify the risk and the associations between the dependent variable and the independent variables. The SPSS software was used to investigate the most reliable coefficient based on the received questionnaires. The obtained results are shown in Appendix 5 and were reported as follows:

Table 9-25: Statistical analysis results from SPSS for pavement strength risk

Model Summary

Model	R	R Square	Adjusted R Square	Std. Error of the Estimate
1	.523a	.274	.220	.10406

a. Predictors: (Constant), X4.2, X4.1

ANOVAa

Model		Sum of Squares	df	Mean Square	F	Sig.
1	Regression	.110	2	.055	5.087	.013b
	Residual	.292	27	.011		
	Total	.403	29			

a. Dependent Variable: Y4: R4.Pavement Strength

b. Predictors: (Constant), X4.2, X4.1as per Table 9-26

coefficientsa

Model		Unstandardised Coefficients		Standardised Coefficients	t	Sig.
		B	Std. Error	Beta		
1	(Constant)	.039	.038		1.018	.318
	X4.1	.468	.155	.520	3.025	.005
	X4.2	.007	.115	.010	.058	.954

a. Dependent Variable: Y4: R4.Pavement Strength

Table 9-26: Pavement strength risks and sub-risks

Y4	X4.1	X4.2
R4.Pavement Strength	R1.Traffic Loading	S22.Insufficient value of Structural Number (SN)

A multiple regression was considered for estimating the regression coefficients

$$\boldsymbol{Y}_{\mathbf{ps}} = B_0 + a_1 X_{i1} + a_2 X_{i2}$$

Equation 9-27: Risk factor coefficients analysis for pavement strength due to climate change impact

The results are shown Table 9-25 to define the relationship between the independent variable sub-risks: traffic loading and insufficient value of structural number (SN), and the dependent variable pavement strength. The quadratic multiple regression model explained 27.4% of the variance of the data set. The model was significant at .013 (P<0.05). The regression coefficient are **a1= 0.468 and a2=0.007**.

$$Y_{\mathrm{ps}=0.039+0.468\times X_{i1}+0.007\times X_{i2}}$$

9.3.2.4. Pavement Ageing

To analyse the risk of climate change on the pavement failure due to pavement ageing, a quadratic multiple regression model was used to quantify the risk and the associations between the dependent variable and the independent variables. The SPSS software was used to investigate the most reliable coefficient based on the received questionnaires. The obtained results are shown in Appendix 5 and were reported as follows:

Table 9-27: Statistical analysis results from SPSS for pavement ageing risk

Model Summary

Model	R	R Square	Adjusted R Square	Std. Error of the Estimate
1	.578a	.334	.227	.10708

a. Predictors: (Constant), X5.4, X5.1, X5.3, X5.2

ANOVA[a]

Model		Sum of Squares	df	Mean Square	F	Sig.
1	Regression	.144	4	.036	3.132	.032b
	Residual	.287	25	.011		
	Total	.430	29			

a. Dependent Variable: Y5: R5.Pavement Ageing

b. Predictors: (Constant), X5.4, X5.1, X5.3, X5.2

Coefficientsa

Model		Unstandardised Coefficients		Standardised Coefficients	t	Sig.
		B	Std. Error	Beta		
1	(Constant)	.042	.044		.955	.348

X5.1	.023	.141	.028	.161	.873
X5.2	.406	.164	.475	2.468	.021
X5.3	.247	.149	.276	1.660	.109
X5.4	-.036	.157	-.042	-.228	.821

a. Dependent Variable: Y5

Table 9-28: Pavement ageing risks and sub-risks

Y5	X5.1	X5.2	X5.3	X5.4
R5.Pavement Ageing	R2.Climate Change	R1.Traffic Loading	R6.Subgrade Soil	R8.Maintenance

$$\boldsymbol{Y}_{\textbf{Ageing}} = \boldsymbol{B_0} + \boldsymbol{a_1} \boldsymbol{X_{i1}} + \boldsymbol{a_2} \boldsymbol{X_{i2}} + \boldsymbol{a_3} \boldsymbol{X_{i3}} + \boldsymbol{a_4} \boldsymbol{X_{i4}}$$

Equation 9-28: Risk factor coefficients analysis for pavement ageing due to climate change impact

The results are shown in Table 9-27 to define the relationship between the independent variable sub-risks: traffic loading, climate change, subgrade soil and maintenance, and the dependent variable pavement ageing. The quadratic multiple regression model explained 33.4% of the variance of the data set. The model was significant at 0.032 (P<0.05). The regression coefficient are **a1=.023, a2=0.406, a3=0.247 and a4=-0.036**.

$$\boldsymbol{Y}_{\textbf{Aging}=\mathbf{0.042}+\mathbf{0.023}\times \boldsymbol{X_{i1}}+\mathbf{0.406}\times \boldsymbol{X_{i2}}+\mathbf{0.247}\times \boldsymbol{X_{i3}}-\mathbf{0.036}\boldsymbol{X_{i4}}}$$

9.3.2.5. Subgrade Soil

To analyse the risk of climate change on the pavement failure due to subgrade soil, a multiple regression model was used to quantify the risk and the associations between the dependent variable and the independent variables. The SPSS software was used to investigate the most reliable coefficient based on the received questionnaires. The obtained results are shown in Appendix 5 and were reported as follows:

Table 9-29: Statistical analysis results from SPSS for subgrade soil risk

Model Summary

Model	R	R Square	Adjusted R Square	Std. Error of the Estimate
1	.542a	.293	.241	.07631

a. Predictors: (Constant), X6.2, X6.1

ANOVAa

Model		Sum of Squares	df	Mean Square	F	Sig.
1	Regression	.065	2	.033	5.602	.009b
	Residual	.157	27	.006		
	Total	.222	29			

a. Dependent Variable: Y6

b. Predictors: (Constant), X6.2, X6.1

Coefficientsa

Model		Unstandardised Coefficients		Standardised Coefficients	t	Sig.
		B	Std. Error	Beta		
1	(Constant)	.053	.025		2.080	.047
	X6.1	.294	.130	.383	2.261	.032
	X6.2	.142	.084	.286	1.692	.102

a. Dependent Variable: Y6

Table 9-30: Subgrade risks and sub-risks

Y6	X6.1	X6.2
R6.Subgrade Soil	S17.Increase Moisture/ Excess water	S13.Selection of construction soil

A multiple regression was considered for estimating the regression coefficients.

$$Y_{\text{sub.s}} = B_0 + a_1 X_{i1} + a_2 X_{i2}$$

Equation: 9-29: Risk factor coefficients analysis for subgrade Soil due to climate change impact

The results are shown in Table 9-29 to define the relationship between the independent variable sub-risks: increased moisture/excess water and selection of construction soil, and the dependent variable subgrade soil. The multiple regression model explained 29.3% of the variance of the data set. The model was significant at 0.009 (P<0.05). The regression coefficient are **a1= 0.294 and a2=0.142**.

$$Y_{\text{sub.s}} = 0.053 + 0.294 \times X_{i1} + 0.142 \times X_{i2}$$

9.3.2.6. Drainage

To analyse the risk of climate change on the pavement failure due to drainage, a multiple regression model was used to quantify the risk and the associations between the dependent variable and the independent variables. The SPSS software was used to investigate the most reliable coefficient based on the received questionnaires. The obtained results are shown in Appendix 5 and were reported as follows:

Table 9-31: Statistical analysis results from SPSS for drainage risk

Model Summary

Model	R	R Square	Adjusted R Square	Std. Error of the Estimate
1	.505a	.255	.200	.114

a. Predictors: (Constant), X7.2, X7.1

ANOVAa

Model		Sum of Squares	df	Mean Square	F	Sig.
1	Regression	.120	2	.060	4.628	.019b
	Residual	.351	27	.013		
	Total	.471	29			

a. Dependent Variable: Y7

b. Predictors: (Constant), X7.2, X7.1

Coefficientsa

Model		Unstandardised Coefficients		Standardised Coefficients	t	Sig.
		B	Std. Error	Beta		
1	(Constant)	.074	.044		1.687	.103
	X7.1	.529	.185	.493	2.858	.008
	X7.2	.026	.113	.040	.233	.818

a. Dependent Variable: Y7

Table 9-32: Drainage risks and sub-risks

Y7	X7.1	X7.2
R7.Drainage	S17.Increase Moisture/ Excess water	S23.Insufficient drainage system

A multiple regression was considered for estimating the regression coefficients.

$$Y_{\mathrm{Dr}} = B_0 + a_1 X_{i1} + a_2 X_{i2}$$

Equation 9-30: Risk factor coefficients analysis for drainage due to climate change impact

The results are shown in Table 9-31 to define the relationship between the independent variable sub-risks: moisture/excess water and insufficient drainage system, and the dependent variable drainage. The multiple regression model explained 25.5% of the variance of the data set. The model was significant at 0.019 ($P<0.05$). The regression coefficient are **a1= 0.529 and a2=0.026**.

$$Y_{\mathrm{Dr}} = 0.074 + 0.529 \times X_{i1} + 0.026 \times X_{i2}$$

9.3.2.7. Maintenance

To analyse the risk of climate change on the pavement failure due to maintenance, a quadratic multiple regression model was used to quantify the risk and the associations between the dependent variable and the independent variables. The SPSS software was used to investigate the most reliable coefficient based on the received questionnaires. The obtained results are shown in Appendix 5 and were reported as follows:

Table 9-33: Results of estimated coefficients and ANOVA test for maintenance risk

Variables Entered/Removed[a]

Model	Variables Entered	Variables Removed	Method
1	X8.3, X8.2, X8.1b		Enter

a. Dependent Variable: Y8

b. All requested variables entered.

Model Summary

Model	R	R Square	Adjusted R Square	Std. Error of the Estimate
1	.328a	.108	.005	.10079

a. Predictors: (Constant), X8.3, X8.2, X8.1

ANOVAa

Model		Sum of Squares	df	Mean Square	F	Sig.
1	Regression	.032	3	.011	1.048	.388b
	Residual	.264	26	.010		
	Total	.296	29			

a. Dependent Variable: Y8

b. Predictors: (Constant), X8.3, X8.2, X8.1

Coefficientsa

Model		Unstandardised Coefficients		Standardised Coefficients	t	Sig.
		B	Std. Error	Beta		
1	(Constant)	.105	.033		3.230	.003
	X8.1	-.062	.150	-.134	-.411	.685
	X8.2	.044	.103	.107	.432	.670
	X8.3	.193	.135	.375	1.425	.166

a. Dependent Variable: Y8

A quadratic multiple regression was considered for estimating the regression coefficients

Table 9-34: Maintenance risks and sub-risks

Y8	X8.1	X8.2	X8.3
R8.Maintenance	S24.Delay maintenance	S25.Maintenance priorities /plan	S26.Limited Budget

$$Y_{\text{Maint}}=B_0+a_1X_{i1}+a_2X_{i2}+a_3X_{i3}$$

Equation 9-31: Risk factor coefficients analysis for maintenance due to climate change impact

The results are shown in Table 9-33 to define the relationship between the independent variable sub-risks: delay maintenance, maintenance priorities/plan and limited budget, and the dependent variable maintenance. The quadratic multiple regression model explained 10.8% of the variance of the data set. The model was not significant at .388 (P<0.05). The regression coefficient are **a1= -0.062, a2=0.044 and a3= 0.193**.

$$Y_{\mathbf{Maint}=0.105-\mathbf{0.062}\times X_{i1}+\mathbf{0.044}\times X_{i2}+0.193\times X_{i3}}$$

9.3.2.8. Construction Quality

To analyse the risk of climate change on the pavement failure due to maintenance, a quadratic multiple regression model was used to quantify the risk and the associations between the dependent variable and the independent variables. The SPSS software was used to investigate the most reliable coefficient based on the received questionnaires. The obtained results are shown in Appendix 5 and were reported as follows:

Table 9-35: Results of estimated coefficients and ANOVA for construction quality Risk

Variables Entered/Removeda

Model	Variables Entered	Variables Removed	Method
1	X9.3, X9.1, X9.2b		Enter

a. Dependent Variable: Y9

b. All requested variables entered.

Model Summary

Model	R	R Square	Adjusted R Square	Std. Error of the Estimate
1	.567a	.322	.243	.13937

a. Predictors: (Constant), X9.3, X9.1, X9.2

ANOVAa

Model		Sum of Squares	df	Mean Square	F	Sig.
1	Regression	.239	3	.080	4.107	.016b
	Residual	.505	26	.019		

Total	.744	29			

a. Dependent Variable: Y9

b. Predictors: (Constant), X9.3, X9.1, X9.2

Coefficients

Model		Unstandardised Coefficients		Standardised Coefficients		
		B	Std. Error	Beta	t	Sig.
1	(Constant)	.121	.048		2.538	.017
	X9.1	.337	.176	.409	1.910	.067
	X9.2	-.304	.287	-.247	-1.059	.299
	X9.3	.450	.169	.485	2.655	.013

a. Dependent Variable: Y9

Table 9-36: Construction quality risks and sub-risks

Y9	X9.1	X9.2	X9.3
R9.Construction Quality	S27.Design and Specification	S28.Construction Process	S29.Construction Management

A quadratic multiple regression was considered for estimating the regression coefficients.

$$Y_{CQ} = B_0 + a_1 X_{i1} + a_2 X_{i2} + a_3 X_{i3}$$

Equation 9-32: Risk factor coefficients analysis for construction quality due to climate change impact

The results are shown in Table 9-35 to define the relationship between the independent variable sub-risks: design and specification, construction process and construction management, and the dependent variable construction quality. The quadratic multiple regression model explained 32.2% of the variance of the data set. The model was significant at .016 ($P<0.05$). The regression coefficient are **a1= 0.337, a2= -0.304 and a3= 0.450**.

$$Y_{CQ} = 0.121 + 0.337 \times X_{i1} - 0.304 \times X_{i2} + 0.450 \times X_{i3}$$

9.3.2.9. Rutting

To analyse the risk of climate change on the pavement failure due to rutting, a quadratic multiple regression model was used to quantify the risk and the associations between the dependent variable and the independent variables. The SPSS software was used to investigate the most reliable coefficient based on the received questionnaires. The obtained results are shown in Appendix 5 and were reported as follows:

Table 9-37: Results of estimated coefficients and ANOVA for rutting risk

Variables Entered/Removed[a]

Model	Variables Entered	Variables Removed	Method
1	X10.5, X10.1, X10.4, X10.2, X10.3b		Enter

a. Dependent Variable: Y10

b. All requested variables entered.

Model Summary

Model	R	R Square	Adjusted R Square	Std. Error of the Estimate
1	.825a	.681	.615	.12087

a. Predictors: (Constant), X10.5, X10.1, X10.4, X10.2, X10.3

ANOVAa

Model		Sum of Squares	df	Mean Square	F	Sig.
1	Regression	.748	5	.150	10.247	.000b
	Residual	.351	24	.015		
	Total	1.099	29			

a. Dependent Variable: Y10

b. Predictors: (Constant), X10.5, X10.1, X10.4, X10.2, X10.3

Coefficientsa

Model		Unstandardised Coefficients		Standardised Coefficients	t	Sig.
		B	Std. Error	Beta		
1	(Constant)	-.062	.054		-1.153	.260
	X10.1	.856	.165	.630	5.204	.000

X10.2	.393	.172	.317	2.281	.032
X10.3	.476	.267	.379	1.784	.087
X10.4	.065	.204	.047	.316	.754
X10.5	-.284	.167	-.296	-1.693	.103

a. Dependent Variable: Y10

Table 9-38 : Rutting risks and sub-risks

Y10	X10.1	X10.2	X10.3	X10.4	X10.5
Rutting	R2.Climate Change	R3.Pavement Composition	R9.Construction Quality	R4.Pavement Strength	R6.Subgrade

A quadratic multiple regression was considered for estimating the regression coefficients.

$$Y_{\text{rut}=B_0+a_1X_{i1}+a_2X_{i2}+a_3X_{i3}+a_4X_{i4}+a_5X_{i5}}$$

Equation 9-33 Risk factor coefficients analysis for rutting due to climate change impact

The results are shown in Table 9-37 to define the relationship between the independent variable sub-risks: climate change, pavement composition, construction quality, pavement strength and subgrade, and the dependent variable rutting. The quadratic multiple regression model explained 68.1% of the variance of the data set. The model was significant at .000 (P<0.05). The regression coefficient are **a1= 0.856, a2= 0.393, a3=0.476, a4=0 .065 and a5=-0.284**.

$$Y_{\text{rut}=-0.062+0.856\times X_{i1}+0.393\times X_{i2}+0.476\times X_{i3}+0.065\times X_{i4}-0.284\times X_{i5}}$$

9.3.2.10. Cracking

To analyse the risk of climate change on the pavement failure due to rutting, a quadratic multiple regression model was used to quantify the risk and the associations between the dependent variable and the independent variables. The SPSS software was used to investigate the most reliable coefficient based on the received questionnaires. The obtained results are shown in Appendix 5 and were reported as follows:

Table 9-39: Results of estimated coefficients and ANOVA for cracking risk

Variables Entered/Removeda

Model	Variables Entered	Variables Removed	Method

1	X11.5, X11.1, X11.2, X11.3, X11.4b		Enter

a. Dependent Variable: Y11

b. All requested variables entered.

Model Summary

Model	R	R Square	Adjusted R Square	Std. Error of the Estimate
1	.686a	.471	.360	.20661

a. Predictors: (Constant), X11.5, X11.1, X11.2, X11.3, X11.4

ANOVAa

Model		Sum of Squares	df	Mean Square	F	Sig.
1	Regression	.911	5	.182	4.267	.006b
	Residual	1.025	24	.043		
	Total	1.935	29			

a. Dependent Variable: Y11

b. Predictors: (Constant), X11.5, X11.1, X11.2, X11.3, X11.4

Coefficientsa

Model		Unstandardised Coefficients		Standardised Coefficients	t	Sig.
		B	Std. Error	Beta		
1	(Constant)	.001	.085		.013	.989
	X11.1	.950	.225	.675	4.226	.000
	X11.2	-.446	.359	-.231	-1.242	.226
	X11.3	.358	.308	.210	1.160	.257
	X11.4	.518	.466	.217	1.111	.278
	X11.5	-.189	.365	-.098	-.516	.610

a. Dependent Variable: Y11

Table 9-40: Cracking risk and sub-risks

Y11	X11.1	X11.2	X11.3	X11.4	X11.5
cracking	R2.Climate Change	R3.Pavement Composition	R9.Construction Quality	R4.Pavement Strength	R6.Subgrade

A quadratic multiple regression was considered for estimating the regression coefficients

$$Y_{\text{crac}} = B_0 + a_1 X_{i1} + a_2 X_{i2} + a_3 X_{i3} + a_4 X_{i4} + a_5 X_{i5}$$

Equation 9-34: Risk factor coefficients analysis for cracking due to climate change impact

The results are shown in Table 9-39 to define the relationship between the independent variable sub-risks: climate change, pavement composition, construction quality, pavement strength and subgrade, and the dependent variable cracking. The quadratic multiple regression model explained 47.1% of the variance of the data set. The model was significant at .006 ($P<0.05$). The regression coefficient are **a1= 0.950, a2= -0.446, a3=0.358, a4=0.518 and a5=-0.189**.

$$Y_{\text{crac}} = 0.001 + 0.950 \times X_{i1} - 0.446 \times X_{i2} + 0.358 \times X_{i3} + 0.518 \times X_{i4} - 0.189 \times X_{i5}$$

9.3.2.11. Vehicle Speed

To analyse the risk of climate change on the pavement failure due to vehicle speed, a quadratic multiple regression model was used to quantify the risk and the associations between the dependent variable and the independent variables. The SPSS software was used to investigate the most reliable coefficient based on the received questionnaires. The obtained results are shown in Appendix 5 and were reported as follows:

Table 9-41: Results of estimated coefficients and ANOVA for vehicle speed risk

Variables Entered/Removed[a]

Model	Variables Entered	Variables Removed	Method
1	X12.3, X12.1, X12.2b		Enter

a. Dependent Variable: Y12

b. All requested variables entered.

Model Summary

Model	R	R Square	Adjusted R Square	Std. Error of the Estimate
1	.578a	.334	.257	.07534

a. Predictors: (Constant), X12.3, X12.1, X12.2

ANOVAa

Model		Sum of Squares	df	Mean Square	F	Sig.
1	Regression	.074	3	.025	4.347	.013b
	Residual	.148	26	.006		
	Total	.222	29			

a. Dependent Variable: Y12

b. Predictors: (Constant), X12.3, X12.1, X12.2

Coefficientsa

Model		Unstandardised Coefficients		Standardised Coefficients	t	Sig.
		B	Std. Error	Beta		
1	(Constant)	.021	.027		.779	.443
	X12.1	.611	.176	.581	3.460	.002
	X12.2	-.001	.149	-.001	-.006	.995
	X12.3	-.007	.117	-.011	-.062	.951

a. Dependent Variable: Y12

Table 9-42: Risks associated with vehicle speed and sub-risks

Y12	X12.1	X12.2	X12.3
S7.Vehicle speed	R5.Pavement Ageing	R7.Drainage	R8.Maintenance

A quadratic multiple regression was considered for estimating the regression coefficients.

$$Y_{\text{Veh}} = B_0 + a_1 X_{i1} + a_2 X_{i2} + a_3 X_{i3}$$

Equation 9-35: Risk factor coefficients analysis for vehicle speed due to climate change impact

The results are shown in Table 9-41 to define the relationship between the independent variable sub-risks: pavement ageing, drainage and maintenance, and the dependent variable vehicle speed. The quadratic multiple regression model explained 33.4% of the variance of the data set. The model was significant at .013 (P<0.05). The regression coefficient are **a1= 0.611, a2= -0.001 and a3=-0.007**.

$$Y_{\text{veh}}=0.021+0.611\times X_{i1}-0.001\times X_{i2}-0.007\times X_{i3}$$

9.3.2.12. Pavement Thickness

To analyse the risk of climate change on the pavement failure due to rutting, a linear regression model was used to quantify the risk and the associations between the dependent variable and the independent variables. The SPSS software was used to investigate the most reliable coefficient based on the received questionnaires. The obtained results are shown in Appendix 5 and were reported as follows:

Table 9-43: Descriptive analysis for data of pavement thickness Risk

Variables Entered/Removed[a]

Model	Variables Entered	Variables Removed	Method
1	X13.1b		Enter

a. Dependent Variable: Y13

b. All requested variables entered.

Model Summary

Model	R	R Square	Adjusted R Square	Std. Error of the Estimate
1	.802a	.644	.631	.12993

a. Predictors: (Constant), X13.1

ANOVAa

Model		Sum of Squares	df	Mean Square	F	Sig.
1	Regression	.854	1	.854	50.558	.000b
	Residual	.473	28	.017		
	Total	1.326	29			

a. Dependent Variable: Y13

b. Predictors: (Constant), X13.1

Coefficientsa

Model		Unstandardised Coefficients		Standardised Coefficients	t	Sig.
		B	Std. Error	Beta		
1	(Constant)	.042	.037		1.142	.263
	X13.1	.839	.118	.802	7.110	.000

a. Dependent Variable: Y13

Table 9-44: Pavement thickness risks and sub-risk

Y13	X13.1
S19.Pavement Thickness	R9.Construction Quality

$$Y_{\mathrm{HS}=B_0+a_1 X_{i1}}$$

Equation 9-36: Risk factor coefficients analysis for Pavement thickness due to climate change impact

The results are shown in Table 9-43 to define the relationship between the independent variable sub-risk: construction quality, and the dependent pavement variable thickness. The regression model explained 64.4% of the variance of the data set. The model was significant at .000 ($P<0.05$). The regression coefficient is **a1= 0.839**.

$$Y_{\mathrm{HS}=0.042+0.839\times X_{i1}}$$

9.4. Modelling and Simulation for Pavement Failure Risk under Climate Change Impact

As was discussed earlier in the above sub-sections, a questionnaire survey was carried out to examine and evaluate the qualitative risk of pavement failure effects with respect to climate change through expert judgement. The purposes of the questionnaire survey are to support the causal loop diagrams formed previously with physical risk causal relationships to match the possible risk scenarios in the developed model in Chapter 6 (modified HDM-4). Such causal relationships with risk variables were measured by the probability method and the multiple-regression analysis method (discussed earlier). Thus, building risk into the stock and flow model is the next important step, which is explained in detail in this section. In addition to CLDs, stock and flow diagrams provide more detailed information on how the variables in the model receive dynamic behaviour. For this sub-section, the stock and flow diagrams were built. Eventually, the system behaviour needs to be reassessed due to the introduction of risk factors. The following sub-sections present the updated risks for the highlighted stock and flow diagrams for the pavement deterioration model with different risk scenarios.

9.4.1. Incorporating Risk into the Pavement Deterioration Model using System Dynamics

The primary objective of this chapter is to determine the deterioration curve using a system dynamics method taking into consideration the risk associated with pavement failure. The pavement deterioration curves based on the change in IRI and PCI using dynamics components for the impact of climate change including all pavement temperature scenarios (2013, 2020, 2040 and 2060) are discussed in Chapter 6. However, in the current chapter, such models are built using a system dynamics method. Deterioration curve was determined under different risk scenarios. It was highlighted in previous sub-sections that there are more than 13 main risk variables associated with pavement failure (Chapter 2); however, only seven main risk variables are used in the system dynamics model to match the modified HDM-4 model to determine change in roughness. These variables are pavement thickness, pavement temperature, pavement ageing, traffic loading, the speed of heavy vehicles, change in rutting and cracking. New stock and flow diagrams were introduced to include the risk variables' impact. Once all these sub-models were united with the associated risks into one model, the model was run for 20 years to project the deterioration curve on pavement condition based on two performance indicators, PCI and IRI.

9.4.1.1. Stock and Flow for Traffic Loading Risk Scenario

Only the risk factors that match the variables generated in the modified HDM-4, which was discussed in Chapter 6 section 6.4.3. are considered. Therefore, the risks associated with pavement thickness, pavement temperature, pavement ageing, traffic loading, the speed of heavy vehicles, change in rutting and cracking are incorporated into the proposed deterioration model. Traffic loading risk is one of the crucial risk components. As was discussed in section 9.3.1.2, the higher the traffic loading, the worse the impacts on pavement condition. Therefore, the stock and flow diagram was prepared to achieved dynamic traffic loading with a range that starts from 0.1 m ESAL to 8 m EASL within 20 years based on the data as discussed in Chapter 5 section 5.6.2. This range is going to change based on the impact of the risk factors. The risk was categorised based on multiple-regression analysis method and probability method. In order to examine the model with different risk factors under the multiple-regression analysis method, it was decided to apply three different experiments for the variable inputs, which are average scenario, minimum scenario and maximum scenario, as per equations 9-37, 9-38 and 9-39. Average

$$Y_{\text{traffic(Averg)}}=0.062-0.103\times X_{i1}+0.225\times X_{i2}-0.067\times X_{i3}+0.036X_{i4}+0.079X_{i5}+0.247X_{i6}+0.379X_{i7}$$

Equation 9-37: Average traffic risk based on the multiple linear regression method

Where, $X_{i1}, X_{i2}, X_{i3}, \ldots$ average

$$Y_{\text{traffic(Max)}}=0.062-0.103\times X_{i1}+0.225\times X_{i2}-0.067\times X_{i3}+0.036X_{i4}+0.079X_{i5}+0.247X_{i6}+0.379X_{i7}$$

Equation 9-38: Maximum traffic risk based on the multiple linear regression method

Where, $X_{i1}, X_{i2}, X_{i3}, \ldots$ Maximum

$$\boldsymbol{Y_{\text{traffic(Min)}}=0.062-0.103\times X_{i1}+0.225\times X_{i2}-0.067\times X_{i3}+0.036X_{i4}+0.079X_{i5}+0.247X_{i6}+0.379X_{i7}}$$

Equation 9-39: Minimum traffic risk based on the multiple linear regression method

Where, $\boldsymbol{X_{i1}, X_{i2}, X_{i3}, \ldots}$ **Minmum**

The magnitude of impacted risk for the multiple-regression analysis method was determined as per Table 9-45 where the risk factor based on method 2 was reported in an earlier sub-section. It was decided to use three different scenarios named maximum risk factor, mean risk factor and minimum risk factor for the multiple-regression analysis method. The results are presented in Table 9-45.

Table 9-45: Traffic loading risk based on multiple-regression analysis with three different measures

	A								
	R1.	**S1**	**S2**	**S3**	**S4**	**S5**	**S6**	**S7**	**Adjusted R Square**
Sig.	Y1	X1.1	X1.2	X1.3	X1.4	X1.5	X1.6	X1.7	
.056[b]	R1.Traffic	S1.High volume of heavy trucks	"S2.Axel Group Type	"S3.Tyer configuration	S4.Gross vehicle mass	S5.Dynamic Wheel Loading	S6.High traffic loading (all vehicles type)	S7.Vehicle speed	**0.250**
Max	0.360	0.720	0.720	0.400	0.720	0.560	0.560	0.360	**constant**
Average	0.162	0.339	0.221	0.087	0.186	0.141	0.189	0.072	

Min	0.010	0.060	0.020	0.010	0.030	0.010	0.010	0.010	
coefficients		-0.103	0.225	-0.067	0.036	0.079	0.247	0.378	.062
Risk (Max)	**0.466**	-0.074	0.162	-0.027	0.026	0.045	0.138	0.136	.062
Risk(Mean)	**0.162**	-0.035	0.050	-0.006	0.007	0.011	0.047	0.027	.062
Risk (Min)	**0.067**	-0.006	0.004	-0.001	0.001	0.001	0.002	0.004	.062

The final results for analysing the risk using two methods, probability and multiple regression, are summarised in the following table, 9-46, and Figure 9-18 represents the range of traffic loading with different risk factors.

Table 9-46: Traffic loading risk measures using two different methods

Method type	**Traffic loading Risk Measure**			
	Risk Type		Factor	R1.
				Y1
Method 1 (regression)	Experiment 1	Risk (Max)	a1	**0.466**
	Experiment 2	Risk (Mean)	a2	**0.162**
	Experiment 3	Risk (Min)	a3	**0.067**
Method 2 (probability)	Experiment 4	Risk Average	a4	**0.176**

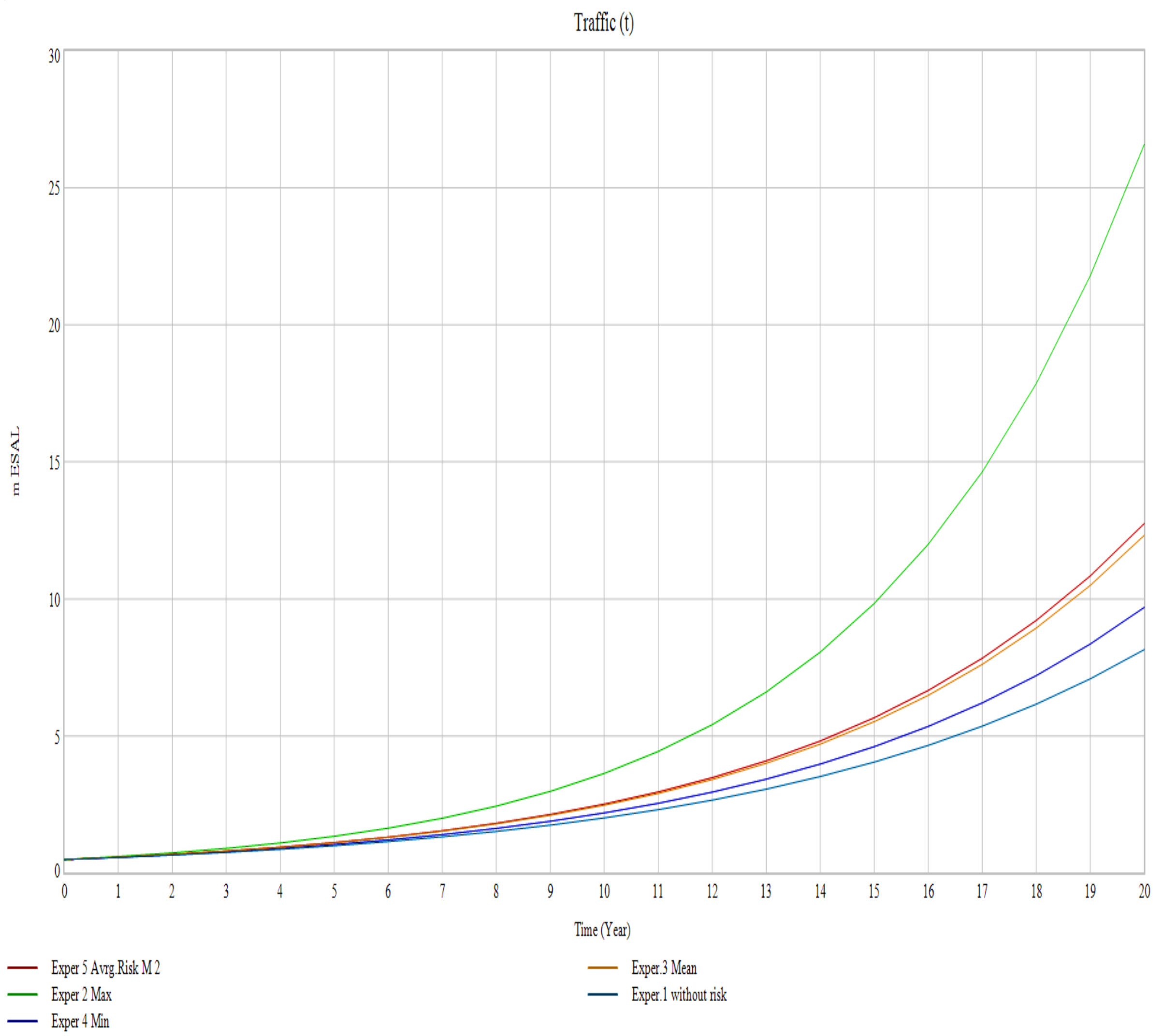

Figure 9-18: Traffic loading range based on different risk factors generated from method 1 and method 2

The relationships between the traffic loading risks and dynamic variables of traffic loading were defined and synchronised through different risk factors using the following equation:

$$y_{R1.T} = Pv.F_T \times \prod_{i=1}^{i=n} R_{R.1T}$$

$$Pv.F_{R1.T} = y_{R1.T} + Pv.F_T$$

Equation 9-40: Equation for risk analysis for traffic loading risk

Thus, the updated model of the stock and flow diagram can be as per the Figure 9-19 below:

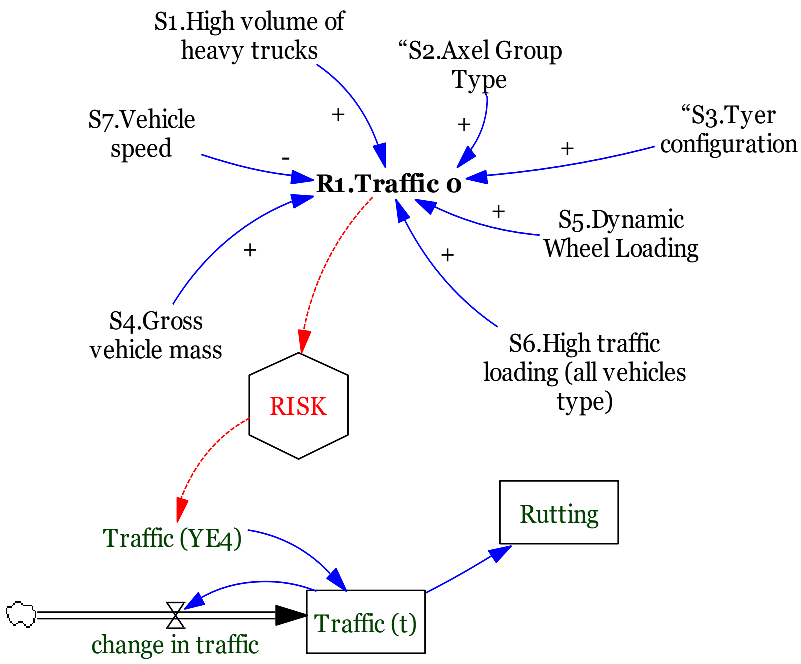

Figure 9-19: Traffic risk scenarios of pavement deterioration model using system dynamics-stock and flow

9.4.2. Stock and Flow for Environmental Loading Risk Scenario

A similar approach to traffic loading was carried out to determine the risk based on multiple-regression analysis method for environmental loading. Tables 9-47 and 9-48 below shows how the results were calculated.

$$Y_{\text{climate(aveg)}}=-0.053-0.988\times X_{i1}+0.193\times X_{i2}+0.090\times X_{i3}+0.660\times X_{i4}+1.527\times X_{i5}-0.524\times X_{i6}+0.203\times X_{i7}-0.160\times X_{i8}+0.672\times X_{i9}+0.216\times X_{i10}$$

Equation 9-41: Average environmental loading risk based on the multiple linear regression method

Where, $X_{i1}, X_{i2}, X_{i3}, \ldots$average

$$Y_{\text{climate(Max)}}=-0.053-0.988\times X_{i1}+0.193\times X_{i2}+0.090\times X_{i3}+0.660\times X_{i4}+1.527\times X_{i5}-0.524\times X_{i6}+0.203\times X_{i7}-0.160\times X_{i8}+0.672\times X_{i9}+0.216\times X_{i10}$$

Equation 9-42: Maximum environmental loading risk based on the multiple linear regression method

Where, $X_{i1}, X_{i2}, X_{i3}, \ldots$Maximum

$$Y_{\text{climate(Min)}}=-0.053-0.988\times X_{i1}+0.193\times X_{i2}+0.090\times X_{i3}+0.660\times X_{i4}+1.527\times X_{i5}-0.524\times X_{i6}+0.203\times X_{i7}-0.160\times X_{i8}+0.672\times X_{i9}+0.216\times X_{i10}$$

Equation 9-43: Minimum environmental loading risk based on the multiple linear regression method

Where, $X_{i1}, X_{i2}, X_{i3}, \ldots$ Minmum

Table 9-47: Environmental loading risk based on regression analysis with three different measures

	B											Adjusted R Square
	R2.	S8	S9	S10	S11	R7	R5	S14	S15	S16	S17	
Sig.	Y2	X2.1	X2.2	X2.3	X2.4	X2.5	X2.6	X2.7	X2.8	X2.9	X2.10	
.005b	R2. Environmental loading	S8.Precipitation	S9.Weathering	S10.High Temperature	S11.Low Temperature	R7.Drainage	R5.Pavement Ageing	S14.Increase oxidation	S15.Increase viscosity and softness	S16.Increase Brittle of asphaltic layer	S17.Increase Moisture/ Excess water	0.500
Max	0.36	0.56	0.56	0.72	0.72	0.56	0.40	0.72	0.56	0.56	0.36	constant
Average	0.16	0.17	0.15	0.31	0.10	0.19	0.17	0.19	0.12	0.20	0.13	
Min	0.01	0.01	0.01	0.01	0.01	0.02	0.01	0.02	0.01	0.01	0.01	
coefficients		-0.99	0.19	0.09	0.66	1.53	-0.52	0.20	-0.16	0.67	0.22	-0.05
Risk (Max)	**1.197**	-0.553	0.108	0.065	0.476	0.855	-0.210	0.146	-0.090	0.376	0.078	-0.05
Risk(Mean)	**0.278**	-0.167	0.028	0.028	0.065	0.289	-0.090	0.039	-0.019	0.133	0.027	-0.05
Risk (Min)	**-0.017**	-0.010	0.002	0.001	0.007	0.031	-0.005	0.004	-0.002	0.007	0.002	-0.05

Table 9-48: Environmental loading risk measures using two different methods

Method type	**Risk Measure**			
	Risk Type		factor	R2. Y2 R2. Environmental loading
Method 1 (Regression)	Experiment 1	Risk (Max)	a1	**1.197**
	Experiment 2	Risk(Mean)	a2	**0.278**
	Experiment 3	Risk (Min)	a3	**-0.017**
Method 2 (Probability)	Experiment 4	Risk Average	a4	**0.172**

Previous stock and flow diagrams for pavement temperature were developed in section 9.2.1. The approach was to structure the pavement temperature model as a dynamic variable that ranges from the 2013 climate condition (current scenario) to the 2060 (future scenario), which is the most critical scenario (worst case scenario). Therefore, the stock and flow model for the pavement temperature was developed to have a range of inputs starting from 69 ºC to 79 ºC over a period of 20 years. The pavement temperature stock and flow model will receive different dynamic behaviours based on four different risk values (a1, a2, a3 and a4), as highlighted in Table 9-48 above. It is suggested that these values will be synchronised with the rate of change of pavement temperature using the following equation, 9-44:

$$y_{R2.CC} = Pv.F_{CC} \times \prod_{i=1}^{i=n} R_{R2.CC}$$

$$Pv.F_{R2.CC} = y_{R2.CC} + Pv.F_{CC}$$

Equation 9-44: Equation for probability risk analysis for environmental loading

The results are shown in Figure 9-20, which represents the pavement temperature stock and flow diagram with different risk factors.

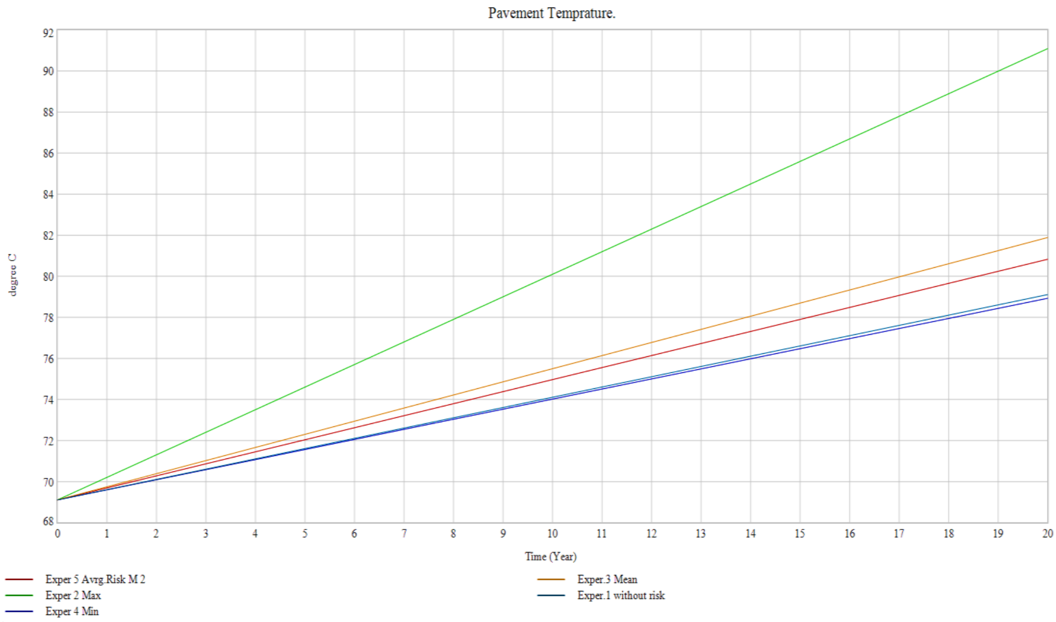

Figure 9-20:Pavement temperature range based on different risk factors generated from method 1 and method 2

9.4.3. Stock and Flow for Pavement Ageing Risk Scenario

As was discussed in section 9.2.1, pavement ageing received a similar analysis to that shown for traffic loading and environmental loading; the results are reported accordingly. The risk is categorised based on multiple-regression analysis method and probability methods. In order to examine the model with different risk factors, it was decided to apply three different scenarios for the variable inputs, which are average scenario, minimum scenario and maximum scenario, as per the following equations.

$$Y_{\text{Ageing(Averg.)}=0.042+0.023\times X_{i1}+0.406\times X_{i2}+0.247\times X_{i3}-0.036X_{i4}}$$

Equation 9-45: Average pavement ageing risk based on the multiple linear regression method

Where, X_{i1},X_{i2},X_{i3},....average

$$Y_{\text{Ageing(Max)}=0.042+0.023\times X_{i1}+0.406\times X_{i2}+0.247\times X_{i3}-0.036X_{i4}}$$

Equation 9-46: Maximum pavement ageing risk based on the multiple linear regression method

Where, X_{i1},X_{i2},X_{i3},....Maximum

$$Y_{\text{Ageing(Min)}=0.042+0.023\times X_{i1}+0.406\times X_{i2}+0.247\times X_{i3}-0.036X_{i4}}$$

Equation 9-47: Minimum pavement ageing risk based on the multiple linear regression method

Where, X_{i1},X_{i2},X_{i3},....Minmum

Maximum risk factor, mean risk factor and minimum risk factor for the multiple-regression analysis method are estimated as per Tables 9-49 and 9-50, where the risk factor based on method 2 was reported in an earlier sub-section.

Table 9-49: Pavement ageing risk based on regression analysis with three different measures

			E			
	R3.	R2	R1	R6	R8	
Sig.	Y5	X5.1	X5.2	X5.3	X5.4	
.032b	R5.Pavement Ageing	R2.Climate Change	R1.Traffic Loading	R6.Subgrade Soil	R8.Maintenance	0.227
Max	0.56	0.72	0.56	0.56	0.56	constant
Average	0.17	0.18	0.21	0.17	0.14	
Min	0.02	0.01	0.02	0.01	0.01	
coefficients		.023	.406	.247	-.036	0.04
Risk (Max)	**0.404**	0.016	0.227	0.138	-0.020	0.04

Risk(Mean)	**0.170**	0.004	0.087	0.041	-0.005	0.04
Risk (Min)	**0.053**	0.0002	0.0081	0.0025	-0.0004	0.04

Table 9-50: Pavement ageing risk measures using two different methods

Method type	Risk Measure			
	Risk Type		factor	R5. Y5 R5.Pavement Ageing
Method 1 (regression)	Experiment 1	Risk (Max)	a1	**0.404**
	Experiment 2	Risk(Mean)	a2	**0.170**
	Experiment 3	Risk (Min)	a3	**0.053**
Method 2 (Probability)	Experiment 4	Risk Average	a4	**0.176**

The previous stock and flow diagram for pavement ageing was built to achieve dynamic variables ranging from eight years to 18 years over a certain period (chosen to be 20 years) as discussed in Chapter 5 section 5.9. The values of both softening point and voids in the mix are determined accordingly (see Chapter 5 sections 5.12 and 5.13). The stock and flow diagrams are updated based on the dynamic behaviour of the pavement deterioration constructs taking into consideration the influence of risks. Four tests were carried out to take into consideration the different risk factors. The updated stock and flow diagram received different dynamic behaviours based on four different risk values (a1, a2, a3 and a4), as highlighted in Table 9-50. It was decided that these values would be synchronised with the rate of change of pavement ageing using the following equation (9-48):

$$y_{R5.PA} = Pv.F_{PA} \times \prod_{i=1}^{i=n} R_{R4.PA}$$

$$Pv.F_{R5.PA} = y_{R5.PA} + Pv.F_{PA}$$

Equation 9-48: Equation for probability risk analysis for Pavement ageing

The results are shown in the figure 9-21 below, which represents the range of pavement ageing with different risk factors. Pavement ageing range based on different risk factors generated from method 1 and method 2 is shown in Figure 9-2.

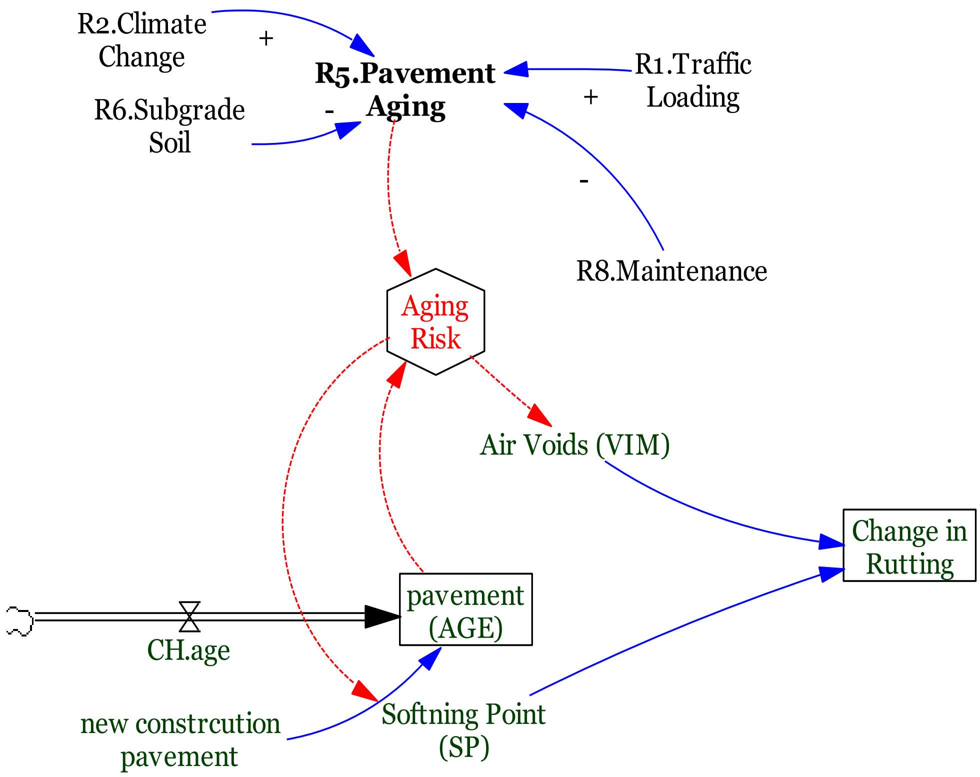

Figure 9-21: Pavement ageing risk scenarios of pavement deterioration model using system dynamics

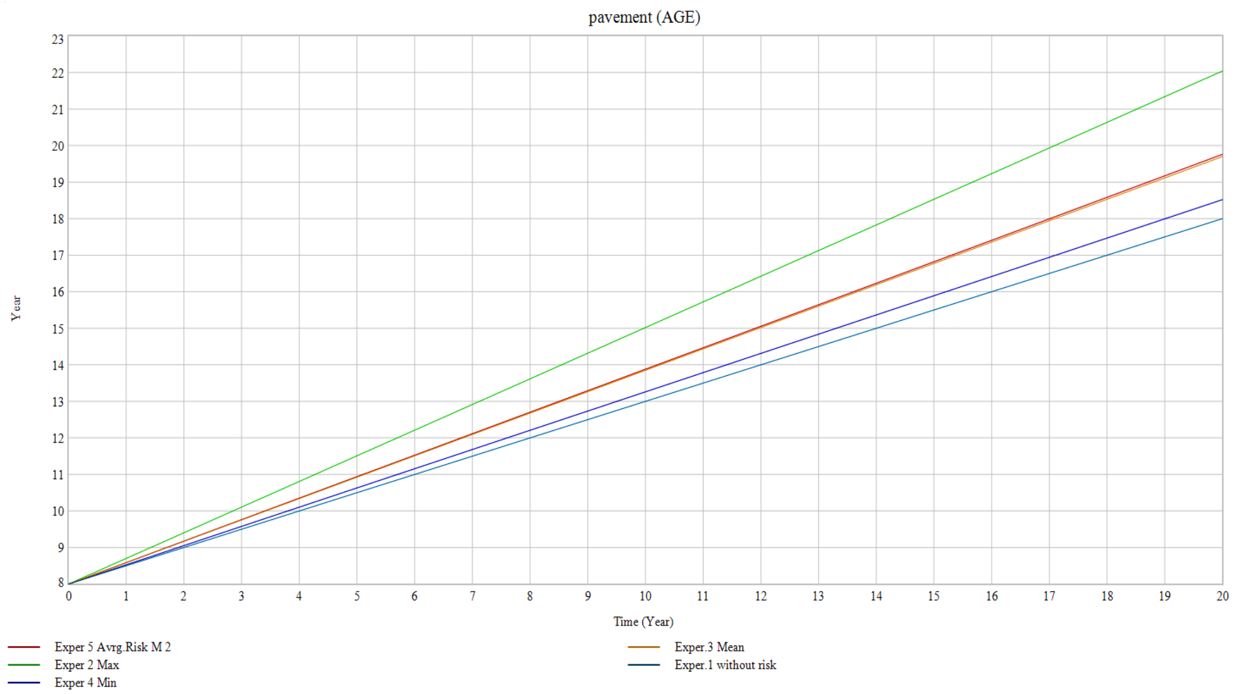

Figure 9-22:Pavement ageing range based on different risk factors generated from method 1 and method 2

9.4.4. Stock and Flow for Pavement Thickness Risk Scenario

The approach in the previous sub-section was applied to pavement thickness analysis and, in order to examine the model with different risk factors for pavement thickness, it was decided to apply three different scenarios for the variable inputs, which are average scenarios, minimum scenarios and maximum scenarios, as per the following equations (9-49, 9-50 and 9-51):

$$\boldsymbol{Y}_{\mathbf{HS(averg.)}}=\mathbf{0.042}+\mathbf{0.839}\times X_{i1}$$

Equation 9-49: Average pavement thickness risk based on the multiple linear regression method

Where, $X_{i1}, X_{i2}, X_{i3}, \ldots$ average

$$\boldsymbol{Y}_{\mathbf{HS(Max)}}=\mathbf{0.042}+\mathbf{0.839}\times X_{i1}$$

Equation 9-50: Maximum Pavement thickness risk based on the multiple linear regression method

Where, $X_{i1}, X_{i2}, X_{i3}, \ldots$ Maximum

$$\boldsymbol{Y}_{\mathbf{HS(Min)}}=\mathbf{0.042}+\mathbf{0.839}\times X_{i1}$$

Equation 9-51: Minimum Pavement thickness risk based on the multiple linear regression method

Where, $X_{i1}, X_{i2}, X_{i3}, \ldots$ Minmum

Maximum risk factor, mean risk factor and minimum risk factor for the multiple-regression analysis method are estimated as per Table 9-51, where the risk factor based on method 2 was reported in an earlier sub-section.

Table 9-51: Pavement thickness risk based on regression analysis with three different measures

	N		
	S7	R2	
Sig.	Y13	X13.1	
.009b	S19.Pavement Thickness	R9.Construction Quality	0.241
Max	0.72	0.72	constant
Average	0.24	0.24	
Min	0.01	0.02	
coefficients		0.84	0.042
Risk (Max)	**0.65**	0.60	0.042
Risk(Mean)	**0.24**	0.20	0.042
Risk (Min)	**0.06**	0.02	0.042

Table 9-52: Pavement thickness risk measures using two different methods

Method type	Pavement Thickness Risk Measure			
	Risk Type		factor	S10 Y13 S19.Pavement Thickness
Method 1 (regression)	Experiment 1	Risk (Max)	a1	**0.646**
	Experiment 2	Risk(Mean)	a2	**0.240**
	Experiment 3	Risk (Min)	a3	**0.059**
Method 2 (Probability)	Experiment 4	Risk Average	a4	**0.237**

In order to build the stock and flow diagram, it is necessary to highlight the rate of change for pavement thickness with respect to risk factors in every interval year and for how many years the model will run and what is the initial value. Thus, to make the model match the real design thickness, it was suggested to use the range between 120 mm (worst case scenario) and 220 mm, then different ranges that occur based on the risk factors, as is shown in the previous figure. The updated stock and flow diagram will receive different dynamic behaviours based on four different risk values (a1, a2, a3 and a4), as highlighted in Table 9-52. It was decided that such values will be synchronised with the rate of change of pavement ageing using the following equation:

$$y_{R.VT} = Pv.F_{VT} \times \prod_{i=1}^{i=n} R_{R.VT}$$

$$Pv.F_{R.VT} = y_{R.VT} + Pv.F_{VT}$$

Equation 9-52: Equation for probability risk analysis for Pavement thickness

The stock and flow was tested, and the highlighted variable becomes a dynamic element as per Figure 9-23 and Figure 9-24 below:

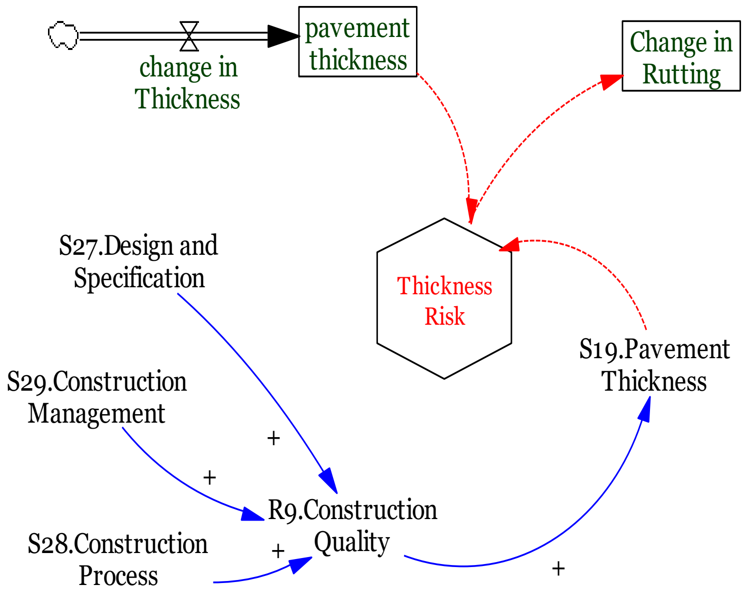

Figure 9-23: Pavement thickness risk scenarios of pavement deterioration model using system dynamics

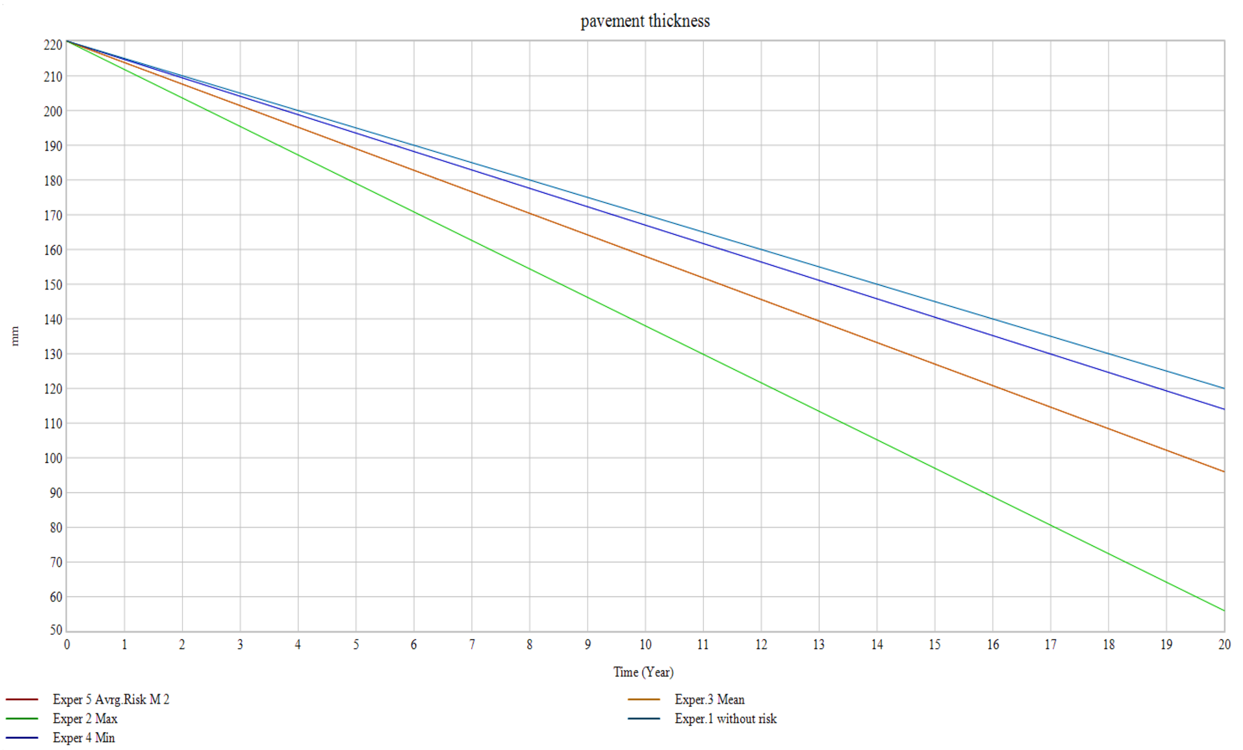

Figure 9-24:Pavement thickness range based on different risk factors generated from method 1 and method 2

9.4.5. Stock and Flow for Vehicle Speed Risk Scenario

The approach in the previous sub-section was applied to the vehicle speed analysis and, in order to examine the model with different risk factors for pavement thickness, it was suggested to apply three different scenarios for the variable inputs, which are average scenarios, minimum scenarios and maximum scenarios as per the following equations:

$$\boldsymbol{Y}_{\mathbf{veh(averag.)}}\mathbf{=0.021+0.611\times}\boldsymbol{X_{i1}}\mathbf{-0.001\times}\boldsymbol{X_{i2}}\mathbf{-0.007\times}\boldsymbol{X_{i3}}$$

Equation 9-53 Average vehicle speed risk based on the multiple linear regression method

Where, X_{i1},X_{i2},X_{i3},....average

$$\boldsymbol{Y}_{\mathbf{veh(Max)}}\mathbf{=0.021+0.611\times}\boldsymbol{X_{i1}}\mathbf{-0.001\times}\boldsymbol{X_{i2}}\mathbf{-0.007\times}\boldsymbol{X_{i3}}$$

Equation 9-54 Maximum vehicle speed risk based on the multiple linear regression method

Where, X_{i1},X_{i2},X_{i3},....Maximum

$$\boldsymbol{Y}_{\mathbf{veh(Min)}}\mathbf{=0.021+0.611\times}\boldsymbol{X_{i1}}\mathbf{-0.001\times}\boldsymbol{X_{i2}}\mathbf{-0.007\times}\boldsymbol{X_{i3}}$$

Equation 9-55 Minimum vehicle speed risk based on the multiple linear regression method

Where, X_{i1},X_{i2},X_{i3},....Minmum

Maximum risk factor, mean risk factor and minimum risk factor for multiple-regression analysis method are determined as per Table 9-53, where risk factor based on method 2 was reported in an earlier sub-section.

Table 9-53: Vehicle speed risk factor based on regression analysis with three different measures

M					
	S7	R2	R1	R6	
Sig.	Y12	X12.1	X12.2	X12.3	Adjusted R Square
.013b	S7.Vehicle speed	R5.Pavement Ageing	R7.Drainage	R8.Maintenance	0.257
Max	0.40000	0.36000	0.40000	0.40000	constant
Average	0.07733	0.09433	0.13467	0.15933	
Min	0.01000	0.01000	0.01000	0.01000	
coefficients		0.61052	-0.00086	-0.00727	0.021
Risk (Max)	**0.23755**	0.21979	-0.00034	-0.00291	0.021
Risk(Mean)	**0.07733**	0.05759	-0.00012	-0.00116	0.021

Risk (Min)	**0.02704**	0.00611	-0.00001	-0.00007	0.021

Table 9-54: Vehicle speed risk measures using two different methods

Method type	**Risk Measure**			
	Risk Type		factor	S7 Y12 S7.Vehicle speed
method 1 (regression)	experiment 1	Risk (Max)	a1	**0.238**
	experiment 2	Risk(Mean)	a2	**0.077**
	experiment 3	Risk (Min)	a3	**0.027**
method 2 (Probability)	experiment 4	Risk Average	a4	**0.129**

Similar to pavement thickness, speed of heavy vehicles was determined to establish an expanded stock and flow diagram that includes risk factors. The analysis in Chapter 5 section 5.7 showed that speed of heavy vehicles depends on whether the vehicle is loaded with goods or not. Heavily loaded vehicles travel more slowly than less heavily laden ones, which means more impact on pavement deterioration. For this reason, to make the speed of heavy vehicles a dynamic variable, it was suggested to range the speed value from 80 km/h to 20 km/h (descending order), which represents a range without risk factors. The updated stock and flow diagram will receive different dynamic behaviours based on four different risk values (a1, a2, a3 and a4), as highlighted in Table 9-54. It is suggested that such values will be synchronised with the rate of change of pavement ageing using the following equation:

$$y_{R.VS} = Pv.F_{VS} \times \prod_{i=1}^{i=n} R_{R.VS}$$

$$Pv.F_{R.VS} = y_{R.VS} + Pv.F_{VS}$$

Equation 9-56: Equation for probability risk analysis for Heavy Vehicle speed risk category

Finally, the stock and flow model for the variable is tested and run for the consecutive 20 years. It was also decided to build the stock and flow model to start with the best scenario and move towards the most critical variable inputs.

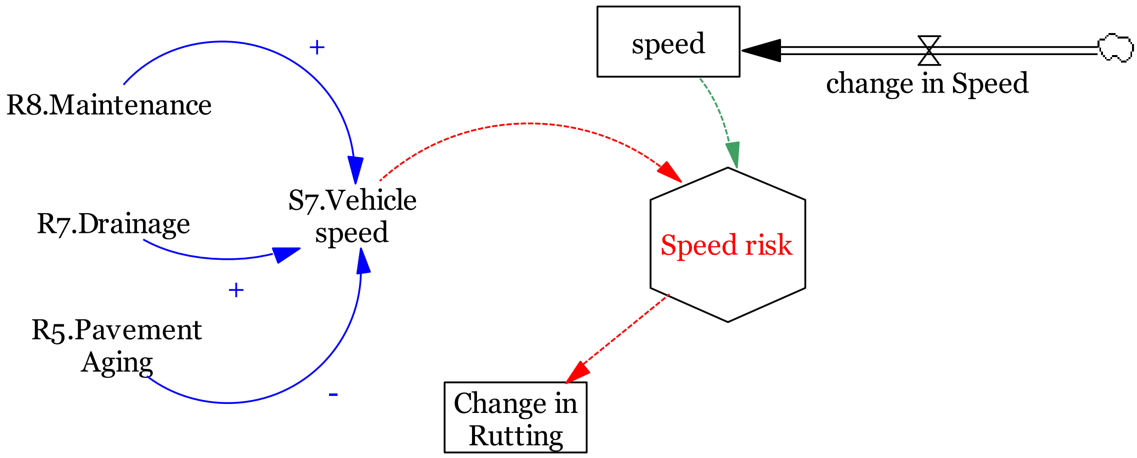

Figure 9-25: Vehicle speed risk scenarios of pavement deterioration model using system dynamics

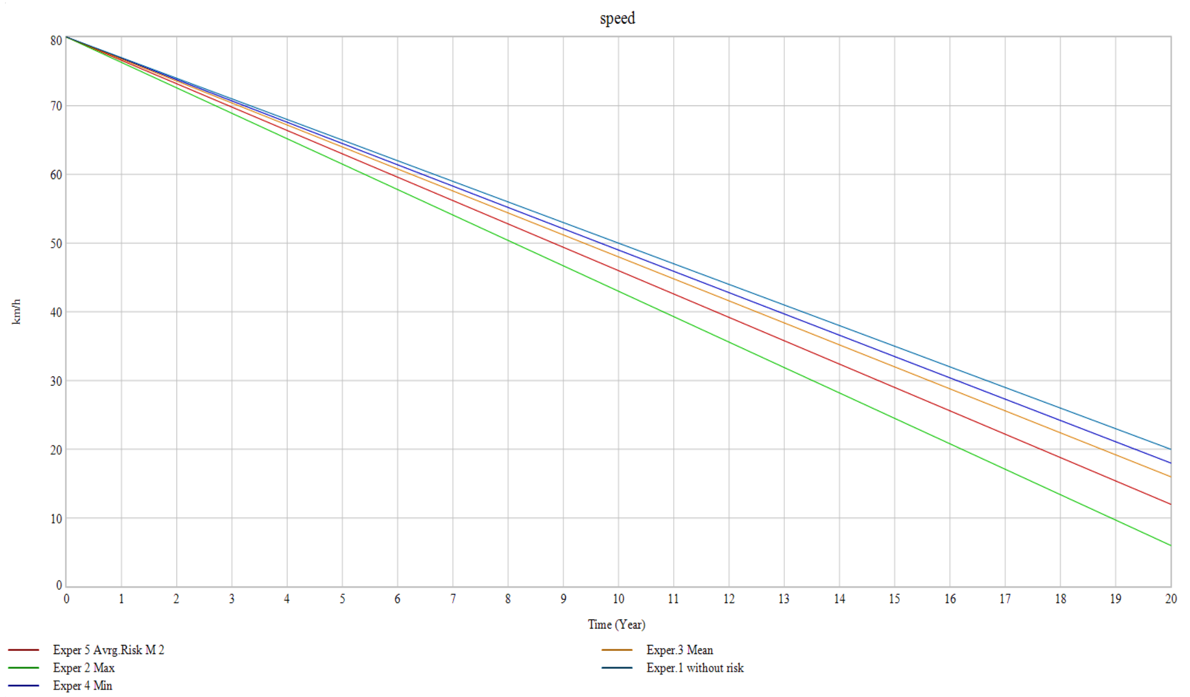

Figure 9-26:Vehicle speed range based on different risk factors generated from method 1 and method 2

9.4.6. Stock and Flow for Rutting Risk Scenario

The approach in the previous sub-section was applied to rutting analysis and, in order to examine the model with different risk factors for pavement thickness, it was suggested to apply three different scenarios for the variable inputs, which are average scenarios, minimum scenarios and maximum scenarios, as per the following equations:

$$\boldsymbol{Y}_{\mathbf{rut(Averg.)}}=-\mathbf{0.062}+\mathbf{0.856}\times X_{i1}+\mathbf{0.393}\times X_{i2}+\mathbf{0.476}\times X_{i3}+\mathbf{0.065}\times X_{i4}-\mathbf{0.284}\times X_{i5}$$

Equation 9-57: Average rutting risk based on the multiple linear regression method

Where, $X_{i1}, X_{i2}, X_{i3}, \ldots$ average

$$\boldsymbol{Y}_{\mathbf{rut(Max)}}=-\mathbf{0.062}+\mathbf{0.856}\times X_{i1}+\mathbf{0.393}\times X_{i2}+\mathbf{0.476}\times X_{i3}+\mathbf{0.065}\times X_{i4}-\mathbf{0.284}\times X_{i5}$$

Equation 9-58: Maximum rutting risk based on the multiple linear regression method

Where, $X_{i1}, X_{i2}, X_{i3}, \ldots$ Maximum

$$\boldsymbol{Y}_{\mathbf{rut(Min)}}=-\mathbf{0.062}+\mathbf{0.856}\times X_{i1}+\mathbf{0.393}\times X_{i2}+\mathbf{0.476}\times X_{i3}+\mathbf{0.065}\times X_{i4}-\mathbf{0.284}\times X_{i5}$$

Equation 9-59: Minimum rutting risk based on the multiple linear regression method

Where, $X_{i1}, X_{i2}, X_{i3}, \ldots$ Minmum

Maximum risk factor, mean risk factor and minimum risk factor for multiple-regression analysis method are determined as per Tables 9-55 and 9-56, where risk factor based on method 2 was reported in an earlier sub-section.

Table 9-55: Rutting risk factor based on regression analysis with three different measures

	H						
	R10.	R2	R3	R9	R4	R6	
Sig.	Y10	X10.1	X10.2	X10.3	X10.4	X10.5	Adjusted R Square
.000b	Rutting	R2.Climate Change	R3.Pavement Composition	R9.Construction Quality	R4.Pavement Strength	R6.Subgrade	.615
Max	0.72	0.72	0.72	0.56	0.56	0.72	constant
Average	0.20	0.15	0.20	0.23	0.21	0.22	
Min	0.01	0.01	0.03	0.05	0.01	0.03	
coefficients		.856	.393	.476	.065	-2.836E-01	-0.06
Risk (Max)	**0.935**	0.617	0.283	0.266	0.036	-0.204	-0.06

Risk(Mean)	**<u>0.204</u>**	0.127	0.080	0.108	0.014	-0.063	-0.06
Risk (Min)	**<u>-0.026</u>**	0.009	0.012	0.024	0.001	-0.009	-0.06

Table 9-56: Rutting risk measures using two different methods

Method type	**Risk Measure**			
	Risk Type		factor	R10. Y10 Rutting
Method 1 (regression)	Experiment 1	Risk (Max)	a1	**<u>0.935</u>**
	Experiment 2	Risk(Mean)	a2	**<u>0.204</u>**
	Experiment 3	Risk (Min)	a3	**<u>-0.026</u>**
Method 2 (Probability)	Experiment 4	Risk Average	a4	**<u>0.203</u>**

The updated stock and flow diagram for rutting will receive different dynamic behaviours based on four different risk values (a1, a2, a3 and a4), as highlighted in Table 9-56. It is suggested that such values will be synchronised with the rate of change of pavement ageing using the following equation:

$$y_{R.rut} = Pv.F_{rut} \times \prod_{i=1}^{i=n} R_{R.rut}$$

$$Pv.F_{R.rut} = y_{R.rut} + Pv.F_{rut}$$

Equation 9-60: Equation for probability risk analysis for rutting

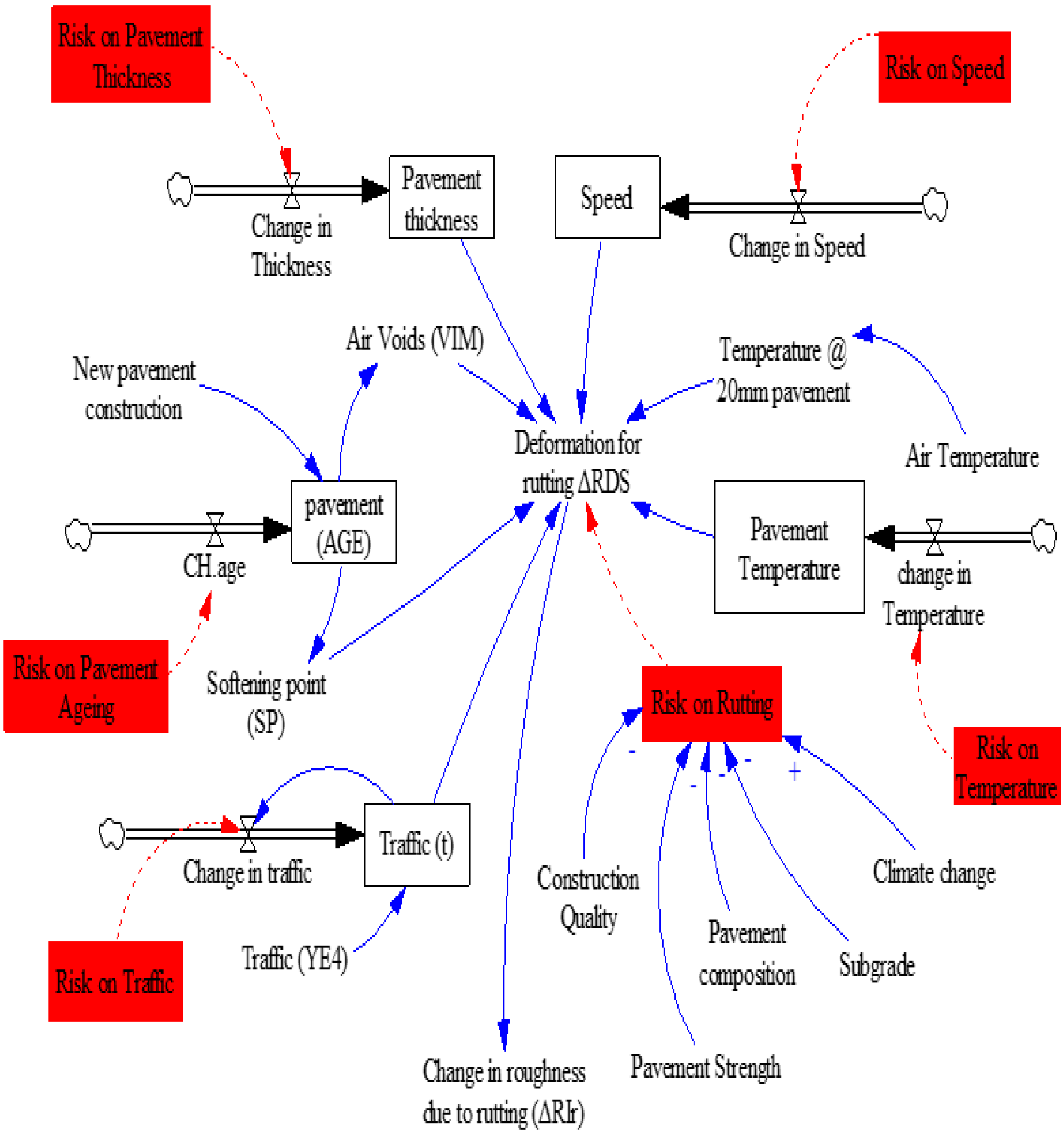

Figure 9-27: Rutting risk scenarios of pavement deterioration model using system dynamics

9.4.7. Stock and Flow for Cracking Risk Scenario

The approach in the previous sub-section was applied to rutting analysis and, in order to examine the model with different risk factors for pavement thickness, it was suggested to apply three different scenarios for the variable inputs, which are average scenarios, minimum scenarios and maximum scenarios, as per the following equations:

$$Y_{\text{crac(averg.)}}=0.001+0.950\times X_{i1}-0.446\times X_{i2}+0.358\times X_{i3}+0.518\times X_{i4}-0.189\times X_{i5}$$

Equation 9-61: Average Cracking risk based on the multiple linear regression method

Where, X_{i1},X_{i2},X_{i3},....average

$$Y_{\text{crac(Max)}}=0.001+0.950\times X_{i1}-0.446\times X_{i2}+0.358\times X_{i3}+0.518\times X_{i4}-0.189\times X_{i5}$$

Equation 9-62: Maximum cracking risk based on the multiple linear regression method

Where, X_{i1},X_{i2},X_{i3},....Maximum

$$Y_{\text{crac(Min)}}=0.001+0.950\times X_{i1}-0.446\times X_{i2}+0.358\times X_{i3}+0.518\times X_{i4}-0.189\times X_{i5}$$

Equation 9-63: Minimum cracking risk based on the multiple linear regression method

Where, X_{i1},X_{i2},X_{i3},....Minmum

Maximum risk factor, mean risk factor and minimum risk factor for multiple-regression analysis method are estimated as per Table 9-57, where risk factor based on method 2 was reported in an earlier sub-section.

Table 9-57: Cracking risk factor based on regression analysis with three different measures

L							
	R11.	R2	R3	R9	R4	R6	
Sig.	Y11	X11.1	X11.2	X11.3	X11.4	X11.5	Adjusted R Square
.000b	Cracking	R2.Climate Change	R3.Pavement Composition	R9.Construction Quality	R4.Pavement Strength	R6.Subgrade	.615
Max	0.80	0.72	0.72	0.56	0.40	0.56	constant
Average	0.30	0.24	0.15	0.18	0.16	0.11	
Min	0.03	0.01	0.01	0.05	0.01	0.01	
coefficients		.950	-.446	.358	.518	-1.886E-01	0.00
Risk (Max)	**0.666**	0.684	-0.321	0.200	0.207	-0.106	0.00
Risk(Mean)	**0.295**	0.231	-0.065	0.065	0.084	-0.021	0.00
Risk (Min)	**0.027**	0.009	-0.004	0.018	0.005	-0.002	0.00

Table 9-58: Cracking risk measures using two different methods

Method type	**Risk Measure**		
	Risk Type	factor	R11.
			Y11
			Cracking

Method 1 (regression)	Experiment 1	Risk (Max)	a1	**0.666**
	Experiment 2	Risk(Mean)	a2	**0.295**
	Experiment 3	Risk (Min)	a3	**0.027**
Method 2 (Probability)	Experiment 4	Risk Average	a4	**0.169**

The updated stock and flow diagram will receive different dynamic behaviours based on four different risk values (a1, a2, a3 and a4), as highlighted in Table 9-58. It was decided that such values will be synchronised with the rate of change of pavement ageing using the following equation:

$$y_{R.cra} = Pv.F_{cra} \times \prod_{i=1}^{i=n} R_{R.cra}$$

$$Pv.F_{R.cra} = y_{R.cra} + Pv.F_{cra}$$

Equation 9-64: Equation for probability risk analysis for cracking

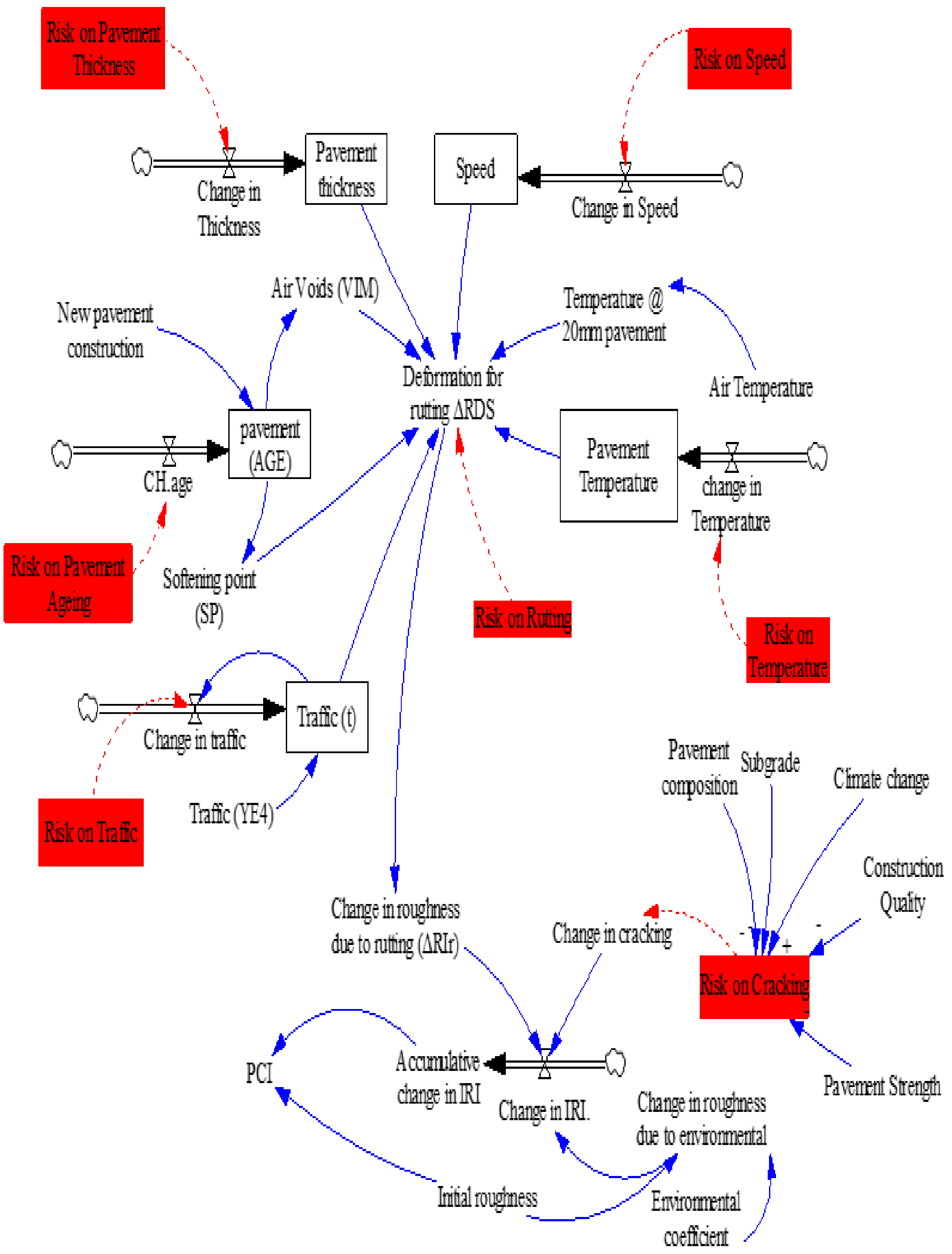

Figure 9-28: Cracking risk scenarios of pavement deterioration model using system dynamics

9.5. Computation of IRI and PCI Deterioration Curve Using System Dynamics

The pavement deterioration curves were based on the change in IRI using dynamic components for the impact of climate change. The main objective was to determine the deterioration curve using a system dynamics method with respect to different risks. Pavement thickness, pavement temperature, pavement ageing, traffic loading, the speed of heavy vehicles and change in rutting are re-assessed by incorporating pavement failure risks. Only those variable risks which are directly linked with dynamic model components were taken into consideration.

9.5.1. IRI and PCI Deterioration Curve Using SystemDynamics without Risk

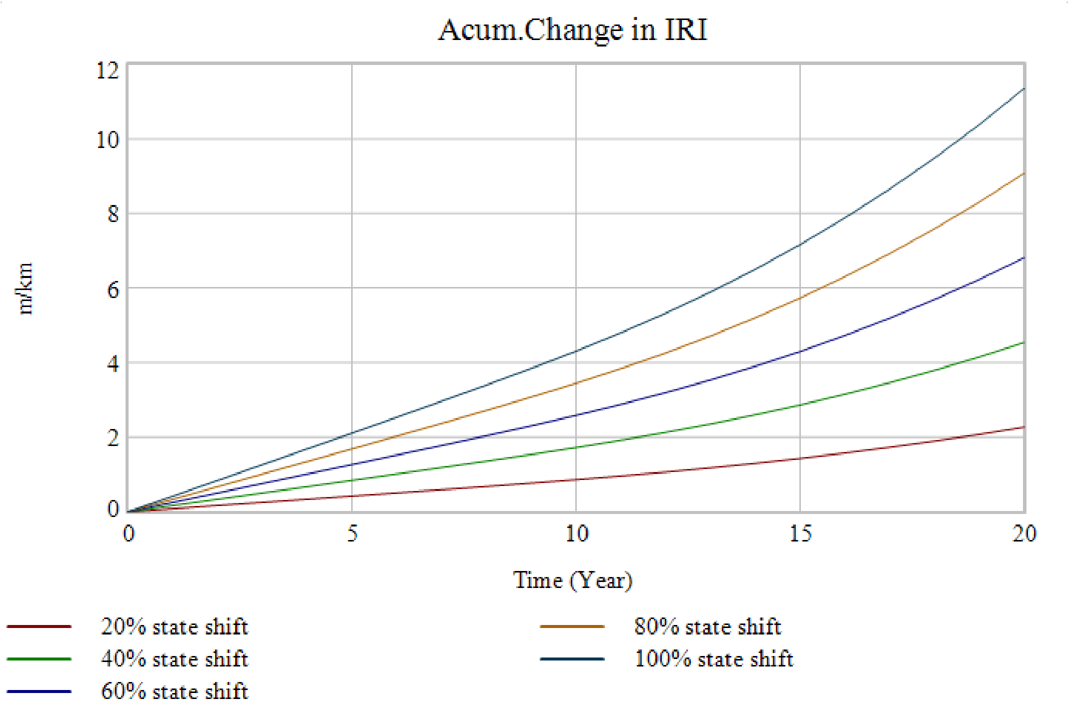

Figure 9-29: Accumulative change in IRI based on different risk scenarios using system dynamics method

The system dynamics model was built to predict the worst pavement condition scenarios that might occur over 20 years. The dynamic variables were defined to range from lower impact scenarios to the worst one. In practice, the pavement condition of the road is going to ultimately fail before reaching these values (IRI =11 m/km). Figure 9-30 showed the different accumulative changes in IRI based on different rates of change. For example, the model was based on the assumption of 100% state condition shift (as yearly rate of change). Partial yearly rates of change with either 80%, 60%, 40% and 20% were also tested. Figure 9-29 also indicated that a 20% yearly rate of change resulted in the lowest change in total roughness (2 m/km) over 20 years. Achieving a 40% state shift recorded change in IRI of nearly 4 m/km after 20 years, which in the opinion of the author seems the most logical approach with which to build the model. However, road designers always depend on the most critical historical data to determine the most acceptable design parameters that allow the road assets to last for the proposed service life period. And, as discussed in Chapter 2, climate change impact is not considered in any current pavement design practice due to the uncertain consequences of such implications and is not part of the historical data. Therefore, with the projection of the worst scenario, it was decided to introduce the pavement deterioration curve in both chapters 8 and 9 based on the worst situation with 100% state shift (rate of change).

Table 9-59: Results generated from Vensim based on deterioration model when all variables are in dynamic mode

Time (Year)	cumulative Change in IRI	IRI (IRla=0.8)	PCI	"Pavement Temperature FROM 2013-2060."
0	0	0.8	100	69.11
1	0.42131	1.22131	82.3	69.61
2	0.84279	1.64279	67.7	70.11
3	1.26454	2.06454	55.7	70.61
4	1.68683	2.48683	45.8	71.11
5	2.11011	2.91011	37.7	71.61
6	2.53523	3.33523	30.9	72.11
7	2.9638	3.7638	25.4	72.61
8	3.39868	4.19868	20.7	73.11
9	3.84459	4.64459	16.9	73.61
10	4.30845	5.10845	13.6	74.11
11	4.7986	5.5986	10.8	74.61
12	5.32323	6.12323	8.5	75.11
13	5.88907	6.68907	6.5	75.61
14	6.50114	7.30114	4.9	76.11
15	7.1633	7.9633	3.6	76.61
16	7.87886	8.67886	2.6	77.11
17	8.65109	9.45109	1.8	77.61
18	9.48352	10.28352	1.2	78.11
19	10.38025	11.18025	0.8	78.61
20	11.34623	12.14623	0.5	79.11

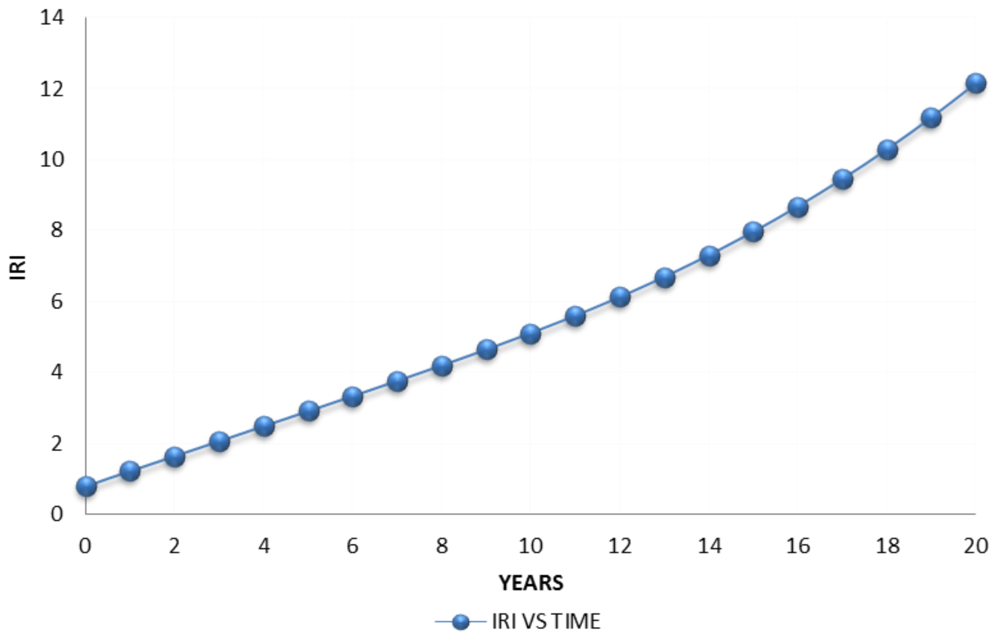

Figure 9-30: Pavement deterioration curve based on IRI using a system dynamics approach based on dynamics change in pavement temperatures

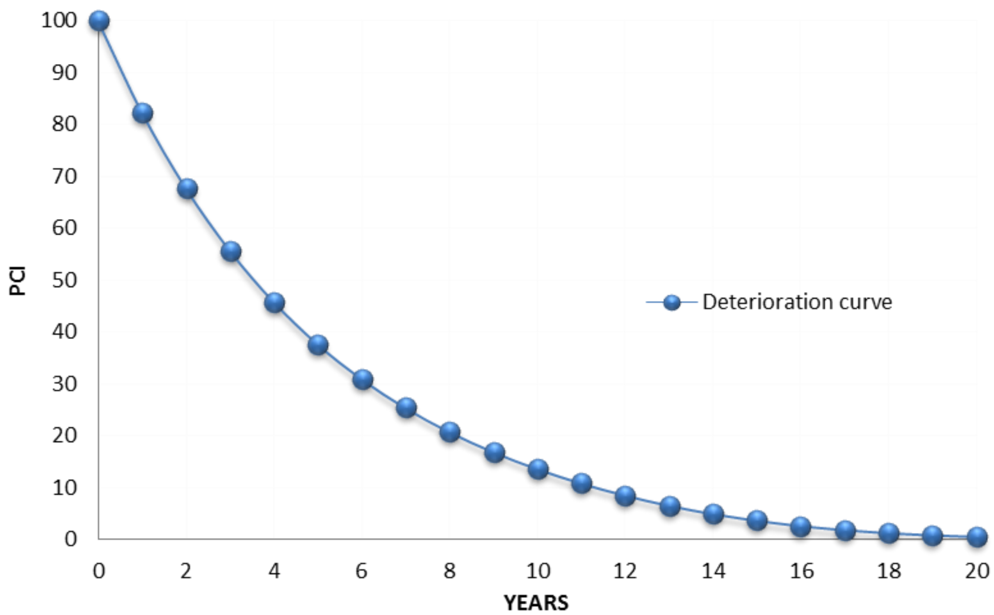

Figure 9-31 Pavement deterioration curve based on IRI using a system dynamics approach based on dynamics change in pavement temperatures

Figures 9-30 and 9-31 represent the deterioration curves concerning the PCI and IRI for the next predicted 20 years for the pavement network of the Ministry of Public Works in the UAE based on a system dynamics method. There are different interpretations of the deterioration predictions function, as was explained in chapters 4 and 8. The presentation of the pavement deterioration predictions curve can be either sigmoid function, traditional S-shaped (Mubaraki 2010) or exponential approach (NAMS 2009). According to the obtained pavement deterioration curve, the expected condition curves showed a logarithmic curve shape because of the data used. The shape of the obtained pavement deterioration curve did not match that found by other researchers, who have found the sigmoid function provides the best interpretation of curve deterioration (Mubaraki, 2010). Nevertheless, the logarithmic curve shape of the deterioration curve can be read as showing that the pavement assets receive a sharp deterioration rate at the start, then a phase of smooth increase takes place till it fails. For example, according to the IRI deterioration curve, achieving an IRI value of 12 m/km is not realistic; most likely, the road failed before reaching this level. According to the IRI international standard, 12 m/km can only be recorded for unpaved roads. Nevertheless, the system showed such a value as a consequence of how the accumulation of stock occurred when the system is in positive (self-reinforcing) mode with unlimited growth if it runs for an undefined period. However, this is not the case, in reality, as the system (pavement condition) either fails before reaching such a state or maintenance intervention occurs to achieve a balancing system.

9.5.2. IRI and PCI Deterioration Curve Using System Dynamics under the Risk of Climate Change

The researcher developed a system dynamics model for pavement failure risk modelling based on the pavement indicators of IRI and PCI as per Chapter 6. Based on the pavement failure risk under climate change impact, a system dynamics model for determining pavement deterioration curves for PCI and IRI was achieved and different risk scenarios were reported as follows:

Table 9-60: Results generated from Vensim based on deterioration model when variables are dynamic based on IRI

	Without Risk	Maximum Risk	Mean Risk	Minimum Risk	Method 2.Average Risk
	Experiment 1	Experiment 2	Experiment 3	Experiment 4	Experiment 5

Time (Year)	Total IRI	Total IRI	Total IRI	Total IRI	Total IRI
0	0.80	0.80	0.80	0.80	0.80
1	1.22	1.31	1.26	1.22	1.25
2	1.64	1.82	1.72	1.64	1.69
3	2.06	2.33	2.17	2.07	2.14
4	2.49	2.85	2.63	2.49	2.59
5	2.91	3.37	3.09	2.91	3.04
6	3.34	3.90	3.56	3.34	3.50
7	3.76	4.45	4.03	3.77	3.96
8	4.20	5.05	4.51	4.21	4.43
9	4.64	5.71	5.02	4.66	4.93
10	5.11	6.44	5.56	5.13	5.47
11	5.60	7.24	6.14	5.64	6.05
12	6.12	8.11	6.78	6.18	6.68
13	6.69	9.07	7.47	6.77	7.37
14	7.30	10.12	8.21	7.40	8.12
15	7.96	11.26	9.03	8.10	8.94
16	8.68	12.50	9.90	8.84	9.84
17	9.45	13.86	10.85	9.65	10.80
18	10.28	15.35	11.88	10.53	11.86
19	11.18	16.98	12.99	11.47	13.00
20	12.15	18.79	14.19	12.49	14.25

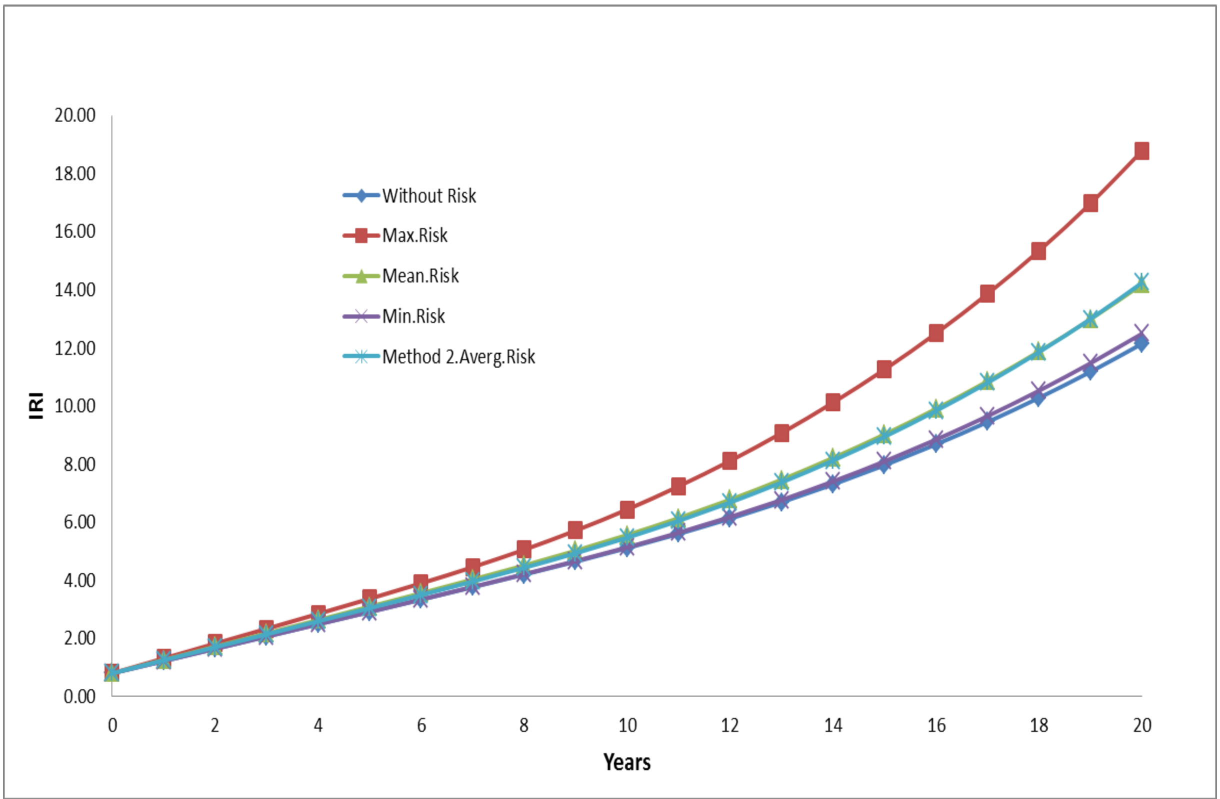

Figure 9-32:Pavement deterioration curve based on IRI under the different risks of climate change (using system dynamics)

Table 9-61: Results generated from Vensim based on deterioration model when variables are dynamic based on PCI

	Without Risk	Maximum Risk	Mean Risk	Minimum Risk	Method 2.Average Risk
	Experiment 1	Experiment 2	Experiment 3	Experiment 4	Experiment 5
Time (Year)	PCI	PCI	PCI	PCI	PCI
0	100	100	100	100	100
1	82.34	79.00	80.97	82.30	81.35
2	67.74	62.36	65.51	67.68	66.12
3	55.72	49.21	52.99	55.65	53.74
4	45.83	38.79	42.84	45.75	43.65
5	37.67	30.51	34.62	37.59	35.43
6	30.94	23.86	27.92	30.85	28.72
7	25.37	18.44	22.45	25.27	23.19
8	20.74	13.97	17.95	20.63	18.61
9	16.87	10.30	14.19	16.74	14.77
10	13.61	7.36	11.05	13.45	11.53
11	10.85	5.08	8.44	10.66	8.82
12	8.51	3.39	6.29	8.29	6.58
13	6.55	2.17	4.57	6.32	4.78
14	4.93	1.34	3.23	4.70	3.37
15	3.63	0.79	2.22	3.41	2.30
16	2.61	0.44	1.48	2.41	1.53
17	1.82	0.24	0.95	1.66	0.97
18	1.24	0.12	0.59	1.11	0.60
19	0.82	0.06	0.35	0.71	0.35
20	0.52	0.02	0.20	0.45	0.20

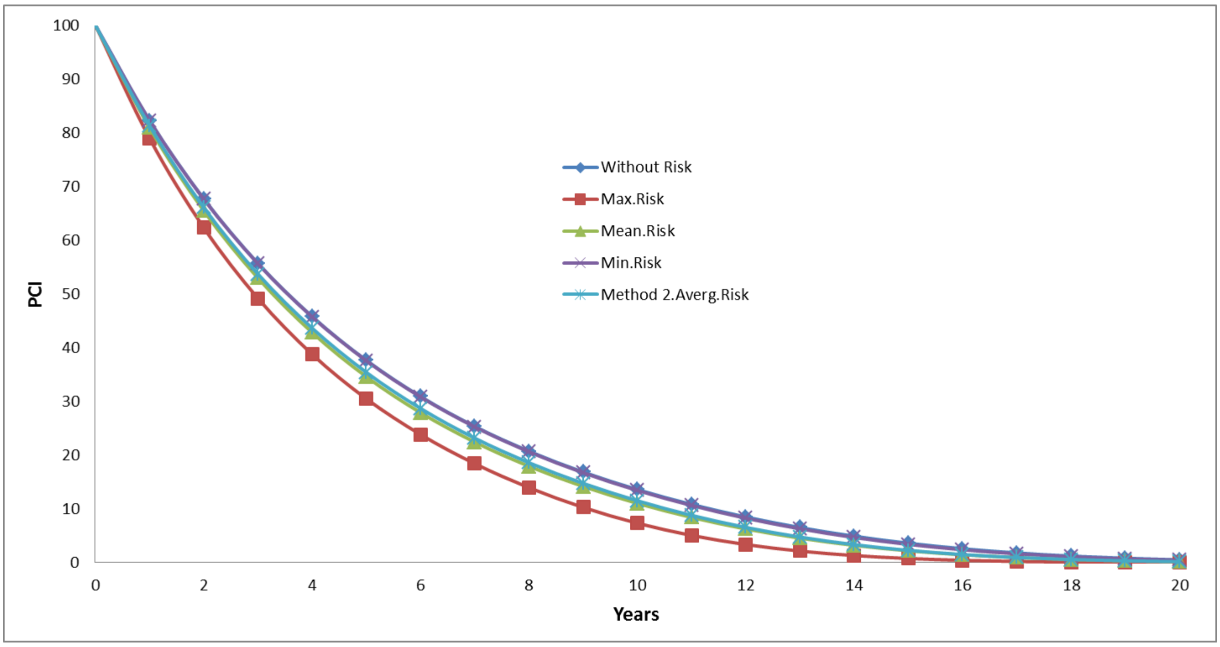

Figure 9-33: Pavement deterioration curve based on IRI under the different risks of climate change (using system dynamics

Figures 9-32 and 9-33 represent the deterioration curves regarding PCI and IRI for the next predicted 20 years for the pavement network of the UAE Ministry of Public Works based on a system dynamics method with different risk scenarios. Overall, the pavement deterioration curve (IRI and PCI) with maximum risk factors received the highest rate of degradation in comparison with other risk scenarios. Moreover, minimum risk scenarios presented a slight change in the rate of deterioration in contrast with the original rate of change (no risk associated).

9.6. Summary

This chapter has demonstrated the results of the system dynamics model. The system dynamics model was built to predict the worst pavement condition scenarios that might occur over 20 years. The dynamic variables were defined to range from lower impact scenarios to the worst one. The pavement deterioration curve (IRI and PCI) with maximum risk factors received the highest rate of degradation in comparison with other risk scenarios.

10. Chapter 10 Measuring Resilience Loss

10.1. Introduction

This chapter’s goal is to measure resilience loss for the pavement network. The pavement deterioration model using Markov chain and system dynamics with parameters developed in chapters 5 and 6 is used to determine the resilience loss. The model in this chapter is formed from two main elements, measuring the main performance by integrating the area under the survival curves and measuring resilience performance loss with respect to 100% performance functionality of the pavement network. The chapter explains the process of developing resilience loss using a Markov chain model with different climate change scenarios, years 2013, 2020, 2040 and 2060. Also, a system dynamics model with different risks associated with climate change is designed. Comparison of the results between the two models is finally reported.

10.2. Measuring Resilience Loss

How to measure resilience is a challenging question (Schoon 2005). Sun, Bocchini and Davison (2018) stated that a resilient transportation infrastructure system indicates that such a system allows for a minor probability of failure, short recovery time and minor impact propagations. Bruneau et al. (2003) were the first to measure resilience quantitatively based on the concept of the resilience triangle and the functionality recovery curve (Sun, Bocchini and Davison 2018). The resilience triangle concept measures a substantial and sudden drop of functionality due to an extreme event at a specific time as well as the gradual recovery of system functionality until it reaches its original function. Sun, Bocchini and Davison (2018) added that resilience triangle measures may comprehensively represent the system’s functionality loss and functionality recovery in terms of speed and duration. They also stated that measuring resilience using a resilience triangle approach may extensively represent the functionality loss. This author agrees with Sun, Bocchini and Davison (2018) and a similar approach is conducted in this study. However, the element of functionality recovery is not considered. Only system functionality loss is determined.

As discussed in Chapter 2 (literature review), current evaluation of resilience transportation infrastructure using qualitative methods can be achieved in a descriptive way where quantitative methods can measure system resilience at infrastructure network level and component level (Sun, Bocchini and Davison 2018). In this study, quantifying the system resilience in terms of functionality at pavement network level is the main objective. Measuring resilience loss is chosen based on future prediction of pavement performance under different climate change impact scenarios (2013, 2020, 2040 and 2060). From the obtained deterioration curves (see chapters 7 and 9), resilience loss will be measured as shown in Figure 10-1. The area under the curve presents the remaining pavement performance. A higher value (area under the curve) indicates that the asset has a high resilience value and a lower value will present low resilience (classified as less than desirable or poor performance). In other words, achieving less resilience loss will indicate that the quality of performance for the pavement network will function sufficiently depending on the age of such assets and the conduction of timely maintenance activities (type, frequency, etc.). However, more resilience loss can occur due to fast deterioration in the pavement network. Nevertheless, Sun, Bocchini and Davison (2018) argued that defining the actual performance is challenging. They listed the challenges based on many uncertain factors, as per the following Table 10-1.

Table 10-1: The challenges in defining actual performance based on many uncertain factors by Sun, Bocchini and Davison (2018)

Factors	Source
Inherent randomness of material properties	*Padgett and DesRoches (2007)*
Structural capacity and demand	*Jia, Tabandeh and Gardoni (2017)*
Unpredictable potential failures of infrastructure systems	*Woods and Wreathall (2003)*
Dynamic characteristics of the surrounding environment	*Archibald (2013)*
And unforeseen human-related factors	*Sheridan (2008)*

Therefore, analysis conducted on resilience loss shows how much performance drops due to the impact of climate change and rate of deterioration but does not indicate if the remaining performance (area under the curve) is resilient enough to continue providing the needed service. The measure of resilience loss is shown in how much drop in functionality occurs over time, assuming the initial pavement network performance is 100%.

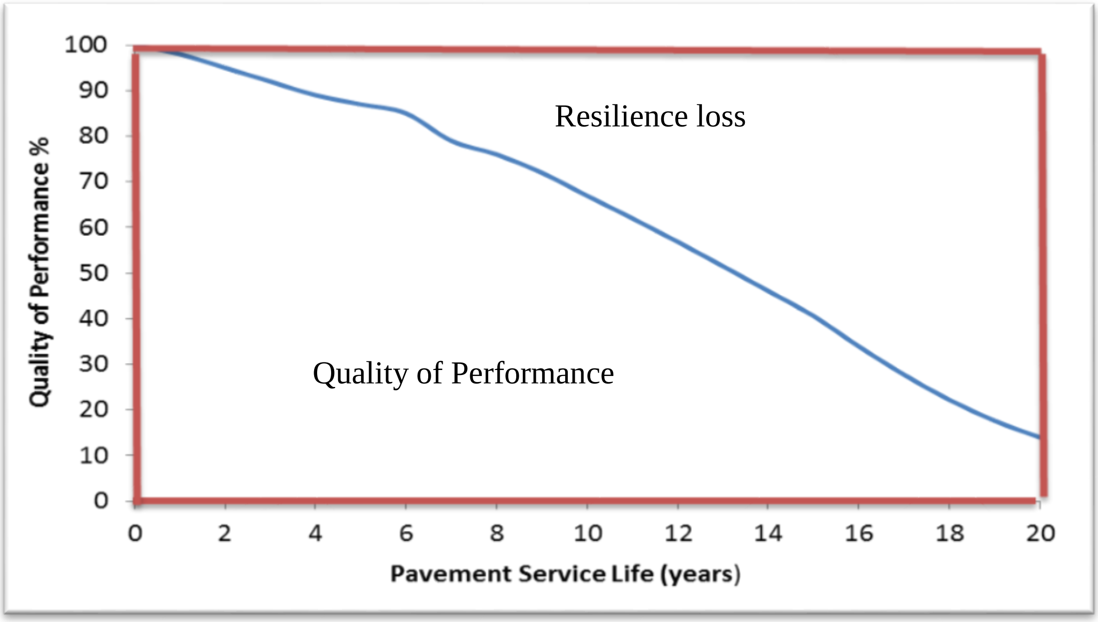

Figure 10-1: Performance without maintenance intervention (recovery)

The resilience triangle theory is applied in this research to measure pavement infrastructure resilience loss through the concept of pavement performance (pavement network functionality). The specific metrics of resilience loss have been developed through the application of a pavement performance prediction model that determines the deterioration curve (survival curve). Such models are built using two different methods, which are Markov and system dynamics (more details were provided in chapters 7, 8 and 9). The data used to measure the pavement network resilience represent the roads and highways under management of the UAE Ministry of Public Works (more details were presented in Chapter 5). Bruneau et al.'s (2003) modified equation is introduced to measure the resilience loss, which indicates that the larger values of resilience loss mean less resilient systems.

$$RL_{Markov.PCI} = Q(t)_{full} - \int_{t0}^{t1} Q(t)dt$$

Equation 10-1:Resilience loss based on Markov chain models

$$RL_{SD.PCI} = Q(t)_{full} - \int_{t0}^{t1} Q(t)dt$$

Equation 10-2: Resilience loss based on system dynamics models

Where,

- t0: The time at which the measure of the performance of the pavement network measure starts.
- t1: The time at which the measure of the performance of the pavement network measure ends.
- Q(t)full: System functionality, which is assumed to be 100% before the degradation in the system.
- $RL_{SD.PCI}$: Resilience loss based on survival curve generated from system dynamics.
- $RL_{Markov.PCI}$: Resilience loss based on survival curve generated from Markov chain.
- $\int_{t0}^{t1} Q(t)dt$: Remaining pavement performance under the survival curve.

In order to measure the performance under the survival curve, a software package named CurveExpert Professional is used. The deterioration curve based on the Pavement Condition Index (PCI) obtained from the Markov chain method (see Chapter 7) and system dynamics method (Chapter 9) is fed into the software. The software integrates the area under the deterioration curve based on four scenarios which indicate the periods of five, 10, 15 and 20 years. The following figure reflects the four different scenarios.

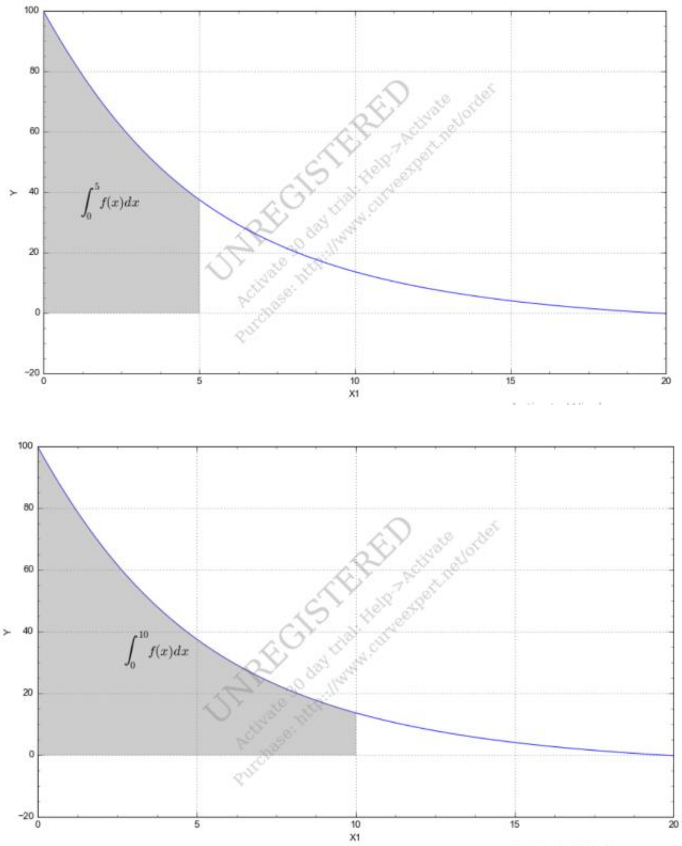

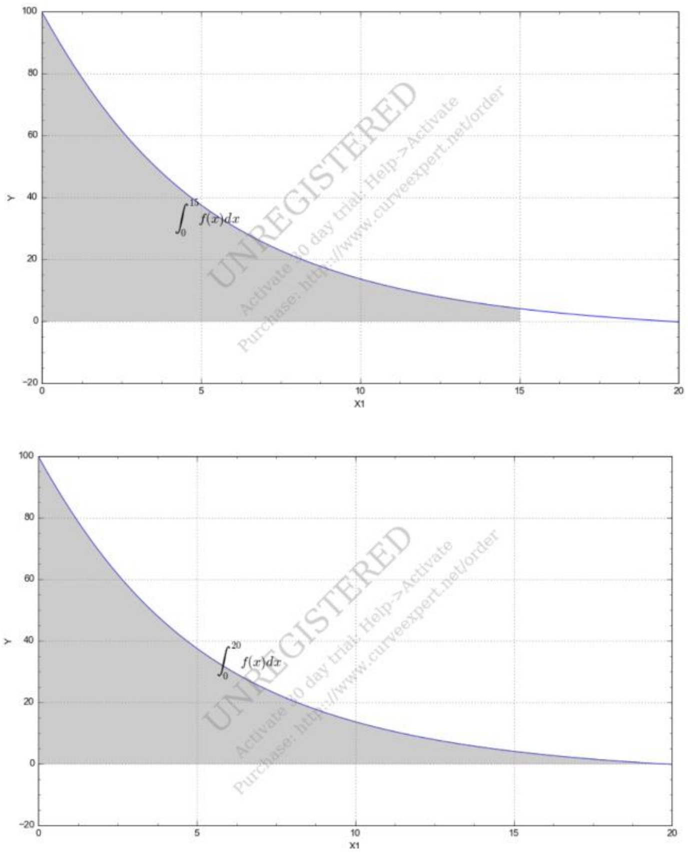

Figure 10-2: Integrating the deterioration curve based on four scenarios which indicate a period of 5 , 10, 15 and 20 years using CurveExpert Professional software

10.3. Measuring Resilience Loss based on a Probabilistic Approach

The Markov chain model was determined in Chapter 7. Results which presented pavement deterioration curves based on the IRI value for different climate change impacts (2013, 2020, 2040 and 2060) were achieved. The deterioration curves for the pavement road network of the UAE Ministry of Public Works with different climate change scenarios were predicted for the 20 years. For the deteriorated pavement curve, the condition curves show a ‘logarithmic’ curve shape as a result of the Markov chain modelling. The PCI which defined one of the performance indicators was determined using the relationship to its roughness, as highlighted in Chapter 6 section 6.5. The results are shown in Table10-2.

Table 10-2: PCI results of Markov chain model using different climate change scenarios

	2013	2020	2040	2060
	PCI	PCI	PCI	PCI

0	95.54	95.54	95.54	95.54
1	92.99	92.41	92.22	92.03
2	90.54	89.46	89.11	88.72
3	88.12	86.59	86.09	85.50
4	85.55	83.54	82.89	82.04
5	82.83	80.33	79.52	78.41
6	80.03	77.09	76.14	74.81
7	77.24	73.95	72.91	71.42
8	74.56	71.02	69.92	68.34
9	72.03	68.35	67.23	65.63
10	69.69	65.96	64.85	63.28
11	67.56	63.86	62.78	61.27
12	65.63	62.02	60.99	59.57
13	63.90	60.42	59.45	58.14
14	62.35	59.04	58.14	56.94
15	60.98	57.86	57.03	55.94
16	59.77	56.85	56.09	55.11
17	58.70	55.98	55.29	54.42
18	57.76	55.25	54.62	53.85
19	56.93	54.62	54.05	53.37
20	56.21	54.08	53.58	52.98

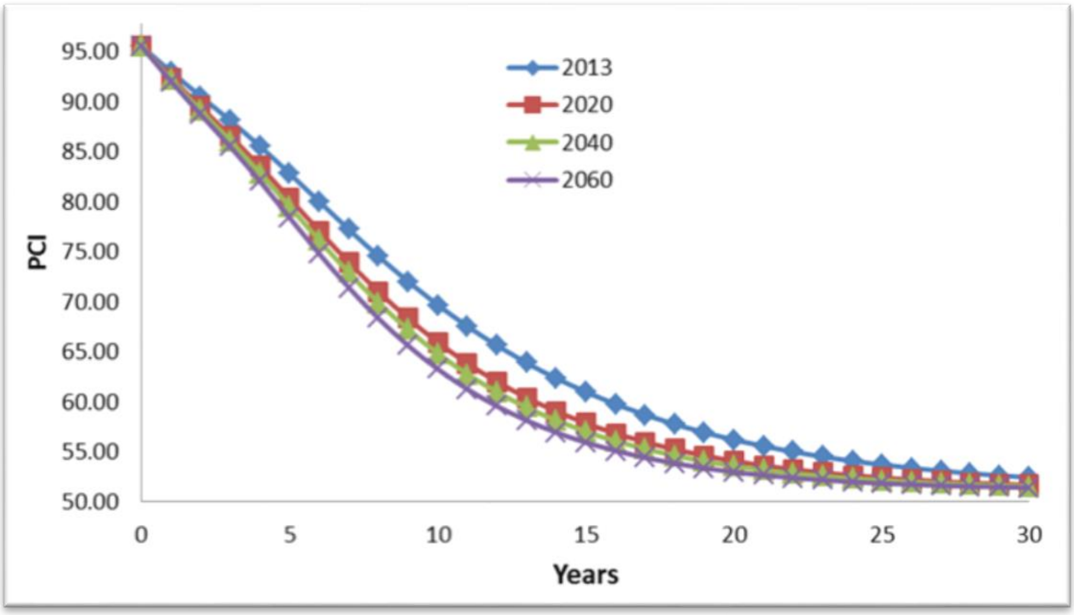

Figure 10-3: Deterioration curve for different climate change scenarios based on Markov chain model

A software package named CurveExpert Professional was used. The deterioration curve based on the PCI obtained from the Markov chain method for different climate change scenarios is based on the following equations:

$$RL_{Markov.PCI.2013} = Q(t)_{full} - \int_{t0}^{t1} Q(t)_{2013} dt$$

Equation 10-3:Resilience loss based on pavement Condition Index with 2013 climate change scenario using Markov chain model

$$RL_{Markov.PCI.2020} = Q(t)_{full} - \int_{t0}^{t1} Q(t)_{2020} dt$$

Equation 10-4:Resilience loss based on pavement Condition Index with 2020 climate change scenario using Markov chain model

$$RL_{Markov.PCI.2040} = Q(t)_{full} - \int_{t0}^{t1} Q(t)_{2040} dt$$

Equation 10-5:Resilience loss based on pavement Condition Index with 2040 climate change scenario using Markov chain model

$$RL_{Markov.PCI.2060} = Q(t)_{full} - \int_{t0}^{t1} Q(t)_{2060} dt$$

Equation 10-6:Resilience loss based on pavement Condition Index with 2060 climate change scenario using Markov chain model

The software integrates the area under deterioration curves based on four scenarios, which indicate a period of five, 10, 15 and 20 years and the remaining pavement performance under the survival curve for different climate change scenarios using the Markov chain method, as per Table 10-3.

Table 10-3: Remaining pavement performance under the survival curve for different climate change scenarios using the Markov chain method

Markov Chain approach (Probabilistic)				
scenarios	case 1 (Year)	case 2 (Year)	case 3 (Year)	case 4 (Year)
	Range 0- 5	0-10	0-15	0-20
2013	446.40	826.47	1151.17	1442.87
2020	439.06	803.43	1110.93	1388.67
2040	436.80	796.18	1098.69	1373.05
2060	433.86	786.32	1081.95	1352.04

It was assumed that the pavement network performance is 100%, which indicates that the PCI value is 100 (based on PCI scale). The total area of performance is a result of multiplying PCI value with pavement service life (in years). Therefore, 'Q(t)full', which is system functionality before the degradation in the pavement network system, is equal to 2000 m^2. Resilience loss for different climate change scenarios and different periods using Markov chain method is presented in Table 10-4.

Table 10-4: Resilience loss for different climate change scenarios and different periods using Markov chain method

Resilience loss based on Markov Chain approach (Probabilistic)				
scenarios	case 1 (Year)	case 2 (Year)	case 3 (Year)	case 4 (Year)
	0-5	0-10	0-15	0-20
2013	53.60	173.53	348.83	557.13
2020	60.94	196.57	389.07	611.33
2040	63.20	203.82	401.31	626.95
2060	66.14	213.68	418.05	647.96

For simplification, the resilience loss is determined in percentage value with respect to 100% pavement network performance. Results are presented in Table 10-5. Plotting a histogram presents a comparison of resilience loss among different climate change scenarios with different pavement service life years, as per Figure 10-4.

Table 10-5: Percentage of resilience loss base on different deterioration curves using Markov chain approach

Percentage of Resilience Loss base on different deterioration curve using Markov Chain approach (Probabilistic)				
scenarios	case 1 (Year)	case 2 (Year)	case 3 (Year)	case 4 (Year)
	0-5	0-10	0-15	0-20
2013	10.72%	17.35%	23.26%	27.86%
2020	12.19%	19.66%	25.94%	30.57%
2040	12.64%	20.38%	26.75%	31.35%
2060	13.23%	21.37%	27.87%	32.40%

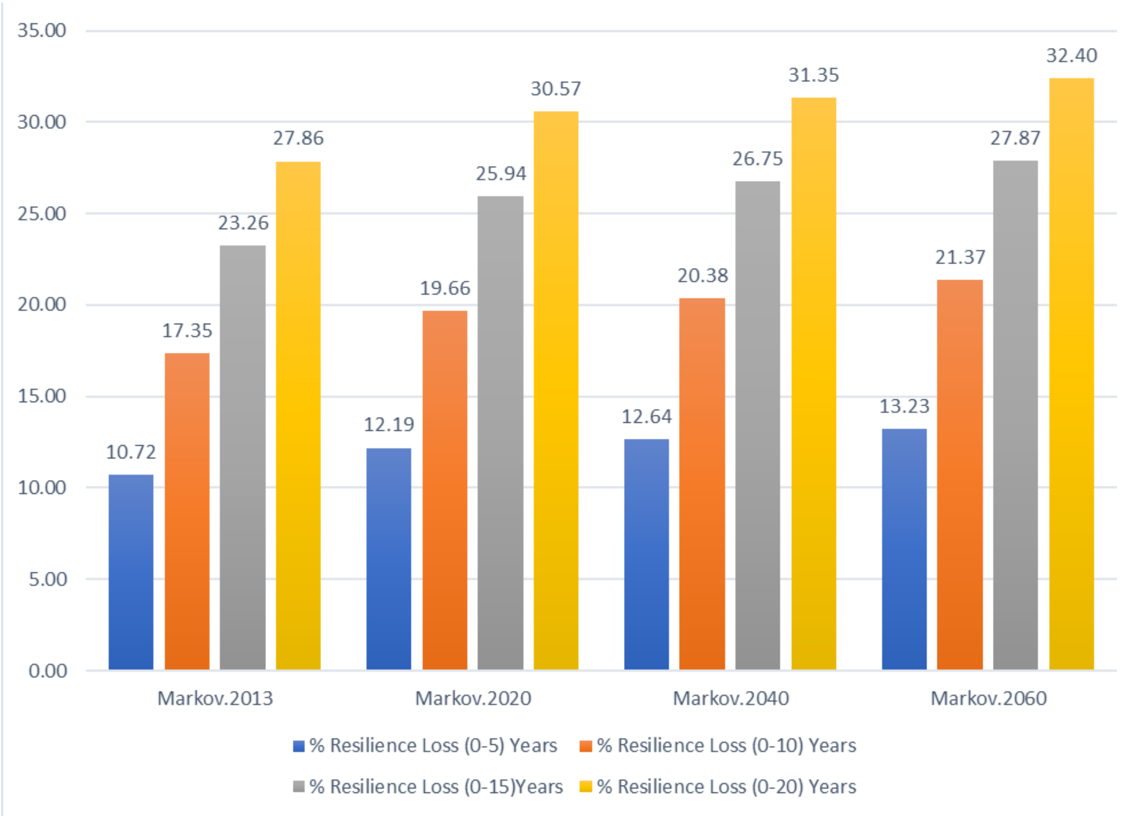

Figure 10-4: Percentage of resilience loss based on Markov chain

The graph represents the evaluation of functionality for the pavement network in terms of resilience loss. Several tests were conducted to evaluate the pavement network under different climate change scenarios. Figure 10-4 captures predictions for resilience loss at different milestones such as five years, 10 years, 15 years and 20 years. According to the five years prediction, the resilience loss scored a range from 10.7% to 13.23% for different climate change scenarios (2013, 2020, 2040 and 2060), whereas the 20 years prediction showed a range between 27.86% to 32.4% resilience loss from the similar scenarios. According to Harvey et al. (2004), a flexible pavement structure is designed to last 20-40 years, providing an adequate service that meets the comfort and safety of drivers. The author decided to measure the resilience loss at a projection of 20 years. In the analysis of Figure 10-4, the resilience loss increases with increase of projection year, which indicates that more degradation to the pavement network has occurred and it has triggered the need for maintenance intervention. On the other hand, the deterioration curve based on the 2060 climate change scenario showed the highest drop in performance which leads to 32.40% resilience loss in comparison with other scenarios.

10.4. Measuring Resilience Loss Based on a System Dynamics Approach

Determination of the deterioration curve using a system dynamics method was achieved in Chapter 9. The pavement deterioration model based on the change in IRI using dynamic components for the impact of climate change including all pavement temperature scenarios (2013, 2020, 2040 and 2060) was established and the results were reported accordingly. The model was run for 20 years to project the deterioration curve on pavement condition based on two performance indicators, PCI and IRI. The system dynamics model for pavement deterioration was introduced with different risk scenarios, as discussed in Chapter 9. Pavement condition index (PCI), which is defined as one of the performance indicators, was determined using the relationship to its roughness, as highlighted in Chapter 6. The results are shown in Table 10-6 and Figure 10-5.

Table 10-6: Results generated from Vensim based on deterioration model when variables are dynamic based on PCI

	Without Risk	**Maximum Risk**	**Mean Risk**	**Minimum Risk**	**Method 2.Average Risk**
	Experiment 1	Experiment 2	Experiment 3	Experiment 4	Experiment 5
Time (Year)	PCI	PCI	PCI	PCI	PCI
0	100	100	100	100	100
1	82.34	79	80.97	82.3	81.35
2	67.74	62.36	65.51	67.68	66.12
3	55.72	49.21	52.99	55.65	53.74
4	45.83	38.79	42.84	45.75	43.65
5	37.67	30.51	34.62	37.59	35.43
6	30.94	23.86	27.92	30.85	28.72
7	25.37	18.44	22.45	25.27	23.19
8	20.74	13.97	17.95	20.63	18.61
9	16.87	10.3	14.19	16.74	14.77
10	13.61	7.36	11.05	13.45	11.53
11	10.85	5.08	8.44	10.66	8.82
12	8.51	3.39	6.29	8.29	6.58
13	6.55	2.17	4.57	6.32	4.78
14	4.93	1.34	3.23	4.7	3.37
15	3.63	0.79	2.22	3.41	2.3
16	2.61	0.44	1.48	2.41	1.53

17	1.82	0.24	0.95	1.66	0.97
18	1.24	0.12	0.59	1.11	0.6
19	0.82	0.06	0.35	0.71	0.35
20	0.52	0.02	0.2	0.45	0.2

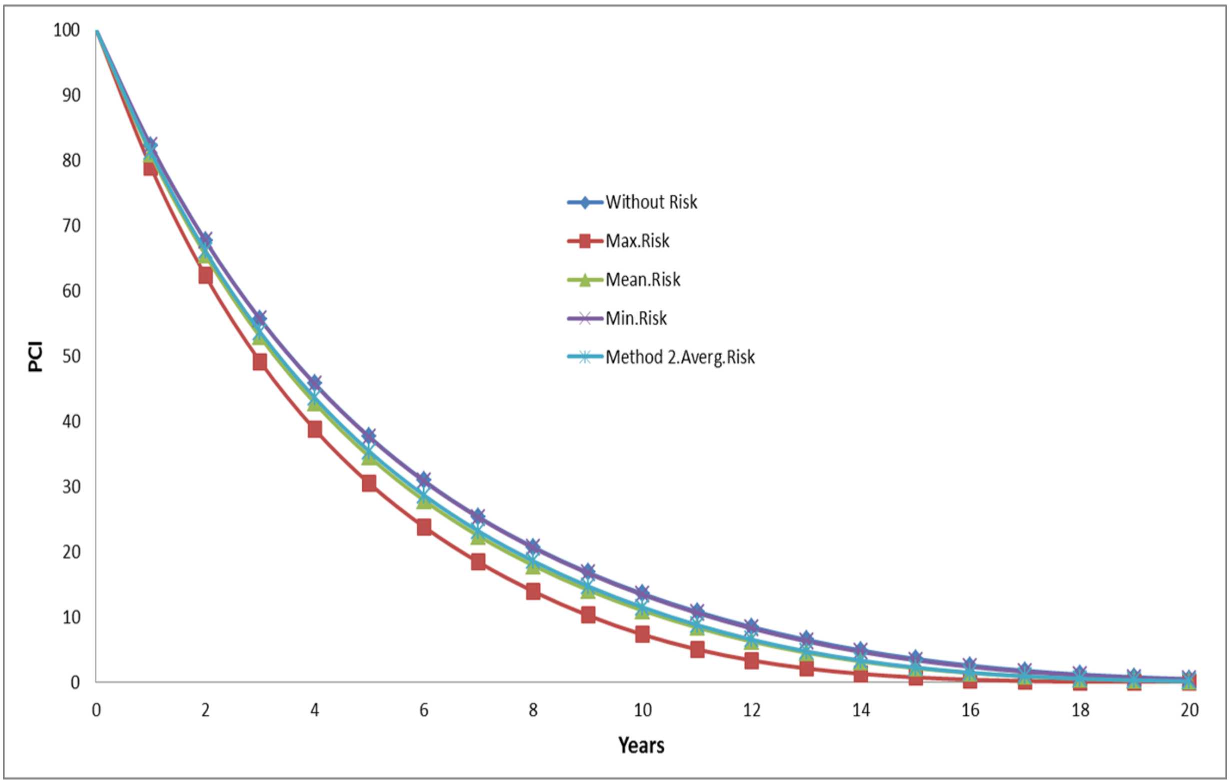

Figure 10-5: Pavement deterioration curves based on IRI under the different risks of climate change (using system dynamics)

Estimation similar to that used for pavement network resilience loss using a Markov chain method was repeated using the deterioration curve generated on the system dynamics model with different risk scenarios. For data analysis, a software package named CurveExpert Professional was used. The deterioration curve based on that the PCI obtained from the system dynamics model for different risks scenarios was fed into the following equations:

$$RL_{SD.no\ Risk} = Q(t)_{full} - \int_{t0}^{t1} Q(t)_{no\ Risk} dt$$

Equation 10-7: Resilience loss based on PCI with no risks scenario using a system dynamics model

$$RL_{SD.Max.R} = Q(t)_{full} - \int_{t0}^{t1} Q(t)_{Max.R} dt$$

Equation 10-8: Resilience loss based on PCI with maximum risks scenario using a system dynamics model

$$RL_{SD.Mean.R} = Q(t)_{full} - \int_{t0}^{t1} Q(t)_{Mean.R} dt$$

Equation 10-9: Resilience loss based on PCI with mean risks scenario using a system dynamics model

$$RL_{SD.Min.R} = Q(t)_{full} - \int_{t0}^{t1} Q(t)_{Min.R} dt$$

Equation 10-10: Resilience loss based on PCI with minimum risks scenario using a system dynamics model

$$RL_{SD.M2.Avg.R} = Q(t)_{full} - \int_{t0}^{t1} Q(t)_{M2.Av.R} dt$$

Equation 10-11: Resilience loss based on PCI with average risks scenario of method 2 using a system dynamics model

The software integrated the area under the survival curves based on four scenarios, which indicate a period of five, 10, 15 and 20 years, and the remaining pavement performance under the survival curve for risk scenarios using the system dynamics model are determined as per Table 10-7.

Table 10-7: Remaining pavement performance under the survival curve for different risks scenarios using system dynamics model

System Dynamics approach				
Scenarios	case 1 (Year)	case 2 (Year)	case 3 (Year)	case 4 (Year)
	0-5	0-10	0-15	0-20
No Risk	319.67	437.97	478.60	486.57
Max.Risk	294.79	377.39	395.32	397.98
Mean.Risk	308.88	412.66	444.21	447.64
Min.Risk	319.54	437.19	477.07	484.37
Averg.M.Risk	311.94	418.99	451.93	455.51

As stated earlier, in the Markov section, 100% performance value over a total period of 20 years (service life) was assumed. The total area of performance was a result of multiplying PCI value with pavement service life (in years). Therefore, ‘Q(t)full’, which is system functionality before the degradation in the pavement network system, was equal to 2000 m^2. . Resilience loss for different climate change scenarios and different periods using system dynamics method is presented in Table 10-8.

Table 10-8: Resilience loss for different risks associated with climate change scenarios and different periods using System Dynamics

Resilience loss based on System Dynamics approach				
Scenarios	case 1 (Year)	case 2 (Year)	case 3 (Year)	case 4 (Year)
	0-5	0-10	0-15	0-20
No Risk	180.33	562.03	1021.40	1513.43
Max.Risk	205.21	622.61	1104.68	1602.02
Mean.Risk	191.12	587.34	1055.79	1552.36
Min.Risk	180.46	562.81	1022.93	1515.63
Averg.M.Risk	188.06	581.01	1048.07	1544.49

Simplification was also conducted for the resilience loss values generated based on the system dynamics model. Percentage value of resilience loss with respect to 100% pavement network performance was achieved. Results are presented in Table 10-9. Plotting the histogram presented a comparison of resilience loss among different risks associated with climate change with different pavement service life years, as per Figure 10-6.

Table 10-9: Percentage of resilience loss base on different deterioration curves using system dynamics Model

Percentage of Resilience Loss base on different deterioration curve using System Dynamics approach				
Scenarios	case 1 (Year)	case 2 (Year)	case 3 (Year)	case 4 (Year)
	0-5	0-10	0-15	0-20
No Risk	36.07%	56.20%	68.09%	75.67%
Max.Risk	41.04%	62.26%	73.65%	80.10%
Mean.Risk	38.22%	58.73%	70.39%	77.62%
Min.Risk	36.09%	56.28%	68.20%	75.78%
Averg.M.Risk	37.61%	58.10%	69.87%	77.22%

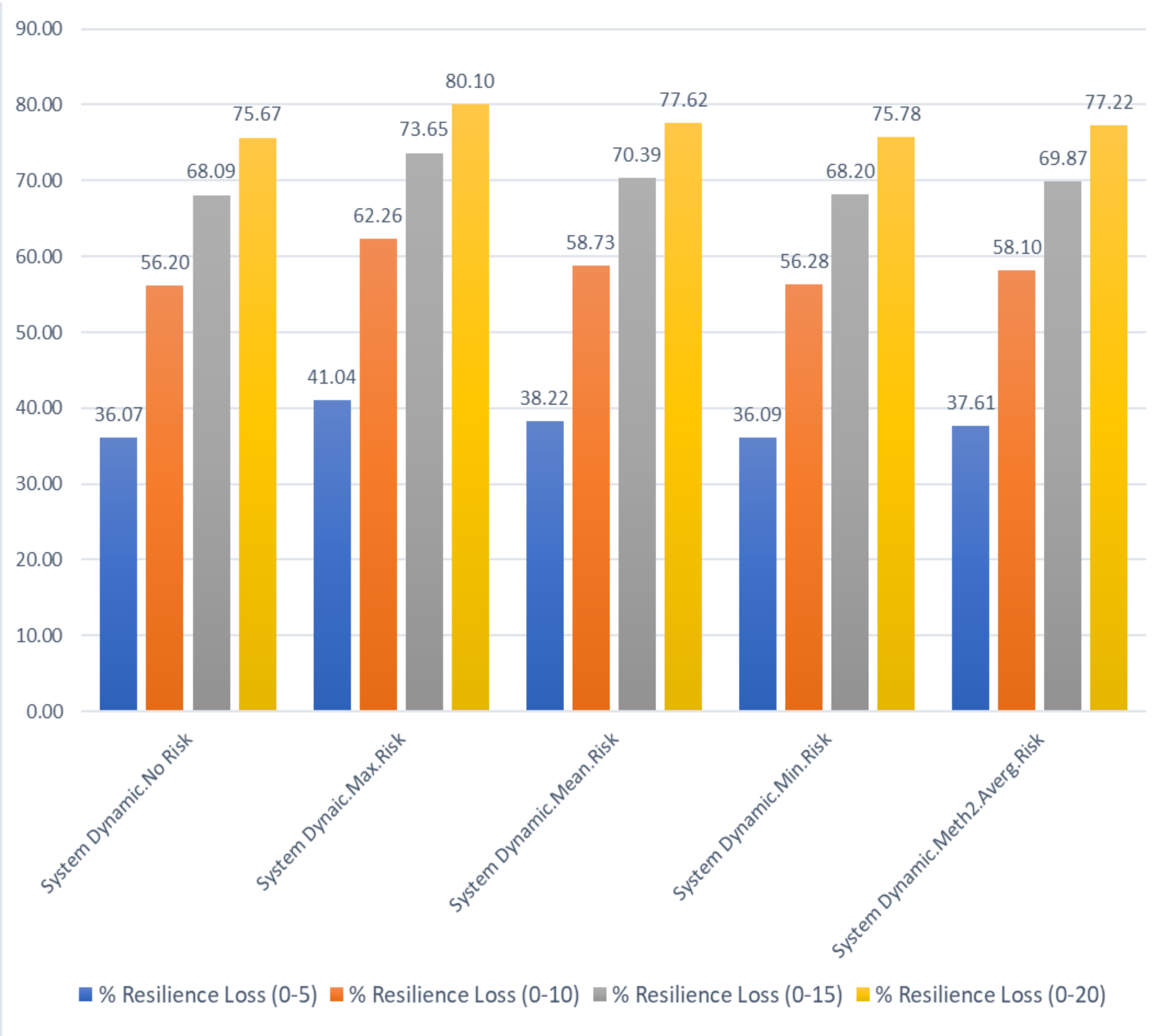

Figure 10-6: Percentage of resilience loss based on system dynamics

The graph represents the evaluation of functionality for the pavement network in terms of resilience loss using a system dynamics model. Several tests were conducted to evaluate the performance of the pavement network under different risks associated with the impact of climate change (see chapters 8 and 9). Figure 10-6 captures predictions for resilience loss at different milestones such as five years, 10 years, 15 years and 20 years. According to the five years prediction, the resilience loss scored a range from 36.9% to 41.04% for different risk scenarios, whereas the 20 years prediction showed a range between 75.67% and 81.0% resilience loss for the same scenarios. The author decided to measure the resilience loss at a projection of 20 years. In the analysis in Figure 10-6, the resilience loss increases with increase of projection year, which indicates that more degradation to the pavement network was occurring and it has triggered the need for maintenance intervention. On the other hand, the deterioration curve based on scenarios of maximum risks associated with climate change showed the highest drop in performance, which led to 80.10% resilience loss in comparison with other risk scenarios.

10.5. Model Checking and Validation

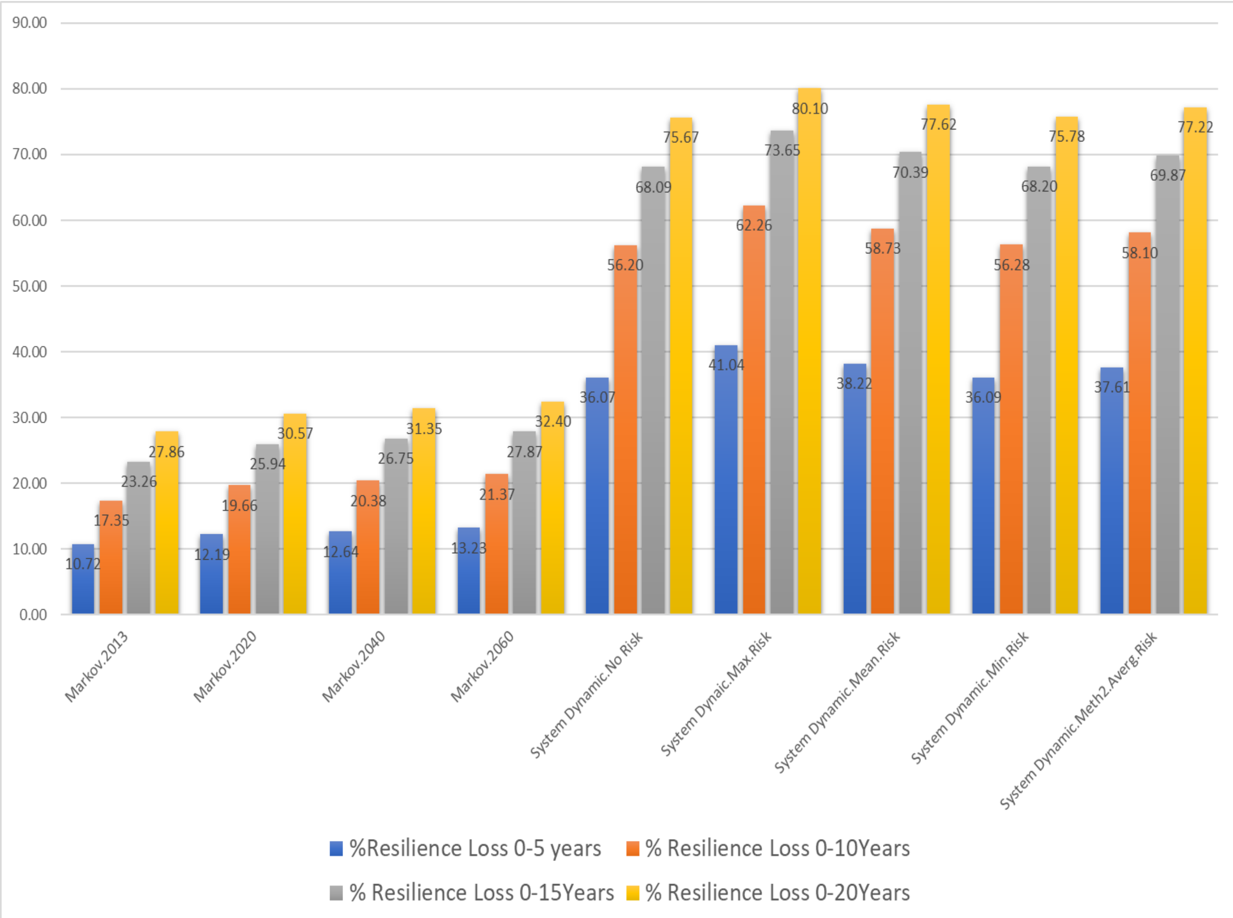

Figure 10-7: The comparison of the results for resilience loss based on system dynamics and Markov chain

The comparison of the results for resilience loss indicated that the system dynamics model achieved the highest drop in pavement network functionality level over the 20 years prediction, showing a range between 75.67% and 81.0% resilience loss with different risk scenarios, whereas the Markov chain model showed a range between 27.86% and 32.4% resilience loss for the same period. Basically, the system dynamics model was built to predict the worst pavement condition scenarios that might occur over 20 years. The dynamic variables such as the pavement thickness, pavement temperature, pavement ageing, traffic loading, the speed of heavy vehicles and change in rutting were defined to range from lower impact scenarios to the worst one. In practice, the pavement section of a typical road is going to fail before reaching the system dynamics model's ultimate values (IRI =11 m/km). The model was built on causal loop diagrams (CLDs) that presented feedback loops which were positive (self-reinforcing). The dynamic variables in the system which link to other variables receive an effect of expansion or increase, which would proportionally lead to an increase in others, which would eventually lead to exponential growth (reinforcing loops). Also, the model was designed on the assumption that the yearly rate of change is a 100% full shift in state of change. Partial yearly changing rates with either 80%, 60%, 40% or 20% were ignored. For example, if a 20% yearly rate of change was used in the model, then a total change of 2 m/km IRI over 20 years would be achieved. Achieving a 40% state of shift for the change in IRI achieved nearly 4 m/km after the 20-year cycle which, in the opinion of the author, seems the most logical approach with which to build the model. A similar approach was followed for the Markov chain model. For instance, the IRI condition states classification selected for the Markov chain (see Chapter 7) was as follows:

Table 10-10: IRI condition states classification used for the Markov chain model

Condition	Range	Average factor
Very good	0-1.25 m/km	0.9 m/km
Good	1.25-1.5 m/km	1.35 m/km
Satisfactory	1.5-1.75 m/km	1.6 m/km
Fair	1.75-2.0 m/km	1.8 m/km
Poor	2.0 above m/km	2.25 m/km

Using those intervals allowed the Markov chain model to capture a pavement deterioration curve with IRI = 2.0459 m/km over the period of 20 years (2013 scenario – see Chapter 7), which is equivalent to PCI 56.21. However, the purpose of the system dynamics model is based on reinforcing loops in order to investigate the ultimate worse-case scenarios. Thus, the drop in pavement network functionality showed a significant drop and scope of 80% resilience loss over 20 years. Generally, an ultimate worse-case scenarios model may help highway designers, who always depend on the most critical historical data, to determine the most acceptable design parameters to incorporate the impact of climate change and consequently measure the resilience loss. And, as discussed in Chapter 3, climate change impact is not considered in any current pavement design practice due to uncertainty about the consequences of such implications, and is not part of the historical data. Therefore, with the projection of the worst scenario, it was decided to introduce the pavement deterioration curve in both chapters 8 and 9 based on the worst situation with 100% state shift (rate of change). For this reason, the resilience loss in the system dynamics model was more complex in comparison with that in the Markov chain model.

10.5.1. Measure Resilience Loss using Markov Chain Model under Worse-Case Scenario

The first step in Markov chain modelling is to evaluate the condition of the asset's elements (Sharabah, Setunge and Zeephongsekul 2006). In practice, pavement condition data can be collected using automated or manual methods. Mandiartha et al. (2017) stated that distributing road conditions into different condition ratings is proven to be a sufficient method to assist highway agencies in deciding a suitable choice of maintenance intervention. For example, the authors applied IRI value condition to build a Markov chain model that can assess the effectiveness of road network pavement maintenance. In this study, for a condition rating system, the feedback from experts was taken into consideration as they stated that UAE roads are considered to be new and most of the IRI value is 1.5 km/m and any value beyond 2.0 m/km is not accepted by the UAE highway agency's standards and regulations. However, to match system dynamics modelling, it is proposed to modify the condition rating system to consider values beyond 2.0 km/m. The new proposed condition rating is shown in Table 10-10.

Table 10-11: New condition rating system for IRI value used validation the comparison between system dynamics and Markov chain

Condition Rating System	Range	New range	Average factor
Very good	0-1.25 m/km	0-1.25 m/km	0.9 m/km
Good	1.25-1.5 m/km	2-4 m/km	3 m/km
Satisfaction	1.5-1.75 m/km	4-6 m/km	5 m/km
Fair	1.75-2.0 m/km	6-8 m/km	7 m/km
Poor	2.0 above m/km	8-12 m/km	10 m/km

Running the Markov chain model with the new condition rating system was achieved using Microsoft Office Excel software. The forecasted period was set for 20 cycles. Each cycle represents a single year. Only the results of determining IRI for the 2013 scenario were considered. The initial state was 1 0 0 0 0 as the assumption was made that the pavement conditions of the study area are in a very good condition state. The results were as per the following Table 10-12 and Figure 10-8 .

Table 10-12: PCI results of Markov chain model using 2013 scenario with new condition rating system

Year	2013
	PCI
0	95.54
1	84.20
2	73.55
3	63.25
4	52.86
5	42.94
6	34.14
7	26.83
8	21.01
9	16.52
10	13.09
11	10.50
12	8.55
13	7.06
14	5.93
15	5.06
16	4.38
17	3.84
18	3.42
19	3.08
20	2.81

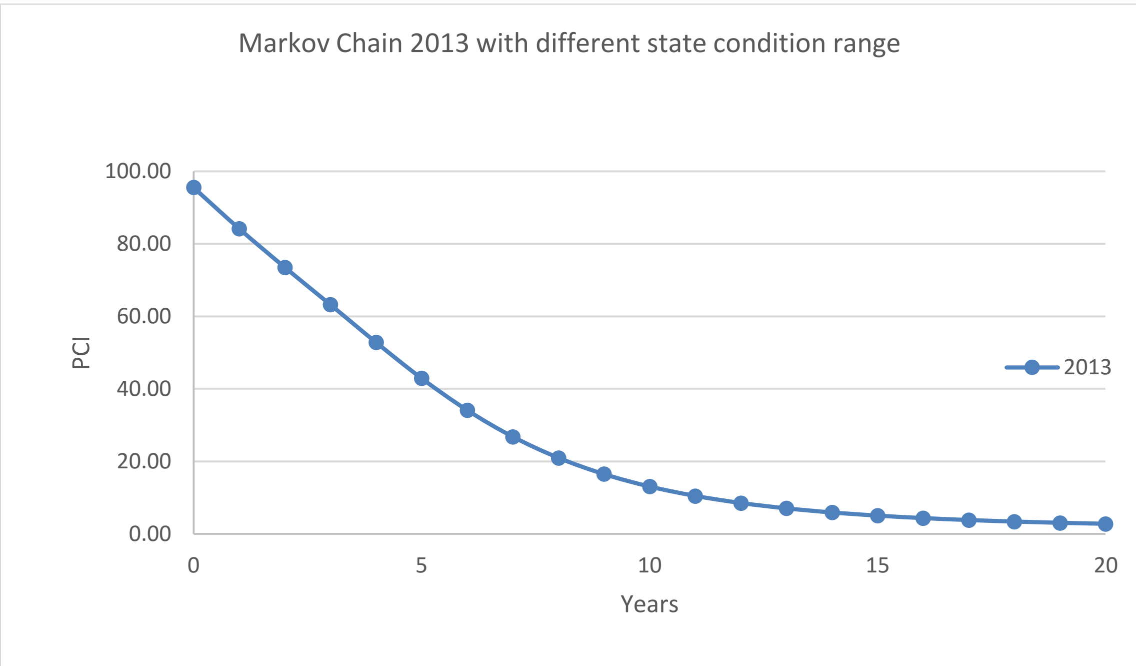

Figure 10-8: Deterioration curve-based Markov chain model 2013 with new state condition range

A software package named CurveExpert Professional was used. The deterioration curve based on that the PCI obtained from the Markov chain method for the 2013 climate change scenario was determined using the following equation:

$$RL_{Markov.PCI.2013.Modefied} = Q(t)_{full} - \int_{t0}^{t1} Q(t)_{2013.modefied}dt$$

Equation 10-12: Resilience loss based on PCI with different risks associated with climate change scenarios using a modified Markov chain model

A similar analysis approach was conducted as per the previous section and the resilience loss of the new modified deterioration curve using a Markov chain model with a new condition rating system was reported. The software integrated the area under the curves based on four scenarios, which indicate a period of five, 10, 15 and 20 years, and the remaining pavement performance under the survival curve for risk scenarios using the system dynamics model were determined as per Tables 10-13, 10-14 and 10-15.

Table 10-13: Remaining pavement performance under the survival curve for different system dynamics model and Markov chain with 2013 scenario (worse case)

		PCI			
Analysis Type		0-5	0-10	0-15	0-20
Modified Markov Chain	**2013**	**343.13**	**470.92**	**513.12**	**528.65**
System Dynamics	No Risk	319.67	437.97	478.60	486.57
	Max.Risk	294.79	377.39	395.32	397.98
	Mean.Risk	308.88	412.66	444.21	447.64
	Min.Risk	319.54	437.19	477.07	484.37
	Averg.M.Risk	311.94	418.99	451.93	455.51

Table 10-14: Resilience loss for different models with new condition rating

		Resilience loss			
Analysis Type		0-5	0-10	0-15	0-20
Modified Markov chain	**2013**	**156.87**	**529.08**	**986.88**	**1471.35**
System Dynamics	No Risk	180.33	562.03	1021.40	1513.43
	Max.Risk	205.21	622.61	1104.68	1602.02
	Mean.Risk	191.12	587.34	1055.79	1552.36
	Min.Risk	180.46	562.81	1022.93	1515.63
	Averg.M.Risk	188.06	581.01	1048.07	1544.49

Table 10-15: Percentage of Resilience Loss base on different deterioration curve

Percentage of Resilience Loss base on different deterioration curve					
Analysis Type		0-5	0-10	0-15	0-20
Modified Markov chain	**Markov.2013**	**31.37%**	**52.91%**	**65.79%**	**73.57%**
System Dynamics	No Risk	36.07%	56.20%	68.09%	75.67%
	Max.Risk	41.04%	62.26%	73.65%	80.10%
	Mean.Risk	38.22%	58.73%	70.39%	77.62%
	Min.Risk	36.09%	56.28%	68.20%	75.78%
	Meth2.Averg.Risk	37.61%	58.10%	69.87%	77.22%

Figure 10-9 presents the comparison of resilience loss between the Markov chain model and the system dynamics model with different risks associated with climate change. The resilience loss scored 73.57% over 20 years for the new modified Markov chain model. This record shows a close value to the range of resilience loss generated from the system dynamics model (range between 75.67% and 81.0% resilience loss).

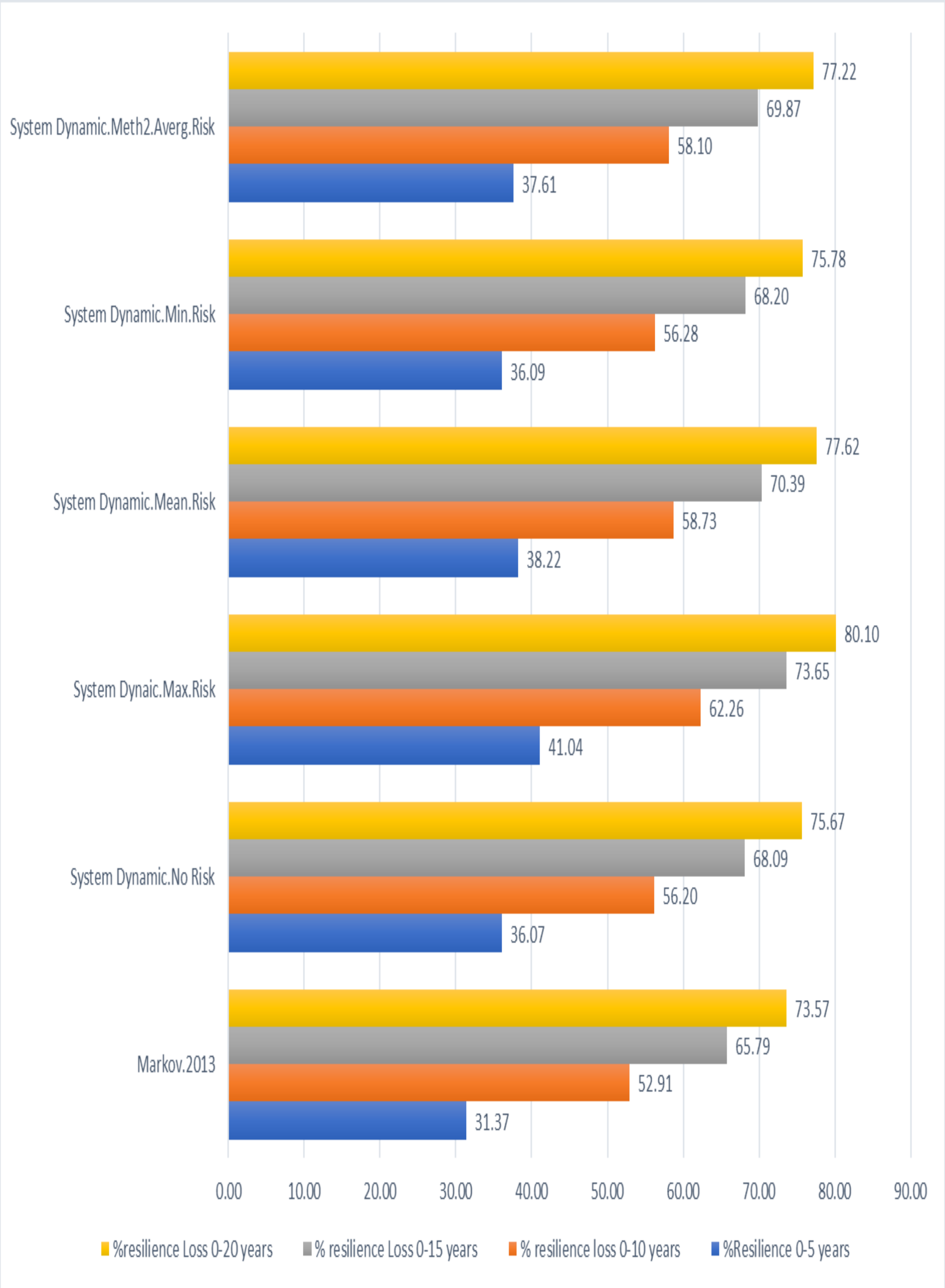

Figure 10-9: Resilience loss comparison between system dynamics model and Markov chain (modified 2013

10.6. Summary

This chapter describes the analysis and results of measuring resilience loss. The findings reveal that the resilience loss increases with increase of projection year, which indicates that more degradation to the pavement network occurred and it has triggered the need for maintenance intervention. The results based on the Markov chain model reported the case of 2060 climate change as the highest drop in performance with 32.40% resilience loss in comparison with other scenarios. The finding for the system dynamics model showed a range between 75.67% and 81.0% resilience loss with different risk scenarios. A comparison between models and validation was also conducted.

11. Chapter 11 Discussion and Conclusion

11.1. Introduction

This chapter presents a discussion of the key research objectives and themes analysed throughout this thesis. The first section presents a discussion on the findings of eight objectives. This is followed by a discussion on the strengths of the research methodology and validation and implications. The last section presents the conclusion of the thesis covering the limitation of the research, summary of contributions and future research and recommendations.

11.2. Main Findings and Summary of Contributions

11.2.1. Objective 1: To Investigate the Impact of Climate Change on Pavements

In Chapter 2, the author pointed out that there are not enough data or adequate guidelines relating to the possible risks associated with the impact of climate change on pavement structure. The first objective in this study sought to expand our understanding of the road infrastructure (existing and future) to better deal with climate change (Cechet, 2005). Limited research has been conducted in the past to study the impact of climate change on pavement performance (Mallick et al. 2014), and increasing disturbance in pavement structure leads to shortening the life of the assets and triggers the need for maintenance. An initial objective of the study was to identify the main climate change risks facing the UAE, which were reported to be heat and water stress, as the area is prone to tremendous rises in both temperatures and increase in water scarcity. For this research, the National Centre of Meteorology and Seismology was the primary source for climate data in the UAE, providing the required information based on Al Ain Airport station including records of evaporation rate, rainfall and air temperature (see Chapter 5 section 5.4). The station is located away from the coast side, which indicates a more arid area. The received data were from years 2003 to 2016. However, the focus was on the highest air temperature record in the UAE, in order to develop the model based on the worst scenarios. The current study found that the maximum air temperature was 50.4 °C, which was recorded in Al Ain in June 2016. The present study was designed to determine the effect of the future predictions of air temperature for the UAE based on climate change. Three different future scenarios (2020, 2040 and 2060-2079) were derived based on the Weather Research and Forecasting (WRF) model and Regional Ocean Model (ROM) (see Chapter 3 section 5.10). In summary, these results showed that the expected maximum air temperatures for the three future different scenarios (2020, 2040 and 2060-2079) were 51.4°C, 52.4°C and 53.4°C respectively. The findings of the current study, which were estimated based on Weather Research and Forecasting (WRF), are consistent with the IPCC (2013) report. This report projected an increase of air temperature in the range from 1.1°C to 6.4°C by the end of the 21st century. Those values were used in developing maximum pavement temperature and Thornthwaite Moisture Index.

11.2.1.1. Thornthwaite Moisture Index (TMI)

Very little was found in the literature on the question of using the Thornthwaite Moisture Index (TMI) in pavement deterioration models. Prior studies such as Sun (2015) and Taylor and Philp (2016) have noted the importance of the Thornthwaite Moisture Index (TMI) in estimating climate variation and its value will differ based on various equations, methods and study periods. The current study used the equations introduced by Mather (1974) and Witczak, Zapata and Houston (2006) to determine the value of Thornthwaite Moisture Index based on the UAE weather data. A comparison was conducted between the two methods with respect to the HDM-4 model. Surprisingly, method 1 was found to be consistent with the default TMI value as per the HDM-4 model. The results obtained from the preliminary analysis of method 1 estimated UAE TMI to be in the range of -96 to -52 based on the current weather data. As mentioned in the literature review, negative TMI values refer to dry soils in arid zones. Regression analysis was used to predict the relationship between the independent variable, which is air temperature, and dependent variable of evaporation rate in order to use the value of evaporation rate for estimating future predicted TMI values. Several experiments were conducted to find the best fit model. Several transformations were considered including log, square roots, etc. The derived model was able to explain 84% of the variation in the existing data. Consequently, the forecasted range of TMI was obtained for the climate scenarios 2020, 2040 and 2060-2079. The most important clinically relevant finding was to set the TMI value of future climate 2020 at -85, TMI 2040 at -90 and TMI -2060 at -96. As mentioned in the literature review, some of the default HDM-4 model selection depends on the application of TMI as the primary climatic factor embodied in the model. This research is in keeping with the findings from Alaswadko (2016), who stated that researchers in Australia and New Zealand developed road deterioration modelling in conjunction with HDM-4 and reported that climate impact (using TMI) made a significant contribution to the model.

11.2.1.2. Pavement Temperature Model

An initial objective of the research was to identify the maximum pavement temperature which would be used as a crucial component in the HDM-4 model. As mentioned in the literature review, hot mix asphalt is classified as a viscoelastic material (viscous and elastic material), which means that pavement material will act as an elastic solid in terms of low temperatures and it will act as a viscous fluid and strain at high temperatures. A strong relationship between air temperature and pavement temperature has been reported in the literature. Out of these studies, the author decided to follow Hassan et al.'s (2004) model, who studied the highest pavement temperature at a depth of 20 mm below the surface. Determination of the maximum pavement temperature based on current UAE weather temperature and future climate change scenarios was achieved (current 69.6°C, 2020 scenario 71.0 °C, 2040 scenario 72.3°C and 2060 scenario 73.6°C). The findings of the current study are consistent with Harun and Morosiuk (1995), who incorporated the element of pavement temperature, which indicates the pavement temperature (in °C) at a depth of 20 mm below the surface, during analysis year in the HDM-4 model, as well as Anyala (2011), who proposed a function of maximum pavement temperature (TPmax) at 20 mm. Therefore, the pavement temperature values were used to build the HDM-4 model and consequently the Markov chain and system dynamics model are comparable to the published literature.

11.2.2. Objective 2: To Develop Deterministic Modelling for Pavement Condition Index

The second objective in this study sought to develop deterministic models for Pavement Condition Index. Prior studies have noted the importance of the pavement condition of asphalt pavement to its roughness. As mentioned in the literature review, Chapter 3 section 3.4.1, PCI values are obtained based on many elements, which are the pavement distress type, severity of distress and assessment of collected distress through visual inspection. However, quantifying procedure for PCI, especially for the pavement network level covering an area the size of a city, is tedious, time-consuming and very costly. Therefore, pavement roughness measure can be used instead of the PCI measure, which quantities physical features of the pavement surface with a cheap solution for picturing the condition of the pavement asset. A strong relationship between IRI and PCI has been reported in the literature, such as by Dewan and Smith (2002) and Lin, Yau and Hsiao (2003), who measured the applicability of IRI as a predictor variable of PCI. Park, Thomas and Lee (2007) also put forward the notion that it is acceptable to use the IRI as a predictor variable of PCI. In this study, the relationship between Pavement Condition Index (PCI) and International Roughness Index (IRI) was tested using the SPSS software program. The data collected from Al Ain City Municipality were prepared and cleaned to remove any invalid data or outliers. This finding supports previous research into this area which links IRI and PCI. The findings of the current study are consistent with those of Park, Thomas and Lee (2007), who developed a regression model of independent variable of IRI and dependent variable of PCI. Their derived model was able to explain 59% of the variation in the existing data. In this study, several experiments were conducted to find the best fit model. Several transformations were considered including log, square roots, etc. The derived model was able to explain 70.9% of the variation in the existing data. These results matched those observed in earlier studies. However, the proposed prediction models produced more realistic and accurate results in comparison to Park, Thomas and Lee's (2007). This is an improvement on the existing knowledge.

11.2.3. Objective 3: To Develop Deterministic Modelling for International Roughness Index (HDM-4)

The third objective in this study sought to develop new deterministic models for International Roughness Index using the HDM-4 model. As mentioned in the literature review in Chapter 3 section 3.4.3, the prediction deterioration model is a mathematical approach that can be applied to forecast how the future pavement is going to deteriorate. The model depends on the existing pavement condition, deterioration factors and previous maintenance (OCED 1987). Three are different categories of deterministic models, mechanistic-empirical models, mechanistic models and empirical models, which were explained in the literature review. The present study was designed to determine the effect of empirical models only. This study set out with the aim of assessing the impact of climate change in a pavement deterioration model through HDM-4. Prior studies that have noted the importance of HDM-4 include Bannour et al. (2017), who stated that the HDM-4 can handle the complex interaction between the environment, vehicles and the pavement structure, and it is one of the most accepted models globally. An objective of the study was to investigate the relationship between pavement distress (rutting, cracking), environmental and structural factors and International Roughness Index (IRI). The default HDM-4 model was able to capture this relationship with respect to climate. However, the model is limited to static climate (averages of past climate records) (Anyala 2011). This study systematically reviewed the data to build an effective and rigorous pavement deterioration model.

New modified HDM-4 equations and coefficients were tested with different inputs of climate change scenarios (pavement temperature). These scenarios were for the years 2013 (current weather data), 2020, 2040 and 2060 (predicted weather data). The current study found that the model for the structural component of roughness was only able to explain 27% of the variation in the existing data, which was insignificant and contributed to the weakness of the results. The proposed improvement was to exclude the structural component of roughness (ΔRls) from the model.

In terms of change in of rutting (ΔRDS), the present study was designed to mimic Anyala's (2011) approach in terms of speed of heavy vehicles, voids in mix (VIM) and softening point (SP) of binder. In this study, the goodness fit of the model was determined The independent variables were traffic (YE4), air voids (VIM%), pavement thickness (HS), softening point (SP), heavy vehicle speed (sh) and maximum pavement temperature (TPmax) and the dependent variable was change in rutting (ΔRDS. Several experiments were conducted to find the best fit model. Several transformations were considered including log, square roots, etc. The derived model was able to explain 60.5% of the variation in the existing data. These findings further support the idea of incorporating the climate change impact into the HDM-4 model. This finding confirms the association between change in rutting (ΔRDS) and other said variables. Moreover, a strong relationship between incremental change in rutting depth (ΔRDS) and rutting component of roughness (ΔRlr) has been reported in the literature as per the HDM-4 model. Another important finding was that such a relationship was tested using non-linear regression analysis. After several experiments were conducted to find the best fit model, the derived model was able to explain 43.1% of the variation in the existing data. The analysis of the cracking component of roughness (ΔRIc) followed a similar approach to that for the rutting component of roughness (ΔRlr) and the model goodness fit was also determined. The independent variable was change in cracking (ΔACRA) and the dependent variable was cracking component of roughness (ΔRIc). Several experiments were conducted to find the best fit model. Finally, the derived model was able to explain 31.3% of the variation in the existing data. There is no estimated coefficient for the environmental component (ΔRIe); therefore, a similar equation to the default HDM-4 was applied. The findings of the current study are consistent with those of Mubaraki (2016), who investigated the relationships of cracking and rutting to IRI values. The results obtained by Mubaraki (2016) proved statistically the existence of significant relationships, as per figures 11-1 and 11-2. However, both studies reported a weak relationship between IRI and cracking and rutting.

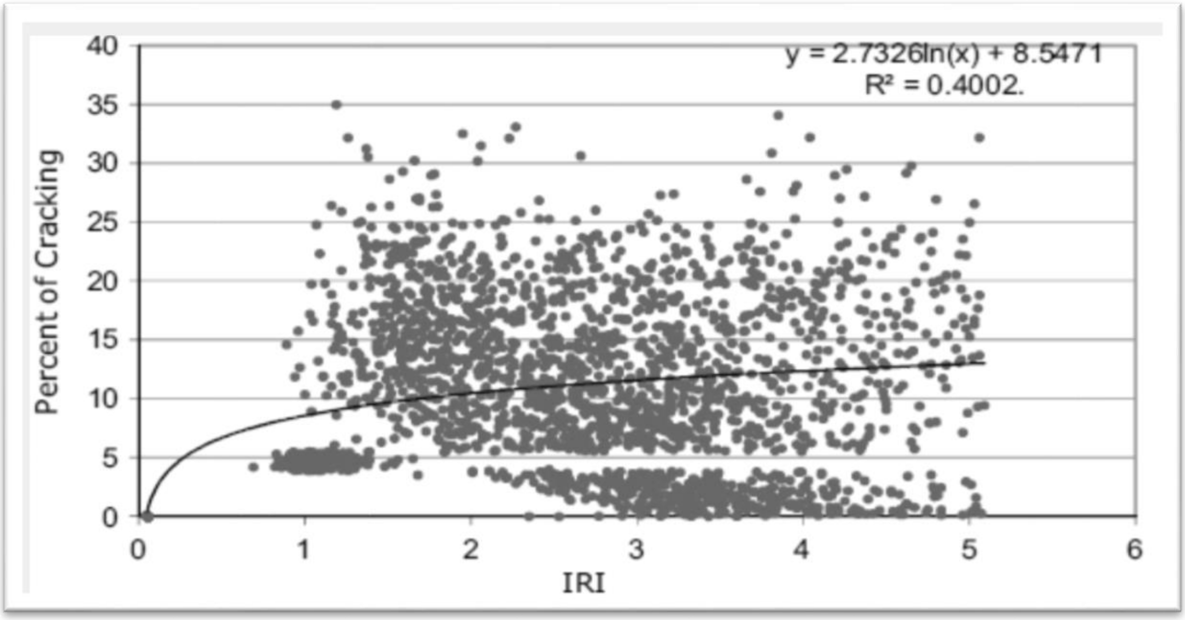

Figure 11-1: IRI and cracking distress density relationship by Mubaraki (2016)

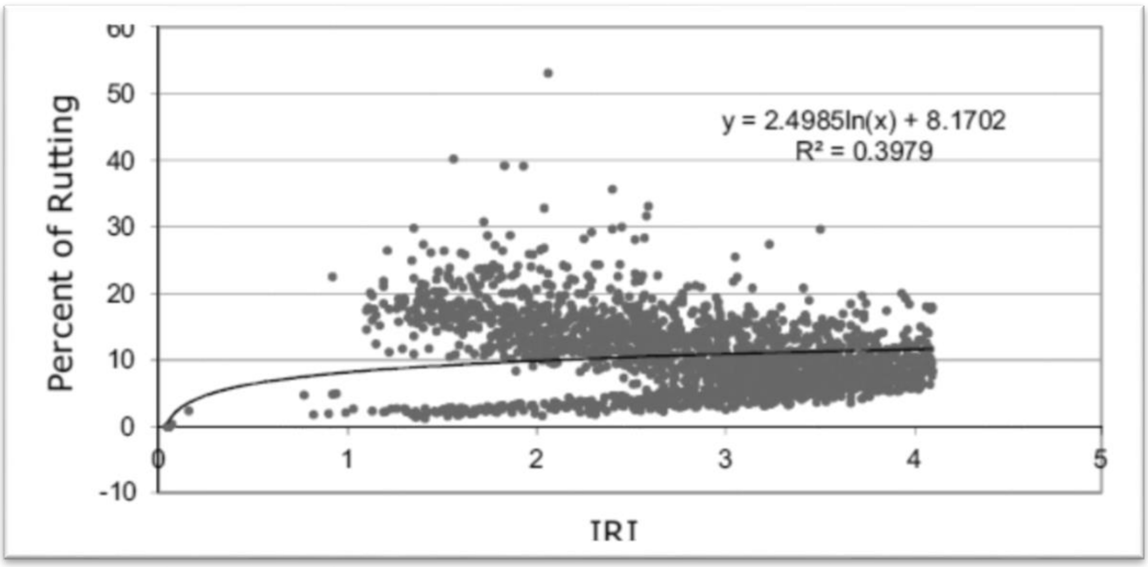

Figure 11-2: IRI and rutting density relationship by Mubaraki (2016)

The modified HDM-4 model was run based on the collected data. Such data represented different road lengths with different variable inputs, such as speed of heavy vehicles, traffic load, pavement thickness, pavement ageing, softening point and voids in mix. It was tested with four different climate change scenarios. Deficiency in the modified HDM-4 was reported as the model scored a higher value of total change on roughness in comparison with the real value, which reached a 50% discrepancy. Bannour et al. (2017) stated that using default equations in HDM-4 without configuration and calibration can generate inaccurate and inadequate pavement performance prediction. Thube (2013) added that the calibration process involves introducing the adjustment factors which are linear multipliers for modifying the predictions to meet the conditions of the selected area. In this study, Bannour et al. (2017) and Thube's (2013) approach was followed by the author. A new, improved equation of total change in roughness ($\Delta RI = \Delta RIc + \Delta RIr + \Delta RIe$) with calibration factor ($\Delta RIc = 0.7$ and $\Delta RIe = 0.5$) was achieved. The model was also tested with different inputs of climate change scenarios (pavement temperature). These scenarios were for the years 2013 (current weather data) and 2020, 2040 and 2060 (prediction scenarios). The combination of results showed a significant difference in total change in roughness with different climate change scenarios. The change in total roughness mainly depended on many variables that affect the deterioration of the road asphaltic pavement. The results have proven that the rate of degradation of pavement assets was increasing with the increase in the pavement temperature (different between 2013, 2020, 2040 and 2060). This finding corroborates the ideas of Zareie, Amin and Amador-Jiménez (2016), who suggested that the IRI progression for projection of regional highways will increase for higher climate change value.

11.2.4. Objective 4: Developing Probabilistic Modelling for International Roughness Index (Modified HDM-4) using Markov Chain

The fourth objective in this study sought to develop probabilistic modelling for International Roughness Index (modified HDM-4) using the Markov chain method. As mentioned in the literature review, Haas (2001) stated that Markov chains are the most accurate techniques for prediction models since the future state of the model element is estimated solely for the current state of the component. Prior studies have noted the importance of Markov chains on the prediction of the next condition state, taking into consideration knowing the current state or condition. In theory, probabilistic models are applied for pavement evaluation at the network level, while the deterministic model is the only appropriate tool for project-level performance. This study set out with the aim of using the homogenous Markov chain to build the deterioration model. It assumed that the initial state probabilities for new pavement condition are 1, 0, 0, . . . , 0.

Very little was found in the literature on the question of pavement condition classification. The present study was designed to determine the effect of the condition rating system, which is a technique of physical deterioration classification to assess the condition of pavement assets. Mandiartha et al. (2017) stated that distributing road conditions into different condition ratings is proven to be a sufficient method to assist highway agencies in deciding on a suitable choice of maintenance intervention. Bryant (2014) investigated different studies regarding bridge assets' management. He showed different condition states and rating applications.

The current study found that the International Roughness Index can be used as the main parameter to reflect the condition of the road assets. The findings of the current study are consistent with those of Mandiartha et al. (2017), who also applied IRI value conditions to build a Markov chain model that can assess the effectiveness of road network pavement maintenance. The selection of five classification conditions (Very good, Good, Satisfactory, Fair, Poor) for this research was consistent with previous classifications shown in Bryant (2014) and NAMS (2009). One of the limitations of the existing literature is the lack of information on the question of building a transition probability matrix from secondary data. The Markov method requires transition probability matrices (TPMs) to express the transition from one pavement condition state to another. For the pavement case, Lytton (1987) defined transition probability matrices (TPMs) as a collection of pavements conditions that will shift from one state of distress to another within an identified period. To conduct a Markov chain, it was crucial to estimate the probability of shifting from one condition state to another, which is usually done by expert judgement or based on the analysis of available previous information (historical data). In this research, both methods were tested and reported. First the approach of expert judgement was tested. Mohseni (2012) stated that, in some industries where not enough data are available to build a TPM, the engineering judgement on the definition of Markov matrices would be the best solution for forecasting the future condition of an element. In this study, the contribution of expert judgement in developing a transition probability matrix which presents the rate of deterioration of the road (flexible pavement) in the UAE was achieved by using a questionnaire. However, the finding was unexpected and suggests that that the impact of future predicted climate change scenarios cannot be incorporated into the model. Thus, the choice of building a transition probability matrix from conditional secondary data was the most suitable decision.

As mentioned in the literature review, the percentage prediction (frequency) method is quite a commonly used method. It requires at least two sets of inspection data without any maintenance interventions. Abaza (2014) used a similar method to estimate the transition probabilities used in the Markovian-based pavement performance prediction models using only two consecutive cycles of pavement distress assessment. The author decided to use regression-based optimisation (expected value) for the deterministic model achieved in Chapter 6 to build the transition probability matrix.

The present study was designed to determine the effect of the regression-based optimisation (expected value) method, which required one set of data and estimates the transition probability matrix by solving the non-linear optimisation problem that minimises the sum of absolute differences between the regression curve that best fits the condition data and the conditions predicted using the Markov chain model.

The current study found that such a method can be adapted based on the modified HDM-4 generated in Chapter 6. A pavement deterioration curve was introduced based on the generated results and by using @RISK software to assess and extract the best-fit probability distribution that captures the deterioration results. The survival probability curves of each pavement deterioration under each climate scenario were obtained and used to estimate the probability of each state in the transition matrix. The analysis was carried out using @RISK, which can automatically derive the correct choice of distribution for a set of given data, taking into consideration that no more than one state deteriorates in each cycle. The probability distribution of the rate of degradation was generated and reported for pavement condition for change in IRI based on four different climate change scenarios. Based on the probability of pavement condition and survival curve for the for change in IRI, the determination of transition probability matrix for four different climate change scenarios (2013, 2020, 2040 and 2060) was achieved.

The main question in this study sought to determine the deterioration curve using a Markov chain model. Running the model was done by using Microsoft Office Excel software. The forecasted period was set for 30 cycles. Each cycle presents a single year. The results of determining the IRI for different climate scenarios were achieved. To observe the trend of the performance over the next 30 years, the results of 2013, 2020, 2040 and 2060 scenarios were plotted into a graph (see Chapter 7 section 7.3). And the probability of the pavement section to be in a state (from 1 to 5) keeps changing over the years. As mentioned in the literature review, there were different interpretations of the deterioration predictions function. Other researchers such as Mubaraki (2010) and Mohseni

(2012) have found the traditional S-shaped or sigmoid function is the best presentation of the pavement deterioration predictions curve. On the other hand, NAMS (2009) put forward the exponential approach to represent the deterioration curve. Surprisingly, the deterioration curve was found to be a logarithmic curve shape as a result of the Markov chain modelling. These results are not consistent with those of other studies which stated that the traditional S-shaped or sigmoid function are the most accepted forms of pavement deterioration curve. Nevertheless, this study's finding is in agreement with Rosa, Liu and Gharaibeh's (2017) findings, which showed a developed empirical model for predicting the International Roughness Index (IRI) over time for network-level pavement management with a logarithmic curve shape especially for low traffic loading conditions, as per Figure 11-3.

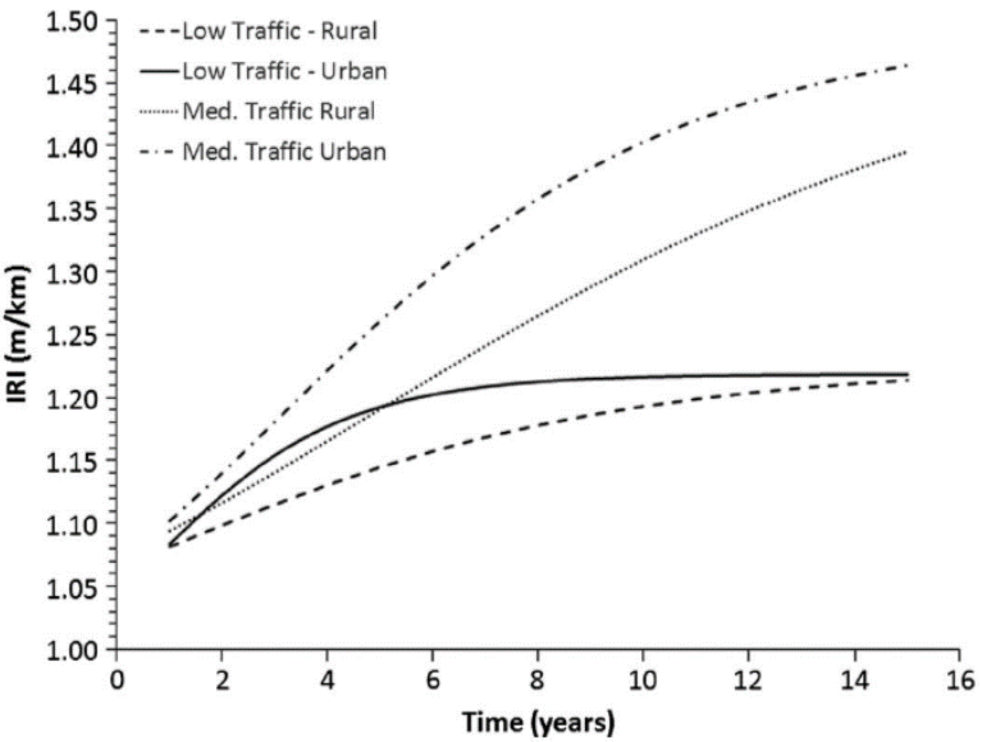

Figure 11-3: IRI under different traffic loads by Rosa et al. (2017)

The logarithmic curve shape of the deterioration curve can be read that pavement assets receive a sharp deterioration rate at the start, then a phase of smooth increase takes place till it reaches a consistent level. The occurrence of such phenomena might be a result of the interpretation of the condition survey data and how such data were being developed in the transition probability matrix. On the other hand, technically, some failure in the pavement can occur as soon as the pavement structure receives traffic loading. This could be due to insufficient pavement strength or construction quality deficiency. Therefore, the rate of deterioration increases faster until consolidation takes place. Moreover, achieving pavement resilience modulus value of 20-35% less than that of its original design value will also increase the probability of cracking and patching areas by more than 17% and the rate of rutting by more than 15 mm. In conclusion, the deterioration curve is shaped according to the data pattern and assumptions made.

On the other hand, the value of IRI for the 2060 scenario case received a faster deterioration rate, while the 2013 case had a lower deterioration rate. Such results conclude that climate change impact can accelerate the rate of degradation for infrastructure assets (pavement in the case study). And such degradation increases with increasing pavement temperature (assuming other variables are consistent). This finding corroborates the ideas of Zareie, Amin and Amador-Jiménez (2016), who suggested that the IRI progression for projection of regional highways will increase for higher climate change value.

11.2.5. Objective 5: Investigation of the Risk of Pavement Failure due to Climate Change

The fifth objective in this study sought to investigate the risk of pavement failure due to climate change. As mentioned in the literature review, pavement failure is a decrease in the serviceability (Kumar and Gupta 2010). This study set out with the aim of assessing the importance of understanding road pavement failure. Schlotjes (2013) stated that pavement failure can be a single risk factor or multiple risk factors. A large and growing body of literature has investigated pavement failure. For example, Haas (2001) listed many risk factors that affect pavement deterioration, which are traffic loading, climate, pavement composition, pavement strength, subgrade soil, maintenance, pavement age and drainage. Al-Arkawazi (2017) introduced five factors, which are traffic volume and load, moisture or water, subgrade soil, construction quality and maintenance. The current study found that nine main risks and 27 sub-risks were related to pavement failure.

The part of the research which related to pavement failure risk was planned and executed to accommodate a rich diversity of opinion for the impact of climate change on pavement structure and function. The present study was designed to determine the opinions collected from specialists and related parties such as contractors, project owners, consultants and operators. An objective of the study was to identify and construct a questionnaire that ascertains the risk associated with pavement failure due to the impact of climate change. The questionnaire was designed through a systematic process showing all the relevant main risks and sub-risks that contribute to pavement failure as derived from the literature. In this study, the questionnaire survey was designed based on the probability rating scaling the risk contribution from 0.1 to 0.72. Even though the target sample was 40 participants, requests to participate in the survey were made to 50 participants working in the asphalt field of the construction in the UAE. However, only 30 returned valid questionnaires with all sections fully responded to.

There are different categories of approaches for risk analysis: deterministic (on numerical computations) and qualitative (based on subjective system). For this research, a deterministic technique was adopted. The results were analysed using a similar approach to that of Jang (2011), who used quadratic multiple regression models to quantify the risk and the functional relations for a dependent risk variable and its independent variables in pavement failure risk. Also, other analyses such as probability measures were conducted. In order to examine the model with different risk factors under the multiple-regression analysis method, it was decided to apply three different experiments for the variable inputs, which are average scenario, minimum scenario and maximum scenario. The final risk factors were constructed on the final product variables. It was decided by the author to only use the risks associated with the main model variables; these variables are pavement thickness, pavement temperature, pavement ageing, traffic loading, the speed of heavy vehicles, change in rutting and cracking. The impacts of the risk associated with the highlighted dynamic variables were then used in the model.

11.2.6. Objective 6: Developing a Casual Loop Diagram for IRI and PCI (Modified HDM-4) Using System Dynamics

The sixth objective in this study sought to develop a casual loop diagram for IRI and PCI (modified HDM-4) using system dynamics. Very little was found in the literature on the question of modelling pavement deterioration using system dynamics. Few prior studies have noted the importance of system dynamics in establishing connections between qualitative and quantitative models and modelling the interdependencies of the various disciplines through loops with respect to the time (Mallick et al. 2015). Causal loop diagrams (CLDs) are responsible for defining theory and interactions among various variables as well as presenting the causes of dynamics (Rashedi and Hegazy 2015). Feedback loops can be either positive (self-reinforcing) or negative (self-correcting or balancing). In this study, the researcher explored the methodology based on the pavement deterioration model developed in Chapter 6. Using system dynamics provided an understanding on how the pavement condition was changing over a period. The modified HDM-4 model developed in Chapter 6 was used to determine the CLDs. CLDs were built to address the component interrelationships, which were based on the developed equations and coefficients for the improved HDM-4 model with calibration and taking into consideration the data described in Chapter 5 and the current literature in Chapter 2. The causal loop diagram for the proposed model was empirically confirmed by Chapter 6 model outputs which were used to examine whether the CLDs could fit to be used in determining pavement condition. All of the model components such as rutting component of roughness, cracking component of roughness and environmental component of roughness including their direct variables and intermediate variables, were included in the causal loop diagram. The modelling of the risk CLDs was also considered through the investigation of the risk associated with pavement failure. The pavement failure risks presented in the literature review by various authors can be considered as incomplete and unrepresentative because the assessment conducted by previous studies only found a single direct risks. A list of generic risk factors has been extracted from various literature reviews and discussed in Chapter 2. The researcher also explored the variables that influence pavement failure and all risk and variables were pictured through a framework of risk CLDs. Therefore, the risk CLDs were modelled based on the significant risk variables that can occur during the pavement life cycle including all risks and their direct and intermediate variables.

11.2.7. Objective 7: Developing a Deterioration Curve for IRI and PCI (Modified HDM-4) Using System Dynamics

The seventh objective in this study sought to develop a deterioration curve for IRI and PCI (modified HDM-4) using system dynamics. Very little was found in the literature on the question of modelling pavement deterioration using system dynamics. The system dynamics model consists of four primary elements named stocks (denote key system variables), flows (variables that generate quantities accumulated into inflows or out of outflows, valves (flow generators) and clouds (entry or exit boundary points in the model) (Rashedi 2016). For this research, it was proposed to use Vensim as the software package for system dynamics modelling. Vensim software consists of various tools such as causal tracing analysis tools, variables diagram tree and SD models that quantify the stock-flow diagram. The proposed model was designed to receive the worst-case scenarios at all levels. In reality, this could not always be the case, as infrastructure highway design is always conducted on maximum historical or predicted data. In this study, a similar approach was carried out by introducing the ultimate values of the variables to seek the stage where the failure could occur under different climate scenarios and with different risk magnitudes. A HDM-4 model was applied to develop models that assess the impact of climate change on road roughness. The developed CLDs were transformed into quantitative stock-flow diagrams to operationalise the model of pavement deterioration (HDM-4). Moreover, it was also decided to investigate the range for every single dynamic variable in the proposed models. These variables were the pavement thickness, pavement temperature, pavement ageing, traffic loading, the speed of heavy vehicles and change in rutting. The worst-case scenario range of the inputs was used to simulate the SD model. All the sub-models were united in one model and the final stock and flow diagram was determined; the model was run for 20 years to project the deterioration curve on pavement condition based on two performance indicators, PCI and IRI, under different risk scenarios. The system dynamics model was built to predict the worst pavement condition scenarios that might occur over 20 years. The dynamic variables were defined to range from lower impact scenarios to the worst one. In practice, the pavement condition is going to ultimately fail before reaching these values (IRI =11 m/km). The model was based on the assumption that, when the yearly rate of change is 100%, then a full shift in state of change will be achieved. Partial yearly rates of change with either 80% , 60%, 40% or 20% were also tested. Achieving a 40% state shift recorded change in IRI with nearly 4 m/km after 20 years, which in the opinion of the author seemed the most logical approach with which to build the model. However, road designers always depend on the most critical historical data to determine the most acceptable design parameters that allow the road assets to last for their proposed service life period. And, as discussed in Chapter 2 section 2.2.5, climate change impact is not considered in any current pavement design practice due to uncertainty about the consequences of such implications and is not part of the historical data. Therefore, with the projection of the worst scenario, it was decided to introduce the pavement deterioration curve in both chapters 8 and 9 based on the worst situation with a 100% state shift (rate of change).

As mentioned in chapters 7 and 9, there were different interpretations of the deterioration predictions function. Other researchers such as Mubaraki (2010) and Mohseni (2012) have found the traditional S-shaped or sigmoid function is the best presentation of pavement deterioration predictions curve. On the other hand, NAMS (2009) put forward the exponential approach to represent the deterioration curve. Surprisingly, the deterioration curve was found to have a logarithmic curve shape as a result of the Markov chain modelling. These results are not consistent with those of other studies which stated that the traditional S-shaped or sigmoid function are the accepted presentation of pavement deterioration. However, this finding is in agreement with Rosa, Liu and Gharaibeh's (2017) findings, which showed a developed empirical model for predicting the International Roughness Index (IRI) over time for network-level pavement management with a logarithmic curve shape especially for low traffic loading conditions

The logarithmic curve shape of the deterioration curve can be read that pavement assets receive a sharp deterioration rate at the start, then a phase of smooth increase takes place till it fails. For example, according to the IRI deterioration curve, achieving an IRI value of 12 m/km is not real; most likely the road failed before reaching this level. According to the IRI international standard, 12 m/km can only be recorded for unpaved roads. Nevertheless, the system shows such a value as a consequence of how the accumulation of stock happens when the system is in positive (self-reinforcing) mode, achieving unlimited growth if it runs for an undefined period. However, this is not the case, in reality; the system (pavement condition) either fails before reaching such a state or maintenance intervention occurs to balance the system. Moreover, the model presented the deterioration curves regarding PCI and IRI with different risk scenarios.

Overall, the pavement deterioration curve (IRI and PCI) with maximum risk factors received the highest rate of degradation in comparison with other risk scenarios. Moreover, minimum risk scenarios presented a slight change in the rate of deterioration in contrast with the original rate of change (no risk associated). This finding corroborates the ideas of Zareie, Amin and Amador-Jiménez (2016), who suggested that the IRI progression for projection of regional highways will increase for higher climate change value.

11.2.8. Objective 8: To Measure Pavement Resilience Loss

The eighth objective in this study sought to measure pavement resilience loss. The literature is sparse on the question of how to measure pavement resilience. Resilience can be considered as the maximum degree of threat mitigation to respond to, minimise or remove long-term impact to property and humans from hazards and the consequences of such risks. Hosseini, Barker and Ramirez-Marquez (2016) suggested four resilience domains, namely social, engineering, economic and organisational. Such classification may differ based on the author's perspective. Hughes and Healy (2014) concluded that these four domains (or dimensions) cannot be assessed or evaluated as one component in terms of system performance. They focused on the area of engineering and felt that the organisational domain is sufficient in terms of the transport system. In this study, resilience is viewed in terms of engineering dimension only. Hosseini, Barker and Ramirez-Marquez (2016) stated that quantitative methods are always interested in engineering systems. For this research, an approach using quantitative methods was selected to measure the pavement resilience. How to quantify resilience is a challenging question (Schoon 2005). Sun, Bocchini and Davison (2018) stated that a resilient transportation infrastructure system indicates that such a system allows for a small probability of failure, redundant connectivity, less recovery time and limited impact propagations. According to Sun, Bocchini and Davison (2018), Bruneau et al. (2003) were the first to measure resilience quantitatively based on the concept of resilience triangle and the functionality recovery curve. The resilience triangle concept measures a substantial and sudden decrease of functionality due to an extreme event at a specific time as well as the gradual recovery of system functionality until it reaches its original function. Sun, Bocchini and Davison (2018) added that the resilience triangle measures may comprehensively represent the system functionality loss, and functionality recovery in terms of the speed and duration. They also stated that measuring resilience using a resilience triangle approach may extensively represent the functionality loss. This author agrees with them,(Sun, Bocchini and Davison 2018) and a similar approach is conducted in this study. However, the element of functionality recovery is not considered. Only system functionality loss is determined. In this study, quantifying the system resilience in terms of functionality at pavement network level was the main objective. Measuring resilience loss was chosen based on future prediction of pavement performance under different climate change impact scenarios (2020, 2040 and 2060). The resilience triangle theory was applied in this research to measure pavement infrastructure resilience loss through the concept of pavement performance (pavement network functionality). The specific measures of resilience loss have been developed through the application of a pavement performance prediction model that determined the deterioration curve (survival curve). Such models are built using two different methods, which are Markov and system dynamics (more details are provided in chapters 7, 8 and 9). The data used to determine the measure for the pavement network resilience represent the roads and highways under the management of the UAE Ministry of Public Works (more details are presented in Chapter 10). The comparison of the results of resilience loss indicated that the system dynamics model achieved the highest drop in pavement network functionality level over the 20 years prediction, showing a range between 75.67% and 81.0% resilience loss with different risk scenarios, whereas the Markov chain model showed a range between 27.86% and 32.4% resilience loss for the same period. The system dynamics model was built to predict the worst pavement condition scenarios that might occur over 20 years. The dynamic variables were defined to range from lower impact scenarios to the worst one and the model was designed on the assumption that the yearly rate of change is a 100% full shift of state of change. Thus, the drop in pavement network functionality showed a significant drop and scope of 80% resilience loss over 20 years. Generally, an ultimate worse scenarios model may help highway designers, who always depend on the most critical historical data, to determine the most acceptable design parameters to incorporate the impact of climate change and consequently measure the resilience loss.

11.3. Strengths of the Research Methodology

There were a number of strengths in the research methodology to achieve the research objectives such as modelling pavement deterioration with respect to climate change and measuring pavement resilience loss. As a result, the author was able to gather an understanding of pavement deterioration modelling in the industry in a comprehensive and realistic manner. Information was gathered from Al Ain City Municipality and the UAE Ministry of Public Works. Different software packages and tools were also used in this research.

A systematic literature review was conducted of studies defining the risks associated with pavement failure of climate change and it was decided that the best method to adopt for this objective was a questionnaire survey. The questionnaire survey was designed based on the probability rating scaling the risk contribution from 0.1 to 0.72. The questionnaire survey was only completed by experts in the area of pavement engineering such as pavement material engineers, highway maintenance contractors, highway maintenance consultants, clients and asset managers.

To date, various methods have been developed and introduced to build a deterministic model. The author aimed to use a number of different methods in order to ensure that the weakness of a particular method did not influence the results. To model pavement performance indicators (IRI and PCI) under the HDM-4 model, the data were analysed using numerical analysis methods which measure different parameters such as the median, standard deviation, skewness and kurtosis, and the mean. All these analyses and tests used SPSS software. SPSS software is widely available, and has been used in many investigational studies. One of the most accepted methods in pavement deterioration is ‘Statistical Regression Analysis’ (Amador-Jiménez and Mrawira 2011). This method was used to define the relationship between different variables in the HDM-4 model, the relationship between IRI and PCI, and to analyse the results generated from the survey questionnaire.

A probabilistic approach using the Markov chain method was another method for determination of the pavement deterioration model. The Markov method requires transition probability matrices (TPMs) to express the transition from one pavement condition state to another. To date, various methods have been developed and introduced to measure to transition probability matrix. In most recent studies, the transition probability matrix has been measured in two different ways. The first method is based on data of pavement condition over a number of years and the second method uses a panel of experts. Both methods were chosen in this research and each had its advantages and drawbacks. However, it was decided that the best method to adopt for this investigation was to build the transition probability matrix from probability distribution of the pavement condition. The collected results from the regression model (modified HDM-4 model) as presented in Chapter 6 were used to define the probability distribution of deterioration for the occurrence of different future climate change impact scenarios. The use of software named @RISK was made to automatically empower the correct choice of distribution for a set of given data. The survival probability curves of each pavement deterioration curve under each climate scenario were used to estimate the probability of each state in the transition matrix. Finally, the Markov chain model was built using Microsoft software package 'Excel'.

A system dynamics method was also used in this research. It consists of elements that shape and investigate a feedback model of strategic systems. This method was crucial to answer the two questions in modelling system dynamics. The first question concerns how to quantify the defined problem (variables) that varies through time, and the second question is about defining a substantial feedback relationship between the variables. To answer these questions, a model which was a simplification of real-world phenomena was the best way to make the problem more understandable. Shire (2018) stated that there is no standard or best modelling process employed by all SD modellers. The proposed system was first drafted on paper in several fashions to achieve the most common, being the casual-loop diagram, then the models were represented in the form of computer code that can be fed into the proposed software package. The Vensim software package was used to build the SD models. It has been extensively applied to build and run system dynamics models (Khan, Luo and Ahmad 2009; Rashedi and Hegazy 2015). The specific measures of resilience were also developed through the application of the pavement performance prediction model (SD and Markov). In theory, there are two important types of pavement prediction models: deterministic and probabilistic. The selection of the probabilistic approach was through the application of the Markov chain technique, while the deterministic approach was applied through the application of system dynamics. In the end, the deterioration curve was obtained for different models and resilience loss was measured using resilience triangle-related theory based on the functionality recovery curve. Sun, Bocchini and Davison (2018) stated that measuring resilience using a resilience triangle approach may extensively represent the functionality loss. A software package named CurveExpert Professional was applied to measure the area under the curve using the generated deterioration pavement curve from the Markov chain model and system dynamics. The area was calculated under different climate scenarios and different risks.

11.4. Validation and Implications

For developing both Markov chain and system dynamics models, it is crucial to ensure that the modified HDM-4 model is validated. Gathered data from the Ministry of Public Works were divided into two groups named backward and forward (see Chapter 5). For the developing models, the analysis was carried out only on data for the backward direction roads (see Chapter 5 section 5.3). Model checking and validation was conducted by testing the modified HDM-4 with the calibrated factor in the forward direction data instead of in the backward direction. For example, the traffic loading data for a road in the forwarding direction differs from that for one on the backward direction. A test was conducted to verify the reliability of the model with different variable inputs. Therefore, a comparison between two means (2013 forward results and 2013 backward results) was conducted using independent T-test. Basically, an independent T-test (analysis of variance) compares the means of two or more independent groups to determine whether there is statistical evidence that the associated population means are significantly different. It is a parametric test. In this case, Sig. = 0.000 (so $p < 0.001$) and the result was significant at the 99.9% level.

Moreover, the modified HDM-4 model was run based on the collected data. Deficiency was reported as the model scored a higher value of total change in roughness in comparison with the real value, which reached a 50% discrepancy. As mentioned in the literature review, Bannour et al. (2017) stated that using default equations in the HDM-4 without configuration and calibration can generate inaccurate and inadequate pavement performance prediction, and Thube (2013) added that the calibration process involves introducing the adjustment factors which are linear multipliers for modifying the predictions to meet the conditions of the selected area. In this study, Thube (2013) and Bannour et al.'s (2017) approach was followed to achieve a new HDM-4 model (details are provided in Chapter 6 section 6.4.3). The model was also retested with different inputs of climate change scenarios (pavement temperature) and found to be acceptable.

According to Sterman (2000), system dynamics model validation comprises two general methods of validation: structural validation and behaviour validation. Structural validation means ensuring that the model achieved the purpose of the objective by capturing and representing the real system scenarios. For example, structural assessment includes using a tree, cause tree, loops, unit check, checking the model and checking the syntax. In this research, the researcher used the Vensim software that provides a variety of structural analysis tools for structural validation. It was then ensured that structural validation requirements were met. Moreover, there was no unit error dimensional analysis step.

The other validation test was extreme condition. The extreme condition test assesses the model's robustness under the extreme values of its parameters (Sterman 2000). It is a test to evaluate the behaviour of the model under the inputs taking on values at extreme conditions. For this research, all the dynamic variables in the model were ranged to the extreme values (see Chapter 9); also, the different risk scenarios associated with climate change impacts were applied. For example, no risk scenario and maximum risk scenario were tested. The system showed robustness and behaved reasonably, disregarding how extreme the inputs are.

To validate the results, for both pavement deterioration models – using the Markov chain model and the system dynamics model – the interpretation of the deterioration predictions function was studied with respect to other researchers' findings. In this study, the deterioration curve was found to be a logarithmic curve shape. This finding is in agreement with Rosa, Liu and Gharaibeh's (2017) findings, which showed a developed empirical model for predicting IRI over time for network-level pavement management with a logarithmic curve shape especially for low traffic loading conditions. Also, the IRI value for the 2060 scenario case received a faster deterioration rate, while the 2013 case had a lower deterioration rate. Such results conclude that climate change impact can accelerate the rate of degradation for infrastructure assets (pavement in the case study). And such degradation increases with increasing pavement temperature (assuming other variables are consistent). This finding corroborates the ideas of Zareie, Amin and Amador-Jiménez (2016), who suggested that the IRI progression for projection of regional highways will increase for higher climate change values.

11.5. Summary of Contribution

This research provides an increased understanding of modelling and managing uncertainty in pavement deterioration models with respect to climate change impacts. It contributes to the existing body of knowledge in the following areas:

(1) A comprehensive literature review to identify and investigate the risk of pavement failure due to climate change, resilience measures, deterministic and probabilistic deterioration models, Markov chain and system dynamics is achieved. Also, definition of climate thresholds, measurement of the pavement temperature, and HDM-4 model are provided.

(2) Demonstrated the first use of the Thornthwaite Moisture Index (TMI) in a UAE pavement deterioration model for climate change impact assessment using data collected from the UAE National Centre of Meteorology

(3) Development of the first Pavement Condition Index model in the UAE using pavement roughness to measure physical features of pavement surface instead of the PCI measure. Such an approach provides a cheap solution for picturing the condition of pavement assets for the UAE road and highway agency. The model computes the IRI value to determine the PCI value for the pavement network.

(4) Development of an improved HDM-4 model that includes a climate variable for considering the contribution of future climate change to the progression of International Roughness Index and Pavement Condition Index. This will consequently empower the road and highway agency of the UAE to plan for future years and to establish the necessary maintenance programmes.

(5) Development of a probabilistic model for International Roughness Index (modified HDM-4) using a Markov chain method which captures pavement deterioration under different climate change scenarios.

(6) Demonstrated the first transition probability matrix built from the best fit of the survival probability distribution curve that captures the deterioration results under each climate scenario in the modified HDM-4 model.

(7) Development of a system dynamics model for International Roughness Index (based on modified HDM-4) that captures pavement deterioration under different risk scenarios. Such a model captures a real system, which assists policy decision makers in devising a pavement intervention programme.

(8) Development of a new tool and method for use in quantitative resilience loss measurements. Such a method provides analytical and numerical approaches to support road maintenance management decisions with respect to future climate predictions.

11.6. Limitations of the Research

A comprehensive piece of research is reflected by the fulfilment of its aim and objectives. The limitations of this research upon which further development can be made are as follows:

(1) The researcher could not obtain more data on some of the pavement features such as softening points, voids in mix, IRI and PCI for more three consecutive years or evaporation rate data. Moreover, participation in the questionnaire survey was limited to 30 participants. There was some resistance to filling in the questionnaire. Also, the questionnaire was designed for those who are in the UAE pavement industry field. To reach more participants was challenging and requires more time. Also, since there were no real data in terms of qualitative risk effects, many parameter values in the system dynamics model heavily relied on the questionnaire survey. Thus, errors might exist in this model of the system dynamics. Obtaining professional software tools such as Vensim, @RISK and CurveExpert Professional was difficult as these software packages were either available only as student versions or as trial versions with limited features.

(2) Very little was found in the literature on the question of how to measure pavement resilience. The proposed modified resilience triangle theory which was applied in this research to measure pavement infrastructure resilience loss through the concept of pavement performance (pavement network functionality) is not supported by any extensive literature and has

potential technical limitations, especially with the assumption made that current pavement performance of the pavement network in the UAE was 100%. In practice, this is not the case and defining the performance of the current pavement network is challenging.

(3) The Markov chain model for determining the pavement degradation was developed based on the assumption that steady transition probabilities occur over time, taking into consideration no change in traffic loading and progressive weakening of the pavement structure. In practice, this is not the case as the magnitude of traffic loading and other factors are not constant values over time. Moreover, the Markov chain process required an enormous number of roughly consistent families related to pavement characteristics which were not available in data from the UAE Ministry of Public Works. Therefore, a regression-based method was used to determine the transition probability matrix.

(4) The investigation of the impact of climate change on pavement structure was limited to the increase in temperature for the HDM-4 model whilst other factors were ignored. Moreover, pavement temperature and Thornthwaite Moisture Index (TMI) were chosen in this research to mainly assess the impact of climate change on the pavement deterioration model. TMI value (current and future) was not used due to fact that the goodness fit and prediction value from change in roughness equations were not in keeping with existing knowledge.

11.7. Recommendations for Future Research

This study has introduced a number of areas that would benefit from further investigation, as follows:

(1) Pavement Condition Index models developed in this research should be utilised to evaluate the pavement structural condition besides the International Roughness Index. Moreover, further study can be proposed to analyse the relationship between IRI and PCI using a probabilistic method with extensive accurate date.

(2) To develop a heterogeneous Markov chain that can capture a different set of transition probabilities for each transition (time interval) within an analysis period for UAE roads and highways.

(3) Investigate further the accuracy of deriving a transition probability matrix using a probability method and regression-based optimisation (expected value) method. Also, to assess the impact of climate change directly on the Markov chain model.

(4) Incorporating more factors of the climate change impact into the HDM-4 model such as flooding instead of increase in temperature to determine the pavement deterioration curve.

(5) Redevelop the Thornthwaite Moisture Index model for the UAE to include more data and investigate new methods to determine the TMI values that fit with UAE weather.

(6) Measure the pavement resilience loss in extreme events and also investigate a method to measure system resilience as a whole rather than just resilience loss.

(7) Develop a pavement deterioration model using the Markov chain method that directly integrates with the system dynamics method.

(8) Measure the risk of pavement failure using a quantitative approach.

11.7.1. Recommendation for industry

This study has also introduced a number of areas that would benefit from further investigation in the industrial level, as follows

1 Develop a cost model of climate change impact on pavement maintenance programmes and deliver more comprehensive information about vulnerable components under the impact of climate change. And evaluate the requirements for achieving better road pavement maintenance strategies and policies that cope with the uncertainties of future climate change.

2 Develop accurate deterioration model that estimates the rate of change of pavement condition for next 30 years using system dynamics tools that capture real system with minimum number of uncertainties.

3 Develop a new decision support tools for the Ministry of Public Works in the UAE and Al Ain City Municipality that integrates both system dynamics and Morkov chain.

References

(OCED) Organization for Economic Co-operation and Development. (1987). *Pavement Management System*.

AASHTO. (1993). *AASHTO Guide for Design of Pavement Structures*. *American Association of State Highway and Transportation Officials*.

Abas, M., Khattak, S. B., Hussain, I., Maqsood, S. & Ahmad, I. (2015). Evaluation of Factors affecting the quality of construction projects. *Technical Journal, University of Engineering and Technology (UET) Taxila, Pakistan, 20(2), pp.115-120.*

Abaza, K. A. (2004). Deterministic performance prediction model for rehabilitation and management of flexible pavement. *International Journal of Pavement Engineering*, vol. 5(2), pp. 111–121.

Abaza, K. A. (2014). Back-calculation of transition probabilities for Markovian-based pavement performance prediction models,. *International Journal of Pavement Engineering*.

Abaza, K. A. (2016). Simplified staged-homogenous Markov model for flexible pavement performance prediction. *Road Materials and Pavement Design*, vol. 17(2), pp. 365–381.

Abaza, K. a., Ashur, S. a. & Al-Khatib, I. a. (2004). Integrated Pavement Management System with a Markovian Prediction Model. *Journal of Transportation Engineering*, vol. 130(1), pp. 24–33.

Abd El-Raof, H. S., Abd El-Hakim, R. T., El-Badawy, S. M. & Afify, H. . (2018). Structural number prediction for flexible pavements using the long term pavement performance data. *International Journal of Pavement Engineering, pp.1-15*.

Abo-hashema, M. (2009). Artificial Neural Network Approach for Overlay Design of Flexible Pavements. *The International Arab Journal of Information Technology*, vol. 6(2), pp. 204–212.

Abo-Hashema, M. . (2013). Modeling Pavement Temperature Prediction using Artificial Neural Networks. *AASCE Proceedings, Airfield and Highway Pavement 2013, pp. 490-505, Los*

Angeles, California, United States.

Abu El-Maaty, E. A., Akal, A. Y. & El-Hamrawy, S. (2016). Management of Highway Projects in Egypt through Identifying Factors Influencing Quality Performance. *Journal of Construction Engineering*, vol. 2016(1), pp. 1–8.

Adlinge, S. S. & Gupta, A. K. (2013). Pavement Deterioration and its Causes. *IOSR Journal of Mechanical & Civil Engineering*.

Al-Abdul Wahhab, H.I. Balghunaim, F. A. (1994). Asphalt Pavement Temperature Related to Arid Saudi Environment. *J. of Materials in Civil Engineering, American Society of Civil Engineers, 6 (1), pp. 1-14.*

Al-Arkawazi, S. A. F. (2017). Flexible Pavement Evaluation: A Case study. *Kurdistan Journal for Applied Research*, vol. 2(3).

Al-Hassan, M. S. A.-H. (1993). *Factors affecting quality of pavement construction in Saudi Arabia*. (Doctoral dissertation, King Fahd University of Petroleum & Minerals).

Al-Omari, B. & Darter, M. I. (1995). Effect of pavement deterioration types on IRI and rehabilitation. *Transportation research record, (1505), pp.57-65.*

Al-Suleiman, T. I. & Shiyab, A. M. S. (2003). Prediction of Pavement Remaining Service Life Using Roughness Data - Case Study in Dubai. *International Journal of Pavement Engineering*, vol. 4(2), pp. 121–129.

Alaswadko, N. H. A. (2016). *Deterioration Modelling of Granular Pavements for Rural Arterial Roads*. *thesis,Faculty of Science, Engineering and Technology Swinburne University of Technology,Melbourne, Australia*. Swinburne University of Technology.

Alaswadko, N., Hassan, R., Meyer, D. & Mohammed, B. (2016). Probabilistic prediction models for crack initiation and progression of spray sealed pavements. *International Journal of Pavement Engineering*. Taylor & Francis, vol. 8436(October), pp. 1–11.

Alaswadko, N., Hassan, R., Meyer, D. & Mohammed, B. (2017). Modelling roughness progression of sealed granular pavements: a new approach. *International Journal of Pavement Engineering*. Taylor & Francis, vol. 8436(April), pp. 1–11.

Albores, P. & Shaw, D. (2008). Government preparedness: Using simulation to prepare for a terrorist attack. *Computers and Operations Research*.

Allen, J. J. & Thompson, M. R. (1974). Resilient response of granular materials subjected to time-dependent lateral stresses. *Transportation Research Record 510*.

Allenby, B. & Fink, J. (2005). Toward inherently secure and resilient societies. *Science*, vol. 309(5737), pp. 1034–1036.

AlRustamani, Z. A. (2014). *Impacts of Climate Change on Urban Development in the Uae: the Case of Dubai*. *United Arab Emirates Uniersity* [online].Available at: http://scholarworks.uaeu.ac.ae/all_theses/29.Acess 10thJune 2017

Alvanchi, A., Lee, S. H. & AbouRizk, S. (2011). Modeling Framework and Architecture of Hybrid System Dynamics and Discrete Event Simulation for Construction. *Computer-Aided Civil and Infrastructure Engineering*.

Alzahrani, A. M. Y. (2015). *Uncovering the Emerging Risks from Climate Change Scenarios and Related Climate Change Risk Management in the Building Sector in the UK Thesis*. University of Liverpool.

Amador-Jiménez, L. E. (Concordia U. & Mrawira, D. (University of N. B. (2012). Bayesian Regression in Pavement Deterioration Modeling: Revisiting the AASHO Road Test Rut Depth Model. *Infraestructura Vial*, vol. 14(25), pp. 28–35.

Amador-Jiménez, L. E. & Mrawira, D. (2009). Roads Performance Modeling and Management System from Two Condition Data Points: Case Study of Costa Rica. *Journal of Transportation Engineering*, vol. 135(12), pp. 999–1007.

Amador-Jiménez, L. E. & Mrawira, D. (2011). Reliability-based initial pavement performance deterioration modelling. *International Journal of Pavement Engineering*, vol. 12(2), pp. 177–186.

Amin, M. S. R. (2015). 'The pavement performance modeling: deterministic vs. stochastic approaches'. , in *Numerical Methods for Reliability and Safety Assessment: Multiscale and Multiphysics Systems*.

Anyala, M. (2011). Investigation of the impact of climate change on road maintenance. *thesis,School of Civil Engineering College of Engineering and Physical Sciences The University of Birmingham*, (May), p. 487 [online].Available at: http://etheses.bham.ac.uk/2815/. Acess 10th December 2016

Anyala, M., Odoki, J. B. & Baker, C. J. (2014). Hierarchical asphalt pavement deterioration model for climate impact studies. *International Journal of Pavement Engineering*, vol. 15(3), pp. 251–266.

Arangi, S. R. & Jain, R. K. (2015). Review Paper on Pavement Temperature Prediction Model for Indian Climatic Condition. *International Journal of Innovative Research in Advanced Engineering (IJIRAE)*, vol. 2(8), pp. 1–9 [online]. Available at: http://www.ijirae.com/volumes/Vol2/iss8/01.AUAE10083.pdf. Acess 15th December 2017

Arce, G. & Zhang, Z. (2019). Skid resistance deterioration model at the network level using Markov chains. *International Journal of Pavement Engineering, pp.1-9.*

Archibald, E. (2013). *Infrastructure resilience at the project level: Considering hazard risk and uncertainty for infrastructure decisions*. University of Delaware.

Archondo-Callao, R. S. & Faiz, A. (1994). *Estimating vehicle operating costs*. Washington, DC: World Bank.

Arimbi, G. (2015). *Network-Level Pavement Performance Prediction Modelling with Markov Chains Predicting the Condition of Road Network*. Delft University of Technology.

Asbahan, R.E. and Vandenbossche, J. M. (2011). Effects of temperature and moisture gradients on slab deformation for jointed plain concrete pavements. *Journal of Transportation Engineering, 137(8), pp.563-570.*

ASTM. (2003). *American Standards for Testing of Materials. D 189; D 240–02; D 4052–96; D 445–03; D 482–74; D 5555–95; D 6751-02; D 93–02a; D 95–990; D 97–02. ASTM International*

ASTM. (2011). D 6433-03-Standard Practice for Roads and Parking Lots Pavement Condition Index Surveys. *ASTM International*.

Austroads. (2012). *The Scoping and Development of Probabilistic Road Deterioration (RD) Models*. *Austroads*.

Austroads. (2018). *Guide to Pavement Technology Part 2: Pavement Structural Design*. *Austroads*.

Azar, A. T. (2012). System dynamics as a useful technique for complex systems. *International Journal of Industrial and Systems Engineering, 10(4), pp.377-410.*

Bae, A., Stoffels, S. M., Antle, C. E. & Lee, S. W. (2008). Observed evidence of subgrade moisture influence on pavement longitudinal profile. *Canadian Journal of Civil Engineering*.

Bagloee, S. A., Sarvi, M., Wolshon, B. & Dixit, V. (2017). Identifying critical disruption scenarios and a global robustness index tailored to real life road networks. *Transportation Research Part E: Logistics and Transportation Review*. Elsevier Ltd, vol. 98(December 2016), pp. 60–81.

Banks, J., Carson, J., Nelson, B. . & Nicol, D. (2004). *Discrete-event system simulation*. Paperback: Prentice Hall.

Bannour, A., El Omari, M., Lakhal, E. K., Afechkar, M., Benamar, A. & Joubert, P. (2017). Optimization of the maintenance strategies of roads in Morocco: calibration study of the degradations models of the highway development and management (HDM-4) for flexible pavements. *International Journal of Pavement Engineering*. Taylor & Francis, vol. 8436(November), pp. 1–10.

Barber, E. S. (1957). Calculation of maximum pavement temperatures from weather reports. *Highway Research Board Bulletin, (168).*

Bayomy F.M. and Abo-Hashema M.A. (2000). Inclusion of the environmental effects in the empirical-mechanistic pavement overlay design system. *in Proceedings of Infra 2000 International Conference, Sound Infrastructure Management, Canada, pp. 465-468.*

Bhamidipati, S. (2015). Simulation framework for asset management in climate-change adaptation of transportation infrastructure. *Transportation Research Procedia*. Elsevier B.V., vol. 8, pp. 17–28.

Bianchini, A. & Bandini, P. (2010). Prediction of pavement performance through neuro-fuzzy reasoning. *Computer-Aided Civil and Infrastructure Engineering*, vol. 25(1), pp. 39–54.

Black, M., Brint, A. T. & Brailsford, J. R. (2005). Comparing Probabilistic Methods for the Asset Management of Distributed Items. *Journal of Infrastructure Systems*.

Bouch, C. J., Rogers, C. D. F., Bryson, J. R., Quinn, A. D., Chapman, D. N., Barber, A. R. G., Jefferson, I., Coaffee, J., Chapman, L., Williams, S. & Baker, C. J. (2012). Resistance and resilience – paradigms for critical local infrastructure. *Proceedings of the Institution of Civil Engineers - Municipal Engineering*.

Bristow, A., Pridmore, A., Tight, M., May, T., Berkhout, F. & Harris, M. (2004). How can we reduce carbon emissions from transport ? How Can We Reduce Carbon Emissions From Transport ? *Tyndall Centre Technical Report 15*, (June).

Bruneau, M., Chang, S. E., Eguchi, R. T., Lee, G. C., O'Rourke, T. D., Reinhorn, A. M., Shinozuka, M., Tierney, K., Wallace, W. A. & Von Winterfeldt, D. (2003). A Framework to Quantitatively Assess and Enhance the Seismic Resilience of Communities. *Earthquake Spectra*, vol. 19(4), pp. 733–752.

Bryant, L. L. H. (2014). *Modelling railway bridge asset management*. (Thesis) University of Nottingham.

Bubshait, A. A. (2002). Quality of Pavement Construction in Saudi Arabia. *Practice Periodical on Structural Design and Construction*.

Burnett, B. H. S. (2001). Analysis Reality and Climate. *National Centre for Policy analysis*, (367), pp. 2–3.

Burnett, S. (2013). A Simplified Numerical Decision Making Toolbox for Physical Asset Management Decisions. *South African Journal of Industrial Engineering*, vol. 25(December), pp. 162–175.

Butt, A. A., Shahin, M. Y., Carpenter, S. H. & Carnahan, J. V. (1994). Application of Markov Process to Pavement Management Systems at Network Level. *3rd International Conference on Managing Pavements*.

Buttlar, William G., and R. R. (1996). Evaluation of empirical and theoretical models to determine asphalt mixture stiffnesses at low temperatures (with discussion). *Journal of the Association of Asphalt Paving Technologists*, (65).

Byrne, M. & Aguiar, G. I. (2010). Impact of climate change on road performance: updating climate information for Australia. *Austroads Publication No. AP-R358-10, Austroads, Sydney, NSW, Australia.*

Cao, M. (2015). Transportation Resilience: A summative review on Definition and Connotation. *International Conference on Automation, Mechanical Control and Computational Engineering.* Atlantis Press.

Carvalho, H., Barroso, A. P., MacHado, V. H., Azevedo, S. & Cruz-Machado, V. (2012). Supply chain redesign for resilience using simulation. *Computers and Industrial Engineering*.

CASRA. (1992). *Pavement Management Systems: Standard Visual Assessment Manual for Flexible Pavements, Technical Methods for Highways (TMH9)*.

Cebon, D. (1999). *Handbook of Vehicle-road Interaction*. *Advances in engineering*. Abingdon : Swets & Zeitlinger, c1999. Series: Advances in Engineering (Lisse, Netherlands).

Cechet, B. (2005). Climate Change Impact on the Pavement Maintenance and Rehabilitation Costs associated with the Australian National Highway Network. *MODSIM05 - International Congress on Modelling and Simulation: Advances and Applications for Management and Decision Making, Proceedings*, pp. 489–496 [online].Available at: file:///C:/Users/Kyle P. Kwiatkowski/Documents/Mendeley Desktop/Cechet - 2005 - Climate Change Impact on the Pavement Maintenance and Rehabilitation Costs associated with the Australian National Highw.pdf. Access 9th July 2017.

Cedergren, H. R. (1987). *Drainage of highway and airfield pavements*.

Chang, S. E. & Shinozuka, M. (2004). Measuring improvements in the disaster resilience of communities. *Earthquake Spectra*.

Chang, S., McDaniels, T., Fox, J., Dhariwal, R. & Longstaff, H. (2014). Toward disaster-resilient cities: characterizing resilience of infrastructure systems with expert judgments. *Risk Anal 2014;34(2):416–34.*

Chapman, L. (2007). Transport and climate change: a review. *Journal of Transport Geography*, vol. 15(5), pp. 354–367.

Cheetham, A., Li, Y., Bekheet, W., Helali, K. & Zaghloul, S. (2007). Enhancement of Arizona Pavement Management System for Construction and Maintenance Activities. *Transportation Research Record: Journal of the Transportation Research Board*.

Chinowsky, P. S., Price, J. C. & Neumann, J. E. (2013). Assessment of climate change adaptation costs for the U.S. road network. *Global Environmental Change*.

Chowdhury, R., Mohamed, M. M. A. & Murad, A. (2016). Variability of Extreme Hydro-Climate Parameters in the North-Eastern Region of United Arab Emirates. *Procedia Engineering*.

Christopher, Barry R. & McGuffey, V. C. (1997). *Pavement subsurface drainage systems*. Transportation Research Board.

Christopher, B., Schwartz, C. & Boudreau, R. (2006). *Geotechnical Aspects of Pavements*. *NHI Course No.132040*.

Church, J. A., White, N. J., Aarup, T., Wilson, W. S., Woodworth, P. L., Domingues, C. M., Hunter, J. R. & Lambeck, K. (2008). Understanding global sea levels: Past, present and future. *Sustainability Science*.

Cimellaro, G. P., Reinhorn, A. M. & Bruneau, M. (2010). Framework for analytical quantification of disaster resilience. *Engineering Structures*. Elsevier Ltd, vol. 32(11), pp. 3639–3649.

Collins, B. (2011). Infrastructure, engineering and climate change adaptation: Ensuring services in an uncertain future. *Royal Academy of Engineering, London.*

Daines, M. E. (1992). The Performance of Hot Rolled Asphalt Containing Crushed Rock Fines, A303 Mere. *A303 Mere. Research Report 298. Transport Research Laboratory. Crowthorne.*

Deacon, J. A., Monismith, C. L. & Harvey, J. T. (2001). *Pay Factors for Asphalt-Concrete Construction: Effect of Construction Quality on Agency Costs*. University of California, Berkely.

Demirel, H., Kompil, M. & Nemry, F. (2015). A framework to analyze the vulnerability of European road networks due to Sea-Level Rise (SLR) and sea storm surges. *Transportation*

Research Part A: Policy and Practice. 81, pp.62-76.

Dempsey, B.J. and Thompson, M. R. (1970). A heat transfer model for evaluating frost action and temperature-related effects in multilayered pavement systems. *Highway Research Record, (342).*

DMRB-UK (2017). Design Manual for Roads and Bridges: Traffic Capacity of Urban Roads. *Vol. 5*

Dewan, S. A. & Smith, R. E. (2002). Estimating IRI from Pavement Distresses to Calculate Vehicle Operating Costs for the Cities and Counties of San Francisco Bay Area. *Transportation Research Record 1816, Transportation Research Board, Washington, DC, 2002*.

DfT, Department for Transport. (2014). *Transport resilience review: a review of the resilience of the transport network to extreme weather events.*

Dong, Q., Huang, B. & Richards, S. H. (2014). Calibration and Application of Treatment Performance Models in a Pavement Management System in Tennessee. *Journal of Transportation Engineering*, vol. 141(2), p. 04014076.

Elghriany, A., Yi, P., Liu, P. & Yu, Q. (2016). Investigation of the effect of pavement roughness on crash rates for rigid pavement. *Journal of Transportation Safety and Security*, vol. 8(2), pp. 164–176.

Enright, M. P. & Frangopol, D. M. (2011). Closure to "Condition Prediction of Deteriorating Concrete Bridges Using Bayesian Updating" by Michael P. Enright and Dan M. Frangopol. *Journal of Structural Engineering*.

Enríquez-de-Salamanca, Á. (2017). Environmental impacts of climate change adaptation of road pavements and mitigation options. *International Journal of Pavement Engineering*. Taylor & Francis, vol. 8436(October), pp. 1–6.

Equivalent Single Axle Load (ESAL). (2018). Pavement Interactive. Access 5 Apr. 2018, *www.pavementinteractive.org/reference-desk/design/design parameters/equivalent-single-axle-load/.*

FHWA. (1993). *PONTIS technical manual, Publ.*

Franchin, P. & Cavalieri, F. (2015). Probabilistic assessment of civil infrastructure resilience to earthquakes. *Computer-Aided Civil and Infrastructure Engineering*, vol. 30(7), pp. 583–600.

Francis, R. & Bekera, B. (2014). A metric and frameworks for resilience analysis of engineered and infrastructure systems. *Reliability Engineering and System Safety*. Elsevier, vol. 121, pp. 90–103.

Freckleton, D., Heaslip, K., Louisell, W. & Collura, J. (2012). Evaluation of Resiliency of Transportation Networks After Disasters. *Transportation Research Record: Journal of the Transportation Research Board*, vol. 2284, pp. 109–116.

Fwa, T. F. (2006). *The Handbook of Engineering of Highway*. *Taylor and Francis*.

George, K. P., Rajagopal, A. S. & Lim, L. K. (1989a). Models for predicting pavement deterioration. *Transportation Research Record, (1215).*

George, K. P., Rajagopal, A. S. & Lim, L. K. (1989b). Models for Predicting Pavement Deterioration. *Transportation Research Record: Journal of the Transportation Research Board*.

Gibbs, M. T. (2009). Resilience: What is it and what does it mean for marine policymakers? *Marine Policy*.

Gillespie, T. D. (1992). *Everything you always wanted to know about the IRI, but were afraid to ask. The University of Michigan Transportation Research Institute. Nebraska.*

Gledhill, R., and Low, L. P. (2010). *Adapting to climate change in the infrastructure sectors*. *Department for Environment, Food and Rural Affairs, London*.

Godschalk, D. R. (2003). Urban Hazard Migration : Creating Resilient Cities. *Natural Hazards Review*, vol. 6988(August), pp. 136–143.

Guan, Y., Drumm, E. C. & Jackson, N. M. (1998). Weighting factors for seasonal subgrade resilient modulus. *Transportation Research Record: Transportation Research Board, 1619, 94–100.*

Ha, S., Kim, K., Jeong, H. & Kim, H. (2017). Reliability approach in economic assessment of adapting infrastructure to climate change. *Journal of Management in Engineering, 33(5), p.04017022.*

Haas, R. (2001). Reinventing the (Pavement Management) Wheel. *Fifth International Conference on Managing Pavements*.

Haas, R., Hudson, W. & Zaniewski, J. (1994). Modern Pavement Management. *Krieger Publishing Company*.

Haimes, Y. Y. (2009). On the Definition of Resilience in Systems. *Risk Analysis: An International Journal, 29(4), pp.498-501.*

Hall, K. T., Correa, C. E. & Simpson, A. L. (2002). *effectiveness of maintenance and rehabilitation options*. *NCHRP Project (2002) 20–50.*

Harun, M.H. and Morosiuk, G. (1995). A Study of the Performance of various Bituminous Surfacings for Use on Climbing Lanes. *H Proceedings of the 8th REAAA Conference, Taipei.*

Harvey, M., Whetton, P., McInnes, K.L., Cechet, B., McGregor, J.L., Nguen, K., Houghton, N., Lester, C., Styles, E. and Michael, N. (2004). *Impact of Climate Change on Road Infrastructure*. *Austroads. Report no. AP-R243/04, Austroads and the Bureau of Transport and Regional Economics, Sydney.*

Hassan, H. F., Al-Nuaimi, A. S., Taha, R. & Jafar, T. M. A. (2004). Development of Asphalt Pavement Temperature Models for. *Journal of Engineering Research*, vol. 2(1), pp. 32–42.

Hassan, R., Lin, O. & Thananjeyan, A. (2017). Probabilistic modelling of flexible pavement distresses for network management. *International Journal of Pavement Engineering*.

Hassan, R., Mcmanus, K. & Holden, J. (2007). Predicting Pavement Deterioration Modes Using Waveband Analysis. *Transportation Research Record: Journal of the Transportation Research Board*.

Holling, C. S. (1973). Resilience and Stability. *Annual Review Ecological System*.

Hollnagel, E. & Woods, D. D. D. (2006). *Epilogue: Resilience engineering precepts*. *Resilience Engineering–Concepts and Precepts, ….*

Homer, J., Sterman, J., Greenwood, B. & Perkola, M. (1993). Delivery time reduction in pulp and paper mill construction projects: A dynamic analysis of alternatives. *In Proceedings of the*

1993 International System Dynamics Conference (pp. 212-221). Cancun, Mexico: Monterey Institute of Technology.

Hong, H. P. & Wang, S. S. (2003). Stochastic modeling of pavement performance. *International Journal of Pavement Engineering*, vol. 4(4), pp. 235–243.

Hosseini, S., Barker, K. & Ramirez-marquez, J. E. (2016). A review of de fi nitions and measures of system resilience. *Reliability Engineering and System Safety*, vol. 145, pp. 47–61.

Hu, X., Zhou, F., Hu, S. & Walubita, L. F. (2009). Proposed Loading Waveforms and Loading Time Equations for Mechanistic-Empirical Pavement Design and Analysis. *Journal of Transportation Engineering*.

Huang, Y. H. (2004). Pavement Analysis and Desig n Second Edition, p. 588 [online].Available at: http://docshare04.docshare.tips/files/14013/140138713.pdf.

Hughes, J. & Healy, K. (2014). *Measuring the resilience of transport infrastructure*.

Hunt, P. D. & Bunker, J. M. (2001). *Analysis of unbound granular pavement deterioration for use in asset management modelling.*

Huntingford, C., Marsh, T., Scaife, A. A., Kendon, E. J., Hannaford, J., Kay, A. L., Lockwood, M., Prudhomme, C., Reynard, N. S., Parry, S., Lowe, J. A., Screen, J. A., Ward, H. C., Roberts, M., Stott, P. A., Bell, V. A., Bailey, M., Jenkins, A., Legg, T., Otto, F. E. L., Massey, N., Schaller, N., Slingo, J. & Allen, M. R. (2014). Potential influences on the United Kingdom's floods of winter 2013/14. *Nature Climate Change*. Nature Publishing Group, vol. 4(9), pp. 769–777.

IPCC. (2007). *Climate Change 2007 Synthesis Report. Contribution of Working Groups I, II and III to the Fourth Assesment Report of the Intergivernmental Panel on Climate Change*. *IPCC.*

IPCC. (2013). *Working Group I Contribution to the IPCC Fifth Assessment Report - Summary for Policymakers*. *Intergovermental Panel on Climate Change*.

ISO. (2018). ISO 31000 Risk management - Principles and guidelines. *International Organization for Standardization*.

ISOHDM. (2002). *HDM-4 Highway development and management model*. *Paris, France:*

International Study of Highway Development and Man- agement, PIARC.

Jang, S. G. (2011). *A Concessionaire Selection Decision Model Development and Application for the PPP Project Procurement*. *Philosophy THESIS*.

Jaroszweski, D.J. (2010). *Climate change and road freight safety: impacts and opportunities*. (Doctoral dissertation, University of Birmingham).

Jaroszweski, D., Hooper, E., Baker, C., Chapman, L. & Quinn, A. (2015). The impacts of the 28 June 2012 storms on UK road and rail transport. *Meteorological Applications*, vol. 22(3), pp. 470–476.

Ji, S. J. (2006). *Investigation of Factors Affecting Resilient Modulus for Hot Mix Asphalt*. University of Canterbury Christchurch, New Zealand.

Jia, G., Tabandeh, A. & Gardoni, P. (2017). Life-cycle analysis of engineering systems: Modeling deterioration, instantaneous reliability, and resilience. *Theory and applications (pp. 465–494). Cham, Switzerland: Springer.*

Jiménez, L.A. and Mrawira, D. (2012). Bayesian regression in pavement deterioration modeling: revisiting the AASHO road test rut depth model. *Infraestructura Vial, 14(25), pp.28-35.*

Jin, Y. and Mukherjee, A. (2014). Markov chain applications in modelling facility condition deterioration. *International Journal of Critical Infrastructures, 10(2), pp.93-112.*

Jones, L. D. & Jefferson, I. (2012). Chapter C5 - Expansive Soils. *Institute of Civil Engineers Manuals series*.

Kahan, J. H., Allen, A. C. & George, J. K. (2009). An Operational Framework for Resilience. *Journal of Homeland Security and Emergency Management*.

Karan, M.A., Haas, R. and Walker, T. (1981). Illustration of pavement management: From data inventory to priority analysis. *Transportation research record, (814).*

Kargah-Ostadi, N., Stoffels, S. & Tabatabaee, N. (2010). Network-Level Pavement Roughness Prediction Model for Rehabilitation Recommendations. *Transportation Research Record: Journal of the Transportation Research Board*.

Karim, C. & Lee, D. (2001). Development of a preventive maintenance strategy for minimizing roughness-related pavement damage. *J. Transport. Res. Board, 2001, The 80th Transportation Research Board Annual Meeting, Washington, D.C.*

Karl, T. R. & Trenberth, K. E. (2003). Modern Global Climate Change. *Science*, vol. 302(5651), pp. 1719–1723.

Keller, G. (2009). *Managerial Statistics*. ICC Macmillan Inc. Lee,.

Khan, F.I. and Haddara, M. M. (2003). Risk-based maintenance (RBM): a quantitative approach for maintenance/inspection scheduling and planning. *Journal of loss prevention in the process industries, 16(6), pp.561-573.*

Khan, S., Luo, Y. & Ahmad, A. (2009). Analysing complex behavior of hydrological systems through a system dynamics approach. *Environ. Model. Software, 24(12), 1363–1372*.

Khraibani, H., Lorino, T., Lepert, P. & Marion, J. M. (2010). Nonlinear mixed-effects model for the evaluation and prediction of pavement deterioration. *Journal of Transportation Engineering, 138(2), pp.149-156.*

Kobayashi, K., Do, M. & Han, D. (2010). Estimation of Markovian transition probabilities for pavement deterioration forecasting. *KSCE Journal of Civil Engineering*, vol. 14(3), pp. 343–351.

Korkiala-Tanttu, L. & Dawson, A. R. (2007). *Relating full-scale pavement rutting to laboratory permanent deformation*.

Kumar Praveen & Gupta Ankit. (2010). *Case Studies on Failure of Bituminous Pavements*. *Case Studies on Failure of Bituminous Pavements*.

Lamptey, G., Labi, S. & Sinha, K. C. (2004). Development of Alternative Pavement Rehabilitation and Maintenance Strategies for Pavement Management. *In 83rd Annual TRB Meeting, Washington, DC.*

Lavin, P. (2003). *Asphalt Pavements: A Practical Guide to Design, Production, and Maintenance for Engineers and Architects.*

Lee, J., Ni, J., Djurdjanovic, D., Qiu, H. & Liao, H. (2006). Intelligent prognostics tools and e-maintenance. *Computers in Industry*.

Lethanh, N. & Adey, B. T. (2013). Use of exponential hidden Markov models for modelling pavement deterioration. *International Journal of Pavement Engineering*, vol. 14(7), pp. 645–654.

Levina, E. & Tirpak, D. (2006). *Adaptation to climate change*. Key Terms. Paris: Organisation For Economic Co-Operation and Development (OECD).

Li, N., Kazmierowski, T. & Sharma, B. (2001). Verification of network level pavement roughness measurements. *The 80th Transportation Research Board Annual Meeting, Washington, D.C.*.

Li, N., W-C, X. & Haas, R. (1996). Reliability-based processing of Markov chains for modelling pavement network deterioration. *Transp Res Rec 1524:203–213*.

Lin, l, Yau, J. & Hsiao, L. (2003). Correlation analysis Between International Roughness Index (IRI) and pavement Distress by Neural Network, J. Transport. *The 82nd Transportation Research Board Annual Meeting, Washington, D.C*.

Lin, H., Cheedella, S., Rushing, J., Anderson, M., Keiser, K. & Graves, S. J. (2005). Mining and analysis of traffic safety and roadway condition data. *46th Annual Transportation Research Forum 2005*.

Loizos, A. & Plati, C. (2008). An alternative approach to pavement roughness evaluation. *International Journal of Pavement Engineering*.

Lorino, T., Lepert, P., Marion, J.-M. & Khraibani, H. (2012). Modeling the Road Degradation Process: Non-linear Mixed Effects Models for Correlation and Heteroscedasticity of Pavement Longitudinal Data. *Procedia - Social and Behavioral Sciences*, vol. 48, pp. 21–29.

Lytton, R. L. (1987). Concepts of Pavement Performance Prediction and Modeling. *Second North American Conference on Managing Pavements*.

MacDonald, M. (2006). *Using SCANNER Data for Maintenance Management on Local Roads.*

Madanat, S. M., Nakat, Z. E. & Sathaye, N. (2005). Development of Empirical-Mechanistic Pavement Performance Models using Data from the Washington State PMS Database.

Institute of Transportation Studies.

Madanat, S., Mishalani, R. & Ibrahim, W. H. W. (2002). Estimation of Infrastructure Transition Probabilities from Condition Rating Data. *Journal of Infrastructure Systems*.

Maguire, B. & Cartwright, S. (2008). Assessing a community's capacity to manage change : A resilience approach to social assessment. *Social Science Program*.

Mahmood, M. S. (2015). *Network - Level Maintenance Decisions for Flexible Pavement Using a Soft Computing-Based Framework*. *PhD Thesis*. *Nottingham Trent University*. Nottingham Trent University.

Mallick, R., Radzicki, M., Daniel, J. & Jacobs, J. (2015). Use of System Dynamics to Understand Long-Term Impact of Climate Change on Pavement Performance and Maintenance Cost. *Transportation Research Record: Journal of the Transportation Research Board*.

Mamlouk, M. S. (1997). General outlook of pavement and vehicle dynamics. *Journal of transportation engineering 123*, (6 (1997): 515-517.).

Mandiartha, P., Duffield, C. F., Thompson, R. G. & Wigan, M. R. (2017). Measuring pavement maintenance effectiveness using Markov Chains analysis. *Structure and Infrastructure Engineering*. Taylor & Francis, vol. 13(7), pp. 844–854.

Mann, A. (2003). *The identification of road sections in Victoria displaying roughness caused by expansive soils*. Swinburne University of Technology.

Mansouri, M., Nilchiani, R. & Mostashari, A. (2010). A policy making framework for resilient port infrastructure systems. *Marine Policy, Vol. 34(2010), p1125–1134.*

Markolf, S. A., Hoehne, C., Fraser, A., Chester, M. V. & Underwood, B. S. (2019). Transportation resilience to climate change and extreme weather events–Beyond risk and robustness. *Transport Policy, 74, pp.174-186.*

Martin, T. C. (2011). Experimental estimation of the relative deterioration of flexible pavements under increased axle loads. *International Journal of Pavement Engineering*.

Martin, T. & Choummanivong, L. (2010). *Interim Network Level Functional Road Deterioration Models*. *Austroads Technical Report*.

Mather, J. R. (1974). *Climatology: Fundamentals and Applications.* McGraw-Hill, New York, USA, pp.113 - 131.

Matic, B., Tepic, J., Sremac, S., Radonjanin, V., Matic, D. & Jovanovic, P. (2012). Development and Evaluation of the model for the Surface Pavement Temperature Prediction, vol. 51(3), pp. 329–332.

Mayada, O., Mostashari, A., Roshanak, N. & Mansouri, M. (2012). A framework for assessing resiliency of maritime. *Maritime Policy & Management, Vol.39 (2012), No.7, p685–703.*

McLean, J. & Ramsay, E. (1996). Interpretations of Road Profile-Roughness Data: Review and Research Needs. *AUSTRALIAN ROAD RESEARCH BOARD.*

Merrill, D., Van Dommelen, A. & Gáspár, L. (2006). A review of practical experience throughout Europe on deterioration in fully-flexible and semi-rigid long-life pavements. *International Journal of Pavement Engineering*.

Metehan, I. & Murat, E. (2016). An integrated graphical user interface for pavement deterioration modeling. *Scientific Research and Essays*, vol. 6(17), pp. 3649–3656.

Meyer, M.D. and Weigel, B. (2010). Climate change and transportation engineering: Preparing for a sustainable future. *Journal of Transportation Engineering, 137(6), pp.393-403.*

Micevski, T., Kuczera, G. & Coombes, P. (2002). Markov Model for Storm Water Pipe Deterioration. *Journal of Infrastructure Systems*.

Mikhail, M. Y. & Mamlouk, M. S. (1998). Effect of traffic load on pavement serviceability in Flexible Pavement Rehabilitation and Maintenance. *ASTM International.*

Miller-Hooks, E., Zhang, X. & Faturechi, R. (2012). Measuring and maximizing resilience of freight transportation networks. *Computers &Operations Research, Vol. 39(2012), p1633–1643.*

Moffatt, M. (2013). *The influence of multiple axle loads on the performance of an unbound granular pavement under accelerated loading*.

Moffatt, M. & Hassan, R. (2006). *Guide to asset management: Part 5e: Cracking*.

Mohseni, H. (2012). *Deterioration prediction of community buildings in Australia*. *School of Civil,* *Environmental and Chemical Engineering, RMIT University*.

Morcous, G. (2006). Performance prediction of bridge deck systems using Markov chains. *Journal of per- formance of Constructed Facilities, 20 (2), 146–155.*

Moreira, A. V., Tinoco, J., Oliveira, J. R. M. & Santos, A. (2016). An application of Markov chains to predict the evolution of performance indicators based on pavement historical data. *International Journal of Pavement Engineering*, (September 2017), pp. 1–12.

Morosiuk, G., Riley, M. & Odoki, J. B. (2004). *Modelling Road Deterioration and Works Effects in HDM-4. Highway development & Management Series*.

Morosiuk, Kerali & Greg. (2000). *The highway development and management tool - HDMV-4. TRL Limited Crowthorne.*

Mubaraki, M. (2016). Highway subsurface assessment using pavement surface distress and roughness data. *International Journal of Pavement Research and Technology*. Chinese Society of Pavement Engineering, vol. 9(5), pp. 393–402.

Mubaraki, M. A. (2010). *Predicting deterioration for the Saudi Arabia Urban Road Network*. *PhD thesis, University of Nottingham*.

Mun, S., Yoo, T. S., Kim, I. S. & Lee, K. B. (2012). Pavement Performance Evaluation of Structural and Functional Conditions.

Murray-Tuite, P. M. (2006). A comparison of transportation network resilience under simulated system optimum and user equilibrium conditions. *Proceedings - Winter Simulation Conference*.

Murray-tuite, P. M. & Tech, V. (2006). Proceedings of the 2006 Winter Simulation Conference L. F. Perrone, F. P. Wieland, J. Liu, B. G. Lawson, D. M. Nicol, and R. M. Fujimoto, eds., pp. 1398–1405.

NAMS. (2009). *Building Condition & Performance Assessment Guidelines.*

National Transport Commission Australia. (2011). *Modelling the marginal cost of road wear*.

Nayel, U. S., Heaslip, K., Brady, B., Louisell, W. C. & Collura, J. (2011). A Case Study of

Transportation Network Resiliency of Santo Domingo. *Dominican Republic, TRB Annual Meeting, 2011*.

NCHRP. (2004). Guide for Mechanistic-Empirical Design of New and Rehabilitated Pavement Structures. *National Cooperative Highway Research Program Transportation Research Board National Research Council*.

NDLI. (1995). *Modelling Road Deterioration and Maintenance Effects in HDM-4.*

Nebojsa, N. & Swart, R. (2000). *Emissions scenarios. Special report of the Intergovernmental panel on climate change*.

Nguyen, B. T. & Mohajerani, A. (2016). Resilient modulus of fine-grained soil and a simple testing and calculation method for determining an average resilient modulus value for pavement design. *Transportation Geotechnics*.

NIAC. (2010). A Framework for Establishing Critical Infrastructure Resilience Goals: Final Report and Recommendations. *National Infrastructure Advisory Council*, pp. 1–73.

Nicholls, J. C., Carswell, I., Thomas, C. & Walter, K. (2007). Durability of Thin Asphalt Surfacing Systems. Part 3: Findings after Six Years Monitoring. *TRL Report TRL660. Transport Research Laboratory. Crowthorne.*

NRC. (1993). *Distress Identification Manual for the Long - Term Pavement Performance Project SHRP-P-338*. National Research Council, Washington, DC.

NRC. (2008). *potential impact of climate change on U.S transportation*. on U.S. transportation. National Research Council. Transportation Research Board, Washington, DC.

Nunn, M., Brown, A. E., Weston, D. & Nicholls, J. C. (1997). Design of Long-Life Flexible Pavements for Heavy Traffic. *TRL Report 250. Transport Research Laboratory. Crowthorne.*

Obaidat, M. T. & Al-kheder, S. A. (2006). Integration of geographic information systems and computer vision systems for pavement distress classification. *Construction and Building Materials*, vol. 20(9), pp. 657–672.

Odoki, J. B., & Kerali, H. R. G. (2006). Analytical framework and model descriptions – Volume 4 of highway development and management series. *Paris: International Study of Highway Development and Management (ISOHDM), World Road Association PIARC.*

Oliver, J. (1999). *The Performance Of Sprayed Seals, ARRB Transport Research. ARRB Transport Research. ARRB Transport Research Ltd, Research Report 326 (extract), Australia.*

Organization for Economic Co-operation and Development & Management System', O. (1987). *Pavement Management System*.

Ortiz-García, J. J., Costello, S. B. & Snaith, M. S. (2006). Derivation of Transition Probability Matrices for Pavement Deterioration Modeling. *Journal of Transportation Engineering*.

Osorio-Lird, A., Chamorro, A., Videla, C., Tighe, S. & Torres-Machi, C. (2018). Application of Markov chains and Monte Carlo simulations for developing pavement performance models for urban network management. *Structure and Infrastructure Engineering*.

Padgett, J. E. & DesRoches, R. (2007). Sensitivity of seismic response and fragility to parameter uncertainty. *Journal of Structural Engineering, 133(12), 1710–1718.*

Paillard, D. (2001). Glacial cycles: toward a new paradigm. *Reviews of Geophysics 39*, (2001), pp. 325–346.

Panayiotou, A. (2017). *Infrastructure as a Financial Asset Class*. (Doctoral dissertation, UCL (University College London)).

Panthi, K. (2009). *A methodological framework for modeling pavement maintenance costs for projects with performance-based contracts*.

Papagiannakis, A. T. & Masad, E. A. (2012). *Pavement Design and Materials*. *Pavement Design and Materials*.

Parasuraman, A., Zeithaml, V. A. & Berry, L. L. (1991). Refinement and reassessment of the SERVQUAL scale. *Journal of Retailing, vol. 67(4), p. 420-50*.

Park, E. S., Smith, R. E., Freeman, T. J. & Spiegelman, C. H. (2008). A Bayesian approach for improved pavement performance prediction. *Journal of Applied Statistics*, vol. 35(11), pp. 1219–1238.

Park, J., Seager, T. P., Rao, P. S. C., Convertino, M. & Linkov, I. (2013). Integrating risk and resilience approaches to catastrophe management in engineering systems. *Risk Analysis*.

Park, K., Thomas, N. E. & Wayne Lee, K. (2007). Applicability of the international roughness index as a predictor of asphalt pavement condition. *Journal of Transportation Engineering, 133(12), pp.706-709.*

Park, S. (2004). Identifying the hazard characteristics of pipes in water distribution systems by using the proportional hazard model: 2. Applications. *KSCE J. of Civil Engineering, Vol. 8, No. 6, pp. 669-677.*

Parzen, E. (1987). *Stochastic Processes*. Oakland.

Paterson, W. (1989). A transferable causal model for predicting roughness progression in flexible pavements. *Transportation Research Record 1215*.

Paterson, W. D. O. (1987). *Road deterioration and maintenance effects : models for planning and management* [online].Available at: http://www-wds.worldbank.org/external/default/WDSContentServer/WDSP/IB/1987/12/01/000009265_3971113151012/Rendered/PDF/multi_page.pdf.

Pavlopoulos, I. (2010). *Impacts of climate change on transportation and infrastructure - A Gulf Coast study*. *Impacts of Climate Change on Transportation and Infrastructure - A Gulf Coast Study*.

Pearson, D. (2011). *Deterioration and Maintenance of Pavements*. *Deterioration and Maintenance of Pavements*.

Petit, J.R., Jouzel, J., Raynaud, D., Barkov, N.I., Barnola, J.-M., Basile, I., Benders, M., Chappellaz, J., Davis, M., Delaygue, G., Delmotte, M., Kotlyakov, V.M., Legrand, M., Lipenkov, V.Y., Lorius, C., Pepin, L., Ritz, C., Saltzman, E. and Stievenard, M. (1999). *Climate and Atmospheric History of the Past 420,000 Years from the Vostok Ice Core*. Edited by Antarctica. Nature Publishing Group.

Porras-Alvarado, J., Zhang, Z. & Salazar, L. (2014). Probabilistic Approach to Modeling Pavement Performance Using IRI Data. *Transportation Research Board 93rd Annual Meeting*.

Pregenzer, A. (2011). Systems resilience: a new analytical framework for nuclear nonproliferation. *Sandia National Laboratories, Albuquerque. New México, 8, pp.1-21.*

Prozzi, J.A. and Madanat, S. M. (2003). Empirical-mechanistic model for estimating pavement roughness. *In 82nd Annual Meeting of Transportation Research Board, Washington, DC.* In 82nd Annual Meeting of Transportation Research Board, Washington, DC.

PWC. (2014). *capital projects and infrastructure spending: Outlook to 2025* [online].Available at: https://www.pwc.com/gx/en/capital-projects-infrastructure/publications/cpi-outlook/assets/cpi-outlook-to-2025.pdf. Acess 12th June 2017

Qi-sen, Z., Yu-liang, C. & Xue-lian, L. (2009). Rutting in Asphalt Pavement under Heavy Load and High Temperature. *GeoHunan International Conference*, pp. 39–48.

Qiao, Y. (2015). Flexible Pavements and Climate Change Impact of Climate Change on the Performance, Maintenance, and Life-Cycle Costs of Flexible Pavements. *thesis,University of Nottingham*, (May).

Qiao, Y., Dawson, A., Parry, T. & Flintsch, G. (2015). Evaluating the effects of climate change on road maintenance intervention strategies and Life-Cycle Costs. *D: Transport and Environment*, pp. 492–503 [online].Available at: http://www.sciencedirect.com/science/article/pii/S1361920915001431.

Qiao, Y., Dawson, A., Parry, T. & Flintsch, G. W. (2016). Immediate effects of some corrective maintenance interventions on flexible pavements. *International Journal of Pavement Engineering*, (May), pp. 1–7.

Raad, L., Minassian, G. H. & Scott Gartin. (1992). *Characterization of saturated granular bases under repeated loads*. .

Ranita Sen. (2012). *Impact of changes in fleet composition and axle loading on pavement profile characteristics*. Swinburne University of Technology, Melbourne, Australia.

Rashedi, R. (2016). *Combined Strategic-Tactical Planning for Facility Rehabilitation Using System Dynamics and Optimization*. *thesis, Waterloo, Ontario, Canada,*.

Rashedi, R. & Hegazy, T. (2015). Holistic Analysis of Infrastructure Deterioration and Rehabilitation

Using System Dynamics. *Journal of Infrastructure Systems*.

Rashidy, R. A. H. El. (2014). *The Resilience of Road Transport Networks Redundancy , Vulnerability and Mobility characteristics*. University of Leeds,(Doctoral dissertation).

Rebecchi, J. and Sharp, K. (2009). *Guide to Pavement Technology: Part 3: Pavement Surfacings.*

Reigle, J. A. (2002). *Development of an integrated project-level pavement management model using risk analysis*.

Roberson, R. & Siekmeier, J. (2002). *Determining material moisture characteristics for pavement drainage and mechanistic empirical design*. *Research Bulletin. Minnesota Department of Transportation. Office of Materials and Road Research*.

Roberts, D. J. & Martin, T. C. (1998). Pavement performance monitoring for network management and life-cycle costing. *In Proceedings, 4th International Conference on Managing Pavements*. Durban, South Africa.

Rochas, C., Kuznecova, C. & Romagnoli, F. (2014). The concept of the system resilience within the infrastructure dimension. *application to a Latvian case. J Clean Prod 2014:1–11*.

Rohde, G. T. (1995). *Modelling Road Deterioration and maintenance effects in HDM-4. Pavement Strength in HDM-4 with FWDs.*

Rolt, J., and Parkman, C. C. (2000). Characterisation of Pavement Strength in HDM-III and Changes Adopted in HDM-4. *Presented at 10th International Conference on the Road Engineering Association of Asia and Australia, Tokyo, Japan.*

Rosa Dalla, F., Liu, L. & Gharaibeh, N. G. (2017). IRI Prediction Model for Use in Network-Level Pavement Management Systems. *Journal of Transportation Engineering, Part B: Pavements*, vol. 143(1), p. 04017001.

Saad, B. (2014). Analysis of excess water impact on the structural performance of flexible pavements. *International Journal of Pavement Engineering*.

Sayers, M. W. (1995). On the calculation of international roughness index from longitudinal road profile. *Transportation Research Record: Journal of the Transportation Research Board*.

Sayers, M. W., Gillespie, T. D. & Queiroz, C. a V. (1986). *The International Road Roughness Experiment - Establishing Correlation and a Calibration Standard for Measurements*. *The World Bank Technical Paper*.

Scherer, W. T. and Glagola, D. M. (1994). Markovian models for bridge maintenance management. *Journal of Transportation Engineering, 120(1):37–51*.

Schlotjes, M. R. (2013). The development of a diagnostic approach to predicting the probability of road pavement failure [online].Available at: http://etheses.bham.ac.uk/4528/2/Decl_IS_Schlotjes13PhD.pdf. Acessed 11TH May 2017

Schlotjes, M. R., Henning, T. F. & Burrow, M. P. (2011). Improved network understanding–a diagnostic approach to the risk of pavement failure. *In Proceedings of the 8th International Conference on Managing Pavement Assets, Santiago, Chile.*

Schoon, M. (2005). *A short historical overview of the concepts of resilience, vulnerability and adaptation (Working Paper W05-4). Workshop in Political Theory and Policy Analysis, Indiana University. (Working Paper W05-4). Workshop in Political Theory and Policy Analysis, Indiana University.*

Schwartz, C.W., and Carvalho, R. L. (2007). *Evaluation of Mechanistic-Empirical Design Procedure.*

Sen, R. (2012). *Impact of changes in fleet composition and axle loading on pavement profile characteristics*. Swinburne University of Technology, Melbourne, Australia.

Shafabakhsh, G. & Tanakizadeh, A. (2015). Investigation of loading features effects on resilient modulus of asphalt mixtures using Adaptive Neuro-Fuzzy Inference System. *Construction and Building Materials*.

Shahin, M. Y. (2005). *Pavement management for airports, roads, and parking lots: Second edition*. *Pavement Management for Airports, Roads, and Parking Lots: Second Edition*.

Sharabah, A., Setunge, S. and Zeephongsekul, P. (2006). Use of Markov chain for deterioration modeling and risk management of infrastructure assets. *International Conference on Information and Automation (pp. 384-389). IEEE.*

Sharp, K. G. (2009). *Guide to pavement technology: part 1: introduction to pavement technology*.

Shepherd, S. P. (2014a). A review of system dynamics models applied in transportation. *Transportmetrica B*.

Shepherd, S. P. (2014b). A review of system dynamics models applied in transportation. *Transportmetrica B*, vol. 2(2), pp. 83–105.

Sheridan, T. B. (2008). Risk, human error, and system resilience: Fundamental ideas. *Fundamental ideas. Psychology, 50(3), 418–426.*

Shire, I. (2018). *Participatory system dynamics modelling approach to safe and efficient staffing level management within hospital pharmacies*. (Doctoral dissertation) Loughborough University.

Shiyab, A. M. S. H. (2007). Optimum Use of the Flexible Pavement Condition Indicators in Pavement Management System. *Curtin University of Technology, Department of Civil Engineering.*

Shiyab, A. M. S. H., Al Fahim, H. A. & Nikraz, H. (2006). New Approaches for Estimation of Flexible Pavemen Remaining Life for the Use of PMS. *22nd ARRB Conference – Research into Practice, Canberra Australia, 2006*.

SOBANJO, J. O. (2011). State transition probabilities in bridge deterioration based on Weibull sojourn times. *Structure and Infrastructure Engineering, 7, 747-764.*

Sorum, N. G., Guite, T. & Martina, N. (2014). Pavement distress: a case study. *vol 3 (2014): 274-284.*

Sousa, J. B., Craus, J. & Carl, L. (1991). *Summary report on permanent deformation in asphalt concrete*.

Sterman, J. D. (2011). *Part I: Managing the Earth's life support systems: The emergence of sustainability science and transdisciplinarity*. *Sustainability Science: The Emerging Paradigm and the Urban Environment*.

Sterman, J. D. J. D. (2000). *Business dynamics: Systems thinking and modeling for a complex world with CD-ROM. Journal of the Operational Research Society*.

Stewart, M. G. & Deng, X. (2015). Climate Impact Risks and Climate Adaptation Engineering for Built Infrastructure. *ASCE-ASME Journal of Risk and Uncertainty in Engineering*

Systems, Part A: Civil Engineering, vol. 1(1), p. 04014001.

Sun, W., Bocchini, P. & Davison, B. D. (2018). Resilience metrics and measurement methods for transportation infrastructure: the state of the art. *Sustainable and Resilient Infrastructure*.

Sun, X. (2015). The impact of climate as expressed by Thornthwaite Moisture Index on residential footing design on expansive soil in Australia, (March).

Tamvakis, P. & Xenidis, Y. (2013). Comparative Evaluation of Resilience Quantification Methods for Infrastructure Systems. *Procedia - Social and Behavioral Sciences*. Elsevier B.V., vol. 74, pp. 339–348.

Taylor, M. A. P. & Philp, M. L. (2015). Investigating the impact of maintenance regimes on the design life of road pavements in a changing climate and the implications for transport policy. *Transport Policy*. Elsevier, vol. 41, pp. 117–135.

Taylor, M. A. P. & Philp, M. L. (2016). Beyond agriculture: A review of the Thornthwaite Moisture Index with respect to road pavements and other infrastructure applications. *International Journal of Sustainable Transportation*. Taylor & Francis, vol. 10(6), pp. 528–540.

The White House. (2014). *An economic analysis of transportation infrastructure investment. Retrieved from https://obamawhitehouse.archives.gov/sites/default/files/ docs/economic_analysis_of_transportation_investments. pdf*.

Thom, N. (2014). *Principles of Pavement Engineering, 2nd Edition*.

Thube, D. T. (2013). Highway development and management model (HDM-4): calibration and adoption for low-volume roads in local conditions. *International Journal ofPavement Engineering, 14 (1), 50–59. doi:10.1080/10298436.2011.606320.*

Toole, T. (2009). *Guide to asset management part 5H: performance modelling. Austroads, Austroads Publication No. AGAM05H-09*.

TRL (Transport Research Laboratory). (1993). *Overseas road note 31: A guide to the structural design of bitumen surfaced roads in tropical and sub-tropical countries*. England, UK.

United Nations. (2014). *Technical report*. Department of Economic and Social Affairs ,New York, US.

USDOC. (2013). *Economic impact of Hurricane Sandy: Potential economic activity lost and gained in New Jersey and New York. United States Department of Commerce (USDOC).*

USDOT. (2016). *National transportation statistics: Bureau of Transportation Statistics* [online].Available at: https://www.rita.dot.gov/bts/sites/rita.dot.gov.bts/files/ publications/transportation_statistics_annual_report/ index.html.

Valor. (2013). *Ministry of Public Works : Preparation and Operation of Pavement and Asset Management System*.

Venturini, S., Alonso, E. J., Khosa, B., Coudel, N., Ferreira, P., Judas, J. & Kerr, O. (2017). *UAE Climate Change Risks & Resilience : An overview of climate change risks to 12 key sectors*.

Vuong, B., Sharp, K. G., Baran, E. & Vertessy, N. J. (1994). Performance of a fine-grained marginal material under accelerated loading. *Proceedings - Conference of the Australian Road Research Board*.

Wang, J. & Yuan, H. (2016). System dynamics approach for investigating the risk effects on schedule delay in infrastructure projects. *Journal of Management in Engineering, 33(1), p.04016029.*

Watanatada, T., Harral, C., Paterson, W., Dhareshwar, A., Bhandari, A. & Tsunokawa, K. (1987). *Description of the HDM-III Model the Highway Design and Maintenance Standards Model*. *Design*.

Watson, R. T. (2001). *IPCC Special Report: Climate Change 200*.

Webb, A. B. (1986). *How to build a quality asphalt pavement*.

Weninger-Vycudil. (2008). Section based probabilistic performance prediction fiction or future? *Proceedings of the 3rd European Pavement and Asset Management Conference, 1–10. Retrieved from http://trid.trb.org/view.aspx?id=1084785*.

White, G. (2016). Challenges for Australian flexible airport pavements. *Australian Geomechanics Journal*.

White, G. & Embleton, K. (2015). Next Generation Binder for Airport Asphalt, (September).

Witczak, M.W., Zapata, C.E. and Houston, W. N. (2006). *Models Incorporated into the Current Enhanced Integrated Climatic Model for Used in Version 1.0 of the ME-PDG. NCHRP 9-23 Project Report*.

Wolff, E. W. (2005). *Understanding the past-climate history from Antarctica*.

Woods, D. & Wreathall, J. (2003). *Managing risk proactively: The emergence of resilience engineering (p. 2003). Columbus, GA: Ohio University*.

World Bank. (2013). *Building resilience: Integrating climate and disaster risk into development.*

Wuebbles, D. J. & Jain, A. K. (2001). Concerns about climate change and the role of fossil fuel use. *Fuel Processing Technology*, vol. 71(1–3), pp. 99–119.

Xu, Z. & Coors, V. (2012). Combining system dynamics model, GIS and 3D visualization in sustainability assessment of urban residential development. *Building and Environment*.

Yang, Y., Gao, X., Lin, W., Timm, D. H., Priest, A. L., Huber, G. A. & Andrewski, D. A. (2006). Perpetual pavement design in China. *Proceedings for the International Conference on Perpetual Pavements, Columbus, OH*, pp. 1–17.

Zareie, A., Amin, M. S. R. & Amador-Jiménez, L. E. (2016). Thornthwaite moisture index modeling to estimate the implication of climate change on pavement deterioration. *J. Transp. Eng., 10.1061 /(ASCE)TE.1943-5436.0000840, 04016007*.

Zhao, S., Liu, X. & Zhuo, Y. (2017). Hybrid Hidden Markov Models for resilience metrics in a dynamic infrastructure system. *Reliability Engineering and System Safety*. Elsevier Ltd, vol. 164(March), pp. 84–97.

Zobel, C. W. (2011). Representing perceived tradeoffs in defining disaster resilience. *Decision Support Systems*.

Zuo, G., Drumm, E. C. & Meier, R. W. (2006). Environmental Effects on the Predicted Service Life of Flexible Pavements. *Journal of Transportation Engineering*.

12. Appendix 1: Additional Data for Chapter 5

Table 12-1: List of assumptions of the study

Component	Assumption/decision	Chapter
Climate change model	Based on the highlighted literature, part of the research is to examine the emerging role of temperature in the context of climate change impact. Therefore, the research only considers the element of increases in temperature. More details are explained in sections 3.2.1 and 5.11.2	Chapter 2 page 24
Climate change model	UAE climate change model outcomes highlighted by Venturini et al. (2017) are applied in this research. More details are provided in sections 3.2.1and 5.10 .	Chapter 2 page 26
Climate change model	For the proposed research, the elements of temperature and Thornthwaite Moisture Index are selected. Further discussion is provided in sections 3.3.2 and 5.11.3.	Chapter 2 page 27
Pavement Structure	Highway pavements are classified into two groups, flexible and rigid. For this research, flexible pavement is selected as it is widely used in the UAE.	Chapter 2 page 28
Pavement Deterioration Distress Risks	Fwa (2006) classified distress into five groups, which are cracking, patching and potholes, surface deformation, surface defects and miscellaneous distresses. However, Rutting and cracking of asphaltic pavements are the two most crucial elements of distress that present overall pavement condition. Rutting and cracking are fundamental modes of deterioration	Chapter 2 page 43
Pavement Performance	There are four general categories of pavement condition used in maintenance planning for pavements: Surface distress (Pavement Condition Index – PCI), Ride quality (International Roughness Index – IRI), Structural capacity (Falling Weight Deflectometer – FWD) and Friction (Skid resistance). IRI and PCI were selected for this research	Chapter 2 page 43
Resilience	Hughes and Healy (2014) mentioned how important the four domains (organisational, engineering, economic and social) of system resilience are. Nevertheless, they concluded that focusing on the area of engineering and organisational system resilience is sufficient in terms of the transport system. In this study, resilience is viewed in terms of the engineering dimension only	Chapter 2 page 56
Deterministic Model	Anyala, Odoki and Baker (2014) and Amin (2015) stated that there are different categories of deterministic models, such as mechanistic-empirical models, mechanistic models and regression or empirical models. However, empirical models are sufficient to study the impact of climate change through the HDM-4 model. Further details are presented in Chapter 5 section 5.11 and Chapter 6 section 6.4.	Chapter 2 page 60
Markov Chain Process	Abaza (2016) stated that the most popular model could be built based on either homogeneous or	Chapter 2 page 64

	heterogeneous type. For this research, the selection of an homogeneous approach for Markov chain analysis is presented in Chapter 7 section 7.2.2	
Markov Chain Process	T The defined transition probability matrix is either a progressive TPM or a sequential TPM . The sequential TPM is applied in this research. More details are provided in Chapter 7.	Chapter 2 page 67
Simulation Models	Various techniques exist to simulate and model the behaviour of an actual system, such as system dynamics (SD), discrete-event simulation (DES) and agent-based simulation (ABS). The author has considered only Vensim as the software package to build the SD models	Chapter 2 page 74
Measure resilience	The resilience triangle theory is applied in this research to study the measured pavement infrastructure resilience loss through the concept of pavement performance.	Chapter 2 page 76
Pavement Temperature Model	Moreover, Hassan et al. (2004) studied the pavement highest temperature at a depth of 20 mm below the ground surface for 445 days of collected data. The study took place in Oman, which is considered to have similar weather conditions to the UAE. Hassan et al.'s (2004) model is used in this research to determine the maximum pavement temperature. Further explanation is provided in Chapter 5 section 5.11.	Chapter 3 page 82
Thornthwaite Moisture Index model for pavements	Equations proposed by Mather (1974) and Witczak, Zapata and Houston (2006) are used to build a new TMI value that matches UAE conditions	Chapter 3 page 85
Change in Rutting (ΔRDS)	For Initial Densification Factor, For this research, an assumption was made that the roads should be designed and built according to standards and specifications with the accepted construction quality. Therefore, the parameter of quality of construction was not considered as a part of the rutting equations.	Chapter 3 page 96
Change in Rutting (ΔRDS)	For Initial Densification Factor , material properties such as Voids in Mix (VIM) and Softening Point (SP) of binder are applied in this research	Chapter 3 page 96
Change in Rutting (ΔRDS)	For Surface Wear Factor, The UAE is located in a hot climate area; therefore, this factor is not considered in the proposed equation. Moreover, Anyala (2011) also did not consider such elements in his model. Therefore, for this research, the study focuses on the UAE, a country with hot climate conditions.	Chapter 3 page 97
Change in Rutting (ΔRDS)	For Structural Deformation Factor, Anyala (2011) did not consider the cracking factor directly in the equation as he focused more on the main components that affect the strength and lead to cracking, such as pavement strength and traffic loading. The author of this research agrees with Anyala's (2011) approach and similar assumptions are included in the proposed model.	Chapter 3 page 97
Change in Rutting (ΔRDS)	For Plastic Deformation Factor, In this research, the assumption was made that most of the roads in the UAE are flat; thus, the gradient element is not considered in the proposed equation of change in	Chapter 3 page 98

	rutting. However, properties of asphalt mix such as asphalt binder viscosity are deemed important	
Change in Rutting (ΔRDS)	For Prediction of Softening Point Value, Anyala, Odoki and Baker (2014) considered softening point in their research model in conjunction with age (AGE) of the asphalt layer. The author follows their proposed equation. The reason behind this is that there are no recorded data that represent the softening point with respect to pavement age in either the Ministry of Public Works or Al Ain City Municipality (Valor 2013)	Chapter 3 page 100
Change in Rutting (ΔRDS)	For Voids in Mix (VIM), Anyala, Odoki and Baker (2014) considered Voids in Mix (VIM in their research model in conjunction with age (AGE) of the asphalt layer. The author follows their proposed equation. The reason behind this is that there are no recorded data that represent the Voids in Mix (VIM) with respect to pavement age in either the Ministry of Public Works or Al Ain City Municipality (Valor 2013)	Chapter 3 page 102
Risk Analysis for Pavement Failure	. There are different methods for risk analysis, deterministic (on numerical computations) and qualitative (based on the subjective system). For this research, the deterministic technique is adopted	Chapter 3 page 107
Delivery of Scope	The study focuses on United Arab Emirates roads taking into consideration only federal roads and highways which are under the jurisdiction of the UAE Ministry of Public Works. Local authority roads are not included, except Al Ain City Municipality roads. The research investigates the main roads with a flexible pavement type. Other types such as composite or concrete are not part of the research scope. The assumption is made that, in general, there is one standard policy and specification for designing and constructing the roads and highways. And the built roads are delivered according to the UAE design standards. The assumption is made that maintenance activities are almost the same across all federal roads. The source of the pavement condition data (IRI, cracking, rutting), Annual Average Daily Traffic (AADT), pavement thickness, pavement age and heavy vehicle speed is the UAE Ministry of Public Works. Three sets of data for consecutive years are available. The data will be used to determine the modified HDM-4, Transition Probability Matrix and Pavement Condition Index. This process is similar to the studies conducted by Anyala (2011) and Abaza (2016). Weather data such as average, minimum and maximum mean monthly temperature and evaporation are collected from the National Centre of Meteorology and Seismology. This process is similar to the study conducted by Anyala (2011). Pavement Condition Index (PCI) data are collected from Al Ain City Municipality. The future rises in UAE temperature are estimated from the forecasting model developed by the Abu Dhabi environmental agency (Venturini et al. 2017), based on three different scenarios, 2020, 2040 and 2060.	Chapter 4 page 123

Maximum pavement temperature is developed based on three future climate change scenarios and calculated accordingly. This process is similar to the study conducted by Hassan et al. (2004).

Determination of the change in roughness is structured based on the modified HDM-4 model. SPSS tools are applied to the model to define the relationship and variable coefficients between dependent and independent variables. A similar method was used by Mubaraki (2010) and Anyala (2011).

The relationship between PCI and IRI is modelled using SPSS. A similar method was used by Park, Thomas and Lee (2007).

The modified equations of change in roughness based on HDM-4 with new coefficients are applied to build a Transition Probability Matrix with different climate change scenarios (2013,2020, 2040 and 2060). The Transition Probability Matrix is delivered using @RISK software. The author modified the approach carried out by Abaza (2016).

For building the Markov chain model, the pavement network in the UAE is assumed to be in excellent condition and classification of pavement condition is made according to IRI classification. A similar approach was defined by the UAE Ministry of Public Works. However, the author modified the classification of condition states based on the literature.

Determination of Markovian deterioration curve based on IRI and PCI with different climate change scenarios (2013,2020, 2040 and 2060) is made. A similar method was used by Arimbi (2015).

Building the system dynamics model through casual loop diagram and stock and flow using variables from the modified HDM-4 model (change in roughness). Modified equations and coefficients are applied to cement the relationship between dynamic variables in the Vensim software. This process is similar to the studies conducted by Mallick et al. (2015) and Rashedi (2016).

Deterioration curve modelling is based on the proposed system dynamics model of PCI and IRI.

Investigation of the risk associated with pavement failure under the impact of climate change is determined from the literature and examined by the survey. Results are analysed using regression method and probability method. This process is similar to the study conducted by Jang (2011).

Risk is incorporated into the built system dynamics methods with different scenarios and the deterioration curve is modelled under different climate change scenarios. This process is similar to the study conducted by Jang (2011).

- Measuring resilience loss of the pavement network in the UAE under different climate change scenarios and different risks by using deterioration curves generated from both system dynamics model and Markov chain model. This process is similar to the

	studies conducted by Bruneau et al. (2003) and Sun, Bocchini and Davison (2018).	
Data	Anyala (2011) also focused on the road used by heavy vehicles is his study. A similar approach is followed in this research.	Chapter 5 page 142
Data	The author was able to estimate the value of IRI, rutting and cracking based on average reading of 5000 meters (more details are provided in Chapter 6 section 6.3).	Chapter 5 page 144
Data	Heavy Vehicle Speed, For this research, the worst case scenario is chosen, which is the minimum travelling speed (heavily loaded vehicles). More details are provided in Chapter 6 section 6.2.2.	Chapter 5 page 151
Data	Data weathering, There are 75 automatic stations for data collection. For this research, Al Ain Airport station was the selected station	Chapter 5 page 154
Data	The selection of the highest air temperature recorded in the UAE was made to develop the model based on the worst case scenarios. Therefore, a maximum air temperature of 50.4 recorded in Al Ain in June 2016 was applied for this research.	Chapter 5 page 159
Data	For TMI, The following results were selected as inputs of TMI value for the three future scenarios as minimum for 2020, average for 2040 and maximum for 2040-2079. More details are provided in Chapter 6 section 6.2.4 and 6.4.	Chapter 5 page 159
System Dynamics	It was highlighted in previous sub-sections that there are more than 13 main risk variables associated with pavement failure (Chapter 2); however, only seven main risk variables are used in the system dynamics model to match the modified HDM-4 model to determine change in roughness. These variables are pavement thickness, pavement temperature, pavement ageing, traffic loading, the speed of heavy vehicles, change in rutting and cracking. New stock and flow diagrams were introduced to include the risk variables' impact. Once all these sub-models were united with the associated risks into one model, the model was run for 20 years to project the deterioration curve on pavement condition based on two performance indicators, PCI and IRI.	Chapter 9 page 319
Measure resilience	It was assumed that the pavement network performance is 100%, which indicates that the PCI value is 100 (based on PCI scale). The total area of performance is a result of multiplying PCI value with pavement service life (in years). Therefore, 'Q(t)full', which is system functionality before the degradation in the pavement network system, is equal to 2000 m^2.	Chapter 9 page 356

Summary of major roads under the jurisdiction of the Ministry of Public Works in the UAE

Table 12-2 : The major roads under the jurisdiction of the Ministry of Public Works in the UAE

Road	Direction
Ittihad road	RAK
Ittihad road	SHA
Manama- RAK Airport	Rak Airport
Manama- RAK Airport	Manama
RAK Airport-Sha'am	Sha'am
RAK Airport-Sha'am	Rak Airport
Sha'am - Oman	
Sheik Mohammed Bin Zayed	RAK
Sheik Mohammed Bin Zayed	SHA
Dhaid - Madam	Madam
Dhaid - Madam	Dhaid
Madam - Shiweb	Shiweb
Madam - Shiweb	Madam
Umm Al Quwaim - Dhaid	Dhaid
Umm Al Quwaim - Dhaid	Umm Al Quwaim
Maliha Rd - Fallah Al Muala Rd	RAK
Maliha Rd - Fallah Al Muala Rd	SHA
Fallah Al Muala Rd - Shk Mohammed Bin Zayed Rd	RAK
Fallah Al Muala Rd - Shk Mohammed Bin Zayed Rd	SHA
Sheikh Khalifa Rd	FUJ
Sheikh Khalifa Rd	DUB
Tawyeen - Dibba	Dibba
Tawyeen - Dibba	Tawyeen
Sharjah - Dhaid	Dhaid

Sharjah - Dhaid	SHA
Dhaid - Masafi	Dhaid
Dhaid - Masafi	Masafi
Masafi - Dibba (from Dibba to Ghona Bridge)	Masafi
Masafi - Dibba (from Dibba to Ghona Bridge)	Dibba
Masafi - Dibba (from Ghona Bridge to Masafi)	
Masafi - Fujairah	FUJ
Masafi - Fujairah	Masafi
Khor Fakkan - Dibba	Khor Fakkan
Khor Fakkan - Dibba	Dibba
Fujairah - Khor Fakkan	Fujairah
Fujairah - Khor Fakkan	Khor Fakkan
Fujairah - Oman	Oman
Fujairah - Oman	FUJ
Fili link	
Dhaid Ring Road	
Dhaid Ring Road	
Masfut link	
Siji link	

A summary of the length of roads used in the study

Table 12-3: The roads to be investigated selected based on the data availability

N	Code	Road	Direction	Length [m]
1	E.11	E-11. Ittihad road	RAK	47,560
2	E.11	E-11. Ittihad road	SHA	47,650
3	E18.1	E-18. Manama- RAK Airport	Rak Airport	41,640

4	E18.1	E-18. Manama- RAK Airport	Manama	41,550
5	E18.2	E-18. RAK Airport-Sha'am	Sha'am	53,360
6	E18.2	E-18. RAK Airport-Sha'am	Rak Airport	53,480
7	E311	E-311. Sheik Mohammed Bin Zayed	SHA	70,950
8	E55.1	E-55. Dhaid - Madam	Madam	48,220
9	E55.1	E-55. Dhaid - Madam	Dhaid	48,230
10	E55.2	E-55. Madam - Shiweb	Shiweb	20,480
11	E55.2	E-55. Madam - Shiweb	Madam	20,460
12	E55.3	E-55. Umm Al Quwaim - Dhaid	Dhaid	49,330
13	E55.3	E-55. Umm Al Quwaim - Dhaid	Umm Al Quwaim	49,330
14	E611.1	E-611. Maliha Rd - Fallah Al Muala Rd	RAK	24,610
15	E611.1	E-611. Maliha Rd - Fallah Al Muala Rd	SHA	24,580
16	E611.2	E-611. Fallah Al Muala Rd - Shk Mohammed Bin Zayed Rd	RAK	15,690
17	E611.2	E-611. Fallah Al Muala Rd - Shk Mohammed Bin Zayed Rd	SHA	15,360
18	E84	E-84. Sheikh Khalifa Rd	FUJ	42,480
19	E84	E-84. Sheikh Khalifa Rd	DUB	41,710
20	E88.1	E-88. Sharjah - Dhaid	Dhaid	35,350
21	E88.1	E-88. Sharjah - Dhaid	SHA	35,390
22	E88.2	E-88. Dhaid - Masafi	Dhaid	31,390
23	E88.2	E-88. Dhaid - Masafi	Masafi	31,370
24	E89.1	E-89. Masafi - Dibba (from Dibba to Ghona Bridge)	Masafi	16,940
25	E89.1	E-89. Masafi - Dibba (from Dibba to Ghona Bridge)	Dibba	16,910
26	E89.3	E-89. Masafi - Fujairah	FUJ	27,940
27	E89.3	E-89. Masafi - Fujairah	Masafi	27,970
28	E99.1	E-99. Khor Fakkan - Dibba	Khor Fakkan	33,830

29	E99.2	E-99. Fujairah - Khor Fakkan	Fujairah	20,820
30	E99.3	E-99. Fujairah - Oman	Oman	15,580
31	Siji link	Siji link		9,930

Roads Classification Group

Table 12-4: Roads classified as forward group 2013

N	Road Code	Road	Direction	Length [m]	Data collection Approach
2	E.11	Ittihad road	SHA	47,650	Forward
4	E18.1	Manama- RAK Airport	Manama	41,550	Forward
6	E18.2	RAK Airport-Sha'am	Rak Airport	53,480	Forward
9	E55.1	Dhaid - Madam	Dhaid	48,230	Forward
11	E55.2	Madam - Shiweb	Madam	20,460	Forward
13	E55.3	Umm Al Quwaim - Dhaid	Umm Al Quwaim	49,330	Forward
15	E611.1	Maliha Rd - Fallah Al Muala Rd	SHA	24,580	Forward
17	E611.2	Fallah Al Muala Rd - Shk Mohammed Bin Zayed Rd	SHA	15,360	Forward
19	E84	Sheikh Khalifa Rd	DUB	41,710	Forward
21	E88.1	Sharjah - Dhaid	SHA	35,390	Forward
23	E88.2	Dhaid - Masafi	Masafi	31,370	Forward
25	E89.1	Masafi - Dibba (from Dibba to Ghona Bridge)	Dibba	16,910	Forward
27	E89.3	Masafi - Fujairah	Masafi	27,970	Forward

Table 12-5:Roads classified as backward group 2013

N	Road Code	Road	Direction	Length [m]	Data collection Approach
1	E.11	Ittihad road	RAK	47,560	Backward
3	E18.1	Manama- RAK Airport	Rak Airport	41,640	Backward
5	E18.2	RAK Airport-Sha'am	Sha'am	53,360	Backward
7	E311	Sheik Mohammed Bin Zayed	SHA	70,950	Backward
8	E55.1	Dhaid - Madam	Madam	48,220	Backward
10	E55.2	Madam - Shiweb	Shiweb	20,480	Backward
12	E55.3	Umm Al Quwaim - Dhaid	Dhaid	49,330	Backward
14	E611.1	Maliha Rd - Fallah Al Muala Rd	RAK	24,610	Backward
16	E611.2	Fallah Al Muala Rd - Shk Mohammed Bin Zayed Rd	RAK	15,690	Backward

18	E84	Sheikh Khalifa Rd	FUJ	42,480	Backward
20	E88.1	Sharjah - Dhaid	Dhaid	35,350	Backward
22	E88.2	Dhaid - Masafi	Dhaid	31,390	Backward
24	E89.1	Masafi - Dibba (from Dibba to Ghona Bridge)	Masafi	16,940	Backward
26	E89.3	Masafi - Fujairah	FUJ	27,940	Backward
28	E99.1	Khor Fakkan - Dibba	Khor Fakkan	33,830	Backward
29	E99.2	Fujairah - Khor Fakkan	Fujairah	20,820	Backward
30	E99.3	Fujairah - Oman	Oman	15,580	Backward
31	Siji link	Siji link		9,930	Backward

IRI value for backward direction-based data collection 2013

Table 12-6: Example of mean IRI value for backward direction based data collection 2013

N	Road Code	Road	RIa
1	E.11	Ittihad road	1.16
3	E18.1	Manama- RAK Airport	0.98
5	E18.2	RAK Airport-Sha'am	1.73
7	E311	Sheik Mohammed Bin Zayed	0.99
8	E55.1	Dhaid - Madam	1.31
10	E55.2	Madam - Shiweb	1.51
12	E55.3	Umm Al Quwaim - Dhaid	1.16
14	E611.1	Maliha Rd - Fallah Al Muala Rd	0.99
16	E611.2	Fallah Al Muala Rd - Shk Mohammed Bin Zayed Rd	1.41
18	E84	Sheikh Khalifa Rd	0.80
20	E88.1	Sharjah - Dhaid	1.20
22	E88.2	Dhaid - Masafi	1.18
24	E89.1	Masafi - Dibba (from Dibba to Ghona Bridge)	1.81
26	E89.3	Masafi - Fujairah	1.42
28	E99.1	Khor Fakkan - Dibba	1.60
29	E99.2	Fujairah - Khor Fakkan	1.33
30	E99.3	Fujairah - Oman	1.61

Annual Daily Traffic (AADT)

Table 12-7: Average daily traffic for backward data collection roads 2013

Backward data collection roads					Average Daily Traffic		
N	**Road Code**	**Road**	**Direction**	**Length [m]**	**A.D.T**	**A.D.T Heavy**	**% Heavy Vehicles**
1	E.11	Ittihad road	RAK	47,560	18351	918	5

3	E18.1	Manama- RAK Airport	Rak Airport	41,640	4025	1146	28
5	E18.2	RAK Airport-Sha'am	Sha'am	53,360	4025	1006	25
7	E311	Sheik Mohammed Bin Zayed	SHA	70,950	65994	4620	7
8	E55.1	Dhaid - Madam	Madam	48,220	6172	123	2
10	E55.2	Madam - Shiweb	Shiweb	20,480	2956	207	7
12	E55.3	Umm Al Quwaim - Dhaid	Dhaid	49,330	4533	91	2
14	E611.1	Maliha Rd - Fallah Al Muala Rd	RAK	24,610	22883	2975	13
16	E611.2	Fallah Al Muala Rd - Shk Mohammed Bin Zayed Rd	RAK	15,690	4880	1074	22
18	E84	Sheikh Khalifa Rd	FUJ	42,480	8332	333	4
20	E88.1	Sharjah - Dhaid	Dhaid	35,350	7931	1190	15
22	E88.2	Dhaid - Masafi	Dhaid	31,390	7078	991	14
24	E89.1	Masafi - Dibba (from Dibba to Ghona Bridge)	Masafi	16,940	2743	82	3
26	E89.3	Masafi - Fujairah	FUJ	27,940	6397	768	12
28	E99.1	Khor Fakkan - Dibba	Khor Fakkan	33,830	14292	429	3
29	E99.2	Fujairah - Khor Fakkan	Fujairah	20,820	17085	683	4
30	E99.3	Fujairah - Oman	Oman	15,580	5249	401	7
31	Siji link	Siji link		9,930	2015	584	29

Table 12-8: Average daily traffic for forward data collection roads 2013

Forward data collection ROADS					Average Daily Traffic		
N	**Road Code**	**Road**	**Direction**	**Length [m]**	**A.D.T**	**A.D.T Heavy**	**% Heavy Vehicles**
2	E.11	Ittihad road	SHA	47,650	18344	1101	6
4	E18.1	Manama- RAK Airport	Manama	41,550	4092	275	6
6	E18.2	RAK Airport-Sha'am	Rak Airport	53,480	4025	1146	28
9	E55.1	Dhaid - Madam	Dhaid	48,230	6314	126	2
11	E55.2	Madam - Shiweb	Madam	20,460	3057	214	7
13	E55.3	Umm Al Quwaim - Dhaid	Umm Al Quwaim	49,330	4583	92	2
15	E611.1	Maliha Rd - Fallah Al Muala Rd	SHA	24,580	23007	3451	15
17	E611.2	Fallah Al Muala Rd - Shk Mohammed Bin Zayed Rd	SHA	15,360	4754	666	14
19	E84	Sheikh Khalifa Rd	DUB	41,710	8946	179	2
21	E88.1	Sharjah - Dhaid	SHA	35,390	7682	768	10
23	E88.2	Dhaid - Masafi	Masafi	31,370	7656	995	13

25	E89.1	Masafi - Dibba (from Dibba to Ghona Bridge)	Dibba	16,910	3049	30	1
27	E89.3	Masafi - Fujairah	Masafi	27,970	6388	575	9

Table 12-9: Annual Daily Traffic (AADT) data for Forward data collection roads

Forward data collection ROADS			**Average Daily Traffic**			**EASL**				
N	**Road Code**	**Road**	**A.D.T**	**A.D.T Heavy**	**% Heavy Vehicles**	**LEF**	**DD**	**Growth factor**	**EASL**	**EASL m/lane**
2	E.11	Ittihad road	18344	1101	6	6.5	0.7	1	1827888	**1.83**
4	E18.1	Manama- RAK Airport	4092	275	6	6.5	0.7	1	407747	**0.41**
6	E18.2	RAK Airport-Sha'am	4025	1146	28	6.5	0.7	1	1871665	**1.87**
9	E55.1	Dhaid - Madam	6314	126	2	6.5	0.7	1	209720	**0.21**
11	E55.2	Madam - Shiweb	3057	214	7	6.5	0.7	1	355384	**0.36**
13	E55.3	Umm Al Quwaim - Dhaid	4583	92	2	6.5	0.7	1	152224	**0.15**
15	E611.1	Maliha Rd - Fallah Al Muala Rd	23007	3451	15	6.5	0.7	1	5731331	**5.73**
17	E611.2	Fallah Al Muala Rd - Shk Mohammed Bin Zayed Rd	4754	666	14	6.5	0.7	1	1105329	**1.11**
19	E84	Sheikh Khalifa Rd	8946	179	2	6.5	0.7	1	297141	**0.30**
21	E88.1	Sharjah - Dhaid	7682	768	10	6.5	0.7	1	1275788	**1.28**
23	E88.2	Dhaid - Masafi	7656	995	13	6.5	0.7	1	1652911	**1.65**
25	E89.1	Masafi - Dibba (from Dibba to Ghona Bridge)	3049	30	1	6.5	0.7	1	50636	**0.05**
27	E89.3	Masafi - Fujairah	6388	575	9	6.5	0.7	1	954798	**0.95**
Heavy Vehicle L.E.F=6.5										
W18=DD*LD*LEF*365*ADT(Heavy)										

Table 12-10: Annual daily traffic (AADT) data for backward data collection roads

Backward data collection			**Average Daily Traffic**			**EASL**				
N	**Road Code**	**Road**	**A.D.T**	**A.D.T Heavy**	**% Heavy Vehicles**	**LEF**	**DD**	**Growth factor**	**EASL**	**EASL m/lane**
1	E.11	Ittihad road	18351	918	5	6.5	0.7	1	1523821	**1.52**

3	E18.1	Manama- RAK Airport	4025	1146	28	6.5	0.7	1	1871665	**1.87**
5	E18.2	RAK Airport-Sha'am	4025	1006	25	6.5	0.7	1	1671130	**1.67**
7	E311	Sheik Mohammed Bin Zayed	65994	4620	7	6.5	0.7	1	7671967	**7.67**
8	E55.1	Dhaid - Madam	6172	123	2	6.5	0.7	1	205003	**0.21**
10	E55.2	Madam - Shiweb	2956	207	7	6.5	0.7	1	343642	**0.34**
12	E55.3	Umm Al Quwaim - Dhaid	4533	91	2	6.5	0.7	1	150564	**0.15**
14	E611.1	Maliha Rd - Fallah Al Muala Rd	22883	2975	13	6.5	0.7	1	4940382	**4.94**
16	E611.2	Fallah Al Muala Rd - Shk Mohammed Bin Zayed Rd	4880	1074	22	6.5	0.7	1	1782981	**1.78**
18	E84	Sheikh Khalifa Rd	8332	333	4	6.5	0.7	1	553495	**0.55**
20	E88.1	Sharjah - Dhaid	7931	1190	15	6.5	0.7	1	1975711	**1.98**
22	E88.2	Dhaid - Masafi	7078	991	14	6.5	0.7	1	1645670	**1.65**
24	E89.1	Masafi - Dibba (from Dibba to Ghona Bridge)	2743	82	3	6.5	0.7	1	136663	**0.14**
26	E89.3	Masafi - Fujairah	6397	768	12	6.5	0.7	1	1274858	**1.27**
28	E99.1	Khor Fakkan - Dibba	14292	429	3	6.5	0.7	1	712063	**0.71**
29	E99.2	Fujairah - Khor Fakkan	17085	683	4	6.5	0.7	1	1134957	**1.13**
30	E99.3	Fujairah - Oman	5249	401	7	6.5	0.7	1	610209	**0.61**
31	Siji link	Siji link	2015	584	29	6.5	0.7	1	970459	**0.97**

Example of Speed measurements for E88 Al Dhaid - Masafi

Table 12-11: Example of speed measurements for E88 Al Dhaid - Masafi

E88 Al Dhaid - Masafi			
Date	**Time**	**Speed(km/h)**	**Axle**
7/8/2013	0:00:13	56	6
7/8/2013	0:00:24	65	6
7/8/2013	0:00:26	80	6
7/8/2013	0:00:42	87	6
7/8/2013	0:01:43	89	6
7/8/2013	0:01:50	81	6
7/8/2013	0:01:53	58	6
7/8/2013	0:03:28	51	6
7/8/2013	0:03:30	59	6
7/8/2013	0:03:35	55	6
7/8/2013	0:04:10	76	6
7/8/2013	0:05:31	74	6
7/8/2013	0:07:18	75	6
7/8/2013	0:07:22	66	6

7/8/2013	0:07:43	69	6
7/8/2013	0:08:13	72	6
7/8/2013	0:08:40	69	6
7/8/2013	0:09:58	86	6
7/8/2013	0:11:19	63	6
7/8/2013	0:12:50	68	6
7/8/2013	0:12:53	67	6
7/8/2013	0:12:59	73	6
7/8/2013	0:13:51	70	6
7/8/2013	0:13:45	65	6
7/8/2013	0:13:50	73	6
7/8/2013	0:14:49	75	6
7/8/2013	0:15:13	73	6
7/8/2013	0:15:40	70	6
7/8/2013	0:15:44	65	6
7/8/2013	0:16:17	53	6
7/8/2013	0:16:34	69	6
		69	

Asphaltic age for roads based on Data collection

Table 12-12: Asphaltic age for roads based on data collection (backward approach)

N	Road Code	Road	construction date	Major rehabilitation	Road age
1	E.11	Ittihad road	2006	no record	11
3	E18.1	Manama- RAK Airport	2006	no record	11
5	E18.2	RAK Airport-Sha'am	2005	no record	12
7	E311	Sheik Mohammed Bin Zayed	2011	no record	6
8	E55.1	Dhaid - Madam	2001	no record	16
10	E55.2	Madam - Shiweb	2001	no record	16
12	E55.3	Umm Al Quwaim - Dhaid	2001	no record	16
14	E611.1	Maliha Rd - Fallah Al Muala Rd	2008	no record	9
16	E611.2	Fallah Al Muala Rd - Shk Mohammed Bin Zayed Rd	2008	no record	9
18	E84	Sheikh Khalifa Rd	2012	no record	5
20	E88.1	Sharjah - Dhaid	2002	no record	15
22	E88.2	Dhaid - Masafi	2002	no record	15
24	E89.1	Masafi - Dibba (from Dibba to Ghona Bridge)	2013	no record	9
26	E89.3	Masafi - Fujairah	1999	no record	18

28	E99.1	Khor Fakkan - Dibba	2000	no record	17
29	E99.2	Fujairah - Khor Fakkan	2000	no record	17
30	E99.3	Fujairah - Oman	2003	no record	19

Table 12-13: Asphaltic age for roads based on data collection (forward approach)

N	Road Code	Road	construction date	Major rehabilitation	road age
2	E.11	Ittihad road	2006	no record	11
4	E18.1	Manama- RAK Airport	2006	no record	11
6	E18.2	RAK Airport-Sha'am	2005	no record	12
9	E55.1	Dhaid - Madam	2001	no record	16
11	E55.2	Madam - Shiweb	2001	no record	16
13	E55.3	Umm Al Quwaim - Dhaid	2001	no record	16
15	E611.1	Maliha Rd - Fallah Al Muala Rd	2008	no record	9
17	E611.2	Fallah Al Muala Rd - Shk Mohammed Bin Zayed Rd	2008	no record	9
19	E84	Sheikh Khalifa Rd	2012	no record	5
21	E88.1	Sharjah - Dhaid	2002	no record	15
23	E88.2	Dhaid - Masafi	2003	no record	14
25	E89.1	Masafi - Dibba (from Dibba to Ghona Bridge)	2013	no record	9
27	E89.3	Masafi - Fujairah	1995	no record	22

Predicted air temperature for the UAE based on three different scenarios (2020, 2040, 2060-2079)

Table 12-14: Predicted air temperature for the UAE based on three different scenarios (2020, 2040, 2060-2079)

Month	**Max month Temp. Current (2010)**	**The highest reading ever in UAE**	**2020**	**2040**	**2060-2079**	**2010**	**2060**	**2080**	**2060-2080**
			Increase by 1°C	**1.5 and 2°C**	**2 and 3°C**	**Tmax**	**Tmax**	**Tmax**	**Tmax**
			Assume =1°C	**Assume =2°C**	**Assume = 3°C**				
Month 6-2017		**50.4**	**51.4**	**52.4**	**53.4**	**<u>69.6</u>**	**<u>71.0</u>**	**<u>72.3</u>**	**<u>73.6</u>**
Jan	30.0	50.4	31.0	32.0	33.0	42.7	44.0	45.4	46.7
Feb	35.1	50.4	36.1	37.1	38.1	49.5	50.8	52.1	53.4
Mar	39.8	50.4	40.8	41.8	42.8	55.7	57.0	58.3	59.6
Apr	43.0	50.4	44.0	45.0	46.0	59.9	61.2	62.5	63.8
May	45.6	50.4	46.6	47.6	48.6	63.3	64.6	65.9	67.3
Jun	48.5	50.4	49.5	50.5	51.5	67.1	68.5	69.8	71.1
Jul	49.2	50.4	50.2	51.2	52.2	68.1	69.4	70.7	72.0
Aug	46.7	50.4	47.7	48.7	49.7	64.8	66.1	67.4	68.7
Sep	45.2	50.4	46.2	47.2	48.2	62.8	64.1	65.4	66.7

Oct	41.3	50.4	42.3	43.3	44.3	57.6	59.0	60.3	61.6
Nov	34.4	50.4	35.4	36.4	37.4	48.5	49.9	51.2	52.5
Dec	31.3	50.4	32.3	33.3	34.3	44.4	45.8	47.1	48.4

Development of Binder Softening Point (SP) for Data collection

Table 12-15: Development of binder softening point (SP) for data collection backward approach

N	Road Code	Road	Construction date	Major rehabilitation	Road age	a1	a2	Softening point
1	E.11	Ittihad road	2006	N/A	11	2.5	70.5	76.5
3	E18.1	Manama- RAK Airport	2006	N/A	11	2.5	70.5	76.5
5	E18.2	RAK Airport-Sha'am	2005	N/A	12	2.5	70.5	76.8
7	E311	Sheik Mohammed Bin Zayed	2011	N/A	6	2.5	70.5	75.0
8	E55.1	Dhaid - Madam	2001	N/A	16	2.5	70.5	77.5
10	E55.2	Madam - Shiweb	2001	N/A	16	2.5	70.5	77.5
12	E55.3	Umm Al Quwaim - Dhaid	2001	N/A	16	2.5	70.5	77.5
14	E611.1	Maliha Rd - Fallah Al Muala Rd	2008	N/A	9	2.5	70.5	76.0
16	E611.2	Fallah Al Muala Rd - Shk Mohammed Bin Zayed Rd	2008	N/A	9	2.5	70.5	76.0
18	E84	Sheikh Khalifa Rd	2012	N/A	5	2.5	70.5	74.6
20	E88.1	Sharjah - Dhaid	2002	N/A	15	2.5	70.5	77.3
22	E88.2	Dhaid - Masafi	2002	N/A	15	2.5	70.5	77.3
24	E89.1	Masafi - Dibba (from Dibba to Ghona Bridge)	2013	N/A	4	2.5	70.5	74.0
26	E89.3	Masafi - Fujairah	1999	N/A	18	2.5	70.5	77.8
28	E99.1	Khor Fakkan - Dibba	2000	N/A	17	2.5	70.5	77.6
29	E99.2	Fujairah - Khor Fakkan	2000	N/A	17	2.5	70.5	77.6
30	E99.3	Fujairah - Oman	2003	N/A	14	2.5	70.5	77.2

Table 12-16: Development of binder softening point (SP) for data collection forward

N	Road Code	Road	Construction date	Major rehabilitation	Road age	a1	a2	Softening point
2	E.11	Ittihad road	2006	N/A	11	2.52	70.5	76.5
4	E18.1	Manama- RAK Airport	2006	N/A	11	2.52	70.5	76.5
6	E18.2	RAK Airport-Sha'am	2005	N/A	12	2.52	70.5	76.8
9	E55.1	Dhaid - Madam	2001	N/A	16	2.52	70.5	77.5
11	E55.2	Madam - Shiweb	2001	N/A	16	2.52	70.5	77.5
13	E55.3	Umm Al Quwaim - Dhaid	2001	N/A	16	2.52	70.5	77.5
15	E611.1	Maliha Rd - Fallah Al Muala Rd	2008	N/A	9	2.52	70.5	76.0
17	E611.2	Fallah Al Muala Rd - Shk Mohammed Bin Zayed Rd	2008	N/A	9	2.52	70.5	76.0
19	E84	Sheikh Khalifa Rd	2012	N/A	5	2.52	70.5	74.6
21	E88.1	Sharjah - Dhaid	2002	N/A	15	2.52	70.5	77.3
23	E88.2	Dhaid - Masafi	2003	N/A	14	2.52	70.5	77.2
25	E89.1	Masafi - Dibba (from Dibba to Ghona Bridge)	2013	N/A	4	2.52	70.5	74.0
27	E89.3	Masafi - Fujairah	1995	N/A	22	2.52	70.5	78.3

Development of Voids in Mix (VIM) based on Data

Table 12-17: Development of voids in mix (VIM) based on data collection backward

N	Road Code	Road	Construction date	Major rehabilitation	Road age	b1	b2	VIM%
1	E.11	Ittihad road	2006	no record	11	-0.07	1.39	1.22
3	E18.1	Manama- RAK Airport	2006	no record	11	-0.07	1.39	1.22
5	E18.2	RAK Airport-Sha'am	2005	no record	12	-0.07	1.39	1.22
7	E311	Sheik Mohammed Bin Zayed	2011	no record	6	-0.07	1.39	1.26
8	E55.1	Dhaid - Madam	2001	no record	16	-0.07	1.39	1.20
10	E55.2	Madam - Shiweb	2001	no record	16	-0.07	1.39	1.20
12	E55.3	Umm Al Quwaim - Dhaid	2001	no record	16	-0.07	1.39	1.20
14	E611.1	Maliha Rd - Fallah Al Muala Rd	2008	no record	9	-0.07	1.39	1.24

16	E611.2	Fallah Al Muala Rd - Shk Mohammed Bin Zayed Rd	2008	no record	9	-0.07	1.39	1.24
18	E84	Sheikh Khalifa Rd	2012	no record	5	-0.07	1.39	1.28
20	E88.1	Sharjah - Dhaid	2002	no record	15	-0.07	1.39	1.20
22	E88.2	Dhaid - Masafi	2002	no record	15	-0.07	1.39	1.20
24	E89.1	Masafi - Dibba (from Dibba to Ghona Bridge)	2013	no record	4	-0.07	1.39	1.29
26	E89.3	Masafi - Fujairah	1999	no record	18	-0.07	1.39	1.19
28	E99.1	Khor Fakkan - Dibba	2000	no record	17	-0.07	1.39	1.19
29	E99.2	Fujairah - Khor Fakkan	2000	no record	17	-0.07	1.39	1.19
30	E99.3	Fujairah - Oman	2003	no record	14	-0.07	1.39	1.21

Table 12-18: Development of voids in mix (VIM) based on data collection Forward

N	Road Code	Road	Construction date	Major rehabilitation	Road age	b1	b2	VIM
2	E.11	Ittihad road	2006	no record	11	-0.07	1.39	1.22
4	E18.1	Manama-RAK Airport	2006	no record	11	-0.07	1.39	1.22
6	E18.2	RAK Airport-Sha'am	2005	no record	12	-0.07	1.39	1.22
9	E55.1	Dhaid - Madam	2001	no record	16	-0.07	1.39	1.20
11	E55.2	Madam - Shiweb	2001	no record	16	-0.07	1.39	1.20
13	E55.3	Umm Al Quwaim - Dhaid	2001	no record	16	-0.07	1.39	1.20
15	E611.1	Maliha Rd - Fallah Al Muala Rd	2008	no record	9	-0.07	1.39	1.24
17	E611.2	Fallah Al Muala Rd - Shk Mohammed Bin Zayed Rd	2008	no record	9	-0.07	1.39	1.24
19	E84	Sheikh Khalifa Rd	2012	no record	5	-0.07	1.39	1.28
21	E88.1	Sharjah - Dhaid	2002	no record	15	-0.07	1.39	1.20
23	E88.2	Dhaid - Masafi	2003	no record	14	-0.07	1.39	1.21
25	E89.1	Masafi - Dibba (from Dibba to Ghona Bridge)	2013	no record	4	-0.07	1.39	1.29

27	E89.3	Masafi - Fujairah	1995	no record	22	-0.07	1.39	1.17

Questionnaires

Job position		Threats	
		Project Manager ( )	Material Technician ( )
		Project Engineer ( )	Maintenance Engineer ( )
		Supplier ( )	Asset Engineer ( )
		Resident Engineer ( )	Asset Manager ( )
		Material Engineer ( )	Road Inspectors ( )
		others :	

experience		experience
		1-2 years ( )
		2-5 years ( )
		6-8 years ( )
		8-12 years ( )
		more than 12 years ( )
		others :

1.Please estimate the likelihood times impact of “**R1.Traffic** “ intensity in conjunction with climate change conditions contribution to the failure of pavement in UAE roads	probability		Threats				
		0.9	0.05 ( )	0.09 ( )	0.18 ( )	0.36 ( )	0.72 ( )
		0.7	0.04 ( )	0.07 ( )	0.14 ( )	0.28 ( )	0.56 ( )
		0.5	0.03 ( )	0.05 ( )	0.1 ( )	0.2 ( )	0.4 ( )
		0.3	0.02 ( )	0.03 ( )	0.06 ( )	0.12 ( )	0.24 ( )
		0.1	0.01 ( )	0.01 ( )	0.02 ( )	0.04 ( )	0.08 ( )

	0.05/Very Low	0.1/Low	0.2/Low	0.4/High	0.8/Very High

2. Please estimate the likelihood times impact of **“S1.High volume of heavy trucks** “In conjunction with climate change conditions contribute the traffic loading that lead to pavement failure

probability		Threats				
	0.9	0.05 ( )	0.09 ( )	0.18 ( )	0.36 ( )	0.72 ( )
	0.7	0.04 ( )	0.07 ( )	0.14 ( )	0.28 ( )	0.56 ( )
	0.5	0.03 ( )	0.05 ( )	0.1 ( )	0.2 ( )	0.4 ( )
	0.3	0.02 ( )	0.03 ( )	0.06 ( )	0.12 ( )	0.24 ( )
	0.1	0.01 ( )	0.01 ( )	0.02 ( )	0.04 ( )	0.08 ( )
		0.05/Very Low	0.1/Low	0.2/Low	0.4/High	0.8/Very High

3. Please estimate the likelihood times impact of **“S2.Axel Group Type** “In conjunction with climate change conditions contribute the traffic loading that lead to pavement failure

probability		Threats				
	0.9	0.05 ( )	0.09 ( )	0.18 ( )	0.36 ( )	0.72 ( )
	0.7	0.04 ( )	0.07 ( )	0.14 ( )	0.28 ( )	0.56 ( )
	0.5	0.03 ( )	0.05 ( )	0.1 ( )	0.2 ( )	0.4 ( )
	0.3	0.02 ( )	0.03 ( )	0.06 ( )	0.12 ( )	0.24 ( )
	0.1	0.01 ( )	0.01 ( )	0.02 ( )	0.04 ( )	0.08 ( )
		0.05/Very Low	0.1/Low	0.2/Low	0.4/High	0.8/Very High

4. Please estimate the likelihood times impact of **“S3.Tyer configuration** “In conjunction with climate change conditions contribute to pavement failure

probability		Threats				
	0.9	0.05 ( )	0.09 ( )	0.18 ( )	0.36 ( )	0.72 ( )
	0.7	0.04 ( )	0.07 ( )	0.14 ( )	0.28 ( )	0.56 ( )
	0.5	0.03 ( )	0.05 ( )	0.1 ( )	0.2 ( )	0.4 ( )
	0.3	0.02 ( )	0.03 ( )	0.06 ( )	0.12 ( )	0.24 ( )
	0.1	0.01 ( )	0.01 ( )	0.02 ( )	0.04 ( )	0.08 ( )
		0.05/Very Low	0.1/Low	0.2/Low	0.4/High	0.8/Very High

5. Please estimate the likelihood times impact of

probability		Threats				
	0.9	0.05	0.09	0.18	0.36	0.72

“S4.Gross vehicle mass “In conjunction with climate change conditions contribute to pavement failure			( )	( )	( )	( )	( )
		0.7	0.04 ( )	0.07 ( )	0.14 ( )	0.28 ( )	0.56 ( )
		0.5	0.03 ( )	0.05 ( )	0.1 ( )	0.2 ( )	0.4 ( )
		0.3	0.02 ( )	0.03 ( )	0.06 ( )	0.12 ( )	0.24 ( )
		0.1	0.01 ( )	0.01 ( )	0.02 ( )	0.04 ( )	0.08 ( )
			0.05/Very Low	0.1/Low	0.2/Low	0.4/High	0.8/Very High

6. Please estimate the likelihood times impact of **“S5.Dynamic Wheel Loading “**In conjunction with climate change conditions contribute to pavement failure	probability		Threats				
		0.9	0.05 ( )	0.09 ( )	0.18 ( )	0.36 ( )	0.72 ( )
		0.7	0.04 ( )	0.07 ( )	0.14 ( )	0.28 ( )	0.56 ( )
		0.5	0.03 ( )	0.05 ( )	0.1 ( )	0.2 ( )	0.4 ( )
		0.3	0.02 ( )	0.03 ( )	0.06 ( )	0.12 ( )	0.24 ( )
		0.1	0.01 ( )	0.01 ( )	0.02 ( )	0.04 ( )	0.08 ( )
			0.05/Very Low	0.1/Low	0.2/Low	0.4/High	0.8/Very High

7. Please estimate the likelihood times impact of **“S6.High traffic loading (all vehicles type “**In conjunction with climate change conditions contribute to pavement failure	probability		Threats				
		0.9	0.05 ( )	0.09 ( )	0.18 ( )	0.36 ( )	0.72 ( )
		0.7	0.04 ( )	0.07 ( )	0.14 ( )	0.28 ( )	0.56 ( )
		0.5	0.03 ( )	0.05 ( )	0.1 ( )	0.2 ( )	0.4 ( )
		0.3	0.02 ( )	0.03 ( )	0.06 ( )	0.12 ( )	0.24 ( )
		0.1	0.01 ( )	0.01 ( )	0.02 ( )	0.04 ( )	0.08 ( )
			0.05/Very Low	0.1/Low	0.2/Low	0.4/High	0.8/Very High

8. Please estimate the likelihood times impact of **“S7.Vehicle speed “**In conjunction with climate change conditions contribute to pavement failure	probability		Threats				
		0.9	0.05 ( )	0.09 ( )	0.18 ( )	0.36 ( )	0.72 ( )
		0.7	0.04 ( )	0.07 ( )	0.14 ( )	0.28 ( )	0.56 ( )
		0.5	0.03	0.05	0.1	0.2	0.4

			( )	( )	( )	( )	( )
		0.3	0.02 ( )	0.03 ( )	0.06 ( )	0.12 ( )	0.24 ( )
		0.1	0.01 ( )	0.01 ( )	0.02 ( )	0.04 ( )	0.08 ( )
			0.05/Very Low	0.1/Low	0.2/Low	0.4/High	0.8/Very High

1. Please estimate the likelihood times impact of **<u>“R2.Climate Change “</u>** will lead to the failure of pavement in UAE roads	probability		Threats				
		0.9	0.05 ( )	0.09 ( )	0.18 ( )	0.36 ( )	0.72 ( )
		0.7	0.04 ( )	0.07 ( )	0.14 ( )	0.28 ( )	0.56 ( )
		0.5	0.03 ( )	0.05 ( )	0.1 ( )	0.2 ( )	0.4 ( )
		0.3	0.02 ( )	0.03 ( )	0.06 ( )	0.12 ( )	0.24 ( )
		0.1	0.01 ( )	0.01 ( )	0.02 ( )	0.04 ( )	0.08 ( )
			0.05/Very Low	0.1/Low	0.2/Low	0.4/High	0.8/Very High

2.Please estimate the likelihood times impact of **“S8.Precipitation “** due to the climate change impact contribute to pavement failure	probability		Threats				
		0.9	0.05 ( )	0.09 ( )	0.18 ( )	0.36 ( )	0.72 ( )
		0.7	0.04 ( )	0.07 ( )	0.14 ( )	0.28 ( )	0.56 ( )
		0.5	0.03 ( )	0.05 ( )	0.1 ( )	0.2 ( )	0.4 ( )
		0.3	0.02 ( )	0.03 ( )	0.06 ( )	0.12 ( )	0.24 ( )
		0.1	0.01 ( )	0.01 ( )	0.02 ( )	0.04 ( )	0.08 ( )
			0.05/Very Low	0.1/Low	0.2/Low	0.4/High	0.8/Very High

3. Please estimate the likelihood times impact of **“S9.Weathering “**due to the climate change contribute to pavement failure	probability		Threats				
		0.9	0.05 ( )	0.09 ( )	0.18 ( )	0.36 ( )	0.72 ( )
		0.7	0.04 ( )	0.07 ( )	0.14 ( )	0.28 ( )	0.56 ( )
		0.5	0.03 ( )	0.05 ( )	0.1 ( )	0.2 ( )	0.4 ( )
		0.3	0.02 ( )	0.03 ( )	0.06 ( )	0.12 ( )	0.24 ( )
		0.1	0.01	0.01	0.02	0.04	0.08

	( )	( )	( )	( )	( )
	0.05/Very Low	0.1/Low	0.2/Low	0.4/High	0.8/Very High

4. Please estimate the likelihood times impact of **“S10.High Temperature “** due climate change contribute to pavement failure

probability	Threats				
0.9	0.05 ( )	0.09 ( )	0.18 ( )	0.36 ( )	0.72 ( )
0.7	0.04 ( )	0.07 ( )	0.14 ( )	0.28 ( )	0.56 ( )
0.5	0.03 ( )	0.05 ( )	0.1 ( )	0.2 ( )	0.4 ( )
0.3	0.02 ( )	0.03 ( )	0.06 ( )	0.12 ( )	0.24 ( )
0.1	0.01 ( )	0.01 ( )	0.02 ( )	0.04 ( )	0.08 ( )
	0.05/Very Low	0.1/Low	0.2/Low	0.4/High	0.8/Very High

5. Please estimate the likelihood times impact of **“S11.Low Temperature “** due to the climate change contribute to pavement failure

probability	Threats				
0.9	0.05 ( )	0.09 ( )	0.18 ( )	0.36 ( )	0.72 ( )
0.7	0.04 ( )	0.07 ( )	0.14 ( )	0.28 ( )	0.56 ( )
0.5	0.03 ( )	0.05 ( )	0.1 ( )	0.2 ( )	0.4 ( )
0.3	0.02 ( )	0.03 ( )	0.06 ( )	0.12 ( )	0.24 ( )
0.1	0.01 ( )	0.01 ( )	0.02 ( )	0.04 ( )	0.08 ( )
	0.05/Very Low	0.1/Low	0.2/Low	0.4/High	0.8/Very High

6. Please estimate the likelihood times impact of **“R7.Drainage “** due to the climate change contribute to pavement failure.

probability	Threats				
0.9	0.05 ( )	0.09 ( )	0.18 ( )	0.36 ( )	0.72 ( )
0.7	0.04 ( )	0.07 ( )	0.14 ( )	0.28 ( )	0.56 ( )
0.5	0.03 ( )	0.05 ( )	0.1 ( )	0.2 ( )	0.4 ( )
0.3	0.02 ( )	0.03 ( )	0.06 ( )	0.12 ( )	0.24 ( )
0.1	0.01 ( )	0.01 ( )	0.02 ( )	0.04 ( )	0.08 ( )
	0.05/Very Low	0.1/Low	0.2/Low	0.4/High	0.8/Very High

prob abili	Threats

7. Please estimate the likelihood times impact of **"R5.Pavement Ageing "** due to the climate change contribute to pavement failure.						
	0.9	0.05 ( )	0.09 ( )	0.18 ( )	0.36 ( )	0.72 ( )
	0.7	0.04 ( )	0.07 ( )	0.14 ( )	0.28 ( )	0.56 ( )
	0.5	0.03 ( )	0.05 ( )	0.1 ( )	0.2 ( )	0.4 ( )
	0.3	0.02 ( )	0.03 ( )	0.06 ( )	0.12 ( )	0.24 ( )
	0.1	0.01 ( )	0.01 ( )	0.02 ( )	0.04 ( )	0.08 ( )
		0.05/Very Low	0.1/Low	0.2/Low	0.4/High	0.8/Very High

8. Please estimate the likelihood times impact of **"S14.Increase oxidation "** due to the climate change contribute to pavement failure.							
	probability		Threats				
		0.9	0.05 ( )	0.09 ( )	0.18 ( )	0.36 ( )	0.72 ( )
		0.7	0.04 ( )	0.07 ( )	0.14 ( )	0.28 ( )	0.56 ( )
		0.5	0.03 ( )	0.05 ( )	0.1 ( )	0.2 ( )	0.4 ( )
		0.3	0.02 ( )	0.03 ( )	0.06 ( )	0.12 ( )	0.24 ( )
		0.1	0.01 ( )	0.01 ( )	0.02 ( )	0.04 ( )	0.08 ( )
			0.05/Very Low	0.1/Low	0.2/Low	0.4/High	0.8/Very High

9. Please estimate the likelihood times impact of **"S15.Increase viscosity and softness "**due to the climate change contribute to pavement failure							
	probability		Threats				
		0.9	0.05 ( )	0.09 ( )	0.18 ( )	0.36 ( )	0.72 ( )
		0.7	0.04 ( )	0.07 ( )	0.14 ( )	0.28 ( )	0.56 ( )
		0.5	0.03 ( )	0.05 ( )	0.1 ( )	0.2 ( )	0.4 ( )
		0.3	0.02 ( )	0.03 ( )	0.06 ( )	0.12 ( )	0.24 ( )
		0.1	0.01 ( )	0.01 ( )	0.02 ( )	0.04 ( )	0.08 ( )
			0.05/Very Low	0.1/Low	0.2/Low	0.4/High	0.8/Very High

10. Please estimate the likelihood times impact of **"S16.Increase Brittle of asphaltic layer "**due to							
	probability		Threats				
		0.9	0.05 ( )	0.09 ( )	0.18 ( )	0.36 ( )	0.72 ( )
		0.7	0.04 ( )	0.07 ( )	0.14 ( )	0.28 ( )	0.56 ( )

climate change contribute to pavement failure		0.5	0.03 ( )	0.05 ( )	0.1 ( )	0.2 ( )	0.4 ( )
		0.3	0.02 ( )	0.03 ( )	0.06 ( )	0.12 ( )	0.24 ( )
		0.1	0.01 ( )	0.01 ( )	0.02 ( )	0.04 ( )	0.08 ( )
			0.05/Very Low	0.1/Low	0.2/Low	0.4/High	0.8/Very High

11. Please estimate the likelihood times impact of **"S17.Increase Moisture/ Excess water "** due to the climate change contribute to pavement failure	probability		Threats				
		0.9	0.05 ( )	0.09 ( )	0.18 ( )	0.36 ( )	0.72 ( )
		0.7	0.04 ( )	0.07 ( )	0.14 ( )	0.28 ( )	0.56 ( )
		0.5	0.03 ( )	0.05 ( )	0.1 ( )	0.2 ( )	0.4 ( )
		0.3	0.02 ( )	0.03 ( )	0.06 ( )	0.12 ( )	0.24 ( )
		0.1	0.01 ( )	0.01 ( )	0.02 ( )	0.04 ( )	0.08 ( )
			0.05/Very Low	0.1/Low	0.2/Low	0.4/High	0.8/Very High

1. Please estimate the likelihood times impact of **"R3.Pavement Composition** "will be affected by climate change conditions leading to the failure of pavement in UAE roads	probability		Threats				
		0.9	0.05 ( )	0.09 ( )	0.18 ( )	0.36 ( )	0.72 ( )
		0.7	0.04 ( )	0.07 ( )	0.14 ( )	0.28 ( )	0.56 ( )
		0.5	0.03 ( )	0.05 ( )	0.1 ( )	0.2 ( )	0.4 ( )
		0.3	0.02 ( )	0.03 ( )	0.06 ( )	0.12 ( )	0.24 ( )
		0.1	0.01 ( )	0.01 ( )	0.02 ( )	0.04 ( )	0.08 ( )
			0.05/Very Low	0.1/Low	0.2/Low	0.4/High	0.8/Very High

2. Please estimate the likelihood times impact of **"S18. Reduction in Material Quality and Properties of Aggregate and soil)** "due to the climate change contribute to pavement failure	probability		Threats				
		0.9	0.05 ( )	0.09 ( )	0.18 ( )	0.36 ( )	0.72 ( )
		0.7	0.04 ( )	0.07 ( )	0.14 ( )	0.28 ( )	0.56 ( )
		0.5	0.03 ( )	0.05 ( )	0.1 ( )	0.2 ( )	0.4 ( )
		0.3	0.02 ( )	0.03 ( )	0.06 ( )	0.12 ( )	0.24 ( )

		0.1	0.01 ( )	0.01 ( )	0.02 ( )	0.04 ( )	0.08 ( )
			0.05/Very Low	0.1/Low	0.2/Low	0.4/High	0.8/Very High

			Threats				
3.Please estimate the likelihood times impact of **"S19.Pavement Thickness** "In conjunction with climate change conditions contribute to pavement failure	probability	0.9	0.05 ( )	0.09 ( )	0.18 ( )	0.36 ( )	0.72 ( )
		0.7	0.04 ( )	0.07 ( )	0.14 ( )	0.28 ( )	0.56 ( )
		0.5	0.03 ( )	0.05 ( )	0.1 ( )	0.2 ( )	0.4 ( )
		0.3	0.02 ( )	0.03 ( )	0.06 ( )	0.12 ( )	0.24 ( )
		0.1	0.01 ( )	0.01 ( )	0.02 ( )	0.04 ( )	0.08 ( )
			0.05/Very Low	0.1/Low	0.2/Low	0.4/High	0.8/Very High

			Threats				
4. Please estimate the likelihood times impact of **"S20.Shortage of Material availability** "due to the climate change contribute to pavement failure	probability	0.9	0.05 ( )	0.09 ( )	0.18 ( )	0.36 ( )	0.72 ( )
		0.7	0.04 ( )	0.07 ( )	0.14 ( )	0.28 ( )	0.56 ( )
		0.5	0.03 ( )	0.05 ( )	0.1 ( )	0.2 ( )	0.4 ( )
		0.3	0.02 ( )	0.03 ( )	0.06 ( )	0.12 ( )	0.24 ( )
		0.1	0.01 ( )	0.01 ( )	0.02 ( )	0.04 ( )	0.08 ( )
			0.05/Very Low	0.1/Low	0.2/Low	0.4/High	0.8/Very High

			Threats				
5. Please estimate the likelihood times impact of **"S21.Bitumen Supply and Quality** "In conjunction with climate change conditions contribute to pavement failure	probability	0.9	0.05 ( )	0.09 ( )	0.18 ( )	0.36 ( )	0.72 ( )
		0.7	0.04 ( )	0.07 ( )	0.14 ( )	0.28 ( )	0.56 ( )
		0.5	0.03 ( )	0.05 ( )	0.1 ( )	0.2 ( )	0.4 ( )
		0.3	0.02 ( )	0.03 ( )	0.06 ( )	0.12 ( )	0.24 ( )
		0.1	0.01 ( )	0.01 ( )	0.02 ( )	0.04 ( )	0.08 ( )
			0.05/Very Low	0.1/Low	0.2/Low	0.4/High	0.8/Very High

1. Please estimate the likelihood times impact of **“R4.Pavement Strength** will be affected by climate change conditions leading to pavement failure

probability	Threats				
0.9	0.05 ( )	0.09 ( )	0.18 ( )	0.36 ( )	0.72 ( )
0.7	0.04 ( )	0.07 ( )	0.14 ( )	0.28 ( )	0.56 ( )
0.5	0.03 ( )	0.05 ( )	0.1 ( )	0.2 ( )	0.4 ( )
0.3	0.02 ( )	0.03 ( )	0.06 ( )	0.12 ( )	0.24 ( )
0.1	0.01 ( )	0.01 ( )	0.02 ( )	0.04 ( )	0.08 ( )
	0.05/Very Low	0.1/Low	0.2/Low	0.4/High	0.8/Very High

2. Please estimate the likelihood times impact of **“R1.Traffic Loading “**In conjunction with climate change conditions contribute the Pavement strength that lead to pavement failure

probability	Threats				
0.9	0.05 ( )	0.09 ( )	0.18 ( )	0.36 ( )	0.72 ( )
0.7	0.04 ( )	0.07 ( )	0.14 ( )	0.28 ( )	0.56 ( )
0.5	0.03 ( )	0.05 ( )	0.1 ( )	0.2 ( )	0.4 ( )
0.3	0.02 ( )	0.03 ( )	0.06 ( )	0.12 ( )	0.24 ( )
0.1	0.01 ( )	0.01 ( )	0.02 ( )	0.04 ( )	0.08 ( )
	0.05/Very Low	0.1/Low	0.2/Low	0.4/High	0.8/Very High

3. Please estimate the likelihood times impact of **“S22.Insufficient value of Structural Number (SN)** “In conjunction with climate change conditions to pavement failure

probability	Threats				
0.9	0.05 ( )	0.09 ( )	0.18 ( )	0.36 ( )	0.72 ( )
0.7	0.04 ( )	0.07 ( )	0.14 ( )	0.28 ( )	0.56 ( )
0.5	0.03 ( )	0.05 ( )	0.1 ( )	0.2 ( )	0.4 ( )
0.3	0.02 ( )	0.03 ( )	0.06 ( )	0.12 ( )	0.24 ( )
0.1	0.01 ( )	0.01 ( )	0.02 ( )	0.04 ( )	0.08 ( )
	0.05/Very Low	0.1/Low	0.2/Low	0.4/High	0.8/Very High

1. Please estimate the likelihood times impact of **“R5.Pavement Ageing “**will be affected by climate change

probability	Threats				
0.9	0.05 ( )	0.09 ( )	0.18 ( )	0.36 ( )	0.72 ( )
0.7	0.04	0.07	0.14	0.28	0.56

conditions leading to the failure of pavement in UAE roads							
			( )	( )	( )	( )	( )
		0.5	0.03 ( )	0.05 ( )	0.1 ( )	0.2 ( )	0.4 ( )
		0.3	0.02 ( )	0.03 ( )	0.06 ( )	0.12 ( )	0.24 ( )
		0.1	0.01 ( )	0.01 ( )	0.02 ( )	0.04 ( )	0.08 ( )
			0.05/Very Low	0.1/Low	0.2/Low	0.4/High	0.8/Very High

2. Please estimate the likelihood times impact of **“R2.Climate Change** “contribute the Pavement Ageing that lead to pavement failure	probability		Threats				
		0.9	0.05 ( )	0.09 ( )	0.18 ( )	0.36 ( )	0.72 ( )
		0.7	0.04 ( )	0.07 ( )	0.14 ( )	0.28 ( )	0.56 ( )
		0.5	0.03 ( )	0.05 ( )	0.1 ( )	0.2 ( )	0.4 ( )
		0.3	0.02 ( )	0.03 ( )	0.06 ( )	0.12 ( )	0.24 ( )
		0.1	0.01 ( )	0.01 ( )	0.02 ( )	0.04 ( )	0.08 ( )
			0.05/Very Low	0.1/Low	0.2/Low	0.4/High	0.8/Very High

3. Please estimate the likelihood times impact of **“R1.Traffic Loading** “In conjunction with climate change conditions contribute the Pavement Ageing that lead to pavement failure	probability		Threats				
		0.9	0.05 ( )	0.09 ( )	0.18 ( )	0.36 ( )	0.72 ( )
		0.7	0.04 ( )	0.07 ( )	0.14 ( )	0.28 ( )	0.56 ( )
		0.5	0.03 ( )	0.05 ( )	0.1 ( )	0.2 ( )	0.4 ( )
		0.3	0.02 ( )	0.03 ( )	0.06 ( )	0.12 ( )	0.24 ( )
		0.1	0.01 ( )	0.01 ( )	0.02 ( )	0.04 ( )	0.08 ( )
			0.05/Very Low	0.1/Low	0.2/Low	0.4/High	0.8/Very High

4. Please estimate the likelihood times impact of **“R6.Subgrade Soil** “In conjunction with climate change conditions contribute the Pavement Ageing that lead to pavement failure	probability		Threats				
		0.9	0.05 ( )	0.09 ( )	0.18 ( )	0.36 ( )	0.72 ( )
		0.7	0.04 ( )	0.07 ( )	0.14 ( )	0.28 ( )	0.56 ( )
		0.5	0.03 ( )	0.05 ( )	0.1 ( )	0.2 ( )	0.4 ( )
		0.3	0.02	0.03	0.06	0.12	0.24

			( )	( )	( )	( )	( )
		0.1	0.01 ( )	0.01 ( )	0.02 ( )	0.04 ( )	0.08 ( )
			0.05/Very Low	0.1/Low	0.2/Low	0.4/High	0.8/Very High

			Threats				
5.Please estimate the likelihood times impact of **“R8.Maintenance “**In conjunction with climate change conditions contribute the Pavement Ageing that lead to pavement failure	probability	0.9	0.05 ( )	0.09 ( )	0.18 ( )	0.36 ( )	0.72 ( )
		0.7	0.04 ( )	0.07 ( )	0.14 ( )	0.28 ( )	0.56 ( )
		0.5	0.03 ( )	0.05 ( )	0.1 ( )	0.2 ( )	0.4 ( )
		0.3	0.02 ( )	0.03 ( )	0.06 ( )	0.12 ( )	0.24 ( )
		0.1	0.01 ( )	0.01 ( )	0.02 ( )	0.04 ( )	0.08 ( )
			0.05/Very Low	0.1/Low	0.2/Low	0.4/High	0.8/Very High

			Threats				
1.Please estimate the likelihood times impact of “**R6.Subgrade Soil** “will be affected by climate change conditions leading to the failure of pavement in UAE roads	probability	0.9	0.05 ( )	0.09 ( )	0.18 ( )	0.36 ( )	0.72 ( )
		0.7	0.04 ( )	0.07 ( )	0.14 ( )	0.28 ( )	0.56 ( )
		0.5	0.03 ( )	0.05 ( )	0.1 ( )	0.2 ( )	0.4 ( )
		0.3	0.02 ( )	0.03 ( )	0.06 ( )	0.12 ( )	0.24 ( )
		0.1	0.01 ( )	0.01 ( )	0.02 ( )	0.04 ( )	0.08 ( )
			0.05/Very Low	0.1/Low	0.2/Low	0.4/High	0.8/Very High

			Threats				
2. Please estimate the likelihood times impact of **“S17.Increase Moisture/ Excess water “**In conjunction with climate change conditions contribute the subgrade that lead to pavement failure	probability	0.9	0.05 ( )	0.09 ( )	0.18 ( )	0.36 ( )	0.72 ( )
		0.7	0.04 ( )	0.07 ( )	0.14 ( )	0.28 ( )	0.56 ( )
		0.5	0.03 ( )	0.05 ( )	0.1 ( )	0.2 ( )	0.4 ( )
		0.3	0.02 ( )	0.03 ( )	0.06 ( )	0.12 ( )	0.24 ( )
		0.1	0.01 ( )	0.01 ( )	0.02 ( )	0.04 ( )	0.08 ( )
			0.05/Very Low	0.1/Low	0.2/Low	0.4/High	0.8/Very High

3. Please estimate the likelihood times impact of **“S13.Selection of construction soil “**In conjunction with climate change conditions contribute the subgrade that lead to pavement failure contribute the Subgrade Soil that lead to pavement failure

probability		Threats				
	0.9	0.05 ( )	0.09 ( )	0.18 ( )	0.36 ( )	0.72 ( )
	0.7	0.04 ( )	0.07 ( )	0.14 ( )	0.28 ( )	0.56 ( )
	0.5	0.03 ( )	0.05 ( )	0.1 ( )	0.2 ( )	0.4 ( )
	0.3	0.02 ( )	0.03 ( )	0.06 ( )	0.12 ( )	0.24 ( )
	0.1	0.01 ( )	0.01 ( )	0.02 ( )	0.04 ( )	0.08 ( )
		0.05/Very Low	0.1/Low	0.2/Low	0.4/High	0.8/Very High

1. Please estimate the likelihood times impact of **“R7.Drainage** “will be affected by climate change conditions leading to the failure of pavement in UAE roads

probability		Threats				
	0.9	0.05 ( )	0.09 ( )	0.18 ( )	0.36 ( )	0.72 ( )
	0.7	0.04 ( )	0.07 ( )	0.14 ( )	0.28 ( )	0.56 ( )
	0.5	0.03 ( )	0.05 ( )	0.1 ( )	0.2 ( )	0.4 ( )
	0.3	0.02 ( )	0.03 ( )	0.06 ( )	0.12 ( )	0.24 ( )
	0.1	0.01 ( )	0.01 ( )	0.02 ( )	0.04 ( )	0.08 ( )
		0.05/Very Low	0.1/Low	0.2/Low	0.4/High	0.8/Very High

2. Please estimate the likelihood times impact of **“S17.Increase Moisture/ Excess water “**In conjunction with climate change conditions contribute the Drainage that lead to pavement failure

probability		Threats				
	0.9	0.05 ( )	0.09 ( )	0.18 ( )	0.36 ( )	0.72 ( )
	0.7	0.04 ( )	0.07 ( )	0.14 ( )	0.28 ( )	0.56 ( )
	0.5	0.03 ( )	0.05 ( )	0.1 ( )	0.2 ( )	0.4 ( )
	0.3	0.02 ( )	0.03 ( )	0.06 ( )	0.12 ( )	0.24 ( )
	0.1	0.01 ( )	0.01 ( )	0.02 ( )	0.04 ( )	0.08 ( )
		0.05/Very Low	0.1/Low	0.2/Low	0.4/High	0.8/Very High

3. Please estimate the likelihood times impact of **“S23.Insufficient drainage**

probability		Threats				
	0.9	0.05 ( )	0.09 ( )	0.18 ( )	0.36 ( )	0.72 ( )

system "In conjunction with climate change conditions contribute to pavement failure		0.7	0.04 ( )	0.07 ( )	0.14 ( )	0.28 ( )	0.56 ( )
		0.5	0.03 ( )	0.05 ( )	0.1 ( )	0.2 ( )	0.4 ( )
		0.3	0.02 ( )	0.03 ( )	0.06 ( )	0.12 ( )	0.24 ( )
		0.1	0.01 ( )	0.01 ( )	0.02 ( )	0.04 ( )	0.08 ( )
			0.05/Very Low	0.1/Low	0.2/Low	0.4/High	0.8/Very High

			Threats				
1.Please estimate the likelihood times impact of "**R8.Maintenance** "will be affected by climate change conditions leading to the failure of pavement in UAE roads	probability	0.9	0.05 ( )	0.09 ( )	0.18 ( )	0.36 ( )	0.72 ( )
		0.7	0.04 ( )	0.07 ( )	0.14 ( )	0.28 ( )	0.56 ( )
		0.5	0.03 ( )	0.05 ( )	0.1 ( )	0.2 ( )	0.4 ( )
		0.3	0.02 ( )	0.03 ( )	0.06 ( )	0.12 ( )	0.24 ( )
		0.1	0.01 ( )	0.01 ( )	0.02 ( )	0.04 ( )	0.08 ( )
			0.05/Very Low	0.1/Low	0.2/Low	0.4/High	0.8/Very High

			Threats				
2. Please estimate the likelihood times impact of "**S24.Delay maintenance** "In conjunction with climate change conditions contribute to pavement failure	probability	0.9	0.05 ( )	0.09 ( )	0.18 ( )	0.36 ( )	0.72 ( )
		0.7	0.04 ( )	0.07 ( )	0.14 ( )	0.28 ( )	0.56 ( )
		0.5	0.03 ( )	0.05 ( )	0.1 ( )	0.2 ( )	0.4 ( )
		0.3	0.02 ( )	0.03 ( )	0.06 ( )	0.12 ( )	0.24 ( )
		0.1	0.01 ( )	0.01 ( )	0.02 ( )	0.04 ( )	0.08 ( )
			0.05/Very Low	0.1/Low	0.2/Low	0.4/High	0.8/Very High

			Threats				
3. Please estimate the likelihood times impact of "**S25.Maintenance priorities /plan** "In conjunction with climate change conditions contribute to pavement failure	probability	0.9	0.05 ( )	0.09 ( )	0.18 ( )	0.36 ( )	0.72 ( )
		0.7	0.04 ( )	0.07 ( )	0.14 ( )	0.28 ( )	0.56 ( )
		0.5	0.03 ( )	0.05 ( )	0.1 ( )	0.2 ( )	0.4 ( )

		0.3	0.02 ( )	0.03 ( )	0.06 ( )	0.12 ( )	0.24 ( )
		0.1	0.01 ( )	0.01 ( )	0.02 ( )	0.04 ( )	0.08 ( )
			0.05/Very Low	0.1/Low	0.2/Low	0.4/High	0.8/Very High

4. Please estimate the likelihood times impact of **“S26.Limited Budget “**In conjunction with climate change conditions contribute to pavement failure	probability		Threats				
		0.9	0.05 ( )	0.09 ( )	0.18 ( )	0.36 ( )	0.72 ( )
		0.7	0.04 ( )	0.07 ( )	0.14 ( )	0.28 ( )	0.56 ( )
		0.5	0.03 ( )	0.05 ( )	0.1 ( )	0.2 ( )	0.4 ( )
		0.3	0.02 ( )	0.03 ( )	0.06 ( )	0.12 ( )	0.24 ( )
		0.1	0.01 ( )	0.01 ( )	0.02 ( )	0.04 ( )	0.08 ( )
			0.05/Very Low	0.1/Low	0.2/Low	0.4/High	0.8/Very High

1. Please estimate the likelihood times impact of **“R9.Construction Quality “**will be affected by climate change conditions leading to the failure of pavement in UAE roads	probability		Threats				
		0.9	0.05 ( )	0.09 ( )	0.18 ( )	0.36 ( )	0.72 ( )
		0.7	0.04 ( )	0.07 ( )	0.14 ( )	0.28 ( )	0.56 ( )
		0.5	0.03 ( )	0.05 ( )	0.1 ( )	0.2 ( )	0.4 ( )
		0.3	0.02 ( )	0.03 ( )	0.06 ( )	0.12 ( )	0.24 ( )
		0.1	0.01 ( )	0.01 ( )	0.02 ( )	0.04 ( )	0.08 ( )
			0.05/Very Low	0.1/Low	0.2/Low	0.4/High	0.8/Very High

2. Please estimate the likelihood times impact of **“S27.Design and Specification “**In conjunction with climate change conditions contribute to pavement failure	probability		Threats				
		0.9	0.05 ( )	0.09 ( )	0.18 ( )	0.36 ( )	0.72 ( )
		0.7	0.04 ( )	0.07 ( )	0.14 ( )	0.28 ( )	0.56 ( )
		0.5	0.03 ( )	0.05 ( )	0.1 ( )	0.2 ( )	0.4 ( )
		0.3	0.02 ( )	0.03 ( )	0.06 ( )	0.12 ( )	0.24 ( )
		0.1	0.01 ( )	0.01 ( )	0.02 ( )	0.04 ( )	0.08 ( )
			0.05/Very Low	0.1/Low	0.2/Low	0.4/High	0.8/Very High

3. Please estimate the likelihood times impact of	probability		Threats				
		0.9	0.05 ( )	0.09 ( )	0.18 ( )	0.36 ( )	0.72 ( )

“**S28.Construction Process** “In conjunction with climate change conditions contribute to pavement failure						
	0.7	0.04 ( )	0.07 ( )	0.14 ( )	0.28 ( )	0.56 ( )
	0.5	0.03 ( )	0.05 ( )	0.1 ( )	0.2 ( )	0.4 ( )
	0.3	0.02 ( )	0.03 ( )	0.06 ( )	0.12 ( )	0.24 ( )
	0.1	0.01 ( )	0.01 ( )	0.02 ( )	0.04 ( )	0.08 ( )
		0.05/Very Low	0.1/Low	0.2/Low	0.4/High	0.8/Very High

4.Please estimate the likelihood times impact of **“S29.Construction Management** “In conjunction with climate change conditions contribute to pavement failure			Threats				
	probability	0.9	0.05 ( )	0.09 ( )	0.18 ( )	0.36 ( )	0.72 ( )
		0.7	0.04 ( )	0.07 ( )	0.14 ( )	0.28 ( )	0.56 ( )
		0.5	0.03 ( )	0.05 ( )	0.1 ( )	0.2 ( )	0.4 ( )
		0.3	0.02 ( )	0.03 ( )	0.06 ( )	0.12 ( )	0.24 ( )
		0.1	0.01 ( )	0.01 ( )	0.02 ( )	0.04 ( )	0.08 ( )
			0.05/Very Low	0.1/Low	0.2/Low	0.4/High	0.8/Very High

1.Please estimate the likelihood times impact of **“Rutting** “will be affected by climate change conditions leading to the failure of pavement in UAE roads			Threats				
	probability	0.9	0.05 ( )	0.09 ( )	0.18 ( )	0.36 ( )	0.72 ( )
		0.7	0.04 ( )	0.07 ( )	0.14 ( )	0.28 ( )	0.56 ( )
		0.5	0.03 ( )	0.05 ( )	0.1 ( )	0.2 ( )	0.4 ( )
		0.3	0.02 ( )	0.03 ( )	0.06 ( )	0.12 ( )	0.24 ( )
		0.1	0.01 ( )	0.01 ( )	0.02 ( )	0.04 ( )	0.08 ( )
			0.05/Very Low	0.1/Low	0.2/Low	0.4/High	0.8/Very High

2. Please estimate the likelihood times impact of **“R2.Climate Change** “contribute the Rutting that lead to pavement failure			Threats				
	probability	0.9	0.05 ( )	0.09 ( )	0.18 ( )	0.36 ( )	0.72 ( )
		0.7	0.04 ( )	0.07 ( )	0.14 ( )	0.28 ( )	0.56 ( )
		0.5	0.03 ( )	0.05 ( )	0.1 ( )	0.2 ( )	0.4 ( )
		0.3	0.02 ( )	0.03 ( )	0.06 ( )	0.12 ( )	0.24 ( )
		0.1	0.01 ( )	0.01 ( )	0.02 ( )	0.04 ( )	0.08 ( )
			0.05/Very Low	0.1/Low	0.2/Low	0.4/High	0.8/Very High

			Threats				
	probability	0.9	0.05	0.09	0.18	0.36	0.72

3. Please estimate the likelihood times impact of **“R3.Pavement Composition** “In conjunction with climate change conditions contribute to Rutting that lead to pavement failure

		( )	( )	( )	( )	( )
	0.7	0.04 ( )	0.07 ( )	0.14 ( )	0.28 ( )	0.56 ( )
	0.5	0.03 ( )	0.05 ( )	0.1 ( )	0.2 ( )	0.4 ( )
	0.3	0.02 ( )	0.03 ( )	0.06 ( )	0.12 ( )	0.24 ( )
	0.1	0.01 ( )	0.01 ( )	0.02 ( )	0.04 ( )	0.08 ( )
		0.05/Very Low	0.1/Low	0.2/Low	0.4/High	0.8/Very High

4. Please estimate the likelihood times impact of **“R9.Construction Quality “I**n conjunction with climate change conditions contribute to Rutting that lead to pavement failure

		Threats				
probability	0.9	0.05 ( )	0.09 ( )	0.18 ( )	0.36 ( )	0.72 ( )
	0.7	0.04 ( )	0.07 ( )	0.14 ( )	0.28 ( )	0.56 ( )
	0.5	0.03 ( )	0.05 ( )	0.1 ( )	0.2 ( )	0.4 ( )
	0.3	0.02 ( )	0.03 ( )	0.06 ( )	0.12 ( )	0.24 ( )
	0.1	0.01 ( )	0.01 ( )	0.02 ( )	0.04 ( )	0.08 ( )
		0.05/Very Low	0.1/Low	0.2/Low	0.4/High	0.8/Very High

5.Please estimate the likelihood times impact of **“R4.Pavement Strength “I**n conjunction with climate change conditions contribute to Rutting that lead to pavement failure

		Threats				
probability	0.9	0.05 ( )	0.09 ( )	0.18 ( )	0.36 ( )	0.72 ( )
	0.7	0.04 ( )	0.07 ( )	0.14 ( )	0.28 ( )	0.56 ( )
	0.5	0.03 ( )	0.05 ( )	0.1 ( )	0.2 ( )	0.4 ( )
	0.3	0.02 ( )	0.03 ( )	0.06 ( )	0.12 ( )	0.24 ( )
	0.1	0.01 ( )	0.01 ( )	0.02 ( )	0.04 ( )	0.08 ( )
		0.05/Very Low	0.1/Low	0.2/Low	0.4/High	0.8/Very High

6. Please estimate the likelihood times impact of **“R6.Subgrade “I**n conjunction with climate change conditions contribute to Rutting that lead to pavement failure

		Threats				
probability	0.9	0.05 ( )	0.09 ( )	0.18 ( )	0.36 ( )	0.72 ( )
	0.7	0.04 ( )	0.07 ( )	0.14 ( )	0.28 ( )	0.56 ( )
	0.5	0.03 ( )	0.05 ( )	0.1 ( )	0.2 ( )	0.4 ( )
	0.3	0.02 ( )	0.03 ( )	0.06 ( )	0.12 ( )	0.24 ( )
	0.1	0.01 ( )	0.01 ( )	0.02 ( )	0.04 ( )	0.08 ( )
		0.05/Very Low	0.1/Low	0.2/Low	0.4/High	0.8/Very High

	prob	Threats

1. Please estimate the likelihood times impact of **“Cracking** “will be affected by climate change conditions contribute to the failure of pavement in UAE roads		0.9	0.05 ( )	0.09 ( )	0.18 ( )	0.36 ( )	0.72 ( )
		0.7	0.04 ( )	0.07 ( )	0.14 ( )	0.28 ( )	0.56 ( )
		0.5	0.03 ( )	0.05 ( )	0.1 ( )	0.2 ( )	0.4 ( )
		0.3	0.02 ( )	0.03 ( )	0.06 ( )	0.12 ( )	0.24 ( )
		0.1	0.01 ( )	0.01 ( )	0.02 ( )	0.04 ( )	0.08 ( )
			0.05/Very Low	0.1/Low	0.2/Low	0.4/High	0.8/Very High

2. Please estimate the likelihood times impact of **“R2.Climate Change** “contribute the Cracking that lead to pavement failure	probability				Threats		
		0.9	0.05 ( )	0.09 ( )	0.18 ( )	0.36 ( )	0.72 ( )
		0.7	0.04 ( )	0.07 ( )	0.14 ( )	0.28 ( )	0.56 ( )
		0.5	0.03 ( )	0.05 ( )	0.1 ( )	0.2 ( )	0.4 ( )
		0.3	0.02 ( )	0.03 ( )	0.06 ( )	0.12 ( )	0.24 ( )
		0.1	0.01 ( )	0.01 ( )	0.02 ( )	0.04 ( )	0.08 ( )
			0.05/Very Low	0.1/Low	0.2/Low	0.4/High	0.8/Very High

3.Please estimate the likelihood times impact of **“R3.Pavement Composition** “In conjunction with climate change conditions contribute to cracking that lead to pavement failure	probability				Threats		
		0.9	0.05 ( )	0.09 ( )	0.18 ( )	0.36 ( )	0.72 ( )
		0.7	0.04 ( )	0.07 ( )	0.14 ( )	0.28 ( )	0.56 ( )
		0.5	0.03 ( )	0.05 ( )	0.1 ( )	0.2 ( )	0.4 ( )
		0.3	0.02 ( )	0.03 ( )	0.06 ( )	0.12 ( )	0.24 ( )
		0.1	0.01 ( )	0.01 ( )	0.02 ( )	0.04 ( )	0.08 ( )
			0.05/Very Low	0.1/Low	0.2/Low	0.4/High	0.8/Very High

4. Please estimate the likelihood times impact of **“R9.Construction Quality** “In conjunction with climate change conditions contribute to cracking that lead to pavement failure	probability				Threats		
		0.9	0.05 ( )	0.09 ( )	0.18 ( )	0.36 ( )	0.72 ( )
		0.7	0.04 ( )	0.07 ( )	0.14 ( )	0.28 ( )	0.56 ( )
		0.5	0.03 ( )	0.05 ( )	0.1 ( )	0.2 ( )	0.4 ( )
		0.3	0.02 ( )	0.03 ( )	0.06 ( )	0.12 ( )	0.24 ( )
		0.1	0.01 ( )	0.01 ( )	0.02 ( )	0.04 ( )	0.08 ( )
			0.05/Very Low	0.1/Low	0.2/Low	0.4/High	0.8/Very High

5. Please estimate the likelihood times impact of **“R4.Pavement Strength** “In conjunction with climate change conditions contribute to cracking that lead to pavement failure

		Threats				
probability	0.9	0.05 ( )	0.09 ( )	0.18 ( )	0.36 ( )	0.72 ( )
	0.7	0.04 ( )	0.07 ( )	0.14 ( )	0.28 ( )	0.56 ( )
	0.5	0.03 ( )	0.05 ( )	0.1 ( )	0.2 ( )	0.4 ( )
	0.3	0.02 ( )	0.03 ( )	0.06 ( )	0.12 ( )	0.24 ( )
	0.1	0.01 ( )	0.01 ( )	0.02 ( )	0.04 ( )	0.08 ( )
		0.05/Very Low	0.1/Low	0.2/Low	0.4/High	0.8/Very High

6. Please estimate the likelihood times impact of **“R6.Subgrade “**In conjunction with climate change conditions contribute to cracking that lead to pavement failure

		Threats				
probability	0.9	0.05 ( )	0.09 ( )	0.18 ( )	0.36 ( )	0.72 ( )
	0.7	0.04 ( )	0.07 ( )	0.14 ( )	0.28 ( )	0.56 ( )
	0.5	0.03 ( )	0.05 ( )	0.1 ( )	0.2 ( )	0.4 ( )
	0.3	0.02 ( )	0.03 ( )	0.06 ( )	0.12 ( )	0.24 ( )
	0.1	0.01 ( )	0.01 ( )	0.02 ( )	0.04 ( )	0.08 ( )
		0.05/Very Low	0.1/Low	0.2/Low	0.4/High	0.8/Very High

1. Please estimate the likelihood times impact of **“Speed of Vehicle “**will be affected by climate change conditions leading c to the failure of pavement in UAE roads

		Threats				
probability	0.9	0.05 ( )	0.09 ( )	0.18 ( )	0.36 ( )	0.72 ( )
	0.7	0.04 ( )	0.07 ( )	0.14 ( )	0.28 ( )	0.56 ( )
	0.5	0.03 ( )	0.05 ( )	0.1 ( )	0.2 ( )	0.4 ( )
	0.3	0.02 ( )	0.03 ( )	0.06 ( )	0.12 ( )	0.24 ( )
	0.1	0.01 ( )	0.01 ( )	0.02 ( )	0.04 ( )	0.08 ( )
		0.05/Very Low	0.1/Low	0.2/Low	0.4/High	0.8/Very High

2.Please estimate the likelihood times impact of **“R5.Pavement Ageing “**In conjunction with climate change conditions contribute to speed of vehicles that lead to pavement failure.

		Threats				
probability	0.9	0.05 ( )	0.09 ( )	0.18 ( )	0.36 ( )	0.72 ( )
	0.7	0.04 ( )	0.07 ( )	0.14 ( )	0.28 ( )	0.56 ( )
	0.5	0.03 ( )	0.05 ( )	0.1 ( )	0.2 ( )	0.4 ( )
	0.3	0.02 ( )	0.03 ( )	0.06 ( )	0.12 ( )	0.24 ( )
	0.1	0.01 ( )	0.01 ( )	0.02 ( )	0.04 ( )	0.08 ( )

	0.05/Very Low	0.1/Low	0.2/Low	0.4/High	0.8/Very High

3. Please estimate the likelihood times impact of **“R7.Drinage** “In conjunction with climate change conditions contribute to speed of vehicles that lead to pavement failure.	probability		Threats				
		0.9	0.05 ( )	0.09 ( )	0.18 ( )	0.36 ( )	0.72 ( )
		0.7	0.04 ( )	0.07 ( )	0.14 ( )	0.28 ( )	0.56 ( )
		0.5	0.03 ( )	0.05 ( )	0.1 ( )	0.2 ( )	0.4 ( )
		0.3	0.02 ( )	0.03 ( )	0.06 ( )	0.12 ( )	0.24 ( )
		0.1	0.01 ( )	0.01 ( )	0.02 ( )	0.04 ( )	0.08 ( )
			0.05/Very Low	0.1/Low	0.2/Low	0.4/High	0.8/Very High

4. Please estimate the likelihood times impact of **“R8.Maintenance** “In conjunction with climate change conditions contribute to speed of vehicles that lead to pavement failure.	probability		Threats				
		0.9	0.05 ( )	0.09 ( )	0.18 ( )	0.36 ( )	0.72 ( )
		0.7	0.04 ( )	0.07 ( )	0.14 ( )	0.28 ( )	0.56 ( )
		0.5	0.03 ( )	0.05 ( )	0.1 ( )	0.2 ( )	0.4 ( )
		0.3	0.02 ( )	0.03 ( )	0.06 ( )	0.12 ( )	0.24 ( )
		0.1	0.01 ( )	0.01 ( )	0.02 ( )	0.04 ( )	0.08 ( )
			0.05/Very Low	0.1/Low	0.2/Low	0.4/High	0.8/Very High

1. Please estimate the likelihood times impact of **“Pavement Thickness** “will be affected by climate change conditions leading to the failure of pavement in UAE roads	probability		Threats				
		0.9	0.05 ( )	0.09 ( )	0.18 ( )	0.36 ( )	0.72 ( )
		0.7	0.04 ( )	0.07 ( )	0.14 ( )	0.28 ( )	0.56 ( )
		0.5	0.03 ( )	0.05 ( )	0.1 ( )	0.2 ( )	0.4 ( )
		0.3	0.02 ( )	0.03 ( )	0.06 ( )	0.12 ( )	0.24 ( )
		0.1	0.01 ( )	0.01 ( )	0.02 ( )	0.04 ( )	0.08 ( )
			0.05/Very Low	0.1/Low	0.2/Low	0.4/High	0.8/Very High

2.Please estimate the likelihood times impact of **“R9.Construction Quality** “In conjunction with climate change conditions contribute to pavement thickness that lead to pavement failure.	probability		Threats				
		0.9	0.05 ( )	0.09 ( )	0.18 ( )	0.36 ( )	0.72 ( )
		0.7	0.04 ( )	0.07 ( )	0.14 ( )	0.28 ( )	0.56 ( )
		0.5	0.03 ( )	0.05 ( )	0.1 ( )	0.2 ( )	0.4 ( )
		0.3	0.02 ( )	0.03 ( )	0.06 ( )	0.12 ( )	0.24 ( )

		0.1	0.01 ( )	0.01 ( )	0.02 ( )	0.04 ( )	0.08 ( )
			0.05/Very Low	0.1/Low	0.2/Low	0.4/High	0.8/Very High

			Threats				
1. Pavement network classified in UAE into 5 condition states: how likely the risk of "Rate of pavement deterioration " **move from Very good condition (PCI =100) to good condition (PCI -80)** Every year because of climate change	probability	0.9	0.05 ( )	0.09 ( )	0.18 ( )	0.36 ( )	0.72 ( )
		0.7	0.04 ( )	0.07 ( )	0.14 ( )	0.28 ( )	0.56 ( )
		0.5	0.03 ( )	0.05 ( )	0.1 ( )	0.2 ( )	0.4 ( )
		0.3	0.02 ( )	0.03 ( )	0.06 ( )	0.12 ( )	0.24 ( )
		0.1	0.01 ( )	0.01 ( )	0.02 ( )	0.04 ( )	0.08 ( )
			0.05/Very Low	0.1/Low	0.2/Low	0.4/High	0.8/Very High

			Threats				
2. Pavement network classified in UAE into 5 condition states: how likely the risk of "Rate of pavement deterioration " **move from good condition (PCI =80) to Satisfaction condition (PCI =60)** Every year. Because of climate change	probability	0.9	0.05 ( )	0.09 ( )	0.18 ( )	0.36 ( )	0.72 ( )
		0.7	0.04 ( )	0.07 ( )	0.14 ( )	0.28 ( )	0.56 ( )
		0.5	0.03 ( )	0.05 ( )	0.1 ( )	0.2 ( )	0.4 ( )
		0.3	0.02 ( )	0.03 ( )	0.06 ( )	0.12 ( )	0.24 ( )
		0.1	0.01 ( )	0.01 ( )	0.02 ( )	0.04 ( )	0.08 ( )
			0.05/Very Low	0.1/Low	0.2/Low	0.4/High	0.8/Very High

			Threats				
3. Pavement network classified in UAE into 5 condition states: how likely the risk of "Rate of pavement deterioration " **move from Satisfaction condition (PCI =60) to poor condition (PCI =40)** Every year because of climate change .	probability	0.9	0.05 ( )	0.09 ( )	0.18 ( )	0.36 ( )	0.72 ( )
		0.7	0.04 ( )	0.07 ( )	0.14 ( )	0.28 ( )	0.56 ( )
		0.5	0.03 ( )	0.05 ( )	0.1 ( )	0.2 ( )	0.4 ( )
		0.3	0.02 ( )	0.03 ( )	0.06 ( )	0.12 ( )	0.24 ( )
		0.1	0.01 ( )	0.01 ( )	0.02 ( )	0.04 ( )	0.08 ( )
			0.05/Very Low	0.1/Low	0.2/Low	0.4/High	0.8/Very High

			Threats				
4. Pavement network classified in UAE into 5 condition states: how likely the risk of "Rate of pavement deterioration " **move from poor condition**	probability	0.9	0.05 ( )	0.09 ( )	0.18 ( )	0.36 ( )	0.72 ( )
		0.7	0.04 ( )	0.07 ( )	0.14 ( )	0.28 ( )	0.56 ( )
		0.5	0.03 ( )	0.05 ( )	0.1 ( )	0.2 ( )	0.4 ( )

(PCI =40) to Failure condition (PCI =<40) Every year because of climate change		0.3	0.02 ( )	0.03 ( )	0.06 ( )	0.12 ( )	0.24 ( )
		0.1	0.01 ( )	0.01 ( )	0.02 ( )	0.04 ( )	0.08 ( )
			0.05/Very Low	0.1/Low	0.2/Low	0.4/High	0.8/Very High

13. Appendix 2: Deterministic Risk Analysis

Traffic

Table 13-1 : Deterministic risk analysis for traffic

A							
R1.	**S1**	**S2**	**S3**	**S4**	**S5**	**S6**	**S7**
Y1	**X1.1**	**X1.2**	**X1.3**	**X1.4**	**X1.5**	**X1.6**	**X1.7**
R1.Traffic	S1.High volume of heavy trucks	“S2.Axel Group Type	“S3.Tyer configuration	S4.Gross vehicle mass	S5.Dynamic Wheel Loading	S6.High traffic loading (all vehicles	S7.Vehicle speed
	0.06	0.28	0.05	0.28	0.03	0.14	0.03
	0.2	0.12	0.06	0.2	0.2	0.2	0.28
	0.1	0.1	0.1	0.2	0.2	0.1	0.01
	0.56	0.2	0.12	0.4	0.1	0.1	0.05
	0.56	0.2	0.1	0.12	0.06	0.1	0.1
	0.56	0.2	0.12	0.28	0.56	0.2	0.01
	0.72	0.28	0.01	0.72	0.28	0.14	0.18
	0.36	0.72	0.01	0.28	0.28	0.36	0.01
	0.36	0.36	0.03	0.03	0.02	0.36	0.02
	0.36	0.2	0.06	0.2	0.05	0.03	0.2
	0.12	0.12	0.05	0.08	0.12	0.14	0.03
	0.06	0.03	0.02	0.03	0.03	0.06	0.06
	0.2	0.12	0.1	0.12	0.08	0.1	0.03
	0.56	0.1	0.28	0.36	0.56	0.56	0.03
	0.28	0.06	0.2	0.26	0.56	0.2	0.12
	0.2	0.02	0.03	0.03	0.03	0.06	0.03
	0.2	0.03	0.01	0.03	0.03	0.01	0.02
	0.28	0.28	0.05	0.28	0.2	0.2	0.14
	0.2	0.1	0.06	0.1	0.28	0.2	0.1
	0.4	0.24	0.2	0.24	0.08	0.36	0.02
	0.56	0.4	0.02	0.1	0.01	0.12	0.01
	0.24	0.28	0.03	0.06	0.01	0.12	0.02
	0.4	0.2	0.02	0.1	0.01	0.28	0.01
	0.4	0.2	0.01	0.06	0.01	0.2	0.01
	0.56	0.28	0.01	0.06	0.03	0.28	0.01
	0.24	0.24	0.01	0.03	0.01	0.14	0.01
	0.4	0.4	0.02	0.1	0.01	0.2	0.2
	0.36	0.4	0.4	0.12	0.06	0.28	0.04
	0.1	0.1	0.14	0.14	0.04	0.04	0.01
	0.56	0.36	0.28	0.56	0.28	0.4	0.36
Average	**0.339**	**0.221**	**0.087**	**0.186**	**0.141**	**0.189**	**0.072**

Climate Change

Table 13-2: Deterministic risk analysis for climate change

				B						
R2.	**S8**	**S9**	**S10**	**S11**	**R7**	**R5**	**S14**	**S15**	**S16**	**S17**
Y2	**X2.1**	**X2.2**	**X2.3**	**X2.4**	**X2.5**	**X2.6**	**X2.7**	**X2.8**	**X2.9**	**X2.10**
R2.Climate Change	S8.Precipitation	S9.Weathering	S10.High Temperature	S11.Low Temperature	R7.Drainage	R5.Pavement Ageing	S14.Increase oxidation	S15.Increase viscosity and softness	S16.Increase Brittle of asphaltic layer	S17.Increase Moisture/ Excess water
	0.01	0.01	0.28	0.03	0.02	0.03	0.03	0.14	0.03	0.05
	0.28	0.4	0.2	0.28	0.14	0.06	0.12	0.2	0.28	0.12
	0.1	0.2	0.2	0.2	0.1	0.2	0.28	0.2	0.2	0.1
	0.1	0.07	0.2	0.05	0.12	0.2	0.2	0.07	0.1	0.14
	0.1	0.1	0.2	0.03	0.12	0.2	0.1	0.05	0.2	0.1
	0.2	0.06	0.36	0.02	0.2	0.1	0.2	0.28	0.28	0.2
	0.4	0.03	0.72	0.01	0.24	0.28	0.72	0.1	0.36	0.01
	0.04	0.14	0.72	0.72	0.05	0.03	0.1	0.03	0.01	0.28
	0.03	0.06	0.1	0.06	0.1	0.06	0.06	0.02	0.06	0.28
	0.1	0.05	0.28	0.2	0.28	0.28	0.12	0.2	0.28	0.1
	0.1	0.06	0.28	0.04	0.4	0.2	0.03	0.03	0.1	0.06
	0.03	0.06	0.2	0.01	0.06	0.06	0.06	0.06	0.06	0.01
	0.1	0.1	0.28	0.12	0.12	0.4	0.06	0.03	0.2	0.06
	0.12	0.4	0.56	0.03	0.05	0.28	0.28	0.2	0.28	0.36
	0.1	0.12	0.28	0.05	0.1	0.1	0.2	0.14	0.07	0.2
	0.02	0.03	0.06	0.1	0.03	0.03	0.1	0.06	0.05	0.03
	0.02	0.01	0.1	0.1	0.03	0.06	0.1	0.03	0.1	0.03
	0.14	0.03	0.28	0.2	0.1	0.14	0.03	0.28	0.2	0.03
	0.03	0.03	0.07	0.02	0.06	0.2	0.2	0.06	0.28	0.28
	0.1	0.4	0.2	0.1	0.05	0.14	0.12	0.2	0.2	0.1
	0.2	0.1	0.28	0.05	0.28	0.28	0.28	0.02	0.36	0.1
	0.24	0.12	0.56	0.01	0.4	0.2	0.2	0.04	0.12	0.06
	0.56	0.28	0.28	0.01	0.36	0.28	0.4	0.06	0.36	0.12
	0.4	0.2	0.56	0.01	0.56	0.2	0.28	0.04	0.28	0.02
	0.28	0.2	0.28	0.01	0.56	0.28	0.28	0.12	0.28	0.06
	0.24	0.24	0.2	0.01	0.36	0.28	0.2	0.1	0.56	0.24
	0.06	0.1	0.28	0.05	0.28	0.1	0.4	0.1	0.03	0.1
	0.56	0.56	0.72	0.28	0.2	0.07	0.28	0.2	0.18	0.28
	0.2	0.01	0.01	0.01	0.1	0.01	0.02	0.01	0.02	0.01
	0.2	0.2	0.56	0.12	0.2	0.4	0.28	0.56	0.4	0.24
Average	**0.169**	**0.146**	**0.310**	**0.098**	**0.189**	**0.172**	**0.191**	**0.121**	**0.198**	**0.126**

Pavement Composition

Table 13-3: Deterministic risk analysis for pavement composition

c				
R3.	S18	S19	S20	S21
Y3	X3.1	X3.2	X3.3	X3.4
R3.Pavement Composition	S18. Reduction in Material Quality and Properties of Aggregate and soil	S19.Pavement Thickness	S20.Shortage of Material availability	S21.Bitumen Supply and Quality
	0.07	0.14	0.03	0.03
	0.28	0.4	0.2	0.28
	0.28	0.2	0.01	0.03
	0.12	0.24	0.07	0.03
	0.1	0.24	0.1	0.06
	0.36	0.06	0.2	0.56
	0.4	0.1	0.03	0.72
	0.03	0.01	0.01	0.01
	0.01	0.01	0.05	0.05
	0.28	0.14	0.12	0.03
	0.4	0.02	0.4	0.4
	0.2	0.12	0.02	0.03
	0.2	0.03	0.2	0.24
	0.4	0.1	0.02	0.56
	0.12	0.04	0.04	0.12
	0.05	0.1	0.06	0.03
	0.2	0.1	0.03	0.03
	0.28	0.28	0.01	0.06
	0.28	0.05	0.01	0.01
	0.28	0.2	0.2	0.24
	0.2	0.4	0.28	0.2
	0.28	0.4	0.12	0.2
	0.28	0.56	0.18	0.36
	0.2	0.56	0.2	0.2
	0.56	0.56	0.2	0.56
	0.14	0.28	0.28	0.36
	0.2	0.4	0.36	0.14
	0.2	0.12	0.02	0.06
	0.24	0.12	0.1	0.2

	0.56	0.4	0.4	0.56
Average	**0.240**	**0.213**	**0.132**	**0.212**

Pavement Strength

Table 13-4: Deterministic risk analysis for pavement strength

D		
R4	**S1**	**S22**
Y4	X4.1	X4.2
R4.Pavement Strength	R1.Traffic Loading	S22.Insufficient value of Structural Number (SN)
	0.28	0.2
	0.36	0.2
	0.2	0.03
	0.05	0.24
	0.1	0.12
	0.03	0.28
	0.28	0.1
	0.28	0.01
	0.36	0.36
	0.2	0.4
	0.2	0.24
	0.2	0.03
	0.12	0.12
	0.4	0.4
	0.2	0.12
	0.06	0.03
	0.03	0.03
	0.36	0.28
	0.02	0.02
	0.12	0.2
	0.28	0.14
	0.12	0.4
	0.2	0.36
	0.2	0.4
	0.28	0.56
	0.1	0.72
	0.03	0.14
	0.06	0.03
	0.2	0.2
	0.56	0.4
Average	**0.196**	**0.225**

Pavement Ageing

Table 13-5: Deterministic risk analysis for pavement ageing

c				
R3.	R2	R1	R6	R8
Y5	X5.1	X5.2	X5.3	X5.4
R5.Pavement Ageing	R2.Climate Change	R1.Traffic Loading	R6.Subgrade Soil	R8.Maintenance
	0.28	0.28	0.03	0.03
	0.28	0.14	0.28	0.12
	0.2	0.2	0.28	0.03
	0.05	0.2	0.24	0.2
	0.1	0.2	0.4	0.1
	0.36	0.2	0.2	0.2
	0.1	0.28	0.1	0.56
	0.72	0.28	0.01	0.28
	0.06	0.36	0.02	0.1
	0.4	0.56	0.24	0.28
	0.12	0.24	0.12	0.4
	0.03	0.06	0.12	0.06
	0.2	0.24	0.2	0.2
	0.28	0.2	0.56	0.07
	0.2	0.28	0.28	0.2
	0.05	0.06	0.05	0.06
	0.1	0.03	0.2	0.03
	0.1	0.56	0.05	0.05
	0.01	0.02	0.1	0.03
	0.02	0.2	0.2	0.4
	0.2	0.12	0.01	0.02
	0.12	0.12	0.02	0.01
	0.2	0.2	0.1	0.05
	0.2	0.12	0.01	0.02
	0.12	0.2	0.28	0.02
	0.4	0.2	0.1	0.05
	0.2	0.12	0.03	0.06
	0.03	0.07	0.2	0.07
	0.06	0.12	0.2	0.12
	0.28	0.56	0.4	0.36
Average	**0.182**	**0.214**	**0.168**	**0.139**

Subgrade Soil

Table 13-6 Deterministic risk analysis for subgrade soil

c		
R3.	S17	S13
Y6	X6.1	X6.2
R6.Subgrade Soil	S17.Increase Moisture/ Excess water	S13.Selection of construction soil
	0.12	0.03
	0.28	0.56
	0.03	0.28
	0.18	0.1
	0.1	0.2
	0.2	0.4
	0.01	0.03
	0.12	0.04
	0.14	0.06
	0.1	0.2
	0.1	0.06
	0.03	0.12
	0.2	0.4
	0.36	0.04
	0.2	0.2
	0.06	0.1
	0.05	0.2
	0.03	0.05
	0.2	0.1
	0.1	0.1
	0.04	0.06
	0.12	0.24
	0.12	0.56
	0.04	0.56
	0.2	0.56
	0.06	0.28
	0.07	0.06
	0.09	0.2
	0.2	0.2
	0.56	0.4
Rate	**0.137**	**0.213**

Drainage

Table 13-7: Deterministic risk analysis for drainage

c		
R3.	S17	S23
Y7	X7.1	X7.2
	S17.Increase Moisture/ Excess water	S23.Insufficient drainage system
R7.Drainage	0.03	0.03
	0.28	0.56
	0.2	0.2
	0.07	0.2
	0.2	0.2
	0.4	0.56
	0.01	0.28
	0.28	0.28
	0.14	0.28
	0.18	0.18
	0.4	0.4
	0.02	0.02
	0.1	0.56
	0.12	0.12
	0.2	0.36
	0.06	0.03
	0.03	0.03
	0.06	0.1
	0.2	0.28
	0.2	0.14
	0.04	0.72
	0.04	0.24
	0.28	0.36
	0.04	0.24
	0.2	0.56
	0.2	0.28
	0.04	0.72
	0.18	0.36
	0.28	0.24
	0.4	0.28
	0.163	**0.294**

Maintenance

Table 13-8: Deterministic risk analysis for maintenance

	c		
R8	S24	S25	S26
Y8	X8.1	X8.2	X8.3
R8.Maintenance	S24.Delay maintenance	S25.Maintenance priorities /plan	S26.Limited Budget
	0.06	0.06	0.1
	0.4	0.4	0.2
	0.01	0.01	0.01
	0.2	0.14	0.2
	0.1	0.1	0.2
	0.56	0.28	0.72
	0.28	0.1	0.56
	0.72	0.12	0.72
	0.72	0.56	0.56
	0.28	0.28	0.2
	0.4	0.4	0.4
	0.06	0.02	0.12
	0.2	0.24	0.2
	0.04	0.2	0.02
	0.12	0.12	0.12
	0.1	0.05	0.06
	0.1	0.05	0.05
	0.02	0.03	0.1
	0.03	0.06	0.06
	0.2	0.2	0.28
	0.56	0.72	0.28
	0.56	0.72	0.12
	0.28	0.36	0.36
	0.56	0.72	0.36
	0.56	0.72	0.18
	0.28	0.18	0.18
	0.06	0.72	0.36
	0.24	0.04	0.02
	0.12	0.12	0.1
	0.4	0.36	0.36
Average	**0.274**	**0.269**	**0.240**

Construction Quality

Table 13-9: Deterministic risk analysis for construction quality

c			
R9	S27	S28	S29
Y9	X9.1	X9.2	X9.3
R9. Construction Quality	S27.Design and Specification	S28.Construction Process	S29.Construction Management
	0.28	0.28	0.28
	0.56	0.56	0.4
	0.03	0.03	0.28
	0.12	0.05	0.05
	0.2	0.1	0.1
	0.72	0.1	0.2
	0.72	0.28	0.1
	0.4	0.4	0.4
	0.28	0.28	0.2
	0.36	0.12	0.28
	0.1	0.1	0.56
	0.12	0.12	0.12
	0.2	0.1	0.56
	0.03	0.06	0.1
	0.12	0.1	0.14
	0.1	0.06	0.03
	0.2	0.05	0.03
	0.03	0.05	0.05
	0.05	0.2	0.2
	0.1	0.05	0.24
	0.28	0.28	0.56
	0.24	0.24	0.04
	0.2	0.12	0.12
	0.08	0.08	0.12
	0.2	0.12	0.12
	0.28	0.2	0.12
	0.28	0.28	0.56
	0.01	0.03	0.05
	0.06	0.1	0.1
	0.56	0.4	0.36
Average	**0.230**	**0.165**	**0.216**

Rutting

Table 13-10: Deterministic risk analysis for rutting

c					
R10.	**R2**	**R3**	**R9**	**R4**	**R6**
Y10	X10.1	X10.2	X10.3	X10.4	X10.5
Rutting	R2.Climate Change	R3.Pavement Composition	R9.Construction Quality	R4.Pavement Strength	R6.Subgrade
	0.28	0.1	0.05	0.03	0.03
	0.24	0.4	0.24	0.2	0.1
	0.2	0.03	0.06	0.2	0.2
	0.1	0.12	0.06	0.2	0.12
	0.2	0.24	0.1	0.1	0.12
	0.28	0.2	0.56	0.56	0.56
	0.03	0.72	0.56	0.4	0.28
	0.72	0.2	0.2	0.01	0.04
	0.14	0.1	0.2	0.28	0.1
	0.28	0.36	0.28	0.28	0.28
	0.1	0.1	0.2	0.2	0.2
	0.06	0.06	0.12	0.12	0.06
	0.2	0.1	0.2	0.4	0.2
	0.14	0.18	0.28	0.24	0.06
	0.2	0.12	0.06	0.12	0.06
	0.2	0.2	0.05	0.1	0.05
	0.2	0.2	0.1	0.1	0.1
	0.05	0.1	0.14	0.05	0.03
	0.06	0.06	0.06	0.2	0.06
	0.2	0.04	0.2	0.12	0.2
	0.01	0.03	0.56	0.24	0.56
	0.06	0.24	0.24	0.4	0.24
	0.02	0.4	0.4	0.28	0.56
	0.02	0.4	0.4	0.24	0.56
	0.1	0.4	0.28	0.2	0.72
	0.02	0.24	0.4	0.1	0.56
	0.01	0.18	0.14	0.07	0.07
	0.03	0.05	0.12	0.12	0.28
	0.02	0.12	0.2	0.28	0.04
	0.28	0.4	0.36	0.56	0.2
Average	**0.148**	**0.203**	**0.227**	**0.213**	**0.221**

Cracking

Table 13-11: Deterministic risk analysis for cracking

R11.	R2	R3	R9	R4	R6
Y11	X11.1	X11.2	X11.3	X11.4	X11.5
	R2.Climate Change	R3.Pavement Composition	R9.Construction Quality	R4.Pavement Strength	R6.Subgrade
Cracking	0.28	0.14	0.28	0.07	0.03
	0.56	0.72	0.28	0.4	0.28
	0.2	0.1	0.2	0.2	0.1
	0.1	0.04	0.05	0.07	0.2
	0.2	0.05	0.05	0.14	0.14
	0.2	0.2	0.36	0.28	0.2
	0.01	0.01	0.2	0.05	0.01
	0.72	0.28	0.28	0.01	0.01
	0.18	0.1	0.28	0.28	0.01
	0.28	0.2	0.12	0.2	0.1
	0.28	0.2	0.56	0.1	0.2
	0.06	0.06	0.12	0.12	0.06
	0.2	0.2	0.4	0.2	0.1
	0.2	0.14	0.14	0.36	0.04
	0.2	0.12	0.06	0.12	0.06
	0.2	0.2	0.05	0.03	0.03
	0.2	0.2	0.1	0.05	0.06
	0.1	0.28	0.05	0.28	0.03
	0.1	0.1	0.05	0.05	0.06
	0.2	0.12	0.2	0.14	0.12
	0.12	0.05	0.06	0.12	0.01
	0.4	0.03	0.06	0.12	0.01
	0.36	0.06	0.05	0.12	0.02
	0.72	0.01	0.06	0.12	0.01
	0.56	0.1	0.2	0.28	0.56
	0.14	0.06	0.12	0.12	0.01
	0.12	0.12	0.06	0.12	0.05
	0.06	0.06	0.06	0.07	0.06
	0.06	0.12	0.4	0.24	0.4
	0.28	0.28	0.56	0.4	0.36
Rate	**0.243**	**0.145**	**0.182**	**0.162**	**0.111**

Vehicle Speed

Table 13-12 Parametric risk analysis for vehicle speed

c			
S7	R2	R1	R6
Y12	X12.1	X12.2	X12.3
S7.Vehicle speed	R5.Pavement Ageing	R7.Drainage	R8.Maintenance
	0.03	0.03	0.03
	0.1	0.14	0.18
	0.1	0.02	0.01
	0.14	0.2	0.12
	0.05	0.2	0.1
	0.02	0.02	0.06
	0.02	0.01	0.1
	0.01	0.01	0.03
	0.06	0.28	0.06
	0.14	0.14	0.28
	0.12	0.12	0.2
	0.06	0.03	0.06
	0.2	0.12	0.12
	0.12	0.2	0.28
	0.12	0.06	0.2
	0.1	0.03	0.06
	0.1	0.03	0.03
	0.28	0.05	0.03
	0.05	0.05	0.05
	0.12	0.2	0.12
	0.01	0.12	0.4
	0.12	0.24	0.24
	0.2	0.4	0.4
	0.01	0.12	0.4
	0.01	0.2	0.12
	0.01	0.1	0.4
	0.01	0.36	0.02
	0.1	0.14	0.14
	0.06	0.14	0.14
	0.36	0.28	0.4
Average	**0.094**	**0.135**	**0.159**

Pavement Thickness

Table 13-13: Parametric risk analysis for Pavement Thickness

c	
S7	R2
Y13	X13.1
S19.Pavement Thickness	R9.Construction Quality
	0.14
	0.4
	0.4
	0.1
	0.2
	0.2
	0.04
	0.2
	0.1
	0.1
	0.05
	0.12
	0.1
	0.05
	0.12
	0.1
	0.1
	0.1
	0.1
	0.02
	0.72
	0.28
	0.28
	0.56
	0.56
	0.36
	0.72
	0.2
	0.12
	0.56
Average	**0.237**

14. Appendix 3: Additional Data for Chapter 6

Change in Roughness- Structural component (ΔRIs) based on Default HDM-4 Model

Table 14-1 : Example of change in roughness -structural (ΔRIs) based on HDM-4 model

Change in roughness structural (ΔRIs) based on HDM-4 model											
N	Road Code	**Road**	**SNPKb**	**m**	**AGE**	**HS**	**Kgs**	**kgm**	**YE4**	**a0**	**ΔRIs**
1	E.11	Ittihad road	3.5	0.008	11	180	1	1	1.52	134	0.121
3	E18.1	Manama- RAK Airport	3.5	0.007	11	160	1	1	1.87	134	0.147
5	E18.2	RAK Airport-Sha'am	3.5	0.013	12	160	1	1	1.67	134	0.141
7	E311	Sheik Mohammed Bin Zayed	3.5	0.007	6	180	1	1	7.67	134	0.582
8	E55.1	Dhaid - Madam	3.5	0.010	16	180	1	1	0.21	134	0.018
10	E55.2	Madam - Shiweb	3.5	0.011	16	180	1	1	0.34	134	0.029
12	E55.3	Umm Al Quwaim - Dhaid	3.5	0.008	16	180	1	1	0.15	134	0.012
18	E84	Sheikh Khalifa Rd	3.5	0.006	5	190	1	1	0.55	134	0.041
20	E88.1	Sharjah - Dhaid	3.5	0.009	15	180	1	1	1.98	134	0.164
22	E88.2	Dhaid - Masafi	3.5	0.009	15	180	1	1	1.65	134	0.136
24	E89.1	Masafi - Dibba (from Dibba to Ghona Bridge)	3.5	0.013	9	160	1	1	0.14	134	0.011
26	E89.3	Masafi - Fujairah	3.5	0.010	18	180	1	1	1.27	134	0.111
28	E99.1	Khor Fakkan - Dibba	3.5	0.012	17	180	1	1	0.71	134	0.063
29	E99.2	Fujairah - Khor Fakkan	3.5	0.010	17	180	1	1	1.13	134	0.097
30	E99.3	Fujairah - Oman	3.5	0.012	19	180	1	1	0.61	134	0.055

Change in Rutting (ΔRDS) based on Default HDM-4

Table 14-2: Change in rutting (ΔRDS) based on HDM-4

plastic deformation for rutting ΔRDS														
Road	**YE4**	**VIM**	**SP**	**HS**	**RIa**	**sh**	**TPm**	**Kr**	**b0**	**b1**	**b2**	**b3**	**b4**	**ΔRDS**
Ittihad road	1.52	1.222	76.54	180	1.160	48	69.64	1	2.46	-0.78	0.71	1.34	-1.26	4.987
Manama- RAK Airport	1.87	1.222	76.54	160	0.980	48	69.64	1	2.46	-0.78	0.71	1.34	-1.26	5.643
RAK Airport-Sha'am	1.67	1.216	76.76	160	1.730	50	69.64	1	2.46	-0.78	0.71	1.34	-1.26	4.894
Sheik Mohammed Bin Zayed	7.67	1.265	75.02	180	0.990	48	69.64	1	2.46	-0.78	0.71	1.34	-1.26	24.767
Dhaid - Madam	0.21	1.196	77.49	180	1.310	44	69.64	1	2.46	-0.78	0.71	1.34	-1.26	0.746
Madam - Shiweb	0.34	1.196	77.49	180	1.510	46	69.64	1	2.46	-0.78	0.71	1.34	-1.26	1.166
Umm Al Quwaim - Dhaid	0.15	1.196	77.49	180	1.160	47	69.64	1	2.46	-0.78	0.71	1.34	-1.26	0.506
Sheikh Khalifa Rd	0.55	1.277	74.56	190	0.802	50	69.64	1	2.46	-0.78	0.71	1.34	-1.26	1.780
Sharjah - Dhaid	1.98	1.200	77.32	180	1.201	40	69.64	1	2.46	-0.78	0.71	1.34	-1.26	7.557
Dhaid - Masafi	1.65	1.200	77.32	180	1.180	43	69.64	1	2.46	-0.78	0.71	1.34	-1.26	5.952
Masafi - Dibba	0.14	1.240	73.99	160	1.806	42	69.64	1	2.46	-0.78	0.71	1.34	-1.26	0.482
Masafi - Fujairah	1.27	1.188	77.78	180	1.416	42	69.64	1	2.46	-0.78	0.71	1.34	-1.26	4.692
Khor Fakkan - Dibba	0.71	1.192	77.64	180	1.601	35	69.64	1	2.46	-0.78	0.71	1.34	-1.26	3.019
Fujairah - Khor Fakkan	1.13	1.192	77.64	180	1.334	38	69.64	1	2.46	-0.78	0.71	1.34	-1.26	4.506
Fujairah - Oman	0.61	1.188	77.95	180	1.610	35	69.64	1	2.46	-0.78	0.71	1.34	-1.26	2.591

Change in Roughness- Rutting (ΔRlr) based on Default HDM-4

Table 14-3: Change in roughness- rutting (ΔRlr) based on HDM-4

Road	ΔRDS	ΔRIr	Kgr	c0
Ittihad road	4.99	0.44	1	0.088
Manama- RAK Airport	5.64	0.50	1	0.088
RAK Airport-Sha'am	4.89	0.43	1	0.088
Sheik Mohammed Bin Zayed	24.77	2.18	1	0.088
Dhaid - Madam	0.75	0.07	1	0.088
Madam - Shiweb	1.17	0.10	1	0.088
Umm Al Quwaim - Dhaid	0.51	0.04	1	0.088
Sheikh Khalifa Rd	1.78	0.16	1	0.088
Sharjah - Dhaid	7.56	0.67	1	0.088
Dhaid - Masafi	5.95	0.52	1	0.088
Masafi - Dibba (from Dibba to Ghona Bridge)	0.48	0.04	1	0.088
Masafi - Fujairah	4.69	0.41	1	0.088
Khor Fakkan - Dibba	3.02	0.27	1	0.088
Fujairah - Khor Fakkan	4.51	0.40	1	0.088
Fujairah - Oman	2.59	0.23	1	0.088

Change in Roughness due to Cracking ΔRIc based on Default HDM-4

Table 14-4: Change in roughness due to cracking ΔRIc based on HDM-4

Road	ΔACRA	kgc	a0	ΔRIc
Ittihad road	3.7	1	0.0066	0.024
Manama- RAK Airport	7.7	1	0.0066	0.051
RAK Airport-Sha'am	4.5	1	0.0066	0.030
Sheik Mohammed Bin Zayed	5.4	1	0.0066	0.036

Dhaid - Madam	10.3	1	0.0066	0.068
Madam - Shiweb	7.7	1	0.0066	0.051
Umm Al Quwaim - Dhaid	3.5	1	0.0066	0.023
Sheikh Khalifa Rd	12.2	1	0.0066	0.081
Sharjah - Dhaid	2.2	1	0.0066	0.014
Dhaid - Masafi	13.0	1	0.0066	0.086
Masafi - Dibba (from Dibba to Ghona Bridge)	14.5	1	0.0066	0.096
Masafi - Fujairah	12.9	1	0.0066	0.085
Khor Fakkan - Dibba	10.1	1	0.0066	0.067
Fujairah - Khor Fakkan	3.3	1	0.0066	0.022
Fujairah - Oman	7.6	1	0.0066	0.050

Change in Roughness due to Environment ΔRIe based on Default HDM-4

Table 14-5 Example of change in roughness due to environment ΔRIe based on HDM-4

Road	ΔRIe	Kgm	m	RIa
Ittihad road	0.010	1	0.0085	1.160
Manama- RAK Airport	0.007	1	0.0072	0.980
RAK Airport-Sha'am	0.022	1	0.0126	1.730
Sheik Mohammed Bin Zayed	0.007	1	0.0072	0.990
Dhaid - Madam	0.013	1	0.0096	1.310
Madam - Shiweb	0.017	1	0.011	1.510
Umm Al Quwaim - Dhaid	0.010	1	0.0085	1.160
Sheikh Khalifa Rd	0.005	1	0.0059	0.802
Sharjah - Dhaid	0.011	1	0.0088	1.201
Dhaid - Masafi	0.010	1	0.0086	1.180
Masafi - Dibba (from Dibba to Ghona Bridge)	0.024	1	0.0132	1.806
Masafi - Fujairah	0.015	1	0.0103	1.416
Khor Fakkan - Dibba	0.019	1	0.0117	1.601
Fujairah - Khor Fakkan	0.013	1	0.0097	1.334
Fujairah - Oman	0.019	1	0.0118	1.610

Total Change in Roughness (ΔRI) based on Default HDM-4

Table 14-6:Total change in roughness (ΔRI) based on HDM-4

Road	ΔRls	ΔRIr	ΔRIc	ΔRIe	ΔRI
Ittihad road	0.120	0.439	0.024	0.010	0.594
Manama- RAK Airport	0.150	0.497	0.051	0.007	0.702

RAK Airport-Sha'am	0.140	0.431	0.030	0.022	0.623
Sheik Mohammed Bin Zayed	0.580	2.180	0.036	0.007	2.804
Dhaid - Madam	0.020	0.066	0.068	0.013	0.164
Madam - Shiweb	0.030	0.103	0.051	0.017	0.200
Umm Al Quwaim - Dhaid	0.010	0.045	0.023	0.010	0.090
Sheikh Khalifa Rd	0.040	0.157	0.081	0.005	0.283
Sharjah - Dhaid	0.160	0.665	0.014	0.011	0.854
Dhaid - Masafi	0.140	0.524	0.086	0.010	0.756
Masafi - Dibba (from Dibba to Ghona Bridge)	0.010	0.042	0.096	0.024	0.174
Masafi - Fujairah	0.110	0.413	0.086	0.015	0.624
Khor Fakkan - Dibba	0.060	0.266	0.067	0.019	0.414
Fujairah - Khor Fakkan	0.100	0.397	0.022	0.013	0.528
Fujairah - Oman	0.060	0.228	0.050	0.019	0.352

Results of Default HDM-4 Model based on 2013 Climate Change scenario

Table 14-7: Results of HDM-4 model based on 2013 climate change scenario

N	Road Code	Road	change in roughness structural (ΔRIs)	change in roughness rutting ΔRIr	change in roughness due to cracking ΔRIc	environmental component of roughness (ΔRIe)	The total incremental change in roughness ΔRI
1	E.11	Ittihad road	0.121	0.439	0.024	0.214	0.798
1	E.11	Ittihad road	0.121	0.439	0.055	0.214	0.829
1	E.11	Ittihad road	0.121	0.439	0.079	0.214	0.853
1	E.11	Ittihad road	0.121	0.439	0.045	0.214	0.820
1	E.11	Ittihad road	0.121	0.439	0.014	0.214	0.789
1	E.11	Ittihad road	0.121	0.439	0.032	0.214	0.806
1	E.11	Ittihad road	0.121	0.439	0.021	0.214	0.796
1	E.11	Ittihad road	0.121	0.439	0.051	0.214	0.825
3	E18.1	Manama- RAK Airport	0.147	0.497	0.020	0.181	0.844
3	E18.1	Manama- RAK Airport	0.147	0.497	0.017	0.181	0.841
3	E18.1	Manama- RAK Airport	0.147	0.497	0.064	0.181	0.889
3	E18.1	Manama- RAK Airport	0.147	0.497	0.042	0.181	0.866
3	E18.1	Manama- RAK Airport	0.147	0.497	0.037	0.181	0.862
3	E18.1	Manama- RAK Airport	0.147	0.497	0.069	0.181	0.893
3	E18.1	Manama- RAK Airport	0.147	0.497	0.014	0.181	0.839
3	E18.1	Manama- RAK Airport	0.147	0.497	0.051	0.181	0.875
5	E18.2	RAK Airport-Sha'am	0.141	0.431	0.030	0.319	0.921
5	E18.2	RAK Airport-Sha'am	0.141	0.431	0.019	0.319	0.910
5	E18.2	RAK Airport-Sha'am	0.141	0.431	0.014	0.319	0.905
5	E18.2	RAK Airport-Sha'am	0.141	0.431	0.040	0.319	0.932
5	E18.2	RAK Airport-Sha'am	0.141	0.431	0.015	0.319	0.906
5	E18.2	RAK Airport-Sha'am	0.141	0.431	0.107	0.319	0.998
5	E18.2	RAK Airport-Sha'am	0.141	0.431	0.028	0.319	0.919

5	E18.2	RAK Airport-Sha'am	0.141	0.431	0.065	0.319	0.956
5	E18.2	RAK Airport-Sha'am	0.141	0.431	0.073	0.319	0.964
7	E311	Sheik Mohammed Bin Zayed	0.582	2.179	0.026	0.183	2.969
7	E311	Sheik Mohammed Bin Zayed	0.582	2.179	0.069	0.183	3.012
7	E311	Sheik Mohammed Bin Zayed	0.582	2.179	0.043	0.183	2.987
7	E311	Sheik Mohammed Bin Zayed	0.582	2.179	0.020	0.183	2.964
7	E311	Sheik Mohammed Bin Zayed	0.582	2.179	0.046	0.183	2.990
7	E311	Sheik Mohammed Bin Zayed	0.582	2.179	0.034	0.183	2.978
7	E311	Sheik Mohammed Bin Zayed	0.582	2.179	0.023	0.183	2.967
7	E311	Sheik Mohammed Bin Zayed	0.582	2.179	0.038	0.183	2.982
7	E311	Sheik Mohammed Bin Zayed	0.582	2.179	0.061	0.183	3.005
7	E311	Sheik Mohammed Bin Zayed	0.582	2.179	0.023	0.183	2.967
7	E311	Sheik Mohammed Bin Zayed	0.582	2.179	0.036	0.183	2.979
8	E55.1	Dhaid - Madam	0.018	0.066	0.068	0.242	0.393
8	E55.1	Dhaid - Madam	0.018	0.066	0.017	0.242	0.343
8	E55.1	Dhaid - Madam	0.018	0.066	0.024	0.242	0.349
8	E55.1	Dhaid - Madam	0.018	0.066	0.024	0.242	0.349
8	E55.1	Dhaid - Madam	0.018	0.066	0.016	0.242	0.341
8	E55.1	Dhaid - Madam	0.018	0.066	0.023	0.242	0.348
8	E55.1	Dhaid - Madam	0.018	0.066	0.041	0.242	0.366
8	E55.1	Dhaid - Madam	0.018	0.066	0.016	0.242	0.341
8	E55.1	Dhaid - Madam	0.018	0.066	0.050	0.242	0.375
8	E55.1	Dhaid - Madam	0.018	0.066	0.056	0.242	0.381
10	E55.2	Madam - Shiweb	0.029	0.103	0.048	0.279	0.459
10	E55.2	Madam - Shiweb	0.029	0.103	0.023	0.279	0.434
10	E55.2	Madam - Shiweb	0.029	0.103	0.058	0.279	0.468
10	E55.2	Madam - Shiweb	0.029	0.103	0.051	0.279	0.462
12	E55.3	Umm Al Quwaim - Dhaid	0.012	0.045	0.023	0.214	0.294
12	E55.3	Umm Al Quwaim - Dhaid	0.012	0.045	0.006	0.214	0.277
12	E55.3	Umm Al Quwaim - Dhaid	0.012	0.045	0.037	0.214	0.309
12	E55.3	Umm Al Quwaim - Dhaid	0.012	0.045	0.027	0.214	0.298
12	E55.3	Umm Al Quwaim - Dhaid	0.012	0.045	0.113	0.214	0.384
12	E55.3	Umm Al Quwaim - Dhaid	0.012	0.045	0.019	0.214	0.290
12	E55.3	Umm Al Quwaim - Dhaid	0.012	0.045	0.058	0.214	0.329
12	E55.3	Umm Al Quwaim - Dhaid	0.012	0.045	0.079	0.214	0.350
12	E55.3	Umm Al Quwaim - Dhaid	0.012	0.045	0.073	0.214	0.344
18	E84	Sheikh Khalifa Rd	0.041	0.157	0.022	0.148	0.368
18	E84	Sheikh Khalifa Rd	0.041	0.157	0.017	0.148	0.362
18	E84	Sheikh Khalifa Rd	0.041	0.157	0.061	0.148	0.407
18	E84	Sheikh Khalifa Rd	0.041	0.157	0.106	0.148	0.452
18	E84	Sheikh Khalifa Rd	0.041	0.157	0.034	0.148	0.380
18	E84	Sheikh Khalifa Rd	0.041	0.157	0.101	0.148	0.447
18	E84	Sheikh Khalifa Rd	0.041	0.157	0.043	0.148	0.388
18	E84	Sheikh Khalifa Rd	0.041	0.157	0.081	0.148	0.426
20	E88.1	Sharjah - Dhaid	0.164	0.665	0.014	0.222	1.065
20	E88.1	Sharjah - Dhaid	0.164	0.665	0.038	0.222	1.089
20	E88.1	Sharjah - Dhaid	0.164	0.665	0.058	0.222	1.109
20	E88.1	Sharjah - Dhaid	0.164	0.665	0.062	0.222	1.113
20	E88.1	Sharjah - Dhaid	0.164	0.665	0.028	0.222	1.078
20	E88.1	Sharjah - Dhaid	0.164	0.665	0.104	0.222	1.155
22	E88.2	Dhaid - Masafi	0.137	0.524	0.090	0.218	0.969
22	E88.2	Dhaid - Masafi	0.136	0.524	0.025	0.218	0.903
22	E88.2	Dhaid - Masafi	0.136	0.524	0.030	0.218	0.908
22	E88.2	Dhaid - Masafi	0.136	0.524	0.032	0.218	0.910
22	E88.2	Dhaid - Masafi	0.136	0.524	0.015	0.218	0.893
22	E88.2	Dhaid - Masafi	0.136	0.524	0.077	0.218	0.955
22	E88.2	Dhaid - Masafi	0.136	0.524	0.065	0.218	0.943
22	E88.2	Dhaid - Masafi	0.136	0.524	0.086	0.218	0.964
24	E89.1	Masafi - Dibba)	0.011	0.042	0.096	0.333	0.483
24	E89.1	Masafi - Dibba	0.011	0.042	0.014	0.333	0.402

24	E89.1	Masafi - Dibba	0.011	0.042	0.050	0.333	0.437
26	E89.3	Masafi - Fujairah	0.111	0.413	0.056	0.261	0.842
26	E89.3	Masafi - Fujairah	0.111	0.413	0.041	0.261	0.826
26	E89.3	Masafi - Fujairah	0.111	0.413	0.029	0.261	0.814
26	E89.3	Masafi - Fujairah	0.111	0.413	0.085	0.261	0.871
28	E99.1	Khor Fakkan - Dibba	0.063	0.266	0.067	0.296	0.691
28	E99.1	Khor Fakkan - Dibba	0.063	0.266	0.047	0.296	0.671
28	E99.1	Khor Fakkan - Dibba	0.063	0.266	0.103	0.296	0.727
28	E99.1	Khor Fakkan - Dibba	0.063	0.266	0.030	0.296	0.654
28	E99.1	Khor Fakkan - Dibba	0.063	0.266	0.023	0.296	0.647
28	E99.1	Khor Fakkan - Dibba	0.063	0.266	0.062	0.296	0.686
28	E99.1	Khor Fakkan - Dibba	0.063	0.266	0.058	0.296	0.682
29	E99.2	Fujairah - Khor Fakkan	0.097	0.397	0.019	0.246	0.759
29	E99.2	Fujairah - Khor Fakkan	0.097	0.397	0.053	0.246	0.793
29	E99.2	Fujairah - Khor Fakkan	0.097	0.397	0.022	0.246	0.761
29	E99.2	Fujairah - Khor Fakkan	0.097	0.397	0.024	0.246	0.764
30	E99.3	Fujairah - Oman	0.055	0.228	0.050	0.297	0.631

Results of default HDM-4 Model based on 2020 Climate change scenario

Table 14-8: Results of HDM-4 model based on 2020 climate change scenario

N	Road Code	Road	change in roughness structural (ΔRIs)	change in roughness rutting ΔRIr	change in roughness due to cracking ΔRIc	environmental component of roughness (ΔRIe)	The total incremental change in roughness ΔRI
1	E.11	Ittihad road	0.8338	0.4504	0.0243	0.2132	1.5218
1	E.11	Ittihad road	0.8338	0.4504	0.0545	0.2132	1.5520
1	E.11	Ittihad road	0.8338	0.4504	0.0792	0.2132	1.5767
1	E.11	Ittihad road	0.8338	0.4504	0.0454	0.2132	1.5429
1	E.11	Ittihad road	0.8338	0.4504	0.0144	0.2132	1.5118
1	E.11	Ittihad road	0.8338	0.4504	0.0318	0.2132	1.5292
1	E.11	Ittihad road	0.8338	0.4504	0.0214	0.2132	1.5188
1	E.11	Ittihad road	0.8338	0.4504	0.0508	0.2132	1.5483
3	E18.1	Manama- RAK Airport	1.0258	0.5097	0.0196	0.1801	1.7352
3	E18.1	Manama- RAK Airport	1.0258	0.5097	0.0167	0.1801	1.7323
3	E18.1	Manama- RAK Airport	1.0258	0.5097	0.0645	0.1801	1.7801
3	E18.1	Manama- RAK Airport	1.0258	0.5097	0.0420	0.1801	1.7576
3	E18.1	Manama- RAK Airport	1.0258	0.5097	0.0372	0.1801	1.7529
3	E18.1	Manama- RAK Airport	1.0258	0.5097	0.0689	0.1801	1.7845
3	E18.1	Manama- RAK Airport	1.0258	0.5097	0.0141	0.1801	1.7297
3	E18.1	Manama- RAK Airport	1.0258	0.5097	0.0510	0.1801	1.7666
5	E18.2	RAK Airport-Sha'am	1.1010	0.4420	0.0296	0.3180	1.8905
5	E18.2	RAK Airport-Sha'am	1.1010	0.4420	0.0193	0.3180	1.8803
5	E18.2	RAK Airport-Sha'am	1.1010	0.4420	0.0141	0.3180	1.8751
5	E18.2	RAK Airport-Sha'am	1.1010	0.4420	0.0404	0.3180	1.9013
5	E18.2	RAK Airport-Sha'am	1.1010	0.4420	0.0149	0.3180	1.8759
5	E18.2	RAK Airport-Sha'am	1.1010	0.4420	0.1072	0.3180	1.9681
5	E18.2	RAK Airport-Sha'am	1.1010	0.4420	0.0282	0.3180	1.8892
5	E18.2	RAK Airport-Sha'am	1.1010	0.4420	0.0650	0.3180	1.9260
5	E18.2	RAK Airport-Sha'am	1.1010	0.4420	0.0729	0.3180	1.9339
7	E311	Sheik Mohammed Bin Zayed	1.6782	2.2368	0.0256	0.1820	4.1225
7	E311	Sheik Mohammed Bin Zayed	1.6782	2.2368	0.0685	0.1820	4.1655
7	E311	Sheik Mohammed Bin Zayed	1.6782	2.2368	0.0427	0.1820	4.1397
7	E311	Sheik Mohammed Bin Zayed	1.6782	2.2368	0.0203	0.1820	4.1172
7	E311	Sheik Mohammed Bin Zayed	1.6782	2.2368	0.0461	0.1820	4.1431
7	E311	Sheik Mohammed Bin Zayed	1.6782	2.2368	0.0339	0.1820	4.1309

7	E311	Sheik Mohammed Bin Zayed	1.6782	2.2368	0.0233	0.1820	4.1203
7	E311	Sheik Mohammed Bin Zayed	1.6782	2.2368	0.0379	0.1820	4.1349
7	E311	Sheik Mohammed Bin Zayed	1.6782	2.2368	0.0609	0.1820	4.1578
7	E311	Sheik Mohammed Bin Zayed	1.6782	2.2368	0.0229	0.1820	4.1199
7	E311	Sheik Mohammed Bin Zayed	1.6782	2.2368	0.0356	0.1820	4.1326
8	E55.1	Dhaid - Madam	0.2888	0.0673	0.0682	0.2408	0.6652
8	E55.1	Dhaid - Madam	0.2888	0.0673	0.0175	0.2408	0.6144
8	E55.1	Dhaid - Madam	0.2888	0.0673	0.0235	0.2408	0.6205
8	E55.1	Dhaid - Madam	0.2888	0.0673	0.0238	0.2408	0.6207
8	E55.1	Dhaid - Madam	0.2888	0.0673	0.0163	0.2408	0.6132
8	E55.1	Dhaid - Madam	0.2888	0.0673	0.0230	0.2408	0.6200
8	E55.1	Dhaid - Madam	0.2888	0.0673	0.0413	0.2408	0.6382
8	E55.1	Dhaid - Madam	0.2888	0.0673	0.0162	0.2408	0.6131
8	E55.1	Dhaid - Madam	0.2888	0.0673	0.0498	0.2408	0.6467
8	E55.1	Dhaid - Madam	0.2888	0.0673	0.0560	0.2408	0.6530
10	E55.2	Madam - Shiweb	0.4676	0.1053	0.0484	0.2776	0.8988
10	E55.2	Madam - Shiweb	0.4676	0.1053	0.0227	0.2776	0.8732
10	E55.2	Madam - Shiweb	0.4676	0.1053	0.0576	0.2776	0.9081
10	E55.2	Madam - Shiweb	0.4676	0.1053	0.0509	0.2776	0.9014
12	E55.3	Umm Al Quwaim - Dhaid	0.2063	0.0457	0.0230	0.2132	0.4882
12	E55.3	Umm Al Quwaim - Dhaid	0.2063	0.0457	0.0060	0.2132	0.4712
12	E55.3	Umm Al Quwaim - Dhaid	0.2063	0.0457	0.0375	0.2132	0.5027
12	E55.3	Umm Al Quwaim - Dhaid	0.2063	0.0457	0.0268	0.2132	0.4920
12	E55.3	Umm Al Quwaim - Dhaid	0.2063	0.0457	0.1128	0.2132	0.5780
12	E55.3	Umm Al Quwaim - Dhaid	0.2063	0.0457	0.0193	0.2132	0.4845
12	E55.3	Umm Al Quwaim - Dhaid	0.2063	0.0457	0.0581	0.2132	0.5233
12	E55.3	Umm Al Quwaim - Dhaid	0.2063	0.0457	0.0788	0.2132	0.5440
12	E55.3	Umm Al Quwaim - Dhaid	0.2063	0.0457	0.0725	0.2132	0.5378
18	E84	Sheikh Khalifa Rd	0.1001	0.1607	0.0219	0.1473	0.4301
18	E84	Sheikh Khalifa Rd	0.1001	0.1607	0.0167	0.1473	0.4249
18	E84	Sheikh Khalifa Rd	0.1001	0.1607	0.0613	0.1473	0.4695
18	E84	Sheikh Khalifa Rd	0.1001	0.1607	0.1063	0.1473	0.5145
18	E84	Sheikh Khalifa Rd	0.1001	0.1607	0.0340	0.1473	0.4422
18	E84	Sheikh Khalifa Rd	0.1001	0.1607	0.1012	0.1473	0.5094
18	E84	Sheikh Khalifa Rd	0.1001	0.1607	0.0428	0.1473	0.4510
18	E84	Sheikh Khalifa Rd	0.1001	0.1607	0.0806	0.1473	0.4889
20	E88.1	Sharjah - Dhaid	2.2658	0.6825	0.0142	0.2208	3.1833
20	E88.1	Sharjah - Dhaid	2.2658	0.6825	0.0383	0.2208	3.2074
20	E88.1	Sharjah - Dhaid	2.2658	0.6825	0.0584	0.2208	3.2275
20	E88.1	Sharjah - Dhaid	2.2658	0.6825	0.0620	0.2208	3.2311
20	E88.1	Sharjah - Dhaid	2.2658	0.6825	0.0275	0.2208	3.1966
20	E88.1	Sharjah - Dhaid	2.2658	0.6825	0.1039	0.2208	3.2729
22	E88.2	Dhaid - Masafi	1.8882	0.5375	0.0905	0.2169	2.7331
22	E88.2	Dhaid - Masafi	1.8882	0.5375	0.0250	0.2169	2.6676
22	E88.2	Dhaid - Masafi	1.8882	0.5375	0.0298	0.2169	2.6724
22	E88.2	Dhaid - Masafi	1.8882	0.5375	0.0319	0.2169	2.6745
22	E88.2	Dhaid - Masafi	1.8882	0.5375	0.0151	0.2169	2.6577
22	E88.2	Dhaid - Masafi	1.8882	0.5375	0.0768	0.2169	2.7194
22	E88.2	Dhaid - Masafi	1.8882	0.5375	0.0652	0.2169	2.7078
22	E88.2	Dhaid - Masafi	1.8882	0.5375	0.0860	0.2169	2.7286
24	E89.1	Masafi - Dibba	0.0532	0.0435	0.0959	0.3320	0.5245
24	E89.1	Masafi - Dibba	0.0532	0.0435	0.0144	0.3320	0.4430
24	E89.1	Masafi - Dibba	0.0532	0.0435	0.0502	0.3320	0.4789
26	E89.3	Masafi - Fujairah	2.5227	0.4237	0.0563	0.2604	3.2631
26	E89.3	Masafi - Fujairah	2.5227	0.4237	0.0408	0.2604	3.2476
26	E89.3	Masafi - Fujairah	2.5227	0.4237	0.0288	0.2604	3.2356
26	E89.3	Masafi - Fujairah	2.5227	0.4237	0.0855	0.2604	3.2923
28	E99.1	Khor Fakkan - Dibba	1.1735	0.2726	0.0668	0.2943	1.8072
28	E99.1	Khor Fakkan - Dibba	1.1735	0.2726	0.0471	0.2943	1.7875

28	E99.1	Khor Fakkan - Dibba	1.1735	0.2726	0.1027	0.2943	1.8431
28	E99.1	Khor Fakkan - Dibba	1.1735	0.2726	0.0300	0.2943	1.7704
28	E99.1	Khor Fakkan - Dibba	1.1735	0.2726	0.0227	0.2943	1.7632
28	E99.1	Khor Fakkan - Dibba	1.1735	0.2726	0.0616	0.2943	1.8020
28	E99.1	Khor Fakkan - Dibba	1.1735	0.2726	0.0582	0.2943	1.7987
29	E99.2	Fujairah - Khor Fakkan	1.8677	0.4069	0.0190	0.2452	2.5388
29	E99.2	Fujairah - Khor Fakkan	1.8677	0.4069	0.0529	0.2452	2.5727
29	E99.2	Fujairah - Khor Fakkan	1.8677	0.4069	0.0216	0.2452	2.5415
29	E99.2	Fujairah - Khor Fakkan	1.8677	0.4069	0.0245	0.2452	2.5443
30	E99.3	Fujairah - Oman	1.4562	0.2340	0.0502	0.2959	2.0362

Results of Default HDM-4 Model based on 2040 Climate Change Scenario

Table 14-9: Results of HDM-4 model based on 2040 climate change scenario

N	Road Code	Road	change in roughness structural (ΔRIs)	change in roughness rutting ΔRIr	change in roughness due to cracking ΔRIc	environmental component of roughness (ΔRIe)	The total incremental change in roughness ΔRI
1	E.11	Ittihad road	0.8267	0.4615	0.0243	0.2123	1.5249
1	E.11	Ittihad road	0.8267	0.4615	0.0545	0.2123	1.5551
1	E.11	Ittihad road	0.8267	0.4615	0.0792	0.2123	1.5798
1	E.11	Ittihad road	0.8267	0.4615	0.0454	0.2123	1.5460
1	E.11	Ittihad road	0.8267	0.4615	0.0144	0.2123	1.5149
1	E.11	Ittihad road	0.8267	0.4615	0.0318	0.2123	1.5323
1	E.11	Ittihad road	0.8267	0.4615	0.0214	0.2123	1.5219
1	E.11	Ittihad road	0.8267	0.4615	0.0508	0.2123	1.5514
3	E18.1	Manama- RAK Airport	1.0171	0.5222	0.0196	0.1794	1.7383
3	E18.1	Manama- RAK Airport	1.0171	0.5222	0.0167	0.1794	1.7354
3	E18.1	Manama- RAK Airport	1.0171	0.5222	0.0645	0.1794	1.7832
3	E18.1	Manama- RAK Airport	1.0171	0.5222	0.0420	0.1794	1.7607
3	E18.1	Manama- RAK Airport	1.0171	0.5222	0.0372	0.1794	1.7559
3	E18.1	Manama- RAK Airport	1.0171	0.5222	0.0689	0.1794	1.7876
3	E18.1	Manama- RAK Airport	1.0171	0.5222	0.0141	0.1794	1.7328
3	E18.1	Manama- RAK Airport	1.0171	0.5222	0.0510	0.1794	1.7697
5	E18.2	RAK Airport-Sha'am	1.0908	0.4529	0.0296	0.3167	1.8899
5	E18.2	RAK Airport-Sha'am	1.0908	0.4529	0.0193	0.3167	1.8796
5	E18.2	RAK Airport-Sha'am	1.0908	0.4529	0.0141	0.3167	1.8744
5	E18.2	RAK Airport-Sha'am	1.0908	0.4529	0.0404	0.3167	1.9007
5	E18.2	RAK Airport-Sha'am	1.0908	0.4529	0.0149	0.3167	1.8753
5	E18.2	RAK Airport-Sha'am	1.0908	0.4529	0.1072	0.3167	1.9675
5	E18.2	RAK Airport-Sha'am	1.0908	0.4529	0.0282	0.3167	1.8885
5	E18.2	RAK Airport-Sha'am	1.0908	0.4529	0.0650	0.3167	1.9253
5	E18.2	RAK Airport-Sha'am	1.0908	0.4529	0.0729	0.3167	1.9332
7	E311	Sheik Mohammed Bin Zayed	1.6704	2.2918	0.0256	0.1812	4.1690
7	E311	Sheik Mohammed Bin Zayed	1.6704	2.2918	0.0685	0.1812	4.2120
7	E311	Sheik Mohammed Bin Zayed	1.6704	2.2918	0.0427	0.1812	4.1862
7	E311	Sheik Mohammed Bin Zayed	1.6704	2.2918	0.0203	0.1812	4.1637
7	E311	Sheik Mohammed Bin Zayed	1.6704	2.2918	0.0461	0.1812	4.1896
7	E311	Sheik Mohammed Bin Zayed	1.6704	2.2918	0.0339	0.1812	4.1774
7	E311	Sheik Mohammed Bin Zayed	1.6704	2.2918	0.0233	0.1812	4.1668
7	E311	Sheik Mohammed Bin Zayed	1.6704	2.2918	0.0379	0.1812	4.1814
7	E311	Sheik Mohammed Bin Zayed	1.6704	2.2918	0.0609	0.1812	4.2043
7	E311	Sheik Mohammed Bin Zayed	1.6704	2.2918	0.0229	0.1812	4.1664
7	E311	Sheik Mohammed Bin Zayed	1.6704	2.2918	0.0356	0.1812	4.1791
8	E55.1	Dhaid - Madam	0.2852	0.0690	0.0682	0.2398	0.6622
8	E55.1	Dhaid - Madam	0.2852	0.0690	0.0175	0.2398	0.6115

8	E55.1	Dhaid - Madam	0.2852	0.0690	0.0235	0.2398	0.6176
8	E55.1	Dhaid - Madam	0.2852	0.0690	0.0238	0.2398	0.6178
8	E55.1	Dhaid - Madam	0.2852	0.0690	0.0163	0.2398	0.6103
8	E55.1	Dhaid - Madam	0.2852	0.0690	0.0230	0.2398	0.6171
8	E55.1	Dhaid - Madam	0.2852	0.0690	0.0413	0.2398	0.6353
8	E55.1	Dhaid - Madam	0.2852	0.0690	0.0162	0.2398	0.6102
8	E55.1	Dhaid - Madam	0.2852	0.0690	0.0498	0.2398	0.6438
8	E55.1	Dhaid - Madam	0.2852	0.0690	0.0560	0.2398	0.6501
10	E55.2	Madam - Shiweb	0.4618	0.1079	0.0484	0.2764	0.8945
10	E55.2	Madam - Shiweb	0.4618	0.1079	0.0227	0.2764	0.8688
10	E55.2	Madam - Shiweb	0.4618	0.1079	0.0576	0.2764	0.9037
10	E55.2	Madam - Shiweb	0.4618	0.1079	0.0509	0.2764	0.8970
12	E55.3	Umm Al Quwaim - Dhaid	0.2037	0.0468	0.0230	0.2123	0.4859
12	E55.3	Umm Al Quwaim - Dhaid	0.2037	0.0468	0.0060	0.2123	0.4688
12	E55.3	Umm Al Quwaim - Dhaid	0.2037	0.0468	0.0375	0.2123	0.5004
12	E55.3	Umm Al Quwaim - Dhaid	0.2037	0.0468	0.0268	0.2123	0.4897
12	E55.3	Umm Al Quwaim - Dhaid	0.2037	0.0468	0.1128	0.2123	0.5757
12	E55.3	Umm Al Quwaim - Dhaid	0.2037	0.0468	0.0193	0.2123	0.4822
12	E55.3	Umm Al Quwaim - Dhaid	0.2037	0.0468	0.0581	0.2123	0.5210
12	E55.3	Umm Al Quwaim - Dhaid	0.2037	0.0468	0.0788	0.2123	0.5417
12	E55.3	Umm Al Quwaim - Dhaid	0.2037	0.0468	0.0725	0.2123	0.5354
18	E84	Sheikh Khalifa Rd	0.0997	0.1647	0.0219	0.1467	0.4331
18	E84	Sheikh Khalifa Rd	0.0997	0.1647	0.0167	0.1467	0.4279
18	E84	Sheikh Khalifa Rd	0.0997	0.1647	0.0613	0.1467	0.4725
18	E84	Sheikh Khalifa Rd	0.0997	0.1647	0.1063	0.1467	0.5174
18	E84	Sheikh Khalifa Rd	0.0997	0.1647	0.0340	0.1467	0.4452
18	E84	Sheikh Khalifa Rd	0.0997	0.1647	0.1012	0.1467	0.5123
18	E84	Sheikh Khalifa Rd	0.0997	0.1647	0.0428	0.1467	0.4539
18	E84	Sheikh Khalifa Rd	0.0997	0.1647	0.0806	0.1467	0.4918
20	E88.1	Sharjah - Dhaid	2.2396	0.6993	0.0142	0.2199	3.1730
20	E88.1	Sharjah - Dhaid	2.2396	0.6993	0.0383	0.2199	3.1971
20	E88.1	Sharjah - Dhaid	2.2396	0.6993	0.0584	0.2199	3.2172
20	E88.1	Sharjah - Dhaid	2.2396	0.6993	0.0620	0.2199	3.2208
20	E88.1	Sharjah - Dhaid	2.2396	0.6993	0.0275	0.2199	3.1863
20	E88.1	Sharjah - Dhaid	2.2396	0.6993	0.1039	0.2199	3.2626
22	E88.2	Dhaid - Masafi	1.8663	0.5508	0.0905	0.2160	2.7236
22	E88.2	Dhaid - Masafi	1.8663	0.5508	0.0250	0.2160	2.6580
22	E88.2	Dhaid - Masafi	1.8663	0.5508	0.0298	0.2160	2.6629
22	E88.2	Dhaid - Masafi	1.8663	0.5508	0.0319	0.2160	2.6650
22	E88.2	Dhaid - Masafi	1.8663	0.5508	0.0151	0.2160	2.6481
22	E88.2	Dhaid - Masafi	1.8663	0.5508	0.0768	0.2160	2.7099
22	E88.2	Dhaid - Masafi	1.8663	0.5508	0.0652	0.2160	2.6983
22	E88.2	Dhaid - Masafi	1.8663	0.5508	0.0860	0.2160	2.7191
24	E89.1	Masafi - Dibba	0.0528	0.0446	0.0959	0.3306	0.5238
24	E89.1	Masafi - Dibba	0.0528	0.0446	0.0144	0.3306	0.4423
24	E89.1	Masafi - Dibba	0.0528	0.0446	0.0502	0.3306	0.4782
26	E89.3	Masafi - Fujairah	2.4877	0.4342	0.0563	0.2593	3.2375
26	E89.3	Masafi - Fujairah	2.4877	0.4342	0.0408	0.2593	3.2220
26	E89.3	Masafi - Fujairah	2.4877	0.4342	0.0288	0.2593	3.2099
26	E89.3	Masafi - Fujairah	2.4877	0.4342	0.0855	0.2593	3.2666
28	E99.1	Khor Fakkan - Dibba	1.1581	0.2793	0.0668	0.2931	1.7973
28	E99.1	Khor Fakkan - Dibba	1.1581	0.2793	0.0471	0.2931	1.7777
28	E99.1	Khor Fakkan - Dibba	1.1581	0.2793	0.1027	0.2931	1.8332
28	E99.1	Khor Fakkan - Dibba	1.1581	0.2793	0.0300	0.2931	1.7605
28	E99.1	Khor Fakkan - Dibba	1.1581	0.2793	0.0227	0.2931	1.7533
28	E99.1	Khor Fakkan - Dibba	1.1581	0.2793	0.0616	0.2931	1.7921
28	E99.1	Khor Fakkan - Dibba	1.1581	0.2793	0.0582	0.2931	1.7888
29	E99.2	Fujairah - Khor Fakkan	1.8432	0.4169	0.0190	0.2442	2.5234
29	E99.2	Fujairah - Khor Fakkan	1.8432	0.4169	0.0529	0.2442	2.5573
29	E99.2	Fujairah - Khor Fakkan	1.8432	0.4169	0.0216	0.2442	2.5260

29	E99.2	Fujairah - Khor Fakkan	1.8432	0.4169	0.0245	0.2442	2.5289
30	E99.3	Fujairah - Oman	1.4349	0.2397	0.0502	0.2947	2.0195

Results of Default HDM-4 Model based on 2060 Climate Change Scenario

Table 14-10: Results of HDM-4 model based on 2060 climate change scenario

N	Road Code	Road	change in roughness structural (ΔRIs)	change in roughness rutting ΔRIr	change in roughness due to cracking ΔRIc	environmental component of roughness (ΔRIe)	The total incremental change in roughness ΔRI
1	E.11	Ittihad road	0.8183	0.4727	0.0243	0.2113	1.5265
1	E.11	Ittihad road	0.8183	0.4727	0.0545	0.2113	1.5567
1	E.11	Ittihad road	0.8183	0.4727	0.0792	0.2113	1.5814
1	E.11	Ittihad road	0.8183	0.4727	0.0454	0.2113	1.5476
1	E.11	Ittihad road	0.8183	0.4727	0.0144	0.2113	1.5166
1	E.11	Ittihad road	0.8183	0.4727	0.0318	0.2113	1.5340
1	E.11	Ittihad road	0.8183	0.4727	0.0214	0.2113	1.5236
1	E.11	Ittihad road	0.8183	0.4727	0.0508	0.2113	1.5530
3	E18.1	Manama- RAK Airport	1.0067	0.5348	0.0196	0.1785	1.7396
3	E18.1	Manama- RAK Airport	1.0067	0.5348	0.0167	0.1785	1.7368
3	E18.1	Manama- RAK Airport	1.0067	0.5348	0.0645	0.1785	1.7845
3	E18.1	Manama- RAK Airport	1.0067	0.5348	0.0420	0.1785	1.7621
3	E18.1	Manama- RAK Airport	1.0067	0.5348	0.0372	0.1785	1.7573
3	E18.1	Manama- RAK Airport	1.0067	0.5348	0.0689	0.1785	1.7890
3	E18.1	Manama- RAK Airport	1.0067	0.5348	0.0141	0.1785	1.7342
3	E18.1	Manama- RAK Airport	1.0067	0.5348	0.0510	0.1785	1.7711
5	E18.2	RAK Airport-Sha'am	1.0787	0.4638	0.0296	0.3151	1.8871
5	E18.2	RAK Airport-Sha'am	1.0787	0.4638	0.0193	0.3151	1.8769
5	E18.2	RAK Airport-Sha'am	1.0787	0.4638	0.0141	0.3151	1.8717
5	E18.2	RAK Airport-Sha'am	1.0787	0.4638	0.0404	0.3151	1.8979
5	E18.2	RAK Airport-Sha'am	1.0787	0.4638	0.0149	0.3151	1.8725
5	E18.2	RAK Airport-Sha'am	1.0787	0.4638	0.1072	0.3151	1.9647
5	E18.2	RAK Airport-Sha'am	1.0787	0.4638	0.0282	0.3151	1.8857
5	E18.2	RAK Airport-Sha'am	1.0787	0.4638	0.0650	0.3151	1.9225
5	E18.2	RAK Airport-Sha'am	1.0787	0.4638	0.0729	0.3151	1.9305
7	E311	Sheik Mohammed Bin Zayed	1.6611	2.3472	0.0256	0.1803	4.2142
7	E311	Sheik Mohammed Bin Zayed	1.6611	2.3472	0.0685	0.1803	4.2571
7	E311	Sheik Mohammed Bin Zayed	1.6611	2.3472	0.0427	0.1803	4.2313
7	E311	Sheik Mohammed Bin Zayed	1.6611	2.3472	0.0203	0.1803	4.2089
7	E311	Sheik Mohammed Bin Zayed	1.6611	2.3472	0.0461	0.1803	4.2347
7	E311	Sheik Mohammed Bin Zayed	1.6611	2.3472	0.0339	0.1803	4.2225
7	E311	Sheik Mohammed Bin Zayed	1.6611	2.3472	0.0233	0.1803	4.2120
7	E311	Sheik Mohammed Bin Zayed	1.6611	2.3472	0.0379	0.1803	4.2265
7	E311	Sheik Mohammed Bin Zayed	1.6611	2.3472	0.0609	0.1803	4.2495
7	E311	Sheik Mohammed Bin Zayed	1.6611	2.3472	0.0229	0.1803	4.2115
7	E311	Sheik Mohammed Bin Zayed	1.6611	2.3472	0.0356	0.1803	4.2242
8	E55.1	Dhaid - Madam	0.2810	0.0707	0.0682	0.2386	0.6585
8	E55.1	Dhaid - Madam	0.2810	0.0707	0.0175	0.2386	0.6078
8	E55.1	Dhaid - Madam	0.2810	0.0707	0.0235	0.2386	0.6138
8	E55.1	Dhaid - Madam	0.2810	0.0707	0.0238	0.2386	0.6140
8	E55.1	Dhaid - Madam	0.2810	0.0707	0.0163	0.2386	0.6065
8	E55.1	Dhaid - Madam	0.2810	0.0707	0.0230	0.2386	0.6133

8	E55.1	Dhaid - Madam	0.2810	0.0707	0.0413	0.2386	0.6315
8	E55.1	Dhaid - Madam	0.2810	0.0707	0.0162	0.2386	0.6064
8	E55.1	Dhaid - Madam	0.2810	0.0707	0.0498	0.2386	0.6401
8	E55.1	Dhaid - Madam	0.2810	0.0707	0.0560	0.2386	0.6463
10	E55.2	Madam - Shiweb	0.4550	0.1105	0.0484	0.2750	0.8889
10	E55.2	Madam - Shiweb	0.4550	0.1105	0.0227	0.2750	0.8632
10	E55.2	Madam - Shiweb	0.4550	0.1105	0.0576	0.2750	0.8981
10	E55.2	Madam - Shiweb	0.4550	0.1105	0.0509	0.2750	0.8914
12	E55.3	Umm Al Quwaim - Dhaid	0.2007	0.0479	0.0230	0.2113	0.4829
12	E55.3	Umm Al Quwaim - Dhaid	0.2007	0.0479	0.0060	0.2113	0.4659
12	E55.3	Umm Al Quwaim - Dhaid	0.2007	0.0479	0.0375	0.2113	0.4974
12	E55.3	Umm Al Quwaim - Dhaid	0.2007	0.0479	0.0268	0.2113	0.4868
12	E55.3	Umm Al Quwaim - Dhaid	0.2007	0.0479	0.1128	0.2113	0.5728
12	E55.3	Umm Al Quwaim - Dhaid	0.2007	0.0479	0.0193	0.2113	0.4792
12	E55.3	Umm Al Quwaim - Dhaid	0.2007	0.0479	0.0581	0.2113	0.5181
12	E55.3	Umm Al Quwaim - Dhaid	0.2007	0.0479	0.0788	0.2113	0.5387
12	E55.3	Umm Al Quwaim - Dhaid	0.2007	0.0479	0.0725	0.2113	0.5325
18	E84	Sheikh Khalifa Rd	0.0993	0.1687	0.0219	0.1460	0.4359
18	E84	Sheikh Khalifa Rd	0.0993	0.1687	0.0167	0.1460	0.4307
18	E84	Sheikh Khalifa Rd	0.0993	0.1687	0.0613	0.1460	0.4752
18	E84	Sheikh Khalifa Rd	0.0993	0.1687	0.1063	0.1460	0.5202
18	E84	Sheikh Khalifa Rd	0.0993	0.1687	0.0340	0.1460	0.4480
18	E84	Sheikh Khalifa Rd	0.0993	0.1687	0.1012	0.1460	0.5151
18	E84	Sheikh Khalifa Rd	0.0993	0.1687	0.0428	0.1460	0.4567
18	E84	Sheikh Khalifa Rd	0.0993	0.1687	0.0806	0.1460	0.4946
20	E88.1	Sharjah - Dhaid	2.2086	0.7162	0.0142	0.2188	3.1577
20	E88.1	Sharjah - Dhaid	2.2086	0.7162	0.0383	0.2188	3.1818
20	E88.1	Sharjah - Dhaid	2.2086	0.7162	0.0584	0.2188	3.2019
20	E88.1	Sharjah - Dhaid	2.2086	0.7162	0.0620	0.2188	3.2055
20	E88.1	Sharjah - Dhaid	2.2086	0.7162	0.0275	0.2188	3.1711
20	E88.1	Sharjah - Dhaid	2.2086	0.7162	0.1039	0.2188	3.2474
22	E88.2	Dhaid - Masafi	1.8405	0.5641	0.0905	0.2149	2.7099
22	E88.2	Dhaid - Masafi	1.8405	0.5641	0.0250	0.2149	2.6444
22	E88.2	Dhaid - Masafi	1.8405	0.5641	0.0298	0.2149	2.6493
22	E88.2	Dhaid - Masafi	1.8405	0.5641	0.0319	0.2149	2.6513
22	E88.2	Dhaid - Masafi	1.8405	0.5641	0.0151	0.2149	2.6345
22	E88.2	Dhaid - Masafi	1.8405	0.5641	0.0768	0.2149	2.6962
22	E88.2	Dhaid - Masafi	1.8405	0.5641	0.0652	0.2149	2.6846
22	E88.2	Dhaid - Masafi	1.8405	0.5641	0.0860	0.2149	2.7055
24	E89.1	Masafi - Dibba	0.0524	0.0457	0.0959	0.3289	0.5228
24	E89.1	Masafi - Dibba	0.0524	0.0457	0.0144	0.3289	0.4413
24	E89.1	Masafi - Dibba	0.0524	0.0457	0.0502	0.3289	0.4771
26	E89.3	Masafi - Fujairah	2.4464	0.4447	0.0563	0.2580	3.2054
26	E89.3	Masafi - Fujairah	2.4464	0.4447	0.0408	0.2580	3.1899
26	E89.3	Masafi - Fujairah	2.4464	0.4447	0.0288	0.2580	3.1778
26	E89.3	Masafi - Fujairah	2.4464	0.4447	0.0855	0.2580	3.2345
28	E99.1	Khor Fakkan - Dibba	1.1400	0.2861	0.0668	0.2916	1.7844
28	E99.1	Khor Fakkan - Dibba	1.1400	0.2861	0.0471	0.2916	1.7647
28	E99.1	Khor Fakkan - Dibba	1.1400	0.2861	0.1027	0.2916	1.8203
28	E99.1	Khor Fakkan - Dibba	1.1400	0.2861	0.0300	0.2916	1.7476
28	E99.1	Khor Fakkan - Dibba	1.1400	0.2861	0.0227	0.2916	1.7404
28	E99.1	Khor Fakkan - Dibba	1.1400	0.2861	0.0616	0.2916	1.7792
28	E99.1	Khor Fakkan - Dibba	1.1400	0.2861	0.0582	0.2916	1.7759
29	E99.2	Fujairah - Khor Fakkan	1.8143	0.4270	0.0190	0.2430	2.5033
29	E99.2	Fujairah - Khor Fakkan	1.8143	0.4270	0.0529	0.2430	2.5372
29	E99.2	Fujairah - Khor Fakkan	1.8143	0.4270	0.0216	0.2430	2.5060
29	E99.2	Fujairah - Khor Fakkan	1.8143	0.4270	0.0245	0.2430	2.5088
30	E99.3	Fujairah - Oman	1.4098	0.2455	0.0502	0.2932	1.9986

Experiment Model 1: Total Change in Roughness 2013

Table 14-11: Experiment model 1-total change in roughness 2013 scenario

N	Road Code	Road	change in roughness structural (ΔRIs)	change in roughness rutting ΔRIr	change in roughness due to cracking ΔRIc	environmental component of roughness (ΔRIe)	The total incremental change in roughness ΔRI
1	E.11	Ittihad road	0.000	0.148	0.277	0.214	0.640
1	E.11	Ittihad road	0.000	0.148	0.378	0.214	0.740
1	E.11	Ittihad road	0.000	0.148	0.368	0.214	0.730
1	E.11	Ittihad road	0.000	0.148	0.361	0.214	0.720
1	E.11	Ittihad road	0.000	0.148	0.216	0.214	0.580
1	E.11	Ittihad road	0.000	0.148	0.314	0.214	0.680
1	E.11	Ittihad road	0.000	0.148	0.260	0.214	0.620
1	E.11	Ittihad road	0.000	0.148	0.373	0.214	0.740
3	E18.1	Manama- RAK Airport	0.000	0.177	0.250	0.181	0.610
3	E18.1	Manama- RAK Airport	0.000	0.177	0.232	0.181	0.590
3	E18.1	Manama- RAK Airport	0.000	0.177	0.384	0.181	0.740
3	E18.1	Manama- RAK Airport	0.000	0.177	0.352	0.181	0.710
3	E18.1	Manama- RAK Airport	0.000	0.177	0.336	0.181	0.690
3	E18.1	Manama- RAK Airport	0.000	0.177	0.383	0.181	0.740
3	E18.1	Manama- RAK Airport	0.000	0.177	0.214	0.181	0.570
3	E18.1	Manama- RAK Airport	0.000	0.177	0.373	0.181	0.730
5	E18.2	RAK Airport-Sha'am	0.000	0.166	0.304	0.319	0.790
5	E18.2	RAK Airport-Sha'am	0.000	0.166	0.248	0.319	0.730
5	E18.2	RAK Airport-Sha'am	0.000	0.166	0.214	0.319	0.700
5	E18.2	RAK Airport-Sha'am	0.000	0.166	0.347	0.319	0.830
5	E18.2	RAK Airport-Sha'am	0.000	0.166	0.220	0.319	0.710
5	E18.2	RAK Airport-Sha'am	0.000	0.166	0.255	0.319	0.740
5	E18.2	RAK Airport-Sha'am	0.000	0.166	0.297	0.319	0.780
5	E18.2	RAK Airport-Sha'am	0.000	0.166	0.384	0.319	0.870
5	E18.2	RAK Airport-Sha'am	0.000	0.166	0.379	0.319	0.860
7	E311	Sheik Mohammed Bin Zayed	0.000	0.197	0.284	0.183	0.660
7	E311	Sheik Mohammed Bin Zayed	0.000	0.197	0.383	0.183	0.760
7	E311	Sheik Mohammed Bin Zayed	0.000	0.197	0.354	0.183	0.730
7	E311	Sheik Mohammed Bin Zayed	0.000	0.197	0.254	0.183	0.630
7	E311	Sheik Mohammed Bin Zayed	0.000	0.197	0.363	0.183	0.740
7	E311	Sheik Mohammed Bin Zayed	0.000	0.197	0.323	0.183	0.700
7	E311	Sheik Mohammed Bin Zayed	0.000	0.197	0.272	0.183	0.650
7	E311	Sheik Mohammed Bin Zayed	0.000	0.197	0.338	0.183	0.720
7	E311	Sheik Mohammed Bin Zayed	0.000	0.197	0.384	0.183	0.760
7	E311	Sheik Mohammed Bin Zayed	0.000	0.197	0.269	0.183	0.650
7	E311	Sheik Mohammed Bin Zayed	0.000	0.197	0.330	0.183	0.710
8	E55.1	Dhaid - Madam	1382.844	0.130	0.383	0.242	1383.600
8	E55.1	Dhaid - Madam	1382.844	0.130	0.237	0.242	1383.450
8	E55.1	Dhaid - Madam	1382.844	0.130	0.273	0.242	1383.490
8	E55.1	Dhaid - Madam	1382.844	0.130	0.274	0.242	1383.490
8	E55.1	Dhaid - Madam	1382.844	0.130	0.229	0.242	1383.440
8	E55.1	Dhaid - Madam	1382.844	0.130	0.270	0.242	1383.490
8	E55.1	Dhaid - Madam	1382.844	0.130	0.349	0.242	1383.570
8	E55.1	Dhaid - Madam	1382.844	0.130	0.228	0.242	1383.440
8	E55.1	Dhaid - Madam	1382.844	0.130	0.371	0.242	1383.590
8	E55.1	Dhaid - Madam	1382.844	0.130	0.380	0.242	1383.600
10	E55.2	Madam - Shiweb	39.303	0.131	0.368	0.279	40.080
10	E55.2	Madam - Shiweb	39.303	0.131	0.268	0.279	39.980
10	E55.2	Madam - Shiweb	39.303	0.131	0.382	0.279	40.100
10	E55.2	Madam - Shiweb	39.303	0.131	0.373	0.279	40.090

12	E55.3	Umm Al Quwaim - Dhaid	16618.860	0.126	0.270	0.214	16619.470
12	E55.3	Umm Al Quwaim - Dhaid	16618.860	0.126	0.154	0.214	16619.350
12	E55.3	Umm Al Quwaim - Dhaid	16618.860	0.126	0.337	0.214	16619.540
12	E55.3	Umm Al Quwaim - Dhaid	16618.860	0.126	0.290	0.214	16619.490
12	E55.3	Umm Al Quwaim - Dhaid	16618.860	0.126	0.219	0.214	16619.420
12	E55.3	Umm Al Quwaim - Dhaid	16618.860	0.126	0.248	0.214	16619.450
12	E55.3	Umm Al Quwaim - Dhaid	16618.860	0.126	0.382	0.214	16619.580
12	E55.3	Umm Al Quwaim - Dhaid	16618.860	0.126	0.369	0.214	16619.570
12	E55.3	Umm Al Quwaim - Dhaid	16618.860	0.126	0.379	0.214	16619.580
18	E84	Sheikh Khalifa Rd	0.243	0.131	0.264	0.148	0.790
18	E84	Sheikh Khalifa Rd	0.243	0.131	0.232	0.148	0.750
18	E84	Sheikh Khalifa Rd	0.243	0.131	0.384	0.148	0.910
18	E84	Sheikh Khalifa Rd	0.243	0.131	0.260	0.148	0.780
18	E84	Sheikh Khalifa Rd	0.243	0.131	0.323	0.148	0.840
18	E84	Sheikh Khalifa Rd	0.243	0.131	0.288	0.148	0.810
18	E84	Sheikh Khalifa Rd	0.243	0.131	0.354	0.148	0.880
18	E84	Sheikh Khalifa Rd	0.243	0.131	0.365	0.148	0.890
20	E88.1	Sharjah - Dhaid	0.000	0.180	0.215	0.222	0.620
20	E88.1	Sharjah - Dhaid	0.000	0.180	0.340	0.222	0.740
20	E88.1	Sharjah - Dhaid	0.000	0.180	0.382	0.222	0.780
20	E88.1	Sharjah - Dhaid	0.000	0.180	0.384	0.222	0.790
20	E88.1	Sharjah - Dhaid	0.000	0.180	0.294	0.222	0.700
20	E88.1	Sharjah - Dhaid	0.000	0.180	0.274	0.222	0.680
22	E88.2	Dhaid - Masafi	0.000	0.162	0.335	0.218	0.720
22	E88.2	Dhaid - Masafi	0.000	0.162	0.280	0.218	0.660
22	E88.2	Dhaid - Masafi	0.000	0.162	0.305	0.218	0.680
22	E88.2	Dhaid - Masafi	0.000	0.162	0.314	0.218	0.690
22	E88.2	Dhaid - Masafi	0.000	0.162	0.221	0.218	0.600
22	E88.2	Dhaid - Masafi	0.000	0.162	0.373	0.218	0.750
22	E88.2	Dhaid - Masafi	0.000	0.162	0.384	0.218	0.760
22	E88.2	Dhaid - Masafi	0.000	0.162	0.350	0.218	0.730
24	E89.1	Masafi - Dibba	16883.818	0.142	0.313	0.333	16884.610
24	E89.1	Masafi - Dibba	16883.818	0.142	0.216	0.333	16884.510
24	E89.1	Masafi - Dibba	16883.818	0.142	0.372	0.333	16884.670
26	E89.3	Masafi - Fujairah	0.003	0.158	0.380	0.261	0.800
26	E89.3	Masafi - Fujairah	0.003	0.158	0.348	0.261	0.770
26	E89.3	Masafi - Fujairah	0.003	0.158	0.300	0.261	0.720
26	E89.3	Masafi - Fujairah	0.003	0.158	0.352	0.261	0.770
28	E99.1	Khor Fakkan - Dibba	0.184	0.173	0.384	0.296	1.040
28	E99.1	Khor Fakkan - Dibba	0.184	0.173	0.365	0.296	1.020
28	E99.1	Khor Fakkan - Dibba	0.184	0.173	0.280	0.296	0.930
28	E99.1	Khor Fakkan - Dibba	0.184	0.173	0.306	0.296	0.960
28	E99.1	Khor Fakkan - Dibba	0.184	0.173	0.268	0.296	0.920
28	E99.1	Khor Fakkan - Dibba	0.184	0.173	0.384	0.296	1.040
28	E99.1	Khor Fakkan - Dibba	0.184	0.173	0.382	0.296	1.030
29	E99.2	Fujairah - Khor Fakkan	0.006	0.171	0.246	0.246	0.670
29	E99.2	Fujairah - Khor Fakkan	0.006	0.171	0.376	0.246	0.800
29	E99.2	Fujairah - Khor Fakkan	0.006	0.171	0.262	0.246	0.690
29	E99.2	Fujairah - Khor Fakkan	0.006	0.171	0.278	0.246	0.700
30	E99.3	Fujairah - Oman	0.646	0.168	0.372	0.297	1.480

Experiment Model 1: Total change in roughness 2020

Table 14-12: Experiment model 1-total change in roughness 2020 scenario

N	Road Code	Road	change in roughness structural (ΔRIs)	change in roughness rutting ΔRIr	change in roughness due to cracking ΔRIc	environmental component of roughness (ΔRIe)	The total incremental change in roughness ΔRI
1	E.11	Ittihad road	0.0004	0.1590	0.2769	0.1838	0.6202
1	E.11	Ittihad road	0.0004	0.1550	0.3784	0.2132	0.7470
1	E.11	Ittihad road	0.0004	0.1550	0.3680	0.2132	0.7366
1	E.11	Ittihad road	0.0004	0.1550	0.3610	0.2132	0.7296
1	E.11	Ittihad road	0.0004	0.1550	0.2160	0.2132	0.5846
1	E.11	Ittihad road	0.0004	0.1550	0.3137	0.2132	0.6823
1	E.11	Ittihad road	0.0004	0.1550	0.2603	0.2132	0.6289
1	E.11	Ittihad road	0.0004	0.1550	0.3727	0.2132	0.7413
3	E18.1	Manama- RAK Airport	0.0001	0.1891	0.2495	0.1801	0.6189
3	E18.1	Manama- RAK Airport	0.0001	0.1891	0.2316	0.1801	0.6010
3	E18.1	Manama- RAK Airport	0.0001	0.1891	0.3843	0.1801	0.7537
3	E18.1	Manama- RAK Airport	0.0001	0.1891	0.3517	0.1801	0.7211
3	E18.1	Manama- RAK Airport	0.0001	0.1891	0.3358	0.1801	0.7052
3	E18.1	Manama- RAK Airport	0.0001	0.1891	0.3825	0.1801	0.7519
3	E18.1	Manama- RAK Airport	0.0001	0.1891	0.2143	0.1801	0.5837
3	E18.1	Manama- RAK Airport	0.0001	0.1891	0.3731	0.1801	0.7425
5	E18.2	RAK Airport-Sha'am	0.0003	0.1763	0.3036	0.3180	0.7982
5	E18.2	RAK Airport-Sha'am	0.0003	0.1763	0.2481	0.3180	0.7427
5	E18.2	RAK Airport-Sha'am	0.0003	0.1763	0.2145	0.3180	0.7091
5	E18.2	RAK Airport-Sha'am	0.0003	0.1763	0.3465	0.3180	0.8411
5	E18.2	RAK Airport-Sha'am	0.0003	0.1763	0.2200	0.3180	0.7146
5	E18.2	RAK Airport-Sha'am	0.0003	0.1763	0.2548	0.3180	0.7494
5	E18.2	RAK Airport-Sha'am	0.0003	0.1763	0.2970	0.3180	0.7916
5	E18.2	RAK Airport-Sha'am	0.0003	0.1763	0.3842	0.3180	0.8788
5	E18.2	RAK Airport-Sha'am	0.0003	0.1763	0.3786	0.3180	0.8732
7	E311	Sheik Mohammed Bin Zayed	0.0000	0.2110	0.2837	0.1820	0.6766
7	E311	Sheik Mohammed Bin Zayed	0.0000	0.2110	0.3828	0.1820	0.7757
7	E311	Sheik Mohammed Bin Zayed	0.0000	0.2110	0.3537	0.1820	0.7466
7	E311	Sheik Mohammed Bin Zayed	0.0000	0.2110	0.2540	0.1820	0.6469
7	E311	Sheik Mohammed Bin Zayed	0.0000	0.2110	0.3628	0.1820	0.7557
7	E311	Sheik Mohammed Bin Zayed	0.0000	0.2110	0.3229	0.1820	0.7158
7	E311	Sheik Mohammed Bin Zayed	0.0000	0.2110	0.2716	0.1820	0.6645
7	E311	Sheik Mohammed Bin Zayed	0.0000	0.2110	0.3382	0.1820	0.7311
7	E311	Sheik Mohammed Bin Zayed	0.0000	0.2110	0.3837	0.1820	0.7767
7	E311	Sheik Mohammed Bin Zayed	0.0000	0.2110	0.2692	0.1820	0.6621
7	E311	Sheik Mohammed Bin Zayed	0.0000	0.2110	0.3296	0.1820	0.7226
8	E55.1	Dhaid - Madam	1388.9022	0.1327	0.3830	0.2408	1389.6587
8	E55.1	Dhaid - Madam	1388.9022	0.1327	0.2366	0.2408	1389.5123
8	E55.1	Dhaid - Madam	1388.9022	0.1327	0.2727	0.2408	1389.5484
8	E55.1	Dhaid - Madam	1388.9022	0.1327	0.2740	0.2408	1389.5497
8	E55.1	Dhaid - Madam	1388.9022	0.1327	0.2287	0.2408	1389.5044
8	E55.1	Dhaid - Madam	1388.9022	0.1327	0.2698	0.2408	1389.5455
8	E55.1	Dhaid - Madam	1388.9022	0.1327	0.3494	0.2408	1389.6251
8	E55.1	Dhaid - Madam	1388.9022	0.1327	0.2281	0.2408	1389.5038
8	E55.1	Dhaid - Madam	1388.9022	0.1327	0.3708	0.2408	1389.6465
8	E55.1	Dhaid - Madam	1388.9022	0.1327	0.3802	0.2408	1389.6559
10	E55.2	Madam - Shiweb	39.4754	0.1345	0.3679	0.2776	40.2554
10	E55.2	Madam - Shiweb	39.4754	0.1345	0.2681	0.2776	40.1556
10	E55.2	Madam - Shiweb	39.4754	0.1345	0.3817	0.2776	40.2692
10	E55.2	Madam - Shiweb	39.4754	0.1345	0.3729	0.2776	40.2603

12	E55.3	Umm Al Quwaim - Dhaid	16691.6629	0.1278	0.2697	0.2132	16692.2737
12	E55.3	Umm Al Quwaim - Dhaid	16691.6629	0.1278	0.1539	0.2132	16692.1578
12	E55.3	Umm Al Quwaim - Dhaid	16691.6629	0.1278	0.3366	0.2132	16692.3405
12	E55.3	Umm Al Quwaim - Dhaid	16691.6629	0.1278	0.2902	0.2132	16692.2941
12	E55.3	Umm Al Quwaim - Dhaid	16691.6629	0.1278	0.2188	0.2132	16692.2227
12	E55.3	Umm Al Quwaim - Dhaid	16691.6629	0.1278	0.2480	0.2132	16692.2519
12	E55.3	Umm Al Quwaim - Dhaid	16691.6629	0.1278	0.3821	0.2132	16692.3861
12	E55.3	Umm Al Quwaim - Dhaid	16691.6629	0.1278	0.3689	0.2132	16692.3728
12	E55.3	Umm Al Quwaim - Dhaid	16691.6629	0.1278	0.3791	0.2132	16692.3830
18	E84	Sheikh Khalifa Rd	0.2441	0.1334	0.2636	0.1473	0.7885
18	E84	Sheikh Khalifa Rd	0.2441	0.1334	0.2318	0.1473	0.7566
18	E84	Sheikh Khalifa Rd	0.2441	0.1334	0.3839	0.1473	0.9088
18	E84	Sheikh Khalifa Rd	0.2441	0.1334	0.2602	0.1473	0.7851
18	E84	Sheikh Khalifa Rd	0.2441	0.1334	0.3233	0.1473	0.8482
18	E84	Sheikh Khalifa Rd	0.2441	0.1334	0.2881	0.1473	0.8129
18	E84	Sheikh Khalifa Rd	0.2441	0.1334	0.3538	0.1473	0.8787
18	E84	Sheikh Khalifa Rd	0.2441	0.1334	0.3648	0.1473	0.8896
20	E88.1	Sharjah - Dhaid	0.0001	0.1918	0.2148	0.2208	0.6275
20	E88.1	Sharjah - Dhaid	0.0001	0.1918	0.3396	0.2208	0.7523
20	E88.1	Sharjah - Dhaid	0.0001	0.1918	0.3823	0.2208	0.7950
20	E88.1	Sharjah - Dhaid	0.0001	0.1918	0.3841	0.2208	0.7968
20	E88.1	Sharjah - Dhaid	0.0001	0.1918	0.2938	0.2208	0.7065
20	E88.1	Sharjah - Dhaid	0.0001	0.1918	0.2738	0.2208	0.6865
22	E88.2	Dhaid - Masafi	0.0003	0.1716	0.3353	0.2169	0.7241
22	E88.2	Dhaid - Masafi	0.0003	0.1716	0.2804	0.2169	0.6692
22	E88.2	Dhaid - Masafi	0.0003	0.1716	0.3049	0.2169	0.6937
22	E88.2	Dhaid - Masafi	0.0003	0.1716	0.3142	0.2169	0.7030
22	E88.2	Dhaid - Masafi	0.0003	0.1716	0.2207	0.2169	0.6095
22	E88.2	Dhaid - Masafi	0.0003	0.1716	0.3727	0.2169	0.7616
22	E88.2	Dhaid - Masafi	0.0003	0.1716	0.3842	0.2169	0.7730
22	E88.2	Dhaid - Masafi	0.0003	0.1716	0.3503	0.2169	0.7391
24	E89.1	Masafi - Dibba	16957.7815	0.1482	0.3135	0.3320	16958.5752
24	E89.1	Masafi - Dibba	16957.7815	0.1482	0.2162	0.3320	16958.4779
24	E89.1	Masafi - Dibba	16957.7815	0.1482	0.3716	0.3320	16958.6333
26	E89.3	Masafi - Fujairah	0.0027	0.1668	0.3805	0.2604	0.8103
26	E89.3	Masafi - Fujairah	0.0027	0.1668	0.3480	0.2604	0.7778
26	E89.3	Masafi - Fujairah	0.0027	0.1668	0.2998	0.2604	0.7296
26	E89.3	Masafi - Fujairah	0.0027	0.1668	0.3520	0.2604	0.7818
28	E99.1	Khor Fakkan - Dibba	0.1844	0.1840	0.3837	0.2943	1.0464
28	E99.1	Khor Fakkan - Dibba	0.1844	0.1840	0.3652	0.2943	1.0279
28	E99.1	Khor Fakkan - Dibba	0.1844	0.1840	0.2801	0.2943	0.9428
28	E99.1	Khor Fakkan - Dibba	0.1844	0.1840	0.3055	0.2943	0.9683
28	E99.1	Khor Fakkan - Dibba	0.1844	0.1840	0.2682	0.2943	0.9309
28	E99.1	Khor Fakkan - Dibba	0.1844	0.1840	0.3840	0.2943	1.0467
28	E99.1	Khor Fakkan - Dibba	0.1844	0.1840	0.3822	0.2943	1.0449
29	E99.2	Fujairah - Khor Fakkan	0.0059	0.1824	0.2461	0.2452	0.6796
29	E99.2	Fujairah - Khor Fakkan	0.0059	0.1824	0.3762	0.2452	0.8097
29	E99.2	Fujairah - Khor Fakkan	0.0059	0.1824	0.2620	0.2452	0.6955
29	E99.2	Fujairah - Khor Fakkan	0.0059	0.1824	0.2778	0.2452	0.7114
30	E99.3	Fujairah - Oman	0.6493	0.1783	0.3715	0.2959	1.4950

Experiment Model 1: Total Change in Roughness 2040

Table 14-13: Experiment model 1-total change in roughness 2040 Scenario

N	Road Code	Road	change in roughness structural (ΔRIs)	change in roughness rutting ΔRIr	change in roughness due to cracking ΔRIc	environmental component of roughness (ΔRIe)	The total incremental change in roughness ΔRI
1	E.11	Ittihad road	0.0004	0.1629	0.2769	0.2123	0.6525
1	E.11	Ittihad road	0.0004	0.1629	0.3784	0.2123	0.7540
1	E.11	Ittihad road	0.0004	0.1629	0.3680	0.2123	0.7436
1	E.11	Ittihad road	0.0004	0.1629	0.3610	0.2123	0.7367
1	E.11	Ittihad road	0.0004	0.1629	0.2160	0.2123	0.5916
1	E.11	Ittihad road	0.0004	0.1629	0.3137	0.2123	0.6893
1	E.11	Ittihad road	0.0004	0.1629	0.2603	0.2123	0.6360
1	E.11	Ittihad road	0.0004	0.1629	0.3727	0.2123	0.7483
3	E18.1	Manama- RAK Airport	0.0001	0.2013	0.2495	0.1794	0.6303
3	E18.1	Manama- RAK Airport	0.0001	0.2013	0.2316	0.1794	0.6124
3	E18.1	Manama- RAK Airport	0.0001	0.2013	0.3843	0.1794	0.7651
3	E18.1	Manama- RAK Airport	0.0001	0.2013	0.3517	0.1794	0.7325
3	E18.1	Manama- RAK Airport	0.0001	0.2013	0.3358	0.1794	0.7166
3	E18.1	Manama- RAK Airport	0.0001	0.2013	0.3825	0.1794	0.7633
3	E18.1	Manama- RAK Airport	0.0001	0.2013	0.2143	0.1794	0.5951
3	E18.1	Manama- RAK Airport	0.0001	0.2013	0.3731	0.1794	0.7539
5	E18.2	RAK Airport-Sha'am	0.0003	0.1872	0.3036	0.3167	0.8077
5	E18.2	RAK Airport-Sha'am	0.0003	0.1872	0.2481	0.3167	0.7523
5	E18.2	RAK Airport-Sha'am	0.0003	0.1872	0.2145	0.3167	0.7186
5	E18.2	RAK Airport-Sha'am	0.0003	0.1872	0.3465	0.3167	0.8507
5	E18.2	RAK Airport-Sha'am	0.0003	0.1872	0.2200	0.3167	0.7241
5	E18.2	RAK Airport-Sha'am	0.0003	0.1872	0.2548	0.3167	0.7589
5	E18.2	RAK Airport-Sha'am	0.0003	0.1872	0.2970	0.3167	0.8012
5	E18.2	RAK Airport-Sha'am	0.0003	0.1872	0.3842	0.3167	0.8884
5	E18.2	RAK Airport-Sha'am	0.0003	0.1872	0.3786	0.3167	0.8828
7	E311	Sheik Mohammed Bin Zayed	0.0000	0.2248	0.2837	0.1812	0.6896
7	E311	Sheik Mohammed Bin Zayed	0.0000	0.2248	0.3828	0.1812	0.7888
7	E311	Sheik Mohammed Bin Zayed	0.0000	0.2248	0.3537	0.1812	0.7597
7	E311	Sheik Mohammed Bin Zayed	0.0000	0.2248	0.2540	0.1812	0.6600
7	E311	Sheik Mohammed Bin Zayed	0.0000	0.2248	0.3628	0.1812	0.7687
7	E311	Sheik Mohammed Bin Zayed	0.0000	0.2248	0.3229	0.1812	0.7289
7	E311	Sheik Mohammed Bin Zayed	0.0000	0.2248	0.2716	0.1812	0.6776
7	E311	Sheik Mohammed Bin Zayed	0.0000	0.2248	0.3382	0.1812	0.7442
7	E311	Sheik Mohammed Bin Zayed	0.0000	0.2248	0.3837	0.1812	0.7897
7	E311	Sheik Mohammed Bin Zayed	0.0000	0.2248	0.2692	0.1812	0.6752
7	E311	Sheik Mohammed Bin Zayed	0.0000	0.2248	0.3296	0.1812	0.7356
8	E55.1	Dhaid - Madam	1395.0124	0.1359	0.3830	0.2398	1395.7711
8	E55.1	Dhaid - Madam	1395.0124	0.1359	0.2366	0.2398	1395.6248
8	E55.1	Dhaid - Madam	1395.0124	0.1359	0.2727	0.2398	1395.6608
8	E55.1	Dhaid - Madam	1395.0124	0.1359	0.2740	0.2398	1395.6621
8	E55.1	Dhaid - Madam	1395.0124	0.1359	0.2287	0.2398	1395.6168
8	E55.1	Dhaid - Madam	1395.0124	0.1359	0.2698	0.2398	1395.6579
8	E55.1	Dhaid - Madam	1395.0124	0.1359	0.3494	0.2398	1395.7375
8	E55.1	Dhaid - Madam	1395.0124	0.1359	0.2281	0.2398	1395.6162
8	E55.1	Dhaid - Madam	1395.0124	0.1359	0.3708	0.2398	1395.7589
8	E55.1	Dhaid - Madam	1395.0124	0.1359	0.3802	0.2398	1395.7683
10	E55.2	Madam - Shiweb	39.6491	0.1382	0.3679	0.2764	40.4316
10	E55.2	Madam - Shiweb	39.6491	0.1382	0.2681	0.2764	40.3317
10	E55.2	Madam - Shiweb	39.6491	0.1382	0.3817	0.2764	40.4453
10	E55.2	Madam - Shiweb	39.6491	0.1382	0.3729	0.2764	40.4365

12	E55.3	Umm Al Quwaim - Dhaid	16765.0945	0.1297	0.2697	0.2123	16765.7062
12	E55.3	Umm Al Quwaim - Dhaid	16765.0945	0.1297	0.1539	0.2123	16765.5904
12	E55.3	Umm Al Quwaim - Dhaid	16765.0945	0.1297	0.3366	0.2123	16765.7731
12	E55.3	Umm Al Quwaim - Dhaid	16765.0945	0.1297	0.2902	0.2123	16765.7267
12	E55.3	Umm Al Quwaim - Dhaid	16765.0945	0.1297	0.2188	0.2123	16765.6553
12	E55.3	Umm Al Quwaim - Dhaid	16765.0945	0.1297	0.2480	0.2123	16765.6845
12	E55.3	Umm Al Quwaim - Dhaid	16765.0945	0.1297	0.3821	0.2123	16765.8186
12	E55.3	Umm Al Quwaim - Dhaid	16765.0945	0.1297	0.3689	0.2123	16765.8054
12	E55.3	Umm Al Quwaim - Dhaid	16765.0945	0.1297	0.3791	0.2123	16765.8156
18	E84	Sheikh Khalifa Rd	0.2452	0.1368	0.2636	0.1467	0.7923
18	E84	Sheikh Khalifa Rd	0.2452	0.1368	0.2318	0.1467	0.7605
18	E84	Sheikh Khalifa Rd	0.2452	0.1368	0.3839	0.1467	0.9126
18	E84	Sheikh Khalifa Rd	0.2452	0.1368	0.2602	0.1467	0.7889
18	E84	Sheikh Khalifa Rd	0.2452	0.1368	0.3233	0.1467	0.8520
18	E84	Sheikh Khalifa Rd	0.2452	0.1368	0.2881	0.1467	0.8168
18	E84	Sheikh Khalifa Rd	0.2452	0.1368	0.3538	0.1467	0.8825
18	E84	Sheikh Khalifa Rd	0.2452	0.1368	0.3648	0.1467	0.8935
20	E88.1	Sharjah - Dhaid	0.0001	0.2042	0.2148	0.2199	0.6390
20	E88.1	Sharjah - Dhaid	0.0001	0.2042	0.3396	0.2199	0.7637
20	E88.1	Sharjah - Dhaid	0.0001	0.2042	0.3823	0.2199	0.8065
20	E88.1	Sharjah - Dhaid	0.0001	0.2042	0.3841	0.2199	0.8083
20	E88.1	Sharjah - Dhaid	0.0001	0.2042	0.2938	0.2199	0.7180
20	E88.1	Sharjah - Dhaid	0.0001	0.2042	0.2738	0.2199	0.6980
22	E88.2	Dhaid - Masafi	0.0003	0.1819	0.3353	0.2160	0.7335
22	E88.2	Dhaid - Masafi	0.0003	0.1819	0.2804	0.2160	0.6786
22	E88.2	Dhaid - Masafi	0.0003	0.1819	0.3049	0.2160	0.7031
22	E88.2	Dhaid - Masafi	0.0003	0.1819	0.3142	0.2160	0.7125
22	E88.2	Dhaid - Masafi	0.0003	0.1819	0.2207	0.2160	0.6189
22	E88.2	Dhaid - Masafi	0.0003	0.1819	0.3727	0.2160	0.7710
22	E88.2	Dhaid - Masafi	0.0003	0.1819	0.3842	0.2160	0.7824
22	E88.2	Dhaid - Masafi	0.0003	0.1819	0.3503	0.2160	0.7485
24	E89.1	Masafi - Dibba	17032.3839	0.1549	0.3135	0.3306	17033.1828
24	E89.1	Masafi - Dibba	17032.3839	0.1549	0.2162	0.3306	17033.0855
24	E89.1	Masafi - Dibba	17032.3839	0.1549	0.3716	0.3306	17033.2410
26	E89.3	Masafi - Fujairah	0.0027	0.1765	0.3805	0.2593	0.8189
26	E89.3	Masafi - Fujairah	0.0027	0.1765	0.3480	0.2593	0.7865
26	E89.3	Masafi - Fujairah	0.0027	0.1765	0.2998	0.2593	0.7382
26	E89.3	Masafi - Fujairah	0.0027	0.1765	0.3520	0.2593	0.7905
28	E99.1	Khor Fakkan - Dibba	0.1852	0.1957	0.3837	0.2931	1.0577
28	E99.1	Khor Fakkan - Dibba	0.1852	0.1957	0.3652	0.2931	1.0392
28	E99.1	Khor Fakkan - Dibba	0.1852	0.1957	0.2801	0.2931	0.9541
28	E99.1	Khor Fakkan - Dibba	0.1852	0.1957	0.3055	0.2931	0.9795
28	E99.1	Khor Fakkan - Dibba	0.1852	0.1957	0.2682	0.2931	0.9422
28	E99.1	Khor Fakkan - Dibba	0.1852	0.1957	0.3840	0.2931	1.0580
28	E99.1	Khor Fakkan - Dibba	0.1852	0.1957	0.3822	0.2931	1.0562
29	E99.2	Fujairah - Khor Fakkan	0.0060	0.1939	0.2461	0.2442	0.6901
29	E99.2	Fujairah - Khor Fakkan	0.0060	0.1939	0.3762	0.2442	0.8202
29	E99.2	Fujairah - Khor Fakkan	0.0060	0.1939	0.2620	0.2442	0.7060
29	E99.2	Fujairah - Khor Fakkan	0.0060	0.1939	0.2778	0.2442	0.7219
30	E99.3	Fujairah - Oman	0.6521	0.1895	0.3715	0.2947	1.5078

Experiment Model 1: Total Change in Roughness 2060

Table 14-14: Experiment model 1-total change in roughness 2060 scenario

N	Road Code	Road	change in roughness structural (ΔRIs)	change in roughness rutting ΔRIr	change in roughness due to cracking ΔRIc	environmental component of roughness (ΔRIe)	The total incremental change in roughness ΔRI
1	E.11	Ittihad road	0.0004	0.1719	0.2769	0.2113	0.6605
1	E.11	Ittihad road	0.0004	0.1719	0.3784	0.2113	0.7619
1	E.11	Ittihad road	0.0004	0.1719	0.3680	0.2113	0.7515
1	E.11	Ittihad road	0.0004	0.1719	0.3610	0.2113	0.7446
1	E.11	Ittihad road	0.0004	0.1719	0.2160	0.2113	0.5995
1	E.11	Ittihad road	0.0004	0.1719	0.3137	0.2113	0.6972
1	E.11	Ittihad road	0.0004	0.1719	0.2603	0.2113	0.6439
1	E.11	Ittihad road	0.0004	0.1719	0.3727	0.2113	0.7563
3	E18.1	Manama- RAK Airport	0.0001	0.2142	0.2495	0.1785	0.6423
3	E18.1	Manama- RAK Airport	0.0001	0.2142	0.2316	0.1785	0.6244
3	E18.1	Manama- RAK Airport	0.0001	0.2142	0.3843	0.1785	0.7771
3	E18.1	Manama- RAK Airport	0.0001	0.2142	0.3517	0.1785	0.7445
3	E18.1	Manama- RAK Airport	0.0001	0.2142	0.3358	0.1785	0.7286
3	E18.1	Manama- RAK Airport	0.0001	0.2142	0.3825	0.1785	0.7754
3	E18.1	Manama- RAK Airport	0.0001	0.2142	0.2143	0.1785	0.6071
3	E18.1	Manama- RAK Airport	0.0001	0.2142	0.3731	0.1785	0.7659
5	E18.2	RAK Airport-Sha'am	0.0003	0.1990	0.3036	0.3151	0.8179
5	E18.2	RAK Airport-Sha'am	0.0003	0.1990	0.2481	0.3151	0.7624
5	E18.2	RAK Airport-Sha'am	0.0003	0.1990	0.2145	0.3151	0.7288
5	E18.2	RAK Airport-Sha'am	0.0003	0.1990	0.3465	0.3151	0.8609
5	E18.2	RAK Airport-Sha'am	0.0003	0.1990	0.2200	0.3151	0.7343
5	E18.2	RAK Airport-Sha'am	0.0003	0.1990	0.2548	0.3151	0.7691
5	E18.2	RAK Airport-Sha'am	0.0003	0.1990	0.2970	0.3151	0.8113
5	E18.2	RAK Airport-Sha'am	0.0003	0.1990	0.3842	0.3151	0.8986
5	E18.2	RAK Airport-Sha'am	0.0003	0.1990	0.3786	0.3151	0.8929
7	E311	Sheik Mohammed Bin Zayed	0.0000	0.2390	0.2837	0.1803	0.7030
7	E311	Sheik Mohammed Bin Zayed	0.0000	0.2390	0.3828	0.1803	0.8021
7	E311	Sheik Mohammed Bin Zayed	0.0000	0.2390	0.3537	0.1803	0.7730
7	E311	Sheik Mohammed Bin Zayed	0.0000	0.2390	0.2540	0.1803	0.6733
7	E311	Sheik Mohammed Bin Zayed	0.0000	0.2390	0.3628	0.1803	0.7821
7	E311	Sheik Mohammed Bin Zayed	0.0000	0.2390	0.3229	0.1803	0.7422
7	E311	Sheik Mohammed Bin Zayed	0.0000	0.2390	0.2716	0.1803	0.6909
7	E311	Sheik Mohammed Bin Zayed	0.0000	0.2390	0.3382	0.1803	0.7575
7	E311	Sheik Mohammed Bin Zayed	0.0000	0.2390	0.3837	0.1803	0.8031
7	E311	Sheik Mohammed Bin Zayed	0.0000	0.2390	0.2692	0.1803	0.6885
7	E311	Sheik Mohammed Bin Zayed	0.0000	0.2390	0.3296	0.1803	0.7489
8	E55.1	Dhaid - Madam	1402.4146	0.1399	0.3830	0.2386	1403.1761
8	E55.1	Dhaid - Madam	1402.4146	0.1399	0.2366	0.2386	1403.0297
8	E55.1	Dhaid - Madam	1402.4146	0.1399	0.2727	0.2386	1403.0658
8	E55.1	Dhaid - Madam	1402.4146	0.1399	0.2740	0.2386	1403.0670
8	E55.1	Dhaid - Madam	1402.4146	0.1399	0.2287	0.2386	1403.0218
8	E55.1	Dhaid - Madam	1402.4146	0.1399	0.2698	0.2386	1403.0629
8	E55.1	Dhaid - Madam	1402.4146	0.1399	0.3494	0.2386	1403.1424
8	E55.1	Dhaid - Madam	1402.4146	0.1399	0.2281	0.2386	1403.0211
8	E55.1	Dhaid - Madam	1402.4146	0.1399	0.3708	0.2386	1403.1639
8	E55.1	Dhaid - Madam	1402.4146	0.1399	0.3802	0.2386	1403.1733
10	E55.2	Madam - Shiweb	39.8594	0.1427	0.3679	0.2750	40.6451
10	E55.2	Madam - Shiweb	39.8594	0.1427	0.2681	0.2750	40.5452
10	E55.2	Madam - Shiweb	39.8594	0.1427	0.3817	0.2750	40.6588
10	E55.2	Madam - Shiweb	39.8594	0.1427	0.3729	0.2750	40.6500

12	E55.3	Umm Al Quwaim - Dhaid	16854.0535	0.1321	0.2697	0.2113	16854.6666
12	E55.3	Umm Al Quwaim - Dhaid	16854.0535	0.1321	0.1539	0.2113	16854.5507
12	E55.3	Umm Al Quwaim - Dhaid	16854.0535	0.1321	0.3366	0.2113	16854.7334
12	E55.3	Umm Al Quwaim - Dhaid	16854.0535	0.1321	0.2902	0.2113	16854.6870
12	E55.3	Umm Al Quwaim - Dhaid	16854.0535	0.1321	0.2188	0.2113	16854.6156
12	E55.3	Umm Al Quwaim - Dhaid	16854.0535	0.1321	0.2480	0.2113	16854.6448
12	E55.3	Umm Al Quwaim - Dhaid	16854.0535	0.1321	0.3821	0.2113	16854.7790
12	E55.3	Umm Al Quwaim - Dhaid	16854.0535	0.1321	0.3689	0.2113	16854.7658
12	E55.3	Umm Al Quwaim - Dhaid	16854.0535	0.1321	0.3791	0.2113	16854.7759
18	E84	Sheikh Khalifa Rd	0.2465	0.1410	0.2636	0.1460	0.7971
18	E84	Sheikh Khalifa Rd	0.2465	0.1410	0.2318	0.1460	0.7653
18	E84	Sheikh Khalifa Rd	0.2465	0.1410	0.3839	0.1460	0.9174
18	E84	Sheikh Khalifa Rd	0.2465	0.1410	0.2602	0.1460	0.7937
18	E84	Sheikh Khalifa Rd	0.2465	0.1410	0.3233	0.1460	0.8568
18	E84	Sheikh Khalifa Rd	0.2465	0.1410	0.2881	0.1460	0.8215
18	E84	Sheikh Khalifa Rd	0.2465	0.1410	0.3538	0.1460	0.8873
18	E84	Sheikh Khalifa Rd	0.2465	0.1410	0.3648	0.1460	0.8983
20	E88.1	Sharjah - Dhaid	0.0001	0.2173	0.2148	0.2188	0.6510
20	E88.1	Sharjah - Dhaid	0.0001	0.2173	0.3396	0.2188	0.7757
20	E88.1	Sharjah - Dhaid	0.0001	0.2173	0.3823	0.2188	0.8185
20	E88.1	Sharjah - Dhaid	0.0001	0.2173	0.3841	0.2188	0.8202
20	E88.1	Sharjah - Dhaid	0.0001	0.2173	0.2938	0.2188	0.7300
20	E88.1	Sharjah - Dhaid	0.0001	0.2173	0.2738	0.2188	0.7100
22	E88.2	Dhaid - Masafi	0.0003	0.1932	0.3353	0.2149	0.7437
22	E88.2	Dhaid - Masafi	0.0003	0.1932	0.2804	0.2149	0.6888
22	E88.2	Dhaid - Masafi	0.0003	0.1932	0.3049	0.2149	0.7133
22	E88.2	Dhaid - Masafi	0.0003	0.1932	0.3142	0.2149	0.7226
22	E88.2	Dhaid - Masafi	0.0003	0.1932	0.2207	0.2149	0.6291
22	E88.2	Dhaid - Masafi	0.0003	0.1932	0.3727	0.2149	0.7811
22	E88.2	Dhaid - Masafi	0.0003	0.1932	0.3842	0.2149	0.7926
22	E88.2	Dhaid - Masafi	0.0003	0.1932	0.3503	0.2149	0.7587
24	E89.1	Masafi - Dibba	17122.7612	0.1627	0.3135	0.3289	17123.5662
24	E89.1	Masafi - Dibba	17122.7612	0.1627	0.2162	0.3289	17123.4689
24	E89.1	Masafi - Dibba	17122.7612	0.1627	0.3716	0.3289	17123.6244
26	E89.3	Masafi - Fujairah	0.0027	0.1872	0.3805	0.2580	0.8283
26	E89.3	Masafi - Fujairah	0.0027	0.1872	0.3480	0.2580	0.7959
26	E89.3	Masafi - Fujairah	0.0027	0.1872	0.2998	0.2580	0.7476
26	E89.3	Masafi - Fujairah	0.0027	0.1872	0.3520	0.2580	0.7998
28	E99.1	Khor Fakkan - Dibba	0.1862	0.2082	0.3837	0.2916	1.0697
28	E99.1	Khor Fakkan - Dibba	0.1862	0.2082	0.3652	0.2916	1.0512
28	E99.1	Khor Fakkan - Dibba	0.1862	0.2082	0.2801	0.2916	0.9660
28	E99.1	Khor Fakkan - Dibba	0.1862	0.2082	0.3055	0.2916	0.9915
28	E99.1	Khor Fakkan - Dibba	0.1862	0.2082	0.2682	0.2916	0.9542
28	E99.1	Khor Fakkan - Dibba	0.1862	0.2082	0.3840	0.2916	1.0700
28	E99.1	Khor Fakkan - Dibba	0.1862	0.2082	0.3822	0.2916	1.0682
29	E99.2	Fujairah - Khor Fakkan	0.0060	0.2062	0.2461	0.2430	0.7013
29	E99.2	Fujairah - Khor Fakkan	0.0060	0.2062	0.3762	0.2430	0.8314
29	E99.2	Fujairah - Khor Fakkan	0.0060	0.2062	0.2620	0.2430	0.7172
29	E99.2	Fujairah - Khor Fakkan	0.0060	0.2062	0.2778	0.2430	0.7330
30	E99.3	Fujairah - Oman	0.6556	0.2014	0.3715	0.2932	1.5217

Deficiency in Experiment Model 1

Table 14-15: Deficiency in experiment model 1,2013 climate change scenario

N	Road Code	Road	change in roughness structural (ΔRIs)	change in roughness rutting ΔRIr	change in roughness due to cracking ΔRIc	environmental component of roughness (ΔRIe)	The total incremental change in roughness ΔRI
8	E55.1	Dhaid - Madam	1382.8443	0.1300	0.3830	0.2418	1383.5991
8	E55.1	Dhaid - Madam	1382.8443	0.1300	0.2366	0.2418	1383.4528
8	E55.1	Dhaid - Madam	1382.8443	0.1300	0.2727	0.2418	1383.4889
8	E55.1	Dhaid - Madam	1382.8443	0.1300	0.2740	0.2418	1383.4901
8	E55.1	Dhaid - Madam	1382.8443	0.1300	0.2287	0.2418	1383.4448
8	E55.1	Dhaid - Madam	1382.8443	0.1300	0.2698	0.2418	1383.4859
8	E55.1	Dhaid - Madam	1382.8443	0.1300	0.3494	0.2418	1383.5655
8	E55.1	Dhaid - Madam	1382.8443	0.1300	0.2281	0.2418	1383.4442
8	E55.1	Dhaid - Madam	1382.8443	0.1300	0.3708	0.2418	1383.5869

Experiment 2: Total Change in Roughness 2013

Table 14-16: Experiment model 2-total change in roughness 2013 climate change scenario

N	Road Code	Road	change in roughness structural (ΔRIs)	change in roughness rutting ΔRIr	change in roughness due to cracking ΔRIc	environmental component of roughness (ΔRIe)	The total incremental change in roughness ΔRI
1	E.11	Ittihad road	0	0.1478	0.2769	0.2141	0.6389
1	E.11	Ittihad road	0	0.1478	0.3784	0.2141	0.7404
1	E.11	Ittihad road	0	0.1478	0.3680	0.2141	0.7299
1	E.11	Ittihad road	0	0.1478	0.3610	0.2141	0.7230
1	E.11	Ittihad road	0	0.1478	0.2160	0.2141	0.5779
1	E.11	Ittihad road	0	0.1478	0.3137	0.2141	0.6757
1	E.11	Ittihad road	0	0.1478	0.2603	0.2141	0.6223
1	E.11	Ittihad road	0	0.1478	0.3727	0.2141	0.7347
3	E18.1	Manama- RAK Airport	0	0.1774	0.2495	0.1809	0.6078
3	E18.1	Manama- RAK Airport	0	0.1774	0.2316	0.1809	0.5899
3	E18.1	Manama- RAK Airport	0	0.1774	0.3843	0.1809	0.7426
3	E18.1	Manama- RAK Airport	0	0.1774	0.3517	0.1809	0.7099
3	E18.1	Manama- RAK Airport	0	0.1774	0.3358	0.1809	0.6940
3	E18.1	Manama- RAK Airport	0	0.1774	0.3825	0.1809	0.7408
3	E18.1	Manama- RAK Airport	0	0.1774	0.2143	0.1809	0.5725
3	E18.1	Manama- RAK Airport	0	0.1774	0.3731	0.1809	0.7314
5	E18.2	RAK Airport-Sha'am	0	0.1660	0.3036	0.3194	0.7890
5	E18.2	RAK Airport-Sha'am	0	0.1660	0.2481	0.3194	0.7335
5	E18.2	RAK Airport-Sha'am	0	0.1660	0.2145	0.3194	0.6998
5	E18.2	RAK Airport-Sha'am	0	0.1660	0.3465	0.3194	0.8319
5	E18.2	RAK Airport-Sha'am	0	0.1660	0.2200	0.3194	0.7053
5	E18.2	RAK Airport-Sha'am	0	0.1660	0.2548	0.3194	0.7401
5	E18.2	RAK Airport-Sha'am	0	0.1660	0.2970	0.3194	0.7824
5	E18.2	RAK Airport-Sha'am	0	0.1660	0.3842	0.3194	0.8696
5	E18.2	RAK Airport-Sha'am	0	0.1660	0.3786	0.3194	0.8640
7	E311	Sheik Mohammed Bin Zayed	0	0.1972	0.2837	0.1827	0.6636
7	E311	Sheik Mohammed Bin Zayed	0	0.1972	0.3828	0.1827	0.7627
7	E311	Sheik Mohammed Bin Zayed	0	0.1972	0.3537	0.1827	0.7336
7	E311	Sheik Mohammed Bin Zayed	0	0.1972	0.2540	0.1827	0.6339
7	E311	Sheik Mohammed Bin Zayed	0	0.1972	0.3628	0.1827	0.7427

7	E311	Sheik Mohammed Bin Zayed	0	0.1972	0.3229	0.1827	0.7029
7	E311	Sheik Mohammed Bin Zayed	0	0.1972	0.2716	0.1827	0.6515
7	E311	Sheik Mohammed Bin Zayed	0	0.1972	0.3382	0.1827	0.7182
7	E311	Sheik Mohammed Bin Zayed	0	0.1972	0.3837	0.1827	0.7637
7	E311	Sheik Mohammed Bin Zayed	0	0.1972	0.2692	0.1827	0.6492
7	E311	Sheik Mohammed Bin Zayed	0	0.1972	0.3296	0.1827	0.7096
8	E55.1	Dhaid - Madam	0	0.1300	0.3830	0.2418	0.7548
8	E55.1	Dhaid - Madam	0	0.1300	0.2366	0.2418	0.6085
8	E55.1	Dhaid - Madam	0	0.1300	0.2727	0.2418	0.6445
8	E55.1	Dhaid - Madam	0	0.1300	0.2740	0.2418	0.6458
8	E55.1	Dhaid - Madam	0	0.1300	0.2287	0.2418	0.6005
8	E55.1	Dhaid - Madam	0	0.1300	0.2698	0.2418	0.6416
8	E55.1	Dhaid - Madam	0	0.1300	0.3494	0.2418	0.7212
8	E55.1	Dhaid - Madam	0	0.1300	0.2281	0.2418	0.5999
8	E55.1	Dhaid - Madam	0	0.1300	0.3708	0.2418	0.7426
8	E55.1	Dhaid - Madam	0	0.1300	0.3802	0.2418	0.7520
10	E55.2	Madam - Shiweb	0	0.1314	0.3679	0.2787	0.7781
10	E55.2	Madam - Shiweb	0	0.1314	0.2681	0.2787	0.6782
10	E55.2	Madam - Shiweb	0	0.1314	0.3817	0.2787	0.7918
10	E55.2	Madam - Shiweb	0	0.1314	0.3729	0.2787	0.7830
12	E55.3	Umm Al Quwaim - Dhaid	0	0.1263	0.2697	0.2141	0.6101
12	E55.3	Umm Al Quwaim - Dhaid	0	0.1263	0.1539	0.2141	0.4943
12	E55.3	Umm Al Quwaim - Dhaid	0	0.1263	0.3366	0.2141	0.6770
12	E55.3	Umm Al Quwaim - Dhaid	0	0.1263	0.2902	0.2141	0.6306
12	E55.3	Umm Al Quwaim - Dhaid	0	0.1263	0.2188	0.2141	0.5592
12	E55.3	Umm Al Quwaim - Dhaid	0	0.1263	0.2480	0.2141	0.5884
12	E55.3	Umm Al Quwaim - Dhaid	0	0.1263	0.3821	0.2141	0.7225
12	E55.3	Umm Al Quwaim - Dhaid	0	0.1263	0.3689	0.2141	0.7093
12	E55.3	Umm Al Quwaim - Dhaid	0	0.1263	0.3791	0.2141	0.7195
18	E84	Sheikh Khalifa Rd	0	0.1305	0.2636	0.1480	0.5421
18	E84	Sheikh Khalifa Rd	0	0.1305	0.2318	0.1480	0.5103
18	E84	Sheikh Khalifa Rd	0	0.1305	0.3839	0.1480	0.6624
18	E84	Sheikh Khalifa Rd	0	0.1305	0.2602	0.1480	0.5387
18	E84	Sheikh Khalifa Rd	0	0.1305	0.3233	0.1480	0.6018
18	E84	Sheikh Khalifa Rd	0	0.1305	0.2881	0.1480	0.5666
18	E84	Sheikh Khalifa Rd	0	0.1305	0.3538	0.1480	0.6323
18	E84	Sheikh Khalifa Rd	0	0.1305	0.3648	0.1480	0.6433
20	E88.1	Sharjah - Dhaid	0	0.1797	0.2148	0.2217	0.6163
20	E88.1	Sharjah - Dhaid	0	0.1797	0.3396	0.2217	0.7411
20	E88.1	Sharjah - Dhaid	0	0.1797	0.3823	0.2217	0.7838
20	E88.1	Sharjah - Dhaid	0	0.1797	0.3841	0.2217	0.7856
20	E88.1	Sharjah - Dhaid	0	0.1797	0.2938	0.2217	0.6953
20	E88.1	Sharjah - Dhaid	0	0.1797	0.2738	0.2217	0.6753
22	E88.2	Dhaid - Masafi	0	0.1619	0.3353	0.2178	0.7150
22	E88.2	Dhaid - Masafi	0	0.1619	0.2804	0.2178	0.6601
22	E88.2	Dhaid - Masafi	0	0.1619	0.3049	0.2178	0.6846
22	E88.2	Dhaid - Masafi	0	0.1619	0.3142	0.2178	0.6940
22	E88.2	Dhaid - Masafi	0	0.1619	0.2207	0.2178	0.6004
22	E88.2	Dhaid - Masafi	0	0.1619	0.3727	0.2178	0.7525
22	E88.2	Dhaid - Masafi	0	0.1619	0.3842	0.2178	0.7639
22	E88.2	Dhaid - Masafi	0	0.1619	0.3503	0.2178	0.7300
24	E89.1	Masafi - Dibba (	0	0.1423	0.3135	0.3334	0.7891
24	E89.1	Masafi - Dibba	0	0.1423	0.2162	0.3334	0.6918
24	E89.1	Masafi - Dibba	0	0.1423	0.3716	0.3334	0.8473
26	E89.3	Masafi - Fujairah	0	0.1578	0.3805	0.2615	0.7997
26	E89.3	Masafi - Fujairah	0	0.1578	0.3480	0.2615	0.7673
26	E89.3	Masafi - Fujairah	0	0.1578	0.2998	0.2615	0.7190
26	E89.3	Masafi - Fujairah	0	0.1578	0.3520	0.2615	0.7712
28	E99.1	Khor Fakkan - Dibba	0	0.1728	0.3837	0.2955	0.8520
28	E99.1	Khor Fakkan - Dibba	0	0.1728	0.3652	0.2955	0.8335

28	E99.1	Khor Fakkan - Dibba	0	0.1728	0.2801	0.2955	0.7484
28	E99.1	Khor Fakkan - Dibba	0	0.1728	0.3055	0.2955	0.7739
28	E99.1	Khor Fakkan - Dibba	0	0.1728	0.2682	0.2955	0.7365
28	E99.1	Khor Fakkan - Dibba	0	0.1728	0.3840	0.2955	0.8523
28	E99.1	Khor Fakkan - Dibba	0	0.1728	0.3822	0.2955	0.8505
29	E99.2	Fujairah - Khor Fakkan	0	0.1713	0.2461	0.2463	0.6637
29	E99.2	Fujairah - Khor Fakkan	0	0.1713	0.3762	0.2463	0.7937
29	E99.2	Fujairah - Khor Fakkan	0	0.1713	0.2620	0.2463	0.6795
29	E99.2	Fujairah - Khor Fakkan	0	0.1713	0.2778	0.2463	0.6954
30	E99.3	Fujairah - Oman	0	0.1678	0.3715	0.2972	0.8365

Experiment Model 2: Total Change in Roughness 2020

Table 14-17: Experiment model 2: total change in roughness 2020 climate change scenario

N	Road Code	Road	change in roughness structural (ΔRIs)	change in roughness rutting ΔRIr	change in roughness due to cracking ΔRIc	environmental component of roughness (ΔRIe)	The total incremental change in roughness ΔRI
1	E.11	Ittihad road	0	0.1590	0.2769	0.1838	0.6198
1	E.11	Ittihad road	0	0.1550	0.3784	0.2132	0.7466
1	E.11	Ittihad road	0	0.1550	0.3680	0.2132	0.7362
1	E.11	Ittihad road	0	0.1550	0.3610	0.2132	0.7292
1	E.11	Ittihad road	0	0.1550	0.2160	0.2132	0.5842
1	E.11	Ittihad road	0	0.1550	0.3137	0.2132	0.6819
1	E.11	Ittihad road	0	0.1550	0.2603	0.2132	0.6285
1	E.11	Ittihad road	0	0.1550	0.3727	0.2132	0.7409
3	E18.1	Manama- RAK Airport	0	0.1891	0.2495	0.1801	0.6188
3	E18.1	Manama- RAK Airport	0	0.1891	0.2316	0.1801	0.6009
3	E18.1	Manama- RAK Airport	0	0.1891	0.3843	0.1801	0.7536
3	E18.1	Manama- RAK Airport	0	0.1891	0.3517	0.1801	0.7210
3	E18.1	Manama- RAK Airport	0	0.1891	0.3358	0.1801	0.7051
3	E18.1	Manama- RAK Airport	0	0.1891	0.3825	0.1801	0.7518
3	E18.1	Manama- RAK Airport	0	0.1891	0.2143	0.1801	0.5836
3	E18.1	Manama- RAK Airport	0	0.1891	0.3731	0.1801	0.7424
5	E18.2	RAK Airport-Sha'am	0	0.1763	0.3036	0.3180	0.7979
5	E18.2	RAK Airport-Sha'am	0	0.1763	0.2481	0.3180	0.7425
5	E18.2	RAK Airport-Sha'am	0	0.1763	0.2145	0.3180	0.7088
5	E18.2	RAK Airport-Sha'am	0	0.1763	0.3465	0.3180	0.8409
5	E18.2	RAK Airport-Sha'am	0	0.1763	0.2200	0.3180	0.7143
5	E18.2	RAK Airport-Sha'am	0	0.1763	0.2548	0.3180	0.7491
5	E18.2	RAK Airport-Sha'am	0	0.1763	0.2970	0.3180	0.7913
5	E18.2	RAK Airport-Sha'am	0	0.1763	0.3842	0.3180	0.8786
5	E18.2	RAK Airport-Sha'am	0	0.1763	0.3786	0.3180	0.8729
7	E311	Sheik Mohammed Bin Zayed	0	0.2110	0.2837	0.1820	0.6766
7	E311	Sheik Mohammed Bin Zayed	0	0.2110	0.3828	0.1820	0.7757
7	E311	Sheik Mohammed Bin Zayed	0	0.2110	0.3537	0.1820	0.7466
7	E311	Sheik Mohammed Bin Zayed	0	0.2110	0.2540	0.1820	0.6469
7	E311	Sheik Mohammed Bin Zayed	0	0.2110	0.3628	0.1820	0.7557
7	E311	Sheik Mohammed Bin Zayed	0	0.2110	0.3229	0.1820	0.7158
7	E311	Sheik Mohammed Bin Zayed	0	0.2110	0.2716	0.1820	0.6645
7	E311	Sheik Mohammed Bin Zayed	0	0.2110	0.3382	0.1820	0.7311
7	E311	Sheik Mohammed Bin Zayed	0	0.2110	0.3837	0.1820	0.7767
7	E311	Sheik Mohammed Bin Zayed	0	0.2110	0.2692	0.1820	0.6621
7	E311	Sheik Mohammed Bin Zayed	0	0.2110	0.3296	0.1820	0.7226
8	E55.1	Dhaid - Madam	0	0.1327	0.3830	0.2408	0.7565
8	E55.1	Dhaid - Madam	0	0.1327	0.2366	0.2408	0.6101

8	E55.1	Dhaid - Madam	0	0.1327	0.2727	0.2408	0.6462
8	E55.1	Dhaid - Madam	0	0.1327	0.2740	0.2408	0.6475
8	E55.1	Dhaid - Madam	0	0.1327	0.2287	0.2408	0.6022
8	E55.1	Dhaid - Madam	0	0.1327	0.2698	0.2408	0.6433
8	E55.1	Dhaid - Madam	0	0.1327	0.3494	0.2408	0.7228
8	E55.1	Dhaid - Madam	0	0.1327	0.2281	0.2408	0.6016
8	E55.1	Dhaid - Madam	0	0.1327	0.3708	0.2408	0.7443
8	E55.1	Dhaid - Madam	0	0.1327	0.3802	0.2408	0.7537
10	E55.2	Madam - Shiweb	0	0.1345	0.3679	0.2776	0.7800
10	E55.2	Madam - Shiweb	0	0.1345	0.2681	0.2776	0.6802
10	E55.2	Madam - Shiweb	0	0.1345	0.3817	0.2776	0.7938
10	E55.2	Madam - Shiweb	0	0.1345	0.3729	0.2776	0.7849
12	E55.3	Umm Al Quwaim - Dhaid	0	0.1278	0.2697	0.2132	0.6108
12	E55.3	Umm Al Quwaim - Dhaid	0	0.1278	0.1539	0.2132	0.4949
12	E55.3	Umm Al Quwaim - Dhaid	0	0.1278	0.3366	0.2132	0.6776
12	E55.3	Umm Al Quwaim - Dhaid	0	0.1278	0.2902	0.2132	0.6312
12	E55.3	Umm Al Quwaim - Dhaid	0	0.1278	0.2188	0.2132	0.5598
12	E55.3	Umm Al Quwaim - Dhaid	0	0.1278	0.2480	0.2132	0.5890
12	E55.3	Umm Al Quwaim - Dhaid	0	0.1278	0.3821	0.2132	0.7232
12	E55.3	Umm Al Quwaim - Dhaid	0	0.1278	0.3689	0.2132	0.7100
12	E55.3	Umm Al Quwaim - Dhaid	0	0.1278	0.3791	0.2132	0.7201
18	E84	Sheikh Khalifa Rd	0	0.1334	0.2636	0.1473	0.5444
18	E84	Sheikh Khalifa Rd	0	0.1334	0.2318	0.1473	0.5125
18	E84	Sheikh Khalifa Rd	0	0.1334	0.3839	0.1473	0.6646
18	E84	Sheikh Khalifa Rd	0	0.1334	0.2602	0.1473	0.5409
18	E84	Sheikh Khalifa Rd	0	0.1334	0.3233	0.1473	0.6041
18	E84	Sheikh Khalifa Rd	0	0.1334	0.2881	0.1473	0.5688
18	E84	Sheikh Khalifa Rd	0	0.1334	0.3538	0.1473	0.6346
18	E84	Sheikh Khalifa Rd	0	0.1334	0.3648	0.1473	0.6455
20	E88.1	Sharjah - Dhaid	0	0.1918	0.2148	0.2208	0.6274
20	E88.1	Sharjah - Dhaid	0	0.1918	0.3396	0.2208	0.7522
20	E88.1	Sharjah - Dhaid	0	0.1918	0.3823	0.2208	0.7949
20	E88.1	Sharjah - Dhaid	0	0.1918	0.3841	0.2208	0.7967
20	E88.1	Sharjah - Dhaid	0	0.1918	0.2938	0.2208	0.7064
20	E88.1	Sharjah - Dhaid	0	0.1918	0.2738	0.2208	0.6864
22	E88.2	Dhaid - Masafi	0	0.1716	0.3353	0.2169	0.7238
22	E88.2	Dhaid - Masafi	0	0.1716	0.2804	0.2169	0.6689
22	E88.2	Dhaid - Masafi	0	0.1716	0.3049	0.2169	0.6934
22	E88.2	Dhaid - Masafi	0	0.1716	0.3142	0.2169	0.7027
22	E88.2	Dhaid - Masafi	0	0.1716	0.2207	0.2169	0.6092
22	E88.2	Dhaid - Masafi	0	0.1716	0.3727	0.2169	0.7612
22	E88.2	Dhaid - Masafi	0	0.1716	0.3842	0.2169	0.7727
22	E88.2	Dhaid - Masafi	0	0.1716	0.3503	0.2169	0.7388
24	E89.1	Masafi - Dibba	0	0.1482	0.3135	0.3320	0.7936
24	E89.1	Masafi - Dibba	0	0.1482	0.2162	0.3320	0.6963
24	E89.1	Masafi - Dibba	0	0.1482	0.3716	0.3320	0.8518
26	E89.3	Masafi - Fujairah	0	0.1668	0.3805	0.2604	0.8076
26	E89.3	Masafi - Fujairah	0	0.1668	0.3480	0.2604	0.7752
26	E89.3	Masafi - Fujairah	0	0.1668	0.2998	0.2604	0.7269
26	E89.3	Masafi - Fujairah	0	0.1668	0.3520	0.2604	0.7791
28	E99.1	Khor Fakkan - Dibba	0	0.1840	0.3837	0.2943	0.8620
28	E99.1	Khor Fakkan - Dibba	0	0.1840	0.3652	0.2943	0.8435
28	E99.1	Khor Fakkan - Dibba	0	0.1840	0.2801	0.2943	0.7584
28	E99.1	Khor Fakkan - Dibba	0	0.1840	0.3055	0.2943	0.7839
28	E99.1	Khor Fakkan - Dibba	0	0.1840	0.2682	0.2943	0.7465
28	E99.1	Khor Fakkan - Dibba	0	0.1840	0.3840	0.2943	0.8623
28	E99.1	Khor Fakkan - Dibba	0	0.1840	0.3822	0.2943	0.8605
29	E99.2	Fujairah - Khor Fakkan	0	0.1824	0.2461	0.2452	0.6737
29	E99.2	Fujairah - Khor Fakkan	0	0.1824	0.3762	0.2452	0.8038
29	E99.2	Fujairah - Khor Fakkan	0	0.1824	0.2620	0.2452	0.6895

29	E99.2	Fujairah - Khor Fakkan	0	0.1824	0.2778	0.2452	0.7054
30	E99.3	Fujairah - Oman	0	0.1783	0.3715	0.2959	0.8458

Experiment Model 2: Total Change in Roughness 2040

Table 14-18: Experiment model 2-total change in roughness 2040 climate change scenario

N	Road Code	Road	change in roughness structural (ΔRIs)	change in roughness rutting ΔRIr	change in roughness due to cracking ΔRIc	environmental component of roughness (ΔRIe)	The total incremental change in roughness ΔRI
1	E.11	Ittihad road	0	0.1629	0.2769	0.2123	0.6522
1	E.11	Ittihad road	0	0.1629	0.3784	0.2123	0.7536
1	E.11	Ittihad road	0	0.1629	0.3680	0.2123	0.7432
1	E.11	Ittihad road	0	0.1629	0.3610	0.2123	0.7363
1	E.11	Ittihad road	0	0.1629	0.2160	0.2123	0.5912
1	E.11	Ittihad road	0	0.1629	0.3137	0.2123	0.6889
1	E.11	Ittihad road	0	0.1629	0.2603	0.2123	0.6356
1	E.11	Ittihad road	0	0.1629	0.3727	0.2123	0.7480
3	E18.1	Manama- RAK Airport	0	0.2013	0.2495	0.1794	0.6302
3	E18.1	Manama- RAK Airport	0	0.2013	0.2316	0.1794	0.6123
3	E18.1	Manama- RAK Airport	0	0.2013	0.3843	0.1794	0.7650
3	E18.1	Manama- RAK Airport	0	0.2013	0.3517	0.1794	0.7324
3	E18.1	Manama- RAK Airport	0	0.2013	0.3358	0.1794	0.7165
3	E18.1	Manama- RAK Airport	0	0.2013	0.3825	0.1794	0.7632
3	E18.1	Manama- RAK Airport	0	0.2013	0.2143	0.1794	0.5950
3	E18.1	Manama- RAK Airport	0	0.2013	0.3731	0.1794	0.7538
5	E18.2	RAK Airport-Sha'am	0	0.1872	0.3036	0.3167	0.8075
5	E18.2	RAK Airport-Sha'am	0	0.1872	0.2481	0.3167	0.7520
5	E18.2	RAK Airport-Sha'am	0	0.1872	0.2145	0.3167	0.7184
5	E18.2	RAK Airport-Sha'am	0	0.1872	0.3465	0.3167	0.8504
5	E18.2	RAK Airport-Sha'am	0	0.1872	0.2200	0.3167	0.7238
5	E18.2	RAK Airport-Sha'am	0	0.1872	0.2548	0.3167	0.7586
5	E18.2	RAK Airport-Sha'am	0	0.1872	0.2970	0.3167	0.8009
5	E18.2	RAK Airport-Sha'am	0	0.1872	0.3842	0.3167	0.8881
5	E18.2	RAK Airport-Sha'am	0	0.1872	0.3786	0.3167	0.8825
7	E311	Sheik Mohammed Bin Zayed	0	0.2248	0.2837	0.1812	0.6896
7	E311	Sheik Mohammed Bin Zayed	0	0.2248	0.3828	0.1812	0.7888
7	E311	Sheik Mohammed Bin Zayed	0	0.2248	0.3537	0.1812	0.7597
7	E311	Sheik Mohammed Bin Zayed	0	0.2248	0.2540	0.1812	0.6600
7	E311	Sheik Mohammed Bin Zayed	0	0.2248	0.3628	0.1812	0.7687
7	E311	Sheik Mohammed Bin Zayed	0	0.2248	0.3229	0.1812	0.7289
7	E311	Sheik Mohammed Bin Zayed	0	0.2248	0.2716	0.1812	0.6776
7	E311	Sheik Mohammed Bin Zayed	0	0.2248	0.3382	0.1812	0.7442
7	E311	Sheik Mohammed Bin Zayed	0	0.2248	0.3837	0.1812	0.7897
7	E311	Sheik Mohammed Bin Zayed	0	0.2248	0.2692	0.1812	0.6752
7	E311	Sheik Mohammed Bin Zayed	0	0.2248	0.3296	0.1812	0.7356
8	E55.1	Dhaid - Madam	0	0.1359	0.3830	0.2398	0.7587
8	E55.1	Dhaid - Madam	0	0.1359	0.2366	0.2398	0.6123
8	E55.1	Dhaid - Madam	0	0.1359	0.2727	0.2398	0.6484
8	E55.1	Dhaid - Madam	0	0.1359	0.2740	0.2398	0.6497
8	E55.1	Dhaid - Madam	0	0.1359	0.2287	0.2398	0.6044
8	E55.1	Dhaid - Madam	0	0.1359	0.2698	0.2398	0.6455
8	E55.1	Dhaid - Madam	0	0.1359	0.3494	0.2398	0.7251
8	E55.1	Dhaid - Madam	0	0.1359	0.2281	0.2398	0.6038
8	E55.1	Dhaid - Madam	0	0.1359	0.3708	0.2398	0.7465
8	E55.1	Dhaid - Madam	0	0.1359	0.3802	0.2398	0.7559
10	E55.2	Madam - Shiweb	0	0.1382	0.3679	0.2764	0.7825

10	E55.2	Madam - Shiweb	0	0.1382	0.2681	0.2764	0.6827
10	E55.2	Madam - Shiweb	0	0.1382	0.3817	0.2764	0.7963
10	E55.2	Madam - Shiweb	0	0.1382	0.3729	0.2764	0.7875
12	E55.3	Umm Al Quwaim - Dhaid	0	0.1297	0.2697	0.2123	0.6118
12	E55.3	Umm Al Quwaim - Dhaid	0	0.1297	0.1539	0.2123	0.4959
12	E55.3	Umm Al Quwaim - Dhaid	0	0.1297	0.3366	0.2123	0.6786
12	E55.3	Umm Al Quwaim - Dhaid	0	0.1297	0.2902	0.2123	0.6322
12	E55.3	Umm Al Quwaim - Dhaid	0	0.1297	0.2188	0.2123	0.5608
12	E55.3	Umm Al Quwaim - Dhaid	0	0.1297	0.2480	0.2123	0.5900
12	E55.3	Umm Al Quwaim - Dhaid	0	0.1297	0.3821	0.2123	0.7242
12	E55.3	Umm Al Quwaim - Dhaid	0	0.1297	0.3689	0.2123	0.7110
12	E55.3	Umm Al Quwaim - Dhaid	0	0.1297	0.3791	0.2123	0.7211
18	E84	Sheikh Khalifa Rd	0	0.1368	0.2636	0.1467	0.5471
18	E84	Sheikh Khalifa Rd	0	0.1368	0.2318	0.1467	0.5153
18	E84	Sheikh Khalifa Rd	0	0.1368	0.3839	0.1467	0.6674
18	E84	Sheikh Khalifa Rd	0	0.1368	0.2602	0.1467	0.5437
18	E84	Sheikh Khalifa Rd	0	0.1368	0.3233	0.1467	0.6069
18	E84	Sheikh Khalifa Rd	0	0.1368	0.2881	0.1467	0.5716
18	E84	Sheikh Khalifa Rd	0	0.1368	0.3538	0.1467	0.6374
18	E84	Sheikh Khalifa Rd	0	0.1368	0.3648	0.1467	0.6483
20	E88.1	Sharjah - Dhaid	0	0.2042	0.2148	0.2199	0.6389
20	E88.1	Sharjah - Dhaid	0	0.2042	0.3396	0.2199	0.7637
20	E88.1	Sharjah - Dhaid	0	0.2042	0.3823	0.2199	0.8064
20	E88.1	Sharjah - Dhaid	0	0.2042	0.3841	0.2199	0.8082
20	E88.1	Sharjah - Dhaid	0	0.2042	0.2938	0.2199	0.7179
20	E88.1	Sharjah - Dhaid	0	0.2042	0.2738	0.2199	0.6979
22	E88.2	Dhaid - Masafi	0	0.1819	0.3353	0.2160	0.7332
22	E88.2	Dhaid - Masafi	0	0.1819	0.2804	0.2160	0.6783
22	E88.2	Dhaid - Masafi	0	0.1819	0.3049	0.2160	0.7028
22	E88.2	Dhaid - Masafi	0	0.1819	0.3142	0.2160	0.7121
22	E88.2	Dhaid - Masafi	0	0.1819	0.2207	0.2160	0.6186
22	E88.2	Dhaid - Masafi	0	0.1819	0.3727	0.2160	0.7707
22	E88.2	Dhaid - Masafi	0	0.1819	0.3842	0.2160	0.7821
22	E88.2	Dhaid - Masafi	0	0.1819	0.3503	0.2160	0.7482
24	E89.1	Masafi - Dibba	0	0.1549	0.3135	0.3306	0.7989
24	E89.1	Masafi - Dibba	0	0.1549	0.2162	0.3306	0.7016
24	E89.1	Masafi - Dibba	0	0.1549	0.3716	0.3306	0.8571
26	E89.3	Masafi - Fujairah	0	0.1765	0.3805	0.2593	0.8162
26	E89.3	Masafi - Fujairah	0	0.1765	0.3480	0.2593	0.7838
26	E89.3	Masafi - Fujairah	0	0.1765	0.2998	0.2593	0.7355
26	E89.3	Masafi - Fujairah	0	0.1765	0.3520	0.2593	0.7877
28	E99.1	Khor Fakkan - Dibba	0	0.1957	0.3837	0.2931	0.8725
28	E99.1	Khor Fakkan - Dibba	0	0.1957	0.3652	0.2931	0.8540
28	E99.1	Khor Fakkan - Dibba	0	0.1957	0.2801	0.2931	0.7689
28	E99.1	Khor Fakkan - Dibba	0	0.1957	0.3055	0.2931	0.7943
28	E99.1	Khor Fakkan - Dibba	0	0.1957	0.2682	0.2931	0.7570
28	E99.1	Khor Fakkan - Dibba	0	0.1957	0.3840	0.2931	0.8728
28	E99.1	Khor Fakkan - Dibba	0	0.1957	0.3822	0.2931	0.8710
29	E99.2	Fujairah - Khor Fakkan	0	0.1939	0.2461	0.2442	0.6842
29	E99.2	Fujairah - Khor Fakkan	0	0.1939	0.3762	0.2442	0.8142
29	E99.2	Fujairah - Khor Fakkan	0	0.1939	0.2620	0.2442	0.7000
29	E99.2	Fujairah - Khor Fakkan	0	0.1939	0.2778	0.2442	0.7159
30	E99.3	Fujairah - Oman	0	0.1895	0.3715	0.2947	0.8556

Experiment Model 2: Total Change in Roughness 2060

Table 14-19: Experiment Model 2-total change in roughness 2060 climate change scenario

N	Road Code	Road	change in roughness structural (ΔRIs)	change in roughness rutting ΔRIr	change in roughness due to cracking ΔRIc	environmental component of roughness (ΔRIe)	The total incremental change in roughness ΔRI
1	E.11	Ittihad road	0	0.1719	0.2769	0.2113	0.6601
1	E.11	Ittihad road	0	0.1719	0.3784	0.2113	0.7615
1	E.11	Ittihad road	0	0.1719	0.3680	0.2113	0.7511
1	E.11	Ittihad road	0	0.1719	0.3610	0.2113	0.7442
1	E.11	Ittihad road	0	0.1719	0.2160	0.2113	0.5991
1	E.11	Ittihad road	0	0.1719	0.3137	0.2113	0.6969
1	E.11	Ittihad road	0	0.1719	0.2603	0.2113	0.6435
1	E.11	Ittihad road	0	0.1719	0.3727	0.2113	0.7559
3	E18.1	Manama- RAK Airport	0	0.2142	0.2495	0.1785	0.6422
3	E18.1	Manama- RAK Airport	0	0.2142	0.2316	0.1785	0.6243
3	E18.1	Manama- RAK Airport	0	0.2142	0.3843	0.1785	0.7770
3	E18.1	Manama- RAK Airport	0	0.2142	0.3517	0.1785	0.7444
3	E18.1	Manama- RAK Airport	0	0.2142	0.3358	0.1785	0.7285
3	E18.1	Manama- RAK Airport	0	0.2142	0.3825	0.1785	0.7752
3	E18.1	Manama- RAK Airport	0	0.2142	0.2143	0.1785	0.6070
3	E18.1	Manama- RAK Airport	0	0.2142	0.3731	0.1785	0.7658
5	E18.2	RAK Airport-Sha'am	0	0.1990	0.3036	0.3151	0.8176
5	E18.2	RAK Airport-Sha'am	0	0.1990	0.2481	0.3151	0.7622
5	E18.2	RAK Airport-Sha'am	0	0.1990	0.2145	0.3151	0.7285
5	E18.2	RAK Airport-Sha'am	0	0.1990	0.3465	0.3151	0.8606
5	E18.2	RAK Airport-Sha'am	0	0.1990	0.2200	0.3151	0.7340
5	E18.2	RAK Airport-Sha'am	0	0.1990	0.2548	0.3151	0.7688
5	E18.2	RAK Airport-Sha'am	0	0.1990	0.2970	0.3151	0.8111
5	E18.2	RAK Airport-Sha'am	0	0.1990	0.3842	0.3151	0.8983
5	E18.2	RAK Airport-Sha'am	0	0.1990	0.3786	0.3151	0.8927
7	E311	Sheik Mohammed Bin Zayed	0	0.2390	0.2837	0.1803	0.7030
7	E311	Sheik Mohammed Bin Zayed	0	0.2390	0.3828	0.1803	0.8021
7	E311	Sheik Mohammed Bin Zayed	0	0.2390	0.3537	0.1803	0.7730
7	E311	Sheik Mohammed Bin Zayed	0	0.2390	0.2540	0.1803	0.6733
7	E311	Sheik Mohammed Bin Zayed	0	0.2390	0.3628	0.1803	0.7821
7	E311	Sheik Mohammed Bin Zayed	0	0.2390	0.3229	0.1803	0.7422
7	E311	Sheik Mohammed Bin Zayed	0	0.2390	0.2716	0.1803	0.6909
7	E311	Sheik Mohammed Bin Zayed	0	0.2390	0.3382	0.1803	0.7575
7	E311	Sheik Mohammed Bin Zayed	0	0.2390	0.3837	0.1803	0.8031
7	E311	Sheik Mohammed Bin Zayed	0	0.2390	0.2692	0.1803	0.6885
7	E311	Sheik Mohammed Bin Zayed	0	0.2390	0.3296	0.1803	0.7489
8	E55.1	Dhaid - Madam	0	0.1399	0.3830	0.2386	0.7614
8	E55.1	Dhaid - Madam	0	0.1399	0.2366	0.2386	0.6151
8	E55.1	Dhaid - Madam	0	0.1399	0.2727	0.2386	0.6512
8	E55.1	Dhaid - Madam	0	0.1399	0.2740	0.2386	0.6524
8	E55.1	Dhaid - Madam	0	0.1399	0.2287	0.2386	0.6071
8	E55.1	Dhaid - Madam	0	0.1399	0.2698	0.2386	0.6483
8	E55.1	Dhaid - Madam	0	0.1399	0.3494	0.2386	0.7278
8	E55.1	Dhaid - Madam	0	0.1399	0.2281	0.2386	0.6065
8	E55.1	Dhaid - Madam	0	0.1399	0.3708	0.2386	0.7493
8	E55.1	Dhaid - Madam	0	0.1399	0.3802	0.2386	0.7586
10	E55.2	Madam - Shiweb	0	0.1427	0.3679	0.2750	0.7856
10	E55.2	Madam - Shiweb	0	0.1427	0.2681	0.2750	0.6858
10	E55.2	Madam - Shiweb	0	0.1427	0.3817	0.2750	0.7994
10	E55.2	Madam - Shiweb	0	0.1427	0.3729	0.2750	0.7906
12	E55.3	Umm Al Quwaim - Dhaid	0	0.1321	0.2697	0.2113	0.6131

12	E55.3	Umm Al Quwaim - Dhaid	0	0.1321	0.1539	0.2113	0.4972
12	E55.3	Umm Al Quwaim - Dhaid	0	0.1321	0.3366	0.2113	0.6799
12	E55.3	Umm Al Quwaim - Dhaid	0	0.1321	0.2902	0.2113	0.6335
12	E55.3	Umm Al Quwaim - Dhaid	0	0.1321	0.2188	0.2113	0.5621
12	E55.3	Umm Al Quwaim - Dhaid	0	0.1321	0.2480	0.2113	0.5913
12	E55.3	Umm Al Quwaim - Dhaid	0	0.1321	0.3821	0.2113	0.7255
12	E55.3	Umm Al Quwaim - Dhaid	0	0.1321	0.3689	0.2113	0.7123
12	E55.3	Umm Al Quwaim - Dhaid	0	0.1321	0.3791	0.2113	0.7224
18	E84	Sheikh Khalifa Rd	0	0.1410	0.2636	0.1460	0.5506
18	E84	Sheikh Khalifa Rd	0	0.1410	0.2318	0.1460	0.5188
18	E84	Sheikh Khalifa Rd	0	0.1410	0.3839	0.1460	0.6709
18	E84	Sheikh Khalifa Rd	0	0.1410	0.2602	0.1460	0.5472
18	E84	Sheikh Khalifa Rd	0	0.1410	0.3233	0.1460	0.6103
18	E84	Sheikh Khalifa Rd	0	0.1410	0.2881	0.1460	0.5750
18	E84	Sheikh Khalifa Rd	0	0.1410	0.3538	0.1460	0.6408
18	E84	Sheikh Khalifa Rd	0	0.1410	0.3648	0.1460	0.6518
20	E88.1	Sharjah - Dhaid	0	0.2173	0.2148	0.2188	0.6509
20	E88.1	Sharjah - Dhaid	0	0.2173	0.3396	0.2188	0.7757
20	E88.1	Sharjah - Dhaid	0	0.2173	0.3823	0.2188	0.8184
20	E88.1	Sharjah - Dhaid	0	0.2173	0.3841	0.2188	0.8202
20	E88.1	Sharjah - Dhaid	0	0.2173	0.2938	0.2188	0.7299
20	E88.1	Sharjah - Dhaid	0	0.2173	0.2738	0.2188	0.7099
22	E88.2	Dhaid - Masafi	0	0.1932	0.3353	0.2149	0.7434
22	E88.2	Dhaid - Masafi	0	0.1932	0.2804	0.2149	0.6885
22	E88.2	Dhaid - Masafi	0	0.1932	0.3049	0.2149	0.7130
22	E88.2	Dhaid - Masafi	0	0.1932	0.3142	0.2149	0.7223
22	E88.2	Dhaid - Masafi	0	0.1932	0.2207	0.2149	0.6288
22	E88.2	Dhaid - Masafi	0	0.1932	0.3727	0.2149	0.7808
22	E88.2	Dhaid - Masafi	0	0.1932	0.3842	0.2149	0.7923
22	E88.2	Dhaid - Masafi	0	0.1932	0.3503	0.2149	0.7584
24	E89.1	Masafi - Dibba	0	0.1627	0.3135	0.3289	0.8050
24	E89.1	Masafi - Dibba	0	0.1627	0.2162	0.3289	0.7077
24	E89.1	Masafi - Dibba	0	0.1627	0.3716	0.3289	0.8632
26	E89.3	Masafi - Fujairah	0	0.1872	0.3805	0.2580	0.8256
26	E89.3	Masafi - Fujairah	0	0.1872	0.3480	0.2580	0.7931
26	E89.3	Masafi - Fujairah	0	0.1872	0.2998	0.2580	0.7449
26	E89.3	Masafi - Fujairah	0	0.1872	0.3520	0.2580	0.7971
28	E99.1	Khor Fakkan - Dibba	0	0.2082	0.3837	0.2916	0.8835
28	E99.1	Khor Fakkan - Dibba	0	0.2082	0.3652	0.2916	0.8650
28	E99.1	Khor Fakkan - Dibba	0	0.2082	0.2801	0.2916	0.7799
28	E99.1	Khor Fakkan - Dibba	0	0.2082	0.3055	0.2916	0.8053
28	E99.1	Khor Fakkan - Dibba	0	0.2082	0.2682	0.2916	0.7680
28	E99.1	Khor Fakkan - Dibba	0	0.2082	0.3840	0.2916	0.8838
28	E99.1	Khor Fakkan - Dibba	0	0.2082	0.3822	0.2916	0.8820
29	E99.2	Fujairah - Khor Fakkan	0	0.2062	0.2461	0.2430	0.6953
29	E99.2	Fujairah - Khor Fakkan	0	0.2062	0.3762	0.2430	0.8254
29	E99.2	Fujairah - Khor Fakkan	0	0.2062	0.2620	0.2430	0.7112
29	E99.2	Fujairah - Khor Fakkan	0	0.2062	0.2778	0.2430	0.7270
30	E99.3	Fujairah - Oman	0	0.2014	0.3715	0.2932	0.8661

Experiment Model 3: Determine Total Change in Roughness 2013

Table 14-20: Experiment model 3-total change in roughness 2013 climate change scenario

N	Road Code	Road	change in roughness structural (ΔRIs)	change in roughness rutting ΔRIr	change in roughness due to cracking ΔRIc	environmental component of roughness (ΔRIe)	The total incremental change in roughness ΔRI
1	E.11	Ittihad road	0	0.1478	0.1938	0.1071	0.4487
1	E.11	Ittihad road	0	0.1478	0.2649	0.1071	0.5198
1	E.11	Ittihad road	0	0.1478	0.2576	0.1071	0.5125
1	E.11	Ittihad road	0	0.1478	0.2527	0.1071	0.5076
1	E.11	Ittihad road	0	0.1478	0.1512	0.1071	0.4061
1	E.11	Ittihad road	0	0.1478	0.2196	0.1071	0.4745
1	E.11	Ittihad road	0	0.1478	0.1822	0.1071	0.4371
1	E.11	Ittihad road	0	0.1478	0.2609	0.1071	0.5158
3	E18.1	Manama- RAK Airport	0	0.1774	0.1747	0.0905	0.4425
3	E18.1	Manama- RAK Airport	0	0.1774	0.1621	0.0905	0.4299
3	E18.1	Manama- RAK Airport	0	0.1774	0.2690	0.0905	0.5368
3	E18.1	Manama- RAK Airport	0	0.1774	0.2462	0.0905	0.5140
3	E18.1	Manama- RAK Airport	0	0.1774	0.2350	0.0905	0.5029
3	E18.1	Manama- RAK Airport	0	0.1774	0.2678	0.0905	0.5356
3	E18.1	Manama- RAK Airport	0	0.1774	0.1500	0.0905	0.4178
3	E18.1	Manama- RAK Airport	0	0.1774	0.2612	0.0905	0.5290
5	E18.2	RAK Airport-Sha'am	0	0.1660	0.2125	0.1597	0.5382
5	E18.2	RAK Airport-Sha'am	0	0.1660	0.1737	0.1597	0.4994
5	E18.2	RAK Airport-Sha'am	0	0.1660	0.1501	0.1597	0.4758
5	E18.2	RAK Airport-Sha'am	0	0.1660	0.2426	0.1597	0.5683
5	E18.2	RAK Airport-Sha'am	0	0.1660	0.1540	0.1597	0.4797
5	E18.2	RAK Airport-Sha'am	0	0.1660	0.1783	0.1597	0.5040
5	E18.2	RAK Airport-Sha'am	0	0.1660	0.2079	0.1597	0.5336
5	E18.2	RAK Airport-Sha'am	0	0.1660	0.2690	0.1597	0.5947
5	E18.2	RAK Airport-Sha'am	0	0.1660	0.2650	0.1597	0.5907
7	E311	Sheik Mohammed Bin Zayed	0	0.1972	0.1986	0.0914	0.4871
7	E311	Sheik Mohammed Bin Zayed	0	0.1972	0.2680	0.0914	0.5565
7	E311	Sheik Mohammed Bin Zayed	0	0.1972	0.2476	0.0914	0.5362
7	E311	Sheik Mohammed Bin Zayed	0	0.1972	0.1778	0.0914	0.4664
7	E311	Sheik Mohammed Bin Zayed	0	0.1972	0.2539	0.0914	0.5425
7	E311	Sheik Mohammed Bin Zayed	0	0.1972	0.2260	0.0914	0.5146
7	E311	Sheik Mohammed Bin Zayed	0	0.1972	0.1901	0.0914	0.4787
7	E311	Sheik Mohammed Bin Zayed	0	0.1972	0.2368	0.0914	0.5253
7	E311	Sheik Mohammed Bin Zayed	0	0.1972	0.2686	0.0914	0.5572
7	E311	Sheik Mohammed Bin Zayed	0	0.1972	0.1884	0.0914	0.4770
7	E311	Sheik Mohammed Bin Zayed	0	0.1972	0.2307	0.0914	0.5193
8	E55.1	Dhaid - Madam	0	0.1300	0.2681	0.1209	0.5190
8	E55.1	Dhaid - Madam	0	0.1300	0.1657	0.1209	0.4165
8	E55.1	Dhaid - Madam	0	0.1300	0.1909	0.1209	0.4418
8	E55.1	Dhaid - Madam	0	0.1300	0.1918	0.1209	0.4427
8	E55.1	Dhaid - Madam	0	0.1300	0.1601	0.1209	0.4110
8	E55.1	Dhaid - Madam	0	0.1300	0.1889	0.1209	0.4398
8	E55.1	Dhaid - Madam	0	0.1300	0.2445	0.1209	0.4954
8	E55.1	Dhaid - Madam	0	0.1300	0.1596	0.1209	0.4105
8	E55.1	Dhaid - Madam	0	0.1300	0.2596	0.1209	0.5105
8	E55.1	Dhaid - Madam	0	0.1300	0.2661	0.1209	0.5170
10	E55.2	Madam - Shiweb	0	0.1314	0.2575	0.1394	0.5283
10	E55.2	Madam - Shiweb	0	0.1314	0.1877	0.1394	0.4584
10	E55.2	Madam - Shiweb	0	0.1314	0.2672	0.1394	0.5379

10	E55.2	Madam - Shiweb	0	0.1314	0.2610	0.1394	0.5318
12	E55.3	Umm Al Quwaim - Dhaid	0	0.1263	0.1888	0.1071	0.4222
12	E55.3	Umm Al Quwaim - Dhaid	0	0.1263	0.1077	0.1071	0.3411
12	E55.3	Umm Al Quwaim - Dhaid	0	0.1263	0.2356	0.1071	0.4690
12	E55.3	Umm Al Quwaim - Dhaid	0	0.1263	0.2031	0.1071	0.4365
12	E55.3	Umm Al Quwaim - Dhaid	0	0.1263	0.1531	0.1071	0.3865
12	E55.3	Umm Al Quwaim - Dhaid	0	0.1263	0.1736	0.1071	0.4069
12	E55.3	Umm Al Quwaim - Dhaid	0	0.1263	0.2675	0.1071	0.5008
12	E55.3	Umm Al Quwaim - Dhaid	0	0.1263	0.2582	0.1071	0.4916
12	E55.3	Umm Al Quwaim - Dhaid	0	0.1263	0.2653	0.1071	0.4987
18	E84	Sheikh Khalifa Rd	0	0.1305	0.1845	0.0740	0.3890
18	E84	Sheikh Khalifa Rd	0	0.1305	0.1623	0.0740	0.3668
18	E84	Sheikh Khalifa Rd	0	0.1305	0.2687	0.0740	0.4733
18	E84	Sheikh Khalifa Rd	0	0.1305	0.1821	0.0740	0.3867
18	E84	Sheikh Khalifa Rd	0	0.1305	0.2263	0.0740	0.4308
18	E84	Sheikh Khalifa Rd	0	0.1305	0.2016	0.0740	0.4062
18	E84	Sheikh Khalifa Rd	0	0.1305	0.2477	0.0740	0.4522
18	E84	Sheikh Khalifa Rd	0	0.1305	0.2554	0.0740	0.4599
20	E88.1	Sharjah - Dhaid	0	0.1797	0.1504	0.1109	0.4410
20	E88.1	Sharjah - Dhaid	0	0.1797	0.2377	0.1109	0.5283
20	E88.1	Sharjah - Dhaid	0	0.1797	0.2676	0.1109	0.5582
20	E88.1	Sharjah - Dhaid	0	0.1797	0.2689	0.1109	0.5595
20	E88.1	Sharjah - Dhaid	0	0.1797	0.2057	0.1109	0.4963
20	E88.1	Sharjah - Dhaid	0	0.1797	0.1917	0.1109	0.4823
22	E88.2	Dhaid - Masafi	0	0.1619	0.2347	0.1089	0.5055
22	E88.2	Dhaid - Masafi	0	0.1619	0.1963	0.1089	0.4671
22	E88.2	Dhaid - Masafi	0	0.1619	0.2134	0.1089	0.4843
22	E88.2	Dhaid - Masafi	0	0.1619	0.2200	0.1089	0.4908
22	E88.2	Dhaid - Masafi	0	0.1619	0.1545	0.1089	0.4253
22	E88.2	Dhaid - Masafi	0	0.1619	0.2609	0.1089	0.5317
22	E88.2	Dhaid - Masafi	0	0.1619	0.2689	0.1089	0.5398
22	E88.2	Dhaid - Masafi	0	0.1619	0.2452	0.1089	0.5160
24	E89.1	Masafi - Dibba	0	0.1423	0.2194	0.1667	0.5284
24	E89.1	Masafi - Dibba	0	0.1423	0.1513	0.1667	0.4603
24	E89.1	Masafi - Dibba	0	0.1423	0.2602	0.1667	0.5691
26	E89.3	Masafi - Fujairah	0	0.1578	0.2663	0.1307	0.5548
26	E89.3	Masafi - Fujairah	0	0.1578	0.2436	0.1307	0.5321
26	E89.3	Masafi - Fujairah	0	0.1578	0.2099	0.1307	0.4984
26	E89.3	Masafi - Fujairah	0	0.1578	0.2464	0.1307	0.5349
28	E99.1	Khor Fakkan - Dibba	0	0.1728	0.2686	0.1478	0.5892
28	E99.1	Khor Fakkan - Dibba	0	0.1728	0.2556	0.1478	0.5762
28	E99.1	Khor Fakkan - Dibba	0	0.1728	0.1961	0.1478	0.5166
28	E99.1	Khor Fakkan - Dibba	0	0.1728	0.2139	0.1478	0.5345
28	E99.1	Khor Fakkan - Dibba	0	0.1728	0.1877	0.1478	0.5083
28	E99.1	Khor Fakkan - Dibba	0	0.1728	0.2688	0.1478	0.5894
28	E99.1	Khor Fakkan - Dibba	0	0.1728	0.2675	0.1478	0.5881
29	E99.2	Fujairah - Khor Fakkan	0	0.1713	0.1723	0.1231	0.4667
29	E99.2	Fujairah - Khor Fakkan	0	0.1713	0.2633	0.1231	0.5578
29	E99.2	Fujairah - Khor Fakkan	0	0.1713	0.1834	0.1231	0.4778
29	E99.2	Fujairah - Khor Fakkan	0	0.1713	0.1945	0.1231	0.4889
30	E99.3	Fujairah - Oman	0	0.1678	0.2601	0.1486	0.5764

Experiment Model 3: Determine Total Change in Roughness 2020

Table 14-21: Experiment model 3-total change in roughness 2020 climate change scenario

N	Road Code	Road	change in roughness structural (ΔRIs)	change in roughness rutting ΔRIr	change in roughness due to cracking ΔRIc	environmental component of roughness (ΔRIe)	The total incremental change in roughness ΔRI
1	E.11	Ittihad road	0	0.1590	0.1938	0.0919	0.4448
1	E.11	Ittihad road	0	0.1550	0.2649	0.1066	0.5265
1	E.11	Ittihad road	0	0.1550	0.2576	0.1066	0.5192
1	E.11	Ittihad road	0	0.1550	0.2527	0.1066	0.5143
1	E.11	Ittihad road	0	0.1550	0.1512	0.1066	0.4128
1	E.11	Ittihad road	0	0.1550	0.2196	0.1066	0.4812
1	E.11	Ittihad road	0	0.1550	0.1822	0.1066	0.4438
1	E.11	Ittihad road	0	0.1550	0.2609	0.1066	0.5225
3	E18.1	Manama- RAK Airport	0	0.1891	0.1747	0.0901	0.4539
3	E18.1	Manama- RAK Airport	0	0.1891	0.1621	0.0901	0.4413
3	E18.1	Manama- RAK Airport	0	0.1891	0.2690	0.0901	0.5482
3	E18.1	Manama- RAK Airport	0	0.1891	0.2462	0.0901	0.5254
3	E18.1	Manama- RAK Airport	0	0.1891	0.2350	0.0901	0.5143
3	E18.1	Manama- RAK Airport	0	0.1891	0.2678	0.0901	0.5470
3	E18.1	Manama- RAK Airport	0	0.1891	0.1500	0.0901	0.4292
3	E18.1	Manama- RAK Airport	0	0.1891	0.2612	0.0901	0.5404
5	E18.2	RAK Airport-Sha'am	0	0.1763	0.2125	0.1590	0.5478
5	E18.2	RAK Airport-Sha'am	0	0.1763	0.1737	0.1590	0.5090
5	E18.2	RAK Airport-Sha'am	0	0.1763	0.1501	0.1590	0.4855
5	E18.2	RAK Airport-Sha'am	0	0.1763	0.2426	0.1590	0.5779
5	E18.2	RAK Airport-Sha'am	0	0.1763	0.1540	0.1590	0.4893
5	E18.2	RAK Airport-Sha'am	0	0.1763	0.1783	0.1590	0.5137
5	E18.2	RAK Airport-Sha'am	0	0.1763	0.2079	0.1590	0.5432
5	E18.2	RAK Airport-Sha'am	0	0.1763	0.2690	0.1590	0.6043
5	E18.2	RAK Airport-Sha'am	0	0.1763	0.2650	0.1590	0.6004
7	E311	Sheik Mohammed Bin Zayed	0	0.2110	0.1986	0.0910	0.5005
7	E311	Sheik Mohammed Bin Zayed	0	0.2110	0.2680	0.0910	0.5699
7	E311	Sheik Mohammed Bin Zayed	0	0.2110	0.2476	0.0910	0.5495
7	E311	Sheik Mohammed Bin Zayed	0	0.2110	0.1778	0.0910	0.4798
7	E311	Sheik Mohammed Bin Zayed	0	0.2110	0.2539	0.0910	0.5559
7	E311	Sheik Mohammed Bin Zayed	0	0.2110	0.2260	0.0910	0.5280
7	E311	Sheik Mohammed Bin Zayed	0	0.2110	0.1901	0.0910	0.4921
7	E311	Sheik Mohammed Bin Zayed	0	0.2110	0.2368	0.0910	0.5387
7	E311	Sheik Mohammed Bin Zayed	0	0.2110	0.2686	0.0910	0.5706
7	E311	Sheik Mohammed Bin Zayed	0	0.2110	0.1884	0.0910	0.4904
7	E311	Sheik Mohammed Bin Zayed	0	0.2110	0.2307	0.0910	0.5327
8	E55.1	Dhaid - Madam	0	0.1327	0.2681	0.1204	0.5212
8	E55.1	Dhaid - Madam	0	0.1327	0.1657	0.1204	0.4187
8	E55.1	Dhaid - Madam	0	0.1327	0.1909	0.1204	0.4440
8	E55.1	Dhaid - Madam	0	0.1327	0.1918	0.1204	0.4449
8	E55.1	Dhaid - Madam	0	0.1327	0.1601	0.1204	0.4132
8	E55.1	Dhaid - Madam	0	0.1327	0.1889	0.1204	0.4420
8	E55.1	Dhaid - Madam	0	0.1327	0.2445	0.1204	0.4976
8	E55.1	Dhaid - Madam	0	0.1327	0.1596	0.1204	0.4127
8	E55.1	Dhaid - Madam	0	0.1327	0.2596	0.1204	0.5127
8	E55.1	Dhaid - Madam	0	0.1327	0.2661	0.1204	0.5192
10	E55.2	Madam - Shiweb	0	0.1345	0.2575	0.1388	0.5308
10	E55.2	Madam - Shiweb	0	0.1345	0.1877	0.1388	0.4609

10	E55.2	Madam - Shiweb	0	0.1345	0.2672	0.1388	0.5405
10	E55.2	Madam - Shiweb	0	0.1345	0.2610	0.1388	0.5343
12	E55.3	Umm Al Quwaim - Dhaid	0	0.1278	0.1888	0.1066	0.4232
12	E55.3	Umm Al Quwaim - Dhaid	0	0.1278	0.1077	0.1066	0.3422
12	E55.3	Umm Al Quwaim - Dhaid	0	0.1278	0.2356	0.1066	0.4700
12	E55.3	Umm Al Quwaim - Dhaid	0	0.1278	0.2031	0.1066	0.4376
12	E55.3	Umm Al Quwaim - Dhaid	0	0.1278	0.1531	0.1066	0.3876
12	E55.3	Umm Al Quwaim - Dhaid	0	0.1278	0.1736	0.1066	0.4080
12	E55.3	Umm Al Quwaim - Dhaid	0	0.1278	0.2675	0.1066	0.5019
12	E55.3	Umm Al Quwaim - Dhaid	0	0.1278	0.2582	0.1066	0.4927
12	E55.3	Umm Al Quwaim - Dhaid	0	0.1278	0.2653	0.1066	0.4998
18	E84	Sheikh Khalifa Rd	0	0.1334	0.1845	0.0737	0.3916
18	E84	Sheikh Khalifa Rd	0	0.1334	0.1623	0.0737	0.3693
18	E84	Sheikh Khalifa Rd	0	0.1334	0.2687	0.0737	0.4758
18	E84	Sheikh Khalifa Rd	0	0.1334	0.1821	0.0737	0.3892
18	E84	Sheikh Khalifa Rd	0	0.1334	0.2263	0.0737	0.4334
18	E84	Sheikh Khalifa Rd	0	0.1334	0.2016	0.0737	0.4087
18	E84	Sheikh Khalifa Rd	0	0.1334	0.2477	0.0737	0.4547
18	E84	Sheikh Khalifa Rd	0	0.1334	0.2554	0.0737	0.4624
20	E88.1	Sharjah - Dhaid	0	0.1918	0.1504	0.1104	0.4526
20	E88.1	Sharjah - Dhaid	0	0.1918	0.2377	0.1104	0.5399
20	E88.1	Sharjah - Dhaid	0	0.1918	0.2676	0.1104	0.5698
20	E88.1	Sharjah - Dhaid	0	0.1918	0.2689	0.1104	0.5711
20	E88.1	Sharjah - Dhaid	0	0.1918	0.2057	0.1104	0.5079
20	E88.1	Sharjah - Dhaid	0	0.1918	0.1917	0.1104	0.4939
22	E88.2	Dhaid - Masafi	0	0.1716	0.2347	0.1084	0.5147
22	E88.2	Dhaid - Masafi	0	0.1716	0.1963	0.1084	0.4763
22	E88.2	Dhaid - Masafi	0	0.1716	0.2134	0.1084	0.4935
22	E88.2	Dhaid - Masafi	0	0.1716	0.2200	0.1084	0.5000
22	E88.2	Dhaid - Masafi	0	0.1716	0.1545	0.1084	0.4346
22	E88.2	Dhaid - Masafi	0	0.1716	0.2609	0.1084	0.5410
22	E88.2	Dhaid - Masafi	0	0.1716	0.2689	0.1084	0.5490
22	E88.2	Dhaid - Masafi	0	0.1716	0.2452	0.1084	0.5252
24	E89.1	Masafi - Dibba	0	0.1482	0.2194	0.1660	0.5336
24	E89.1	Masafi - Dibba	0	0.1482	0.1513	0.1660	0.4655
24	E89.1	Masafi - Dibba	0	0.1482	0.2602	0.1660	0.5743
26	E89.3	Masafi - Fujairah	0	0.1668	0.2663	0.1302	0.5633
26	E89.3	Masafi - Fujairah	0	0.1668	0.2436	0.1302	0.5406
26	E89.3	Masafi - Fujairah	0	0.1668	0.2099	0.1302	0.5068
26	E89.3	Masafi - Fujairah	0	0.1668	0.2464	0.1302	0.5433
28	E99.1	Khor Fakkan - Dibba	0	0.1840	0.2686	0.1471	0.5998
28	E99.1	Khor Fakkan - Dibba	0	0.1840	0.2556	0.1471	0.5868
28	E99.1	Khor Fakkan - Dibba	0	0.1840	0.1961	0.1471	0.5272
28	E99.1	Khor Fakkan - Dibba	0	0.1840	0.2139	0.1471	0.5451
28	E99.1	Khor Fakkan - Dibba	0	0.1840	0.1877	0.1471	0.5189
28	E99.1	Khor Fakkan - Dibba	0	0.1840	0.2688	0.1471	0.6000
28	E99.1	Khor Fakkan - Dibba	0	0.1840	0.2675	0.1471	0.5987
29	E99.2	Fujairah - Khor Fakkan	0	0.1824	0.1723	0.1226	0.4772
29	E99.2	Fujairah - Khor Fakkan	0	0.1824	0.2633	0.1226	0.5683
29	E99.2	Fujairah - Khor Fakkan	0	0.1824	0.1834	0.1226	0.4883
29	E99.2	Fujairah - Khor Fakkan	0	0.1824	0.1945	0.1226	0.4995
30	E99.3	Fujairah - Oman	0	0.1783	0.2601	0.1480	0.5864

Experiment Model 3: Determine Total Change in Roughness 2040

Table 14-22: Experiment 3-total change in roughness 2040 climate change scenario

N	Road Code	Road	change in roughness structural (ΔRIs)	change in roughness rutting ΔRIr	change in roughness due to cracking ΔRIc	environmental component of roughness (ΔRIe)	The total incremental change in roughness ΔRI
1	E.11	Ittihad road	0	0.1629	0.1938	0.1062	0.4629
1	E.11	Ittihad road	0	0.1629	0.2649	0.1062	0.5339
1	E.11	Ittihad road	0	0.1629	0.2576	0.1062	0.5266
1	E.11	Ittihad road	0	0.1629	0.2527	0.1062	0.5218
1	E.11	Ittihad road	0	0.1629	0.1512	0.1062	0.4202
1	E.11	Ittihad road	0	0.1629	0.2196	0.1062	0.4887
1	E.11	Ittihad road	0	0.1629	0.1822	0.1062	0.4513
1	E.11	Ittihad road	0	0.1629	0.2609	0.1062	0.5300
3	E18.1	Manama- RAK Airport	0	0.2013	0.1747	0.0897	0.4657
3	E18.1	Manama- RAK Airport	0	0.2013	0.1621	0.0897	0.4531
3	E18.1	Manama- RAK Airport	0	0.2013	0.2690	0.0897	0.5600
3	E18.1	Manama- RAK Airport	0	0.2013	0.2462	0.0897	0.5372
3	E18.1	Manama- RAK Airport	0	0.2013	0.2350	0.0897	0.5261
3	E18.1	Manama- RAK Airport	0	0.2013	0.2678	0.0897	0.5588
3	E18.1	Manama- RAK Airport	0	0.2013	0.1500	0.0897	0.4410
3	E18.1	Manama- RAK Airport	0	0.2013	0.2612	0.0897	0.5522
5	E18.2	RAK Airport-Sha'am	0	0.1872	0.2125	0.1583	0.5581
5	E18.2	RAK Airport-Sha'am	0	0.1872	0.1737	0.1583	0.5192
5	E18.2	RAK Airport-Sha'am	0	0.1872	0.1501	0.1583	0.4957
5	E18.2	RAK Airport-Sha'am	0	0.1872	0.2426	0.1583	0.5881
5	E18.2	RAK Airport-Sha'am	0	0.1872	0.1540	0.1583	0.4995
5	E18.2	RAK Airport-Sha'am	0	0.1872	0.1783	0.1583	0.5239
5	E18.2	RAK Airport-Sha'am	0	0.1872	0.2079	0.1583	0.5535
5	E18.2	RAK Airport-Sha'am	0	0.1872	0.2690	0.1583	0.6145
5	E18.2	RAK Airport-Sha'am	0	0.1872	0.2650	0.1583	0.6106
7	E311	Sheik Mohammed Bin Zayed	0	0.2248	0.1986	0.0906	0.5139
7	E311	Sheik Mohammed Bin Zayed	0	0.2248	0.2680	0.0906	0.5833
7	E311	Sheik Mohammed Bin Zayed	0	0.2248	0.2476	0.0906	0.5630
7	E311	Sheik Mohammed Bin Zayed	0	0.2248	0.1778	0.0906	0.4932
7	E311	Sheik Mohammed Bin Zayed	0	0.2248	0.2539	0.0906	0.5693
7	E311	Sheik Mohammed Bin Zayed	0	0.2248	0.2260	0.0906	0.5414
7	E311	Sheik Mohammed Bin Zayed	0	0.2248	0.1901	0.0906	0.5055
7	E311	Sheik Mohammed Bin Zayed	0	0.2248	0.2368	0.0906	0.5521
7	E311	Sheik Mohammed Bin Zayed	0	0.2248	0.2686	0.0906	0.5840
7	E311	Sheik Mohammed Bin Zayed	0	0.2248	0.1884	0.0906	0.5038
7	E311	Sheik Mohammed Bin Zayed	0	0.2248	0.2307	0.0906	0.5461
8	E55.1	Dhaid - Madam	0	0.1359	0.2681	0.1199	0.5239
8	E55.1	Dhaid - Madam	0	0.1359	0.1657	0.1199	0.4215
8	E55.1	Dhaid - Madam	0	0.1359	0.1909	0.1199	0.4467
8	E55.1	Dhaid - Madam	0	0.1359	0.1918	0.1199	0.4476
8	E55.1	Dhaid - Madam	0	0.1359	0.1601	0.1199	0.4159
8	E55.1	Dhaid - Madam	0	0.1359	0.1889	0.1199	0.4447
8	E55.1	Dhaid - Madam	0	0.1359	0.2445	0.1199	0.5004
8	E55.1	Dhaid - Madam	0	0.1359	0.1596	0.1199	0.4155
8	E55.1	Dhaid - Madam	0	0.1359	0.2596	0.1199	0.5154
8	E55.1	Dhaid - Madam	0	0.1359	0.2661	0.1199	0.5219
10	E55.2	Madam - Shiweb	0	0.1382	0.2575	0.1382	0.5339
10	E55.2	Madam - Shiweb	0	0.1382	0.1877	0.1382	0.4641
10	E55.2	Madam - Shiweb	0	0.1382	0.2672	0.1382	0.5436
10	E55.2	Madam - Shiweb	0	0.1382	0.2610	0.1382	0.5374

12	E55.3	Umm Al Quwaim - Dhaid	0	0.1297	0.1888	0.1062	0.4247
12	E55.3	Umm Al Quwaim - Dhaid	0	0.1297	0.1077	0.1062	0.3436
12	E55.3	Umm Al Quwaim - Dhaid	0	0.1297	0.2356	0.1062	0.4715
12	E55.3	Umm Al Quwaim - Dhaid	0	0.1297	0.2031	0.1062	0.4390
12	E55.3	Umm Al Quwaim - Dhaid	0	0.1297	0.1531	0.1062	0.3890
12	E55.3	Umm Al Quwaim - Dhaid	0	0.1297	0.1736	0.1062	0.4095
12	E55.3	Umm Al Quwaim - Dhaid	0	0.1297	0.2675	0.1062	0.5034
12	E55.3	Umm Al Quwaim - Dhaid	0	0.1297	0.2582	0.1062	0.4941
12	E55.3	Umm Al Quwaim - Dhaid	0	0.1297	0.2653	0.1062	0.5012
18	E84	Sheikh Khalifa Rd	0	0.1368	0.1845	0.0734	0.3947
18	E84	Sheikh Khalifa Rd	0	0.1368	0.1623	0.0734	0.3724
18	E84	Sheikh Khalifa Rd	0	0.1368	0.2687	0.0734	0.4789
18	E84	Sheikh Khalifa Rd	0	0.1368	0.1821	0.0734	0.3923
18	E84	Sheikh Khalifa Rd	0	0.1368	0.2263	0.0734	0.4365
18	E84	Sheikh Khalifa Rd	0	0.1368	0.2016	0.0734	0.4118
18	E84	Sheikh Khalifa Rd	0	0.1368	0.2477	0.0734	0.4578
18	E84	Sheikh Khalifa Rd	0	0.1368	0.2554	0.0734	0.4655
20	E88.1	Sharjah - Dhaid	0	0.2042	0.1504	0.1099	0.4645
20	E88.1	Sharjah - Dhaid	0	0.2042	0.2377	0.1099	0.5518
20	E88.1	Sharjah - Dhaid	0	0.2042	0.2676	0.1099	0.5818
20	E88.1	Sharjah - Dhaid	0	0.2042	0.2689	0.1099	0.5830
20	E88.1	Sharjah - Dhaid	0	0.2042	0.2057	0.1099	0.5198
20	E88.1	Sharjah - Dhaid	0	0.2042	0.1917	0.1099	0.5058
22	E88.2	Dhaid - Masafi	0	0.1819	0.2347	0.1080	0.5246
22	E88.2	Dhaid - Masafi	0	0.1819	0.1963	0.1080	0.4862
22	E88.2	Dhaid - Masafi	0	0.1819	0.2134	0.1080	0.5033
22	E88.2	Dhaid - Masafi	0	0.1819	0.2200	0.1080	0.5099
22	E88.2	Dhaid - Masafi	0	0.1819	0.1545	0.1080	0.4444
22	E88.2	Dhaid - Masafi	0	0.1819	0.2609	0.1080	0.5508
22	E88.2	Dhaid - Masafi	0	0.1819	0.2689	0.1080	0.5589
22	E88.2	Dhaid - Masafi	0	0.1819	0.2452	0.1080	0.5351
24	E89.1	Masafi - Dibba	0	0.1549	0.2194	0.1653	0.5396
24	E89.1	Masafi - Dibba	0	0.1549	0.1513	0.1653	0.4715
24	E89.1	Masafi - Dibba	0	0.1549	0.2602	0.1653	0.5804
26	E89.3	Masafi - Fujairah	0	0.1765	0.2663	0.1296	0.5724
26	E89.3	Masafi - Fujairah	0	0.1765	0.2436	0.1296	0.5497
26	E89.3	Masafi - Fujairah	0	0.1765	0.2099	0.1296	0.5160
26	E89.3	Masafi - Fujairah	0	0.1765	0.2464	0.1296	0.5525
28	E99.1	Khor Fakkan - Dibba	0	0.1957	0.2686	0.1465	0.6109
28	E99.1	Khor Fakkan - Dibba	0	0.1957	0.2556	0.1465	0.5979
28	E99.1	Khor Fakkan - Dibba	0	0.1957	0.1961	0.1465	0.5383
28	E99.1	Khor Fakkan - Dibba	0	0.1957	0.2139	0.1465	0.5561
28	E99.1	Khor Fakkan - Dibba	0	0.1957	0.1877	0.1465	0.5300
28	E99.1	Khor Fakkan - Dibba	0	0.1957	0.2688	0.1465	0.6111
28	E99.1	Khor Fakkan - Dibba	0	0.1957	0.2675	0.1465	0.6098
29	E99.2	Fujairah - Khor Fakkan	0	0.1939	0.1723	0.1221	0.4882
29	E99.2	Fujairah - Khor Fakkan	0	0.1939	0.2633	0.1221	0.5793
29	E99.2	Fujairah - Khor Fakkan	0	0.1939	0.1834	0.1221	0.4994
29	E99.2	Fujairah - Khor Fakkan	0	0.1939	0.1945	0.1221	0.5105
30	E99.3	Fujairah - Oman	0	0.1895	0.2601	0.1473	0.5968

Experimental Model 3: Determine Total Change in Roughness 2060

Table 14-23: Experiment 3- total change in roughness 2060 climate change scenario

	Road Code	Road	change in roughness structural (ΔRIs)	change in roughness rutting ΔRIr	change in roughness due to cracking ΔRIc	environmental component of roughness (ΔRIe)	The total incremental change in roughness ΔRI
1	E.11	Ittihad road	0	0.1719	0.1938	0.1056	0.4714
1	E.11	Ittihad road	0	0.1719	0.2649	0.1056	0.5424
1	E.11	Ittihad road	0	0.1719	0.2576	0.1056	0.5351
1	E.11	Ittihad road	0	0.1719	0.2527	0.1056	0.5302
1	E.11	Ittihad road	0	0.1719	0.1512	0.1056	0.4287
1	E.11	Ittihad road	0	0.1719	0.2196	0.1056	0.4971
1	E.11	Ittihad road	0	0.1719	0.1822	0.1056	0.4598
1	E.11	Ittihad road	0	0.1719	0.2609	0.1056	0.5384
3	E18.1	Manama- RAK Airport	0	0.2142	0.1747	0.0892	0.4781
3	E18.1	Manama- RAK Airport	0	0.2142	0.1621	0.0892	0.4656
3	E18.1	Manama- RAK Airport	0	0.2142	0.2690	0.0892	0.5725
3	E18.1	Manama- RAK Airport	0	0.2142	0.2462	0.0892	0.5496
3	E18.1	Manama- RAK Airport	0	0.2142	0.2350	0.0892	0.5385
3	E18.1	Manama- RAK Airport	0	0.2142	0.2678	0.0892	0.5712
3	E18.1	Manama- RAK Airport	0	0.2142	0.1500	0.0892	0.4535
3	E18.1	Manama- RAK Airport	0	0.2142	0.2612	0.0892	0.5646
5	E18.2	RAK Airport-Sha'am	0	0.1990	0.2125	0.1575	0.5690
5	E18.2	RAK Airport-Sha'am	0	0.1990	0.1737	0.1575	0.5302
5	E18.2	RAK Airport-Sha'am	0	0.1990	0.1501	0.1575	0.5066
5	E18.2	RAK Airport-Sha'am	0	0.1990	0.2426	0.1575	0.5991
5	E18.2	RAK Airport-Sha'am	0	0.1990	0.1540	0.1575	0.5105
5	E18.2	RAK Airport-Sha'am	0	0.1990	0.1783	0.1575	0.5349
5	E18.2	RAK Airport-Sha'am	0	0.1990	0.2079	0.1575	0.5644
5	E18.2	RAK Airport-Sha'am	0	0.1990	0.2690	0.1575	0.6255
5	E18.2	RAK Airport-Sha'am	0	0.1990	0.2650	0.1575	0.6215
7	E311	Sheik Mohammed Bin Zayed	0	0.2390	0.1986	0.0901	0.5278
7	E311	Sheik Mohammed Bin Zayed	0	0.2390	0.2680	0.0901	0.5971
7	E311	Sheik Mohammed Bin Zayed	0	0.2390	0.2476	0.0901	0.5768
7	E311	Sheik Mohammed Bin Zayed	0	0.2390	0.1778	0.0901	0.5070
7	E311	Sheik Mohammed Bin Zayed	0	0.2390	0.2539	0.0901	0.5831
7	E311	Sheik Mohammed Bin Zayed	0	0.2390	0.2260	0.0901	0.5552
7	E311	Sheik Mohammed Bin Zayed	0	0.2390	0.1901	0.0901	0.5193
7	E311	Sheik Mohammed Bin Zayed	0	0.2390	0.2368	0.0901	0.5659
7	E311	Sheik Mohammed Bin Zayed	0	0.2390	0.2686	0.0901	0.5978
7	E311	Sheik Mohammed Bin Zayed	0	0.2390	0.1884	0.0901	0.5176
7	E311	Sheik Mohammed Bin Zayed	0	0.2390	0.2307	0.0901	0.5599
8	E55.1	Dhaid - Madam	0	0.1399	0.2681	0.1193	0.5273
8	E55.1	Dhaid - Madam	0	0.1399	0.1657	0.1193	0.4248
8	E55.1	Dhaid - Madam	0	0.1399	0.1909	0.1193	0.4501
8	E55.1	Dhaid - Madam	0	0.1399	0.1918	0.1193	0.4509
8	E55.1	Dhaid - Madam	0	0.1399	0.1601	0.1193	0.4192
8	E55.1	Dhaid - Madam	0	0.1399	0.1889	0.1193	0.4480
8	E55.1	Dhaid - Madam	0	0.1399	0.2445	0.1193	0.5037
8	E55.1	Dhaid - Madam	0	0.1399	0.1596	0.1193	0.4188
8	E55.1	Dhaid - Madam	0	0.1399	0.2596	0.1193	0.5187
8	E55.1	Dhaid - Madam	0	0.1399	0.2661	0.1193	0.5253
10	E55.2	Madam - Shiweb	0	0.1427	0.2575	0.1375	0.5377
10	E55.2	Madam - Shiweb	0	0.1427	0.1877	0.1375	0.4679
10	E55.2	Madam - Shiweb	0	0.1427	0.2672	0.1375	0.5474
10	E55.2	Madam - Shiweb	0	0.1427	0.2610	0.1375	0.5412

12	E55.3	Umm Al Quwaim - Dhaid	0	0.1321	0.1888	0.1056	0.4265
12	E55.3	Umm Al Quwaim - Dhaid	0	0.1321	0.1077	0.1056	0.3454
12	E55.3	Umm Al Quwaim - Dhaid	0	0.1321	0.2356	0.1056	0.4733
12	E55.3	Umm Al Quwaim - Dhaid	0	0.1321	0.2031	0.1056	0.4408
12	E55.3	Umm Al Quwaim - Dhaid	0	0.1321	0.1531	0.1056	0.3908
12	E55.3	Umm Al Quwaim - Dhaid	0	0.1321	0.1736	0.1056	0.4113
12	E55.3	Umm Al Quwaim - Dhaid	0	0.1321	0.2675	0.1056	0.5052
12	E55.3	Umm Al Quwaim - Dhaid	0	0.1321	0.2582	0.1056	0.4960
12	E55.3	Umm Al Quwaim - Dhaid	0	0.1321	0.2653	0.1056	0.5031
18	E84	Sheikh Khalifa Rd	0	0.1410	0.1845	0.0730	0.3985
18	E84	Sheikh Khalifa Rd	0	0.1410	0.1623	0.0730	0.3762
18	E84	Sheikh Khalifa Rd	0	0.1410	0.2687	0.0730	0.4827
18	E84	Sheikh Khalifa Rd	0	0.1410	0.1821	0.0730	0.3961
18	E84	Sheikh Khalifa Rd	0	0.1410	0.2263	0.0730	0.4403
18	E84	Sheikh Khalifa Rd	0	0.1410	0.2016	0.0730	0.4156
18	E84	Sheikh Khalifa Rd	0	0.1410	0.2477	0.0730	0.4617
18	E84	Sheikh Khalifa Rd	0	0.1410	0.2554	0.0730	0.4693
20	E88.1	Sharjah - Dhaid	0	0.2173	0.1504	0.1094	0.4771
20	E88.1	Sharjah - Dhaid	0	0.2173	0.2377	0.1094	0.5644
20	E88.1	Sharjah - Dhaid	0	0.2173	0.2676	0.1094	0.5943
20	E88.1	Sharjah - Dhaid	0	0.2173	0.2689	0.1094	0.5956
20	E88.1	Sharjah - Dhaid	0	0.2173	0.2057	0.1094	0.5323
20	E88.1	Sharjah - Dhaid	0	0.2173	0.1917	0.1094	0.5184
22	E88.2	Dhaid - Masafi	0	0.1932	0.2347	0.1074	0.5353
22	E88.2	Dhaid - Masafi	0	0.1932	0.1963	0.1074	0.4969
22	E88.2	Dhaid - Masafi	0	0.1932	0.2134	0.1074	0.5141
22	E88.2	Dhaid - Masafi	0	0.1932	0.2200	0.1074	0.5206
22	E88.2	Dhaid - Masafi	0	0.1932	0.1545	0.1074	0.4552
22	E88.2	Dhaid - Masafi	0	0.1932	0.2609	0.1074	0.5616
22	E88.2	Dhaid - Masafi	0	0.1932	0.2689	0.1074	0.5696
22	E88.2	Dhaid - Masafi	0	0.1932	0.2452	0.1074	0.5458
24	E89.1	Masafi - Dibba	0	0.1627	0.2194	0.1644	0.5466
24	E89.1	Masafi - Dibba	0	0.1627	0.1513	0.1644	0.4784
24	E89.1	Masafi - Dibba	0	0.1627	0.2602	0.1644	0.5873
26	E89.3	Masafi - Fujairah	0	0.1872	0.2663	0.1290	0.5825
26	E89.3	Masafi - Fujairah	0	0.1872	0.2436	0.1290	0.5598
26	E89.3	Masafi - Fujairah	0	0.1872	0.2099	0.1290	0.5260
26	E89.3	Masafi - Fujairah	0	0.1872	0.2464	0.1290	0.5625
28	E99.1	Khor Fakkan - Dibba	0	0.2082	0.2686	0.1458	0.6226
28	E99.1	Khor Fakkan - Dibba	0	0.2082	0.2556	0.1458	0.6096
28	E99.1	Khor Fakkan - Dibba	0	0.2082	0.1961	0.1458	0.5501
28	E99.1	Khor Fakkan - Dibba	0	0.2082	0.2139	0.1458	0.5679
28	E99.1	Khor Fakkan - Dibba	0	0.2082	0.1877	0.1458	0.5418
28	E99.1	Khor Fakkan - Dibba	0	0.2082	0.2688	0.1458	0.6228
28	E99.1	Khor Fakkan - Dibba	0	0.2082	0.2675	0.1458	0.6216
29	E99.2	Fujairah - Khor Fakkan	0	0.2062	0.1723	0.1215	0.5000
29	E99.2	Fujairah - Khor Fakkan	0	0.2062	0.2633	0.1215	0.5910
29	E99.2	Fujairah - Khor Fakkan	0	0.2062	0.1834	0.1215	0.5111
29	E99.2	Fujairah - Khor Fakkan	0	0.2062	0.1945	0.1215	0.5222
30	E99.3	Fujairah - Oman	0	0.2014	0.2601	0.1466	0.6081

15. Appendix 4: Additional Data for Chapter 7

Measure Transition Probability Matrix based on Experts (Questionnaire Results)

Table 15-1: The questionnaire results based on a sample of 30 experts

State 1	State 2	State 3	State 4
Rate of deterioration in state 1	Rate of deterioration in state 2	Rate of deterioration in state 3	Rate of deterioration in state 4
0.05	0.05	0.02	0.02
0.28	0.2	0.18	0.2
0.2	0.03	0.06	0.01
0.03	0.01	0.01	0.03
0.05	0.01	0.05	0.05
0.2	0.2	0.12	0.28
0.05	0.03	0.05	0.03
0.04	0.04	0.04	0.01
0.36	0.14	0.36	0.12
0.1	0.1	0.2	0.2
0.1	0.1	0.1	0.1
0.03	0.03	0.03	0.03
0.2	0.1	0.2	0.2
0.07	0.05	0.18	0.28
0.04	0.04	0.06	0.06
0.03	0.03	0.06	0.12
0.03	0.03	0.06	0.12
0.1	0.03	0.02	0.03
0.06	0.04	0.04	0.2
0.28	0.14	0.28	0.14
0.72	0.28	0.28	0.28
0.28	0.28	0.12	0.2
0.36	0.28	0.2	0.4
0.28	0.28	0.28	0.28
0.06	0.2	0.28	0.36
0.56	0.36	0.14	0.4
0.72	0.28	0.28	0.72
0.02	0.02	0.02	0.02
0.01	0.01	0.01	0.01

0.1	0.1	0.12	0.1
0.180	**0.116**	**0.128**	**0.167**
Average			

Table 15-2: Questionnaire questions to determine the change in condition state

1. Pavement network classified in UAE into 5 condition states: how likely the risk of "Rate of pavement deterioration " **move from Very good condition to good condition** Every year

probability		Threats				
	0.9	0.05 ( )	0.09 ( )	0.18 ( )	0.36 ( )	0.72 ( )
	0.7	0.04 ( )	0.07 ( )	0.14 ( )	0.28 ( )	0.56 ( )
	0.5	0.03 ( )	0.05 ( )	0.1 ( )	0.2 ( )	0.4 ( )
	0.3	0.02 ( )	0.03 ( )	0.06 ( )	0.12 ( )	0.24 ( )
	0.1	0.01 ( )	0.01 ( )	0.02 ( )	0.04 ( )	0.08 ( )
		0.05/Very Low	0.1/Low	0.2/Low	0.4/High	0.8/Very High

2. Pavement network classified in UAE into 5 condition states: how likely the risk of "Rate of pavement deterioration " **move from good condition) to Satisfaction** Every year.

probability		Threats				
	0.9	0.05 ( )	0.09 ( )	0.18 ( )	0.36 ( )	0.72 ( )
	0.7	0.04 ( )	0.07 ( )	0.14 ( )	0.28 ( )	0.56 ( )
	0.5	0.03 ( )	0.05 ( )	0.1 ( )	0.2 ( )	0.4 ( )
	0.3	0.02 ( )	0.03 ( )	0.06 ( )	0.12 ( )	0.24 ( )
	0.1	0.01 ( )	0.01 ( )	0.02 ( )	0.04 ( )	0.08 ( )
		0.05/Very Low	0.1/Low	0.2/Low	0.4/High	0.8/Very High

3. Pavement network classified in UAE into 5 condition states: how likely the risk of "Rate of pavement deterioration " **move from Satisfaction condition to poor condition** Every year .

probability		Threats				
	0.9	0.05 ( )	0.09 ( )	0.18 ( )	0.36 ( )	0.72 ( )
	0.7	0.04 ( )	0.07 ( )	0.14 ( )	0.28 ( )	0.56 ( )
	0.5	0.03 ( )	0.05 ( )	0.1 ( )	0.2 ( )	0.4 ( )
	0.3	0.02 ( )	0.03 ( )	0.06 ( )	0.12 ( )	0.24 ( )
	0.1	0.01 ( )	0.01 ( )	0.02 ( )	0.04 ( )	0.08 ( )
		0.05/Very Low	0.1/Low	0.2/Low	0.4/High	0.8/Very High

4. Pavement network classified in UAE into 5 condition states: how likely the risk of "Rate of pavement deterioration "

probability		Threats				
	0.9	0.05 ( )	0.09 ( )	0.18 ( )	0.36 ( )	0.72 ( )
	0.7	0.04 ( )	0.07 ( )	0.14 ( )	0.28 ( )	0.56 ( )
	0.5	0.03	0.05	0.1	0.2	0.4

move from poor condition to Failure condition Every year c		( )	( )	( )	( )	( )
	0.3	0.02 ( )	0.03 ( )	0.06 ( )	0.12 ( )	0.24 ( )
	0.1	0.01 ( )	0.01 ( )	0.02 ( )	0.04 ( )	0.08 ( )
		0.05/Very Low	0.1/Low	0.2/Low	0.4/High	0.8/Very High

Results from the Deterministic Model (Modified HDM-4) used to Estimate the Transition Probability Matrix

Table 15-3: Results from the deterministic model used to estimate the transition probability matrix

N	Road Code	Road	initial roughness	Change in roughness (ΔRIe(k = 0.5) and (ΔRIc (k=0.7)	(Ria+ ΔRI) 2013	Change in roughness (ΔRIe(k = 0.5) and (ΔRIc (k=0.7)	(Ria+ ΔRI) 2020	Change in roughness(ΔRIe(k = 0.5) and (ΔRIc (k=0.7)	(Ria+ ΔRI) 2040	Change in roughness (ΔRIe(k = 0.5) and (ΔRIc (k=0.7)	(Ria+ ΔRI) 2060
			RIa	**2013**		**2020**		**2040**		**2060**	
1	E.11	Ittihad road	1.16	0.449	1.609	0.455	1.615	0.463	1.623	0.471	1.631
1	E.11	Ittihad road	1.16	0.52	1.68	0.526	1.686	0.534	1.694	0.542	1.702
1	E.11	Ittihad road	1.16	0.512	1.672	0.519	1.679	0.527	1.687	0.535	1.695
1	E.11	Ittihad road	1.16	0.508	1.668	0.514	1.674	0.522	1.682	0.53	1.69
1	E.11	Ittihad road	1.16	0.406	1.566	0.413	1.573	0.42	1.58	0.429	1.589
1	E.11	Ittihad road	1.16	0.474	1.634	0.481	1.641	0.489	1.649	0.497	1.657
1	E.11	Ittihad road	1.16	0.437	1.597	0.444	1.604	0.451	1.611	0.46	1.62
1	E.11	Ittihad road	1.16	0.516	1.676	0.522	1.682	0.53	1.69	0.538	1.698
3	E18.1	Manama- RAK Airport	0.98	0.442	1.422	0.454	1.434	0.466	1.446	0.478	1.458
3	E18.1	Manama- RAK Airport	0.98	0.43	1.41	0.441	1.421	0.453	1.433	0.466	1.446
3	E18.1	Manama- RAK Airport	0.98	0.537	1.517	0.548	1.528	0.56	1.54	0.572	1.552
3	E18.1	Manama- RAK Airport	0.98	0.514	1.494	0.525	1.505	0.537	1.517	0.55	1.53
3	E18.1	Manama- RAK Airport	0.98	0.503	1.483	0.514	1.494	0.526	1.506	0.539	1.519
3	E18.1	Manama- RAK Airport	0.98	0.536	1.516	0.547	1.527	0.559	1.539	0.571	1.551
3	E18.1	Manama- RAK Airport	0.98	0.418	1.398	0.429	1.409	0.441	1.421	0.453	1.433
3	E18.1	Manama- RAK Airport	0.98	0.529	1.509	0.54	1.52	0.552	1.532	0.565	1.545
5	E18.2	RAK Airport- Sha'am	1.73	0.538	2.268	0.548	2.278	0.558	2.288	0.569	2.299
5	E18.2	RAK Airport- Sha'am	1.73	0.499	2.229	0.509	2.239	0.519	2.249	0.53	2.26
5	E18.2	RAK Airport- Sha'am	1.73	0.476	2.206	0.485	2.215	0.496	2.226	0.507	2.237
5	E18.2	RAK Airport- Sha'am	1.73	0.568	2.298	0.578	2.308	0.588	2.318	0.599	2.329
5	E18.2	RAK Airport- Sha'am	1.73	0.48	2.21	0.489	2.219	0.5	2.23	0.51	2.24
5	E18.2	RAK Airport- Sha'am	1.73	0.504	2.234	0.514	2.244	0.524	2.254	0.535	2.265

5	E18.2	RAK Airport-Sha'am	1.73	0.534	2.264	0.543	2.273	0.553	2.283	0.564	2.294
5	E18.2	RAK Airport-Sha'am	1.73	0.595	2.325	0.604	2.334	0.615	2.345	0.625	2.355
5	E18.2	RAK Airport-Sha'am	1.73	0.591	2.321	0.6	2.33	0.611	2.341	0.622	2.352
7	E311	Sheik Mohammed Bin Zayed	0.99	0.487	1.477	0.501	1.49	0.514	1.504	0.528	1.518
7	E311	Sheik Mohammed Bin Zayed	0.99	0.557	1.546	0.57	1.56	0.583	1.573	0.597	1.587
7	E311	Sheik Mohammed Bin Zayed	0.99	0.536	1.526	0.55	1.539	0.563	1.553	0.577	1.567
7	E311	Sheik Mohammed Bin Zayed	0.99	0.466	1.456	0.48	1.47	0.493	1.483	0.507	1.497
7	E311	Sheik Mohammed Bin Zayed	0.99	0.543	1.532	0.556	1.546	0.569	1.559	0.583	1.573
7	E311	Sheik Mohammed Bin Zayed	0.99	0.515	1.504	0.528	1.518	0.541	1.531	0.555	1.545
7	E311	Sheik Mohammed Bin Zayed	0.99	0.479	1.469	0.492	1.482	0.505	1.495	0.519	1.509
7	E311	Sheik Mohammed Bin Zayed	0.99	0.525	1.515	0.539	1.529	0.552	1.542	0.566	1.556
7	E311	Sheik Mohammed Bin Zayed	0.99	0.557	1.547	0.571	1.56	0.584	1.574	0.598	1.588
7	E311	Sheik Mohammed Bin Zayed	0.99	0.477	1.467	0.49	1.48	0.504	1.494	0.518	1.508
7	E311	Sheik Mohammed Bin Zayed	0.99	0.519	1.509	0.533	1.523	0.546	1.536	0.56	1.55
8	E55.1	Dhaid - Madam	1.31	0.519	1.829	0.521	1.831	0.524	1.834	0.527	1.837
8	E55.1	Dhaid - Madam	1.31	0.417	1.727	0.419	1.729	0.421	1.731	0.425	1.735
8	E55.1	Dhaid - Madam	1.31	0.442	1.752	0.444	1.754	0.447	1.757	0.45	1.76
8	E55.1	Dhaid - Madam	1.31	0.443	1.753	0.445	1.755	0.448	1.758	0.451	1.761
8	E55.1	Dhaid - Madam	1.31	0.411	1.721	0.413	1.723	0.416	1.726	0.419	1.729
8	E55.1	Dhaid - Madam	1.31	0.44	1.75	0.442	1.752	0.445	1.755	0.448	1.758
8	E55.1	Dhaid - Madam	1.31	0.495	1.805	0.498	1.808	0.5	1.81	0.504	1.814
8	E55.1	Dhaid - Madam	1.31	0.411	1.721	0.413	1.723	0.415	1.725	0.419	1.729
8	E55.1	Dhaid - Madam	1.31	0.51	1.82	0.513	1.823	0.515	1.825	0.519	1.829
8	E55.1	Dhaid - Madam	1.31	0.517	1.827	0.519	1.829	0.522	1.832	0.525	1.835
10	E55.2	Madam - Shiweb	1.51	0.528	2.038	0.531	2.041	0.534	2.044	0.538	2.048
10	E55.2	Madam - Shiweb	1.51	0.458	1.968	0.461	1.971	0.464	1.974	0.468	1.978
10	E55.2	Madam - Shiweb	1.51	0.538	2.048	0.54	2.05	0.544	2.054	0.547	2.057
10	E55.2	Madam - Shiweb	1.51	0.532	2.042	0.534	2.044	0.537	2.047	0.541	2.051
12	E55.3	Umm Al Quwaim - Dhaid	1.16	0.422	1.582	0.423	1.583	0.425	1.585	0.427	1.587
12	E55.3	Umm Al Quwaim - Dhaid	1.16	0.341	1.501	0.342	1.502	0.344	1.504	0.345	1.505
12	E55.3	Umm Al Quwaim - Dhaid	1.16	0.469	1.629	0.47	1.63	0.471	1.631	0.473	1.633

12	E55.3	Umm Al Quwaim - Dhaid	1.16	0.436	1.596	0.438	1.598	0.439	1.599	0.441	1.601
12	E55.3	Umm Al Quwaim - Dhaid	1.16	0.386	1.546	0.388	1.548	0.389	1.549	0.391	1.551
12	E55.3	Umm Al Quwaim - Dhaid	1.16	0.407	1.567	0.408	1.568	0.409	1.569	0.411	1.571
12	E55.3	Umm Al Quwaim - Dhaid	1.16	0.501	1.661	0.502	1.662	0.503	1.663	0.505	1.665
12	E55.3	Umm Al Quwaim - Dhaid	1.16	0.492	1.652	0.493	1.653	0.494	1.654	0.496	1.656
12	E55.3	Umm Al Quwaim - Dhaid	1.16	0.499	1.659	0.5	1.66	0.501	1.661	0.503	1.663
18	E84	Sheikh Khalifa Rd	0.8	0.389	1.191	0.392	1.193	0.395	1.196	0.399	1.2
18	E84	Sheikh Khalifa Rd	0.8	0.367	1.168	0.369	1.171	0.372	1.174	0.376	1.178
18	E84	Sheikh Khalifa Rd	0.8	0.473	1.275	0.476	1.277	0.479	1.28	0.483	1.284
18	E84	Sheikh Khalifa Rd	0.8	0.387	1.188	0.389	1.191	0.392	1.194	0.396	1.198
18	E84	Sheikh Khalifa Rd	0.8	0.431	1.232	0.433	1.235	0.437	1.238	0.44	1.242
18	E84	Sheikh Khalifa Rd	0.8	0.406	1.208	0.409	1.21	0.412	1.213	0.416	1.217
18	E84	Sheikh Khalifa Rd	0.8	0.452	1.254	0.455	1.256	0.458	1.259	0.462	1.263
18	E84	Sheikh Khalifa Rd	0.8	0.46	1.261	0.462	1.264	0.466	1.267	0.469	1.271
20	E88.1	Sharjah - Dhaid	1.2	0.441	1.642	0.453	1.654	0.465	1.666	0.477	1.678
20	E88.1	Sharjah - Dhaid	1.2	0.528	1.729	0.54	1.741	0.552	1.753	0.564	1.766
20	E88.1	Sharjah - Dhaid	1.2	0.558	1.759	0.57	1.771	0.582	1.783	0.594	1.795
20	E88.1	Sharjah - Dhaid	1.2	0.559	1.761	0.571	1.772	0.583	1.784	0.596	1.797
20	E88.1	Sharjah - Dhaid	1.2	0.496	1.697	0.508	1.709	0.52	1.721	0.532	1.734
20	E88.1	Sharjah - Dhaid	1.2	0.482	1.683	0.494	1.695	0.506	1.707	0.518	1.72
22	E88.2	Dhaid - Masafi	1.18	0.506	1.685	0.515	1.695	0.525	1.704	0.535	1.715
22	E88.2	Dhaid - Masafi	1.18	0.467	1.647	0.476	1.656	0.486	1.666	0.497	1.677
22	E88.2	Dhaid - Masafi	1.18	0.484	1.664	0.493	1.673	0.503	1.683	0.514	1.694
22	E88.2	Dhaid - Masafi	1.18	0.491	1.671	0.5	1.68	0.51	1.69	0.521	1.7
22	E88.2	Dhaid - Masafi	1.18	0.425	1.605	0.435	1.614	0.444	1.624	0.455	1.635
22	E88.2	Dhaid - Masafi	1.18	0.532	1.712	0.541	1.721	0.551	1.731	0.562	1.741
22	E88.2	Dhaid - Masafi	1.18	0.54	1.72	0.549	1.729	0.559	1.739	0.57	1.749
22	E88.2	Dhaid - Masafi	1.18	0.516	1.696	0.525	1.705	0.535	1.715	0.546	1.726
24	E89.1	Masafi - Dibba	1.81	0.528	2.334	0.534	2.34	0.54	2.346	0.547	2.352
24	E89.1	Masafi - Dibba	1.81	0.46	2.266	0.465	2.271	0.472	2.277	0.478	2.284
24	E89.1	Masafi - Dibba	1.81	0.569	2.375	0.574	2.38	0.58	2.386	0.587	2.393
26	E89.3	Masafi - Fujairah	1.42	0.555	1.971	0.563	1.98	0.572	1.989	0.582	1.999
26	E89.3	Masafi - Fujairah	1.42	0.532	1.949	0.541	1.957	0.55	1.966	0.56	1.976
26	E89.3	Masafi - Fujairah	1.42	0.498	1.915	0.507	1.923	0.516	1.932	0.526	1.942
26	E89.3	Masafi - Fujairah	1.42	0.535	1.951	0.543	1.96	0.553	1.969	0.563	1.979
28	E99.1	Khor Fakkan - Dibba	1.6	0.589	2.19	0.6	2.201	0.611	2.212	0.623	2.224
28	E99.1	Khor Fakkan - Dibba	1.6	0.576	2.177	0.587	2.188	0.598	2.199	0.61	2.211

28	E99.1	Khor Fakkan - Dibba	1.6	0.517	2.118	0.527	2.128	0.538	2.139	0.55	2.151
28	E99.1	Khor Fakkan - Dibba	1.6	0.534	2.135	0.545	2.146	0.556	2.157	0.568	2.169
28	E99.1	Khor Fakkan - Dibba	1.6	0.508	2.109	0.519	2.12	0.53	2.131	0.542	2.143
28	E99.1	Khor Fakkan - Dibba	1.6	0.589	2.19	0.6	2.201	0.611	2.212	0.623	2.224
28	E99.1	Khor Fakkan - Dibba	1.6	0.588	2.189	0.599	2.2	0.61	2.211	0.622	2.223
29	E99.2	Fujairah - Khor Fakkan	1.33	0.467	1.801	0.477	1.811	0.488	1.822	0.5	1.834
29	E99.2	Fujairah - Khor Fakkan	1.33	0.558	1.892	0.568	1.902	0.579	1.913	0.591	1.925
29	E99.2	Fujairah - Khor Fakkan	1.33	0.478	1.812	0.488	1.822	0.499	1.833	0.511	1.845
29	E99.2	Fujairah - Khor Fakkan	1.33	0.489	1.823	0.499	1.834	0.51	1.845	0.522	1.856
30	E99.3	Fujairah - Oman	1.61	0.576	2.186	0.586	2.196	0.597	2.207	0.608	2.218

Building the Transition Probability Matrix for 2020

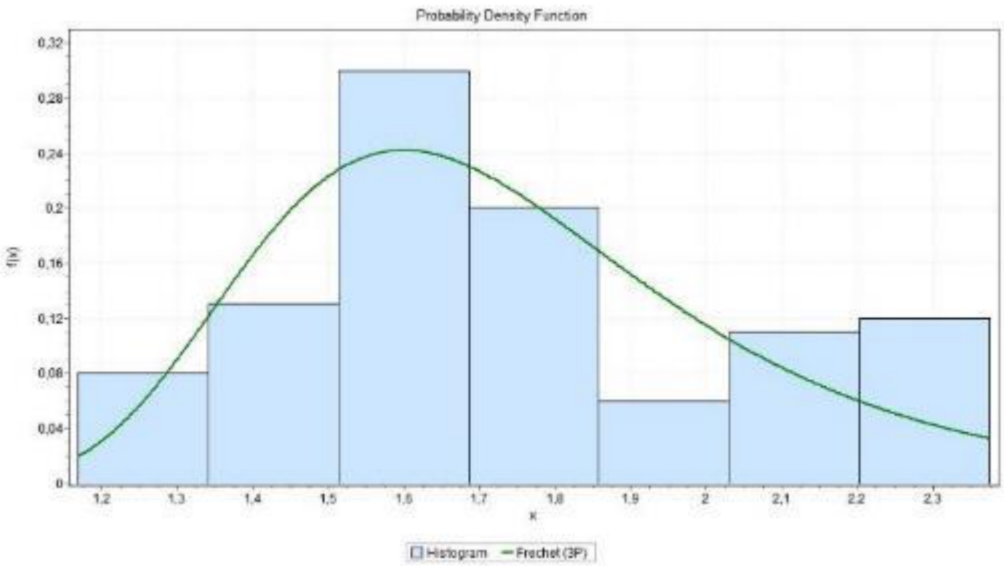

Figure 15-1: Probability of pavement condition for change in IRI based on 2020 obtained results from the modified HDM-4 model

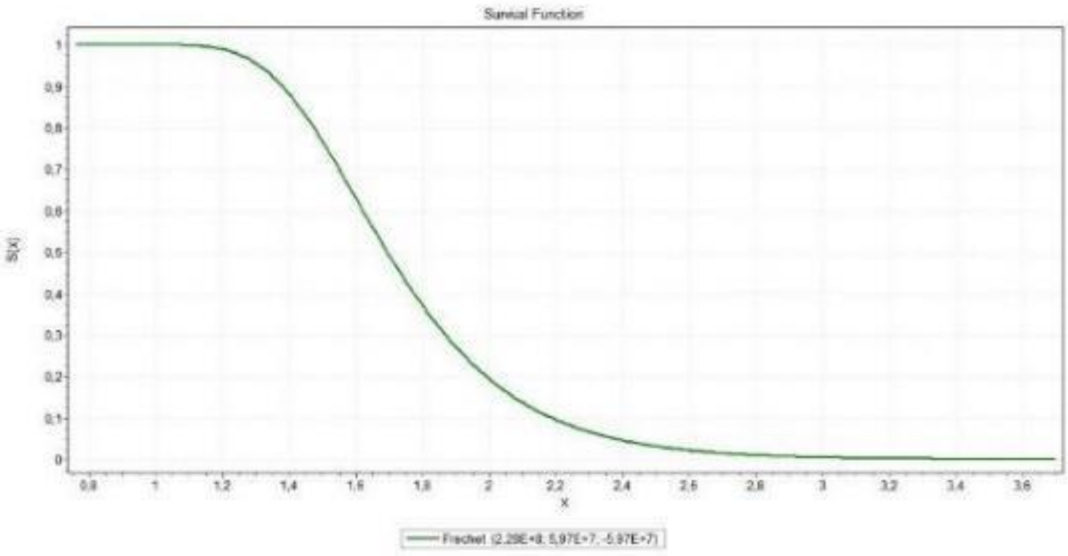

Figure 15-2: Survival curve for Change in IRI based on 2020 obtained results from the modified HDM-4 model

Building the Transition Probability Matrix for 2040

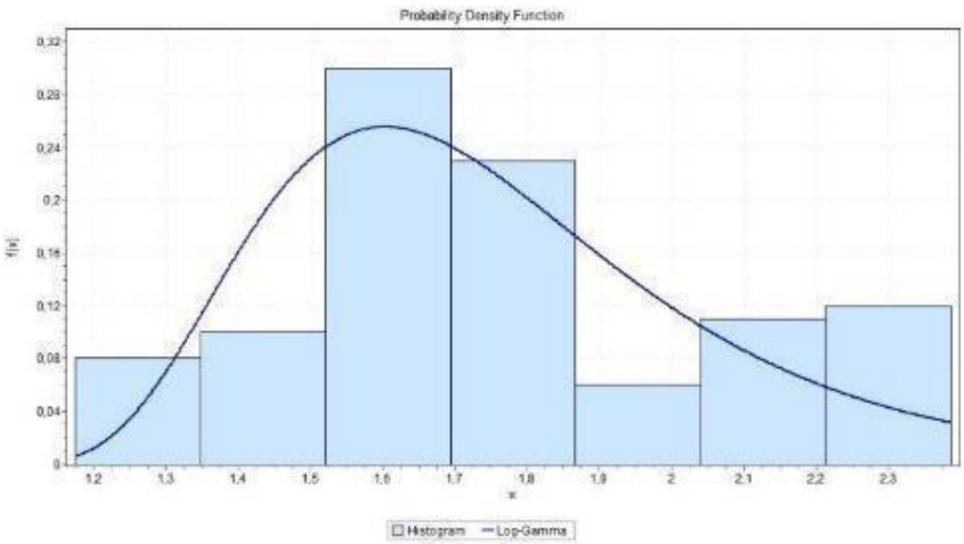

Figure 15-3: Probability of pavement condition for change in IRI based on 2040 obtained results from the modified HDM-4 model

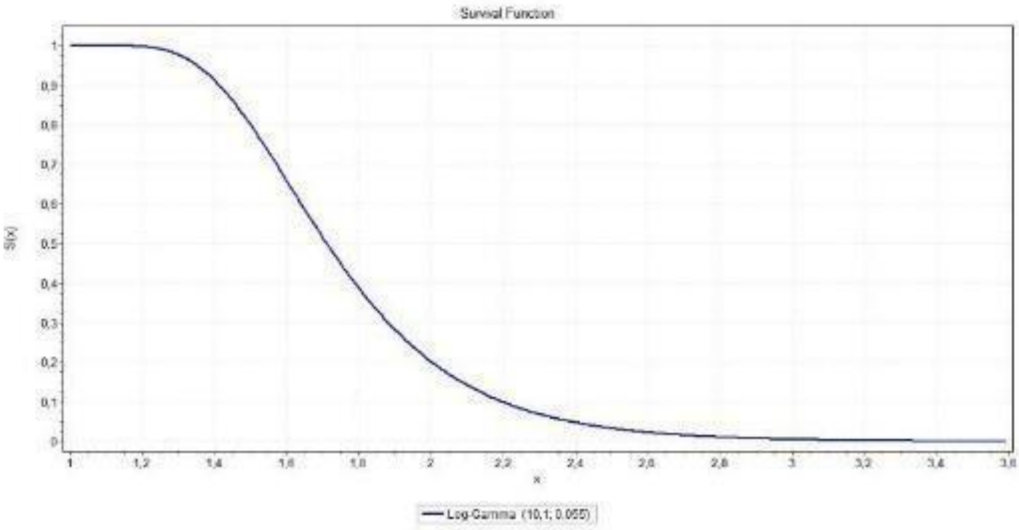

Figure 15-4: Survival curve for change in IRI based on 2040 obtained results from the modified HDM-4 model

Building the Transition Probability Matrix for 2060

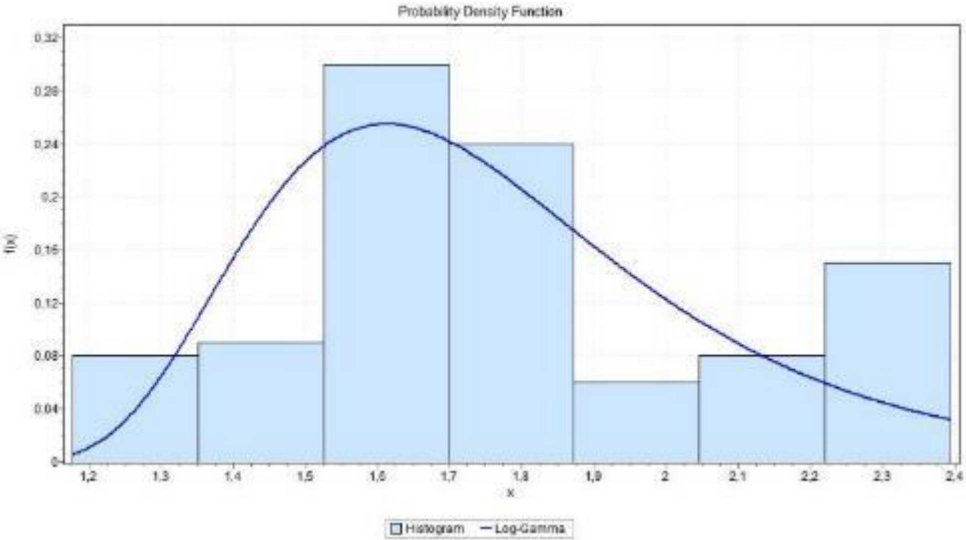

Figure 15-5: Probability of pavement condition for change in IRI based on 2060 obtained results from the modified HDM-4 model

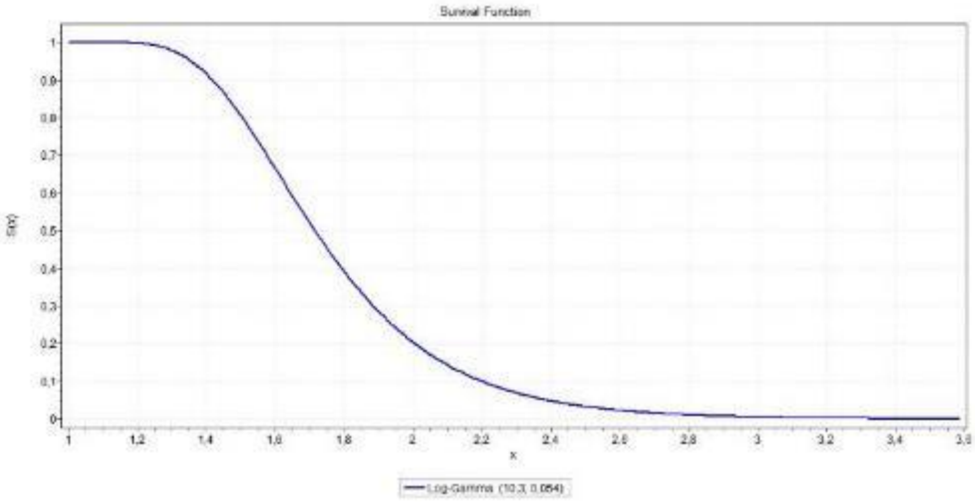

Figure 15-6: Survival curve for change in IRI based on 2060 obtained results from the modified HDM-4 model

International Roughness Index (IRI) 2013 based on Markov Chain Model for 30-year cycle

Table 15-4: International roughness index (IRI) 2013 based on Markov chain model for 30-year cycle

Years /cycle	State 1	State 2	State 3	State 4	State 5	IRI
0	1	0	0	0	0	0.9000
1	0.8700	0.1300	0.0000	0.0000	0.0000	0.9585
2	0.7569	0.2158	0.0273	0.0000	0.0000	1.0162
3	0.6585	0.2689	0.0584	0.0142	0.0000	1.0747
4	0.5729	0.2980	0.0845	0.0332	0.0114	1.1385
5	0.4984	0.3099	0.1031	0.0506	0.0379	1.2084
6	0.4336	0.3096	0.1146	0.0638	0.0784	1.2828
7	0.3773	0.3010	0.1200	0.0723	0.1294	1.3593
8	0.3282	0.2868	0.1208	0.0769	0.1873	1.4357
9	0.2855	0.2693	0.1182	0.0782	0.2488	1.5102
10	0.2484	0.2498	0.1133	0.0771	0.3113	1.5814
11	0.2161	0.2297	0.1068	0.0743	0.3730	1.6486
12	0.1880	0.2095	0.0995	0.0704	0.4325	1.7112
13	0.1636	0.1900	0.0918	0.0658	0.4888	1.7689
14	0.1423	0.1713	0.0839	0.0609	0.5415	1.8217
15	0.1238	0.1539	0.0763	0.0558	0.5902	1.8697
16	0.1077	0.1376	0.0689	0.0508	0.6349	1.9130
17	0.0937	0.1227	0.0620	0.0460	0.6755	1.9520
18	0.0815	0.1092	0.0555	0.0414	0.7123	1.9869

19	0.0709	0.0968	0.0496	0.0372	0.7455	2.0181
20	0.0617	0.0857	0.0441	0.0332	0.7752	2.0459
21	0.0537	0.0757	0.0392	0.0296	0.8018	2.0706
22	0.0467	0.0668	0.0347	0.0263	0.8255	2.0924
23	0.0406	0.0589	0.0307	0.0233	0.8465	2.1117
24	0.0354	0.0518	0.0271	0.0206	0.8651	2.1288
25	0.0308	0.0455	0.0239	0.0182	0.8816	2.1438
26	0.0268	0.0399	0.0210	0.0161	0.8962	2.1570
27	0.0233	0.0350	0.0185	0.0141	0.9091	2.1687
28	0.0203	0.0307	0.0162	0.0124	0.9204	2.1789
29	0.0176	0.0269	0.0142	0.0109	0.9303	2.1878
30	0.0153	0.0235	0.0125	0.0096	0.9391	2.1957

International Roughness Index (IRI) 2020 based on Markov Chain Model for 30-year cycle

Table 15-5: International roughness index (IRI) 2020 based on Markov chain model for 30-year cycle

Years/ cycle	State 1	State 2	State 3	State 4	State 5	IRI
0	1	0	0	0	0	0.9000
1	0.8400	0.1600	0.0000	0.0000	0.0000	0.9720
2	0.7056	0.2560	0.0384	0.0000	0.0000	1.0421
3	0.5927	0.3075	0.0787	0.0211	0.0000	1.1125
4	0.4979	0.3285	0.1092	0.0475	0.0169	1.1899
5	0.4182	0.3293	0.1280	0.0696	0.0549	1.2745
6	0.3513	0.3172	0.1366	0.0843	0.1106	1.3635
7	0.2951	0.2973	0.1376	0.0920	0.1780	1.4532
8	0.2479	0.2731	0.1333	0.0941	0.2516	1.5406
9	0.2082	0.2473	0.1255	0.0921	0.3269	1.6233
10	0.1749	0.2212	0.1158	0.0875	0.4006	1.7001
11	0.1469	0.1961	0.1052	0.0812	0.4706	1.7702
12	0.1234	0.1726	0.0944	0.0741	0.5355	1.8334
13	0.1037	0.1509	0.0839	0.0667	0.5948	1.8897
14	0.0871	0.1313	0.0740	0.0595	0.6482	1.9395
15	0.0731	0.1137	0.0648	0.0526	0.6958	1.9832
16	0.0614	0.0981	0.0564	0.0461	0.7379	2.0213
17	0.0516	0.0844	0.0489	0.0403	0.7748	2.0544
18	0.0434	0.0724	0.0423	0.0350	0.8070	2.0831
19	0.0364	0.0620	0.0364	0.0302	0.8350	2.1078

20	0.0306	0.0529	0.0313	0.0261	0.8592	2.1290
21	0.0257	0.0451	0.0268	0.0224	0.8800	2.1472
22	0.0216	0.0384	0.0229	0.0192	0.8980	2.1628
23	0.0181	0.0326	0.0195	0.0164	0.9133	2.1761
24	0.0152	0.0277	0.0166	0.0140	0.9264	2.1874
25	0.0128	0.0235	0.0141	0.0119	0.9377	2.1970
26	0.0107	0.0199	0.0120	0.0102	0.9472	2.2052
27	0.0090	0.0168	0.0102	0.0086	0.9553	2.2122
28	0.0076	0.0142	0.0086	0.0073	0.9622	2.2180
29	0.0064	0.0120	0.0073	0.0062	0.9681	2.2230
30	0.0054	0.0102	0.0062	0.0053	0.9731	2.2272

International Roughness Index (IRI) 2040 based on Markov Chain Model for 30-year cycle

Table 15-6: International roughness index (IRI) 2040 based on Markov chain approach for 30 years

Years /cycle	state 1	state 2	state 3	state 4	state 5	IRI
0	1	0	0	0	0	0.90000
1	0.83000	0.17000	0.00000	0.00000	0.00000	0.97650
2	0.68890	0.26860	0.04250	0.00000	0.00000	1.05062
3	0.57179	0.31856	0.08585	0.02380	0.00000	1.12487
4	0.47458	0.33613	0.11741	0.05260	0.01928	1.20681
5	0.39390	0.33277	0.13569	0.07575	0.06188	1.29645
6	0.32694	0.31654	0.14290	0.09038	0.12324	1.39019
7	0.27136	0.29299	0.14201	0.09720	0.19644	1.48393
8	0.22523	0.26587	0.13573	0.09799	0.27517	1.57433
9	0.18694	0.23769	0.12619	0.09463	0.35455	1.65910
10	0.15516	0.21005	0.11495	0.08865	0.43120	1.73688
11	0.12878	0.18391	0.10309	0.08121	0.50300	1.80707
12	0.10689	0.15983	0.09134	0.07316	0.56878	1.86956
13	0.08872	0.13804	0.08015	0.06505	0.62804	1.92462
14	0.07364	0.11861	0.06977	0.05724	0.68073	1.97273
15	0.06112	0.10148	0.06035	0.04995	0.72710	2.01445
16	0.05073	0.08650	0.05193	0.04329	0.76756	2.05044
17	0.04210	0.07350	0.04447	0.03730	0.80262	2.08132
18	0.03495	0.06228	0.03794	0.03199	0.83284	2.10771
19	0.02901	0.05265	0.03227	0.02733	0.85875	2.13019
20	0.02407	0.04442	0.02736	0.02326	0.88089	2.14927
21	0.01998	0.03741	0.02314	0.01974	0.89973	2.16543

22	0.01659	0.03145	0.01953	0.01671	0.91572	2.17908
23	0.01377	0.02641	0.01646	0.01411	0.92925	2.19060
24	0.01143	0.02215	0.01384	0.01190	0.94068	2.20029
25	0.00948	0.01855	0.01163	0.01001	0.95032	2.20844
26	0.00787	0.01553	0.00975	0.00841	0.95843	2.21527
27	0.00653	0.01298	0.00817	0.00706	0.96525	2.22101
28	0.00542	0.01085	0.00684	0.00592	0.97097	2.22581
29	0.00450	0.00906	0.00572	0.00496	0.97576	2.22982
30	0.00374	0.00756	0.00478	0.00415	0.97978	2.23318

International Roughness Index (IRI) 2060 based on Markov Chain model for 30-year cycle

Table 15-7 : International roughness index (IRI) 2060 based on Markov chain approach for 30 years

Years/ cycle	state 1	state 2	state 3	state 4	state 5	IRI
0	1	0	0	0	0	0.900
1	0.82000	0.18000	0.00000	0.00000	0.00000	0.98100
2	0.67240	0.27720	0.05040	0.00000	0.00000	1.06002
3	0.55137	0.32062	0.09878	0.02923	0.00000	1.13973
4	0.45212	0.33009	0.13126	0.06285	0.02368	1.22895
5	0.37074	0.31905	0.14756	0.08807	0.07459	1.32682
6	0.30401	0.29645	0.15131	0.10232	0.14592	1.42840
7	0.24929	0.26816	0.14655	0.10720	0.22880	1.52862
8	0.20441	0.23795	0.13664	0.10537	0.31563	1.62366
9	0.16762	0.20812	0.12401	0.09927	0.40098	1.71113
10	0.13745	0.18002	0.11036	0.09079	0.48139	1.78984
11	0.11271	0.15435	0.09676	0.08126	0.55493	1.85947
12	0.09242	0.13142	0.08386	0.07156	0.62075	1.92025
13	0.07578	0.11126	0.07202	0.06223	0.67871	1.97274
14	0.06214	0.09375	0.06140	0.05359	0.72912	2.01771
15	0.05096	0.07868	0.05204	0.04579	0.77253	2.05596
16	0.04179	0.06582	0.04389	0.03888	0.80962	2.08832
17	0.03426	0.05492	0.03686	0.03284	0.84112	2.11558
18	0.02810	0.04571	0.03086	0.02762	0.86772	2.13845
19	0.02304	0.03797	0.02576	0.02315	0.89009	2.15757
20	0.01889	0.03148	0.02145	0.01934	0.90884	2.17352
21	0.01549	0.02607	0.01782	0.01611	0.92450	2.18679
22	0.01270	0.02156	0.01478	0.01340	0.93756	2.19781
23	0.01042	0.01781	0.01225	0.01112	0.94841	2.20695
24	0.00854	0.01470	0.01013	0.00922	0.95742	2.21451

25	0.00700	0.01212	0.00837	0.00763	0.96488	2.22077
26	0.00574	0.00999	0.00691	0.00630	0.97106	2.22593
27	0.00471	0.00822	0.00570	0.00520	0.97616	2.23020
28	0.00386	0.00677	0.00470	0.00429	0.98038	2.23371
29	0.00317	0.00557	0.00387	0.00354	0.98386	2.23661
30	0.00260	0.00458	0.00318	0.00292	0.98672	2.23899

Deterioration curves

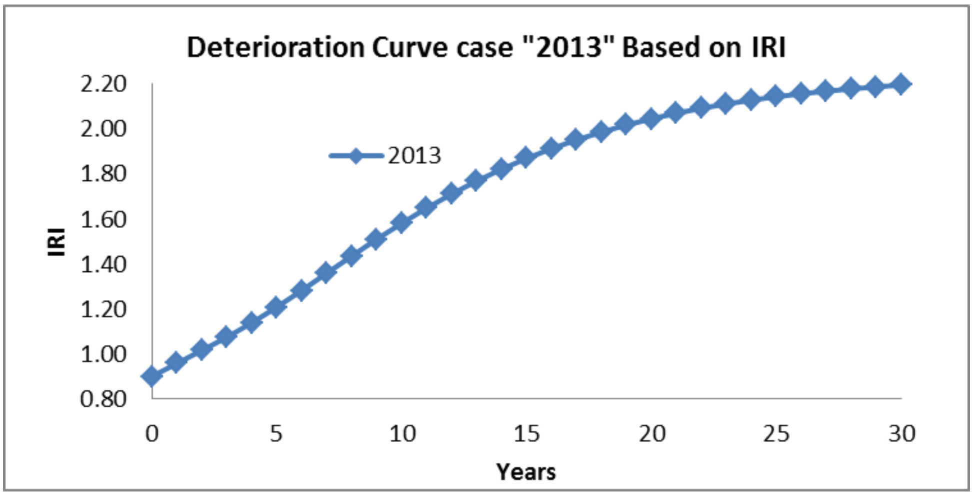

Figure 15-7: Deterioration curve case "2013 scenario" Based on IRI

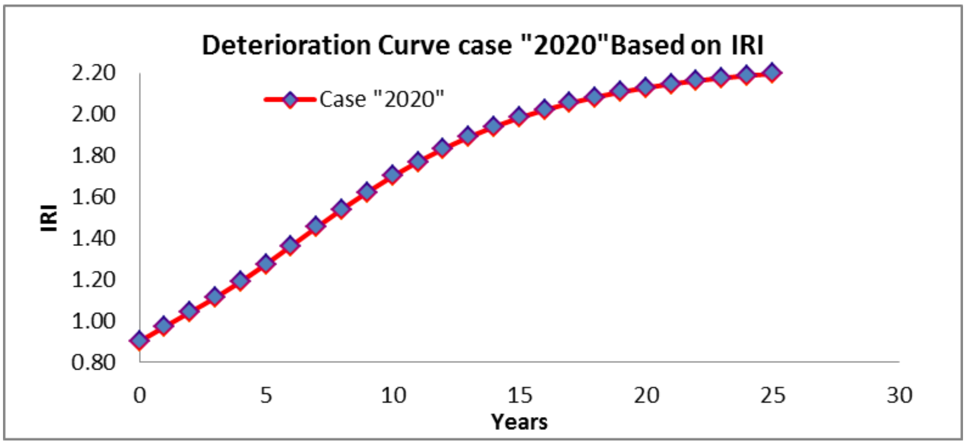

Figure 15-8: Deterioration curve case "2020 scenario" Based on IRI

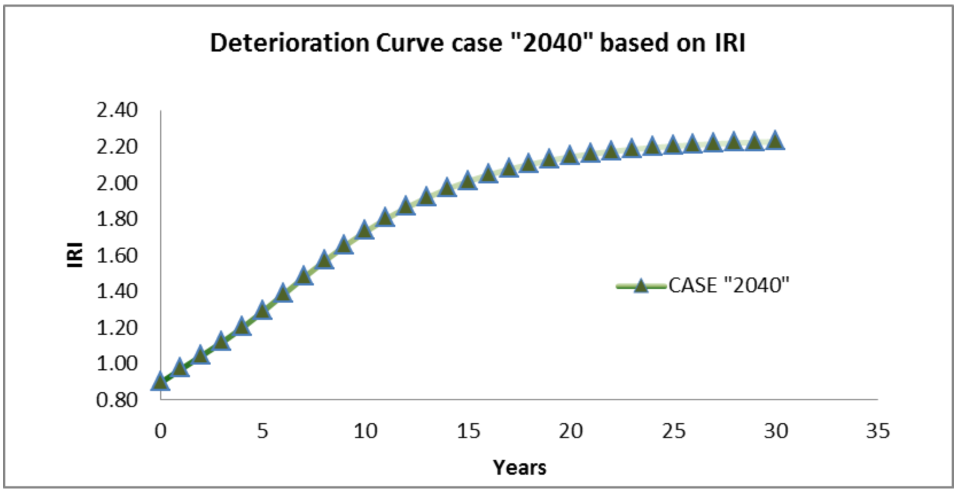

Figure 15-9: Deterioration curve case "2040 scenario" Based on IRI

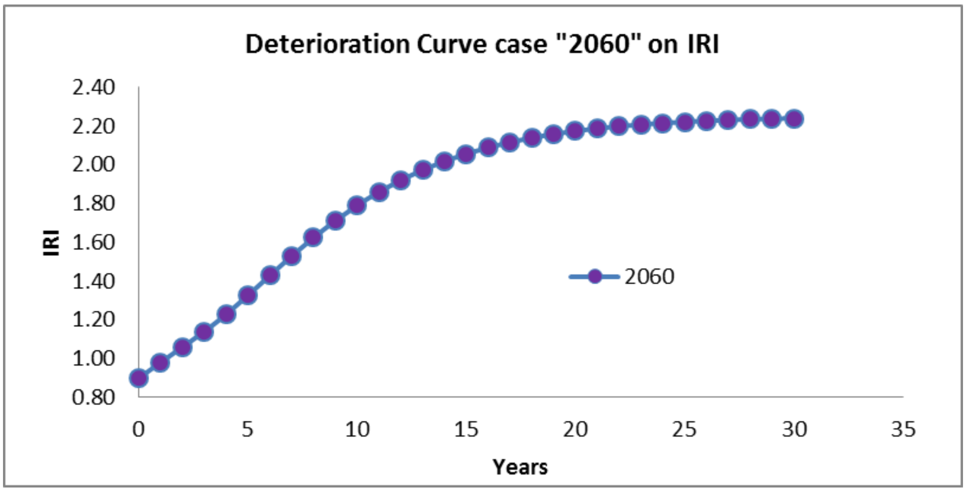

Figure 15-10: Deterioration curve case "2060 scenario" based on IRI

Output results for 20 years -Markov chain 2013

Table 15-8: Model output results for 30 years based on 2013 scenarios

vector (1)
0.87
0.13
0
0
0

Output (1-step) transition matrix					
	1	**2**	**3**	**4**	**5**
1	0.87	0.13	0	0	0
2	0	0.79	0.21	0	0
3	0	0	0.48	0.52	0
4	0	0	0	0.2	0.8
5	0	0	0	0	1

2
0.7569
0.2158
0.0273
0
0

Output (2-step) transition matrix					
	1	**2**	**3**	**4**	**5**
1	0.7569	0.2158	0.0273	0	0
2	0	0.6241	0.2667	0.1092	0
3	0	0	0.2304	0.3536	0.416
4	0	0	0	0.04	0.96
5	0	0	0	0	1

3
0.658503
0.268879
0.058422
0.014196
0

Output (3-step) transition matrix					
	1	**2**	**3**	**4**	**5**
1	0.658503	0.268879	0.058422	0.014196	0
2	0	0.493039	0.259077	0.160524	0.08736
3	0	0	0.110592	0.190528	0.69888
4	0	0	0	0.008	0.992
5	0	0	0	0	1

4
0.572898
0.29802
0.084507
0.033219
0.011357

Output (4-step) transition matrix					
	1	**2**	**3**	**4**	**5**
1	0.572898	0.29802	0.084507	0.033219	0.011357
2	0	0.389501	0.227895	0.166825	0.215779
3	0	0	0.053084	0.095613	0.851302
4	0	0	0	0.0016	0.9984
5	0	0	0	0	1

5
0.498421
0.309912
0.103148

Output (5-step) transition matrix					
	1	**2**	**3**	**4**	**5**
1	0.498421	0.309912	0.103148	0.050587	0.037932
2	0	0.307706	0.191185	0.15187	0.349239
3	0	0	0.02548	0.046726	0.927793

		1	2	3	4	5
0.050587	4	0	0	0	0.00032	0.99968
0.037932	5	0	0	0	0	1

6	Output (6-step) transition matrix					
		1	2	3	4	5
0.433626	1	0.433626	0.309625	0.114592	0.063754	0.078402
0.309625	2	0	0.243087	0.156387	0.12979	0.470735
0.114592	3	0	0	0.012231	0.022595	0.965174
0.063754	4	0	0	0	6.4E-05	0.999936
0.078402	5	0	0	0	0	1

7	Output (7-step) transition matrix					
		1	2	3	4	5
0.377255	1	0.377255	0.300976	0.120026	0.072339	0.129405
0.300976	2	0	0.192039	0.126114	0.107279	0.574568
0.120026	3	0	0	0.005871	0.010879	0.98325
0.072339	4	0	0	0	1.28E-05	0.999987
0.129405	5	0	0	0	0	1

8	Output (8-step) transition matrix					
		1	2	3	4	5
0.328212	1	0.328212	0.286814	0.120817	0.076881	0.187276
0.286814	2	0	0.151711	0.100863	0.087035	0.660391
0.120817	3	0	0	0.002818	0.005229	0.991953
0.076881	4	0	0	0	2.56E-06	0.999997
0.187276	5	0	0	0	0	1

9	Output (9-step) transition matrix					
		1	2	3	4	5
0.285544	1	0.285544	0.26925	0.118223	0.078201	0.248781
0.26925	2	0	0.119852	0.080274	0.069856	0.730019
0.118223	3	0	0	0.001353	0.002511	0.996136
0.078201	4	0	0	0	5.12E-07	1
0.248781	5	0	0	0	0	1

10	Output (10-step) transition matrix					
		1	2	3	4	5
0.248423	1	0.248423	0.249829	0.11329	0.077116	0.311342
0.249829	2	0	0.094683	0.0637	0.055713	0.785904
0.11329	3	0	0	0.000649	0.001206	0.998145

0.077116	4	0	0	0	1.02E-07	1
0.311342	5	0	0	0	0	1

11	Output (11-step) transition matrix					
		1	2	3	4	5
0.216128	1	0.216128	0.22966	0.106843	0.074334	0.373035
0.22966	2	0	0.074799	0.050459	0.044267	0.830474
0.106843	3	0	0	0.000312	0.000579	0.99911
0.074334	4	0	0	0	2.05E-08	1
0.373035	5	0	0	0	0	1

12	Output (12-step) transition matrix					
		1	2	3	4	5
0.188032	1	0.188032	0.209528	0.099513	0.070425	0.432502
0.209528	2	0	0.059092	0.039928	0.035092	0.865888
0.099513	3	0	0	0.00015	0.000278	0.999573
0.070425	4	0	0	0	4.1E-09	1
0.432502	5	0	0	0	0	1

13	Output (13-step) transition matrix					
		1	2	3	4	5
0.163588	1	0.163588	0.189971	0.091767	0.065832	0.488842
0.189971	2	0	0.046682	0.031575	0.027781	0.893962
0.091767	3	0	0	7.18E-05	0.000133	0.999795
0.065832	4	0	0	0	8.19E-10	1
0.488842	5	0	0	0	0	1

14	Output (14-step) transition matrix					
		1	2	3	4	5
0.142321	1	0.142321	0.171344	0.083942	0.060885	0.541508
0.171344	2	0	0.036879	0.024959	0.021975	0.916187
0.083942	3	0	0	3.45E-05	6.4E-05	0.999902
0.060885	4	0	0	0	1.64E-10	1
0.541508	5	0	0	0	0	1

15	Output (15-step) transition matrix					
		1	2	3	4	5
0.123819	1	0.123819	0.153863	0.076274	0.055827	0.590216
0.153863	2	0	0.029134	0.019725	0.017374	0.933767
0.076274	3	0	0	1.65E-05	3.07E-05	0.999953
0.055827	4	0	0	0	3.28E-11	1

0.590216	5	0	0	0	0	1

16	Output (16-step) transition matrix					
		1	2	3	4	5
0.107723	1	0.107723	0.137648	0.068923	0.050828	0.634878
0.137648	2	0	0.023016	0.015586	0.013732	0.947666
0.068923	3	0	0	7.94E-06	1.47E-05	0.999977
0.050828	4	0	0	0	6.55E-12	1
0.634878	5	0	0	0	0	1

17	Output (17-step) transition matrix					
		1	2	3	4	5
0.093719	1	0.093719	0.122746	0.061989	0.046006	0.67554
0.122746	2	0	0.018183	0.012315	0.010851	0.958651
0.061989	3	0	0	3.81E-06	7.08E-06	0.999989
0.046006	4	0	0	0	1.31E-12	1
0.67554	5	0	0	0	0	1

18	Output (18-step) transition matrix					
		1	2	3	4	5
0.081535	1	0.081535	0.109153	0.055532	0.041435	0.712345
0.109153	2	0	0.014364	0.009729	0.008574	0.967332
0.055532	3	0	0	1.83E-06	3.4E-06	0.999995
0.041435	4	0	0	0	2.62E-13	1
0.712345	5	0	0	0	0	1

19	Output (19-step) transition matrix					
		1	2	3	4	5
0.070936	1	0.070936	0.09683	0.049577	0.037163	0.745493
0.09683	2	0	0.011348	0.007687	0.006774	0.974191
0.049577	3	0	0	8.78E-07	1.63E-06	0.999997
0.037163	4	0	0	0	5.24E-14	1
0.745493	5	0	0	0	0	1

20	Output (20-step) transition matrix					
		1	2	3	4	5
0.061714	1	0.061714	0.085718	0.044131	0.033213	0.775224
0.085718	2	0	0.008965	0.006073	0.005352	0.979611
0.044131	3	0	0	4.22E-07	7.83E-07	0.999999

		1	2	3	4	5
0.033213	4	0	0	0	1.05E-14	1
0.775224	5	0	0	0	0	1

21	Output (21-step) transition matrix					
		1	2	3	4	5
0.053691	1	0.053691	0.07574	0.039184	0.029591	0.801794
0.07574	2	0	0.007082	0.004797	0.004228	0.983892
0.039184	3	0	0	2.02E-07	3.76E-07	0.999999
0.029591	4	0	0	0	2.1E-15	1
0.801794	5	0	0	0	0	1

22	Output (22-step) transition matrix					
		1	2	3	4	5
0.046711	1	0.046711	0.066814	0.034714	0.026294	0.825467
0.066814	2	0	0.005595	0.00379	0.00334	0.987275
0.034714	3	0	0	9.71E-08	1.8E-07	1
0.026294	4	0	0	0	4.19E-16	1
0.825467	5	0	0	0	0	1

23	Output (23-step) transition matrix					
		1	2	3	4	5
0.040639	1	0.040639	0.058856	0.030694	0.02331	0.846502
0.058856	2	0	0.00442	0.002994	0.002639	0.989947
0.030694	3	0	0	4.66E-08	8.66E-08	1
0.02331	4	0	0	0	8.39E-17	1
0.846502	5	0	0	0	0	1

24	Output (24-step) transition matrix					
		1	2	3	4	5
0.035356	1	0.035356	0.051779	0.027093	0.020623	0.86515
0.051779	2	0	0.003492	0.002365	0.002085	0.992058
0.027093	3	0	0	2.24E-08	4.16E-08	1
0.020623	4	0	0	0	1.68E-17	1
0.86515	5	0	0	0	0	1

25	Output (25-step) transition matrix					
		1	2	3	4	5
0.03076	1	0.03076	0.045502	0.023878	0.018213	0.881648
0.045502	2	0	0.002759	0.001869	0.001647	0.993726
0.023878	3	0	0	1.07E-08	1.99E-08	1
0.018213	4	0	0	0	3.36E-18	1

0.881648

5	0	0	0	0	1

26

0.026761
0.039945
0.021017
0.016059
0.896218

Output (26-step) transition matrix					
	1	**2**	**3**	**4**	**5**
1	0.026761	0.039945	0.021017	0.016059	0.896218
2	0	0.002179	0.001476	0.001301	0.995043
3	0	0	5.16E-09	9.57E-09	1
4	0	0	0	6.71E-19	1
5	0	0	0	0	1

27

0.023282
0.035036
0.018477
0.014141
0.909065

Output (27-step) transition matrix					
	1	**2**	**3**	**4**	**5**
1	0.023282	0.035036	0.018477	0.014141	0.909065
2	0	0.001722	0.001166	0.001028	0.996084
3	0	0	2.47E-09	4.6E-09	1
4	0	0	0	1.34E-19	1
5	0	0	0	0	1

28

0.020255
0.030705
0.016226
0.012436
0.920378

Output (28-step) transition matrix					
	1	**2**	**3**	**4**	**5**
1	0.020255	0.030705	0.016226	0.012436	0.920378
2	0	0.00136	0.000921	0.000812	0.996907
3	0	0	1.19E-09	2.21E-09	1
4	0	0	0	2.68E-20	1
5	0	0	0	0	1

29

0.017622
0.02689
0.014237
0.010925
0.930326

Output (29-step) transition matrix					
	1	**2**	**3**	**4**	**5**
1	0.017622	0.02689	0.014237	0.010925	0.930326
2	0	0.001074	0.000728	0.000641	0.997556
3	0	0	5.7E-10	1.06E-09	1
4	0	0	0	5.37E-21	1
5	0	0	0	0	1

30

0.015331
0.023534
0.01248
0.009588
0.939066

Output (30-step) transition matrix					
	1	**2**	**3**	**4**	**5**
1	0.015331	0.023534	0.01248	0.009588	0.939066
2	0	0.000849	0.000575	0.000507	0.998069
3	0	0	2.74E-10	5.08E-10	1
4	0	0	0	1.07E-21	1
5	0	0	0	0	1

Output Results for 20 years -Markov Chain 2020

Table 15-9: Model output results for 30 years based on 2020 scenarios

vector (1)		Output (1-step) transition matrix				
		1	2	3	4	5
0.84	1	0.84	0.16	0	0	0
0.16	2	0	0.76	0.24	0	0
0	3	0	0	0.45	0.55	0
0	4	0	0	0	0.2	0.8
0	5	0	0	0	0	1

2		Output (2-step) transition matrix				
		1	2	3	4	5
0.7056	1	0.7056	0.256	0.0384	0	0
0.256	2	0	0.5776	0.2904	0.132	0
0.0384	3	0	0	0.2025	0.3575	0.44
0	4	0	0	0	0.04	0.96
0	5	0	0	0	0	1

3		Output (3-step) transition matrix				
		1	2	3	4	5
0.5927039	1	0.592704	0.307456	0.07872	0.02112	0
0.307456	2	0	0.438976	0.269304	0.18612	0.1056
0.07872	3	0	0	0.091125	0.182875	0.726
0.02112	4	0	0	0	0.008	0.992
0	5	0	0	0	0	1

4		Output (4-step) transition matrix				
		1	2	3	4	5
0.4978713	1	0.497871	0.328499	0.109213	0.04752	0.016896
0.3284992	2	0	0.333622	0.226541	0.185341	0.254496
0.1092134	3	0	0	0.041006	0.086694	0.8723
0.04752	4	0	0	0	0.0016	0.9984
0.016896	5	0	0	0	0	1

5		Output (5-step) transition matrix				
		1	2	3	4	5

		1	2	3	4	5
0.4182118	1	0.418212	0.329319	0.127986	0.069571	0.054912
0.3293188	2	0	0.253553	0.182013	0.161666	0.402769
0.1279858	3	0	0	0.018453	0.039892	0.941655
0.0695714	4	0	0	0	0.00032	0.99968
0.054912	5	0	0	0	0	1

6	Output (6-step) transition matrix					
		1	2	3	4	5
0.3512979	1	0.351298	0.317196	0.13663	0.084306	0.110569
0.3171962	2	0	0.1927	0.142758	0.13244	0.532102
0.1366301	3	0	0	0.008304	0.018127	0.973569
0.0843065	4	0	0	0	6.4E-05	0.999936
0.1105691	5	0	0	0	0	1

7	Output (7-step) transition matrix					
		1	2	3	4	5
0.2950903	1	0.29509	0.297277	0.137611	0.092008	0.178014
0.2972768	2	0	0.146452	0.110489	0.105005	0.638054
0.1376106	3	0	0	0.003737	0.008193	0.988071
0.0920079	4	0	0	0	1.28E-05	0.999987
0.1780143	5	0	0	0	0	1

8	Output (8-step) transition matrix					
		1	2	3	4	5
0.2478758	1	0.247876	0.273145	0.133271	0.094087	0.251621
0.2731448	2	0	0.111303	0.084869	0.08177	0.722058
0.1332712	3	0	0	0.001682	0.003694	0.994625
0.0940874	4	0	0	0	2.56E-06	0.999997
0.2516206	5	0	0	0	0	1

9	Output (9-step) transition matrix					
		1	2	3	4	5
0.2082157	1	0.208216	0.24725	0.125527	0.092117	0.326891
0.2472502	2	0	0.084591	0.064904	0.063032	0.787474
0.1255268	3	0	0	0.000757	0.001664	0.99758
0.0921167	4	0	0	0	5.12E-07	1
0.3268906	5	0	0	0	0	1

10	Output (10-step) transition matrix					
		1	2	3	4	5

0.1749012
0.2212246
0.1158271
0.0874631
0.4005839

1	0.174901	0.221225	0.115827	0.087463	0.400584
2	0	0.064289	0.049508	0.048303	0.837899
3	0	0	0.000341	0.000749	0.998911
4	0	0	0	1.02E-07	1
5	0	0	0	0	1

11

0.146917
0.1961149
0.1052161
0.0811975
0.4705543

Output (11-step) transition matrix

	1	**2**	**3**	**4**	**5**
1	0.146917	0.196115	0.105216	0.081198	0.470554
2	0	0.04886	0.037708	0.03689	0.876542
3	0	0	0.000153	0.000337	0.99951
4	0	0	0	2.05E-08	1
5	0	0	0	0	1

12

0.1234103
0.172554
0.0944148
0.0741084
0.5355123

Output (12-step) transition matrix

	1	**2**	**3**	**4**	**5**
1	0.12341	0.172554	0.094415	0.074108	0.535512
2	0	0.037133	0.028695	0.028118	0.906054
3	0	0	6.9E-05	0.000152	0.999779
4	0	0	0	4.1E-09	1
5	0	0	0	0	1

13

0.1036646
0.1508867
0.0838996
0.0667498
0.594799

Output (13-step) transition matrix

	1	**2**	**3**	**4**	**5**
1	0.103665	0.150887	0.0839	0.06675	0.594799
2	0	0.028221	0.021825	0.021406	0.928548
3	0	0	3.1E-05	6.83E-05	0.999901
4	0	0	0	8.19E-10	1
5	0	0	0	0	1

14

0.0870783
0.1312602
0.0739676
0.0594948
0.6481989

Output (14-step) transition matrix

	1	**2**	**3**	**4**	**5**
1	0.087078	0.13126	0.073968	0.059495	0.648199
2	0	0.021448	0.016594	0.016285	0.945673
3	0	0	1.4E-05	3.07E-05	0.999955
4	0	0	0	1.64E-10	1
5	0	0	0	0	1

15

Output (15-step) transition matrix

	1	**2**	**3**	**4**	**5**

			1	2	3	4	5
0.0731457		1	0.073146	0.11369	0.064788	0.052581	0.695795
0.1136903		2	0	0.016301	0.012615	0.012384	0.958701
0.0647879		3	0	0	6.28E-06	1.38E-05	0.99998
0.0525812		4	0	0	0	3.28E-11	1
0.6957947		5	0	0	0	0	1

16	Output (16-step) transition matrix					
		1	2	3	4	5
0.0614424	1	0.061442	0.098108	0.05644	0.04615	0.73786
0.098108	2	0	0.012388	0.009589	0.009415	0.968608
0.0564402	3	0	0	2.83E-06	6.22E-06	0.999991
0.0461496	4	0	0	0	6.55E-12	1
0.7378596	5	0	0	0	0	1

17	Output (17-step) transition matrix					
		1	2	3	4	5
0.0516116	1	0.051612	0.084393	0.048944	0.040272	0.774779
0.0843928	2	0	0.009415	0.007288	0.007157	0.97614
0.048944	3	0	0	1.27E-06	2.8E-06	0.999996
0.040272	4	0	0	0	1.31E-12	1
0.7747793	5	0	0	0	0	1

18	Output (18-step) transition matrix					
		1	2	3	4	5
0.0433538	1	0.043354	0.072396	0.042279	0.034974	0.806997
0.0723964	2	0	0.007156	0.005539	0.00544	0.981865
0.0422791	3	0	0	5.73E-07	1.26E-06	0.999998
0.0349736	4	0	0	0	2.62E-13	1
0.8069969	5	0	0	0	0	1

19	Output (19-step) transition matrix					
		1	2	3	4	5
0.0364172	1	0.036417	0.061958	0.036401	0.030248	0.834976
0.0619579	2	0	0.005438	0.00421	0.004135	0.986217
0.0364007	3	0	0	2.58E-07	5.67E-07	0.999999
0.0302482	4	0	0	0	5.24E-14	1
0.8349758	5	0	0	0	0	1

20	Output (20-step) transition matrix

		1	2	3	4	5
0.0305904	1	0.03059	0.052915	0.03125	0.02607	0.859174
0.0529147	2	0	0.004133	0.0032	0.003142	0.989525
0.0312502	3	0	0	1.16E-07	2.55E-07	1
0.02607	4	0	0	0	1.05E-14	1
0.8591744	5	0	0	0	0	1

Output (21-step) transition matrix

21		1	2	3	4	5
0.025696	1	0.025696	0.04511	0.026762	0.022402	0.88003
0.0451097	2	0	0.003141	0.002432	0.002388	0.992039
0.0267621	3	0	0	5.22E-08	1.15E-07	1
0.0224016	4	0	0	0	2.1E-15	1
0.8800304	5	0	0	0	0	1

Output (22-step) transition matrix

22		1	2	3	4	5
0.0215846	1	0.021585	0.038395	0.022869	0.019199	0.897952
0.0383947	2	0	0.002387	0.001848	0.001815	0.993949
0.0228693	3	0	0	2.35E-08	5.17E-08	1
0.0191995	4	0	0	0	4.19E-16	1
0.8979517	5	0	0	0	0	1

Output (23-step) transition matrix

23		1	2	3	4	5
0.0181311	1	0.018131	0.032634	0.019506	0.016418	0.913311
0.0326335	2	0	0.001814	0.001405	0.00138	0.995402
0.0195059	3	0	0	1.06E-08	2.32E-08	1
0.016418	4	0	0	0	8.39E-17	1
0.9133112	5	0	0	0	0	1

Output (24-step) transition matrix

24		1	2	3	4	5
0.0152301	1	0.01523	0.027702	0.01661	0.014012	0.926446
0.0277024	2	0	0.001379	0.001068	0.001048	0.996505
0.0166097	3	0	0	4.75E-09	1.05E-08	1
0.0140118	4	0	0	0	1.68E-17	1
0.9264457	5	0	0	0	0	1

Output (25-step) transition matrix

25		1	2	3	4	5

0.0127933	1	0.012793	0.023491	0.014123	0.011938	0.937655
0.0234907	2	0	0.001048	0.000811	0.000797	0.997344
0.0141229	3	0	0	2.14E-09	4.71E-09	1
0.0119377	4	0	0	0	3.36E-18	1
0.9376552	5	0	0	0	0	1

26	Output (26-step) transition matrix					
		1	2	3	4	5
0.0107464	1	0.010746	0.0199	0.011993	0.010155	0.947205
0.0198998	2	0	0.000796	0.000617	0.000606	0.997981
0.0119931	3	0	0	9.63E-10	2.12E-09	1
0.0101552	4	0	0	0	6.71E-19	1
0.9472054	5	0	0	0	0	1

27	Output (27-step) transition matrix					
		1	2	3	4	5
0.0090269	1	0.009027	0.016843	0.010173	0.008627	0.95533
0.0168433	2	0	0.000605	0.000469	0.00046	0.998466
0.0101728	3	0	0	4.33E-10	9.53E-10	1
0.0086272	4	0	0	0	1.34E-19	1
0.9553295	5	0	0	0	0	1

28	Output (28-step) transition matrix					
		1	2	3	4	5
0.0075826	1	0.007583	0.014245	0.00862	0.007321	0.962231
0.0142452	2	0	0.00046	0.000356	0.00035	0.998834
0.0086202	3	0	0	1.95E-10	4.29E-10	1
0.0073205	4	0	0	0	2.68E-20	1
0.9622313	5	0	0	0	0	1

29	Output (29-step) transition matrix					
		1	2	3	4	5
0.0063694	1	0.006369	0.01204	0.007298	0.006205	0.968088
0.0120396	2	0	0.00035	0.000271	0.000266	0.999114
0.0072979	3	0	0	8.77E-11	1.93E-10	1
0.0062052	4	0	0	0	5.37E-21	1
0.9680877	5	0	0	0	0	1

30	Output (30-step) transition matrix					
		1	2	3	4	5

0.0053503	1	0.00535	0.010169	0.006174	0.005255	0.973052
0.0101692	2	0	0.000266	0.000206	0.000202	0.999327
0.0061736	3	0	0	3.95E-11	8.69E-11	1
0.0052549	4	0	0	0	1.07E-21	1
0.9730519	5	0	0	0	0	1

Output Results for 20 years - Markov Chain 2040

Table 15-10: Model output results for 30 years based on 2040 scenarios

vector (1)	Output (1-step) transition matrix					
		1	**2**	**3**	**4**	**5**
0.83	**1**	0.83	0.17	0	0	0
0.17	**2**	0	0.75	0.25	0	0
0	**3**	0	0	0.44	0.56	0
0	**4**	0	0	0	0.19	0.81
0	**5**	0	0	0	0	1

2	Output (2-step) transition matrix					
		1	**2**	**3**	**4**	**5**
0.6889	**1**	0.6889	0.2686	0.0425	0	0
0.2686	**2**	0	0.5625	0.2975	0.14	0
0.0425	**3**	0	0	0.1936	0.3528	0.4536
0	**4**	0	0	0	0.0361	0.9639
0	**5**	0	0	0	0	1

3	Output (3-step) transition matrix					
		1	**2**	**3**	**4**	**5**
0.571787	**1**	0.571787	0.318563	0.08585	0.0238	0
0.318563	**2**	0	0.421875	0.271525	0.1932	0.1134
0.08585	**3**	0	0	0.085184	0.175448	0.739368
0.0238	**4**	0	0	0	0.006859	0.993141
0	**5**	0	0	0	0	1

4	Output (4-step) transition matrix					
		1	**2**	**3**	**4**	**5**
0.474583	**1**	0.474583	0.336126	0.117415	0.052598	0.019278
0.336126	**2**	0	0.316406	0.22494	0.188762	0.269892
0.117415	**3**	0	0	0.037481	0.081038	0.881481
0.052598	**4**	0	0	0	0.001303	0.998697

0.019278	5	0	0	0	0	1

5	Output (5-step) transition matrix					
		1	2	3	4	5
0.393904	1	0.393904	0.332774	0.135694	0.075746	0.061882
0.332774	2	0	0.237305	0.178075	0.161831	0.422789
0.135694	3	0	0	0.016492	0.036387	0.947122
0.075746	4	0	0	0	0.000248	0.999752
0.061882	5	0	0	0	0	1

6	Output (6-step) transition matrix					
		1	2	3	4	5
0.32694	1	0.32694	0.316544	0.142899	0.09038	0.123237
0.316544	2	0	0.177979	0.137679	0.13047	0.553872
0.142899	3	0	0	0.007256	0.016149	0.976595
0.09038	4	0	0	0	4.7E-05	0.999953
0.123237	5	0	0	0	0	1

7	Output (7-step) transition matrix					
		1	2	3	4	5
0.27136	1	0.27136	0.292988	0.142011	0.097196	0.196445
0.292988	2	0	0.133484	0.105073	0.10189	0.659553
0.142011	3	0	0	0.003193	0.007132	0.989675
0.097196	4	0	0	0	8.94E-06	0.999991
0.196445	5	0	0	0	0	1

8	Output (8-step) transition matrix					
		1	2	3	4	5
0.225229	1	0.225229	0.265872	0.135732	0.097994	0.275173
0.265872	2	0	0.100113	0.079603	0.0782	0.742084
0.135732	3	0	0	0.001405	0.003143	0.995452
0.097994	4	0	0	0	1.7E-06	0.999998
0.275173	5	0	0	0	0	1

9	Output (9-step) transition matrix					
		1	2	3	4	5
0.18694	1	0.18694	0.237693	0.12619	0.094629	0.354548
0.237693	2	0	0.075085	0.060054	0.059436	0.805426
0.12619	3	0	0	0.000618	0.001384	0.997998
0.094629	4	0	0	0	3.23E-07	1

0.354548	5	0	0	0	0	1

10	Output (10-step) transition matrix					
		1	2	3	4	5
0.15516	1	0.15516	0.21005	0.114947	0.088646	0.431197
0.21005	2	0	0.056314	0.045195	0.044923	0.853569
0.114947	3	0	0	0.000272	0.000609	0.999119
0.088646	4	0	0	0	6.13E-08	1
0.431197	5	0	0	0	0	1

11	Output (11-step) transition matrix					
		1	2	3	4	5
0.128783	1	0.128783	0.183914	0.103089	0.081213	0.503
0.183914	2	0	0.042235	0.033964	0.033844	0.889956
0.103089	3	0	0	0.00012	0.000268	0.999612
0.081213	4	0	0	0	1.16E-08	1
0.503	5	0	0	0	0	1

12	Output (12-step) transition matrix					
		1	2	3	4	5
0.10689	1	0.10689	0.159829	0.091338	0.07316	0.568783
0.159829	2	0	0.031676	0.025503	0.02545	0.91737
0.091338	3	0	0	5.27E-05	0.000118	0.999829
0.07316	4	0	0	0	2.21E-09	1
0.568783	5	0	0	0	0	1

13	Output (13-step) transition matrix					
		1	2	3	4	5
0.088719	1	0.088719	0.138043	0.080146	0.06505	0.628043
0.138043	2	0	0.023757	0.01914	0.019117	0.937985
0.080146	3	0	0	2.32E-05	5.19E-05	0.999925
0.06505	4	0	0	0	4.21E-10	1
0.628043	5	0	0	0	0	1

14	Output (14-step) transition matrix					
		1	2	3	4	5
0.073637	1	0.073637	0.118614	0.069775	0.057241	0.680733
0.118614	2	0	0.017818	0.014361	0.014351	0.95347
0.069775	3	0	0	1.02E-05	2.28E-05	0.999967
0.057241	4	0	0	0	7.99E-11	1
0.680733	5	0	0	0	0	1

15
0.061118
0.101479
0.060355
0.04995
0.727098

Output (15-step) transition matrix

	1	2	3	4	5
1	0.061118	0.101479	0.060355	0.04995	0.727098
2	0	0.013363	0.010773	0.010769	0.965094
3	0	0	4.49E-06	1E-05	0.999985
4	0	0	0	1.52E-11	1
5	0	0	0	0	1

16
0.050728
0.086499
0.051926
0.043289
0.767558

Output (16-step) transition matrix

	1	2	3	4	5
1	0.050728	0.086499	0.051926	0.043289	0.767558
2	0	0.010023	0.008081	0.008079	0.973817
3	0	0	1.97E-06	4.42E-06	0.999994
4	0	0	0	2.88E-12	1
5	0	0	0	0	1

17
0.042104
0.073498
0.044472
0.037303
0.802622

Output (17-step) transition matrix

	1	2	3	4	5
1	0.042104	0.073498	0.044472	0.037303	0.802622
2	0	0.007517	0.006061	0.00606	0.980361
3	0	0	8.68E-07	1.95E-06	0.999997
4	0	0	0	5.48E-13	1
5	0	0	0	0	1

18
0.034947
0.062282
0.037942
0.031992
0.832837

Output (18-step) transition matrix

	1	2	3	4	5
1	0.034947	0.062282	0.037942	0.031992	0.832837
2	0	0.005638	0.004546	0.004546	0.98527
3	0	0	3.82E-07	8.56E-07	0.999999
4	0	0	0	1.04E-13	1
5	0	0	0	0	1

19
0.029006
0.052652
0.032265
0.027326

Output (19-step) transition matrix

	1	2	3	4	5
1	0.029006	0.052652	0.032265	0.027326	0.858751
2	0	0.004228	0.00341	0.00341	0.988952
3	0	0	1.68E-07	3.77E-07	0.999999
4	0	0	0	1.98E-14	1

0.858751	5	0	0	0	0	1

20	Output (20-step) transition matrix					
		1	2	3	4	5
0.024075	1	0.024075	0.04442	0.02736	0.02326	0.880885
0.04442	2	0	0.003171	0.002557	0.002557	0.991714
0.02736	3	0	0	7.4E-08	1.66E-07	1
0.02326	4	0	0	0	3.76E-15	1
0.880885	5	0	0	0	0	1

21	Output (21-step) transition matrix					
		1	2	3	4	5
0.019982	1	0.019982	0.037408	0.023143	0.019741	0.899726
0.037408	2	0	0.002378	0.001918	0.001918	0.993786
0.023143	3	0	0	3.25E-08	7.29E-08	1
0.019741	4	0	0	0	7.14E-16	1
0.899726	5	0	0	0	0	1

22	Output (22-step) transition matrix					
		1	2	3	4	5
0.016585	1	0.016585	0.031453	0.019535	0.016711	0.915716
0.031453	2	0	0.001784	0.001439	0.001439	0.995339
0.019535	3	0	0	1.43E-08	3.21E-08	1
0.016711	4	0	0	0	1.36E-16	1
0.915716	5	0	0	0	0	1

23	Output (23-step) transition matrix					
		1	2	3	4	5
0.013766	1	0.013766	0.026409	0.016459	0.014115	0.929252
0.026409	2	0	0.001338	0.001079	0.001079	0.996504
0.016459	3	0	0	6.3E-09	1.41E-08	1
0.014115	4	0	0	0	2.58E-17	1
0.929252	5	0	0	0	0	1

24	Output (24-step) transition matrix					
		1	2	3	4	5
0.011425	1	0.011425	0.022147	0.013844	0.011899	0.940685
0.022147	2	0	0.001003	0.000809	0.000809	0.997378
0.013844	3	0	0	2.77E-09	6.21E-09	1
0.011899	4	0	0	0	4.9E-18	1
0.940685	5	0	0	0	0	1

25
0.009483
0.018553
0.011628
0.010013
0.950323

Output (25-step) transition matrix					
	1	2	3	4	5
1	0.009483	0.018553	0.011628	0.010013	0.950323
2	0	0.000753	0.000607	0.000607	0.998034
3	0	0	1.22E-09	2.73E-09	1
4	0	0	0	9.31E-19	1
5	0	0	0	0	1

26
0.007871
0.015527
0.009754
0.008414
0.958434

Output (26-step) transition matrix					
	1	2	3	4	5
1	0.007871	0.015527	0.009754	0.008414	0.958434
2	0	0.000564	0.000455	0.000455	0.998525
3	0	0	5.37E-10	1.2E-09	1
4	0	0	0	1.77E-19	1
5	0	0	0	0	1

27
0.006533
0.012983
0.008174
0.007061
0.965249

Output (27-step) transition matrix					
	1	2	3	4	5
1	0.006533	0.012983	0.008174	0.007061	0.965249
2	0	0.000423	0.000341	0.000341	0.998894
3	0	0	2.36E-10	5.29E-10	1
4	0	0	0	3.36E-20	1
5	0	0	0	0	1

28
0.005422
0.010848
0.006842
0.005919
0.970969

Output (28-step) transition matrix					
	1	2	3	4	5
1	0.005422	0.010848	0.006842	0.005919	0.970969
2	0	0.000317	0.000256	0.000256	0.99917
3	0	0	1.04E-10	2.33E-10	1
4	0	0	0	6.38E-21	1
5	0	0	0	0	1

29
0.004501
0.009058
0.005722
0.004956
0.975763

Output (29-step) transition matrix					
	1	2	3	4	5
1	0.004501	0.009058	0.005722	0.004956	0.975763
2	0	0.000238	0.000192	0.000192	0.999378
3	0	0	4.57E-11	1.02E-10	1
4	0	0	0	1.21E-21	1
5	0	0	0	0	1

30
0.003735
0.007558
0.004782
0.004146
0.979778

Output (30-step) transition matrix					
	1	2	3	4	5
1	0.003735	0.007558	0.004782	0.004146	0.979778
2	0	0.000179	0.000144	0.000144	0.999533
3	0	0	2.01E-11	4.51E-11	1
4	0	0	0	2.3E-22	1
5	0	0	0	0	1

Markov Chain Model for 2060 scenarios

Table 15-11: Model output results for 30 years based on 2060 scenarios

vector (1)
0.82
0.18
0
0
0

Output (1-step) transition matrix					
	1	2	3	4	5
1	0.82	0.180000007	0	0	0
2	0	0.720000029	0.280000001	0	0
3	0	0	0.419999987	0.579999983	0
4	0	0	0	0.189999998	0.81
5	0	0	0	0	1

2
0.6724
0.2772
0.0504
0
0

Output (2-step) transition matrix					
	1	2	3	4	5
1	0.6724	0.277200013	0.050400004	0	0
2	0	0.518400013	0.319200009	0.162399992	0
3	0	0	0.176399991	0.353799969	0.4698
4	0	0	0	0.0361	0.9639
5	0	0	0	0	1

3
0.551368
0.320616
0.098784
0.029232
0

Output (3-step) transition matrix					
	1	2	3	4	5
1	0.551368	0.320616007	0.098784007	0.029231999	0
2	0	0.373248011	0.279216021	0.215991989	0.131544
3	0	0	0.074087992	0.169533983	0.756378
4	0	0	0	0.006859	0.993141
5	0	0	0	0	1

4
0.452122

Output (4-step) transition matrix					
	1	2	3	4	5
1	0.452122	0.330089778	0.131261766	0.062848799	0.023678

		1	2	3	4	5
0.33009	2	0	0.268738568	0.221780181	0.202983752	0.306497
0.131262	3	0	0	0.031116955	0.07518249	0.8937
0.062849	4	0	0	0	0.00130321	0.998697
0.023678	5	0	0	0	0	1

5	Output (5-step) transition matrix					
		1	2	3	4	5
0.37074	1	0.37074	0.319046557	0.147555083	0.08807309	0.074585
0.319047	2	0	0.193491772	0.168394491	0.167199403	0.470914
0.147555	3	0	0	0.01306912	0.032332506	0.954598
0.088073	4	0	0	0	0.00024761	0.999752
0.074585	5	0	0	0	0	1

6	Output (6-step) transition matrix					
		1	2	3	4	5
0.304007	1	0.304007	0.296446681	0.151306167	0.102315821	0.145925
0.296447	2	0	0.139314085	0.124903388	0.129436672	0.606346
0.151306	3	0	0	0.00548903	0.013723265	0.980788
0.102316	4	0	0	0	4.70459E-05	0.999953
0.145925	5	0	0	0	0	1

7	Output (7-step) transition matrix					
		1	2	3	4	5
0.249285	1	0.249285	0.268162817	0.146553665	0.107197568	0.2288
0.268163	2	0	0.100306146	0.091467373	0.097036928	0.71119
0.146554	3	0	0	0.002305393	0.005791058	0.991903
0.107198	4	0	0	0	8.93872E-06	0.999991
0.2288	5	0	0	0	0	1

8	Output (8-step) transition matrix					
		1	2	3	4	5
0.204414	1	0.204414	0.237948626	0.136638135	0.105368651	0.315631
0.237949	2	0	0.07222043	0.06650202	0.07148809	0.789789
0.136638	3	0	0	0.000968265	0.002437429	0.996594
0.105369	4	0	0	0	1.69836E-06	0.999998
0.315631	5	0	0	0	0	1

9	Output (9-step) transition matrix					
		1	2	3	4	5
0.16762	1	0.16762	0.20811756	0.124013633	0.09927015	0.400979

		1	2	3	4	5
0.208118	2	0	0.051998712	0.048152573	0.052153908	0.847695
0.124014	3	0	0	0.000406671	0.001024705	0.998569
0.09927	4	0	0	0	3.22688E-07	1
0.400979	5	0	0	0	0	1

10		Output (10-step) transition matrix				
		1	2	3	4	5
0.137448	1	0.137448	0.18001616	0.110358641	0.090789221	0.481388
0.180016	2	0	0.037439074	0.034783721	0.037837733	0.88994
0.110359	3	0	0	0.000170802	0.000430563	0.999399
0.090789	4	0	0	0	6.13107E-08	1
0.481388	5	0	0	0	0	1

11		Output (11-step) transition matrix				
		1	2	3	4	5
0.112707	1	0.112707	0.154352292	0.096755154	0.081257954	0.554927
0.154352	2	0	0.026956135	0.025092104	0.027363727	0.920588
0.096755	3	0	0	7.17368E-05	0.000180872	0.999747
0.081258	4	0	0	0	1.1649E-08	1
0.554927	5	0	0	0	0	1

12		Output (12-step) transition matrix				
		1	2	3	4	5
0.09242	1	0.09242	0.131420985	0.083855808	0.071556993	0.620746
0.131421	2	0	0.019408418	0.018086404	0.019752529	0.942753
0.083856	3	0	0	3.01295E-05	7.59731E-05	0.999894
0.071557	4	0	0	0	2.21331E-09	1
0.620746	5	0	0	0	0	1

13		Output (13-step) transition matrix				
		1	2	3	4	5
0.075784	1	0.075784	0.111258723	0.072017312	0.062232189	0.678707
0.111259	2	0	0.013974061	0.013030647	0.014243093	0.958752
0.072017	3	0	0	1.26544E-05	3.191E-05	0.999955
0.062232	4	0	0	0	4.2053E-10	1
0.678707	5	0	0	0	0	1

14		Output (14-step) transition matrix				
		1	2	3	4	5
0.062143	1	0.062143	0.093747482	0.061399713	0.05359415	0.729115
0.093747	2	0	0.010061325	0.00938561	0.010263963	0.970289

		1	2	3	4	5
0.0614	3	0	0	5.31484E-06	1.34024E-05	0.999981
0.053594	4	0	0	0	7.99007E-11	1
0.729115	5	0	0	0	0	1

15	Output (15-step) transition matrix					
		1	2	3	4	5
0.050957	1	0.050957	0.078683972	0.052037176	0.045794714	0.772527
0.078684	2	0	0.007244154	0.006759128	0.007393806	0.978603
0.052037	3	0	0	2.23223E-06	5.62907E-06	0.999992
0.045795	4	0	0	0	1.51811E-11	1
0.772527	5	0	0	0	0	1

16	Output (16-step) transition matrix					
		1	2	3	4	5
0.041785	1	0.041785	0.065824807	0.043887127	0.03888255	0.80962
0.065825	2	0	0.005215791	0.004867197	0.005325117	0.984592
0.043887	3	0	0	9.37537E-07	2.36422E-06	0.999997
0.038883	4	0	0	0	2.88441E-12	1
0.80962	5	0	0	0	0	1

17	Output (17-step) transition matrix					
		1	2	3	4	5
0.034264	1	0.034264	0.054915186	0.036863539	0.032842211	0.841115
0.054915	2	0	0.00375537	0.003504644	0.003834747	0.988905
0.036864	3	0	0	3.93766E-07	9.92973E-07	0.999999
0.032842	4	0	0	0	5.48039E-13	1
0.841115	5	0	0	0	0	1

18	Output (18-step) transition matrix					
		1	2	3	4	5
0.028096	1	0.028096	0.045706417	0.03085894	0.027620869	0.867718
0.045706	2	0	0.002703866	0.002523454	0.002761296	0.992011
0.030859	3	0	0	1.65382E-07	4.17049E-07	0.999999
0.027621	4	0	0	0	1.04127E-13	1
0.867718	5	0	0	0	0	1

19	Output (19-step) transition matrix					
		1	2	3	4	5
0.023039	1	0.023039	0.037965957	0.025758551	0.023146147	0.89009

		1	2	3	4	5
0.037966	2	0	0.001946784	0.001816934	0.00198825	0.994248
0.025759	3	0	0	6.94602E-08	1.75161E-07	1
0.023146	4	0	0	0	1.97842E-14	1
0.89009	5	0	0	0	0	1

20	Output (20-step) transition matrix					
		1	2	3	4	5
0.018892	1	0.018892	0.031482507	0.021449061	0.019337725	0.908839
0.031483	2	0	0.001401684	0.001308212	0.001431589	0.995859
0.021449	3	0	0	2.91733E-08	7.35674E-08	1
0.019338	4	0	0	0	3.759E-15	1
0.908839	5	0	0	0	0	1

21	Output (21-step) transition matrix					
		1	2	3	4	5
0.015491	1	0.015491	0.026067957	0.017823707	0.01611462	0.924502
0.026068	2	0	0.001009213	0.000941921	0.001030765	0.997018
0.017824	3	0	0	1.22528E-08	3.08983E-08	1
0.016115	4	0	0	0	7.14209E-16	1
0.924502	5	0	0	0	0	1

22	Output (22-step) transition matrix					
		1	2	3	4	5
0.012703	1	0.012703	0.021557383	0.014784985	0.013399526	0.937555
0.021557	2	0	0.000726633	0.000678186	0.000742159	0.997853
0.014785	3	0	0	5.14617E-09	1.29773E-08	1
0.0134	4	0	0	0	1.357E-16	1
0.937555	5	0	0	0	0	1

23	Output (23-step) transition matrix					
		1	2	3	4	5
0.010416	1	0.010416	0.017807847	0.012245761	0.0111212	0.948409
0.017808	2	0	0.000523176	0.000488296	0.000534358	0.998454
0.012246	3	0	0	2.16139E-09	5.45046E-09	1
0.011121	4	0	0	0	2.5783E-17	1
0.948409	5	0	0	0	0	1

24	Output (24-step) transition matrix					
		1	2	3	4	5
0.008541	1	0.008541	0.014696606	0.010129417	0.009215568	0.957417
0.014697	2	0	0.000376687	0.000351573	0.00038474	0.998887

0.010129	3	0	0	9.07784E-10	2.2892E-09	1
0.009216	4	0	0	0	4.89876E-18	1
0.957417	5	0	0	0	0	1

25	Output (25-step) transition matrix					
		1	**2**	**3**	**4**	**5**
0.007004	**1**	0.007004	0.01211902	0.008369406	0.007626019	0.964882
0.012119	**2**	0	0.000271214	0.000253133	0.000277013	0.999199
0.008369	**3**	0	0	3.81269E-10	9.61462E-10	1
0.007626	**4**	0	0	0	9.30765E-19	1
0.964882	**5**	0	0	0	0	1

26	Output (26-step) transition matrix					
		1	**2**	**3**	**4**	**5**
0.005743	**1**	0.005743	0.009986416	0.006908477	0.006303198	0.971059
0.009986	**2**	0	0.000195274	0.000182256	0.00019945	0.999423
0.006908	**3**	0	0	1.60133E-10	4.03814E-10	1
0.006303	**4**	0	0	0	1.76845E-19	1
0.971059	**5**	0	0	0	0	1

27	Output (27-step) transition matrix					
		1	**2**	**3**	**4**	**5**
0.004709	**1**	0.004709	0.00822401	0.005697757	0.005204523	0.976164
0.008224	**2**	0	0.000140598	0.000131224	0.000143604	0.999585
0.005698	**3**	0	0	6.72559E-11	1.69602E-10	1
0.005205	**4**	0	0	0	3.36006E-20	1
0.976164	**5**	0	0	0	0	1

28	Output (28-step) transition matrix					
		1	**2**	**3**	**4**	**5**
0.003862	**1**	0.003862	0.006768995	0.004695782	0.004293558	0.98038
0.006769	**2**	0	0.00010123	9.44815E-05	0.000103395	0.999701
0.004696	**3**	0	0	2.82475E-11	7.12328E-11	1
0.004294	**4**	0	0	0	6.38411E-21	1
0.98038	**5**	0	0	0	0	1

29	Output (29-step) transition matrix					
		1	**2**	**3**	**4**	**5**
0.003167	**1**	0.003167	0.005568798	0.003867547	0.003539329	0.983858
0.005569	**2**	0	7.28858E-05	6.80267E-05	7.44443E-05	0.999785
0.003868	**3**	0	0	1.18639E-11	2.99178E-11	1

		1	2	3	4	5
0.003539	4	0	0	0	1.21298E-21	1
0.983858	5	0	0	0	0	1

30		Output (30-step) transition matrix				
		1	2	3	4	5
0.002597	1	0.002597	0.004579534	0.003183634	0.002915649	0.986725
0.00458	2	0	5.24778E-05	4.89792E-05	5.35999E-05	0.999845
0.003184	3	0	0	4.98286E-12	1.25655E-11	1
0.002916	4	0	0	0	2.30467E-22	1
0.986725	5	0	0	0	0	1

16. Appendix 5 : Additional Data for Chapter 9

Model Equations input check

Example:

Table 16-1: Equations from system dynamics that shape the model

(01) "Acum.Change in IRI"= INTEG (Change in IRI, 0)

Units: m/km

(02) Air Temperature = 54.3

Units: C

(03) "Air Voids (VIM)"= (LN("pavement (AGE)"+0.0001)*-0.07)+1.39

Units: percentage

(04) "CH.age"= 0

Units: years

(05) change in roughness due environmental= 0.5*environmental coefficient*initial Roughness

Units: m/km

(06) change in cracking= 3.68289

Units: mm

(07) Change in IRI= change in roughness due enviromental+change in roughness due to cracking+"Change in roughness (ΔRIr)"

Units: mm

(08) "Change in roughness (ΔRIr)"= (0.061*LN(Rutting)+0.16)

Units: m/km

(09) change in roughness due to cracking= ((-0.003*change in cracking^2)+(0.058*change in cracking)+0.104)*0.7

Units: m/km

(10) change in Temprature=0

Units: C

(11) change in traffic="Traffic (t)"*0.15

Units: EASLm/lane

(12) environmental coefficient= 0.182

Units: Dmnl

(13) FINAL TIME = 20

Units: Year The final time for the simulation.

(14) initial Roughness= 1.16

Units: m/km

(15) INITIAL TIME = 0

Units: Year The initial time for the simulation.

(16) new construction pavement=11

Units: years

(17) "pavement (AGE)"= INTEG (

"CH.age", new construction pavement)

Units: years

(18) "Pavement Temprature."= INTEG (change in Temprature, 0)

Units: C

(19) "pavement thickness (HS)"=180

Units: mm

(20) PCI= 144.932*EXP(-0.463*("Acum.Change in IRI"+0.8))

Units: Dmnl

(21) Rutting= (11.863*("Traffic (t)"^0.835))*("Speed (sh)"^-5.244)*("pavement thickness (HS)" ^-7.234)*(("Softening Point (SP)"/"Air Voids (VIM)")^-3.131)*("Temprature@20mmpavement"^15.729) + (11.863*0.045)+"Pavement Temprature."

Units: mm

(22) SAVEPER = TIME STEP

Units: Year [0,?] The frequency with which output is stored.

(23) "Softening Point (SP)"=((LN("pavement (AGE)"+0.0001))*2.5)+70.5

Units: C

(24) "Speed (sh)"=48

Units: km/h

(25) "Temprature @ 20mm pavement"=3.16+(1.319*Air Temprature)

Units: C

(26) TIME STEP = 1 Units: Year [0,?]

The time step for the simulation.

(27) "Traffic (t)"= INTEG (change in traffic,"Traffic (YE4)")

Units: m ESAL

(28) "Traffic (YE4)"= (5000*365*0.06*0.7*6.5)/1e+06

Units: EASLm/lane

Model Testing for temperature

Table 16-2: Air temperature data with forecasted climate change scenarios

month	**2003-2017 Al Ain**				
	Max	Mean Max	Mean	Mean Min	Min
	31.7	24.9	17.8	11.2	4.6
February	37.4	27.8	20.3	13.3	4.7
March	40.1	32.3	24	16.2	7.4
April	45.2	37.4	28.7	20.4	11.8
May	49.2	42.7	33.3	24.5	17.7
June	50.9	45	35.4	26.9	21.4
July	51.3	45.7	37.2	30	22.6
August	50.2	45.7	37.3	30.4	25.3

September	48.5	43	34.1	26.6	20.2
October	45.7	38.7	29.9	22.2	15.7
November	37.8	32.3	24.5	17.5	11.1
December	37	27.2	19.6	12.8	5.8

Month	**Max (2003-2017)**	**Climate 2020**	**Climate 2040**	**Climate 2060**	
		Increase by 1°C	**1.5 and 2°C**	**2 and 3°C**	
		Assume =1	**Assume =2**	**Assume = 3**	
January	31.7	32.7	33.7	34.7	
February	37.4	38.4	39.4	40.4	
March	40.1	41.1	42.1	43.1	
April	45.2	46.2	47.2	48.2	
May	49.2	50.2	51.2	52.2	
June	50.9	51.9	52.9	53.9	
July	51.3	52.3	53.3	54.3	
August	50.2	51.2	52.2	53.2	
September	48.5	49.5	50.5	51.5	
October	45.7	46.7	47.7	48.7	
November	37.8	38.8	39.8	40.8	
December	37	38	39	40	

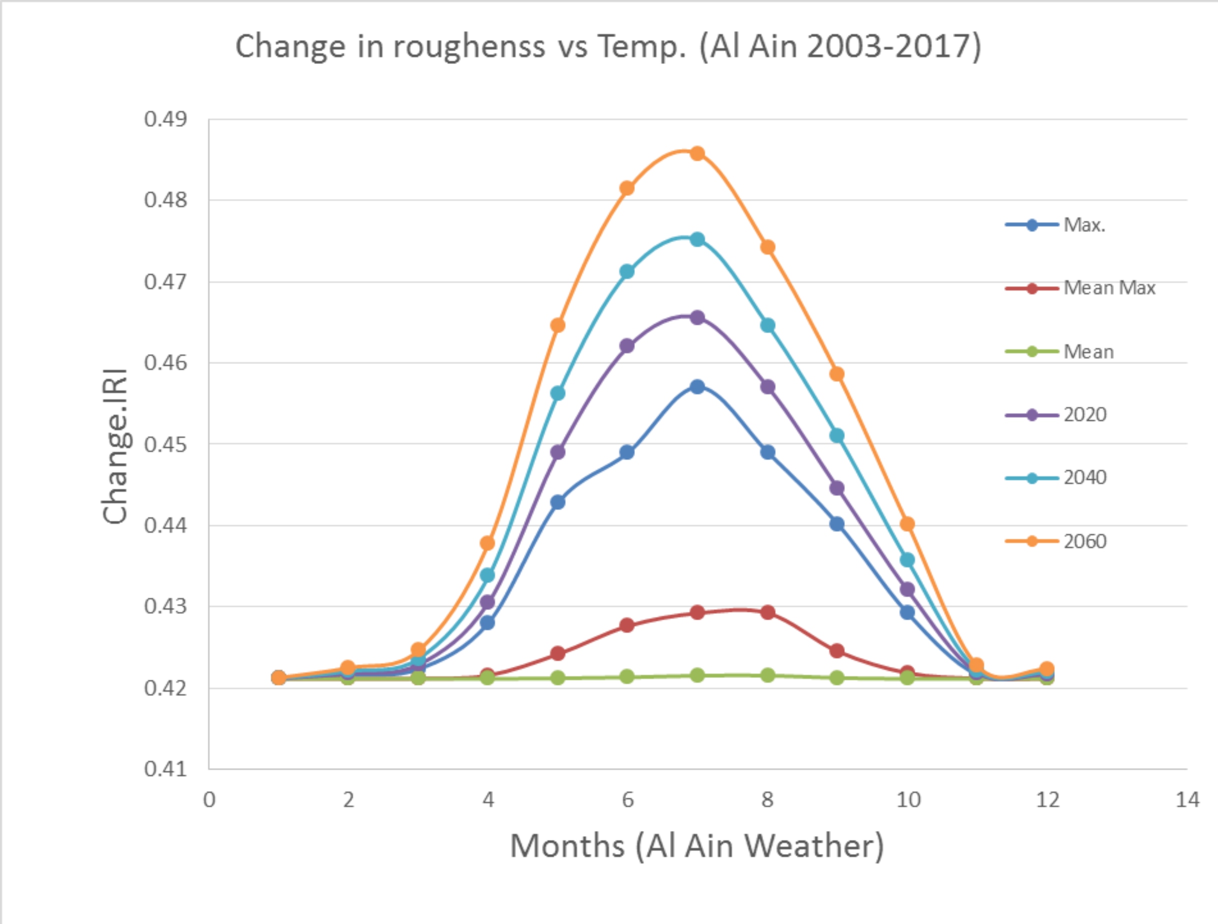

Figure 16-1: Change in roughness vs different temperature scenarios (Al Ain 2003-2017) based on the system dynamics model

Table 16-3 Output results of change in roughness generated from Vensim based on constant variables

Variables are not dynamics				
Time (Year)	**2060**	**2040**	**2020**	**2013**
0	0.485775	0.475171	0.465562	0.457042
1	0.485775	0.475171	0.465562	0.457042
2	0.485775	0.475171	0.465562	0.457042
3	0.485775	0.475171	0.465562	0.457042
4	0.485775	0.475171	0.465562	0.457042
5	0.485775	0.475171	0.465562	0.457042
6	0.485775	0.475171	0.465562	0.457042
7	0.485775	0.475171	0.465562	0.457042
8	0.485775	0.475171	0.465562	0.457042
9	0.485775	0.475171	0.465562	0.457042
10	0.485775	0.475171	0.465562	0.457042
11	0.485775	0.475171	0.465562	0.457042
12	0.485775	0.475171	0.465562	0.457042
13	0.485775	0.475171	0.465562	0.457042

14	0.485775	0.475171	0.465562	0.457042
15	0.485775	0.475171	0.465562	0.457042
16	0.485775	0.475171	0.465562	0.457042
17	0.485775	0.475171	0.465562	0.457042
18	0.485775	0.475171	0.465562	0.457042
19	0.485775	0.475171	0.465562	0.457042
20	0.485775	0.475171	0.465562	0.457042

Experiment 1 (Run the Model with Traffic Loading as the only Dynamic Variable and other Components are not Included)

Table 16-4: Results generated from Vensim based on deterioration model when traffic is the only dynamic variable

Time (Year)	**2013**	**2020**	**2040**	**2060**	**"Traffic (t)"**
	Change in IRI	Change in IRI	Change in IRI	Change in IRI	
0	0.436	0.4402	0.4454	0.4516	0.5
1	0.438	0.4422	0.4478	0.4545	0.57
2	0.439	0.4444	0.4505	0.4576	0.66
3	0.441	0.4467	0.4533	0.4609	0.76
4	0.443	0.4493	0.4563	0.4644	0.87
5	0.446	0.4520	0.4595	0.4681	1
6	0.448	0.4549	0.4630	0.4720	1.15
7	0.451	0.4581	0.4666	0.4762	1.33
8	0.453	0.4614	0.4704	0.4805	1.52
9	0.457	0.4650	0.4745	0.4850	1.75
10	0.460	0.4687	0.4787	0.4897	2.02
11	0.463	0.4727	0.4832	0.4946	2.32
12	0.467	0.4768	0.4878	0.4997	2.67
13	0.471	0.4812	0.4926	0.5049	3.07
14	0.475	0.4857	0.4977	0.5103	3.53
15	0.479	0.4905	0.5028	0.5159	4.05
16	0.484	0.4954	0.5082	0.5215	4.66
17	0.488	0.5005	0.5136	0.5274	5.36
18	0.493	0.5058	0.5193	0.5333	6.17
19	0.498	0.5112	0.5250	0.5393	7.09
20	0.503	0.5168	0.5309	0.5455	8.15

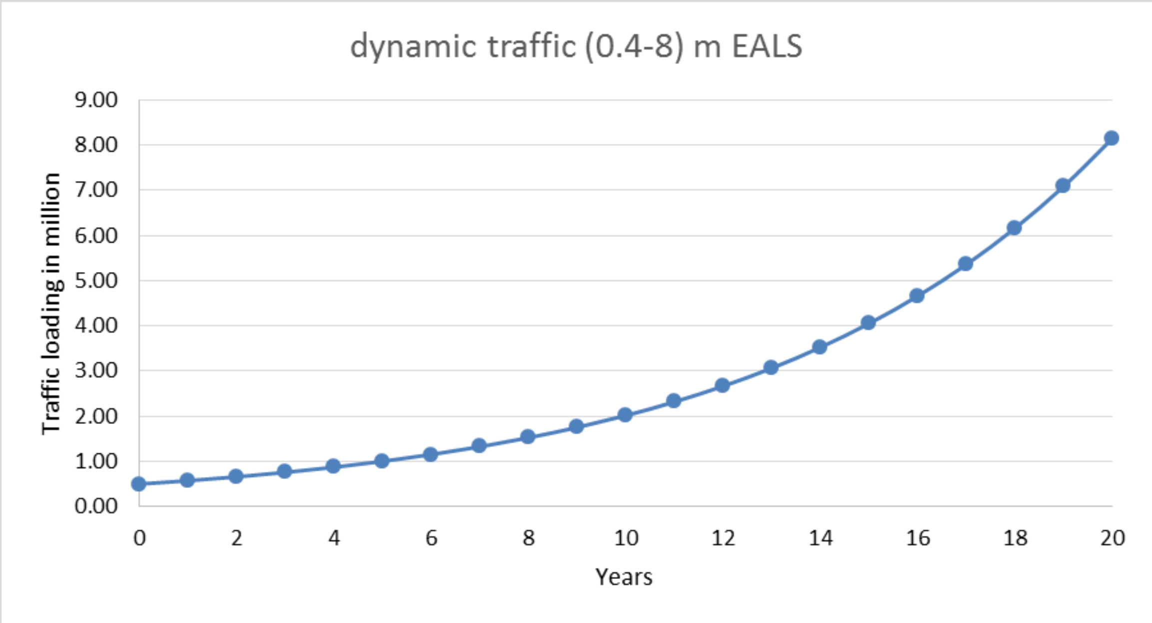

Figure 16-2: Traffic variable limitation over 20 forecasted years with no risk

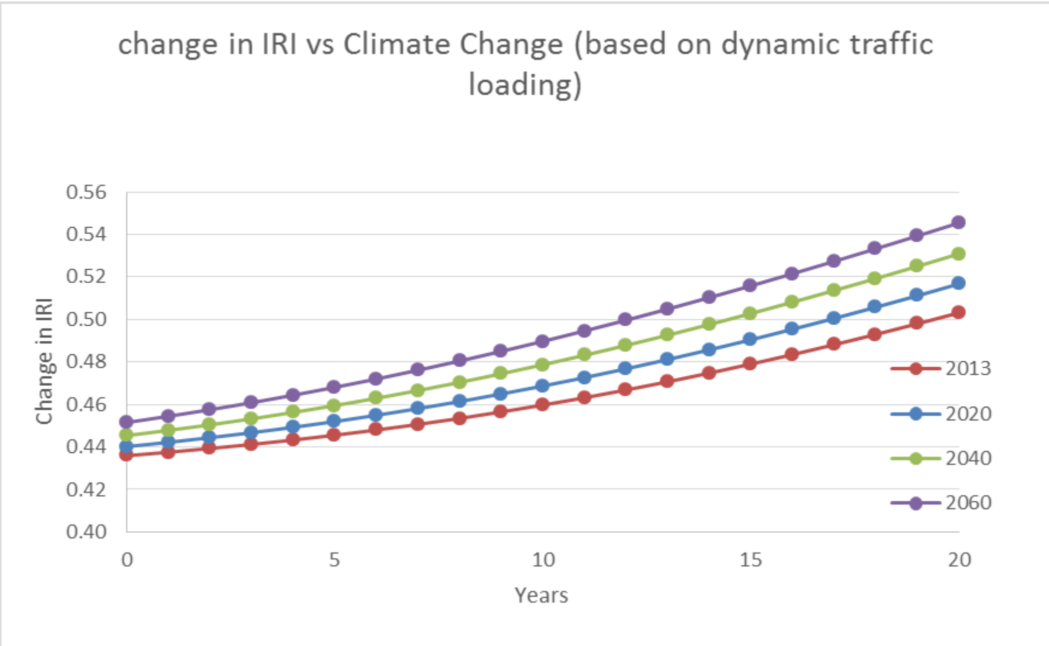

Figure 16-3: Change in IRI vs climate change (based on dynamic traffic loading) with no risk

Experiment 2 (Run the Model with Traffic Loading and Speed of Heavy vehicles as the only Dynamic variables and the others not Included)

Table 16-5: Results generated from Vensim based on deterioration model when traffic and speed are the dynamic variables

	Case 2		2013	2020	2040	2060
Time (Year)	Speed kn/h	Traffic	Change in IRI	Change in IRI	Change in IRI	Change in IRI
0	80	0.50	0.4223	0.4226	0.4231	0.4238
1	77	0.57	0.4227	0.4232	0.4239	0.4247
2	74	0.66	0.4233	0.4240	0.4249	0.4261
3	71	0.76	0.4241	0.4251	0.4263	0.4279
4	68	0.87	0.4253	0.4266	0.4283	0.4305
5	65	1.00	0.4270	0.4288	0.4312	0.4341
6	62	1.15	0.4294	0.4319	0.4351	0.4390
7	59	1.33	0.4328	0.4363	0.4406	0.4457
8	56	1.52	0.4377	0.4424	0.4480	0.4547
9	53	1.75	0.4445	0.4508	0.4580	0.4664
10	50	2.02	0.4540	0.4620	0.4711	0.4812
11	47	2.32	0.4667	0.4766	0.4876	0.4994
12	44	2.67	0.4831	0.4950	0.5077	0.5210
13	41	3.07	0.5036	0.5172	0.5314	0.5460
14	38	3.53	0.5284	0.5434	0.5587	0.5742
15	35	4.05	0.5572	0.5732	0.5893	0.6054
16	32	4.66	0.5900	0.6067	0.6234	0.6399
17	29	5.36	0.6268	0.6439	0.6609	0.6777
18	26	6.17	0.6678	0.6852	0.7024	0.7193
19	23	7.09	0.7135	0.7311	0.7484	0.7654
20	20	8.15	0.7651	0.7827	0.8001	0.8171

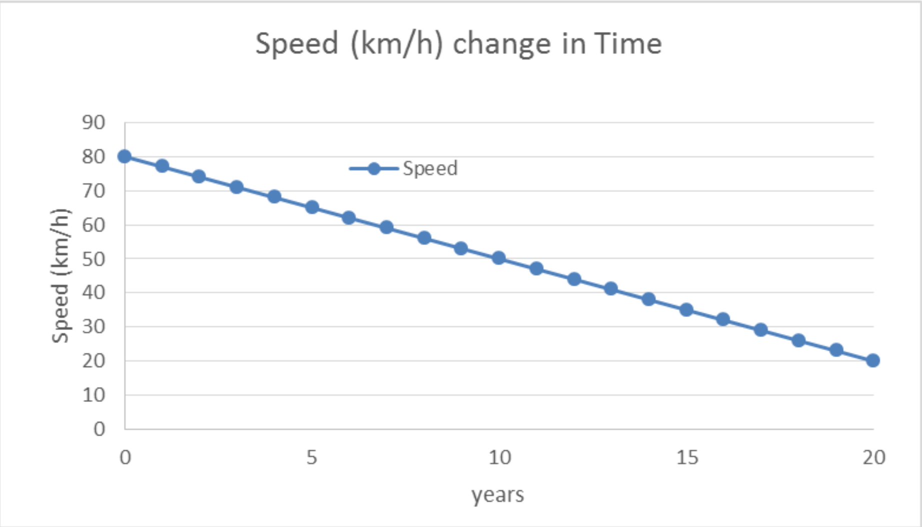

Figure 16-4: Speed (km/h) change in time range over 20 forecasted years with no risk

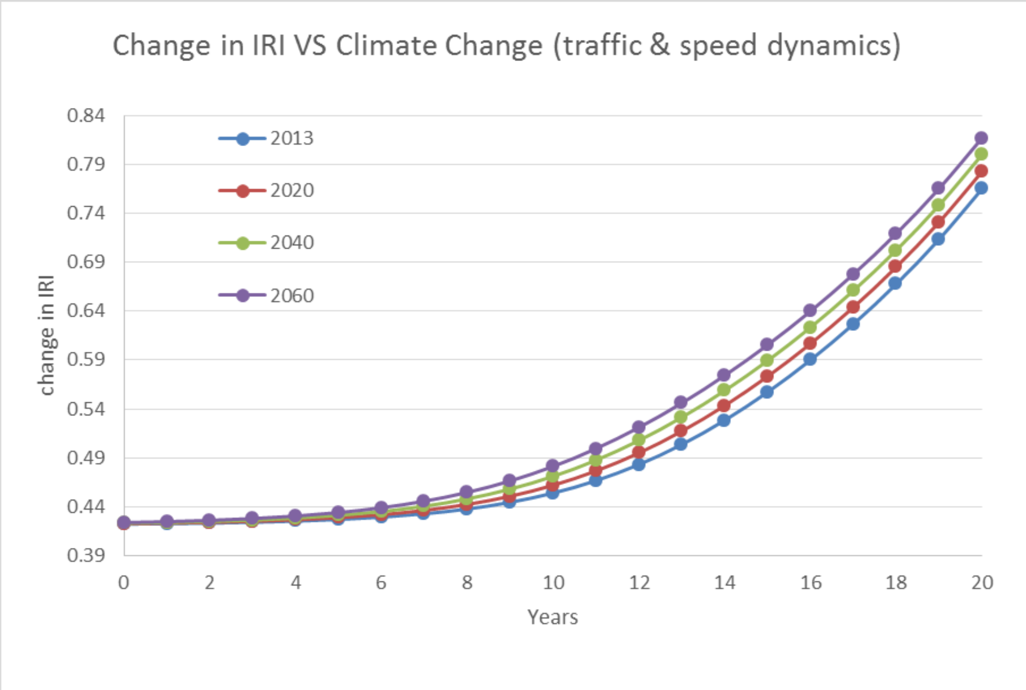

Figure 16-5: Change in IRI vs climate change (based on dynamic traffic loading and speed)

Experiment 3 (Run the Model with Traffic Loading, Speed of Heavy Vehicles and Pavement Thickness as the only Dynamic Variables and others not Included

Table 16-6: Results generated from Vensim based on deterioration model when traffic, speed and thickness are the dynamic variables

Time (Year)	Speed kn/h	Traffic	thickness	2013	2020	2040	2060
				Change in IRI	Change in IRI	Change in IRI	Change in IRI
0	80	0.50	220	0.4214	0.4215	0.4216	0.4217
1	77	0.57	215	0.4216	0.4217	0.4219	0.4221
2	74	0.66	210	0.4218	0.4221	0.4224	0.4228
3	71	0.76	205	0.4223	0.4227	0.4232	0.4239
4	68	0.87	200	0.4231	0.4237	0.4246	0.4257
5	65	1.00	195	0.4245	0.4255	0.4269	0.4287
6	62	1.15	190	0.4268	0.4286	0.4309	0.4338
7	59	1.33	185	0.4309	0.4338	0.4375	0.4420
8	56	1.52	180	0.4377	0.4424	0.4480	0.4547
9	53	1.75	175	0.4488	0.4558	0.4640	0.4732
10	50	2.02	170	0.4658	0.4756	0.4865	0.4982
11	47	2.32	165	0.4898	0.5023	0.5155	0.5294
12	44	2.67	160	0.5209	0.5355	0.5505	0.5658
13	41	3.07	155	0.5582	0.5742	0.5904	0.6065

14	38	3.53	150	0.6006	0.6175	0.6342	0.6509
15	35	4.05	145	0.6472	0.6645	0.6816	0.6985
16	32	4.66	140	0.6976	0.7151	0.7324	0.7494
17	29	5.36	135	0.7519	0.7695	0.7868	0.8039
18	26	6.17	130	0.8104	0.8281	0.8454	0.8625
19	23	7.09	125	0.8740	0.8917	0.9090	0.9261
20	20	8.15	120	0.9438	0.9615	0.9789	0.9959

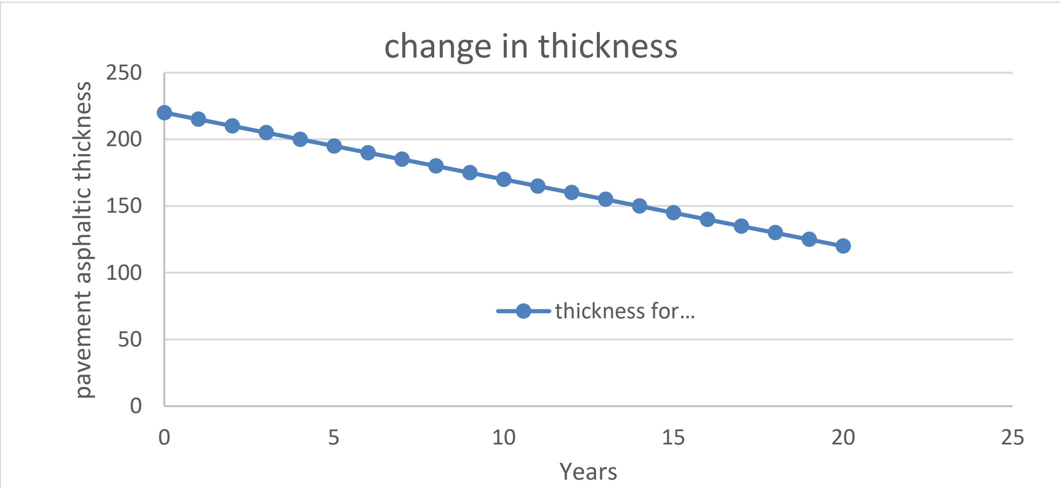

Figure 16-6: Pavement thickness range in mm over 20 forecasted years

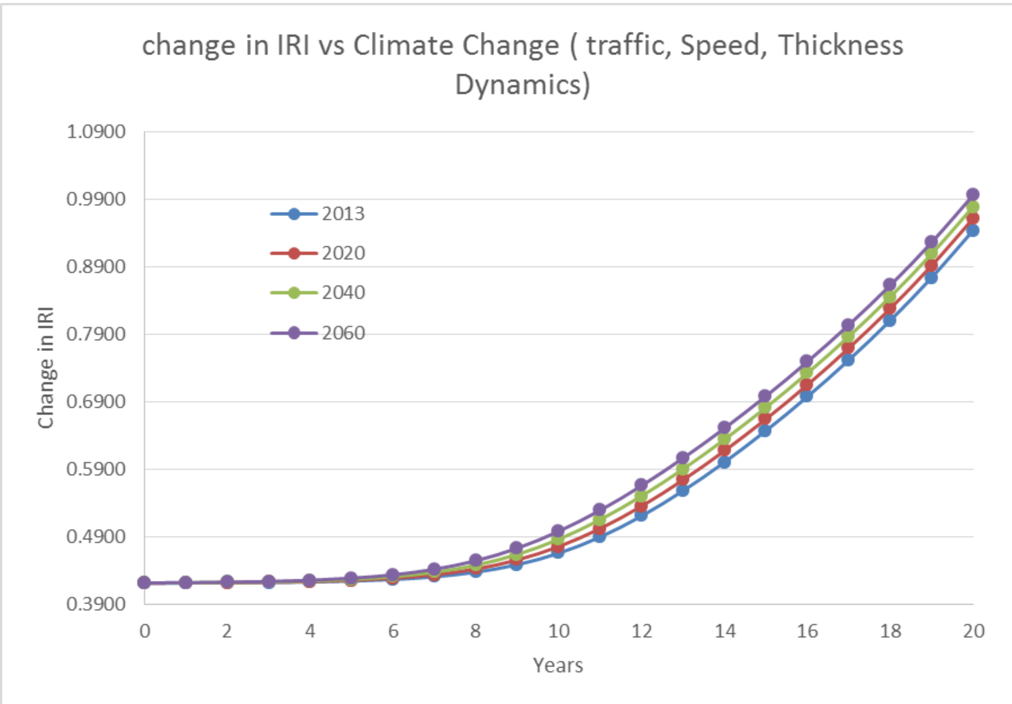

Figure 16-7: Change in IRI vs climate change (based on dynamic traffic loading, pavement thickness and speed with no risk)

Experiment 4 (Run the Model with Traffic loading, Speed of heavy Vehicles, Pavement thickness and Pavement Ageing as the only Dynamic variable and others not included)

Table 16-7: Results generated from Vensim based on deterioration model when traffic ,speed, pavement ageing and thickness are dynamic variables

Time (Year)	Speed kn/h	Traffic	aging	thickness	2013	2020	2040	2060
					Change in IRI	Change in IRI	Change in IRI	Change in IRI
0	80	0.50	8.00	220	0.4214	0.4215	0.4216	0.4218
1	77	0.57	8.50	215	0.4216	0.4217	0.4219	0.4222
2	74	0.66	9.00	210	0.4219	0.4221	0.4225	0.4229
3	71	0.76	9.50	205	0.4223	0.4228	0.4233	0.4240
4	68	0.87	10.00	200	0.4231	0.4238	0.4247	0.4258
5	65	1.00	10.50	195	0.4245	0.4256	0.4270	0.4288
6	62	1.15	11.00	190	0.4268	0.4286	0.4309	0.4338
7	59	1.33	11.50	185	0.4307	0.4337	0.4373	0.4417
8	56	1.52	12.00	180	0.4373	0.4419	0.4475	0.4541
9	53	1.75	12.50	175	0.4480	0.4549	0.4629	0.4720
10	50	2.02	13.00	170	0.4643	0.4739	0.4846	0.4961
11	47	2.32	13.50	165	0.4874	0.4997	0.5128	0.5264
12	44	2.67	14.00	160	0.5176	0.5320	0.5469	0.5620
13	41	3.07	14.50	155	0.5539	0.5699	0.5859	0.6020
14	38	3.53	15.00	150	0.5955	0.6123	0.6291	0.6456
15	35	4.05	15.50	145	0.6414	0.6587	0.6758	0.6926
16	32	4.66	16.00	140	0.6912	0.7087	0.7260	0.7429
17	29	5.36	16.50	135	0.7449	0.7625	0.7798	0.7969
18	26	6.17	17.00	130	0.8029	0.8206	0.8379	0.8550
19	23	7.09	17.50	125	0.8659	0.8836	0.9010	0.9181
20	20	8.15	18.00	120	0.9353	0.9530	0.9703	0.9874

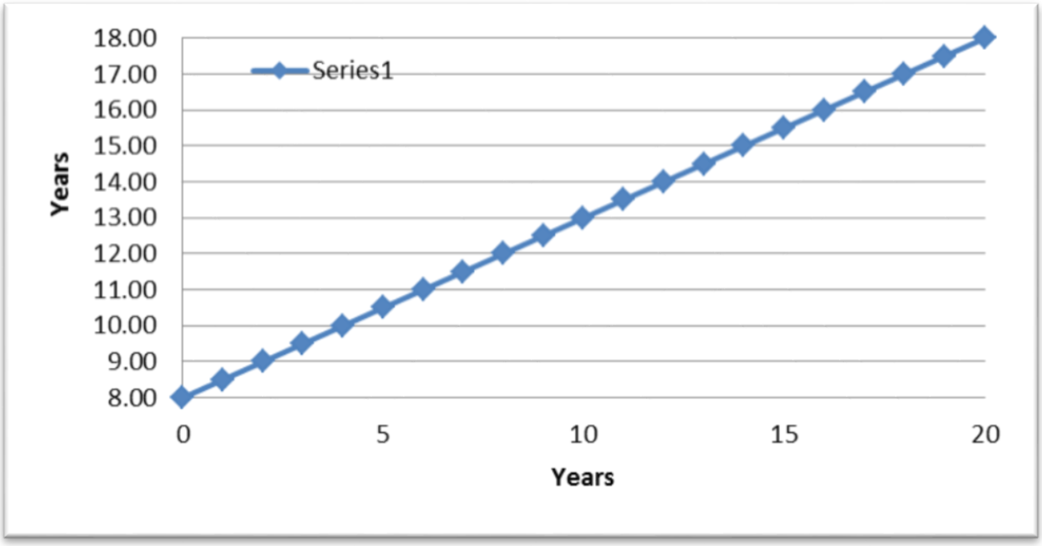

Figure 16-8: Pavement ageing range in years over 20 forecasted years

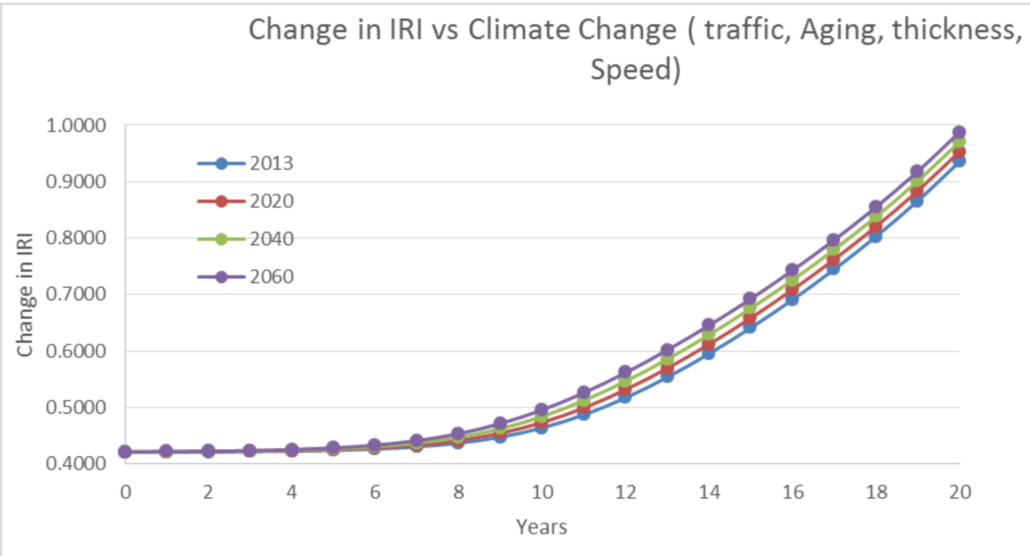

Figure 16-9: Change in IRI vs climate change (based on dynamic traffic loading, pavement thickness, pavement ageing and speed) with no risk

Test 1 Vensim

- Generated from Vensim based on deterioration model when traffic, speed, pavement ageing and thickness are the dynamic variables, and temperature is a constant value with 4 different climate change scenarios (2013, 2020, 2040 and2060)

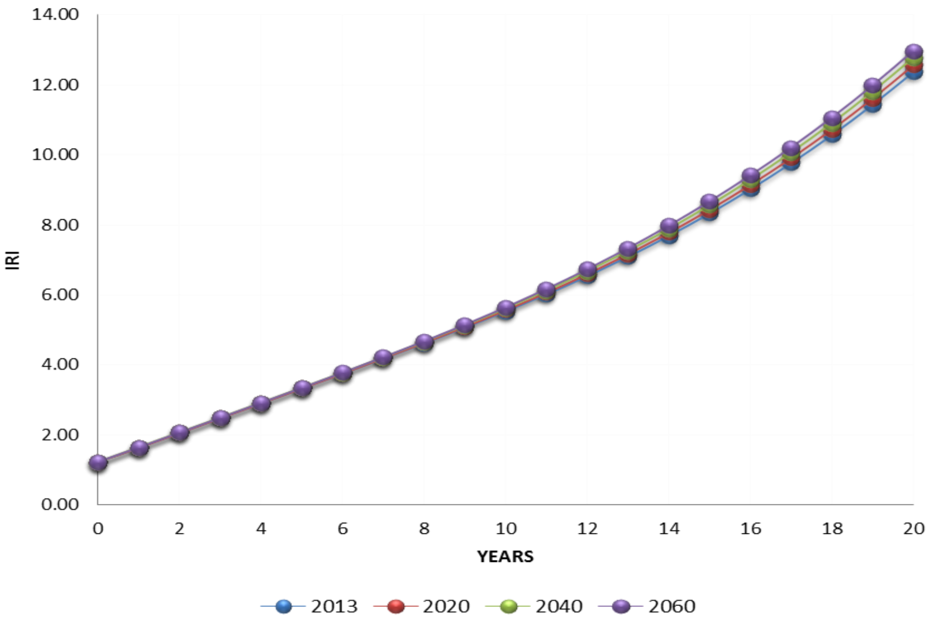

Figure 16-10: Different deterioration curve of IRI Based on climate change scenario using system dynamics with no risk

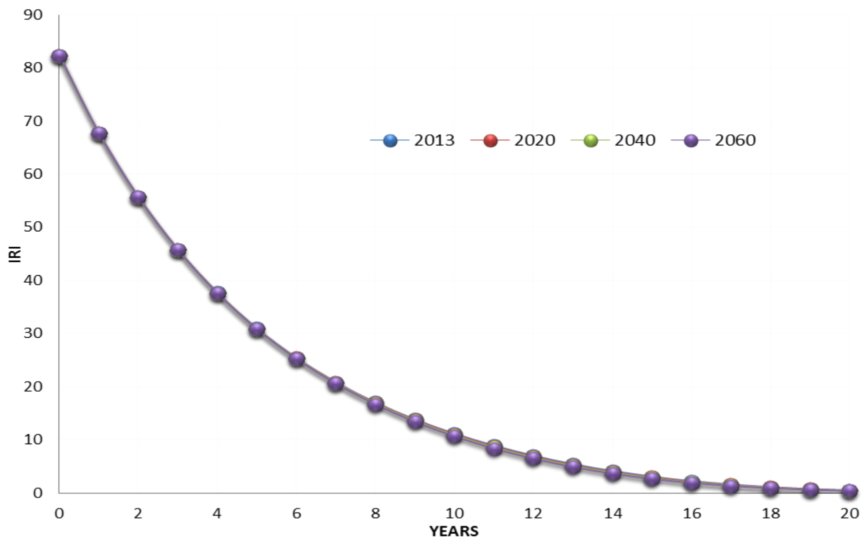

Figure 16-11: Different deterioration curve of PCI based on climate change scenario using system dynamics with no risk

Table 16-8 Change in IRI value based on state shift

	Change in IRI				
Time (Year)	20% state shift	40% state shift	60% state shift	80% state shift	100% state shift
0	0.000	0.000	0.000	0.000	0.000
1	0.084	0.169	0.253	0.337	0.421
2	0.169	0.337	0.506	0.674	0.843
3	0.253	0.506	0.759	1.012	1.265
4	0.337	0.675	1.012	1.349	1.687
5	0.422	0.844	1.266	1.688	2.110
6	0.507	1.014	1.521	2.028	2.535
7	0.593	1.186	1.778	2.371	2.964
8	0.680	1.359	2.039	2.719	3.399
9	0.769	1.538	2.307	3.076	3.845
10	0.862	1.723	2.585	3.447	4.308
11	0.960	1.919	2.879	3.839	4.799
12	1.065	2.129	3.194	4.259	5.323
13	1.178	2.356	3.533	4.711	5.889
14	1.300	2.600	3.901	5.201	6.501
15	1.433	2.865	4.298	5.731	7.163
16	1.576	3.152	4.727	6.303	7.879
17	1.730	3.460	5.191	6.921	8.651
18	1.897	3.793	5.690	7.587	9.484
19	2.076	4.152	6.228	8.304	10.380
20	2.269	4.538	6.808	9.077	11.346

Part A modelling with Risk : Deterministic Risk Analysis

Descriptive Analysis for the Traffic Loading Risk and Sub-risk

Table 16-9: Descriptive analysis for data of traffic loading risk for multiple-regression analysis method

		Y1	X1.1	X1.2	X1.3	X1.4	X1.5	X1.6	X1.7
N	Valid	30	30	30	30	30	30	30	30
Mean		.1620	.3387	.2207	.0867	.1857	.1407	.1893	.0717
Std. Error of Mean		.01797	.03295	.02697	.01772	.02976	.03098	.02297	.01644
Median		.1400	.3600	.2000	.0500	.1200	.0600	.1700	.0300
Mode		.10	.56	.20	.01	.03	.01	.20	.01
Std. Deviation		.09845	.18049	.14774	.09704	.16302	.16966	.12583	.09002
Variance		.010	.033	.022	.009	.027	.029	.016	.008
Skewness		.426	.225	1.284	1.768	1.660	1.569	1.038	1.819
Std. Error of Skewness		.427	.427	.427	.427	.427	.427	.427	.427
Kurtosis		-.734	-.903	3.089	2.929	3.186	1.644	1.173	2.914
Std. Error of Kurtosis		.833	.833	.833	.833	.833	.833	.833	.833
Range		.35	.66	.70	.39	.69	.55	.55	.35
Minimum		.01	.06	.02	.01	.03	.01	.01	.01
Maximum		.36	.72	.72	.40	.72	.56	.56	.36
Sum		4.86	10.16	6.62	2.60	5.57	4.22	5.68	2.15
Percentiles	25	.1000	.2000	.1000	.0200	.0600	.0275	.1000	.0100
	50	.1400	.3600	.2000	.0500	.1200	.0600	.1700	.0300
	75	.2500	.5600	.2800	.1200	.2800	.2200	.2800	.1050

Table 16-10: Results of Estimated coefficients and ANOVA for Traffic Risk.

Variables Entered/Removed[a]

Model	Variables Entered	Variables Removed	Method
1	X1.7, X1.2, X1.3, X1.5, X1.1, X1.6, X1.4[b]		Enter

a. Dependent Variable: Y1

b. All requested variables entered.

Descriptive Analysis for the Environmental Loading Risk and Sub-risk

Table 16-11: Descriptive analysis for data of Climate Risk for multiple-regression analysis method

		Y2	X2.1	X2.2	X2.3	X2.4	X2.5	X2.6	X2.7	X2.8	X2.9	X2.10
N	**Valid**	30	30	30	30	30	30	30	30	30	30	30
Mean		.2783	.1687	.1457	.3100	.0977	.1890	.1717	.1910	.1210	.1977	.1257
Std. Error of Mean		.04477	.02730	.02553	.03634	.02598	.02790	.02023	.02691	.02102	.02475	.01836
Median		.2200	.1000	.1000	.2800	.0500	.1200	.2000	.2000	.0850	.2000	.1000
Mode		.56	.10	.03[a]	.28	.01	.10	.20[a]	.28	.20	.28	.10
Std. Deviation		.24520	.14954	.13984	.19903	.14231	.15282	.11080	.14738	.11511	.13554	.10057
Variance		.060	.022	.020	.040	.020	.023	.012	.022	.013	.018	.010
Skewness		.528	1.365	1.438	.866	3.185	1.071	.335	1.649	2.100	.551	.772
Std. Error of Skewness		.427	.427	.427	.427	.427	.427	.427	.427	.427	.427	.427
Kurtosis		-1.158	1.439	1.603	-.076	12.504	.391	-.774	4.456	6.196	.044	-.555
Std. Error of Kurtosis		.833	.833	.833	.833	.833	.833	.833	.833	.833	.833	.833
Range		.70	.55	.55	.71	.71	.54	.39	.70	.55	.55	.35
Minimum		.02	.01	.01	.01	.01	.02	.01	.02	.01	.01	.01
Maximum		.72	.56	.56	.72	.72	.56	.40	.72	.56	.56	.36
Sum		8.35	5.06	4.37	9.30	2.93	5.67	5.15	5.73	3.63	5.93	3.77
Percentiles	25	.0500	.0550	.0450	.2000	.0100	.0600	.0600	.0900	.0375	.0675	.0450
	50	.2200	.1000	.1000	.2800	.0500	.1200	.2000	.2000	.0850	.2000	.1000
	75	.5600	.2400	.2000	.4100	.1200	.2800	.2800	.2800	.2000	.2800	.2100

Table 16-12: Results of Estimated coefficients and ANOVA for Climate Risk.

Variables Entered/Removed[a]

Model	Variables Entered	Variables Removed	Method
1	X2.10, X2.1, X2.6, X2.8, X2.4, X2.7, X2.5, X2.2, X2.3, X2.9b		Enter

a. Dependent Variable: Y2

b. All requested variables entered.

Descriptive Analysis for the Pavement Composition Risk and Sub-risk

Table 16-13: Descriptive analysis for data of pavement composition risk for multiple-regression analysis method

		Y3	X3.1	X3.2	X3.3	X3.4
N	Valid	30	30	30	30	30
Mean		.1497	.2400	.2127	.1317	.2120
Std. Error of Mean		.01839	.02492	.03158	.02209	.03792
Median		.1200	.2200	.1400	.1000	.1700
Mode		.12	.28	.40	.20	.03
Std. Deviation		.10074	.13651	.17296	.12098	.20770
Variance		.010	.019	.030	.015	.043
Skewness		1.070	.570	.767	.889	.984
Std. Error of Skewness		.427	.427	.427	.427	.427
Kurtosis		.597	.445	-.551	-.166	-.126
Std. Error of Kurtosis		.833	.833	.833	.833	.833
Range		.39	.55	.55	.39	.71
Minimum		.01	.01	.01	.01	.01
Maximum		.40	.56	.56	.40	.72
Sum		4.49	7.20	6.38	3.95	6.36
Percentiles	25	.1000	.1350	.0900	.0275	.0300
	50	.1200	.2200	.1400	.1000	.1700
	75	.2000	.2800	.4000	.2000	.3600

Table 16-14: Results of estimated coefficients and ANOVA for Pavement composition Risk

Variables Entered/Removed[a]

Model	Variables Entered	Variables Removed	Method
1	X3.4, X3.2, X3.3, X3.1b		Enter

a. Dependent Variable: Y3

b. All requested variables entered.

Descriptive Analysis for the Pavement Strength Risk and Sub-risk

Table 16-15: Descriptive analysis for data of pavement strength risk for multiple-regression analysis method

		Y4	X4.1	X4.2
N	Valid	30	30	30
Mean		.1323	.1960	.2253
Std. Error of Mean		.02151	.02392	.03212
Median		.1000	.2000	.2000
Mode		.10	.20	.03[a]
Std. Deviation		.11782	.13103	.17591
Variance		.014	.017	.031
Skewness		1.948	.698	.867
Std. Error of Skewness		.427	.427	.427
Kurtosis		4.734	.455	.636
Std. Error of Kurtosis		.833	.833	.833
Range		.53	.54	.71
Minimum		.03	.02	.01
Maximum		.56	.56	.72
Sum		3.97	5.88	6.76
Percentiles	25	.0575	.0900	.0825
	50	.1000	.2000	.2000
	75	.2000	.2800	.3700

Table 16-16 : Results of estimated coefficients and ANOVA for pavement strength risk

Variables Entered/Removed[a]

Model	Variables Entered	Variables Removed	Method
1	X4.2, X4.1b		Enter

a. Dependent Variable: Y4

b. All requested variables entered.

Descriptive Analysis for the Pavement Ageing Risk and Sub-risk

Table 16-17: Descriptive analysis for data of pavement ageing risk for multiple-regression analysis method

		Y5	X5.1	X5.2	X5.3	X5.4
N	Valid	30	30	30	30	30
Mean		.1697	.1823	.2140	.1677	.1393
Std. Error of Mean		.02224	.02758	.02605	.02482	.02581
Median		.1400	.1600	.2000	.1600	.0700
Mode		.20	.20	.20	.20	.03[a]
Std. Deviation		.12181	.15108	.14267	.13592	.14135
Variance		.015	.023	.020	.018	.020
Skewness		1.440	1.690	1.274	.941	1.441
Std. Error of Skewness		.427	.427	.427	.427	.427
Kurtosis		2.680	4.264	1.583	.916	1.506
Std. Error of Kurtosis		.833	.833	.833	.833	.833
Range		.54	.71	.54	.55	.55
Minimum		.02	.01	.02	.01	.01
Maximum		.56	.72	.56	.56	.56
Sum		5.09	5.47	6.42	5.03	4.18
Percentiles	25	.1000	.0600	.1200	.0450	.0300
	50	.1400	.1600	.2000	.1600	.0700
	75	.2000	.2800	.2800	.2500	.2000

Table 16-18: Results of estimated coefficients and ANOVA for pavement ageing risk

Variables Entered/Removed[a]

Model	Variables Entered	Variables Removed	Method
1	X5.4, X5.1, X5.3, X5.2b		Enter

a. Dependent Variable: Y5

b. All requested variables entered.

Descriptive Analysis for the Subgrade Soil Risk and Sub-risk

Table 16-19: Descriptive analysis for data of subgrade soil Risk for multiple-regression analysis method

		Y6	X6.1	X6.2
N	Valid	30	30	30
Mean		.1233	.1370	.2130
Std. Error of Mean		.01599	.02081	.03224
Median		.1100	.1100	.2000
Mode		.20	.20	.20
Std. Deviation		.08759	.11399	.17656
Variance		.008	.013	.031
Skewness		.440	2.034	.936
Std. Error of Skewness		.427	.427	.427
Kurtosis		-1.176	5.706	-.310
Std. Error of Kurtosis		.833	.833	.833
Range		.27	.55	.53
Minimum		.01	.01	.03
Maximum		.28	.56	.56
Sum		3.70	4.11	6.39
Percentiles	25	.0450	.0575	.0600
	50	.1100	.1100	.2000
	75	.2000	.2000	.3100

Table 16-20: Results of estimated coefficients and ANOVA for subgrade soil risk

Variables Entered/Removeda

Model	Variables Entered	Variables Removed	Method
1	X6.2, X6.1b		Enter

a. Dependent Variable: Y6

b. All requested variables entered.

Descriptive Analysis for the Drainage Risk and Sub-Risk

Table 16: Descriptive analysis for data of drainage soil risk multiple-regression analysis method

		Y7	X7.1	X7.2
N	Valid	30	30	30
Mean		.17	.1627	.2937
Std. Error of Mean		.023	.02169	.03549
Median		.13	.1800	.2800
Mode			.20	.28
Std. Deviation		.127	.11881	.19436
Variance		.016	.014	.038
Skewness		1.286	.554	.687
Std. Error of Skewness		.427	.427	.427
Kurtosis		1.878	-.551	-.074
Std. Error of Kurtosis		.833	.833	.833
Range		1	.39	.70
Minimum			.01	.02
Maximum		1	.40	.72
Sum		5	4.88	8.81
Percentiles	25	.06	.0400	.1700
	50	.13	.1800	.2800
	75	.21	.2200	.3700

Descriptive Analysis for the Maintenance Risk and Sub-risk

Table 16-21: Descriptive analysis for data of maintenance Risk multiple-regression analysis method

		Y8	X8.1	X8.2	X8.3
N	Valid	30	30	30	30
Mean		.1467	.2740	.2693	.2400
Std. Error of Mean		.01845	.04006	.04464	.03588
Median		.1200	.2200	.1900	.2000
Mode		.12	.56	.72	.20
Std. Deviation		.10104	.21943	.24448	.19650
Variance		.010	.048	.060	.039
Skewness		.661	.645	.927	1.128
Std. Error of Skewness		.427	.427	.427	.427
Kurtosis		-.350	-.791	-.481	.683
Std. Error of Kurtosis		.833	.833	.833	.833
Range		.39	.71	.71	.71
Minimum		.01	.01	.01	.01
Maximum		.40	.72	.72	.72
Sum		4.40	8.22	8.08	7.20
Percentiles	25	.0600	.0900	.0600	.1000
	50	.1200	.2200	.1900	.2000
	75	.2400	.4400	.4000	.3600

Descriptive Analysis for the Construction Quality Risk and Sub-risk

Table 16-22: Descriptive analysis for data of construction quality risk for multiple-regression analysis method

		Y9	X9.1	X9.2	X9.3
N	Valid	30	30	30	30
Mean		.2457	.2303	.1647	.2157
Std. Error of Mean		.02925	.03556	.02380	.03151
Median		.2800	.2000	.1100	.1300
Mode		.28[a]	.20[a]	.10	.12
Std. Deviation		.16021	.19477	.13035	.17260
Variance		.026	.038	.017	.030
Skewness		.068	1.272	1.339	.983
Std. Error of Skewness		.427	.427	.427	.427
Kurtosis		-.814	1.104	1.547	-.193
Std. Error of Kurtosis		.833	.833	.833	.833

Range		.55	.71	.53	.53
Minimum		.01	.01	.03	.03
Maximum		.56	.72	.56	.56
Sum		7.37	6.91	4.94	6.47
Percentiles	25	.0600	.0950	.0600	.1000
	50	.2800	.2000	.1100	.1300
	75	.3700	.2800	.2800	.3000

Descriptive Analysis for the Rutting Risk and Sub-risk

Table 16-23: Descriptive analysis for data of rutting risk for multiple-regression analysis method

		Y10	X10.1	X10.2	X10.3	X10.4	X10.5
N	Valid	30	30	30	30	30	30
Mean		.2037	.1483	.2030	.2273	.2133	.2213
Std. Error of Mean		.03554	.02617	.02868	.02832	.02569	.03706
Median		.1700	.1200	.1800	.2000	.2000	.1600
Mode		.20	.20	.10[a]	.20	.20	.20[a]
Std. Deviation		.19468	.14331	.15709	.15512	.14072	.20301
Variance		.038	.021	.025	.024	.020	.041
Skewness		1.440	2.225	1.421	.898	.969	1.149
Std. Error of Skewness		.427	.427	.427	.427	.427	.427
Kurtosis		1.709	7.787	2.526	.016	.724	.096
Std. Error of Kurtosis		.833	.833	.833	.833	.833	.833
Range		.71	.71	.69	.51	.55	.69
Minimum		.01	.01	.03	.05	.01	.03
Maximum		.72	.72	.72	.56	.56	.72
Sum		6.11	4.45	6.09	6.82	6.40	6.64
Percentiles	25	.0500	.0300	.1000	.1000	.1000	.0600
	50	.1700	.1200	.1800	.2000	.2000	.1600
	75	.2800	.2000	.2700	.3000	.2800	.2800

Descriptive Analysis for the Cracking Risk and Sub-risk

Table 16-24: Descriptive analysis for data of cracking risk for multiple-regression analysis method

		Y11	X11.1	X11.2	X11.3	X11.4	X11.5
N	Valid	30	30	30	30	30	30
Mean		.2953	.2430	.1450	.1820	.1620	.1110
Std. Error of Mean		.04716	.03352	.02449	.02767	.01980	.02449
Median		.1800	.2000	.1200	.1200	.1200	.0600
Mode		.12	.20	.20	.05[a]	.12	.01
Std. Deviation		.25833	.18359	.13413	.15155	.10845	.13415
Variance		.067	.034	.018	.023	.012	.018
Skewness		.790	1.438	2.852	1.190	.832	1.932
Std. Error of Skewness		.427	.427	.427	.427	.427	.427
Kurtosis		-.994	1.619	11.303	.680	-.167	3.666
Std. Error of Kurtosis		.833	.833	.833	.833	.833	.833
Range		.77	.71	.71	.51	.39	.55
Minimum		.03	.01	.01	.05	.01	.01
Maximum		.80	.72	.72	.56	.40	.56
Sum		8.86	7.29	4.35	5.46	4.86	3.33
Percentiles	25	.1000	.1150	.0600	.0600	.0700	.0175
	50	.1800	.2000	.1200	.1200	.1200	.0600
	75	.5600	.2800	.2000	.2800	.2500	.1550

Descriptive Analysis for the Vehicle Speed Risk and Sub-risk

Table 16-25: Descriptive analysis for data of vehicle speed risk for multiple-regression analysis method

		Y12	X12.1	X12.2	X12.3
N	Valid	30	30	30	30
Mean		.0773	.0943	.1347	.1593
Std. Error of Mean		.01596	.01517	.01915	.02404
Median		.0550	.1000	.1200	.1200
Mode		.01	.01	.20	.40
Std. Deviation		.08741	.08312	.10490	.13170
Variance		.008	.007	.011	.017
Skewness		2.274	1.467	.821	.862
Std. Error of Skewness		.427	.427	.427	.427
Kurtosis		6.089	2.728	.195	-.544

Std. Error of Kurtosis		.833	.833	.833	.833
Range		.39	.35	.39	.39
Minimum		.01	.01	.01	.01
Maximum		.40	.36	.40	.40
Sum		2.32	2.83	4.04	4.78
Percentiles	25	.0100	.0200	.0300	.0575
	50	.0550	.1000	.1200	.1200
	75	.1000	.1200	.2000	.2500

Descriptive Analysis for the Pavement Thickness Risk and Sub-risk

Table 16-26: Descriptive analysis for data of pavement thickness risk

		Y13	X13.1
N	Valid	30	30
Mean		.2403	.2367
Std. Error of Mean		.03904	.03735
Median		.1400	.1300
Mode		.10	.10
Std. Deviation		.21386	.20456
Variance		.046	.042
Skewness		.969	1.213
Std. Error of Skewness		.427	.427
Kurtosis		-.188	.374
Std. Error of Kurtosis		.833	.833
Range		.71	.70
Minimum		.01	.02
Maximum		.72	.72
Sum		7.21	7.10
Percentiles	25	.0900	.1000
	50	.1400	.1300
	75	.4000	.3700

Risk Measure Input based on the Deterministic Model

Traffic

Table 16-27: Traffic risk based on regression analysis with three different measures

A									**Adjusted R Square**
	R1.	**S1**	**S2**	**S3**	**S4**	**S5**	**S6**	**S7**	
Sig.	Y1	X1.1	X1.2	X1.3	X1.4	X1.5	X1.6	X1.7	
.056[b]	R1.Traffic	S1.High volume of heavy trucks	"S2.Axel Group Type	"S3.Tyer configuration	S4.Gross vehicle mass	S5.Dynamic Wheel Loading	S6.High traffic loading (all vehicles type)	S7.Vehicle speed	**0.250**
Max	0.360	0.720	0.720	0.400	0.720	0.560	0.560	0.360	constant
Average	0.162	0.339	0.221	0.087	0.186	0.141	0.189	0.072	
Min	0.010	0.060	0.020	0.010	0.030	0.010	0.010	0.010	
coefficients		-0.103	0.225	-0.067	0.036	0.079	0.247	0.378	.062
Risk (Max)	**0.466**	-0.074	0.162	-0.027	0.026	0.045	0.138	0.136	.062
Risk(Mean)	**0.162**	-0.035	0.050	-0.006	0.007	0.011	0.047	0.027	.062
Risk (Min)	**0.067**	-0.006	0.004	-0.001	0.001	0.001	0.002	0.004	.062

Climate Change

Table 16-28: Climate change risk based on regression analysis with three different measures

B											**Adjusted R Square**
	R2.	S8	S9	S10	S11	R7	R5	S14	S15	S16	S17	
Sig.	Y2	X2.1	X2.2	X2.3	X2.4	X2.5	X2.6	X2.7	X2.8	X2.9	X2.10	
.005b	R2.Climate Change	S8.Precipitation	S9.Weathering	S10.High Temperature	S11.Low Temperature	R7.Drainage	R5.Pavement Ageing	S14.Increase oxidation	S15.Increase viscosity and softness	S16.Increase Brittle of asphaltic layer	S17.Increase Moisture/ Excess water	0.500
Max	0.36	0.56	0.56	0.72	0.72	0.56	0.40	0.72	0.56	0.56	0.36	constant
Average	0.16	0.17	0.15	0.31	0.10	0.19	0.17	0.19	0.12	0.20	0.13	
Min	0.01	0.01	0.01	0.01	0.01	0.02	0.01	0.02	0.01	0.01	0.01	
coefficients		-0.99	0.19	0.09	0.66	1.53	-0.52	0.20	-0.16	0.67	0.22	-0.05
Risk (Max)	**1.197**	-0.553	0.108	0.065	0.476	0.855	-0.210	0.146	-0.090	0.376	0.078	-0.05
Risk(Mean)	**0.278**	-0.167	0.028	0.028	0.065	0.289	-0.090	0.039	-0.019	0.133	0.027	-0.05
Risk (Min)	**-0.017**	-0.010	0.002	0.001	0.007	0.031	-0.005	0.004	-0.002	0.007	0.002	-0.05

Pavement Composition

Table 16-29: Pavement composition risk based on regression analysis with three different measures

	B					
	R3.	S18	S19	S20	S21	
Sig.	Y3	X3.1	X3.2	X3.3	X3.4	Adjusted R Square
.067b	R3.Pavement Composition	S18. Reduction in Material Quality and Properties of Aggregate and soil	S19.Pavement Thickness	S20.Shortage of Material availability	S21.Bitumen Supply and Quality	0.173
Max	0.36	0.56	0.56	0.40	0.72	constant
Average	0.162	0.24	0.21	0.13	0.21	
Min	0.01	0.01	0.01	0.01	0.01	
coefficients		.273	.193	-.064	7.057E-05	0.05
Risk (Max)	**0.287**	0.153	0.108	-0.026	0.000	0.05
Risk(Mean)	**0.150**	0.065	0.041	-0.008	0.000	0.05
Risk (Min)	**0.056**	0.003	0.002	-0.001	0.000	0.05

Pavement Strength

Table 16-30: Pavement strength risk based on regression analysis with three different measures

	B			
	R4	S1	S22	
Sig.	Y4	X4.1	X4.2	Adjusted R Square
.067b	R4.Pavement Strength	R1.Traffic Loading	S22.Insufficient value of Structural Number (SN)	0.173
Max	0.36	0.56	0.72	constant
Average	0.16	0.20	0.23	
Min	0.01	0.02	0.01	
coefficients		0.47	0.01	0.04
Risk (Max)	**0.306**	0.26	0.005	0.04
Risk(Mean)	**0.132**	0.09	0.002	0.04
Risk (Min)	**0.049**	0.01	0.000	0.04

Pavement Ageing

Table 16-31: Pavement ageing risk based on regression analysis with three different measures

E						
	R3.	R2	R1	R6	R8	
Sig.	Y5	X5.1	X5.2	X5.3	X5.4	Adjusted R Square
.032b	R5.Pavement Ageing	R2.Climate Change	R1.Traffic Loading	R6.Subgrade Soil	R8.Maintenance	0.227
Max	0.56	0.72	0.56	0.56	0.56	constant
Average	0.17	0.18	0.21	0.17	0.14	
Min	0.02	0.01	0.02	0.01	0.01	
coefficients		.023	.406	.247	-.036	0.04
Risk (Max)	**0.404**	0.016	0.227	0.138	-0.020	0.04
Risk(Mean)	**0.170**	0.004	0.087	0.041	-0.005	0.04
Risk (Min)	**0.053**	0.0002	0.0081	0.0025	-0.0004	0.04

Subgrade soil

Table 16-32: Subgrade soil risk based on regression analysis with three different measures

E				
	R3.	S17	S13	
Sig.	Y6	X6.1	X6.2	Adjusted R Square
.009b	R6.Subgrade Soil	S17.Increase Moisture/ Excess water	S13.Selection of construction soil	0.241
Max	0.28	0.56	0.56	constant
Average	0.12	0.14	0.21	
Min	0.01	0.01	0.03	
coefficients		0.29	0.14	0.053
Risk (Max)	**0.30**	0.16	0.08	0.053
Risk(Mean)	**0.12**	0.04	0.03	0.053
Risk (Min)	**0.06**	0.00	0.00	0.053

Drainage

Table 16-33: Drainage risk based on regression analysis with three different measures

	Risk			
	R3.	S17	S23	
Sig.	Y7	X7.1	X7.2	Adjusted R Square
.019b	R7.Drainage	S17.Increase Moisture/ Excess water	S23.Insufficient drainage system	0.200
Max	0.56	0.40	0.72	constant
Average	0.17	0.16	0.29	
Min	0.03	0.01	0.02	
coefficients		.529	.026	0.074
Risk (Max)	**0.304**	0.211	0.019	0.074
Risk(Mean)	**0.167**	0.086	0.008	0.074
Risk (Min)	**0.079**	0.005	0.001	0.074

Maintenance

Table 16-34: Maintenance risk factor based on regression analysis with three different measures

	F				
	R8	S24	S25	S26	
Sig.	Y8	X8.1	X8.2	X8.3	Adjusted R Square
.388b	R8.Maintenance	S24.Delay maintenance	S25.Maintenance priorities /plan	S26.Limited Budget	0.005
Max	0.40	0.72	0.72	0.72	constant
Average	0.15	0.27	0.27	0.24	
Min	0.01	0.01	0.01	0.01	
coefficients		-.062	.044	.193	0.11
Risk (Max)	**0.232**	-0.044	0.032	0.139	0.11
Risk(Mean)	**0.147**	-0.017	0.012	0.046	0.11
Risk (Min)	**0.107**	-0.001	0.000	0.002	0.11

Construction Quality

Table 16-35: Construction quality risk factor based on regression analysis with three different measures

G					
	R9	S27	S28	S29	Adjusted R Square
Sig.	Y9	X9.1	X9.2	X9.3	
.016b	R9.Construction Quality	S27.Design and Specification	S28.Construction Process	S29.Construction Management	0.243
Max	0.56	0.72	0.56	0.56	constant
Average	0.25	0.23	0.16	0.22	
Min	0.01	0.01	0.03	0.03	
coefficients		.337	-.304	.450	0.12
Risk (Max)	**0.445**	0.242	-0.170	0.252	0.12
Risk(Mean)	**0.246**	0.078	-0.050	0.097	0.12
Risk (Min)	**0.129**	0.003	-0.009	0.013	0.12

Rutting

Table 16-36: Rutting risk factor based on regression analysis with three different measures

	H						
	R10.	R2	R3	R9	R4	R6	
Sig.	Y10	X10.1	X10.2	X10.3	X10.4	X10.5	Adjusted R Square
.000b	Rutting	R2.Climate Change	R3.Pavement Composition	R9.Construction Quality	R4.Pavement Strength	R6.Subgrade	.615
Max	0.72	0.72	0.72	0.56	0.56	0.72	constant
Average	0.20	0.15	0.20	0.23	0.21	0.22	
Min	0.01	0.01	0.03	0.05	0.01	0.03	
coefficients		.856	.393	.476	.065	-2.836E-01	-0.06
Risk (Max)	**0.935**	0.617	0.283	0.266	0.036	-0.204	-0.06
Risk(Mean)	**0.204**	0.127	0.080	0.108	0.014	-0.063	-0.06
Risk (Min)	**-0.026**	0.009	0.012	0.024	0.001	-0.009	-0.06

Cracking

Table 16-37: Cracking risk factor based on regression analysis with three different measures

			L				
	R11.	R2	R3	R9	R4	R6	
Sig.	Y11	X11.1	X11.2	X11.3	X11.4	X11.5	Adjusted R Square
.000b	Cracking	R2.Climate Change	R3.Pavement Composition	R9.Construction Quality	R4.Pavement Strength	R6.Subgrade	.615
Max	0.80	0.72	0.72	0.56	0.40	0.56	constant
Average	0.30	0.24	0.15	0.18	0.16	0.11	
Min	0.03	0.01	0.01	0.05	0.01	0.01	
coefficients		.950	-.446	.358	.518	-1.886E-01	0.00
Risk (Max)	**0.666**	0.684	-0.321	0.200	0.207	-0.106	0.00
Risk(Mean)	**0.295**	0.231	-0.065	0.065	0.084	-0.021	0.00
Risk (Min)	**0.027**	0.009	-0.004	0.018	0.005	-0.002	0.00

Vehicle Speed

Table 16-38: Vehicle speed risk factor based on regression analysis with three different measures

			M		
	S7	R2	R1	R6	
Sig.	Y12	X12.1	X12.2	X12.3	Adjusted R Square
.013b	S7.Vehicle speed	R5.Pavement Ageing	R7.Drainage	R8.Maintenance	0.257
Max	0.40000	0.36000	0.40000	0.40000	constant
Average	0.07733	0.09433	0.13467	0.15933	
Min	0.01000	0.01000	0.01000	0.01000	
coefficients		0.61052	-0.00086	-0.00727	0.021
Risk (Max)	**0.23755**	0.21979	-0.00034	-0.00291	0.021
Risk(Mean)	**0.07733**	0.05759	-0.00012	-0.00116	0.021
Risk (Min)	**0.02704**	0.00611	-0.00001	-0.00007	0.021

Pavement thickness

Table 16-39: Pavement thickness risk factor based on regression analysis with three different measures

	N		
	S7	R2	
Sig.	Y13	X13.1	
.009b	S19.Pavement Thickness	R9.Construction Quality	0.241
Max	0.72	0.72	constant
Average	0.24	0.24	
Min	0.01	0.02	
coefficients		0.84	0.042
Risk (Max)	**<u>0.65</u>**	0.60	0.042
Risk(Mean)	**<u>0.24</u>**	0.20	0.042
Risk (Min)	**<u>0.06</u>**	0.02	0.042

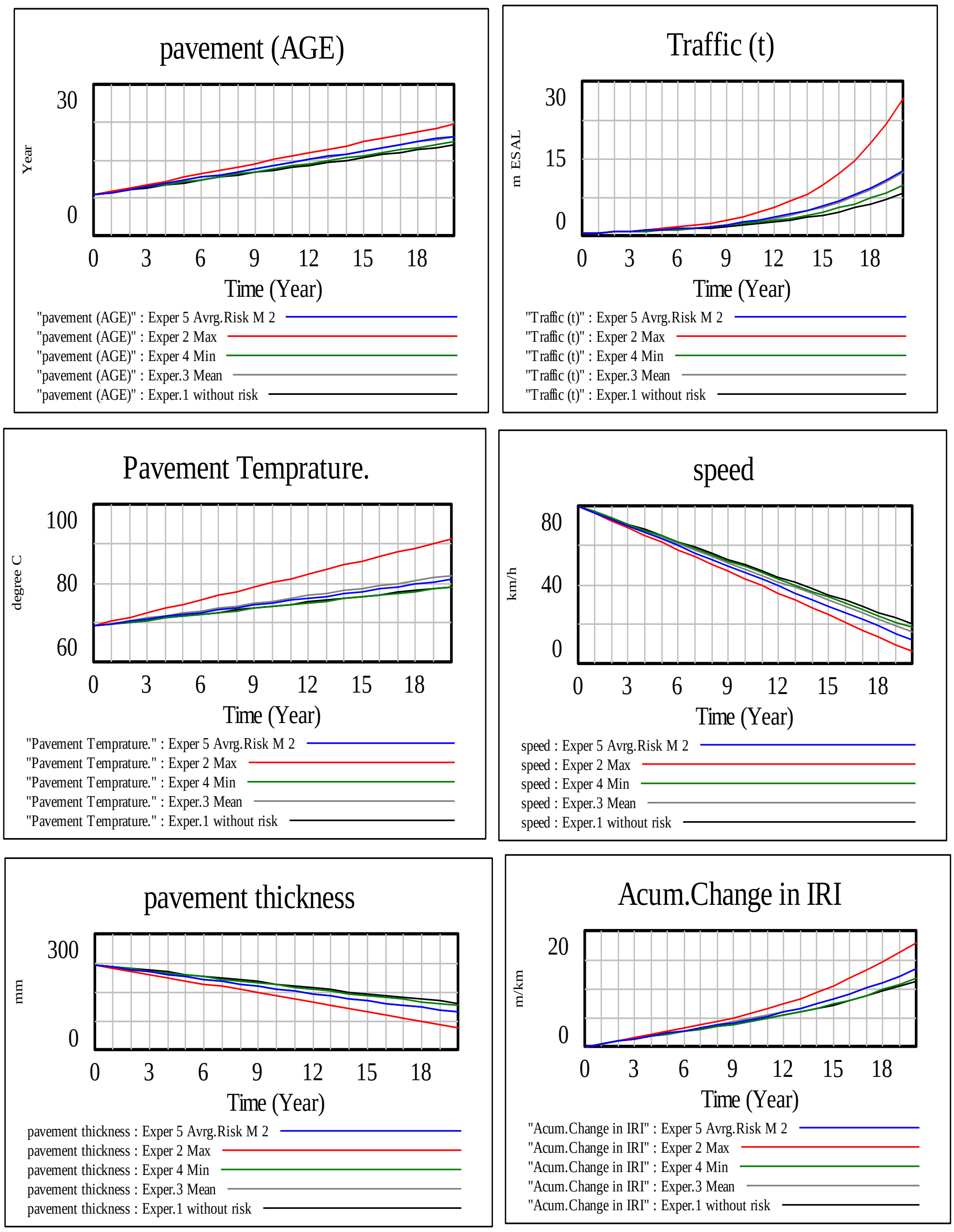

Figure 16-12: System dynamics results for different variables with different risk scenarios

Table 16-40: All risk measures based on two methods: regression and probability

Method type	Risk Measure															
	Risk Type		factor	R1.	R2.	R3.	R4	R5.	R6.	R7.	R8	R9	R10.	R11.	S7	S10
				Y1	Y2	Y3	Y4	Y5	Y6	Y7	Y8	Y9	Y10	Y11	Y12	Y13
				R1.Traffic	R2.Climate Change	R3.Pavement Composition	R4.Pavement Strength	R5.Pavement Ageing	R6.Subgrade Soil	R7.Drainage	R8.Maintenance	R9.Construction Quality	Rutting	Cracking	S7.Vehicle speed	S19.Pavement Thickness
Method 1 (regression)	Experiment 1	Risk (Max)	a1	0.466	1.197	0.287	0.306	0.404	0.297	0.304	0.232	0.445	0.935	0.666	0.238	0.646
	Experiment 2	Risk(Mean)	a2	0.162	0.278	0.150	0.132	0.170	0.123	0.167	0.147	0.246	0.204	0.295	0.077	0.240
	Experiment 3	Risk (Min)	a3	0.067	-0.017	0.056	0.049	0.053	0.060	0.079	0.107	0.129	-0.026	0.027	0.027	0.059
Method 2 (probability)	Experiment 4	Risk Average	a4	0.176	0.1718	0.199	0.211	0.176	0.175	0.228	0.261	0.204	0.203	0.169	0.129	0.237

Experiment 1: System Dynamics Model (without Risk Factor)

Table 16-41: Case 1 without risk

Case 1 Without Risk			
Time (Year)	Change in IRI	Total IRI	PCI
0	0.00	0.80	100
1	0.42	1.22	82.3
2	0.84	1.64	67.7
3	1.26	2.06	55.7
4	1.69	2.49	45.8
5	2.11	2.91	37.7
6	2.54	3.34	30.9
7	2.96	3.76	25.4
8	3.40	4.20	20.7
9	3.84	4.64	16.9
10	4.31	5.11	13.6
11	4.80	5.60	10.8
12	5.32	6.12	8.5
13	5.89	6.69	6.5
14	6.50	7.30	4.93
15	7.16	7.96	3.63
16	7.88	8.68	2.61
17	8.65	9.45	1.82
18	9.48	10.28	1.24
19	10.38	11.18	0.82
20	11.35	12.15	0.52

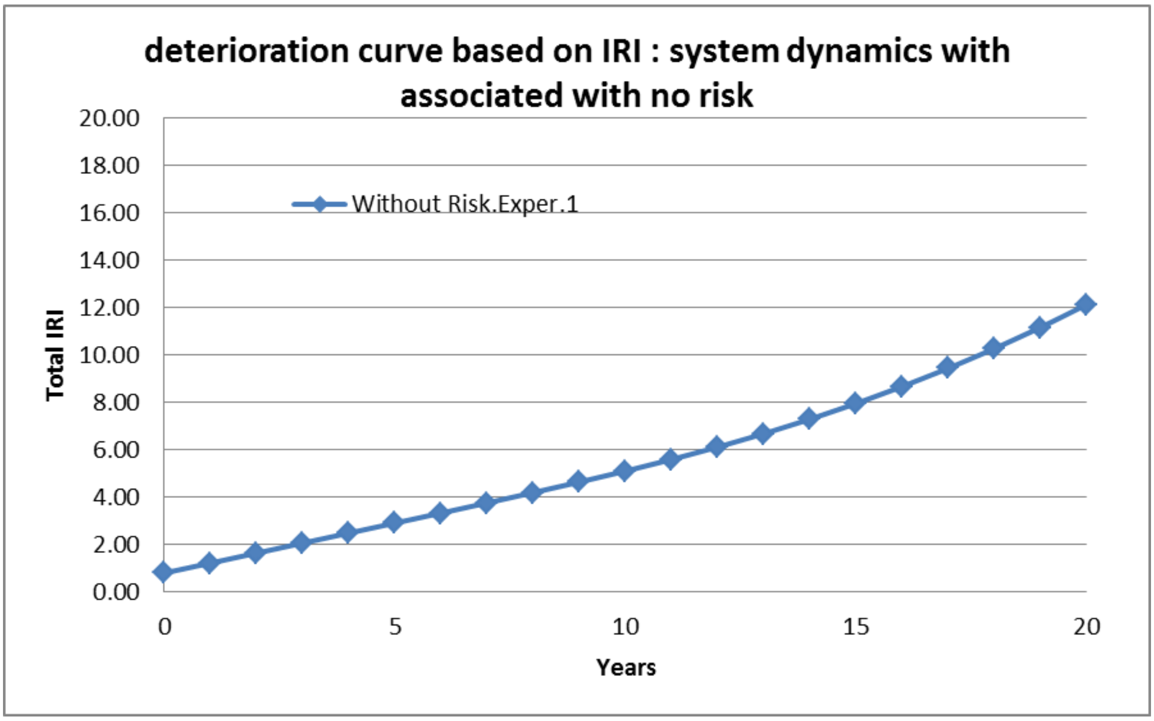

Figure 16-13: Deterioration curve based on IRI using system dynamics model with no risk

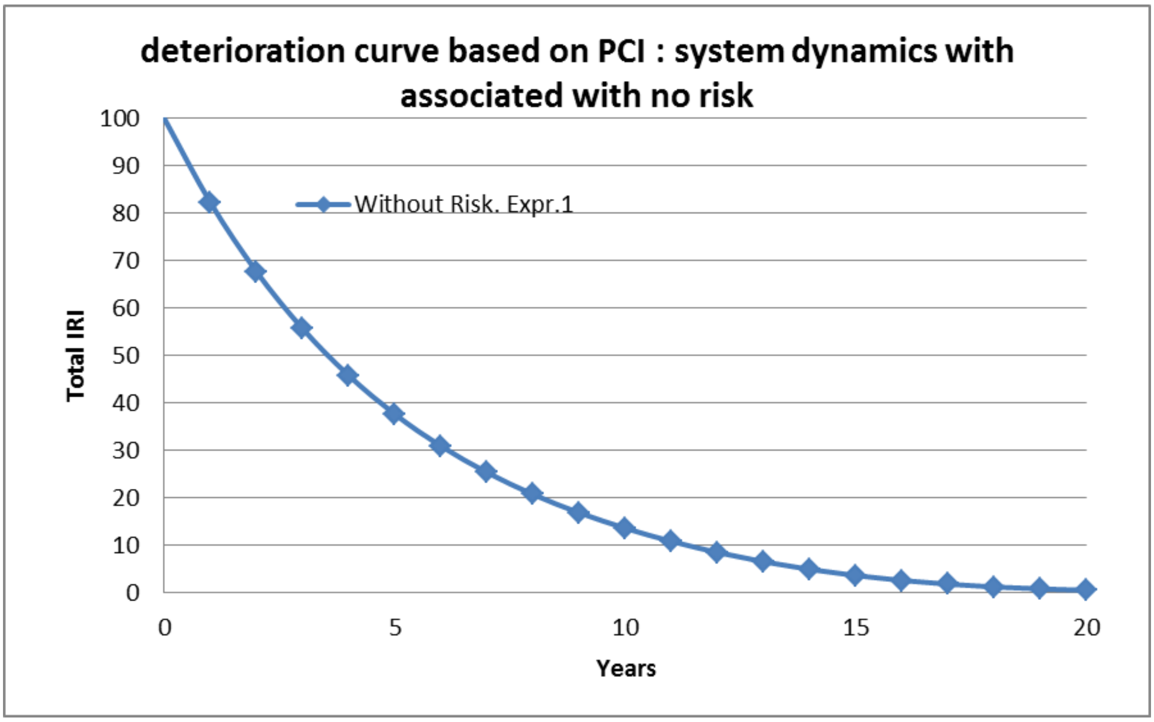

Figure 16-14: Deterioration curve based on PCI using system dynamics model with no risk

Experiment 2 (with Maximum Risk factor Based on Regression Analysis Method)

Table 16-42: Case 2 maximum risk

Case 2 Maximum Risk			
Time (Year)	Change in IRI	Total IRI	PCI
0	0.00	0.80	100
1	0.51	1.31	79.0
2	1.02	1.82	62.4
3	1.53	2.33	49.2
4	2.05	2.85	38.8
5	2.57	3.37	30.5
6	3.10	3.90	23.9
7	3.65	4.45	18.4
8	4.25	5.05	14.0
9	4.91	5.71	10.3
10	5.64	6.44	7.4
11	6.44	7.24	5.1
12	7.31	8.11	3.4
13	8.27	9.07	2.2
14	9.32	10.12	1.34
15	10.46	11.26	0.79
16	11.70	12.50	0.44
17	13.06	13.86	0.24
18	14.55	15.35	0.12
19	16.18	16.98	0.06
20	17.99	18.79	0.02

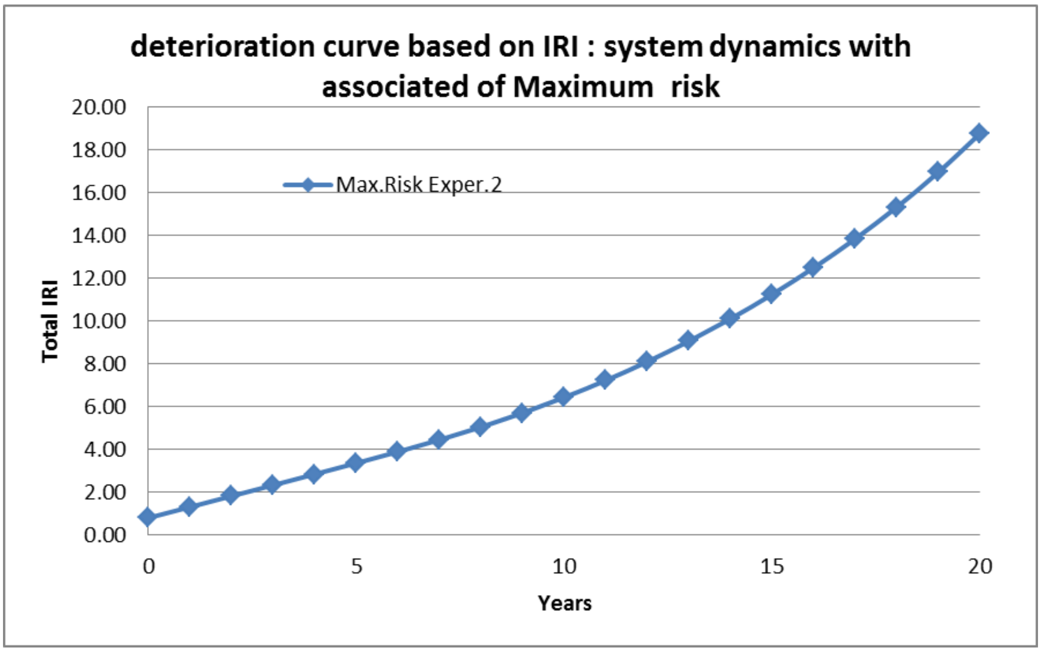

Figure 16-15:Deterioration curve based on IRI using system dynamics model with maximum risk

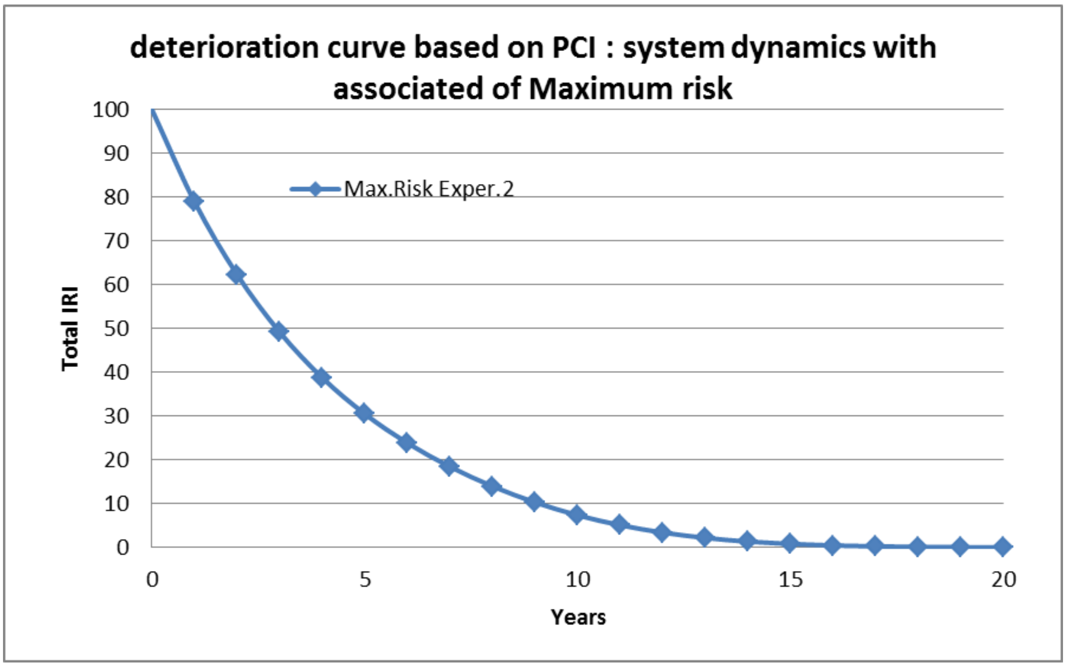

Figure 16-16:Deterioration curve based on PCI using system dynamics model with maximum risk

Experiment 3 (with Mean Risk Factor based on Regression Analysis Method)

Table 16-43: Case 3 mean risk

Case 3 Mean Risk			
Time (Year)	Change in IRI	Total IRI	PCI
0	0.00	0.80	100
1	0.46	1.26	81.0
2	0.92	1.72	65.5
3	1.37	2.17	53.0
4	1.83	2.63	42.8
5	2.29	3.09	34.6
6	2.76	3.56	27.9
7	3.23	4.03	22.5
8	3.71	4.51	17.9
9	4.22	5.02	14.2
10	4.76	5.56	11.1
11	5.34	6.14	8.4
12	5.98	6.78	6.3
13	6.67	7.47	4.6
14	7.41	8.21	3.23
15	8.23	9.03	2.22
16	9.10	9.90	1.48
17	10.05	10.85	0.95
18	11.08	11.88	0.59
19	12.19	12.99	0.35
20	13.39	14.19	0.20

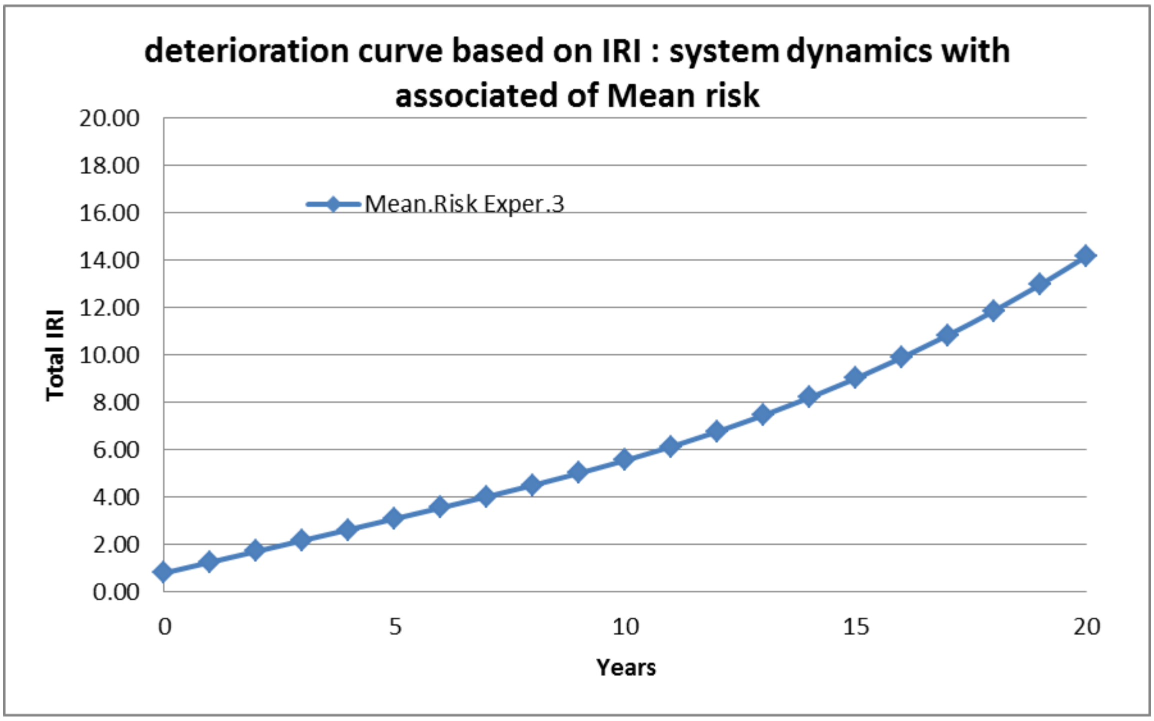

Figure 16-17:Deterioration curve based on IRI using system dynamics model with mean risk

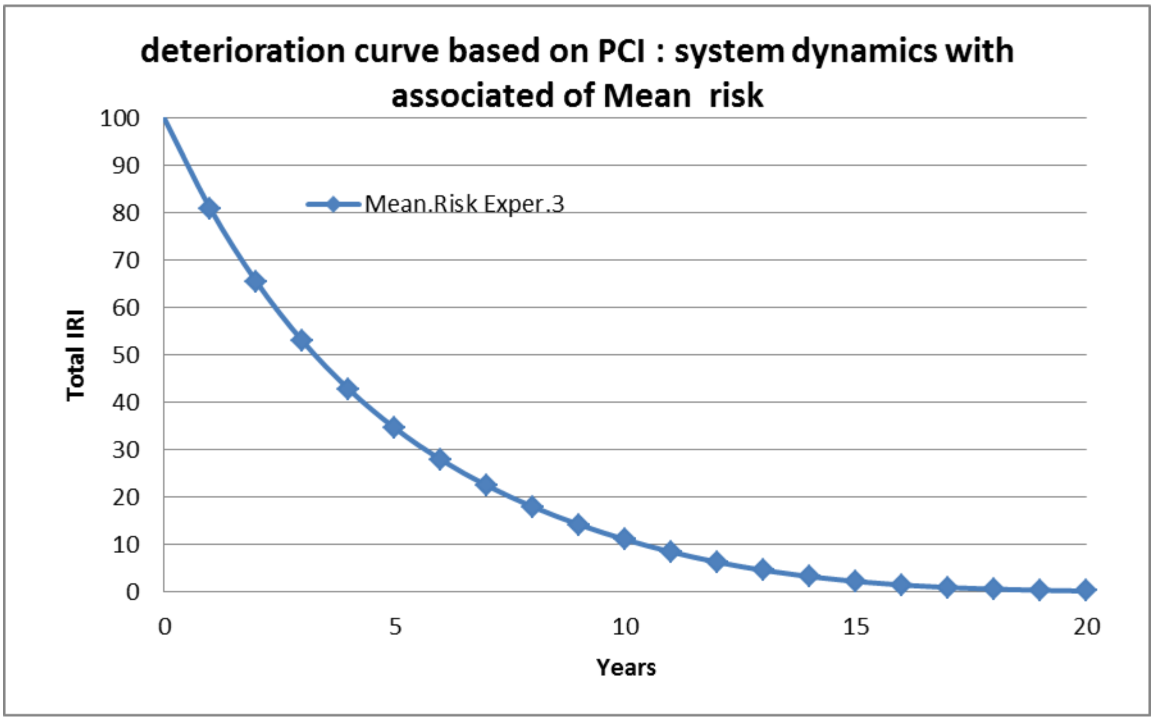

Figure 16-18:Deterioration curve based on PCI using system dynamics model with mean risk

Experiment 4 (with Minimum Risk Factor based on Regression Analysis Method)

Table 16-44:Case 4 minimum risk

Case Minimum Risk			
Time (Year)	Change in IRI	Total IRI	PCI
0	0.00	0.80	100
1	0.42	1.22	82.3
2	0.84	1.64	67.7
3	1.27	2.07	55.7
4	1.69	2.49	45.7
5	2.11	2.91	37.6
6	2.54	3.34	30.9
7	2.97	3.77	25.3
8	3.41	4.21	20.6
9	3.86	4.66	16.7
10	4.33	5.13	13.5
11	4.84	5.64	10.7
12	5.38	6.18	8.3
13	5.97	6.77	6.3
14	6.60	7.40	4.70
15	7.30	8.10	3.41
16	8.04	8.84	2.41
17	8.85	9.65	1.66
18	9.73	10.53	1.11
19	10.67	11.47	0.71
20	11.69	12.49	0.45

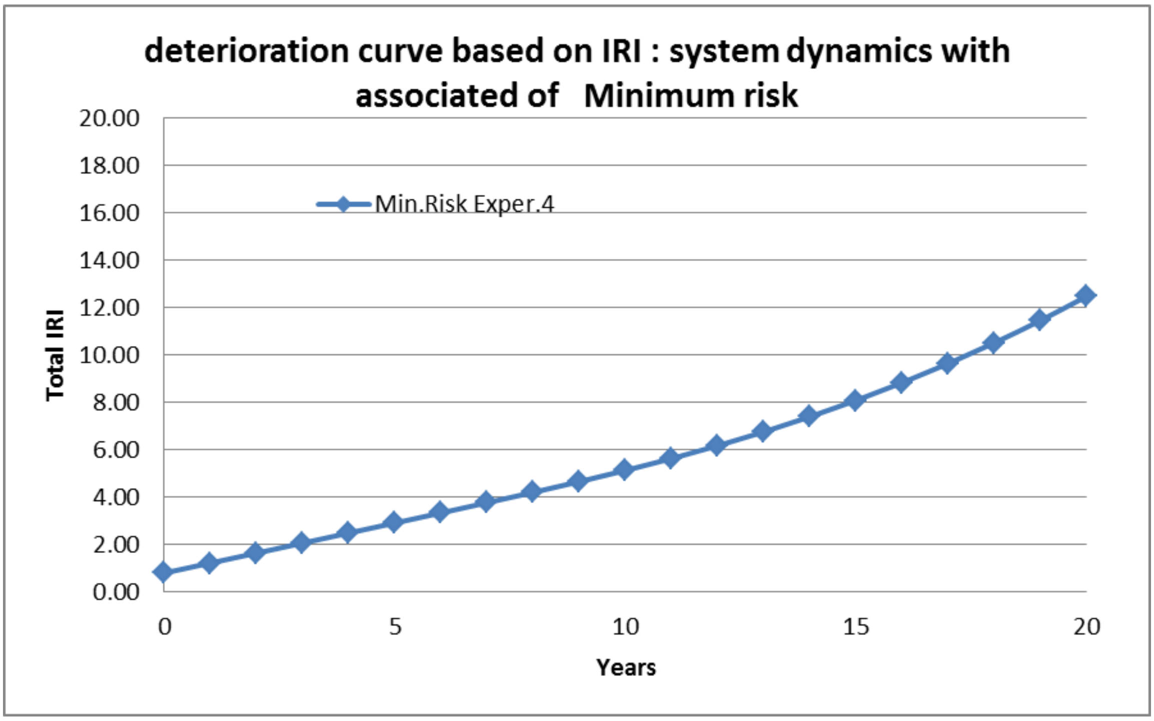

Figure 16-19:Deterioration curve based on IRI using system dynamics model with minimum risk

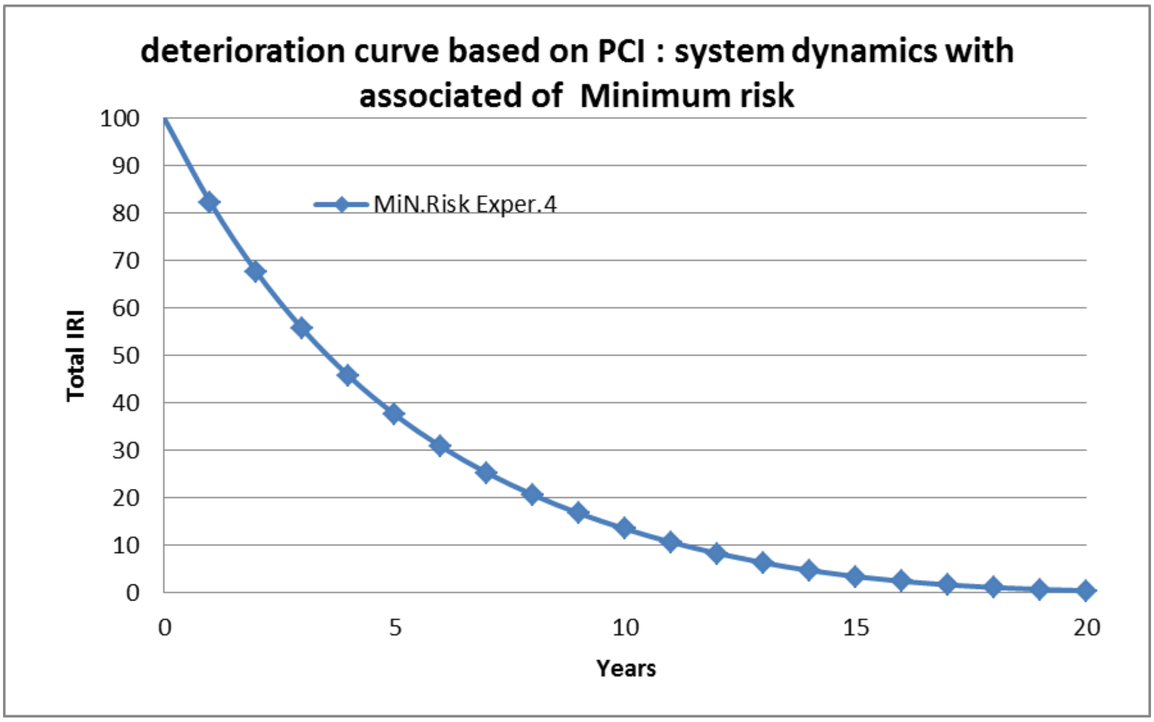

Figure 16-20:Deterioration curve based on PCI using system dynamics model with minimum risk

Experiment 5 (with Average Risk Factor Based on Probability Analysis Method 2)

Table 16-45: Case 5 average risk based on method 2

Case 3 Method 2.Average Risk			
Time (Year)	Change in IRI	Total IRI	PCI
0	0.00	0.80	100
1	0.45	1.25	81.3
2	0.89	1.69	66.1
3	1.34	2.14	53.7
4	1.79	2.59	43.7
5	2.24	3.04	35.4
6	2.70	3.50	28.7
7	3.16	3.96	23.2
8	3.63	4.43	18.6
9	4.13	4.93	14.8
10	4.67	5.47	11.5
11	5.25	6.05	8.8
12	5.88	6.68	6.6
13	6.57	7.37	4.8
14	7.32	8.12	3.37
15	8.14	8.94	2.30
16	9.04	9.84	1.53
17	10.00	10.80	0.97
18	11.06	11.86	0.60
19	12.20	13.00	0.35
20	13.45	14.25	0.20

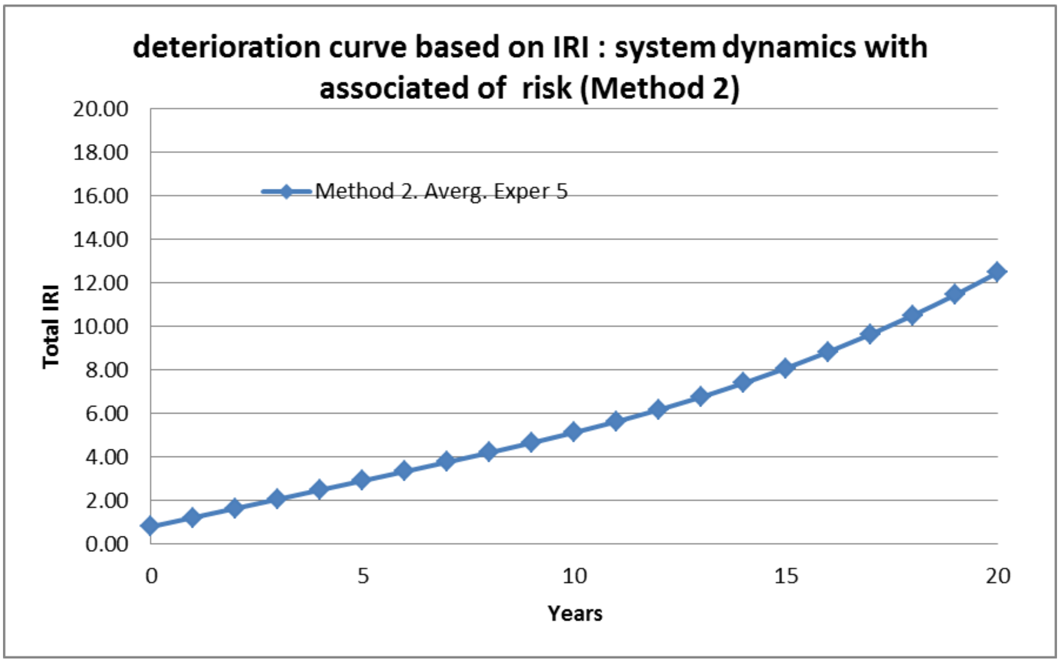

Figure 16-21:Deterioration curve based on IRI using system dynamics model with average risk based on method 2

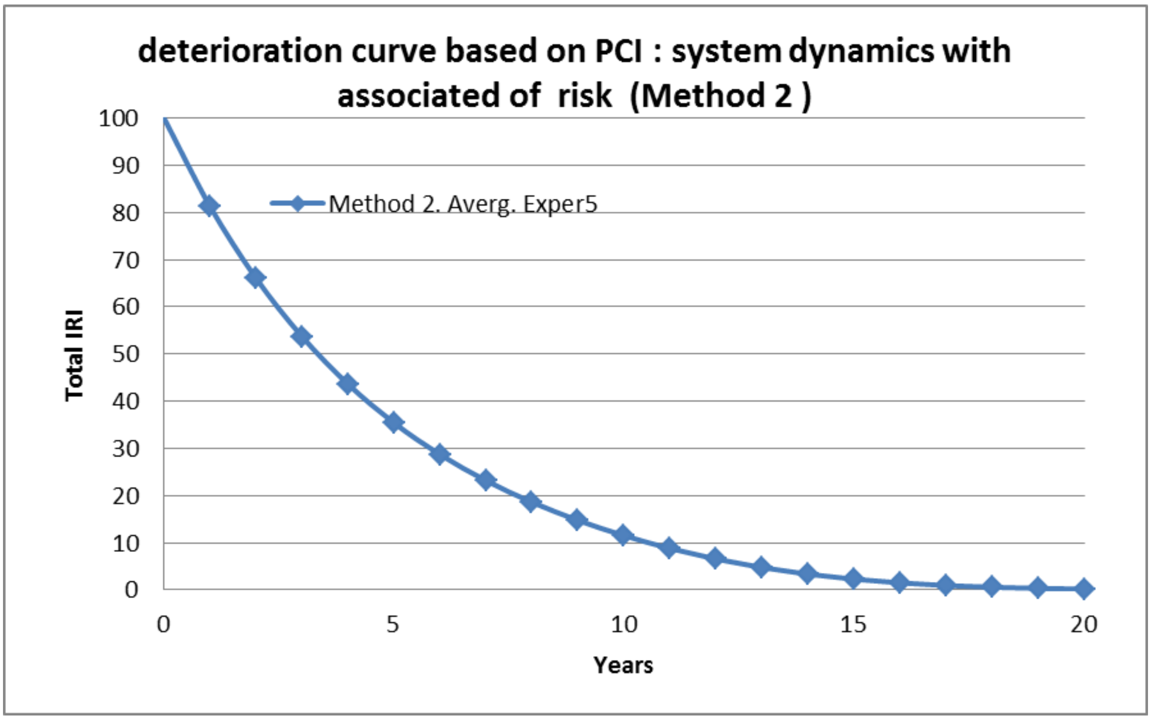

Figure 16-22:Deterioration curve based on PCI using system dynamics model with average risk based on method 2